HELDER FILIPE DOS SANTOS VIANA

MODELLING AND MAPPING ABOVEGROUND BIOMASS FOR ENERGY USAGE AND CARBON STORAGE ASSESSMENT IN MEDITERRANEAN ECOSYSTEMS

DOCTORAL DEGREE IN AGRICULTURAL AND FORESTRY SCIENCES

Supervisor: Professor Doutor José Tadeu Marques Aranha

UNIVERSIDADE DE TRÁS-OS-MONTES E ALTO DOURO

VILA REAL, 2012

Este trabalho foi expressamente elaborado como tese original com o objectivo da obtenção do grau de Doutor em Ciências Agronómicas e Florestais ao abrigo do Decreto-Lei n.º 74/2006, de 24 de Março, alterado pelo Decreto-Lei n.º 107/2008, de 25 de Junho, e pelo Decreto-Lei n.º 230/2009, de 14 de Setembro.

Acknowledgments

These lines that often go unnoticed to readers are perhaps the most complex to write. Given the dynamics involved in a task of this nature, as well the extended period of time for its realization, there were many people who, somehow, gave their contribution. Some people who were important in the beginning were replaced by others during the work. However, whether it was directly about the work, whether it was indirectly about several issues which are part of the individual, all contributions were important. So, my first thanks generic and abstract go to all those who, at some point, gave me encouragement to continue and go further.

In order to express adequately my gratitude to some people who gave me support during my research studies and made this thesis possible, the next lines will be written in Portuguese.

Ao Prof. Doutor José Aranha (Departamento de Ciências Florestais e Arquitectura Paisagista, Escola de Ciências Agrárias e Veterinárias da Universidade de Trás-os-Montes e Alto Douro), pela orientação, apoio, revisão de trabalhos e pela amizade que sempre emprestou nos momentos difíceis, e nos muito difíceis, que existiram ao longo destes vários anos.

Ao Prof. Doutor Domingos Lopes (Departamento de Ciências Florestais e Arquitectura Paisagista, Escola de Ciências Agrárias e Veterinárias da Universidade de Trás-os-Montes e Alto Douro), pela co-orientação no âmbito da bolsa da Fundação para a Ciência e a Tecnologia, que em dado momento foi cirúrgica para continuar o percurso, pelo incentivo, motivação, estabelecimento de pontes, cedência de contactos e amizade prestada.

Ao Prof. Doutor Warren B. Cohen (USDA Forest Service) pela co-orientação no âmbito da bolsa da Fundação para a Ciência e a Tecnologia, pela ajuda na revisão de trabalhos e por ter sido co-autor de artigos científicos publicados.

Ao Prof. Doutor José Luís Lousada (Departamento de Ciências Florestais e Arquitectura Paisagista, Escola de Ciências Agrárias e Veterinárias da Universidade de Trás-os-Montes e Alto Douro), pela ponte criada com a Escuela Universitaria de

Ingeniería Técnica Forestal da Universidade de Vigo, pelo auxílio na medição das densidades das amostras de biomassa e por ter sido co-autor de um artigo científico publicado.

Ao Prof. Doutor Luis Ortiz Torres (Escuela Universitaria de Ingeniería Técnica Forestal. Universidade de Vigo) por me ter recebido em Pontevera-Vigo e por ter sido co-autor de um artigo científico publicado.

Ao Doutor Daniel Vega-Nieva (Escuela Universitaria de Ingeniería Técnica Forestal. Universidade de Vigo), pela estreita colaboração enquanto co-autor de um artigo científico publicado.

Ao Prof. Doutor Carlos Pacheco Marques (Departamento de Ciências Florestais e Arquitectura Paisagista, Escola de Ciências Agrárias e Veterinárias da Universidade de Trás-os-Montes e Alto Douro) por ter tido a amabilidade de fazer uma recomendação para obtenção de uma bolsa de investigação científica.

Ao Investigador Doutor Paulo Fernandes (Departamento de Ciências Florestais e Arquitectura Paisagista, Escola de Ciências Agrárias e Veterinárias da Universidade de Trás-os-Montes e Alto Douro) por ter tido a amabilidade de fazer uma recomendação para obtenção de uma bolsa de investigação científica, pela cedência de bibliografia e por ter sido co-autor de um artigo publicado.

Ao Prof. Doutor Salvador Malheiro (Departamento de Engenharias, Escola de Ciências e Tecnologia da Universidade de Trás-os-Montes e Alto Douro), pela disponibilização de meios para medição dos poderes caloríficos das amostras de biomassa.

Ao Eng.º Cristóvão Santos (Departamento de Engenharias, Escola de Ciências e Tecnologia da Universidade de Trás-os-Montes e Alto Douro), pela sempre pronta ajuda e pelos ensinamentos que permitiram avaliar os poderes caloríficos das amostras de biomassa.

Ao Sr. Armindo Teixeira, assistente operacional do Laboratório de Produtos Florestais (Departamento de Ciências Florestais e Arquitectura Paisagista, Escola de Ciências Agrárias e Veterinárias, UTAD), pela ajuda e aconselhamento na preparação das amostras de biomassa para posterior análise termo-físico-químicas.

Às diversas empresas florestais que fizeram os abates dos pinheiros e eucaliptos agradeço terem acolhido, colaborado e permitido que se fizessem as medições de campo e pesagens da biomassa florestal.

Aos alunos e estagiários, hoje Licenciados, Bruno Abrantes, José Rocha, Henrique Silva, Carlos Carvalho e Mauro Santos, que parcialmente, em maior ou menor grau, foram participando nos fastidiosos trabalhos de campo como a medição, pesagem e separação das componentes de biomassa. Aos alunos e estagiários, hoje Licenciados, Carla Marques, Sara Dias, Ângelo Correia, Marco Cruz, Rogério Queirós, Ricardo Correia, que para além do maior volume de trabalho de campo colaboraram nas análises laboratoriais dos parâmetros termo-físico-químicos. A base de dados recolhida, que foi o cerne deste trabalho, não teria sido possível construir sem esta preciosa colaboração.

Ao Eng.º Rui Rocha da LECO Instrumentos, S.A., pela ajuda na avaliação química elementar das amostras de biomassa.

Ao Sr. Carlos Matos, técnico assistente, (Departamento de Química da Universidade de Trás-os-Montes e Alto Douro), pela realização das análises químicas das amostras de biomassa.

Aos Revisores anónimos das revistas e dos encontros científicos, aos quais submetemos parte dos estudos realizados, agradecemos os comentários e sugestões que contribuíram para a redacção desta tese.

À Escola Superior Agrária de Viseu do Instituto Superior Politécnico de Viseu (ESAV-IPV) pela flexibilidade na elaboração dos horários de docência no decurso dos trabalhos de Doutoramento.

Ao Eng.º Edgar Santos, amigo de longa data pelo apoio, pela leitura e revisão do Inglês da tese.

Às minhas colegas (ESAV-IPV), e fundamentalmente amigas Dr.ª Ana Liza Oliveira, Dr.ª Carla Santos e Engª Daniela Costa, cujo esplendor de brilho estelar desvanece os dias de trovoada.

Ao Prof. Doutor José Luís Pereira (ESAV-IPV), colega e amigo, pelas sugestões de organização da tese.

Ao Doutor João Mesquita (ESAV-IPV), colega e amigo, pela leitura e revisão do Inglês de partes da tese.

Ao Eng.º Pedro Cardoso, colega e amigo, pela leitura e revisão do Inglês da tese.

Ao Eng.º João Paulo Gouveia (ESAV-IPV), colega e amigo, e Dr.ª Ana Marques agradeço o apoio na árdua jornada.

Ao Eng.º António José Almeida, pela amizade e terapêuticas horas de convívio.

A todos aqueles que de alguma forma contribuíram para a realização desta tese.

Por último, àqueles que em última instância, mesmo que em silêncio, estão sempre lá a desejar-nos o melhor, os meus avós, pais, irmãos, cunhadas e sobrinhos com um especial beijo à minha irmã Cláudia que me soube surpreender.

Support Funding

The research described in this thesis was financially supported by a grant, ref: SFRH/PROTEC/49626/2009, for the period 2009-2012, from the Portuguese Science and Technology Foundation (FCT/MCTES, Portugal) and Polytechnic Institute of Viseu (IPV) The financial support included the tuition fees and 50 % reduction of the teaching workload.

Apoios de impressão da Tese:
"Este trabalho é financiado por Fundos FEDER através do Programa Operacional Factores de Competitividade - COMPETE e por Fundos Nacionais através da FCT - Fundação para a Ciência e a Tecnologia no âmbito do projecto FCOMP-01-0124-FEDER-022692".

Supervisor: Prof. Doutor José Tadeu Marques Aranha from Departamento de Ciências Florestais e Arquitectura Paisagista da Universidade de Trás-os-Montes e Alto Douro.

Co-supervisor: Prof. Doutor Domingos Manuel Mendes Lopes from Departamento de Ciências Florestais e Arquitectura Paisagista da Universidade de Trás-os-Montes e Alto Douro.

Co-supervisor: Prof. Doutor Warren B. Cohen from College of Forestry of Oregon State University.

Abstract

Estimates of aboveground biomass stocks are essential for studying the ecosystems dynamics as carbon sinks and consequent role in mitigating climate change. This is particularly important in Mediterranean ecosystems, since it is widely recognized their greater vulnerability to prospective climate change. Moreover, due to efforts in fossil fuels replacement the use of biomass to energy purposes has been increasing. As a consequence, measurements of aboveground biomass and knowledge of biomass characteristics and properties are needed for achieving accurate estimates. In this context, a study was carried out in the main Portuguese forest ecosystems: Maritime pine (*Pinus pinaster* Aiton) and Eucalyptus (*Eucalyptus globulus* Labill.) stands and in shrubland areas. Within these ecosystems-types located in the North-Center region of Portugal an exhaustive field wok were conducted, since 2006, to collect the data used in this research.

By means of destructive sampling technique a specific system of additive nonlinear allometric equations was developed for estimating maritime pine and eucalyptus aboveground biomass stocks and a set of specific equations were established to predict the shrubland aboveground biomass. To spatially assess the aboveground biomass stocks of forest stands and shrubland in this characteristic region, different mapping approaches based in inventory data, remote sensing imagery and spatial predictions models were investigated and compared. Apart from other physical and chemical properties determinations, carbon content in tree biomass components and shrub pool was achieved showing that the ecosystems studied store important amounts of carbon. The fuelwood characteristics and biomass combustion properties of maritime pine, eucalyptus and main native woody shrub species were evaluated and the potential of forest biomass for energy production at industrial scale in Portugal was assessed.

The developed specific equation models in conjunction with the studied mapping techniques and with the values found in this research, *inter alia*, of carbon fraction of dry matter and heating values per tree component are an important contribute to estimate more accurately the carbon uptake and the energy potential of the studied ecosystems.

Key-Words: Additive equations, Biomass, Bioenergy, Carbon, Forest Inventory, GIS, Heating value, Remote Sensing.

Resumo

A quantificação da biomassa dos espaços florestais é essencial para a investigação da dinâmica dos ecossistemas como sumidouro de carbono e consequente papel na mitigação das alterações climáticas. Este conhecimento é particularmente importante nos ecossistemas mediterrânicos, uma vez que é amplamente reconhecida a sua maior vulnerabilidade às previstas alterações climáticas. Adicionalmente, a utilização de biomassa para produção de energia tem vindo a aumentar nos últimos anos com o intuito de substituir o consumo de energia, proveniente de fontes fósseis não renováveis. Consequentemente, as avaliações de biomassa bem como o estudo das suas características e propriedades são necessárias para se atingiram estimativas o mais correctas possíveis.

Neste contexto, foi delineado um estudo, desde 2006, nas espécies mais representativas dos ecossistemas florestais de Portugal: o pinheiro-bravo (*Pinus pinaster* Aiton) e o eucalipto (*Eucalyptus globulus* Labill.), bem como nas espécies arbustivas lenhosas que compõem as áreas mais significativas de matorral. No Norte e Centro do país, foram instaladas parcelas de inventário onde se fizeram diversas medições dendrométricas e, utilizando o método destrutivo, foram feitas pesagens da biomassa aérea das espécies mencionadas. Por ajustamento simultâneo foram desenvolvidos dois sistemas de equações para estimativa da biomassa das componentes de pinheiro bravo e das componentes de eucalipto, observando a aditividade das estimativas das componentes individuais. Foram também desenvolvidas diversas equações para estimativa da biomassa de matorral utilizando diferentes variáveis independentes. Com o intuito de fazer a quantificação espacial da biomassa florestal foram investigados diferentes métodos de mapeamento, combinando dados de inventário florestal convencional, dados obtidos em imagens de satélite e modelos de predição espacial, incluindo a geoestatística.

A biomassa florestal e arbustiva foi caracterizada e as propriedades avaliadas por análises termo-físico-químicas. Desta forma, foi possível avaliar o carbono acumulado quer na biomassa das diferentes fracções da árvore, quer nas principais espécies arbustivas lenhosas características destes ecossistemas. Os resultados mostraram que os valores diferem da fracção de 50%, usualmente considerada em diversos estudos. Com a obtenção destes valores, é possível fazer estimativas mais precisas da acumulação de carbono e consequentes emissões de dióxido de carbono para a atmosfera.

A avaliação dos poderes caloríficos da biomassa das diferentes componentes de pinheiro-bravo, eucalipto e matos, permite avaliar com maior rigor o potencial desta biomassa para fins energéticos. O potencial da biomassa de pinheiro-bravo e eucalipto para produção de energia, em centrais de biomassa dedicadas, foi avaliado para Portugal. A análise mostrou que para suprir as necessidades previstas para os projectos em curso terão de ser consideradas outras fontes de combustível.

O conjunto de modelos alométricos desenvolvidos associados aos métodos de mapeamento investigados e às medições das fracções de carbono e poderes caloríficos específicos para cada componente das espécies de pinheiro-bravo, eucalipto, bem como para as arbustivas lenhosas, são um contributo para se obter com maior exactidão o carbono capturado e o potencial energético da biomassa dos principais ecossistemas florestais da região Norte e Centro de Portugal.

Palavras-Chave: Ajustamento simultâneo, Biomassa, Bioenergia, Carbono, Inventário Florestal, Poderes caloríficos, Detecção Remota, SIG

List of Publications

The content of this thesis was, fully or partially, published in the following scientific manuscripts, book chapter and in conference proceedings, ordered in reverse chronological order of their writing.

Viana, H., Vega-Nieva, D., Ortiz Torres, L., Lousada, J., Aranha, J., 2012. Fuel characterization and biomass combustion properties of selected native woody shrub species from central Portugal and NW Spain. Fuel 102, 737-745. (JCR® $IF_{5\text{-year (cites in 2011)}}$: 3.791; Q_1).

Viana, H., Aranha, J., Lopes, D., Cohen, W.B., 2012. Estimation of crown biomass of *Pinus pinaster* stands and shrubland above-ground biomass using forest inventory data, remotely sensed imagery and spatial prediction models. Ecological Modelling 226, 22-35. (JCR® $IF_{5\text{-year (cites in 2011)}}$: 2.714; Q_2).

Viana, H., Lopes, D., Aranha, J., 2011. Assessment of Forest Aboveground Biomass Stocks and Dynamics with Inventory Data, Remotely Sensed Imagery and Geostatistics, in: Shaukat, S.S. (ed.), Progress in Biomass and Bioenergy Production. InTech, pp. 107-130. ISBN: 978-953-307-491-7.

Aranha, J., Calvão, A., Lopes, D., Viana, H., 2011. Quantificação da biomassa consumida nos últimos 20 anos de fogos florestais no Norte de Portugal. Info 26, 44-49.

Viana H.; Aranha J.; Lopes D., 2011. Dedicated Biomass Plants for Combined Heat & Power (CHP). The Portuguese National Strategy. 19th European Biomass Conference and Exhibition. ETA-Florence Renewable Energies. Berlin, Germany. June 6-10.

Viana, H., Cohen, W.B., Lopes, D., Aranha, J., 2010. Assessment of forest biomass for use as energy. GIS-based analysis of geographical availability and locations of wood-fired power plants in Portugal. Applied Energy 87, 2551-2560. (JCR® IF_{2011}: 5.106; Q_1).

Viana, H., Dias, S., Marques, C., Cruz, M., Lopes, D., Aranha, J., 2009. Estabelecimento de modelos alométricos para predição da biomassa aérea da *Pinus Pinaster*. Actas do 6º Congresso Florestal Nacional. Ponta Delgada, Açores. 6-9 Outubro., pp. 771-775.

Viana, H., Dias, S., Marques, C., Cruz, M., Lopes, D., Aranha, J., 2009. Estabelecimento de modelos alométricos para predição da biomassa aérea de *Eucalyptus globulus*. Actas do 6º Congresso Florestal Nacional. Ponta Delgada, Açores. 6-9 Outubro, pp. 765-770.

Viana, H., Fernandes, P., Rocha, R., Lopes, D., Aranha, J., 2009. Alometria, Dinâmicas da Biomassa e do Carbono Fixado em Algumas Espécies Arbustivas de Portugal 6º Congresso Florestal Nacional. Ponta Delgada, Açores. 6-9 Outubro, pp. 244-252.

Viana, H., Lopes, D., Aranha, J., 2009. Predição de biomassa arbustiva lenhosa empregando dados de inventário e o índice de diferença normalizada extraído em imagens Landsat 5 TM, ISPV Millenium. 37.

Helder Viana contributed with idea, method, and experimental work to all publications except the following, whose initial idea and method was from José Aranha: Aranha, J., Calvão, A., Lopes, D., Viana, H., 2011. Quantificação da biomassa consumida nos últimos 20 anos de fogos florestais no Norte de Portugal. Info 26, 44-49.

Table of Contents

List of Figures

List of Tables

1

Introduction

1.1 Climate change and Terrestrial Carbon Processes

Climate change, which discussion has been done worldwide, is recognized by the Intergovernmental Panel on Climate Change (IPCC, 2011) as one of the great challenges of the 21st century. The global response to climate change, started in 1992 with the United Nations Framework Convention on Climate Change (UNFCCC) (United Nations, 1992) and strengthened by the commitment established with the Kyoto Protocol, in 1997 (United Nations, 1998), formally recognized the need of reduce and prevent anthropogenic emissions of greenhouse gases (GHG), where the carbon dioxide (CO_2) sequestration in marine and terrestrial ecosystems receive particular attention.

Terrestrial ecological systems, in which carbon is retained in live biomass, decomposing organic matter, and soil, play an important role in the global carbon cycle (IPCC, 2000a). The dynamics of terrestrial ecosystems depend on interactions between a number of biogeochemical cycles, particularly the carbon cycle, nutrient cycles, and the hydrological cycle, all of which may be modified by human actions (IPCC, 2000a).

The carbon cycle is the fluxes of carbon among four main reservoirs: fossil carbon, the atmosphere, the oceans, and the terrestrial biosphere (Figure 1.1). A wide range of direct and indirect measurements confirm that the atmospheric mixing ratio of CO_2 has increased globally by 36%, from a range of 275 to 285 ppm (ppm = parts per million) in the pre-industrial Era (usually dated from 1750) to 379 ppm in 2005, as concluded in the IPCC Fourth Assessment Report (AR4) (Forster et al., 2007), and continued to grow to over 390 ppm (39%) above pre-industrial levels, by the end of 2010 (IPCC, 2011). The annual growth rate of atmospheric CO_2 was 2.36±0.09 ppm in 2010, one of the largest growth rates in the past decade. The average for the decade 2000-2009 was 1.9±0.1 ppm per year, 1.5±0.1 ppm for the decade 1990-1999, and 1.6±0.1 for the decade 1980-1989. The present concentration is the highest during at least the last 800,000 years (GCP, 2012). The accumulation of atmospheric CO_2 in 2010 was 5.0±0.2 PgC (1 Pg = Petagram = 1Gigatonne = 1 billion metric tons = 1×10^{15} g), with a total cumulative of 157.5 PgC since the beginning of atmospheric high precision measurements in 1959 and 237 PgC since 1750.

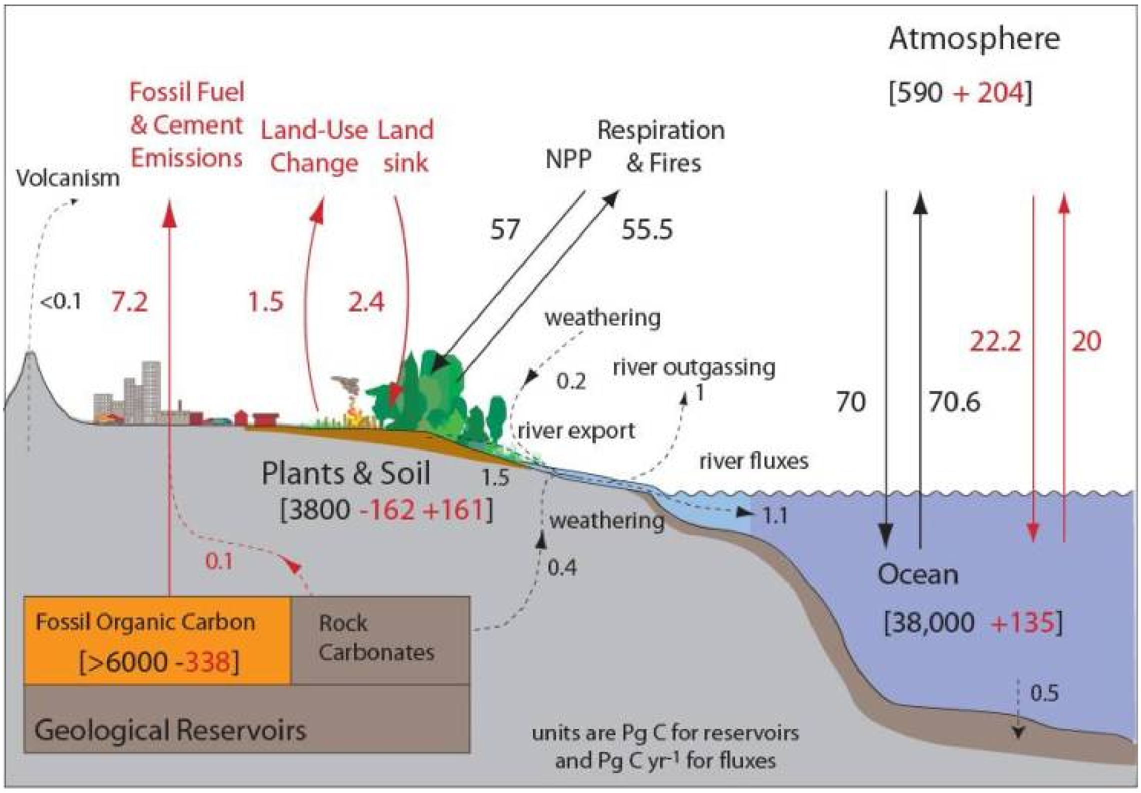

Figure 1.1 - Annual carbon cycle (Average for the time period 2000-2005).

Source: Adapted from PMEL Carbon Group (2012).

Note: The numbers in square brackets shows the pre-industrial carbon values storage plus the balance after the human emissions. The exchanges of CO_2 between different pools of carbon indicate the effects that the human emissions have had on the carbon cycle. The exchanges are in pentagrams of carbon per year (PgC yr^{-1}).

The rates of atmospheric CO_2 accumulation are influenced by both the anthropogenic emissions and the net uptake by natural sinks (ocean and land) (GCP, 2012). Hence, uncertainties in the individual numbers of carbon budget are large as it remains difficult to quantify the influences of the separate but interactive several processes (e.g. forest regrowth, CO_2 fertilization of plant growth, the interaction with other biogeochemical cycles) in the fluxes among the main carbon reservoirs (Schimel, 1995).

1.2 Fossil Fuel and Cement CO_2 Emissions

Among the many human activities that produce Greenhouse Gases, the use of energy represents by far the largest source of emissions. GHG emissions from the energy sector are dominated by the direct combustion of fuels. Since the Industrial Revolution, annual CO_2 emissions from fuel combustion increased from near zero to concerning values. The annual emission rate from fossil fuel burning (plus a small contribution from cement production) averaged 5.4 ± 0.3 PgC yr^{-1} during 1980 to 1989, 6.3 ± 0.4 PgC yr^{-1} during 1990 to 1999 (Prentice et al., 2001) and 7.2± 0.3 PgC yr^{-1} in 2000–2005 (IPCC, 2007b). However, the increasing rate of growth of CO_2 emissions averaged 7.9 PgC yr^{-1} (29 Pg CO_2) in 2009 (IEA, 2011b) and in 2010 reached 9.1±0.5 PgC (33.4 Pg CO_2) (Peters et al., 2012).

Accordingly IEA (2011b) statistics, CO_2 from energy represents about 83% of the anthropogenic GHG emissions for the Annex I countries of the United Nations Framework Convention on Climate Change and about 65% of global emissions (IEA, 2011b). Activities related to land-use, primarily tropical deforestation and biomass burning are responsible for the rest of the emissions. However, according to the rates of anthropogenic CO_2 emissions reported, for 2010 (Boden et al., 2011; Peters et al., 2012), 91% (9.1±0.5 PgC yr^{-1}; 33.4 Pg CO_2) are due to fossil fuel and Cement burning and 9% are due to land-use change (0.9±0.7 PgC yr^{-1}; 3.3 Pg CO_2) leading to total emissions (including fossil fuel and land-use change) of 10.0±0.9 PgC yr^{-1}. These differences and discrepancies in estimates of carbon emissions have been reported and analysed in order to understand how uncertain are estimates of CO_2 emissions (e. g. IPCC, 2000b; Houghton, 2003b; IPCC, 2006b; Marland et al., 2009). In general, the uncertainties of quantified emission are attributed to the uncertainties of statistics independently reported by the largest contributing organizations under the UNFCCC (UNFCCC, 2012) and the Kyoto Protocol, which depend on the quality and availability of sufficient data and comparable methods to estimate emissions (IEA, 2011b).

1.3 Land Use, Land-Use Change, and Forestry (LULUCF) on Greenhouse Gas Sources and Sinks

Since the Kyoto Protocol (United Nations, 1998) that Land Use, Land-Use Change and Forestry (LULUCF) activities received special concern as one of the major sources and sinks of GHG emissions. According to the Kyoto Protocol, signatories countries (Annex I) are required to report afforestation, reforestation and deforestation since 1990 (Article 3.3). Parties can elect to report emissions and removals from any of the following other human-induced activities since 1990 (Art. 3.4): Forest Management, Cropland Management, Grassland Management and Re-vegetation. The methodologies to estimate emissions and removals of GHG are described in the methodological guidelines by IPCC (IPCC, 2003, 2006a), which will be addressed in section 1.6.

Changes in land use and management affect the amount of carbon in plant biomass and soils (Prentice et al., 2001). During the last two centuries, soils have lost a considerable amount of C due to land use changes and expansion of agriculture. These losses from soils are clearly of concern in relation to future productivity and environment (Nieder and Benbi, 2008). The uncertainty on Land Use, Land-Use Change, and Forestry (LULUCF) emissions is the highest of any flux component of the global carbon budget. Since in the past decades, the CO_2 flux caused by land-use changes has been dominated by tropical deforestation (Denman et al., 2007; Havemann, 2009), the large uncertainties in emission estimates arise from inadequate data on the carbon density of forests and the regional rates of deforestation (Baccini et al., 2012).

The average annual global carbon budgets for 1980–1989 and 1989-1998 were estimated in 1.7±0.8 PgC yr^{-1} and 1.6±0.8 PgC yr^{-1}, respectively (IPCC, 2000a). For the period between 2000-2010 (Figure 1.2) the average rate of carbon emissions due to LULUCF account around 11% (1.0±0.7 PgC yr^{-1}) as the fossil fuel rate are estimated in 89% (7.9±0.5 PgC yr^{-1}) (Boden et al., 2011; Peters et al., 2012). However, different estimates of the land use flux than those reported in the Third Assessment Report (TAR) (Prentice et al., 2001) were updated for the 1980s and for the 1990s (2.0 ± 0.8 PgC yr^{-1} and 2.2 ± 0.8 PgC yr^{-1}, respectively (Houghton, 2003a), which gives even more higher carbon losses from tropical deforestation (Denman et al., 2007). Although the uncertainty in the net CO_2 emissions due to land-use change is large, the estimated net emissions for the decade of 2000 reveal a decline trend from the emissions due to land-use change. Carbon losses occur through decreased vegetation productivity, increased respiration, deforestation, biomass combustion and other poor land management practices. The implementation of new land policies, higher law enforcement to stop illegal deforestation, and new afforestation and regrowth of previously deforested areas could all have contributed to this decline (GCP, 2012).

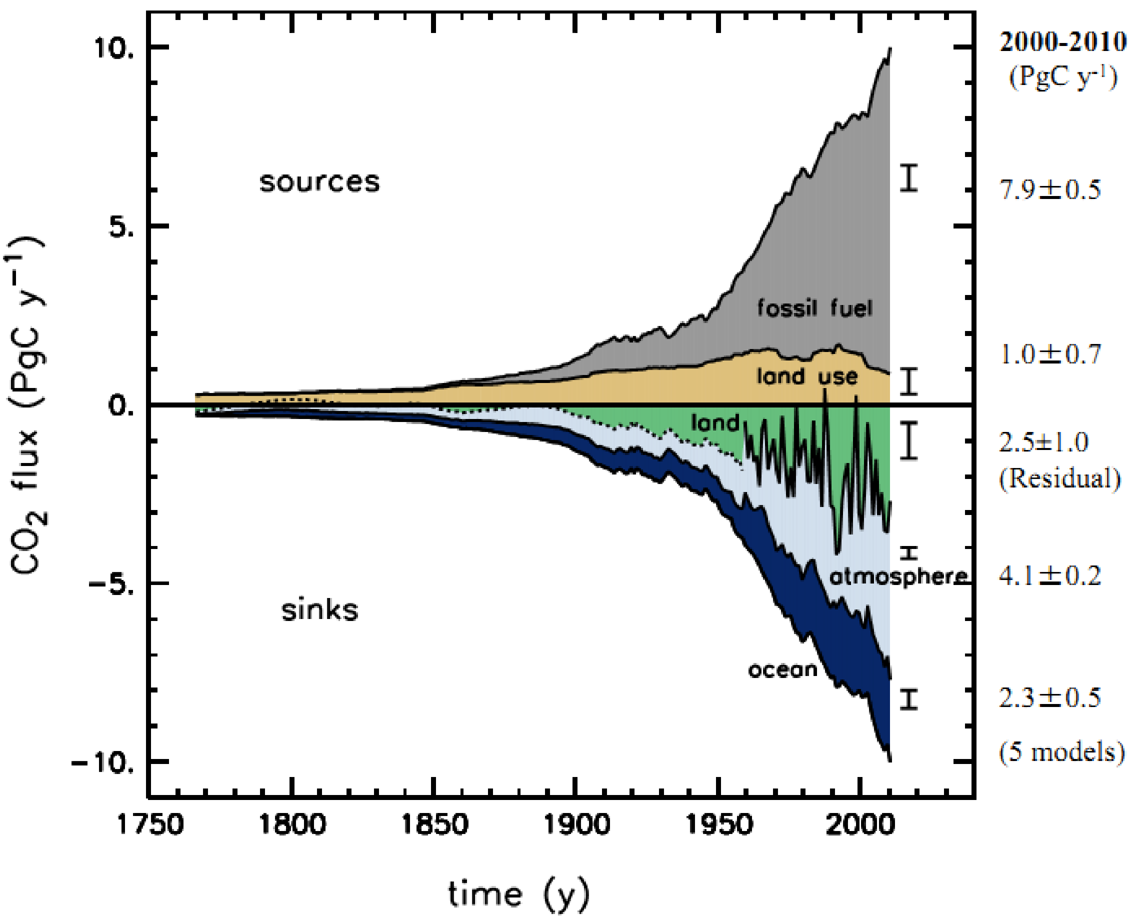

Figure 1.2 - Human Perturbation of the Global Carbon Budget.
Source: Adapted from Global Carbon Project (2012).

Accordingly the Global Forest Resources Assessment 2010 (FRA 2010) the afforestation and natural expansion of forests in some countries and regions have reduced the net loss of forest area significantly at the global level. The net change in forest area in the period 2000-2010 is estimated at -5.2 million hectares per year, down from -8.3 million hectares per year in the period 1990–2000. Additionally, during 2005-2010, the area of planted forest increased by about 5 million hectares per year (FAO, 2010a). In fact, during the last decades, terrestrial ecosystems may have served as a small net sink for CO_2. This terrestrial sink seems to have occurred in spite of net emissions into the atmosphere from land-use change, primarily in the tropics. The net terrestrial carbon uptake, that approximately balances the emissions from land-use change in the tropics, results from land-use practices and natural regrowth in middle and high latitudes, the indirect effects of human activities (e.g., atmospheric CO_2 fertilization and nutrient deposition), and changing climate (both natural and anthropogenic). It is presently not possible to determine the relative importance of these different processes, which also vary from region to region (IPCC, 2000a). Hence, understanding CO_2 capture and storage as well how human activities change carbon stocks in the main pools (fossil carbon, the atmosphere, the oceans, and the terrestrial biosphere) and exchanges between them through LULUCF, among other activities has been the focus of scientific research.

1.4 Role of forests in carbon capture and storage

Quantifying the substantial roles of forests as carbon stores, as sources of carbon emissions and as carbon sinks has become one of the keys to understanding and influencing the global carbon cycle (FAO, 2010a). The biosphere constitutes a carbon sink that absorbed about 2.5 ± 1.0 PgC yr^{-1} from 2000 to 2010 (Figure 1.2). However, the potential of carbon storage varies in the various terrestrial ecosystems (Pan et al., 2011). Forests play a major role in global carbon cycle because they cover around 31 per cent (over 4 billion hectares) of terrestrial lands (FAO, 2010a) and contain more carbon per unit area than any other land types, accounting for 60% of total of carbon in terrestrial vegetation (FAO, 2001). The Global Forest Resources Assessment (FRA) 2010 estimates that the world's forests store more than 650 Gt of carbon, being that 286 Gt (44%) of carbon are captured in their biomass alone (FAO, 2010a). Furthermore, as soils are the largest carbon reservoir of the terrestrial carbon cycle (FAO, 2001, 2004, 2010a), forest soils are of major importance for carbon store, accounting for 292.5 (Gt) 45% of total of carbon soil pool. The remaining 11% is stored in dead wood and litter.

While sustainable management, planting and rehabilitation of forests can conserve or increase forest carbon stocks, deforestation, degradation and poor forest management reduce them. For the entire world, carbon stocks in forest biomass decreased by an estimated 0.5 Gt annually during the period 2005–2010, mainly because of a reduction in the global forest area (FAO, 2010a). Hence, enhancing carbon uptake through afforestation and sustainable forest management, and Reducing Emissions from Deforestation and Forest Degradation (REDD) (UN-REDD Programme, 2009) has been an effort measure to mitigate elevated atmospheric CO_2 concentration.

Carbon sequestration rates vary depending on plant species, soil type, region, climate, topography and management practices that can affect plant productivity, so the carbon storage of forests may change substantially with forest ecosystems on a community scale (Van Der Valk, 2009). Carbon begins its cycle through forest ecosystems (Figure 1.3) when plants assimilate atmospheric CO_2 through photosynthesis and convert it to biomass (Klass, 1998; Nieder and Benbi, 2008). Usually about half the gross photosynthetic products produced (GPP) are expended by plants in autotrophic respiration (Ra) for the synthesis and maintenance of living cells, releasing CO_2 back into the atmosphere. The remaining carbon products (GPP - Ra) go into net primary production (NPP): foliage, branches, stems, roots, and plant reproductive organs (Waring and Running, 2007). Annual primary production (NPP) represents the net amount of carbon sequestered into dry matter during a year (Melillo et al., 1993; Roy and Saugier, 2001) and is equivalent to total carbon uptake through photosynthesis minus the loss through autotrophic respiration. At the local scale, NPP can be defined and measured in terms of either biomass or CO_2 exchange, though measurements based on biomass data are by far the most common (Field et al., 1995). In practice, NPP is estimated by summing the growth of all tissue (change in live biomass plus litter) produced during a year (Waring and Running, 2007).

Biomass can be defined as the total amount of live and inert organic matter aboveground and belowground in a particular ecosystem. Changes in time of the quantity of biomass per unit area (biomass density) are a direct measure of carbon sequestration or loss between terrestrial ecosystems and the atmosphere. Thus, it can be used to determine the amount of carbon emitted to the atmosphere (as CO_2, CO, and CH_4 through burning and decay) when ecosystems are disturbed (Houghton et al., 2009). Therefore, a global assessment of biomass and its dynamics is an essential input to climate change forecasting models and mitigation and adaptation strategies (e.g. GTOS, 2009; GCOS, 2011).

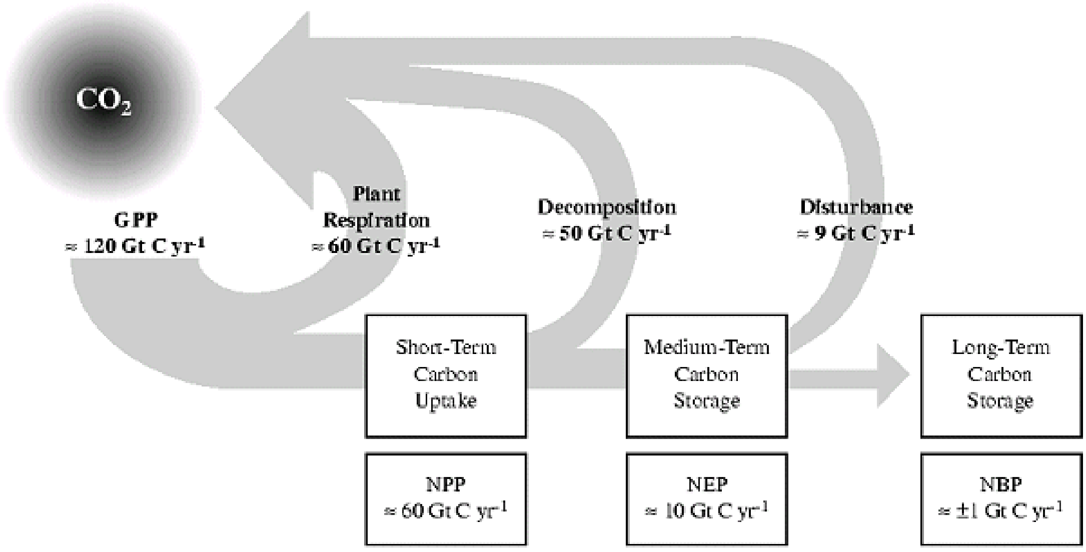

Figure 1.3 - Global Terrestrial carbon balance simplified.

Source: Adapted from IPCC (2000a).

Note: Plant (autotrophic) respiration releases CO_2 to the atmosphere, reducing GPP to NPP and resulting in short-term carbon uptake. Decomposition (heterotrophic respiration) of litter and soils in excess of that resulting from disturbance further releases CO_2 to the atmosphere, reducing NPP to NEP and resulting in medium-term carbon uptake. Disturbance from both natural and anthropogenic sources (e.g., harvest) leads to further release of CO_2 to the atmosphere by additional heterotrophic respiration and combustion-which, in turn, leads to long-term carbon storage.

1.5 Biomass energy and climate change

As previous mentioned, recent data confirm that consumption of fossil fuels resulting from the provision of energy services accounts for the majority of global anthropogenic GHG emissions, with over 90% in 2010, (Peters et al., 2012). In order to mitigate GHG emissions from the energy system while still satisfying the global demand for energy services, several possible options were assessed in the IPCC Fourth Assessment Report (AR4) (IPCC, 2007a). These options includes carbon capture and storage (CCS) and Renewable Energy (RE) as reviewed in the IPCC Special Report on Renewable Energy Sources and Climate Change Mitigation (SRREN) (IPCC, 2011). A particular emphasis has been given to Bioenergy since a variety of biomass feedstocks, including forest, agricultural and livestock residues; short-rotation forest plantations; energy crops; the organic component of municipal solid waste; and other organic waste streams can be directly used to produce electricity or heat, or can be used to create gaseous, liquid, or solid fuels. Highlights of the most significant developments and perspectives of the bioenergy sector can be consulted in several recent reports (e.g. Bogdanski et al., 2011; European Commission, 2011a; GBEP, 2011; IEA, 2011a; IPCC, 2011).

On a global basis, it is estimated that of the total 492 Exajoules (EJ) of primary energy supply in 2008 RE accounted for 12.9% where the biomass contributed with 10.2%. A first qualitative understanding of biomass technical potentials can be gained from considering the total annual aboveground net primary production (NPP) on the Earth's terrestrial surface. This is estimated to be about 35 Gt carbon, or 1,260 EJ yr^{-1}, assuming an average carbon content of 50% and 18 GJ ton^{-1} average heating value. Comparing with the world primary energy supply of about 500 EJ yr^{-1} in 2009 (IEA, 2011b) total terrestrial aboveground NPP is larger than what is required to meet society's energy demand (IPCC, 2011).

Despite the technical potentials and factors such as sustainability, concerns public acceptance, system integration and infrastructure constraints, or economic factors could limit to the continued growth of some individual RE technologies they continue to have significant opportunities for increased deployment (IPCC, 2011). In the case of energy production from biomass, the potential is recognized (e.g. Klass, 1998; Hakkila and Parikka, 2002; IEAGHG, 2011) and several policies are being adopted, leading to the development of new and safer energy sources, thus contributing to reducing dependence on fossil fuels and the consequent reduction of GHG emissions. The European Union (EU) has been a pioneer in taking effective steps on promoting biomass energy, having started from the 90's a strategy on climate and energy (Commission of the European Communities, 1996; European Commission, 1997, 2001b, 2001a; Commission of the European Communities, 2005, 2008b, 2008a; European Parliament, 2009; European Commission, 2011b, 2011a). As result, EU member countries with forest resources have been implementing several projects for energy production (Combined Heat and Power, CHP) from biomass (e.g. Viana et al., 2010).

Biomass is generally indicated as having no net release of CO_2 or "carbon neutral" meaning that carbon emitted by biomass burning for power won't contribute to climate change. It is assumed that if biomass is harvested and subsequently regrows without an overall loss of carbon stocks, there would be no net CO_2 emissions over a full harvest/growth cycle. In this way, land can be used continuously for the production of biomass energy to avoid fossil fuel CO_2 emissions. By contrast, using land to grow carbon stocks to be conserved thereafter can only be a temporary measure to limit fossil fuel use (IPCC, 2000a). However, this issue is not consensual as the CO_2 emissions released in the growth, harvest and transport the biomass for use as a fuel source are not accounted to the carbon footprint of biomass (e.g. Johnson, 2009; Biomass Energy Resource Center et al., 2012). The need to include land use and land-use change emissions of the biomass energy system in the GHG emission balances had already been identified by the IPCC Special Report of LULUCF of (IPCC, 2000a). Broad agreement about the advantages of biomass energy can be achieved in the future, with the view of the development of technologies to the carbon capture and storage emissions from biomass combustion (see Kraxner et al., 2003; IPCC, 2005; Biorecro AB and Global CCS Institute, 2010). These technologies, known as Bio-energy with carbon capture and storage (BECCS), could achieve a permanent net removal of CO_2 from the atmosphere, or *negative CO_2 emissions* (IEAGHG, 2011; IEA, 2012).

The use of forest biomass as an alternative, or complement, to the conventional energy sources can contribute to meeting our energy needs, and so pressure reduction on the consumption of fossil fuels accomplishing the recognized positive effects in the climate change.

1.6 Measuring aboveground forest biomass

Accurate quantitative estimation of forest biomass, expressed in terms of dry weight of living organisms, is important for analysing ecosystem productivity and also for assessing energy potential and the role of forests in the carbon cycle (FAO, 2010a).

As result of the UNFCCC (United Nations, 1992) and the Kyoto Protocol (United Nations, 1998) all member countries should assess and report national GHG emissions regularly. Emissions or removals of CO_2 in the LULUCF (IPCC, 2003) sector are estimated on the basis of changes of carbon stocks in the different pools (above-ground and below-ground biomass; dead organic matter as dead wood and litter; and soil organic matter). Generally, the aboveground biomass comprise all biomass of living vegetation, both woody and herbaceous, above the soil including stems, stumps, branches, bark, seeds, and foliage (IPCC, 2006a). Regarding forest biomass, countries must submit estimates of emissions and removals of carbon reflected as stock changes in forests.

As described in section 1.4, carbon stocks in forest ecosystems can be obtained directly by carbon flux measurements (which are currently expensive and difficult to apply at scale) or more generally applied by indirectly measuring the amount of biomass. According the Good Practice Guidance for Land Use, Land-Use Change and Forestry (GPG-LULUCF) (IPCC, 2003), later updated in the IPCC (2006a) guidelines for estimating and reporting national inventories of anthropogenic GHG emissions and removals in the Agriculture, Forestry and Other Land Use (AFOLU) sector, the annual changes in biomass stocks can be assessed either as the difference between biomass growth (above-ground and below-ground) and loss (harvest, mortality and natural disturbances), called *Gain-Loss Method* or "*Default method*", or as the change in the total biomass carbon stock between two consecutive forest inventories, called *Stock-Difference Method*. Where very accurate forest inventories are available the stock-difference method provides more reliable estimates (IPCC, 2006a) so it is preferable for estimating the annual carbon stock changes, and so the emissions and removals of carbon, from LULUCF/AFOLU activities.

There are four main methods to estimate and monitor biomass and combinations thereof, (GTOS, 2009): (a) *In situ* destructive direct biomass measurement; (b) *In situ* non-destructive biomass estimations (using equations or conversion factors); (c) Inference from remote sensing and (d) Models.

In situ destructive direct biomass measurement is the most direct and accurate method for quantifying biomass within a small unit area, but it is very hard, time consuming and cost effective, so impracticable to apply in large scale. Models, which are generally empirical, are used mainly to extrapolate biomass over time and/or space from a limited dataset. Their use is limited and with inherent inaccuracies. The use of remote sensing is increasingly growing and has been incorporated in forest inventories, to map land use/cover or biomass measurement. It will be addressed in section 1.8. Thus, assessments of biomass and carbon stocks and changes, focus on total biomass, biomass growth and biomass removals (harvest), including non-merchantable components, expressed in tons of dry-weight, is done essentially based on non-destructive field measurements (*diameter at breast height*, *height*, or other tree or stand variable) in sample plots. In practice, the data collected in forest inventories are generally used to calculate the amount of biomass according two ways (Brown, 2002; IPCC, 2006a; Somogyi et al., 2007; Petersson et al., 2012):

(i) as forest inventories and operational records usually document growing stock, net annual increment or wood removals in volume (m^3) of merchantable stem wood of merchantable volume, the first approach consist in applying biomass factors (BF) to convert and if necessary expand or reduce the available stem volume to the all tree biomass.

(ii) the second approach uses species-specific biomass equations (BE) to directly estimate the entire aboveground biomass of tree components such as tree tops, branches, twigs and foliage. When it is intended to estimate belowground biomass stumps and below-ground components (roots) specific equations are used to this purpose.

Biomass factors (BF) are often referred in literature as biomass expansions factors (BEF). However, for the same designation we can find different concepts (e.g. Brown et al., 1989; Brown, 1997; Soares and Tomé, 2004; Navar Chaidez, 2008). A distinction and clarification should be made since there are different types of BF (Somogyi et al., 2007; Somogyi et al., 2008). Some BF converts and expand the merchantable stem volume to the total biomass dry weight as other BF only expand the available variable (merchantable volume, biomass increment or biomass stock) to total biomass. So, following IPCC (2006a):

(i) Biomass Expansion Factors (BEF) expand the dry weight of the merchantable volume of growing stock, net annual increment, or wood removals, to account for non-merchantable components of the tree, stand, and forest. Before applying such BEFs, merchantable volume (m^3) must be converted to dry-weight (tonne) by multiplying with a conversion factor known as basic wood density (D) in ($t\ m^{-3}$). BEFs are dimensionless since they convert between units of weight.

(ii) Biomass Conversion and Expansion Factors (BCEF) calculated as: BCEF = BEF x D, combine conversion and expansion. They have the dimension ($t\ m^{-3}$) and transform in one single multiplication growing stock, net annual increment, or wood removals (m^3) directly into above-ground biomass, above-ground biomass growth, or biomass removals (t).

BCEFs are more convenient than BEF as they can be applied directly to volume-based forest inventory data and operational records without the need of having to resort to basic wood densities. Several default BCEF and default BEF and Basic wood density (D) are available for different forest type and climatic zone by IPCC (2006a), IPCC (2003) and FAO (2010a). As BEF and Basic wood density (D) vary by forest type, age, growing conditions, stand density and climate, several specific BCEF and BEF have being developed for specific forest and species at national, regional or local scale (e.g. Brown, 1997; Schroeder et al., 1997; Levy et al., 2004; Soares and Tomé, 2004; Somogyi et al., 2008; Teobaldelli et al., 2009; Pajtík et al., 2011).

Despite the utility of BF to estimate AGB, mainly when the information of forest inventories is scarce or aggregated by stand-level volume, biomass estimates based on forest inventories and biomass equations are more accurate than estimations derived from regional or global BF (GTOS, 2009). The more these equations are accurate (derived from a large enough number of trees) and able to predict biomass per tree fraction, the more accurate will be the biomass estimates and hence the carbon in biomass. Hence, allometric equations calibrated to national, regional or local circumstances (e.g. Parresol, 2001; Jenkins et al., 2004; Zianis et al., 2005) for direct estimation of biomass are essential and their use is recommended in several Manuals and Guidelines of forest biomass and Carbon measurements (IPCC, 2006a; Pearson et al., 2007; Walker et al., 2011). Additionally, as the assessment for energy purposes is increasingly necessary, the development of equations for predicting biomass per tree fraction allows also to accurately determine the energy potential of forest ecosystems.

Several studies evaluating the performance of BCEF concluded that total biomass estimates can carry a considerable bias (Soares and Tomé, 2004; Dutca et al., 2010; Pajtík et al., 2011; Petersson et al., 2012). Due to their relatively low accuracy, estimates based on BCEF are not appropriate for assessing changes in specific ecosystems. Therefore, when no representative biomass equations are available, some authors suggest that appropriate BF should be used, such as regional or national BCEF (IPCC, 2006a; GTOS, 2009), age-dependent BCEFs (Lehtonen et al., 2004; Soares and Tomé, 2004; Jalkanen et al., 2005; Petersson et al., 2012) and BCEFs developed based on dry weights and with locally basic wood densities.

Achieved the aboveground biomass stocks (biomass density, Mg ha^{-1}) the carbon stock density per unit area (Mg C ha^{-1}), are then converted to carbon values using the carbon fraction of dry matter, known as carbon conversion factor (CF). Some studies, manuals and reports (e.g. Páscoa and Salazar, 2006; FAO, 2010b; Pereira et al., 2010) consider the CF of 0.5, or the default values suggested in the IPCC Good Practice Guidance (IPCC, 2003, 2006a). However, these values vary considerably above or below 0.5, as they depend of the specie and the tree component, as shown by several studies (e.g. Núñez-Regueira et al., 2003; Demirbas, 2004; Lopes, 2005; Vassilev et al., 2010). Hence, appropriate specific CFs should be found in order to minimize the uncertainties in estimates of forest carbon biomass.

The total carbon stock is then converted to tons of CO_2 equivalent by multiplying it by 3.67 (44/12) (IPCC, 2006a; Pearson et al., 2007; ANSAB et al., 2010).

In conclusion, in order to minimize the many uncertainties (Nabuurs et al., 2008; Baccini et al., 2012) in estimates of forest biomass carbon pools, such as the amount of forest biomass, appropriate data of forest density and current annual increment of stems, biomass conversion and expansion factors, allometric equations, wood density and carbon fraction should be developed and used.

1.7 Forest understory and shrubland vegetation

Forest understory, and mainly shrubland vegetation, constitutes a significant part of the ecosystems and plays a multiplicity of functions (Waring and Running, 2007) in biodiversity (Pérez-Devesa et al., 2008), biogeochemical cycling of carbon and ultimately global climate change (Riera et al., 2007). This role is even more important in Mediterranean ecosystems given to the special climate and soils conditions (Rambal, 2001; Van Der Valk, 2009). Although shrub vegetation is significantly involved in the carbon cycle in Mediterranean ecosystems, the knowledge on the amount of carbon they store is still very little. Hence, quantifying the amounts of biomass as well the study of characteristics and properties of the major woody shrub species is fundamental to assess carbon stocks in these ecosystems.

In the Guidelines for National Greenhouse Gas Inventories (IPCC, 2006a) is stated that if forest understory is a relatively small component of the aboveground biomass carbon pool, it is acceptable for the methodologies and associated data used in some tiers to exclude it from the account of carbon emissions. As for shrubland biomass, IPCC Guidelines (IPCC, 2006a) only provides an approach for estimating non-CO_2 emissions resulting from fires. This method allows estimating non-CO_2 emissions due to losses in biomass stocks from burning, but there is no reference to any methodology for estimating the carbon stored in shrubland biomass stocks. However, an increasing attention has been given to this vegetation and some National Forest Inventories (NFI) start including specific information.

The assessment of shrub vegetation biomass has been made by diverse indirect ways, mainly by using remote sensing based approaches (Rahman et al., 2005; Shoshany and Karnibad, 2011; Viana et al., 2012). However, the better accuracies are achieved with *in situ* direct destructive sampling measurements, and by applying shrub biomass allometric equations. These methodologies are recommended in some Measurement Guidelines for the Sequestration of Forest Carbon (e.g. Pearson et al., 2007) and several equations have been developed for many years (Whittaker and Woodwell, 1968; Brown, 1976; Uresk et al., 1977). Thus, the investigation, either direct or indirect methods, are essential in order to pursue more accurate estimates regarding each specific vegetation and ecosystem. Furthermore, the development of biomass equations to assess biomass stocks and the knowledge of characteristics and properties of this biomass is crucial, concerning to carbon balance account, but also for evaluation for energy purposes. In fact, several projects aims to use this vegetation for energy production (see Viana et al., 2010; Aranha et al., 2011).

1.8 Remote sensing and spatial prediction of biomass

The need of gathering data and assessing changes in structure and functioning of ecosystems on a regular basis, in large scales, and with the best possible accuracy is, undoubtedly, a subject that has attracted the attention of many researchers. Assessments aboveground biomass stocks and increment data is one of the subjects more studied given their fundamental role in terrestrial ecosystems. However, the approaches for measuring these resources by traditional inventories don't predict the variables spatially. Moreover, some remote places cannot be assessed to perform direct measurements. Hence, remote sensing and other spatial predictions approaches, either alone or combined, have been introduced in assessment and mapping of biomass.

Remote sensing, the process of imaging the interactions between electromagnetic energy and matter at selected wavelengths, has the ability to monitor terrestrial ecosystems at various temporal and spatial scales and has been widely tested for land cover mapping and forestry applications (Patenaude et al., 2005). Remote sensing approaches have being incorporated into operational forest inventories (McRoberts et al., 2010), and have become the primary source for biomass estimation (Lu, 2006). Remote sensing data may provide a useful contribute in many ways such as, land cover discrimination or above-ground forest carbon stocks estimation. For example:

Remote sensing was included since several years as a complementary part of Global Forest Resources Assessment (FRA) reports. Currently, a global remote sensing survey is being carried out as a part of FRA 2010 in order to provide information on the spatial distribution of forests, forest land cover, and land-use change dynamics such as deforestation, afforestation and natural expansion of forests, at the biome, regional and global level (FAO, 2010a). Moreover, the National Forest Monitoring and Assessment (NFMA) programme at FAO is developing cost-effective methodologies that include both remote sensing techniques and systematic field data collections to assess and monitor the multiple benefits from forests (and other natural resources) at the country level, in order to support national policy processes (FAO, 2010a; FAO and ECJRC, 2011). Remote sensing has also been used for measuring biomass stocks, biomass changes and carbon stocks in forests (e.g. Brown, 2002; Filella et al., 2004), and a range of remote data collection technologies are available including satellite imagery to aerial photo-imagery from low flying airplanes as described by Patenaude et al. (2005), Lu (2006) and McRoberts et al. (2010).

Although land-cover change and forest variables can be inferred using satellite data, remote sensing products carry an inherent inaccuracy (Strahler et al., 2006). Hence, several spatial predictions methods (e.g. Halls, 2005) need to be investigated and tested in order to include it in the operational assessment of aboveground biomass research.

References

ANSAB, FECOFUN, ICIMOD, NORAD, 2010. Forest Carbon Stock Measurement Guidelines for measuring carbon stocks in community-managed forests. Asia Network for Sustainable Agriculture and Bioresources (ANSAB), Federation of Community Forest Users, N.F., International Centre for Integrated Mountain Development (ICIMOD), Norwegian Agency for Development Cooperation (NORAD). Available online at: *http://www.ansab.org/wp-content/uploads/2010/08/Carbon-Measurement-Guideline-REDD-final.pdf*, (Accessed May 2012).

Aranha, J., Calvão, A., Lopes, D., Viana, H., 2011. Quantificação da biomassa consumida nos últimos 20 anos de fogos florestais no Norte de Portugal. Info 26, 44-49.

Baccini, A., Goetz, S.J., Walker, W.S., Laporte, N.T., Sun, M., Sulla-Menashe, D., Hackler, J., Beck, P.S.A., Dubayah, R., Friedl, M.A., Samanta, S., Houghton, R.A., 2012. Estimated carbon dioxide emissions from tropical deforestation improved by carbon-density maps. Nature Clim. Change 2, 182-185.

Biomass Energy Resource Center, Forest Guild, Spatial Informatics Group, 2012. Biomass Supply and Carbon Accounting for Southeastern Forests, National Wildlife Federation and Southern Environmental Law Center. Available online at: *http://www.southernenvironment.org/uploads/fck/file/biomass/biomass-carbon-study-021412-FINAL.pdf*, (Accessed May 2012).

Biorecro AB, Global CCS Institute, 2010. Global Status of BECCS Projects 2010, Global CCS Institute commissioned, Australia, Sweden. Available online at: *http://cdn.globalccsinstitute.com/sites/default/files/publications/13516/gccsi-biorecro-global-status-beccs-110302-report.pdf*, (Accessed May 2012).

Boden, T.A., Marland, G., Andres, R.J., 2011. Global, Regional, and National Fossil-Fuel CO_2 Emissions. Carbon Dioxide Information Analysis Center, Oak Ridge National Laboratory, U.S. Department of Energy, Oak Ridge, Tenn., U.S.A. doi 10.3334/CDIAC/00001_V2011.

Bogdanski, A., Dubois, O., Jamieson, C., Krell, R., 2011. Making Integrated Food-Energy Systems Work for People and Climate - An Overview, Climate, Energy and Tenure Division (NRC) publications. Environment and Natural Resources Management Working Paper, 45, Food and Agriculture Organization of the United Nations, Rome, pp. 116. Available online at: *http://www.fao.org/docrep/013/i2044e/i2044e.pdf*, (Accessed May 2012).

Brown, J.K., 1976. Estimating shrub biomass from basal stem diameters. Canadian Journal of Forest Research 6, 153-158.

Brown, S., Gillespie, A.J.R., Lugo, A.E., 1989. Biomass Estimation Methods for Tropical Forests with Applications to Forest Inventory Data. Forest Science 35, 881-902.

Brown, S., 1997. Estimating Biomass and Biomass Change of Tropical Forests: A Primer (FAO Forestry Paper - 134). Food and Agriculture Organization of the United Nations. Available online at: *http://www.fao.org/docrep/W4095E/W4095E00.htm*, (Accessed May 2012).

Brown, S., 2002. Measuring carbon in forests: current status and future challenges. Environmental Pollution 116, 363-372.

Commission of the European Communities, 1996. Communication from the Commission. Energy for the Future: Renewable Sources of Energy. Green Paper for a Community Strategy. COM(96) 576 final. Brussels.

Commission of the European Communities, 2005. Communication from the Commission. Biomass action plan. COM(2005) 628 final. Brussels.

Commission of the European Communities, 2008a. Communication from the Commission to the European Parliament, the Council, the European Economic and Social Committee and the Committee of the Regions. Second Strategic

Energy Review - An EU energy security and solidarity action plan. COM(2008) 781 final. Brussels.

Commission of the European Communities, 2008b. Communication from the Commission to the European Parliament, the Council, the European Economic and Social Committee and the Committee of the Regions - 20 20 by 2020 - Europe's climate change opportunity. COM(2008) 30 final. Brussels.

Demirbas, A., 2004. Combustion characteristics of different biomass fuels. Progress in Energy and Combustion Science 30, 219-230.

Denman, K.L., G. Brasseur, A. Chidthaisong, P. Ciais, P.M. Cox, R.E. Dickinson, D. Hauglustaine, C. Heinze, E. Holland, D. Jacob, U. Lohmann, S Ramachandran, P.L. da Silva Dias, Zhang, S.C.W.a.X., 2007. Couplings Between Changes in the Climate System and Biogeochemistry. In: Climate Change 2007: The Physical Science Basis. Contribution of Working Group I to the Fourth Assessment Report of the Intergovernmental Panel on Climate Change [Solomon, S., D. Qin, M. Manning, Z. Chen, M. Marquis, K.B. Averyt, M.Tignor and H.L. Miller (eds.)]. Cambridge University Press, Cambridge, United Kingdom and New York, NY, USA.

Dutca, I., Abrudan, I.V., Stancioiu, P.T., Blujdea, V., 2010. Biomass Conversion and Expansion Factors for Young Norway Spruce (Picea abies (L) Karst) Trees Planted on Non-Forest Lands in Eastern Carpathians. . Notulae Botanicae Horti Agrobotanici Cluj-Napoca 38(3), 286-292.

European Commission, 1997. Communication from the Commission. Energy for the Future: Renewable Sources of Energy. White Paper for a Community Strategy and Action Plan: COM(97)599 final. Brussels, Belgium.

European Commission, 2001a. Directive of the European Parliament and the Council on the promotion of electricity produced from renewable energy sources in the internal electricity market, Directive 2001/77/EC, Brussels, Belgium.

European Commission, 2001b. Green Paper: Towards a European strategy for the security of energy supply. COM(2000)769 final, Brussels.

European Commission, 2011a. Communication from the commission to the European Parliament, the council, the european economic and social Committee and the committee of the regions. Energy Roadmap 2050. COM(2011) 885/2, Brussels, Belgium.

European Commission, 2011b. Communication from the Commission to the European Parliament and the Council. Renewable Energy: Progressing towards the 2020 target. COM(2011) 31 final, Brussels, Belgium.

European Parliament, 2009. Directive 2009/28/EC of the European Parliament and of the Council of 23 April 2009, on the promotion of the use of energy from renewable sources and amending and subsequently repealing Directives 2001/77/EC and 2003/30/EC.

FAO, 2001. Soil carbon sequestration for improved land management. World Soil Resources Reports 96. Available online at: *ftp://ftp.fao.org/agl/agll/docs/wsrr96e.pdf*, (Accessed May 2012).

FAO, 2004. Carbon sequestration in dryland soils. World soil resources reports 102, pp. 129.

FAO, 2010a. Global Forest Resources Assessment 2010. Main report. FORESTRY PAPER 163. Food and Agriculture Organization of the United Nations, pp. 343. Available online at: *http://www.fao.org/docrep/013/i1757e/i1757e.pdf*, (Accessed May 2012).

FAO, 2010b. Global Forest Resources Assessment 2010. Country Report, Portugal. FRA2010/167, Food and Agriculture Organization of the United Nations, Forestry Department, Rome, pp. 58. Available online at: *http://www.fao.org/docrep/013/al602E/al602E.pdf*, (Accessed May 2012).

FAO, ECJRC, 2011. Global forest land-use change from 1990 to 2005. Initial results from a global remote sensing survey, Food and Agriculture Organization of the United Nations, EC Joint Research Centre,pp. 8. Available online at: *http://foris.fao.org/static/data/fra2010/RSS_Summary_Report_lowres.pdf*, (Accessed May 2012).

Field, C.B., Randerson, J.T., Malmström, C.M., 1995. Global net primary production: Combining ecology and remote sensing. Remote Sensing of Environment 51, 74-88.

Filella, I., Peñuelas, J., Llorens, L., Estiarte, M., 2004. Reflectance assessment of seasonal and annual changes in biomass and CO_2 uptake of a Mediterranean shrubland submitted to experimental warming and drought. Remote Sensing of Environment 90, 308-318.

Forster, P., Ramaswamy, V., Artaxo, P., Berntsen, T., Betts, R., Fahey, D.W., Haywood, J., Lean, J., Lowe, D.C., Myhre, G., Nganga, J., Prinn, R., Raga, G., Schulz, M., R. Van Dorland, 2007. Changes in Atmospheric Constituents and in Radiative Forcing. In: Climate Change 2007: The Physical Science Basis. Contribution of Working Group I to the Fourth Assessment Report of the Intergovernmental Panel on Climate Change [Solomon, S., D. Qin, M. Manning, Z. Chen, M. Marquis, K.B. Averyt, M.Tignor and H.L. Miller (eds.)]. Cambridge University Press, Cambridge, United Kingdom and New York, NY, USA.

GBEP, 2011. The Global Bioenergy Partnership Sustainability Indicators for Bioenergy. First edition, Food and Agricultural Organization of the United Nations (FAO), Climate, Energy and Tenure Division, Rome, pp. 211. Available online at: *http://www.globalbioenergy.org/programmeofwork/task-force-on-sustainability/gbep-report-on-sustainability-indicators-for-bioenergy/en/*, (Accessed May 2012).

GCOS, 2011. Systematic observation requirements for satellite-based data products for climate. Supplemental details to the satellite-based component of the "Implementation Plan for the Global Observing System for Climate in Support of the UNFCCC (2010 Update)" World Meteorological Organization. Global Climate Observing System (GCOS). Available online at: *http://www.wmo.int/pages/prog/gcos/Publications/gcos-154.pdf*, (Accessed May 2012).

GCP, 2012. Global Carbon Project 2001-2012. Carbon Budget Highlights. Available online at: *http://www.globalcarbonproject.org/carbonbudget/index.htm*, (Accessed May 2012).

GTOS, 2009. Biomass. Assessment of the status of the development of the standards for the terrestrial essential climate variables. Global Terrestrial Observing System. GTOS 67, T12, Version 10. GTOS Secretariat. NRL, Food and Agriculture Organization of the United Nations, Rome. Available online at: *http://www.fao.org/gtos/doc/ECVs/T12/T12.pdf*, (Accessed May 2012).

Hakkila, P., Parikka, M., 2002. Fuel Resources from the forest, in: Richardson, J., Björheden, R., Hakkila, P., Lowe, A.T., Smith, C.T. (eds.), Bioenergy from Sustainable Forestry. Guiding Principles and Practice, vol. 71. Kluwer Academic Publishers.

Halls, P., 2005. Spatial Information and the Environment. INNOVATIONS IN GIS 8. Taylor & Francis, London and New York, pp. 288.

Havemann, T., 2009. Measuring and Monitoring Terrestrial Carbon. The State of the Science and Implications for Policy Makers The Terrestrial Carbon Group. The United Nations Collaborative Programme on Reducing Emissions from Deforestation and Forest Degradation in Developing Countries Available online at: *http://www.un-redd.org/*, (Accessed May 2012).

Houghton, R.A., 2003a. Revised estimates of the annual net flux of carbon to the atmosphere from changes in land use and land management 1850–2000. Tellus B 55, 378-390.

Houghton, R.A., 2003b. Why are estimates of the terrestrial carbon balance so different? Global Change Biology 9, 500-509.

Houghton, R.A., Hall, F., Goetz, S.J., 2009. Importance of biomass in the global carbon cycle. J. Geophys. Res. 114, G00E03.

IEA, 2011a. Technology Roadmap. Biofuels for Transport, International Energy Agency. Renewable Energy Division, Paris, France, pp. 52. Available online at: *http://www.iea.org/papers/2011/biofuels_roadmap.pdf*, (Accessed May 2012).

IEA, 2011b. CO_2 Emissions from Fuel Combustion 2011 - Highlights, OECD/IEA, Paris, pp. 134. Available online at: *http://www.iea.org/co2highlights/co2highlights.pdf*, (Accessed May 2012).

IEA, 2012. A Policy Strategy for Carbon Capture and Storage. Information paper, International Energy Agency, Paris, France, pp. 56. Available online at: *http://www.iea.org/papers/2012/policy_strategy_for_ccs.pdf*, (Accessed May 2012).

IEAGHG, 2011. Potential for biomass and carbon dioxide capture and storage. Available online at: *http://www.eenews.net/assets/2011/08/04/document_cw_01.pdf*, (Accessed May 2012).

IPCC, 2000a. Land Use, Land-Use Change, and Forestry. A Special Report of the Intergovernmental Panel on Climate Change, in: Watson, R.T., Noble, I.R., Bolin, B., Ravindranath, N.H., Verardo, D.J., Dokken, D.J. (eds.). Cambridge University Press, UK, pp. 388. Available online at: *http://www.ipcc.ch/ipccreports/sres/land_use/*, (Accessed May 2012).

IPCC, 2000b. Good Practice Guidance and Uncertainty Management in National Greenhouse Gas Inventories. IPCC National Greenhouse Gas Inventories

Programme, Cambridge University Press, UK. Available online at: *http://www.ipcc-nggip.iges.or.jp/public/gp/english/*, (Accessed May 2012).

IPCC, 2003. Good Practice Guidance for Land Use, Land-Use Change and Forestry, in: Jim Penman, M.G., Taka Hiraishi, Thelma Krug, Dina Kruger, Riitta Pipatti, Leandro Buendia, Kyoko Miwa, Todd Ngara, Kiyoto Tanabe, Fabian Wagner (ed.). Institute for Global Environmental Strategies (IGES). Hayama, Kanagawa, Japan. Available online at: *http://www.ipcc-nggip.iges.or.jp/public/gpglulucf/gpglulucf_contents.html*, (Accessed May 2012).

IPCC, 2005. Carbon Dioxide Capture and Storage. Cambridge University Press, UK, pp. 431.

IPCC, 2006a. 2006 IPCC guidelines for national greenhouse gas inventories. Volume 4, Agriculture, forestry and other land use, Cambridge University Press, UK. Available online at: *http://www.ipcc-nggip.iges.or.jp/public/2006gl/vol4.html*, (Accessed May 2012).

IPCC, 2006b. 2006 IPCC guidelines for national greenhouse gas inventories. Volume 1: General Guidance and Reporting. Chapter 3: Uncertainties, Cambridge University Press, UK. Available online at: *http://www.ipcc-nggip.iges.or.jp/public/2006gl/pdf/1_Volume1/V1_3_Ch3_Uncertainties.pdf*, (Accessed May 2012).

IPCC, 2007a. Contribution of Working Groups I, II and III to the Fourth Assessment Report of the Intergovernmental Panel on Climate Change. Intergovernmental Panel on Climate Change, Geneva, Switzerland, pp. 104.

IPCC, 2007b. Summary for Policymakers. In: Climate Change 2007: The Physical Science Basis. Contribution of Working Group I to the Fourth Assessment Report of the Intergovernmental Panel on Climate Change [Solomon, S., D. Qin, M. Manning, Z. Chen, M. Marquis, K.B. Averyt, M.Tignor and H.L. Miller (eds.)]. Cambridge University Press, Cambridge, United Kingdom and New York, NY, USA.

IPCC, 2011. Special Report on Renewable Energy Sources and Climate Change Mitigation. Prepared by Working Group III of the Intergovernmental Panel on Climate Change. Cambridge University Press, Cambridge, United Kingdom and New York, NY, USA, pp. 1075.

Jalkanen, A., Mäkipää, R., Ståhl, G., Lehtonen, A., Petersson, H., 2005. Estimation of the biomass stock of trees in Sweden: comparison of biomass equations and age-dependent biomass expansion factors. Ann. For. Sci. 62, 845-851.

Jenkins, J.C., Chojnacky, D.C., Heath, L.S., Birdsey, R.A., 2004. Comprehensive Database of Diameter-based Biomass Regressions for North American Tree Species. GTR-NE-319, USDA Forest Service, Northeastern Research Station. Available online at: *http://www.fs.fed.us/ne/global/pubs/books/dia_biomass/index*, (Accessed May 2012).

Johnson, E., 2009. Goodbye to carbon neutral: Getting biomass footprints right. Environmental Impact Assessment Review 29, 165-168.

Klass, D.L., 1998. Chapter 2 - Biomass as an Energy Resource: Concept and Markets, Biomass for Renewable Energy, Fuels, and Chemicals. Academic Press, San Diego, pp. 29-50.

Kraxner, F., Nilsson, S., Obersteiner, M., 2003. Negative emissions from BioEnergy use, carbon capture and sequestration (BECS)—the case of biomass production by sustainable forest management from semi-natural temperate forests. Biomass and Bioenergy 24, 285-296.

Lehtonen, A., Mäkipää, R., Heikkinen, J., Sievänen, R., Liski, J., 2004. Biomass expansion factors (BEFs) for Scots pine, Norway spruce and birch according to stand age for boreal forests. Forest Ecology and Management 188, 211-224.

Levy, P.E., Hale, S.E., Nicoll, B.C., 2004. Biomass expansion factors and root : shoot ratios for coniferous tree species in Great Britain. Forestry 77, 421-430.

Lopes, D., Estimating Net Primary Production in *Eucalyptus globulus* and *Pinus pinaster* Ecosystems in Portugal, Kingston University, PhD Thesis, England, 2005.

Lu, D., 2006. The potential and challenge of remote sensingbased biomass estimation. International Journal of Remote Sensing 27, 1297-1328.

Marland, G., Hamal, K., Jonas, M., 2009. How Uncertain Are Estimates of CO_2 Emissions? Journal of Industrial Ecology 13, 4-7.

McRoberts, R.E., Cohen, W.B., Næsset, E., Stehman, S.V., Tomppo, E.O., 2010. Using remotely sensed data to construct and assess forest attribute maps and related spatial products. Scandinavian Journal of Forest Research 25, 340-367.

Melillo, J.M., McGuire, A.D., Kicklighter, D.W., Moore, B., Vorosmarty, C.J., Schloss, A.L., 1993. Global climate change and terrestrial net primary production. Nature 363, 234-240.

Nabuurs, G.J., van Putten, B., Knippers, T.S., Mohren, G.M.J., 2008. Comparison of uncertainties in carbon sequestration estimates for a tropical and a temperate forest. Forest Ecology and Management 256, 237-245.

Navar Chaidez, J., 2008. Allometric equations and expansion factors for tropical dry trees of eastern Sinaloa, Mexico,10. Tropical and Subtropical Agroecosystems, North America. Available online at: *http://www.ccba.uady.mx/ ojs/index.php/TSA/article/view/5,* (Accessed May 2012).

Nieder, R., Benbi, D.K., 2008. Carbon and Nitrogen in the Terrestrial Environment. Springer.

Núñez-Regueira, L., Rodríguez-Añón, J., Proupín, J., Romero-García, A., 2003. Energy evaluation of forest residues originated from pine in Galicia. Bioresource Technology 88, 121-130.

Pajtík, J., Konôpka, B., Lukac, M., 2011. Individual biomass factors for beech, oak and pine in Slovakia: a comparative study in young naturally regenerated stands. Trees - Structure and Function 25, 277-288.

Pan, Y., Birdsey, R.A., Fang, J., Houghton, R., Kauppi, P.E., Kurz, W.A., Phillips, O.L., Shvidenko, A., Lewis, S.L., Canadell, J.G., Ciais, P., Jackson, R.B., Pacala, S.W., McGuire, A.D., Piao, S., Rautiainen, A., Sitch, S., Hayes, D., 2011. A Large and Persistent Carbon Sink in the World’s Forests. Science 333, 988-993.

Parresol, B.R., 2001. Additivity of nonlinear biomass equations. Canadian Journal of Forest Research 31, 865-878.

Páscoa, F., Salazar, P., 2006. Manual de Procedimentos para Aplicação de Indicadores de Gestão Florestal Sustentável. Federação dos Produtores Florestais de Portugal, Conselho Nacional da Floresta, Lisboa, pp. 48.

Patenaude, G., Milne, R., Dawson, T.P., 2005. Synthesis of remote sensing approaches for forest carbon estimation: reporting to the Kyoto Protocol. Environmental Science & Policy 8, 161-178.

Pearson, T.R.H., Brown, S.L., Birdsey, R.A., 2007. Measurement Guidelines for the Sequestration of Forest Carbon. Technical Report NRS-18. United States Department of Agriculture. Forest Service. Northern Research Station General.

Available online at: *http://www.nrs.fs.fed.us/pubs/gtr/gtr_nrs18.pdf*, (Accessed May 2012).

Pereira, T.C., Seabra, T., Maciel, H., Torres, P., 2010. Portuguese National Inventory Report on Greenhouse Gases 1990-2008. Submitted under the United Nations Framework Convention on Climate Change and the Kyoto protocol, Agência Portuguesa do Ambiente Amadora, Portugal. Available online at: *http://unfccc.int/files/national_reports/annex_i_ghg_inventories/national_inventories_submissions/application/zip/prt-2010-crf-25may.zip*, (May 2012).

Pérez-Devesa, M., Cortina, J., Vilagrosa, A., Vallejo, R., 2008. Shrubland management to promote Quercus suber L. establishment. Forest Ecology and Management 255, 374-382.

Peters, G.P., Marland, G., Le Quere, C., Boden, T., Canadell, J.G., Raupach, M.R., 2012. Rapid growth in CO_2 emissions after the 2008-2009 global financial crisis. Nature Clim. Change 2, 2-4.

Petersson, H., Holm, S., Ståhl, G., Alger, D., Fridman, J., Lehtonen, A., Lundström, A., Mäkipää, R., 2012. Individual tree biomass equations or biomass expansion factors for assessment of carbon stock changes in living biomass – A comparative study. Forest Ecology and Management 270, 78-84.

PMEL Carbon Group, 2012. The Carbon Cycle. NOAA Pacific Marine Environmental Laboratory. Available online at: *http://www.pmel.noaa.gov/co2/story/Carbon+Cycle*, (Accessed May 2012).

Prentice, I.C., Farquhar, G.D., Fasham, M.J.R., Goulden, M.L., Heimann, M., Jaramillo, V.J., Kheshgi, H.S., Quéré, C.L., Scholes, R.J., Wallace, D.W.R., 2001. The Carbon Cycle and Atmospheric Carbon Dioxide, in: Pitelka, L., Rojas, A.R. (eds.), Climate Change 2001. Working Group I: The Scientific Basis. IPCC Third Assessment Report: Climate Change 2001. Cambridge University Press, UK, pp. 185-237. Available online at: *http://www.ipcc.ch/ipccreports/tar/wg1/pdf/TAR-03.PDF*, (Accessed May 2012).

Rahman, M.M., Csaplovics, E., Koch, B., 2005. An efficient regression strategy for extracting forest biomass information from satellite sensor data. International Journal of Remote Sensing 26, 1511-1519.

Rambal, S., 2001. Hierarchy and productivity of Mediterraneantype ecosystems, in: Roy J, S.B., Mooney HA (ed.), Terrestrial Global Productivity. Academic Press, San Diego, pp. 315-344.

Riera, P., Peñuelas, J., Farreras, V., Estiarte, M., 2007. Valuation of Climate-Change Effects on Mediterranean Shrublands. Ecological Applications 17, 91-100.

Roy, J., Saugier, B., 2001. 1 - Terrestrial Primary Productivity: Definitions and Milestones, in: Roy J, S.B., Mooney HA (ed.), Terrestrial Global Productivity. Academic Press, San Diego, pp. 1-6.

Schimel, D.S., 1995. Terrestrial ecosystems and the carbon cycle. Global Change Biology 1, 77-91.

Schroeder, P., Brown, S., Mo, J., Birdsey, R., Cieszewski, C., 1997. Biomass Estimation for Temperate Broadleaf Forests of the United States Using Inventory Data. Forest Science 43, 424-434.

Shoshany, M., Karnibad, L., 2011. Mapping shrubland biomass along Mediterranean climatic gradients: The synergy of rainfall-based and NDVI-based models. International Journal of Remote Sensing 32, 9497-9508.

Soares, P., Tomé, M., 2004. Analysis of the effectiveness of biomass expansion factors to estimate stand biomass. International Conference on Modelling Forest Production. University of Natural Resources and Applied Life Sciences, Vienna, Austria. Available online at: *http://www.isa.utl.pt/cef/globland/projecto2_portugues/Relatorio_Progresso_2004/ANEXO%2011_proceedingsICMFP.pdf*, (Accessed May 2012).

Somogyi, Z., Cienciala, E., Mäkipää, R., Muukkonen, P., Lehtonen, A., Weiss, P., 2007. Indirect methods of large-scale forest biomass estimation. European Journal of Forest Research 126, 197-207.

Somogyi, Z., Teobaldelli, M., Federici, S., Matteucci, G., Pagliari, V., Grassi, G., Seufert, G., 2008. Allometric biomass and carbon factors database. iForest - Biogeosciences and Forestry 1, 107-113.

Strahler, A.H., Boschetti, L., Foody, G.M., Friedl, M.A., Hansen, M.C., Herold, M., Mayaux, P., Morisette, J.T., Stehman, S.V., Woodcock, C.E., 2006. Global land cover validation: Recommendations for evaluation and accuracy assessment of global land cover maps. European Communities. Office for Official Publications of the European Communities, Luxembourg. Available online at: *http://nofc.cfs.nrcan.gc.ca/gofc-gold/Report%20Series/GOLD_25.pdf*, (Accessed May 2012).

Teobaldelli, M., Somogyi, Z., Migliavacca, M., Usoltsev, V.A., 2009. Generalized functions of biomass expansion factors for conifers and broadleaved by stand age, growing stock and site index. Forest Ecology and Management 257, 1004-1013.

UN-REDD Programme, 2009. The United Nations Collaborative Programme on Reducing Emissions from Deforestation and Forest Degradation in Developing Countries. Available online at: *http://www.un-redd.org/Home/tabid/565/Default.aspx*, (Accessed May 2012).

UNFCCC, 2012. Greenhouse Gas Inventory Data. United Nations Framework Convention on Climate Change. Available online at: *http://unfccc.int/ghg_data/items/3800.php*, (Accessed May 2012).

United Nations, 1992. United Nations Framework Convention on Climate Change. FCCC/INFORMAL/84. GE.05-62220 (E) 200705. Available online at: *http://unfccc.int/resource/docs/convkp/conveng.pdf*, (Accessed May 2012).

United Nations, 1998. Kyoto Protocol to the United Nations Framework Convention on Climate Change, pp. 21. Available online at: *http://unfccc.int/resource/docs/convkp/kpeng.pdf*, (Accessed May 2012).

Uresk, D., Gilbert, R., Menke, J., 1977. Sampling big sagebrush for phytomass. J. Range Manag. 30 311-314.

Van Der Valk, A., 2009. Forest Ecology: Recent Advances in Plant Ecology. Springer.

Vassilev, S.V., Baxter, D., Andersen, L.K., Vassileva, C.G., 2010. An overview of the chemical composition of biomass. Fuel 89, 913-933.

Viana, H., Cohen, W.B., Lopes, D., Aranha, J., 2010. Assessment of forest biomass for use as energy. GIS-based analysis of geographical availability and locations of wood-fired power plants in Portugal. Applied Energy 87, 2551-2560.

Viana, H., Aranha, J., Lopes, D., Cohen, W.B., 2012. Estimation of crown biomass of *Pinus pinaster* stands and shrubland above-ground biomass using forest inventory data, remotely sensed imagery and spatial prediction models. Ecological Modelling 226, 22-35.

Walker, W., A. Baccini, Nepstad, M., Horning, N., Knight, D., Braun, E., Bausch, A., 2011. Field Guide for Forest Biomass and Carbon Estimation. Version 1.0. Woods Hole Research Center. Falmouth, Massachusetts, USA. Available online at: *http://www.whrc.org/resources/fieldguides/carbon/pdf/FieldGuide.pdf*, (Accessed May 2012).

Waring, R.H., Running, S.W., 2007. Forest Ecosystems: Analysis at Multiple Scales. Elsevier/Academic Press, pp. 420.

Whittaker, R.H., Woodwell, G.M., 1968. Dimension and production relations of trees and shrubs in the brookhaven forest, New York. Journal of Ecology 56, 1-25.

Zianis, D., Muukkonen, P., Mäkipää, R., Mencuccini, M., 2005. Biomass and stem volume equations for tree species in Europe, Silva Fennica Monographs 4. Finnish Society of Forest Science, p. 63.

2

Purpose of Study

2.1 Aims

The general aim of this thesis is to contribute to a deeper understanding of the aboveground biomass role of the main Portuguese forest species (*Pinus pinaster* Aiton and *Eucalyptus globulus* Labill.) and woody vegetation of shrubland areas characteristics of North-Center Portugal, in the carbon cycle and as potential source of fuel for energy purposes, by providing a specific set of tools regionally developed in the North-Center region of Portugal. In order to concretize the general aim the study examines a set of subjects:

- to develop a specific system of nonlinear allometric equation for estimating the aboveground biomass stocks of maritime pine tree components, in the North-Center region of Portugal;

- to develop a specific system of nonlinear allometric equation for estimating the aboveground biomass stocks of eucalyptus tree components, in the North-Center region of Portugal;

- to develop specific allometric equations for estimating the shrubland biomass stocks, in the North-Center region of Portugal;

- to evaluate the fuelwood characteristic and ash properties of maritime pine and eucalyptus species, in the North-Center region of Portugal;

- to evaluate the fuelwood characteristic and biomass combustion properties of main native woody shrub species from North-Center region of Portugal and NW Spain;

- to investigate different approaches to spatially assess aboveground biomass stocks of forest stands and shrubland of Mediterranean ecosystems using inventory data, remote sensing and spatial predictions models;

- to assess the potential of forest biomass for combined heat and power (CHP) production at industrial scale in Portugal.

2.2 Thesis outline

This thesis is based on the contribution of three scientific papers published, four papers in the submission stage, and several papers published in conference proceedings and presented at various scientific events.

The work is divided into 11 chapters: 1-Introduction, 2-Purpose of Study, 3 to 9 present the research work, 10-Conclusions and 11-Future Work. The main contributions of the present thesis can be summarized in three main questions as follows:

How to accurately estimate aboveground biomass stocks in Mediterranean vegetation?

Chapters 3 and 4 - present a set of specific allometric equations for estimating the aboveground biomass stocks, of tree component, of the most representative forest cover types in Portugal.

Chapter 5 - presents a set of specific allometric equations for estimating the aboveground biomass stocks of shrubland vegetation.

Chapter 8 - presents a comparative study of different approaches to spatially predict and map aboveground biomass stocks in forest stands and shrubland. These approaches can be, ultimately, used to map carbon stocks.

How to accurately estimate carbon uptake in Mediterranean vegetation using appropriate biomass estimates and carbon fraction?

Chapters 3, 4, 5 and 8 - present the tools to estimate and map aboveground biomass and, ultimately, the carbon stocks in forest and shrubland cover types.

Chapter 6 - evaluates the fuelwood characteristics and properties of maritime pine and eucalyptus presenting, apart from other measurements, the carbon fraction values and wood densities, for each tree component.

Chapter 7 - evaluates the fuelwood characteristics and properties of the five most common native woody shrub species presents, apart from other measurements, the carbon fraction values and wood densities.

What is the potential of maritime pine, eucalyptus and shrubland aboveground biomass for use as energy in Portugal?

Chapters 3, 4, 5 and 8 - present the tools to estimate and map aboveground biomass stocks in forest (maritime pine, eucalyptus) and shrubland cover types.

Chapter 6 - evaluates the fuelwood characteristics and properties of maritime pine and eucalyptus, presenting the calorific values of each biomass tree component.

Chapter 7 - evaluates the fuelwood characteristics, ash characteristics and biomass combustion properties of the five most common native woody shrub species presenting the calorific values and analysing the feasibility of using this biomass as fuelwood. Moreover, the analysis of ashes resulting from combustion is done in order to assess their potential application to the soils as fertilizer.

Chapter 9 - assess the forest biomass potential of the Portuguese maritime pine and eucalyptus forests for use as energy.

3

Additive nonlinear biomass equations for *Pinus pinaster* Aiton in Portugal

Data from this chapter contributed for the following publications:

[Annex A] Viana, H., Dias, S., Marques, C., Cruz, M., Lopes, D., Aranha, J., 2009. Estabelecimento de modelos alométricos para predição da biomassa aérea da *Pinus Pinaster*. Actas do 6º Congresso Florestal Nacional, Ponta Delgada, Açores. 6-9 Outubro., pp. 771-775.

[Annex B.1] Viana, H., Cohen, W.B., Lopes, D., Aranha, J., 2010. Assessment of forest biomass for use as energy. GIS-based analysis of geographical availability and locations of wood-fired power plants in Portugal. Applied Energy 87, 2551-2560.

[Annex B.2] Viana H.; Aranha J.; Lopes D., 2011, Dedicated Biomass Plants for Combined Heat & Power (CHP). The Portuguese National Strategy. 19th European Biomass Conference and Exhibition. ETA-Florence Renewable Energies. Berlin, Germany. June 6-10.

[Annex C.1] Viana, H., Aranha, J., Lopes, D., Cohen, W.B., 2012. Estimation of crown biomass of *Pinus pinaster* stands and shrubland above-ground biomass using forest inventory data, remotely sensed imagery and spatial prediction models. Ecological Modelling 226, 22-35.

[Annex C.2] Viana, H., Lopes, D., Aranha, J., 2011. Assessment of Forest Aboveground Biomass Stocks and Dynamics with Inventory Data, Remotely Sensed Imagery and Geostatistics, in: Shaukat, S.S. (ed.), Progress in Biomass and Bioenergy Production. InTech, pp. 107-130.

Abstract

A system of additive nonlinear equations was derived to estimate the aboveground biomass components of the maritime pine (*Pinus pinaster*) species. Data from 162 trees was collected within 16 stands in the North-Center region of Portugal. The weight of entire aboveground tree biomass (stem and crown) was determined in the field using destructive approach. The components of 77 trees were separated, weighted and the moister content of each component was determined in laboratory. The fresh, the air dry and oven dry biomass weights of each tree component (stem wood, stem bark, top, branches and needles) were estimated and modelled as a function of diameter at breast height (d_{bh}) and height (h) of tree. A nonlinear simultaneous system was developed and fitted by the nonlinear seemingly unrelated regression (NSUR) approach. The means of achieved statistics showed a good fit of the models and the additivity property among components and total tree biomass is satisfied. The remaining 85 trees weighted in the field were used as validation dataset to validate the crown, the stem and total aboveground biomass estimates. The results confirmed the good adjustment of the derived equation system. The comparison with models from other authors, to estimate aboveground biomass components of maritime pine showed discrepancies in some tree biomass components predictions. This indicates that special attention must be given in the generalization of biomass equations developed in a specific site. The equations developed in this study to estimate biomass components can be applied to other maritime pine stands under the assumption that the populations being studied are similar regarding to the stand characteristics.

Keywords: Additive equations, aboveground biomass, nonlinear seemingly unrelated regression, maritime pine

3.1 Introduction

According to the most recent National Forest Inventory (5º NFI 2005/2006), maritime pine (*Pinus pinaster* Aiton) is the main forest species in Portugal, with 885,000 hectares. Along with *Eucalyptus globulus* (around 739,000 hectares) comprise 51.2% of the Portuguese forest cover (approximately 3.4 million hectares) (DNGF, 2010). Occurring by regeneration or plantation, maritime pine is mainly used for pulp and chipboard industry or other biomass consuming industries. By this fact, the quantification of pine wood was, during many years, focused to calculate the traditional merchantable volume, while the interest in measurements of biomass weight only recently gained more interest. As stated by Laar and Akça (2007), the estimation of stand volume based on sample tree measurements has a long tradition (e.g. Draudt, 1860; Kopezky, 1899; Gehrhardt, 1909) as opposed to the estimation of the weight, which is much more recent, partly because timber is usually sold on a volume basis and partly because the volume of standing trees can be estimated more easily than their weight. On the other hand, with the increasing interest in studies with purpose to estimate the forest productivity (Lopes, 2005), studies to quantify the contribution of forests in the global carbon cycle (Hese et al., 2005), or the use of the so-called primary residues for use as energy (e.g. Viana et al., 2010), the estimation of the aboveground biomass (AGB) weight gained more interest.

The use of allometric equations adjusted for each specific location, based on destructive sampling would be the most accurate. However, given the labour and time consuming involved in the development of these equations, most studies rely on pre-established equations to other locations. The most common procedure of developing these equations is to adjust the aboveground total tree biomass or tree biomass components (e.g. stem wood, stem bark, tops, branches, leaves), using dendrometric parameters as independent variables.

Usually, the equation for each component is estimated separately and independent of the other equation, through least squares regression. Consequently, the lack of additivity among the tree component equations is observed while the desirable is that the sum of predictions for the biomass regression components equals the prediction for the total tree (Parresol, 1999). Procedures for forcing additivity have been proposed on a system of biomass equations, as described by (Parresol, 1999), both linear and nonlinear (Kozak, 1970; Chiyenda and Kozak, 1984; Cunia and Briggs, 1984, 1985; Reed and Green, 1985).

As demonstrated by (Parresol, 1999, 2001) a system of additive biomass equations when estimated accounting the contemporaneous correlation among the tree biomass components, for using joint-generalized least squares regression, has been proven to provide a gain in parameter estimation efficiency as it allows to impose restrictions that involve parameters in different equations. This method, whose seminal work was provided by Zellner (1962) is also known as seemingly unrelated regression (SUR), or nonlinear seemingly unrelated regression (NSUR) if using nonlinear models. In SUR estimation the different equations are specified in one system and estimated simultaneously as compared to ordinary least squares (OLS) where each of the models is estimated separately and independent of the other equation (Moon and Perron, 2008).

This approach has been used extensively in several studies for different tree species, in recent years (Parresol, 1999, 2001; Carvalho and Parresol, 2003; Bi et al., 2004; Lambert et al., 2005; Bi et al., 2010; Goicoa et al., 2011; Ruiz-Peinado et al., 2011). Concerning maritime pine, despite some equation are available to estimate the tree aboveground biomass components (e.g. Porté et al., 2002; Zianis et al., 2005), few studies applied the seemingly unrelated regression technique (e.g. Balboa-Murias et al., 2006; Shaiek et al., 2011). In Portugal most maritime pine biomass equations reported in the literature are non-additive and estimated using least squares regression and log transformed data (e.g. Arthur D. Little International Inc., 1985; Silva et al., 1991; Barreto, 2005; Lopes, 2005; Viana et al., 2009; Viana et al., 2012). However, only few were developed under the seemingly unrelated regression technique (Páscoa et al., 2004; Faias, 2009; DNGF, 2010).

The purposes of this study were (1) to develop a system of nonlinear allometric equation for estimating and predicting the fresh and dry weight of aboveground maritime pine biomass components in the North-Center region of Portugal, and (2) to compare and validate the existent aboveground biomass equations from other authors.

3.2 Methods and data

3.2.1 Field data

Biomass data used to develop the system of equations was collected, during 2007, in the most representative native maritime pine forests, within 16 logging sites, located in North-Center Portugal, extending from 39º 11' 53" N, 06º 14' 17' W to 42º 50' 50" N, 08º 19' 02" W (Figure 3.1). The maritime pine stands occur mainly in the North and Center of Portugal as ecological conditions limit their growth in the south.

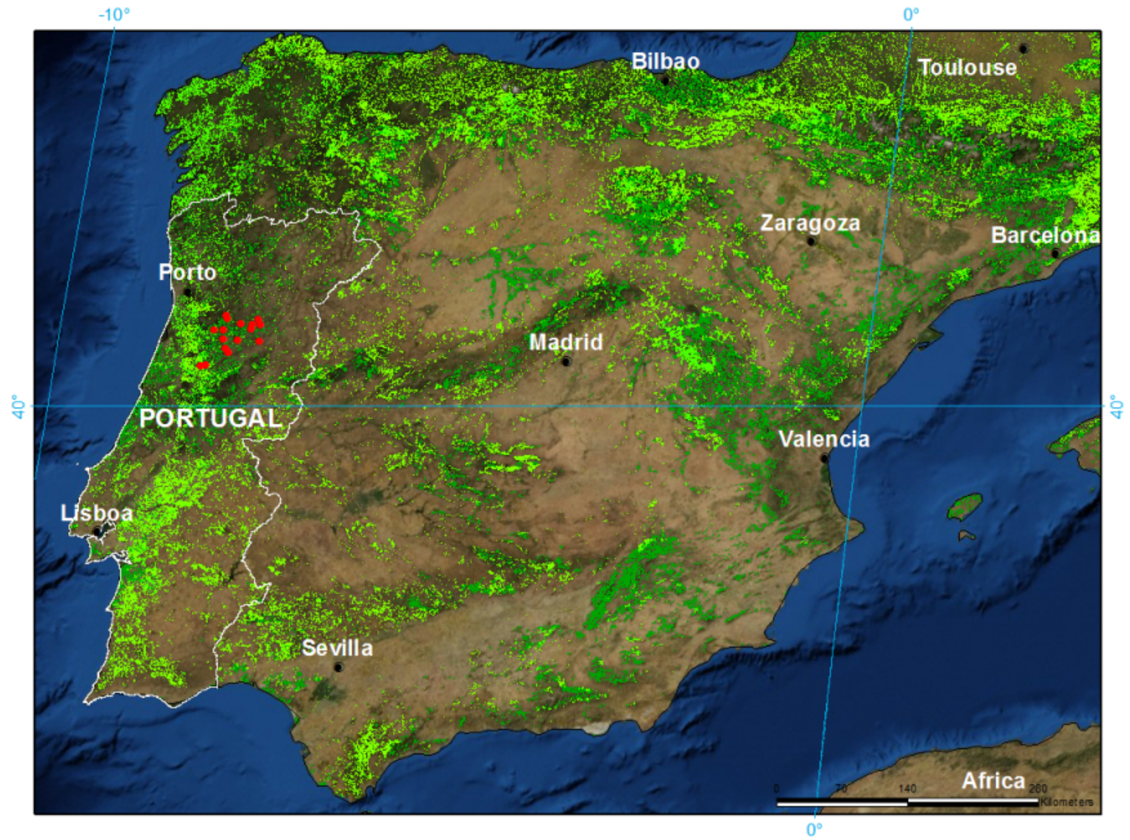

Figure 3.1 - Location of the maritime pine stands sampled for the data acquisition.

A circular temporary sample plot within a fixed-area of 500m^2 was established, in each site, and the dendrometric parameters: diameter at breast height (d_{bh}), total height of the tree (h) and canopy height (hc), crown horizontal projection (Crp) were measured and the structural stand variables such as number of trees per hectare (N), dominant tree height class (h_{dom}), basal area (G), stand age (t), crown closure class (Cc) and site index (SI) calculated.

Through a destructive approach, a total of 162 trees (around 10 trees per stand, representing all the present class diameters) were felled, and tree bole diameters (d_h)

over bark and heights (h_d) were measured directly on the stem with a caliper and a tape with 1 cm accuracy. By rigorous cubage, the merchantable volume (m^3) was obtained summing the bole sections volumes, evaluated with Smalian's formula (Meyer, 1953; Avery and Burkhart, 1983; Husch et al., 2003). The total volume (m^3) was achieved by adding the tip volume calculated as the volume of a cone. For the purpose of this work we considered as merchantable limit the top height up to the diameter of 7 cm. Bark thickness of the sample trees was also measured at the ends of each log, allowing to calculate the volume of wood (under bark).

The entire biomass was then weighted in site for the total 162 sample trees. From each tree all cut branches, including twigs, and tops covered with needles, were recovered and weighed directly in order to obtain the total crown's fresh weight.

A subsample of 77 trees (at least one tree per class diameter in each plot) was selected and the weight of individual components of the crown (branches, needles and tops) was achieved. The remaining 85 trees weighted in the field were used to validate the final models for the crown biomass, stem biomass and the total aboveground biomass. In each tree one live branch (twigs and meddles) was randomly collected at each whorl level, starting from the base up to the top height of the living crown, giving an average of 28.6% of the living branches for the 77 trees and the top recovered. Three discs of the stem, including wood and bark, were taken from the base, middle and top of each tree. All samples were placed into hermetically closed containers to prevent moisture loss, labelled and sent to the laboratory for separation and weighting of the components, on the day of sample collection. The proportion of each component in the total fresh weight was obtained by the ratio of each component sample and the total fresh biomass sample weight.

In order to achieve the biomass dry weights of each component of the respective tree, the moisture content (MC) was determined after air dry at ≈ 12% MC, and after oven dry. It should be noted that the air dried biomass is the MC in equilibrium with the outdoor atmosphere of this particular area. The amount of time to air-dry depends on the species, the tree component, the weather conditions, etc. At the season of measurements (summer), in the Portuguese conditions, we assume that the MC of biomass is approximately 12%. The oven dried biomass consists in the drying of the biomass sample in a drying oven at a temperature within the range of (105 ± 2°C) in air atmosphere until constant mass is achieved, following the European Standard CEN EN 14774-1:2009 (CEN EN 14774-1:2009). Digital scales with 0.001g precision were used for weightings. Additionally, the biomass density was determined to each component by measuring mass (weight) and volume by water displacement technique and expressed as weight per unit volume (Tsoumis, 1991). Density was calculated to the fresh biomass (D) with moisture content as received, Density to the air dried biomass at 12% of moisture ($D_{12\%}$), and the basic Density (D_b) with the biomass oven dried.

3.2.2 Fitting and comparison for each biomass tree component model

The allometric equations to include in the nonlinear simultaneous equation system were selected by comparing several models, for each biomass tree component. Equations to predict individual tree volume and aboveground biomass components and total tree biomass are reported in the literature by several authors since many years: Schumacher and Hall (1933); Stoate (1945); Näslund (1947); Spurr (1952); Meyer (1953); Takata (1958); Prodan (1965); Honer (1967); Ogaya (1968); Loetsch et al. (1973); Burkhart (1977); Avery and Burkhart (1983); Clutter et al. (1983); Marklund (1987; 1988); Prodan (1997); Husch et al. (2003); Zianis et al. (2005). Databases of treewise volume and biomass equations are also available for European tree species (Metla Project 3306, 2006) and for North American Tree Species (Jenkins et al., 2004).

These reviewed models as well as others applied for fitting maritime pine stem volume (Freire et al., 2003; Alegria, 2011; Alegria and Tomé, 2011) and maritime pine biomass components, (Arthur D. Little International Inc., 1985; Silva et al., 1991; Porté et al., 2002; Páscoa et al., 2004; Merino et al., 2005; Faias, 2009; DNGF, 2010; Shaiek et al., 2011) and variants of these models not reported in literature were tested in order to estimate all the biomass components.

The independent variables to include in the regression models were: diameter at breast height (d_{bh}) and total height (h), W_i=f(d ,h), and combinations of these two dendrometric parameters. Although there are variables that best fitted some biomass components (e.g. Biomass of tops), as the total height of tops or the total height of crown's tree, we decided to include in the regression models only these two dendrometric parameters as independent variables, as they are easily measured in field inventory surveys, apart from other reasons presented by Clutter et al. (1983).

Several models were tested and those with best results for each biomass components were chosen to include into the simultaneous system. However, Table 3.1

only presents the nonlinear models with best performance for all the biomass component adjustment stage.

Table 3.1 - Best candidate models.

Model	Equation	Reference
1	$W_i = \beta_1 d^{\beta_2} h^{\beta_3}$	(Schumacher and Hall, 1933)
2	$W_i = \beta_1 d^{\beta_2}$	(Husch et al., 2003)
3	$W_i = \beta_1 (d^2 h)^{\beta_2}$	(Spurr, 1952)
4	$W_i = \beta_0 + \beta_1 d^{\beta_2} h^{\beta_3}$	(Burkhart, 1977)
5	$W_i = \dfrac{d^2}{\beta_0 + \beta_1 (\frac{1}{h})}$	(Honer, 1967)
6	$W_i = \dfrac{d^2}{\beta_0 + \beta_1 d}$	(Takata, 1958)
7	$W_i = d^2 (\beta_0 + \beta_1 h)$	(Ogaya, 1968)
8	$W_i = e^{(\beta_0 + \beta_1 (lnd) + \beta_2 h)}$	(Freire et al., 2003)
9	$W_i = \beta_0 + \beta_1 d^{\beta_2}$	modified from (Husch et al., 2003)
10	$\mathrm{W_i} = \beta_0 + \beta_1 \left(\frac{1}{d}\right) + \beta_2 \left(\frac{1}{d^2}\right)$	adapted from (Curtis, 1967)
11	$W_i = e^{\ln\left(\beta_0 + \beta_1 (\frac{1}{d})\right)}$	
12	$W_i = e^{\ln\left(\beta_0 + \beta_1 (\frac{1}{d^2})\right)}$	
13	$W_i = \beta_1 e^{\left(\beta_2 (\frac{1}{d})\right)}$	
14	$W_i = \beta_1 e^{\beta_2 * (\frac{1}{d} - \beta_3)}$	
15	$W_i = \beta_1 e^{\left(\beta_2 (\frac{1}{d}) + \beta_3 (\frac{1}{d^2})\right)}$	
16	$W_i = \beta_1 e^{\left(\beta_2 (\frac{1}{d}) + \beta_3 (\frac{1}{h})\right)}$	
17	$W_i = \beta_1 e^{\left(\beta_2 (\frac{1}{d^2}) + \beta_3 (\frac{1}{h})\right)}$	

Where: W_i is the biomass (kg tree^{-1}); *d* is the diameter at breast height (cm), (*h)* is the total height of tree (m) and $\beta_0, \beta_1, \beta_2, \beta_3$ are the equation parameters

The non-linear models, for each component, were fitted by nonlinear regression solved by the Gauss-Newton algorithm using the NLIN procedure of the SAS version 9.1 software (SAS Institute Inc., 2004). The initial values of models parameters (β_j) provided to begin the iterations were obtained by log transforming the equations and applying OLS using the SAS REG procedure for fitting (SAS Institute Inc., 2004), and also defining a grid search with a range of starting values in the iterative phase of the NLIN procedure.

The residuals $e_i = (y_i - \hat{y}_i)$ (difference between the observed and fitted values) were calculated for each equation, and the graph analysis (e.g. scatterplots of residuals against the predicted values; scatterplots of residuals against individual predictors; histogram of residuals) and the statistics of regression residuals were examined to check that model assumptions were satisfied (Ostrom, 1990; Rawlings et al., 1998; Ritz and Streibig, 2008). To select the best biomass component model which best fitted the data the following statistical criteria obtained from the residuals of each model were analysed and compared (Sit and Poulin-Costello, 1994): model bias (Bias), mean absolute error (MAE); residual mean squares error (MSE) defined as the mean of the predicted residual sum of squares (PRESS or commonly SSE); root mean squared error (RMSE); coefficient of determination (R^2); and adjusted coefficient of determination (R^2_{adj}), (Eqs. 1-6). Akaike's information criterion (AIC) (Akaike, 1974), which is an index to test and compare the goodness of fit of different models with a different number of parameters, was additionally calculated (Beal, 2005) (Eq. 7). AIC simultaneously maximizes the model fit and minimizes the number of parameters, such the model with the lowest value of AIC is considered the best (Motulsky and Christopoulos, 2003). The best model, for each tree component, was selected based in a ranking of the previous described statistics.

$$Bias = \frac{\sum_1^n (y_i - \hat{y}_i)}{n} = \frac{\sum_1^n (e_i)}{n} \quad [1]$$

$$MAE = \frac{\sum_1^n |y_i - \hat{y}_i|}{n} = \frac{\sum_1^n |e_i|}{n} \quad [2]$$

$$MSE = \frac{SSE}{n-p} = \frac{\sum_1^n (y_i - \hat{y}_i)^2}{n-p} = \frac{\sum_1^n (e_i)^2}{n-p} \quad [3]$$

$$RMSE = \sqrt{MSE} \quad [4]$$

$$R^2 = 1 - \frac{SSE}{SST_{corrected}} = 1 - \frac{\sum_1^n (y_i - \hat{y}_i)^2}{\sum_1^n (y_i - \bar{y})^2} \quad [5]$$

$$R^2_{adj} = 1 - \frac{SSE\,(n-1)}{SST_{corrected}\,(n-p)} = 1 - \left[(1 - R^2)\,\frac{n-1}{n-p}\right] \quad [6]$$

$$AIC = n\,\ln(MSE) + 2\,p \quad [7]$$

where: y_i is the observed value; $\hat{y}_i$ is the predicted value for observation *i*; $\bar{y}$ is the mean of the observed values; *n* is the number of observations used to fit the model and *p* is the number of parameters fitted by the regression.

It should be noted that in nonlinear regression R^2 value is not readily defined. One of the problems with the R^2 definition is that it requires the presence of an intercept, which most nonlinear models do not have. A measure, relatively closely corresponding to R^2 in the nonlinear case is Pseudo-R^2 (Eqs 5 and 6), where SST is the corrected total sum of squares ($SST_{corrected}$) (Schabenberger and Pierce, 2002).

3.2.3 Additive nonlinear simultaneous system specification and modelling

Following Parresol (1999, 2001) a system of six nonlinear regression functions was specified such that (i) each component regression contains its own independent variables, and the total-tree regression is a function of all independent variables used; (ii) each regression can use its own weight function; and (iii) the additivity is insured by setting constraints (i.e., restrictions) on the regression coefficients. This model specification with cross-equation constraints on the structural parameters and cross-equation error correlation with an additive error structure, reported by Cunia and Briggs (1984, 1985) and Reed and Green (1985) as a method of forcing additivity among biomass equations, is written as follows (Eq. 8):

$$
\begin{aligned}
W_{wood} &= f_1(x_{1j}, \beta_{1j}) + \varepsilon_1 \\
W_{bark} &= f_2(x_{2j}, \beta_{b2j}) + \varepsilon_2 \\
W_{top} &= f_3(x_{3j}, \beta_{3j}) + \varepsilon_3 \\
W_{branches} &= f_4(x_{4j}, \beta_{4j}) + \varepsilon_4 \\
W_{needles} &= f_5(x_{5j}, \beta_{5j}) + \varepsilon_5 \\
W_{total} &= f_6(x_{1j}, x_{2j}, x_{3j}, x_{4j}, x_{5j}, \beta_1, \beta_2, \beta_3, \beta_4, \beta_5) + \varepsilon_{total}
\end{aligned}
\tag{8}
$$

where: W, is the biomass of each tree component and the total AGB (ton ha^{-1}) , which is a function $(f_1, \ldots, f_6)$ of a set of independent variables $(x_{1j}, \ldots, x_{6j})$ and a set of parameters $(\beta_{1j}, \ldots, \beta_{6j})$ and $(\varepsilon_1, \ldots, \varepsilon_6)$ is the error component.

The set of equations were fitted to the data of each tree component with the PROC MODEL procedure of SAS (SAS Institute Inc., 2004) using joint generalized least squares more commonly called nonlinear seemingly unrelated regressions (NSUR). The theoretical statistics behind this approach can be better understood in the literature (e.g. Zellner, 1962; Srivastava and Giles, 1987; Bartels, 2006; Moon and Perron, 2008).

Heteroscedasticity typically occurs in biomass data, that is, the error variance is not constant over all observations. The assumption of homoscedasticity of residuals was examined using the White's test (White, 1980). To overcome the problem of heteroscedasticity, and by this way improve the efficiency of the estimates, weight variables were used in the model equations to stabilize the variance (i.e. weighted nonlinear least squares (Cohen et al., 2003). In biomass data, it is usually assumed that the error's variance can be modelled as a power function of the independent variables. However, depending on the model fitted to the data, some biomass tree components can present combined heteroscedasticity trends (Parresol, 1999, 2001). The weight functions, for each equation of the NSUR system were derived by modelling the estimated errors ($\hat{e}_i^2$) of the unweighted model as the dependent variable in the error variance model, upon applying ordinary least squares (OLS), as:

$$\hat{e}_i^2 = \gamma(X_i)^k \qquad [9]$$

or, in the natural logarithm (ln):

$$\ln \hat{e}_i^2 = \ln \gamma + k \ln(X_i) \qquad [10]$$

After modelling the error structure to correct the heteroscedasticity, the weighting functions $1/(X_i)^k$ were specified in the system and the iterated seemingly unrelated regression in the SAS MODEL procedure (SAS Institute Inc., 2004) was carried out.

3.3 Results and discussion

3.3.1 Characteristics of maritime pine stands

The descriptive statistics of pine stands, measured during field work and recorded in the inventory dataset, are presented in Table 3.2.

Table 3.2 - Descriptive statistics of maritime pine stands.

Stands	N (trees ha^{-1})	t (year)	h_{dom} (m)	d_{dom} (cm)	BA (m^2 ha^{-1})	V (m^3 ha^{-1})	SI (m)	WRS
1	700	52	21.5	48.6	59.2	439.2	19	0.18
2	800	40	24.7	41.9	55.8	406.1	24	0.14
3	600	51	21.9	41.4	49.7	460.0	19	0.19
4	600	44	21.6	37.6	50.5	265.2	20	0.19
5	600	42	19.6	37.7	43.4	274.5	18	0.21
6	600	54	21.6	40.8	43.4	540.6	19	0.19
7	620	26	18.2	31.6	30.9	208.2	20	0.22
8	460	39	15.8	40.0	38.6	231.7	15	0.30
9	900	20	13.1	18.4	16.7	96.3	16	0.26
10	620	20	10.8	21.5	15.4	61.6	14	0.37
11	460	51	20.9	33.7	29.3	261.2	19	0.22
12	2020	27	13.3	18.1	30.1	82.5	15	0.17
13	460	60	29.7	57.2	66.9	312.5	25	0.16
14	520	48	21.8	44.4	43.1	126.5	20	0.20
15	980	26	15.7	36.5	36.7	94.8	18	0.20
16	720	35	20.1	30.9	31.0	117.3	20	0.19
Mean	729	40	19.4	36.3	41.9	248.64	19	0.21
Min	460	20	10.8	18.1	15.4	61.60	14	0.14
Max	2020	60	29.7	57.2	89.2	540.59	25	0.37
SD	375.6	12.7	4.8	10.6	18.5	150.51	3	0.06

Where: N is the number of trees per hectares; t is the stand mean age; h_{dom} is the dominant height; d_{dom} is the dominant diameter at breast height; BA is the basal area; V is the stand commercial volume; SI is the site index and WRS is the Wilson's relative spacing index (Wilson, 1946).

These stands are pure self-thinned even-aged with ages ranging between 20 and 60 years. The stand stocking is similar in all stands except in stands 11 to 14. Stand number 12 is composed by trees with small diameters and total heights, which is reflected in the observed low volumes (82.5 m^3 ha^{-1}). Site index, calculated by the equation developed by Páscoa (1987) at the reference age of 50 years. According to the defined site quality classes: inferior <14; moderated 14-18 and superior ≥ 18, the forest stands are in the moderated and superior site quality. The Wilson's relative spacing index, which according the maritime pine yield tables of Oliveira (1985) for this region (North-Center Portugal) should be 0.23 (moderated SI), shows for stands with the same dominant height, that some stands are understocked as others are overstocked.

Figure 3.2 shows the percentage of fresh biomass components measured in the trees (under the bars) of each one of the 16 sample plots. The last column is the percentage of the total tress (77). The mean distribution of the components is similar in all the stands, except in the stands 9 and 10. Comparing with the other stands, these are younger (t=20), with trees with smaller dimensions (d_{dom} and h_{dom}) and with higher Wilson's relative spacing index (Table 3.2). Hence, given the lower competition, the trees have bigger crowns in proportion with the stem.

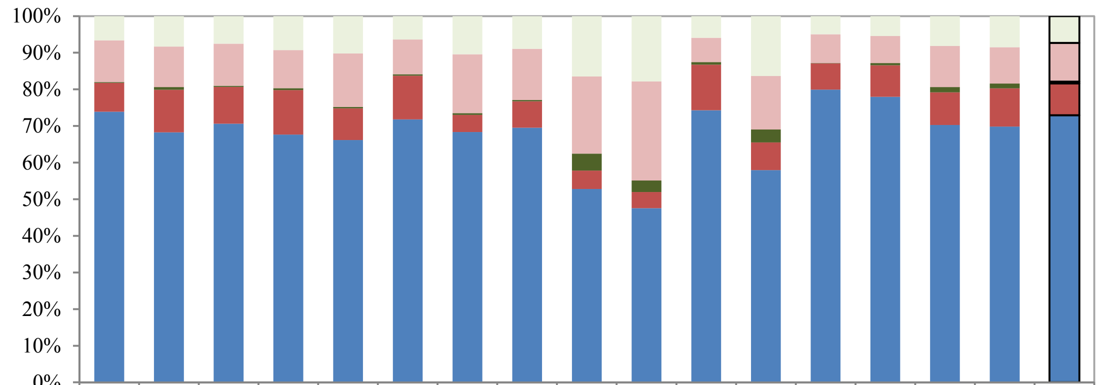

	6	5	5	5	5	5	4	4	4	4	5	5	5	5	5	5	77
Needles	6.6	8.3	7.5	9.3	10.2	6.4	10.4	8.9	16.5	17.9	5.9	16.4	4.9	5.4	8.2	8.5	7.3
Branches	11.4	11.1	11.5	10.4	14.6	9.5	16.1	14.0	21.0	27.0	6.6	14.6	7.9	7.4	11.2	9.9	10.6
Tops	0.2	0.8	0.3	0.5	0.4	0.4	0.5	0.4	4.7	3.1	0.7	3.5	0.1	0.6	1.4	1.3	0.5
Bark	7.9	11.6	10.0	12.1	8.6	11.9	4.7	7.2	5.0	4.4	12.4	7.6	7.1	8.6	8.9	10.4	8.7
Wood	73.9	68.3	70.6	67.6	66.2	71.8	68.3	69.5	52.8	47.6	74.3	57.9	79.9	78.0	70.3	69.9	72.9

Figure 3.2 - Proportion of the maritime pine biomass tree components in the measured sample plots.

3.3.2 Nonlinear models fitted to each biomass tree component

The models previous presented in Table 3.1 were fitted to all the biomass tree components, for fresh weight, air dried weight and oven dry weight. Only the statistics from the models with best performance are presented in Tables 3.3 to 3.7. The entire AGB was also fitted and the statistics presented in Table 3.8.

The models that bets fitted the data of each component, according to the rank of the computed statistics, are shaded in the tables. Attending to the AIC criterion for the wood stem biomass, the model 8 was the best fitted for all biomass weights (fresh, air dried, and oven dried); for the bark stem biomass the model 5 was the selected. The adjustment of the top biomass presented lower performances comparatively to the other biomass components, with model 16 presenting the best performance. For the branches biomass, the model 1 fitted better the fresh biomass, the model 2 fitted better the air dried biomass and the model 9 fitted better the oven dried biomass (model 4 did not converged). For the needles, model 7 fitted better the fresh and air dried biomass and model 2 fitted better the oven dried biomass. Nevertheless, as can be seen in Tables 3.3 to 3.8, the several models fitted well the biomass components. Thus, in order to maintain the parsimony in the nonlinear simultaneous system, a model with the same functional form could be selected to fit the wood stem, barks stem, branches and needles biomass. As example, see model 1 for the mentioned biomass components whose performance did not differ substantially from the best fitted models.

Regarding the development of regression models, about the decisions of which independent variables should be included in the models, the form that the variables should take and the functional form of the models, Rawlings et al. (1998) addresses that the objective of basic research is to obtain realistic models. In the same direction, Barreto (2004) makes a critical analysis of some allometric models to estimate the stem volume of maritime pine where argues that, despite the development of increasingly sophisticated computational methods, the researcher should not forget the tree geometrical coherence and the fundamental basis of the stands ecology. Nevertheless, accounting the considerations above, for the purpose of this work, we decided to include in the simultaneous system model the equations with the best performance obtained in the independent adjustment phase of each biomass component. The potential use of the final system equations should attend to the stand characteristics where this data was collected.

Table 3.3 - Statistics of the best fitted models to the wood stem biomass.

Model	***Mean***	***MAE***	***MSE***	***RMSE***	***RMSE (%)***	R^2	R^2_{adj}	***AIC***
Fresh weight								
1	446.2	41.96	4140.80	64.35	14.22	0.9871	0.9866	644.25
2	437.6	69.35	12155.20	110.25	24.36	0.9616	0.9605	726.20
3	445.8	42.10	4112.80	64.13	14.17	0.9870	0.9866	642.76
4	452.6	40.91	4023.10	63.43	14.02	0.9876	0.9871	642.98
5	448.1	40.74	3980.10	63.09	13.94	0.9874	0.9871	640.23
6	447.2	40.44	4023.00	63.43	14.02	0.9873	0.9869	641.06
7	449.5	42.80	4343.50	65.91	14.56	0.9863	0.9859	646.96
8	451.3	37.87	3629.20	60.24	13.31	0.9887	0.9882	634.09
Air dried weight								
1	265.4	25.90	1416.40	37.64	13.97	0.9874	0.9869	561.64
2	260.5	39.90	3965.80	62.97	23.38	0.9643	0.9634	639.95
3	265.4	25.91	1397.70	37.39	13.88	0.9874	0.9871	559.65
4	269.3	25.02	1369.50	37.01	13.74	0.9880	0.9875	560.00
5	267.1	25.30	1393.80	37.33	13.86	0.9875	0.9871	559.44
6	266.0	25.00	1359.50	36.87	13.69	0.9878	0.9874	557.52
7	268.0	26.43	1498.90	38.72	14.37	0.9865	0.9862	565.03
8	268.3	23.77	1263.70	35.55	13.20	0.9888	0.9883	552.86
Oven dried weight								
1	231.6	22.90	1294.20	35.97	15.35	0.9846	0.9839	554.69
2	227.3	36.18	3246.00	56.97	24.31	0.9608	0.9597	624.53
3	231.4	22.92	1278.70	35.76	15.26	0.9845	0.9841	552.80
4	234.3	22.95	1277.50	35.74	15.25	0.9850	0.9844	554.65
5	232.3	22.69	1259.70	35.49	15.15	0.9848	0.9844	551.65
6	231.7	22.39	1253.80	35.41	15.11	0.9848	0.9844	551.29
7	233.2	23.21	1322.20	36.36	15.52	0.9840	0.9836	555.38
8	234.0	21.43	1170.20	34.21	14.60	0.9860	0.9855	546.94

Note: values of calculated statistics (Mean, MAE, MSE and RMSE) are in kg tree^{-1}.

Table 3.4 - Statistics of the best fitted models to the bark stem biomass.

Model	*Mean*	*MAE*	*MSE*	*RMSE*	*RMSE (%)*	R^2	R^2_{adj}	*AIC*
Fresh weight								
1	54.2	8.61	171.00	13.08	24.27	0.9453	0.9431	398.87
2	53.8	9.36	187.50	13.69	25.42	0.9392	0.9376	404.99
3	54.4	9.25	182.30	13.50	25.06	0.9409	0.9393	402.81
4	53.9	8.34	172.80	13.15	24.40	0.9455	0.9432	400.61
5	53.8	8.51	168.70	12.99	24.11	0.9453	0.9438	396.85
6	53.7	9.25	195.60	13.99	25.96	0.9366	0.9349	408.23
7	54.0	8.79	170.00	13.04	24.20	0.9449	0.9434	397.45
8	54.3	8.88	172.10	13.12	24.35	0.9450	0.9427	399.36
Air dried weight								
1	48.3	7.67	135.80	11.65	24.28	0.9453	0.9431	381.10
2	48.0	8.34	148.90	12.20	25.42	0.9392	0.9376	387.22
3	48.5	8.24	144.70	12.03	25.06	0.9409	0.9393	385.04
4	48.0	7.43	137.20	11.71	24.40	0.9455	0.9432	382.84
5	47.9	7.58	133.90	11.57	24.11	0.9453	0.9438	379.07
6	47.9	8.24	155.30	12.46	25.96	0.9366	0.9349	390.45
7	48.1	7.83	135.00	11.62	24.20	0.9449	0.9434	379.68
8	48.4	7.92	136.70	11.69	24.36	0.9450	0.9427	381.59
Oven dried weight								
1	42.1	6.69	103.20	10.16	24.28	0.9453	0.9431	359.94
2	41.8	7.27	113.10	10.63	25.42	0.9392	0.9376	366.06
3	42.3	7.19	110.00	10.49	25.07	0.9409	0.9393	363.88
4	41.8	6.48	104.20	10.21	24.40	0.9455	0.9432	361.68
5	41.8	6.61	101.80	10.09	24.11	0.9453	0.9438	357.92
6	41.7	7.18	118.00	10.86	25.96	0.9366	0.9349	369.30
7	41.9	6.83	102.60	10.13	24.21	0.9449	0.9434	358.52
8	42.2	6.90	103.80	10.19	24.35	0.9450	0.9427	360.43

Note: values of calculated statistics (Mean, MAE, MSE and RMSE) are in kg tree^{-1}.

Table 3.5 - Statistics of the best fitted models to the top biomass.

Model	*Mean*	*MAE*	*MSE*	*RMSE*	*RMSE (%)*	R^2	R^2_{adj}	*AIC*
Fresh weight								
10	3.1	0.57	0.57	0.76	23.57	0.6387	0.6338	-41.06
11	3.1	0.57	0.55	0.74	24.13	0.6599	0.6507	-43.71
12	3.1	0.57	0.54	0.74	23.45	0.6584	0.6539	-45.41
13	3.1	0.57	0.54	0.74	23.53	0.6563	0.6470	-44.94
14	3.1	0.57	0.54	0.74	23.53	0.6563	0.6470	-44.94
15	3.1	0.57	0.55	0.74	23.65	0.6572	0.6432	-43.15
16	3.1	0.52	0.47	0.69	21.97	0.7044	0.6922	-54.54
17	3.1	0.61	0.59	0.77	24.54	0.6311	0.6160	-37.49
Air dried weight								
10	1.6	0.29	0.15	0.39	23.37	0.6667	0.6623	-142.08
11	1.6	0.29	0.14	0.38	24.09	0.6905	0.6821	-145.78
12	1.6	0.29	0.14	0.38	23.26	0.6894	0.6853	-147.52
13	1.6	0.29	0.15	0.38	23.38	0.6862	0.6778	-146.73
14	1.6	0.29	0.15	0.38	23.38	0.6862	0.6778	-146.73
15	1.6	0.29	0.15	0.38	23.47	0.6877	0.6749	-145.09
16	1.6	0.26	0.13	0.36	22.06	0.7244	0.7130	-154.70
17	1.6	0.31	0.16	0.40	24.82	0.6510	0.6366	-136.53
Oven dried weight								
10	1.1	0.20	0.07	0.27	23.38	0.6905	0.6821	-200.13
11	1.1	0.20	0.07	0.27	24.09	0.6862	0.6778	-201.09
12	1.1	0.20	0.07	0.27	23.25	0.6894	0.6853	-201.87
13	1.1	0.20	0.07	0.27	23.38	0.6862	0.6778	-201.09
14	1.1	0.20	0.08	0.28	23.38	0.6667	0.6623	-196.44
15	1.1	0.20	0.07	0.27	23.48	0.6877	0.6749	-199.45
16	1.1	0.18	0.06	0.25	22.05	0.7244	0.7130	-209.06
17	1.2	0.22	0.08	0.28	24.82	0.6510	0.6366	-190.88

Note: values of calculated statistics (Mean, MAE, MSE and RMSE) are in kg tree^{-1}.

Table 3.6 - Statistics of the best fitted models to the branches biomass.

Model	*Mean*	*MAE*	*MSE*	*RMSE*	*RMSE (%)*	R^2	R^2_{adj}	*AIC*
Fresh weight								
1	64.5	19.61	804.30	28.36	43.21	0.8304	0.8235	518.07
2	64.7	20.04	817.30	28.59	43.56	0.8254	0.8206	518.34
3	65.2	22.20	992.60	31.51	48.00	0.7879	0.7822	533.30
5	67.4	20.51	833.90	28.88	44.00	0.8218	0.8170	519.88
6	63.2	22.33	1055.60	32.49	49.50	0.7744	0.7683	538.04
7	66.7	20.55	833.60	28.87	43.99	0.8219	0.8171	519.86
8	64.4	19.73	814.80	28.54	43.49	0.8282	0.8212	519.06
9	65.6	20.29	821.90	28.67	43.68	0.8267	0.8221	519.73
Air dried weight								
1	40.0	12.39	325.90	18.05	43.94	0.8369	0.8302	448.50
2	40.1	12.44	325.70	18.05	43.92	0.8348	0.8303	447.49
3	40.5	13.61	388.80	19.72	47.99	0.8028	0.7974	461.13
5	41.8	13.00	343.60	18.54	45.11	0.8257	0.8210	451.61
6	39.2	13.63	407.40	20.18	49.13	0.7934	0.7878	464.72
7	41.7	12.91	339.20	18.42	44.83	0.8280	0.8233	450.61
8	40.0	12.41	328.60	18.13	44.12	0.8355	0.8288	449.15
9	41.1	12.63	323.80	17.99	43.80	0.8379	0.8335	448.02
Oven dried weight								
1	28.7	9.19	177.90	13.34	44.83	0.8403	0.8338	401.90
2	28.8	9.17	176.70	13.29	44.68	0.8392	0.8349	400.43
3	29.1	9.80	208.90	14.45	48.58	0.8099	0.8048	413.31
5	30.1	9.63	190.90	13.82	44.29	0.8263	0.8217	406.35
6	28.2	9.83	215.90	14.69	46.44	0.8036	0.7983	415.85
7	30.1	9.54	187.30	13.69	49.39	0.8296	0.8250	404.88
8	28.7	9.16	178.90	13.38	46.00	0.8394	0.8328	402.34
9	29.7	9.26	173.60	13.18	44.96	0.8442	0.8400	400.01

Note: values of calculated statistics (Mean, MAE, MSE and RMSE) are in kg tree^{-1}.

Table 3.7 - Statistics of the best fitted models to the needles biomass.

Model	*Mean*	*MAE*	*MSE*	*RMSE*	*RMSE (%)*	R^2	R^2_{adj}	*AIC*
Fresh weight								
1	45.5	11.92	277.10	16.65	36.75	0.8170	0.8095	436.02
2	45.6	12.34	283.00	16.82	37.14	0.8105	0.8054	436.68
3	45.8	13.36	331.40	18.20	40.19	0.7782	0.7722	448.82
4	45.3	11.99	280.00	16.73	36.95	0.8176	0.8101	437.77
5	44.6	12.03	281.70	16.78	37.06	0.8114	0.8063	436.33
6	44.3	13.94	371.60	19.28	42.56	0.7513	0.7445	457.64
7	44.8	12.10	275.60	16.60	36.65	0.8155	0.8105	434.64
8	45.4	12.04	277.70	16.66	36.79	0.8166	0.8091	436.18
Air dried weight								
1	22.0	5.65	64.54	8.03	36.87	0.8182	0.8107	323.82
2	22.0	5.79	64.63	8.04	36.90	0.8155	0.8105	322.96
3	22.0	6.36	73.90	8.60	39.46	0.7890	0.7833	333.28
4	21.8	5.71	64.98	8.06	37.00	0.8194	0.8120	325.30
5	21.5	5.68	65.59	8.10	37.17	0.8128	0.8077	324.09
6	21.4	6.69	82.04	9.06	41.57	0.7658	0.7595	341.33
7	21.5	5.69	64.45	8.03	36.85	0.8160	0.8110	322.74
8	21.9	5.68	64.50	8.03	36.86	0.8183	0.8109	323.77
Oven dried weight	45.5	11.92	277.10	16.65		0.8170	0.8095	436.02
1	19.5	5.03	51.85	7.20	44.22	0.8165	0.8089	306.97
2	19.6	5.16	51.74	7.19	44.18	0.8144	0.8094	305.84
3	19.6	5.65	58.71	7.66	47.06	0.7894	0.7837	315.56
4	19.4	5.07	52.17	7.22	44.36	0.8179	0.8104	308.39
5	19.1	5.06	52.73	7.26	44.60	0.8108	0.8057	307.30
6	19.1	5.95	64.93	8.06	49.48	0.7671	0.7608	323.31
7	19.1	5.07	51.87	7.20	44.23	0.8139	0.8089	306.02
8	19.5	5.05	51.81	7.20	44.20	0.8166	0.8091	306.90

Note: values of calculated statistics (Mean, MAE, MSE and RMSE) are in kg tree^{-1}.

Table 3.8 - Statistics of the best fitted models to the entire aboveground biomass.

Model	*Mean*	*MAE*	*MSE*	*RMSE*	*RMSE (%)*	R^2	R^2_{adj}	*AIC*
Fresh weight								
1	610.6	60.82	7857.60	88.64	14.29	0.9846	0.9840	693.57
2	602.9	82.86	15548.60	124.69	20.10	0.9691	0.9683	745.16
3	612.1	61.47	8082.50	89.90	14.49	0.9840	0.9835	694.78
4	620.5	58.87	7473.00	86.45	13.93	0.9856	0.9850	690.66
5	612.7	61.59	8011.90	89.51	14.43	0.9841	0.9837	694.10
6	607.9	61.56	8160.00	90.33	14.56	0.9838	0.9834	695.51
7	616.9	60.46	7787.00	88.24	14.22	0.9845	0.9841	691.91
8	615.9	55.92	6956.80	83.41	13.44	0.9864	0.9858	684.20
Air dried weight								
1	375.7	35.91	2731.90	52.27	13.69	0.9859	0.9853	612.22
2	371.1	49.56	5450.60	73.83	19.34	0.9715	0.9707	664.44
3	376.8	36.37	2874.90	53.62	14.04	0.9850	0.9846	615.19
4	381.8	34.22	2582.00	50.81	13.31	0.9869	0.9863	608.83
5	377.8	36.15	2831.80	53.21	13.94	0.9852	0.9848	614.02
6	374.0	36.79	2903.40	53.88	14.11	0.9848	0.9844	615.94
7	380.2	35.39	2746.60	52.41	13.73	0.9856	0.9852	611.67
8	378.8	33.21	2430.50	49.30	12.91	0.9875	0.9869	603.22
Oven dried weight								
1	322.0	30.02	2156.40	46.44	14.36	0.9848	0.9841	594.01
2	317.9	42.19	4297.00	65.55	20.27	0.9692	0.9684	646.13
3	322.8	30.67	2215.70	47.07	14.56	0.9841	0.9837	595.13
4	326.4	29.32	2086.50	45.68	14.13	0.9855	0.9849	592.42
5	323.0	30.34	2192.30	46.82	14.48	0.9843	0.9839	594.31
6	320.5	31.23	2246.00	47.39	14.66	0.9839	0.9835	596.18
7	325.0	29.52	2130.70	46.16	14.28	0.9847	0.9843	592.12
8	324.7	27.96	1932.10	43.96	13.59	0.9863	0.9858	585.55

Note: values of calculated statistics (Mean, MAE, MSE and RMSE) are in kg tree^{-1}.

3.3.3 Additive nonlinear simultaneous biomass equations system fitted by NSUR

The unweighted models included into the additive simultaneous system to be fitted by the nonlinear seemingly unrelated regression approach (NSUR) are (Eq. 11):

$$W_{wood} = e^{\,(\beta_{10}+\beta_{11}(lnd)+\beta_{12}h)}$$
$$W_{bark} = \frac{d^2}{\beta_{20} + \beta_{21}(\frac{1}{h})}$$
$$W_{top} = \beta_{31}\, e^{\left(\beta_{32}\left(\frac{1}{d}\right)+\beta_{33}\left(\frac{1}{h}\right)\right)}$$
$$W_{branches} = \beta_{41} d^{\beta_{42}} h^{\beta_{43}}$$
$$W_{needles} = \beta_{51} d^{\beta_{52}} h^{\beta_{53}}$$
$$W_{AGB} = W_{wood} + W_{bark} + W_{top} + W_{branches} + W_{needles} \qquad [11]$$

where: W, is the biomass of each tree component (kg $tree^{-1}$) , *d* is the diameter at breast height of the tree, *h* is the total height of the tree and β_{1x}..., β_{5x} are the coefficients of the regressions

The previous models, excepting model 16 for tops estimation, exhibit heteroscedasticity, so the standard errors of regression coefficients are biased, as they are if residuals are non-normal, thus leading to less accurate inferences. The distribution of the residuals *(ê)* versus the independent variables (*d, h*) is presented in Figures 3.3 to 3.7. As the behaviour is the same for fresh and dried biomass, only the scatterplots for the fresh biomass are presented.

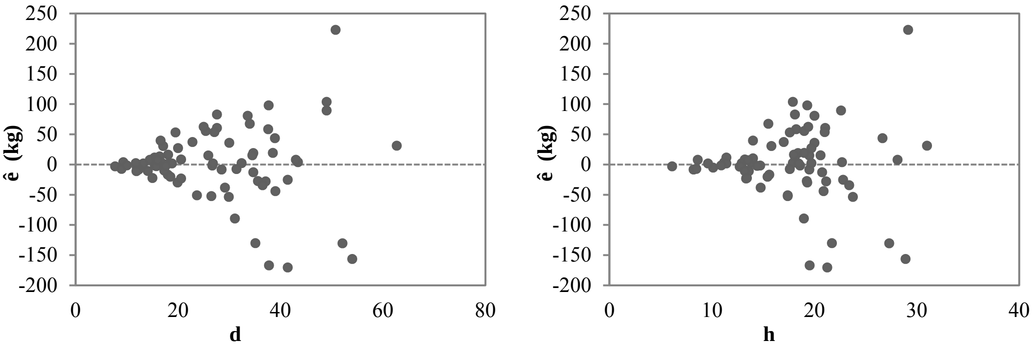

Figure 3.3 - Scatterplots of wood biomass residuals with the independent variables of the unweighted model.

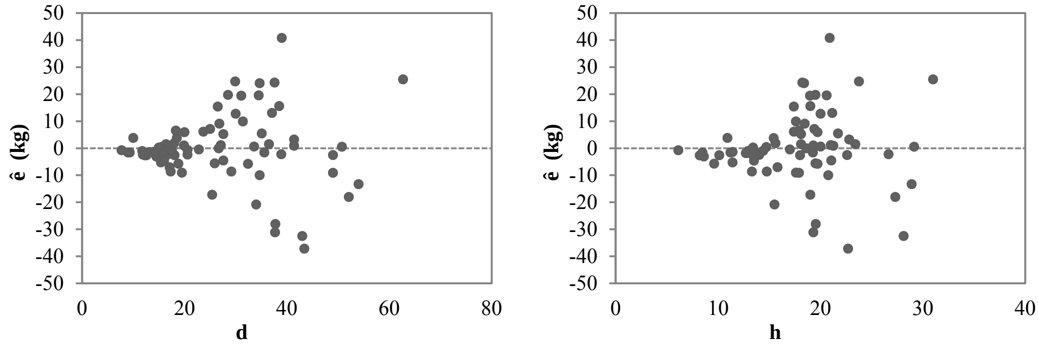

Figure 3.4 - Scatterplots of bark biomass residuals with the independent variables of the unweighted model.

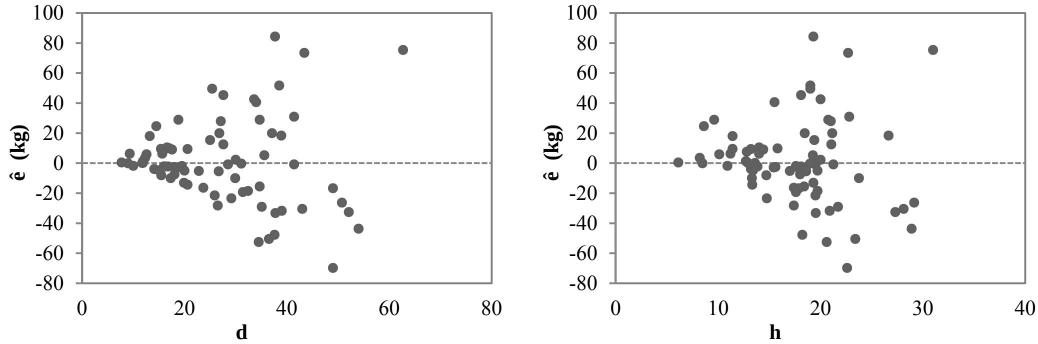

Figure 3.5 - Scatterplots of branches biomass residuals with the independent variables of the unweighted model.

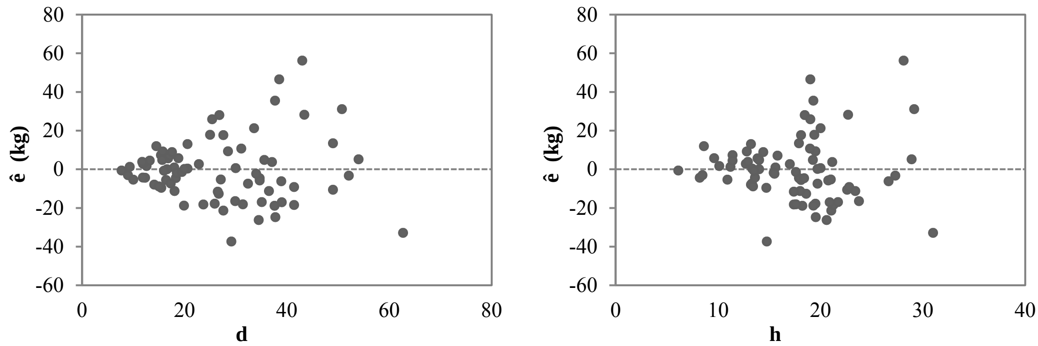

Figure 3.6 - Scatterplots of needles biomass residuals with the independent variables of the unweighted model.

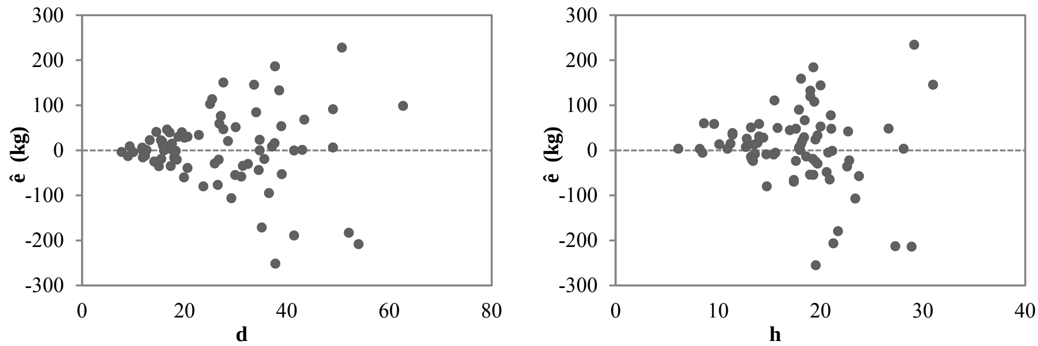

Figure 3.7 - Scatterplots of AGB biomass residuals with the independent variables of the unweighted model.

Weights to correct for heteroscedasticity for NSUR system were derived modelling the error function (Eq. 10) and using AIC criterion to select the better function (see Parresol (1999, 2001), as explained in methods and data section.

The parameter estimates and standard errors, of the nonlinear unweighted models (NLIN procedure) and of the additive nonlinear simultaneous equation system (NSUR procedure) (Eq. 11) are presented in Tables 3.9 to 3.11, for fresh, air and oven dry biomass, respectively. The standard errors decreased from the NLIN unweighted estimates to the NSUR estimates, in almost all parameters. The process of simultaneous estimation reduces the confidence and prediction intervals of the biomass estimations resulting from the smaller variance obtained by the application of the NSUR estimation method, which considers the contemporaneous correlation among the components, and so achieving more efficient parameter estimates (Parresol, 2001).

The parameters to estimate the fresh and air dried biomass were determined, since this information may be useful in some circumstances. For example, in case of transport of biomass under these conditions, or if estimates of biomass, exposed to outdoor conditions, are required in studies where biomass will be used for energy purposes. However, the MC(%) of fresh biomass has large fluctuations between different trees, even from the same species. On the other hand, the air dried biomass will lose its free water depending on the climate conditions in each particular region. By the exposed the developed equations for predicting the fresh and air dried biomass should be applied only to estimate maritime pine biomass under the same conditions of the data used in this research.

Table 3.9 - Parameter estimates and standard errors of the nonlinear unweighted models and of the NSUR system for fresh maritime pine biomass.

		NLIN unweighted		NSUR	
Tree component	**Parameter**	**Estimate**	**Std Err**	**Estimate**	**Std Err**
	β_{10}	-1.8537	0.2041	-2.00744	0.094
Wood	β_{11}	2.0310	0.0731	2.08258	0.045
	β_{12}	0.0499	0.0039	0.04846	0.004
Bark	B_{20}	-1.8537	1.4165	8.75499	1.462
	B_{21}	2.0310	33.92	149.828	32.222
	B_{31}	0.0499	0.1437	1.96420	0.132
Top	B_{32}	16.4046	1.4315	16.20735	1.290
	B_{33}	-5.1615	1.5854	-5.14422	1.410
	B_{41}	0.0561	0.0309	0.17042	0.078
Branches	B_{42}	2.4181	0.2194	2.64723	0.176
	B_{43}	-0.3967	0.2655	-1.02947	0.279
	B_{51}	0.2622	0.1216	0.28747	0.1096
Needles	B_{52}	1.8953	0.1811	2.17987	0.1614
	B_{53}	-0.4091	0.2423	-0.77437	0.2436

Note: parameters estimates from equations presented in Eq.11

Table 3.10 - Parameter estimates and standard errors of the nonlinear unweighted models and of the NSUR system for air dried maritime pine biomass.

		NLIN unweighted		NSUR	
Tree component	**Parameter**	**Estimate**	**Std Err**	**Estimate**	**Std Err**
	β_{10}	-2.4509	0.2030	-2.34783	0.088
Wood	β_{11}	2.0702	0.0724	2.01303	0.043
	β_{12}	0.0470	0.0038	0.05166	0.003
Bark	B_{20}	10.6646	1.5898	10.32865	1.512
	B_{21}	150.50	38.06	158.990	34.267
	B_{31}	0.9519	0.0707	1.03447	0.067
Top	B_{32}	16.6817	1.4095	16.91328	1.254
	B_{33}	-4.6459	1.5403	-5.91660	1.385
	B_{41}	0.0188	0.0105	0.06470	0.028
Branches	B_{42}	2.4785	0.2271	2.50346	0.161
	B_{43}	-0.2648	0.2711	-0.69424	0.260
	B_{51}	0.1074	0.0500	0.10970	0.043
Needles	B_{52}	1.8204	0.1826	2.02956	0.164
	B_{53}	-0.2668	0.2460	-0.52216	0.249

Note: parameters estimates from equations presented in Eq.11

Table 3.11 - Parameter estimates and standard errors of the nonlinear unweighted models and of the NSUR system for oven dried maritime pine biomass.

		NLIN unweighted		NSUR	
Tree component	**Parameter**	**Estimate**	**Std Err**	**Estimate**	**Std Err**
	β_{10}	-2.4421	0.2230	-2.51510	0.107
Wood	β_{11}	2.0267	0.0798	2.02707	0.054
	β_{12}	0.0475	0.0043	0.05050	0.004
Bark	B_{20}	12.2353	1.8239	11.07610	1.666
	B_{21}	172.70	43.67	196.9906	37.787
	B_{31}	0.6688	0.0497	0.75410	0.050
Top	B_{32}	16.6818	1.4095	16.81587	1.262
	B_{33}	-4.6460	1.5403	-6.46652	1.417
	B_{41}	0.0083	0.0048	0.09558	0.024
Branches	B_{42}	2.5568	0.2348	2.65915	0.137
	B_{43}	-0.1968	0.2765	-1.11584	0.180
	B_{51}	0.0919	0.0431	0.12551	0.035
Needles	B_{52}	1.8029	0.1842	2.15321	0.154
	B_{53}	-0.2334	0.2487	-0.74649	0.210

Note: parameters estimates from equations presented in Eq.11

3.3.4 NSUR System evaluation

The statistics of the fitted additive nonlinear simultaneous equations system (NSUR system) to predict the fresh, air and oven dried biomass tree components of maritime pine are presented in Table 3.12. Figure 3.8 shows the scatterplots of biomass measured in the field versus the predicted biomass by NSUR system, for fresh and air and oven dried weights. As depicted in the figure the equations system fitted well the maritime pine biomass data components. The model efficiency of tops, branches and needles models were lower compared with the other biomass tree components (Table 3.12), due to the larger variability of the crowns biomass components (top, branches and needles) from tree to tree comparing with the wood stem and bark stem biomass. Even so, the achieved models revealed a good performance. The efficiencies of equation for estimating fresh biomass of tops, branches and leaves were R^2= 0.7036; 0.8129 and 0.8097, respectively; for air dried biomass R^2= 0.7196; 0.8241 and 0.8148, respectively; and for oven dried biomass R^2= 0.7132; 0.7883 and 0.8039, respectively. The overall model efficiency for the AGB estimation was R^2 = 0.986, 0.988 and 0.986, respectively.

Table 3.12 - Statistics of the fitted additive nonlinear simultaneous equations system.

Tree component	**Mean**	**MAE**	**MSE**	**RMSE**	**RMSE (%)**	$\mathbf{R^2}$	$\mathbf{R^2_{aj}}$
Fresh weight							
Wood	452.21	38.10	3634.50	60.29	13.3	0.9884	0.9884
Bark	53.82	8.50	167.30	12.93	24.0	0.9451	0.9451
Top	3.20	0.57	0.466	0.683	21.8	0.7036	0.7016
Branches	65.47	19.59	869.70	29.49	44.9	0.8129	0.8117
Needles	45.41	12.01	282.40	16.80	37.1	0.8097	0.8084
AGB	620.11	53.83	7135.40	84.47	13.6	0.9868	0.9856
Air dried weight							
Wood	268.64	23.89	1269.80	35.63	13.2	0.9885	0.9884
Bark	47.77	7.56	132.30	11.50	24.0	0.9453	0.9453
Top	1.66	0.28	0.129	0.359	22.0	0.7196	0.7177
Branches	40.96	12.12	344.50	18.56	45.2	0.8241	0.8229
Needles	21.75	6.11	64.46	8.03	36.9	0.8148	0.8135
AGB	380.78	31.39	2463.30	49.63	13.0	0.9880	0.9869
Oven dried weight							
Wood	232.97	21.73	1178.70	34.33	14.7	0.9857	0.9856
Bark	41.81	6.60	101.10	10.05	24.0	0.9449	0.9449
Top	1.16	0.20	0.065	0.255	22.3	0.7132	0.7113
Branches	29.53	8.96	231.20	15.21	51.1	0.7883	0.7869
Needles	19.62	5.50	54.31	7.37	45.3	0.8039	0.8026
AGB	325.10	26.91	1969.50	44.38	13.7	0.9868	0.9857

Note: values of calculated statistics (Mean, MAE, MSE and RMSE) are in kg $tree^{-1}$.

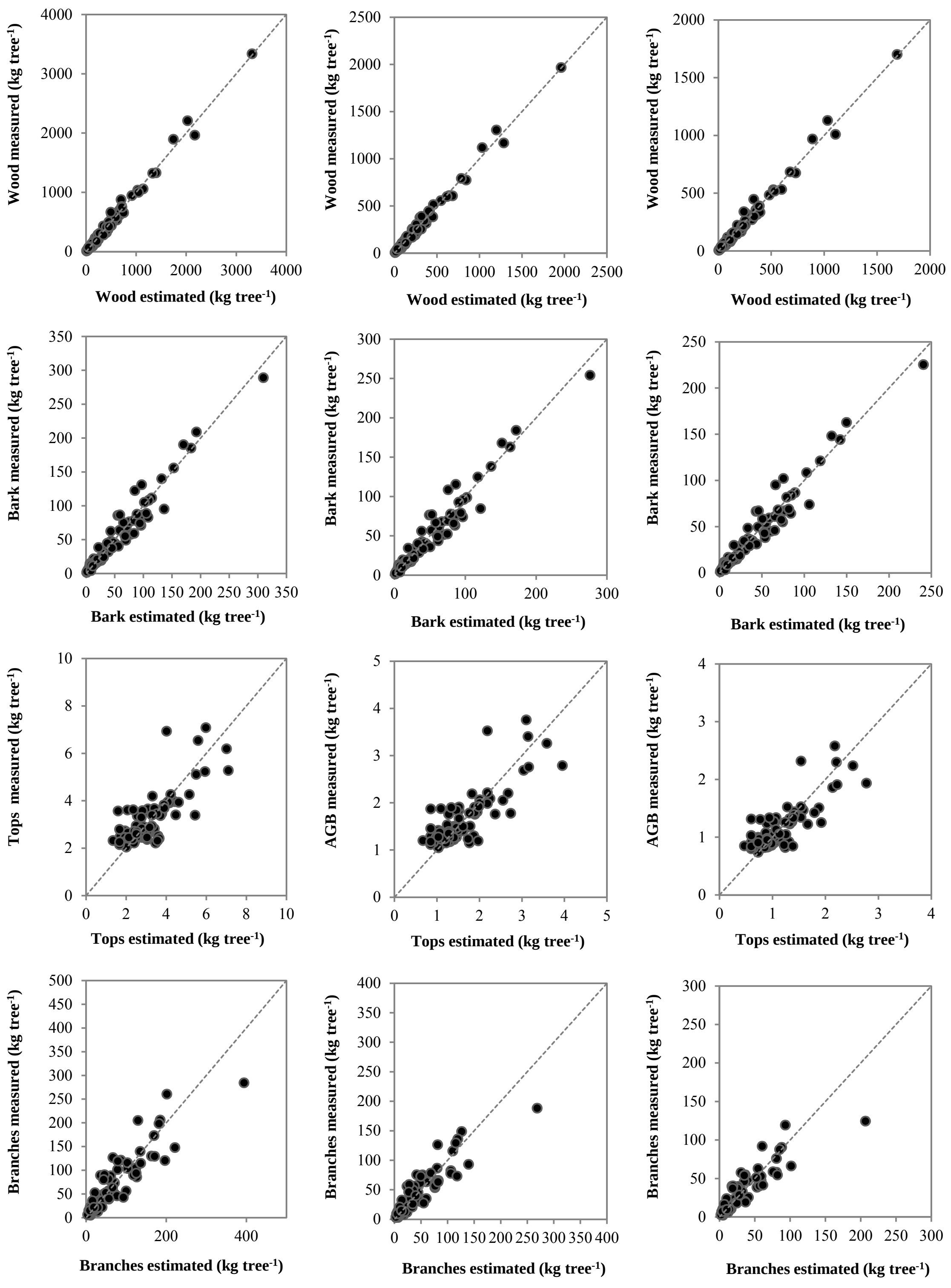

(A) (B) (C)

Figure 3.8 - Scatterplots of the measured versus predicted maritime pine biomass components fitted by the NSUR system.

(A) fresh biomass, (B) air dried biomass, (C) oven dried biomass

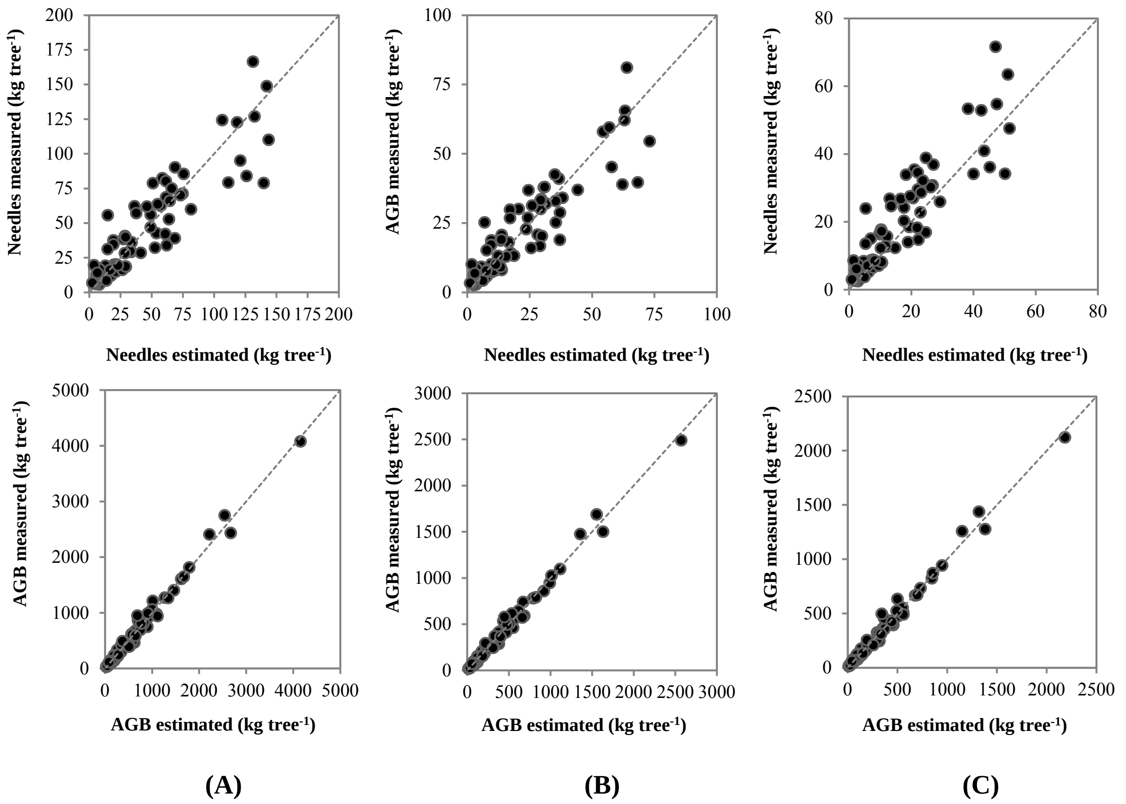

Figure 3.8 - Scatterplots of the measured versus predicted maritime pine biomass components fitted by the NSUR system (cont.).

(A) fresh biomass, (B) air dried biomass, (C) oven dried biomass

The NSUR system equations was additionally validated using the dataset constituted by the 85 trees only weighted in loco during the field work. The derived equations were applied to this dataset and the biomass of wood stem, bark stem, crown stem (sum of branches, tops and needles) and total AGB biomass was calculated. The scatterplots (Figure 3.9) showing the relation of the measured versus the estimated biomass of maritime pine components reveals the good performance of the adjusted models.

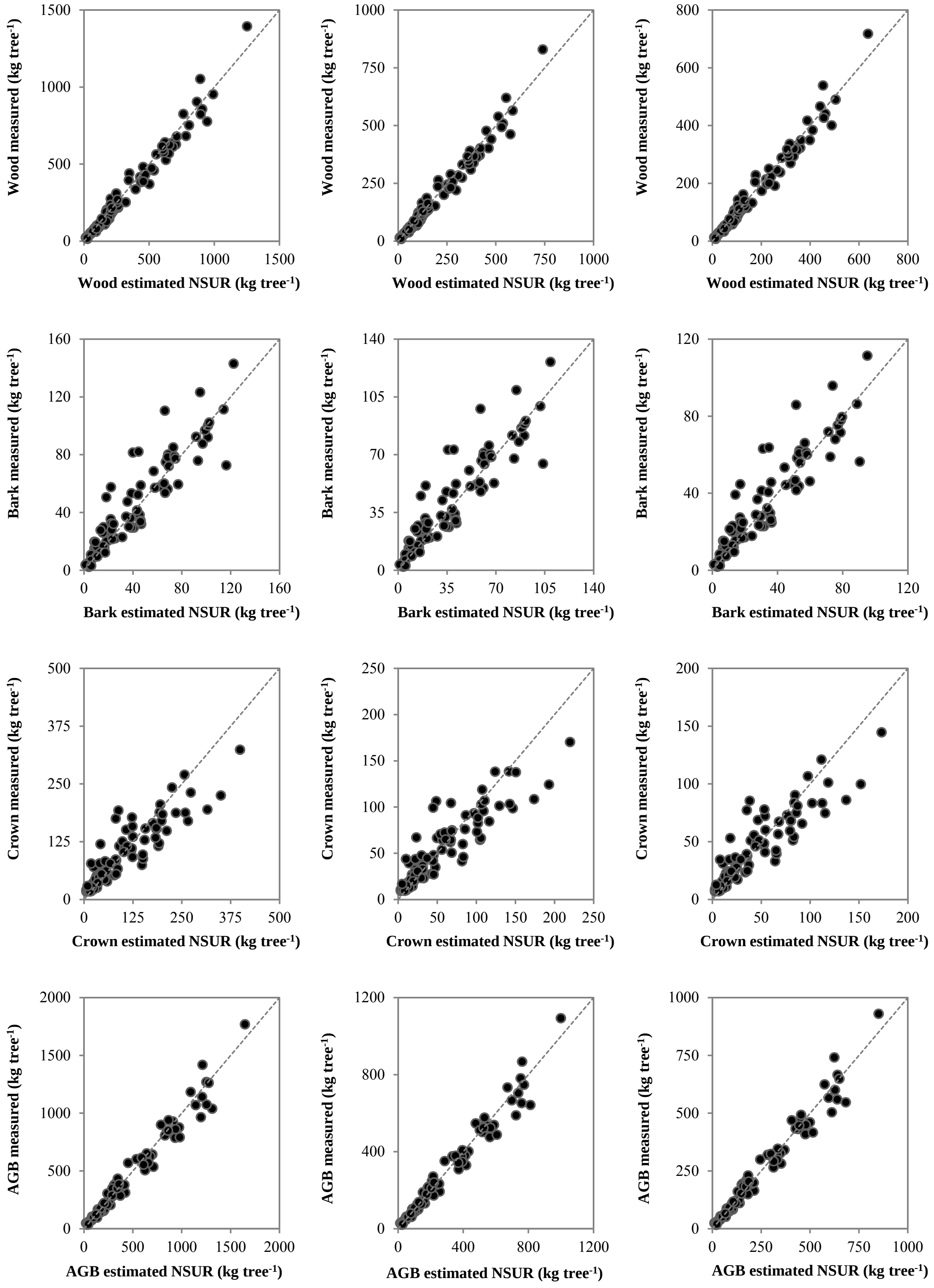

(A) **(B)** **(C)**

Figure 3.9 - Scatterplots of the measured versus predicted maritime pine biomass components fitted by the NSUR system in the validation dataset.

(A) fresh biomass (B) air dried biomass and (C) oven dried biomass.

3.3.5 Comparison with other biomass equations for maritime pine

The developed NSUR models were compared with equations adjusted by other authors for maritime pine in Portugal. The NSUR models fitted for the oven dried biomass were compared with equations, which were adjusted using seemingly unrelated regressions procedures, from Páscoa et al. (2004), from (DNGF, 2010) and from Faias (2009) (Table 3.13 and Figures 3.10 and 3.11). The NSUR models fitted for the fresh biomass weight were compared with a set of equations developed by Barreto (2005) using the Gompertz function (Gompertz, 1825) to indirectly estimate the fresh biomass components of maritime pine to a given age (Table 3.13 and Figure 3.12). Additional comparisons were made with equations from Arthur D. Little International Inc. (1985), Silva et al. (1991), and Lopes (2005) fitted by OLS regression analysis, for the fresh and dry crowns' biomass (Table 3.13 and Figure 3.13). As can be seen in Table 3.13 and Figures 3.10 to 3.12, the biomass equations show differences in the predictions, which are more evident for the branches and needles tree components. These discrepancies can be explained by the specific characteristics of the trees and stands where the data, used in the model adjustments, were collected, which have distinct growth conditions and silvicultural management. In fact, as stated by Barreto (2004) each tree and stand, even of the same species, is the result of a combination unique of genetic, ecological and environmental factors, which makes it possible to establish as many models as the multiplicity of possible combinations. Hence, following this assumption, the generalization of equations developed to a particular tree dataset could be misleading. Beyond this point, the sampling process, to calculate the weight of biomass components, and the determination of moister content, to obtain the biomass dry weight, can also contribute to the discrepancies in the equations. These reasons seem to be more evident in the equation from Páscoa et al. (2004), since it makes the worst estimates for the present data (e.g. branches and needles). Analysing the results from equations developed by Barreto (2005) to the fresh biomass components (Table 3.13 and Figure 3.12), it can be seen that for branches and needles predictions the discrepancies are evident. However, the estimates for the total aboveground biomass reveal a good performance confirming the theory explained in his work. The comparisons with estimates from Arthur D. Little International Inc. (1985), Silva et al. (1991) and Lopes (2005) equations, adjusted by OLS regression analysis, shown a good performance of the fitted models (Figure 3.13 and Table 3.13).

Table 3.13 - Statistics of the estimates obtained by NSUR System and equations from other authors.

Tree component	**Mean**	**MAE**	**MSE**	**RMSE**	**RMSE (%)**
(Páscoa et al., 2004)					
Wood	544.4	310.1	152291.2	390.2	166.5
Bark	33.6	12.5	425.2	20.6	49.3
Top	12.1	10.9	285.2	16.9	1475.6
Branches	68.8	39.8	3743.6	61.2	205.7
Needles	35.9	22.8	2602.8	51.0	313.3
AGB	323.4	371.4	234714.5	484.5	149.8
(Faias, 2009)					
Wood	182.6	57.7	12595.7	112.2	47.9
Bark	36.6	8.7	157.1	12.5	30.0
Branches	53.7	25.4	1994.2	44.7	150.1
Needles	19.1	5.4	54.7	7.4	45.4
AGB	291.9	44.2	6393.7	80.0	24.7
(DNGF, 2010)					
Wood	307.2	73.0	12862.1	113.4	48.4
Bark	47.9	9.1	188.8	13.7	32.8
Branches	51.1	23.7	1878.9	43.3	145.7
Needles	14.6	4.2	38.3	6.2	38.0
AGB	420.8	98.4	25803.2	160.6	49.7
(Barreto, 2005)					
Wood	406.0	84.8	15424.4	124.2	27.4
Bark	69.8	22.8	2131.0	46.2	85.7
Branches	74.4	24.9	1114.9	33.4	50.9
Needles	27.7	18.7	731.9	27.1	59.7
AGB	550.2	105.1	21540.8	146.8	23.7
(Arthur D. Little International Inc., 1985)					
Crown (fresh)	108.0	28.8	1656.9	40.7	35.7
Crown (dry)	45.5	12.6	343.6	18.5	39.3
(Silva et al., 1991)					
Crown (fresh)	98.8	32.4	2319.0	48.2	42.2
Crown (dry)	41.9	13.6	453.8	21.3	45.2
(Lopes, 2005)					
Crown (dry)	61.3	18.4	725.5	26.9	57.1
NSUR (fresh)					
Wood	452.2	38.1	3634.5	60.3	13.3
Bark	53.8	8.5	167.3	12.9	24.0
Top	3.2	0.6	0.5	0.7	21.8
Branches	65.5	19.6	869.7	29.5	44.9
Needles	45.4	12.0	282.4	16.8	37.1
AGB	620.1	53.8	7135.4	84.5	13.6
NSUR (Oven dry)					
Wood	233.0	21.7	1178.7	34.3	14.7
Bark	41.8	6.6	101.1	10.1	24.0
Top	1.2	0.2	0.1	0.3	22.3
Branches	29.5	9.0	231.2	15.2	51.1
Needles	19.6	5.5	54.3	7.4	45.3
AGB	325.1	26.9	1969.5	44.4	13.7

Note: values of calculated statistics (Mean, MAE, MSE and RMSE) are in kg $tree^{-1}$.

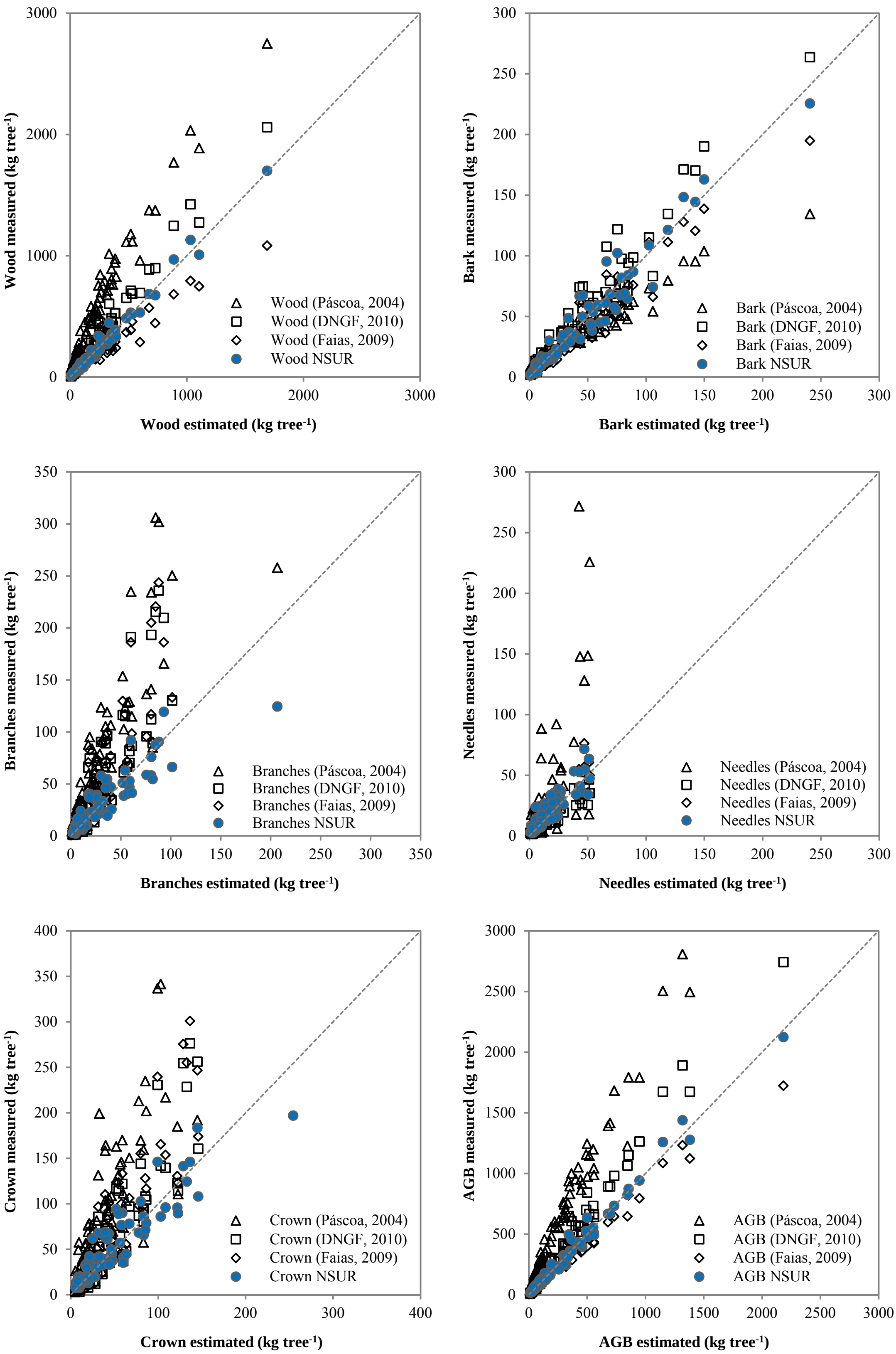

Figure 3.10 - Scatterplots comparing the maritime pine biomass estimates from NSUR equation system and from equations adjusted by other authors.

Note: The Crown and AGB biomass estimates are the sum of the biomass tree components.

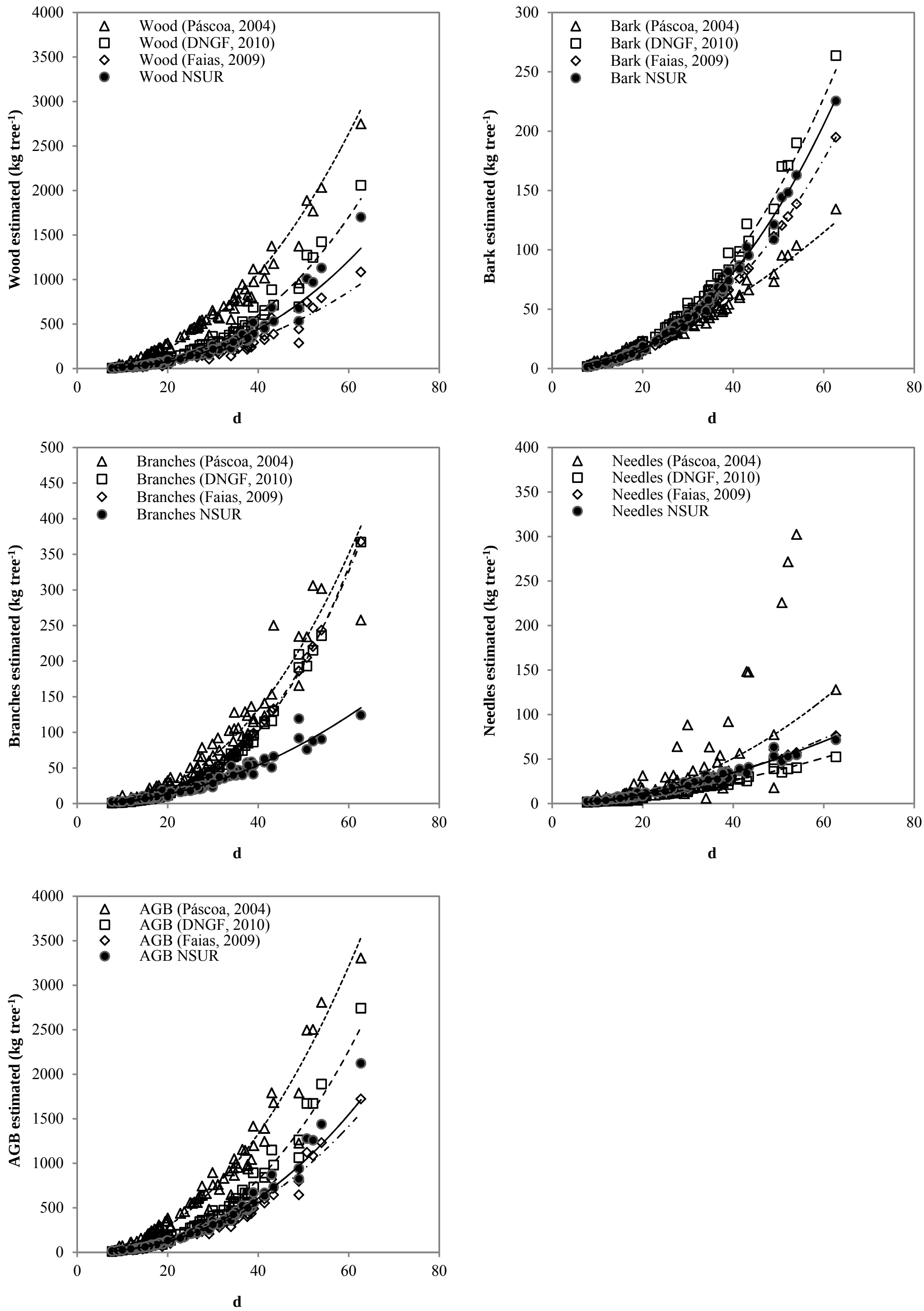

Figure 3.11 - Relationships between the maritime pine biomass estimates by the NSUR equations system and the diameter at breast height.

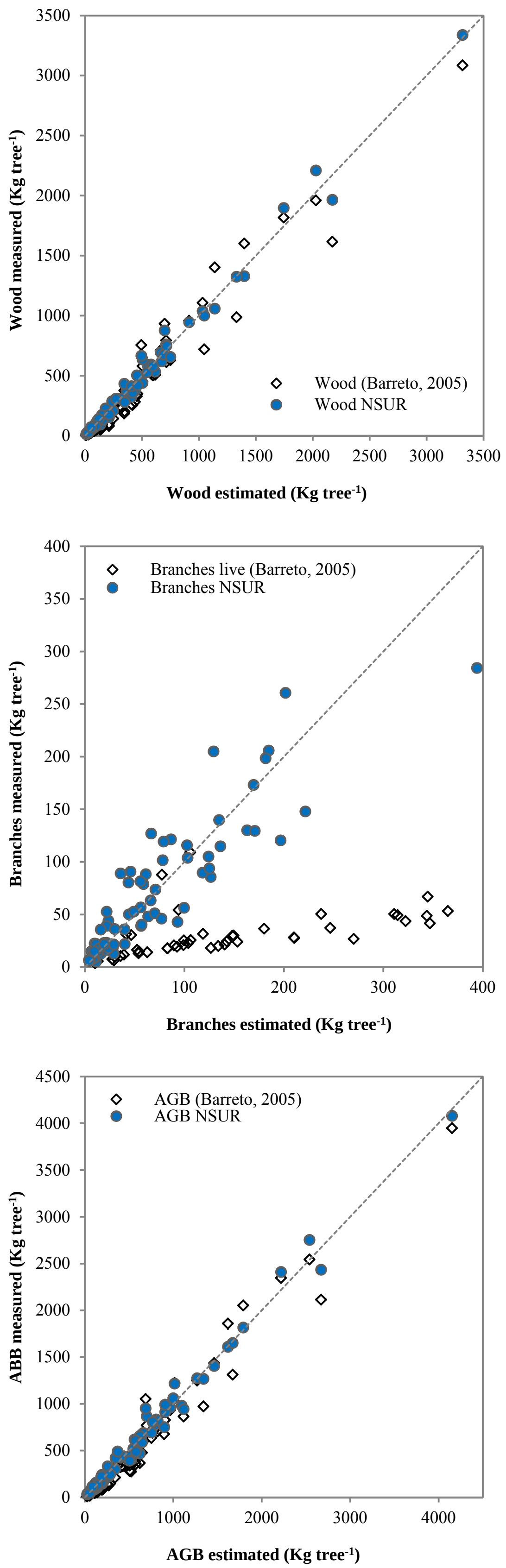

Figure 3.12 - Scatterplots comparing the maritime pine fresh biomass estimates from NSUR system and from equations adjusted by Barreto (2005).

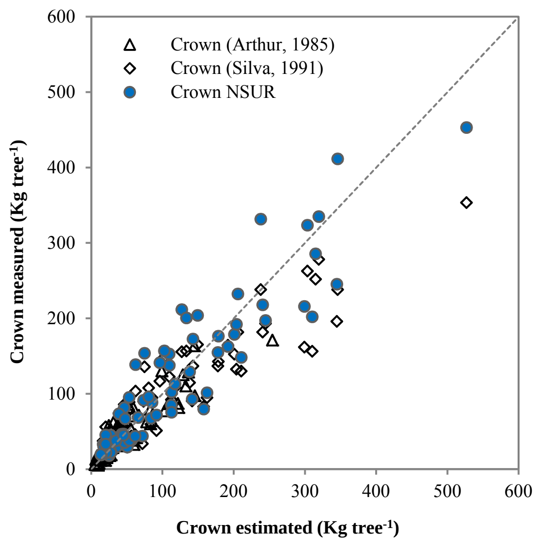

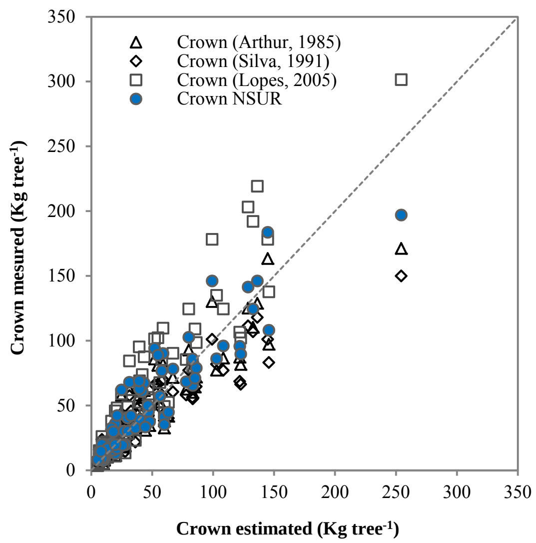

Figure 3.13 - Scatterplots comparing the maritime pine crowns biomass estimates from NSUR equation system and from equations adjusted by OLS from other authors.

(a) fresh weight; (b) oven dry weight.

Note: The NSUR Crown biomass estimates are the sum of the biomass tree components (top, branches and needles). The equations adjusted by OLS regression analysis are from Arthur D. Little International Inc. (1985), Silva et al. (1991) and Lopes (2005).

3.4 Conclusion

New equations to estimate components of tree's biomass were developed for maritime pine in North-Center region of Portugal. The nonlinear simultaneous system fitted by nonlinear seemingly unrelated regression method guarantees the property of additivity among the components of tree biomass and total tree biomass. The equations derived by NSUR method predict the tree biomass components more efficiently then the nonlinear models developed independently to each component of tree biomass. As demonstrated by (Parresol, 1999) the gain in the accuracies has an important implication in forest inventory estimates because less variations are obtained in reliability analysis.

The comparisons between equations derived for maritime pine lead to state that the generalization of equations derived to a specific site should be made prudently. The indiscriminate application in forest inventories of biomass equations, fitted for a specific site, can generate completely erroneous estimates, particularly in estimating the individual components of the tree. Hence, the set of equations derived in this study are suitable to estimate the aboveground biomass components in maritime stands with the same characteristics. Their use generalized to other regions or to a national scale can lead to a consistent inaccuracy of the estimates.

References

Akaike, H., 1974. A new look at the statistical model identification. Automatic Control, IEEE Transactions on 19, 716-723.

Alegria, C., 2011. Modelling merchantable volumes for uneven aged maritime pine (*Pinus pinaster* Aiton) stands established by natural regeneration in the central Portugal. Annals of Forest Research 54(2), 197-214.

Alegria, C., Tomé, M., 2011. A set of models for individual tree merchantable volume prediction for *Pinus pinaster* Aiton in central inland of Portugal. European Journal of Forest Research 130, 871-879.

Arthur D. Little International Inc., 1985. Resíduos florestais para produção de energia em Portugal, Tecninvest, SARL ed.

Avery, T.E., Burkhart, H.E., 1983. Forest measurements. McGraw-Hill, pp. 331.

Balboa-Murias, M.Á., Rodríguez-Soalleiro, R., Merino, A., Álvarez-González, J.G., 2006. Temporal variations and distribution of carbon stocks in aboveground biomass of radiata pine and maritime pine pure stands under different silvicultural alternatives. Forest Ecology and Management 237, 29-38.

Barreto, L.S., 2004. A Inteligibilidade da Equação do Volume da Árvore. Research Paper SB-04/04. Departamento de Engenharia Florestal, Instituto Superior de Agronomia, Universidade Técnica de Lisboa, Lisboa, p. 17.

Barreto, L.S., 2005. Pinhais Bravos - Ecologia e Gestão. Departamento de Engenharia Florestal, Instituto Superior de Agronomia, Universidade Técnica de Lisboa, Lisboa, p. 162.

Bartels, R., 2006. Seemingly Unrelated Regressions, Encyclopedia of Environmetrics. John Wiley & Sons, Ltd.

Beal, D.J., 2005. SAS Code to Select the Best Multiple Linear Regression Model for Multivariate Data Using Information Criteria, Science Applications International Corporation. Available online at: *http://analytics.ncsu.edu/sesug/2005/ SA01_05.PDF*, (Accessed January 2012).

Bi, H., Turner, J., Lambert, M.J., 2004. Additive biomass equations for native eucalypt forest trees of temperate Australia. Trees - Structure and Function 18, 467-479.

Bi, H., Long, Y., Turner, J., Lei, Y., Snowdon, P., Li, Y., Harper, R., Zerihun, A., Ximenes, F., 2010. Additive prediction of aboveground biomass for *Pinus* *radiata* (D. Don) plantations. Forest Ecology and Management 259, 2301-2314.

Burkhart, H.E., 1977. Cubic foot volume of loblolly pine to any merchantable top diameter. Southern Journal of Applied Forestry 1(2), 7-9.

Carvalho, J.P., Parresol, B.R., 2003. Additivity in tree biomass components of Pyrenean oak (Quercus pyrenaica Willd.). Forest Ecology and Management 179, 269-276.

CEN EN 14774-1:2009, Solid biofuels - Determination of moisture content – Oven dry method - Part 1: Total moisture - Reference method.

Chiyenda, S.S., Kozak, A., 1984. Additivity of component biomass regression equations when the underlying model is linear. Canadian Journal of Forest Research 14, 441-446.

Clutter, J.L., Fortson, J.C., Pienaar, L.V., Brister, G.H., Bailey, R.L., 1983. Timber management - a quantitative approach. John Wiley & Sons, New York, pp. 333.

Cohen, J., Cohen, P., West, S.G., Aiken, L.S., 2003. Applied Multiple Regression/Correlation Analysis for the Behavioral Sciences, Third ed. Lawrence Erlbaum Associates, Inc., Publishers, London.

Cunia, T., Briggs, R.D., 1984. Forcing additivity of biomass tables: some empirical results. Canadian Journal of Forest Research 14, 376-384.

Cunia, T., Briggs, R.D., 1985. Forcing additivity of biomass tables-use of the generalized least-square method. Canadian Journal of Forest Research 15, 23-28.

Curtis, R.O., 1967. Height-Diameter and Height-Diameter-Age Equations For Second-Growth Douglas-Fir. Forest Science 13, 365-375.

DNGF, 2010. 5º Inventário Florestal Nacional. Portugal Continental. 2005-2006. Relatório Final, Direcção Nacional de Gestão Florestal (DNGF). Autoridade Florestal Nacional. Ministério da Agricultura do Desenvolvimento Rural e das Pescas, Lisboa.

Draudt, 1860. Die Ermittlung der Holzmassen. Giessen.

Faias, S., Analysis of Biomass Expansion Factors for the most important tree species in Portugal, Instituto Superior de Agronomia. Universidade Técnica de Lisboa, MSc, Lisboa, 2009, pp. 48.

Freire, J., Tomé, M., Tavares, M., 2003. Equação de Volume Local para a *Pinus pinaster* Aiton na Serra da Lousã. Silva Lusitana 11(2), 207-215.

Gehrhardt, E., 1909. Die Bestandeswachstumsgesetze und ihre Anwendung zur Aufstellung von Ertragstafeln. AFJZ, pp. 117-128.

Goicoa, T., Militino, A., Ugarte, M., 2011. Modelling aboveground tree biomass while achieving the additivity property. Environmental and Ecological Statistics 18, 367-384.

Gompertz, B., 1825. On the Nature of the Function Expressive of the Law of Human Mortality, and on a New Mode of Determining the Value of Life Contingencies. Philosophical Transactions of the Royal Society of London 115, 513-585.

Hese, S., Lucht, W., Schmullius, C., Barnsley, M., Dubayah, R., Knorr, D., Neumann, K., Riedel, T., Schröter, K., 2005. Global biomass mapping for an improved understanding of the CO_2 balance--the Earth observation mission Carbon-3D. Remote Sensing of Environment 94, 94-104.

Honer, T.G., 1967. Standard volume tables and merchantable conversion factors for the commercial tree species of Central and Eastern Canada. Information Report FMR-X-5, Forest Management Research and Service Institute, Ottawa, Ontario, p. 21.

Husch, B., Beers, T.W., Kershaw, J.A., 2003. Forest mensuration, 4th ed. John Wiley & Sons, New Jersey, pp. 443.

Jenkins, J.C., Chojnacky, D.C., Heath, L.S., Birdsey, R.A., 2004. Comprehensive Database of Diameter-based Biomass Regressions for North American Tree Species. GTR-NE-319, USDA Forest Service, Northeastern Research Station. Available online at: *http://www.fs.fed.us/ne/global/pubs/books/dia_biomass/index*, (Accessed May 2012).

Kopezky, R., 1899. Neue Verfahren der Bestandsmassen-Ermittlung Centralblatt für das gesamte Forstwesen. 25, 471-495.

Kozak, A., 1970. Methods for ensuring additivity of biomass components by regression analysis. The Forestry Chronicle 46, 402-404.

Laar, A.V., Akça, A., 2007. Forest mensuration. Springer.

Lambert, M.C., Ung, C.H., Raulier, F., 2005. Canadian national tree aboveground biomass equations. Canadian Journal of Forest Research 35, 1996-2018.

Loetsch, F., Haller, K.E., Zöhrer, F., 1973. Forest inventory: Inventory data collected by terrestrial measurements. BLV Verlagsgesellschaft, Munchen, pp. 469

Lopes, D., Estimating Net Primary Production in *Eucalyptus globulus* and *Pinus pinaster* Ecosystems in Portugal, Kingston University, PhD Thesis, England, 2005.

Marklund, L.G., 1987. Biomass functions for Norway spruce (Picea abies (l.) Karst.) in Sweden. Sveriges lantbruksuniversitet, Institutionen för skogstaxer-ing, Rapport 43., pp. 127.

Marklund, L.G., 1988. Biomass functions for pine, spruce and birch in Sweden. Report 45, Department of Forest Survey, The Swedish University of Agricultural Sciences. [in Swedish with an English summary] pp. 73.

Merino, A., Balboa, M.A., Rodríguez Soalleiro, R., González, J.G.Á., 2005. Nutrient exports under different harvesting regimes in fast-growing forest plantations in southern Europe. Forest Ecology and Management 207, 325-339.

Metla Project 3306, Database of treewise volume- and biomass equations for common European tree species, Available online at: *http://www.metla.fi/ hanke/ 3306/tietokanta.htm*, (Accessed May 2012).

Meyer, H.A., 1953. Forest mensuration. Pennsylvania Valley Publishers, Inc., pp. 357.

Moon, H.R., Perron, B., 2008. seemingly unrelated regressions, in: Durlauf, S.N., Blume, L.E. (eds.), The New Palgrave Dictionary of Economics. Palgrave Macmillan, Basingstoke.

Motulsky, H., Christopoulos, A., 2003. Fitting models to biological data using linear e nonlinear regression: a pratical guide to curve fitting. GraphPad Software Inc., San Diego CA, pp. 351.

Näslund, M., 1947. Funktioner och tabeller för kubering av stående träd. Tall, gran och björk i södra Sverige samt i hela landet. (Functions and tables for computing of the cubic volume of standing trees. Pine. spruce and birch In southern Sweden. and in the whole of Sweden). (In Swedish with English summary). Meddelanden från Statens Skogsforskningsinstitut (National Forest Research Institute), Stockholm, Sweden, p. 81.

Ogaya, N., Kubierungsformeln und Bestandesmassenformeln, Univ. Freiburg i. Br., Thesis, 1968, pp. 85.

Oliveira, A.C., 1985. Tabela de produção geral para o pinheiro bravo das regiões montanas e submontanas. INIC.DGF, Lisboa, pp. 38.

Ostrom, C.W., 1990. Time series analysis: regression techniques. Sage Publications.

Parresol, B.R., 1999. Assessing tree and stand biomass: a review with examples and critical comparisons. J For Sci 45, 573-593.

Parresol, B.R., 2001. Additivity of nonlinear biomass equations. Canadian Journal of Forest Research 31, 865-878.

Páscoa, F., Estrutura, Crescimento e Produção em Povoamentos de Pinheiro Bravo. Um Modelo de Simulação. Tese de Doutoramento, ISA/UTL, Lisboa 1987, pp. 241.

Páscoa, F., Martins, F., González, R.S., João, C., 2004. Estabelecimento simultâneo de equações de biomassa para o pinheiro-bravo. II simposio Iberoamericano sobre Gestión y Economía Forestal, Barcelona, pp. 1-18. 18-20 Septiembre.

Porté, A., Trichet, P., Bert, D., Loustau, D., 2002. Allometric relationships for branch and tree woody biomass of Maritime pine (*Pinus pinaster* Aït.). Forest Ecology and Management 158, 71-83.

Prodan, M., 1965. Holzmesslehre. J. D. Sauerlaender´s Verlag, Frankfurt, pp. 644.

Prodan, M., Peters, R., Cox, F., Real, P., 1997. Mensura forestal. GTZ, FmbH: Instituto Interamericano de Cooperación para la Agricultura (IICA), San José, Costa Rica, pp. 586.

Rawlings, J.O., Pantula, S.G., Dickey, D.A., 1998. Applied Regression Analysis: A Research Tool, Second ed. Springer-Verlag New York, Inc.

Reed, D.D., Green, E.J., 1985. A method of forcing additivity of biomass tables when using nonlinear models. Canadian Journal of Forest Research 15, 1184-1187.

Ritz, C., Streibig, J.C., 2008. Nonlinear regression with R. Springer, pp. 144.

Ruiz-Peinado, R., Rio, M.d., Montero, G., 2011. New models for estimating the carbon sink capacity of Spanish softwood species. Forest Systems 2011 20, 176-188.

SAS Institute Inc., 2004. SAS/ETS ® 9.1 User's Guide. Volumes 1 and 2. SAS Institute Inc. Cary, New York.

Schabenberger, O., Pierce, F.J., 2002. Contemporary statistical models for the plant and soil sciences. CRC PRESS, Boca Raton.

Schumacher, F.X., Hall, F., 1933. Logarithmic expression of timber-tree volume. Journal of Agriculture Research 47(9), 719-734.

Shaiek, O., Loustau, D., Trichet, P., Meredieu, C., Bachtobji, B., Garchi, S., El Aouni, M., 2011. Generalized biomass equations for the main aboveground biomass components of maritime pine across contrasting environments. Annals of Forest Science 68, 443-452.

Silva, R., Tavares, M., Páscoa, F., 1991. Residual Biomass of Forest Stands. *Pinus pinaster* Ait. and *Eucaliptus globulus* Labill. 10th World Forestry Congress, 5, Food and Agriculture Organization of the United Nations, Paris.

Sit, V., Poulin-Costello, M., 1994. Catalogue of curves for curve fitting. Biometics Information. Handbook nº 4. Forest Science Research Branch. Ministry of Forests, Province of British Columbia, pp. 116.

Spurr, S.H., 1952. Forest inventory. Ronald Press, New York, pp. 476.

Srivastava, V.K., Giles, D.A., 1987. Seemingly unrelated regression equations models: estimation and inference, Dekker, New York.

Stoate, T.N., 1945. The Use of a Volume Equation in Pine Stands. Australian Forestry 9, 48-52.

Takata, K., 1958. Construction of universal diameter-height-curves. Journal of Japanese Forest Society 40: 1, 1-6.

Tsoumis, G.T., 1991. Science and Technology of wood. Structures, Properties, Utilization. Van Nostrand Reinhold, New York.

Viana, H., Dias, S., Marques, C., Cruz, M., Lopes, D., Aranha, J., 2009. Estabelecimento de modelos alométricos para predição da biomassa aérea da *Pinus Pinaster*. Actas do 6º Congresso Florestal Nacional. Ponta Delgada, Açores. 6-9 Outubro, pp. 771-775.

Viana, H., Cohen, W.B., Lopes, D., Aranha, J., 2010. Assessment of forest biomass for use as energy. GIS-based analysis of geographical availability and locations of wood-fired power plants in Portugal. Applied Energy 87, 2551-2560.

Viana, H., Aranha, J., Lopes, D., Cohen, W.B., 2012. Estimation of crown biomass of *Pinus pinaster* stands and shrubland above-ground biomass using forest inventory data, remotely sensed imagery and spatial prediction models. Ecological Modelling 226, 22-35.

White, H., 1980. A heteroskedastic-consistent covariance matrix estimator and a direct test of heteroskedasticity. Econometrica 48, 817-838.

Wilson, F.G., 1946. Numerical Expression of Stocking in Terms of Height. Journal of Forestry 44, 758-761.

Zellner, A., 1962. An Efficient Method of Estimating Seemingly Unrelated Regression Equations and Tests of Aggregation Bias. Journal of the American Statistical Association 57, 348–368.

Zianis, D., Muukkonen, P., Mäkipää, R., Mencuccini, M., 2005. Biomass and stem volume equations for tree species in Europe, Silva Fennica Monographs 4. Finnish Society of Forest Science, p. 63.

4

Additive nonlinear biomass equations for *Eucalyptus globulus* Labill. in Portugal

---

Data from this chapter contributed for the following publications:

[Annex D] Viana, H., Dias, S., Marques, C., Cruz, M., Lopes, D., Aranha, J., 2009. Estabelecimento de modelos alométricos para predição da biomassa aérea de *Eucalyptus globulus*. Actas do 6º Congresso Florestal Nacional,. Ponta Delgada, Açores. 6-9 Outubro, pp. 765-770.

[Annex B.1] Viana, H., Cohen, W.B., Lopes, D., Aranha, J., 2010. Assessment of forest biomass for use as energy. GIS-based analysis of geographical availability and locations of wood-fired power plants in Portugal. Applied Energy 87, 2551-2560.

[Annex B.2] Viana H.; Aranha J.; Lopes D., 2011, Dedicated Biomass Plants for Combined Heat & Power (CHP). The Portuguese National Strategy. 19th European Biomass Conference and Exhibition. ETA-Florence Renewable Energies. Berlin, Germany. June 6-10.

Abstract

A system of additive nonlinear simultaneous equation system was derived to estimate the aboveground biomass components of planted blue-gum eucalyptus (*Eucalyptus globulus* Labill.) species. Data from 104 trees was collected within 11 eucalyptus stands in the North-Center region of Portugal. Using the destructive approach the weight of entire aboveground tree biomass was determined in the field. In order to obtain the biomass weight per tree fraction (stem wood, stem bark, tops, branches and leaves) a subsample of 51 trees was selected and the fresh biomass collected, separated and weighted. The moister content was determined and the biomass after air dry and oven dry was calculated for each tree component. The fresh and dried biomass weights were used to derive an additive nonlinear simultaneous equation system using the nonlinear seemingly unrelated regression (NSUR) method as a function of diameter at breast height and tree height. The achieved statistics showed a good fit of the models and the additivity property among components and total tree biomass was satisfied. In addition, the remaining 53 trees, weighted in the field work, were used to validate the crown and total aboveground biomass estimated by the derived equations system. The comparison with models from other authors, to estimate the aboveground biomass components of eucalyptus, showed discrepancies in some tree biomass components predictions. This indicates that biomass equations derived to a specific site should not be generalized to other regions without having special attention to the stand characteristics where those equations were developed.

Keywords: Additive equations, aboveground biomass, nonlinear seemingly unrelated regression, *Eucalyptus globulus* Labill.

4.1 Introduction

Eucalyptus species (*Eucalyptus globulus* Labill.) are extensively managed in Portugal. Introduced in Portugal in 1852-1854 (Radich, 2007), nowadays is the second species, after *Pinus pinaster,* occupying around 739,000 hectares (23.3%) of the total Portuguese forest (approximately 3.4 million thousand hectares) (DNGF, 2010).

The high productivity of eucalyptus (e.g. 16 to 24 ton ha^{-1} yr^{-1} in Center-littoral of Portugal, (Fabião, 1986)), makes these species an essential feedstock for pulp industry. Additionally, being the Net Ecosystem Productivity of eucalyptus, the highest of European forests (e.g. 939 g C m^{-2} yr^{-1}, (Pereira, 2007)), makes these species of great interest when determining the CO_2 balance of ecosystems and quantify the contribution of forests in the global carbon cycle. On the other hand, the eucalyptus harvesting produces big amounts of forest residues, which has great importance for use as energy (Viana et al., 2010). Thus, the knowledge of the aboveground biomass (AGB), and the tree biomass components is essential for studying these subjects.

The most practical and expedite method to quantify the tree biomass weight is to apply specific allometric equations using dendrometric parameters as independent variables. Equations for predicting eucalyptus aboveground biomass in Portugal were previous presented by Arthur D. Little International Inc. (1985) and Silva et al. (1991) to estimate the crown biomass; and by Fabião (1986) to estimate stem, branches and leaves biomass components. Usually, the models fitted for each biomass component are derived separately and independent of the others equations, through least squares regression. Consequently, the lack of additivity among the tree's components equations is observed, while the desirable is that the sum of predictions for the biomass regression components equals the prediction for the total tree (Parresol, 1999). This approach, known as seemingly unrelated regression (SUR), or nonlinear seemingly unrelated regression (NSUR) if using nonlinear models, has been increasingly applied in recent years (Parresol, 1999, 2001; Carvalho and Parresol, 2003; Bi et al., 2004; Lambert et al., 2005; Bi et al., 2010; Goicoa et al., 2011). Equations using this approach to predict *Eucalyptus globulus* biomass components were developed by António et al. (2007) and from (DNGF, 2010). These models are global as they were adjusted with data from the whole country, so a local validation in North-Center region of Portugal is needed.

The purposes of this study were (1) to develop a system of nonlinear allometric equation for estimating the fresh and dry weight of aboveground biomass and biomass components (stem wood, stem bark, top, branches and leaves) of *Eucalyptus globulus* Labill. in the North-Center region of Portugal; and (2) compare and validate the previous fitted models with biomass equations derived by other authors.

4.2 Methods and data

4.2.1 Field data

The biomass data used to fit a nonlinear simultaneous equation system to estimate eucalyptus biomass tree components and total aboveground biomass was collected, during 2007, within 11 planted eucalyptus stands in the North-Center Portugal, extending from 39º 11' 53" N, 06º 14' 17' W to 42º 50' 50" N, 08º 19' 02" W (Figure 4.1).

Figure 4.1 - Location of the eucalyptus sample plots.

A circular temporary sample plot within a fixed-area of $500m^2$ was established, in each site, and the dendrometric parameters: diameter at breast height (d_{bh}), total height of the tree (h) and canopy height (hc), crown horizontal projection (Crp) were measured and the structural stand variables such as number of trees per hectare (N), dominant tree height class (h_{dom}), basal area (G), stand age (t), crown closure class (Cc) and site index (SI) calculated.

Through a destructive approach, a total of 104 trees (around 10 trees per stand, representing all the present class diameters) were felled, and tree bole diameters (d_h) over bark and heights (h_d) were measured directly on the stem with a caliper and a tape with 1 mm accuracy. By rigorous cubage, the merchantable volume (m^3) was obtained summing the bole sections volumes, evaluated with Smalian's formula (Meyer, 1953; Avery and Burkhart, 1983; Husch et al., 2003). The total volume (m^3) was achieved by adding the tip volume calculated as the volume of a cone. For the purpose of this work we considered as merchantable limit the top height up to the diameter of 5 cm. The bark thickness was also measured at the ends of each log, allowing calculates the volume of wood (under bark).

The entire biomass was then weighted in site for all the 104 trees. From each tree, all cutted branches and top, covered with leaves, were recovered and weighed directly in order to obtain the total crown's fresh weight. In order to achieve the weight of individual components of the crown (branches, leaves and top) a subsample of 51 trees (at least one tree per class diameter in each plot) was used. In the selected trees around 50% of crown biomass (including the top, branches and leaves) was randomly collected. Three discs of the stem, including wood and bark, were cut from the base, middle and top of each tree. All biomass samples were placed into hermetically closed containers to prevent moisture loss, labelled and sent to the laboratory for separation and weighting of the components, on the day of sample collection. The proportion of each component in the total fresh weight was obtained by the ratio of each component sample and the total fresh biomass sample weight.

The remaining 53 trees weighted in the field were used to evaluate the derived models, namely the ability for predicting the crown biomass, the stem biomass (stem wood and stem bark) and the total aboveground biomass. This validation procedure was used as a complement to the statistics obtained in the fitting stage and used to validate the derived equations (section 4.2.2).

In order to achieve the biomass dry weights (air and oven dried) of each tree's component, the moisture content (MC%) was determined after air dry, which is assumed around 12%. The oven dry biomass was then calculated at a temperature within the range of ($105 \pm 2°C$), following the European Standard CEN EN 14774-

1:2009 (CEN EN 14774-1:2009). Digital scales with 0.001g precision were used for weightings. Additionally, the biomass density was determined to each component by measuring mass (weight) and volume by water displacement technique and is expressed as weight per unit volume (Tsoumis, 1991). Density was calculated to the fresh biomass (D) with moisture content as received, Density to the air dried biomass at 12% of moisture ($D_{12\%}$), and the basic Density (D_b) with the biomass oven dried.

4.2.2 Fitting and comparison for each biomass tree component model

To fit each biomass tree component several allometric equations, compiled in the literature, were tested: Schumacher and Hall (1933); Stoate (1945); Näslund (1947); Spurr (1952); Meyer (1953); Takata (1958); Prodan (1965); Honer (1967); Ogaya (1968); Loetsch et al. (1973); Burkhart (1977); Avery and Burkhart (1983); Clutter et al. (1983); Marklund (1987; 1988); Prodan (1997); Husch et al. (2003); Jenkins et al. (2004). Zianis et al. (2005) and Metla Project 3306 (2006). The models to estimate the AGB biomass and biomass of tree components of eucalyptus adjusted by Arthur D. Little International Inc. (1985), Silva et al. (1991); Fabião (1986); António et al. (2007) and (DNGF, 2010) were also tested. As the performance of these models was very low in fitting the biomass of top, variants of these models were also tested for this biomass tree component estimation.

The independent variables to include in the regression models were diameter at breast height *(d)* and total height (h), W_i=f(d ,h), and combinations of these two dendrometric parameters. Although there are variables that best fitted some biomass components (e.g. Biomass of tops), as the total height of tops or the total height of crown's tree, we decided to include in the regression models only this two dendrometric parameters as independent variables, as they are easily measured in field inventory surveys, apart from other reasons presented by Clutter et al. (1983). The models with better performance in the adjustment stage are summarized in Table 4.1.

Table 4.1 - Best candidate models to fit Eucalyptus biomass tree components.

Model	Equation	Reference
1	$W_i = \beta_1 d^{\beta_2} h^{\beta_3}$	(Schumacher and Hall, 1933)
2	$W_i = \beta_1 d^{\beta_2}$	(Husch et al., 2003)
3	$W_i = \beta_1 (d^2 h)^{\beta_2}$	(Spurr, 1952)
4	$W_i = \beta_0 + \beta_1 d^{\beta_2} h^{\beta_3}$	(Burkhart, 1977)
5	$W_i = \dfrac{d^2}{\beta_0 + \beta_1 (\frac{1}{h})}$	(Honer, 1967)
6	$W_i = \dfrac{d^2}{\beta_0 + \beta_1 d}$	(Takata, 1958)
7	$W_i = d^2(\beta_0 + \beta_1 h)$	(Ogaya, 1968)
8	$W_i = e^{(\beta_0 + \beta_1 (lnd) + \beta_2 h)}$	(Freire et al., 2003)
9	$W_i = e^{\left(\beta_0 + \beta_1 \frac{d}{(d+\beta_2)}\right)}$	

Where: W_i is the biomass (kg tree^{-1}); d is the diameter at breast height (cm), (h) is the total height of tree (m) and the $\beta_0, \beta_1, \beta_2, \beta_3$ are the equation parameters .

As in Chapter 3, the previous presented models, were fitted by nonlinear regression solved by the Gauss-Newton algorithm using the NLIN procedure of the SAS version 9.1 software (SAS Institute Inc., 2004). The initial values of models parameters (β_j) provided to begin the iterations were obtained by log transforming the equations and applying OLS using the SAS REG procedure for fitting (SAS Institute Inc., 2004), and also defining a grid search with a range of starting values in the iterative phase of the NLIN procedure.

In order to check if models' assumptions were satisfied (Ostrom, 1990; Rawlings et al., 1998; Ritz and Streibig, 2008), the residuals $e_i = (y_i - \hat{y}_i)$ (difference between the observed and fitted values) were calculated for each equation, and the graphical analysis (e.g. scatterplots of residuals against the predicted values; scatterplots of residuals against individual predictors; histogram of residuals) and the statistics of regression residuals were examined.

The selection of the best model was done by analysing and comparing the following statistical criteria obtained from the residuals (Sit and Poulin-Costello, 1994): model bias (Bias), mean absolute error (MAE); residual mean squares error (MSE) defined as the mean of the predicted residual sum of squares (PRESS or commonly SSE); root mean squared error (RMSE). The coefficient of determination (R^2); and adjusted coefficient of determination (R^2_{adj}), which in the nonlinear case is the Pseudo-R^2, where SST is the corrected total sum of squares ($SST_{corrected}$) (Schabenberger and Pierce, 2002) were also calculated (Eqs. 1-6).

To test and compare the goodness of fit of different models with a different number of parameters the Akaike's information criterion (AIC) (Akaike, 1974) was additionally calculated (Beal, 2005) (Eq. 7). AIC simultaneously maximizes the model fit and minimizes the number of parameters such that the model with the lowest value of AIC is considered the best (Motulsky and Christopoulos, 2003). As presented in Chapter 3, the equations 1 to 7 are written as:

$$Bias = \frac{\sum_1^n (y_i - \hat{y}_i)}{n} = \frac{\sum_1^n (e_i)}{n} \quad [1]$$

$$MAE = \frac{\sum_1^n |y_i - \hat{y}_i|}{n} = \frac{\sum_1^n |e_i|}{n} \quad [2]$$

$$MSE = \frac{SSE}{n-p} = \frac{\sum_1^n (y_i - \hat{y}_i)^2}{n-p} = \frac{\sum_1^n (e_i)^2}{n-p} \quad [3]$$

$$RMSE = \sqrt{MSE} \quad [4]$$

$$R^2 = 1 - \frac{SSE}{SST_{corrected}} = 1 - \frac{\sum_1^n (y_i - \hat{y}_i)^2}{\sum_1^n (y_i - \bar{y})^2} \quad [5]$$

$$R^2_{adj} = 1 - \frac{SSE\,(n-1)}{SST_{corrected}\,(n-p)} = 1 - \left[(1 - R^2)\,\frac{n-1}{n-p}\right] \quad [6]$$

$$AIC = n\,\ln(MSE) + 2\,p \quad [7]$$

where: y_i is the observed value; $\hat{y}_i$ is the predicted value for observation *i*; $\bar{y}$ is the mean of the observed values; *n* is the number of observations used to fit the model and *p* is the number of parameters fitted by the regression.

The described statistics were ranked in order to achieve the best model and select, for each biomass tree component, the equation to include in the nonlinear simultaneous equation system.

4.2.3 Additive nonlinear simultaneous system specification and modelling

Procedures for forcing additivity have been proposed on a system of biomass equations, as described by (Parresol, 1999), both linear and non-linear (Kozak, 1970; Chiyenda and Kozak, 1984; Cunia and Briggs, 1984, 1985; Reed and Green, 1985). Following Parresol (1999, 2001) a system of six nonlinear regression functions was specified such that (i) each component regression contains its own independent variables, and the total-tree regression is a function of all independent variables used; (ii) each regression can use its own weight function; and (iii) the additivity is insured by setting constraints (i.e., restrictions) on the regression coefficients. This model specification with cross-equation constraints on the structural parameters and cross-equation error correlation with an additive error structure, as a method of forcing additivity among biomass equations, is written as follows (Eq. 8):

$$
\begin{aligned}
W_{wood} &= f_1(x_{1j}, \beta_{1j}) + \varepsilon_1 \\
W_{bark} &= f_2(x_{2j}, \beta_{b2j}) + \varepsilon_2 \\
W_{top} &= f_3(x_{3j}, \beta_{3j}) + \varepsilon_3 \\
W_{branches} &= f_4(x_{4j}, \beta_{4j}) + \varepsilon_4 \\
W_{needles} &= f_5(x_{5j}, \beta_{5j}) + \varepsilon_5 \\
W_{total} &= f_6(x_{1j}, x_{2j}, x_{3j}, x_{4j}, x_{5j}, \beta_1, \beta_2, \beta_3, \beta_4, \beta_5) + \varepsilon_{total} \qquad [8]
\end{aligned}
$$

where: W, is the biomass of each tree component and the total AGB (ton ha^{-1}) , which is a function $(f_1, \dots, f_6)$ of a set of independent variables $(x_{1j}, \dots, x_{6j})$ and a set of parameters $(\beta_{1j}, \dots, \beta_{6j})$ and $(\varepsilon_1, \dots, \varepsilon_6)$ is the error component.

Following the same procedures of chapter 3, the set of equations was fitted with the PROC MODEL procedure of SAS (SAS Institute Inc., 2004) using joint generalized least squares more commonly called nonlinear seemingly unrelated regressions (NSUR). The theoretical statistics behind this approach can be better understood in the literature (e.g. Zellner, 1962; Srivastava and Giles, 1987; Bartels, 2006; Moon and Perron, 2008).

The assumption of homoscedasticity of residuals was examined with the White's test (White, 1980). To overcome the problem of heteroscedasticity, which typically occurs in biomass data, and by this way improving the efficiency of the estimates, weight variables were used in the model equations to stabilize the variance (i.e. weighted nonlinear least squares (Cohen et al., 2003). In biomass data, it is usually assumed that the variance of the error can be modelled as a power function of the independent variables. However, depending on the model fitted to the data, some biomass tree components can present combined heteroscedasticity trends (Parresol, 1999, 2001). The weight functions, for each equation of the NSUR system were derived by modelling the estimated errors ($\hat{e}_i^2$) of the unweighted model as the dependent variable in the error variance model, upon applying ordinary least squares (OLS), as:

$$\hat{e}_i^2 = \gamma(X_i)^k \qquad [9]$$

or, in the natural logarithm (ln):

$$\ln \hat{e}_i^2 = \ln \gamma + k \ln(X_i) \qquad [10]$$

After modelling the error structure to correct the heteroscedasticity, the weighting functions $1/(X_i)^k$ were specified in the system and the iterated seemingly unrelated regression in the SAS MODEL procedure (SAS Institute Inc., 2004) was carried out.

4.3 Results and discussion

4.3.1 Characteristics of eucalyptus stands

The descriptive statistics of eucalyptus stands, measured during field work and recorded in the inventory dataset, are presented in Table 4.2.

Table 4.2 - Descriptive statistics of eucalyptus stands.

	Site	N (trees ha^{-1})	t (year)	d_{bh} (cm)	h (m)	h_{dom} (m)	d_{dom} (cm)	BA (m^2 ha^{-1})	SI (m)
1	Cambra (Vouzela)	1400	11	14.7	20.0	21.3	19.6	27.8	20.1
2	Parada (Carregal do Sal)	1000	11	18.5	21.1	24.8	25.7	33.8	23.4
3	Castelo de Penalva (Penalva do Castelo)	1300	11	18.8	19.4	24.2	21.1	29.7	22.9
4	Pinheiro Ázere (Santa Comba Dão)	1300	11	11.9	16.8	20.8	15.8	15.1	19.6
5	Currelos (Carregal do Sal)	2100	11	13.6	16.1	18.3	16.8	33.5	17.3
6	Sobral (Mortágua)	800	10	12.8	13.6	19.8	16.3	11.3	19.8
7	Cepões (Viseu)	2440	8	11.1	6.9	17.1	20.7	30.9	19.5
8	Dardavaz (Tondela)	800	10	12.9	9.7	19.5	19.0	12.6	19.5
9	Santa Comba Dão	800	13	15.4	16.2	25.9	24.1	17.4	22.3
10	Baiões (São Pedro do Sul)	1320	13	12.6	12.7	23.9	22.8	23.6	20.5
11	Queiriga (Vila Nova de Paiva)	1420	13	14.8	13.9	18.4	23.9	27.4	15.8
	Mean	1335	11.1	14.3	15.1	21.3	20.5	23.9	20.1
	Min	800	8.0	11.1	6.9	17.1	15.8	11.3	15.8
	Max	2440	13.0	18.8	21.1	25.9	25.7	33.8	23.4
	SD	528.3	1.5	2.5	4.3	3.0	3.4	8.4	2.3

Where: *N* is the number of stems per hectares; *t* is the stand mean age; d_{bh} is the diameter at breast height; *h* is the mean height; h_{dom} is the dominant height; d_{dom} is the dominant diameter at breast height; *BA* is the basal area; *SI* is the site index.

The studied eucalyptus stands range from 8 to 13 years with stocking ranging between 800 and 2440 trees per hectare. The site index was calculated by the equation developed by (DNGF, 2010) at the reference age of 10 years. According to the defined site quality classes: inferior <12; low-moderated=16; moderated-height=20 and superior

≥ 24, the forest stands are in the moderated-height site quality, except stands 1 and 5 which is included in the low-moderated class.

The proportion of the biomass components in the trees, calculated for each sample plot, is shown in Figure 4.2. Under the bars are presented the number of trees sampled in each stand. The last column is the average proportion of all 51 sampled trees. The mean distribution of the biomass components is similar for all the stands, except for stand 5 were the wood stem presents lower proportion and the leaves higher proportion, comparing to the other stands.

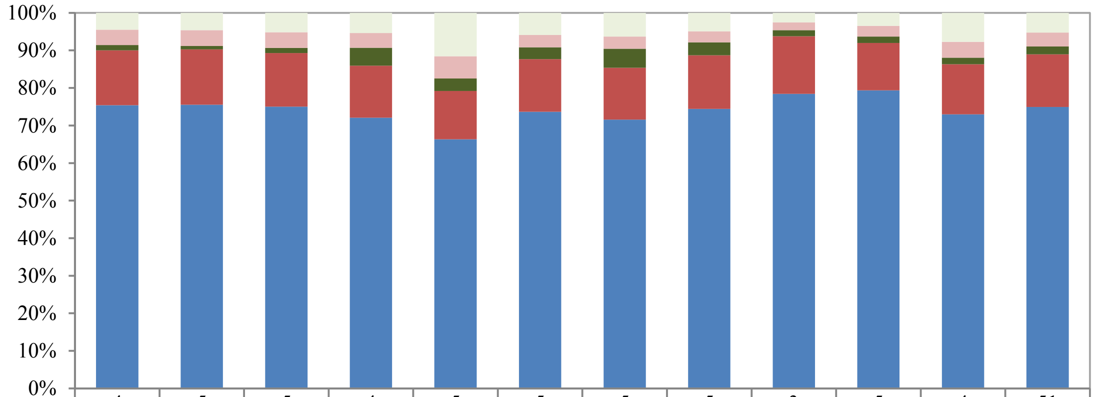

	4	5	5	4	5	5	5	5	3	5	4	51
Leaves	4.5	4.6	5.2	5.4	11.6	5.9	6.3	4.9	2.5	3.5	7.7	5.2
Branches	4.1	4.2	4.1	3.9	5.9	3.3	3.2	2.9	2.1	2.9	4.2	3.7
Top	1.4	0.9	1.4	4.8	3.3	3.2	5.1	3.4	1.6	1.7	1.7	2.1
Bark	14.6	14.7	14.3	13.8	12.9	14.0	13.8	14.3	15.3	12.6	13.3	14.0
Wood	75.4	75.5	75.0	72.1	66.3	73.6	71.6	74.4	78.4	79.4	73.0	74.9

Figure 4.2 - Proportion of the eucalyptus biomass tree components in the measured sample plots.

4.3.2 Nonlinear models fitted to each biomass tree component

The models from Table 4.1 were fitted to the biomass tree components, and total aboveground biomass for fresh, air dried and oven dried weights. The statistics from the unweighted models with best performance are presented in Tables 4.3 to 4.8. The models fitted for the tops biomass estimation presented lower performances comparatively to the models fitted for estimating the other biomass components, so only the five best fitted models are presented (Table 4.5).

The models that better fitted the data of each biomass component, according to the ranking of the computed statistics are shaded in the tables.

The model 8 presented better performances for fitting all the biomass tree components, in fresh and dry weight, except for fitting the bark and top biomass, where the models and model 1 presented the best performance (Table 4.4 and 4.5). However, as can be seen by the achieved statistics, model 8 presented very similar performance in the fitting stage. Thus, in order to maintain the parsimony in the additive nonlinear simultaneous equation system (section 4.3.3) by using equations with the same functional form, the model 8 was selected for fitting all the biomass tree components.

Table 4.3 - Statistics of the fitted models to the wood stem biomass.

Model	Mean	MAE	MSE	RMSE	RMSE (%)	R^2	R^2_{adj}	AIC
Fresh weight								
1	188.1	20.10	1429.60	37.81	20.26	0.959	0.956	560.7
2	189.2	24.22	1669.40	40.86	21.89	0.951	0.949	572.3
3	187.2	19.63	1479.40	38.46	20.61	0.956	0.954	563.0
4	186.6	19.02	1443.60	37.99	20.36	0.959	0.956	561.9
5	189.0	20.42	1435.80	37.89	20.31	0.958	0.956	560.7
6	186.4	19.35	1485.00	38.54	20.65	0.956	0.954	563.3
7	189.8	20.87	1406.90	37.51	20.10	0.958	0.957	559.1
8	188.3	20.44	1382.60	37.18	19.93	0.960	0.957	558.2
Air dried weight								
1	152.6	16.32	941.80	30.69	20.26	0.959	0.956	528.6
2	153.6	19.65	1099.80	33.16	21.90	0.951	0.949	540.1
3	151.9	15.93	974.60	31.22	20.61	0.956	0.954	530.8
4	151.5	15.44	951.00	30.84	20.36	0.959	0.956	529.7
5	153.4	16.57	945.90	30.76	20.31	0.958	0.956	528.5
6	151.3	15.70	978.30	31.28	20.65	0.956	0.954	531.1
7	154.1	16.94	926.90	30.45	20.10	0.958	0.957	527.0
8	152.8	16.59	910.80	30.18	19.93	0.960	0.957	526.0
Oven dried weight								
1	113.5	12.23	425.90	20.64	18.17	0.968	0.966	467.5
2	114.7	16.15	647.50	25.45	22.40	0.950	0.948	499.4
3	113.4	12.28	418.20	20.45	18.01	0.968	0.967	465.7
4	113.6	12.26	435.00	20.86	18.36	0.968	0.966	469.5
5	113.7	12.29	419.30	20.48	18.03	0.968	0.966	465.9
6	113.5	12.26	418.00	20.45	18.00	0.968	0.967	465.7
7	114.4	12.24	420.90	20.52	18.06	0.968	0.966	466.2
8	113.8	12.39	402.70	20.07	17.67	0.970	0.968	463.2

Note: values of calculated statistics (Mean, MAE, MSE and RMSE) are in kg tree^{-1}.

Table 4.4 - Statistics of the fitted models to the bark stem biomass.

Model	**Mean**	**MAE**	**MSE**	**RMSE**	**RMSE (%)**	R^2	R^2_{adj}	**AIC**
Fresh weight								
1	35.3	2.88	17.07	4.13	11.84	0.984	0.983	219.8
2	35.4	3.64	24.33	4.93	14.14	0.977	0.976	246.7
3	35.1	2.74	19.62	4.43	12.69	0.981	0.980	230.1
4	34.9	2.67	16.19	4.02	11.53	0.985	0.984	216.1
5	35.2	2.87	17.04	4.13	11.83	0.984	0.983	219.2
6	34.9	2.59	20.57	4.54	13.00	0.980	0.979	233.8
7	35.2	2.88	16.60	4.07	11.68	0.984	0.983	217.3
8	35.3	2.88	16.61	4.08	11.68	0.984	0.983	217.7
Air dried weight								
1	13.7	1.11	2.61	1.61	11.91	0.984	0.983	75.2
2	13.8	1.42	3.70	1.92	14.19	0.976	0.975	101.7
3	13.7	1.05	2.99	1.73	12.75	0.981	0.980	85.3
4	13.6	1.03	2.47	1.57	11.59	0.985	0.984	71.3
5	13.7	1.11	2.60	1.61	11.90	0.983	0.983	74.6
6	13.5	1.00	3.14	1.77	13.06	0.980	0.979	88.9
7	13.7	1.11	2.54	1.59	11.76	0.984	0.983	72.8
8	13.7	1.11	2.55	1.60	11.77	0.984	0.983	73.3
Oven dried weight								
1	11.4	0.92	1.81	1.34	11.91	0.984	0.983	47.0
2	11.5	1.19	2.57	1.60	14.19	0.976	0.975	73.5
3	11.4	0.88	2.07	1.44	12.75	0.981	0.980	57.1
4	11.3	0.86	1.71	1.31	11.59	0.985	0.984	43.1
5	11.4	0.92	1.80	1.34	11.90	0.983	0.983	46.4
6	11.3	0.83	2.18	1.47	13.06	0.980	0.979	60.8
7	11.4	0.93	1.76	1.33	11.76	0.984	0.983	44.6
8	11.4	0.93	1.77	1.33	11.77	0.984	0.983	45.1

Note: values of calculated statistics (Mean, MAE, MSE and RMSE) are in kg tree^{-1}.

Table 4.5 - Statistics of the fitted models to the top biomass.

Model	Mean	MAE	MSE	RMSE	RMSE (%)	R^2	R^2_{adj}	AIC
Fresh weight								
1	5.2	0.60	0.62	0.79	15.09	0.823	0.812	-35.4
2	5.2	0.61	0.67	0.82	15.70	0.804	0.796	-29.7
3	5.2	0.64	0.80	0.89	17.10	0.768	0.758	-16.5
8	5.2	0.61	0.64	0.80	15.38	0.816	0.804	-32.5
12	5.2	0.65	0.92	0.96	18.41	0.731	0.720	-5.2
Air dried weight								
1	4.2	0.49	0.41	0.64	15.09	0.823	0.812	-67.6
2	4.2	0.49	0.44	0.67	15.70	0.804	0.796	-61.9
3	4.2	0.52	0.53	0.72	17.10	0.768	0.758	-48.7
8	4.2	0.50	0.42	0.65	15.38	0.816	0.804	-64.7
12	4.2	0.53	0.52	0.72	17.06	0.769	0.764	-49.1
Oven dried weight								
1	3.1	0.39	0.26	0.51	16.23	0.802	0.790	-102.1
2	3.1	0.41	0.35	0.59	18.68	0.733	0.722	-80.9
3	3.1	0.45	0.42	0.65	20.56	0.676	0.663	-66.2
8	3.1	0.41	0.29	0.54	17.16	0.779	0.765	-93.5
12	3.1	0.44	0.35	0.59	18.72	0.737	0.720	-80.2

Note: values of calculated statistics (Mean, MSE and RMSE) are in kg tree^{-1}.

Table 4.6 - Statistics of the fitted models to the branches biomass.

Model	Mean	MAE	MSE	RMSE	RMSE (%)	R^2	R^2_{adj}	AIC
Fresh weight								
1	9.3	2.06	8.46	2.91	31.41	0.898	0.892	165.8
2	9.3	2.32	10.21	3.20	34.51	0.875	0.870	179.9
3	9.1	2.73	15.42	3.93	42.40	0.811	0.803	211.5
4	9.3	2.02	8.60	2.93	31.66	0.899	0.893	167.4
5	9.9	2.53	10.69	3.27	35.31	0.869	0.864	183.4
6	8.9	2.77	15.73	3.97	42.83	0.807	0.799	213.1
7	9.9	2.53	10.58	3.25	35.13	0.870	0.865	182.6
8	9.3	2.04	8.29	2.88	31.09	0.900	0.894	164.2
Air dried weight								
1	5.7	1.25	3.13	1.77	31.38	0.900	0.893	89.2
2	5.6	1.36	3.65	1.91	33.86	0.881	0.876	100.5
3	5.6	1.64	5.50	2.35	41.59	0.820	0.812	132.2
4	5.6	1.24	3.20	1.79	31.70	0.900	0.893	91.2
5	6.0	1.48	3.95	1.99	35.24	0.871	0.865	106.7
6	5.4	1.65	5.57	2.36	41.86	0.817	0.810	133.2
7	6.0	1.48	3.92	1.98	35.13	0.871	0.866	106.2
8	5.6	1.24	3.07	1.75	31.05	0.902	0.895	87.6
Oven dried weight								
1	5.0	1.13	2.52	1.59	31.73	0.919	0.914	72.5
2	5.0	1.20	2.89	1.70	33.99	0.905	0.901	82.7
3	4.9	1.46	4.33	2.08	41.61	0.858	0.852	113.9
4	5.0	1.13	2.57	1.60	32.06	0.898	0.891	74.5
5	5.3	1.31	3.16	1.78	35.54	0.896	0.892	89.6
6	4.8	1.46	4.38	2.09	41.82	0.857	0.851	114.6
7	5.3	1.31	3.15	1.77	35.45	0.897	0.893	89.1
8	5.0	1.13	2.47	1.57	31.40	0.921	0.916	70.9

Note: values of calculated statistics (Mean, MAE, MSE and RMSE) are in kg tree^{-1}.

Table 4.7 - Statistics of the fitted models to the biomass of leaves.

Model	Mean	MAE	MSE	RMSE	RMSE (%)	R^2	R^2_{adj}	AIC
Fresh weight								
1	13.1	3.91	31.71	5.63	43.08	0.794	0.781	267.5
2	13.1	4.50	48.83	6.99	53.45	0.676	0.662	300.3
3	13.0	5.03	62.38	7.90	60.42	0.586	0.569	319.2
4	13.1	3.90	32.38	5.69	43.53	0.794	0.781	269.5
5	13.8	4.52	41.62	6.45	49.35	0.724	0.712	288.0
6	12.3	5.00	67.13	8.19	62.67	0.554	0.536	324.8
7	14.2	4.46	36.09	6.01	45.96	0.760	0.750	277.1
8	13.0	3.80	30.15	5.49	42.00	0.804	0.791	263.6
Air dried weight								
1	7.3	2.24	10.36	3.22	44.24	0.792	0.779	181.3
2	7.3	2.54	16.16	4.02	55.25	0.669	0.655	215.2
3	7.2	2.87	20.70	4.55	62.55	0.576	0.558	234.3
4	7.3	2.25	10.58	3.25	44.70	0.792	0.779	183.3
5	7.7	2.59	13.85	3.72	51.15	0.716	0.705	203.3
6	6.8	2.84	22.10	4.70	64.62	0.547	0.529	239.3
7	7.9	2.57	12.12	3.48	47.85	0.752	0.741	193.0
8	7.2	2.17	9.85	3.14	43.14	0.802	0.790	177.5
Oven dried weight								
1	6.7	2.08	8.85	2.97	44.38	0.793	0.780	169.2
2	6.7	2.34	13.85	3.72	55.52	0.669	0.656	203.3
3	6.7	2.66	17.78	4.22	62.90	0.576	0.558	222.5
4	6.7	2.08	9.04	3.01	44.84	0.793	0.780	171.2
5	7.1	2.40	11.89	3.45	51.45	0.716	0.704	191.6
6	6.3	2.63	18.93	4.35	64.91	0.548	0.529	227.4
7	7.3	2.38	10.44	3.23	48.20	0.751	0.741	181.5
8	6.7	2.01	8.42	2.90	43.28	0.803	0.791	165.4

Note: values of calculated statistics (Mean, MAE, MSE and RMSE) are in kg tree^{-1}.

Table 4.8 - Statistics of the fitted models to the aboveground biomass.

Model	*Mean*	*MAE*	*MSE*	*RMSE*	*RMSE (%)*	R^2	R^2_{adj}	*AIC*
Fresh weight								
1	250.2	23.65	1756.10	41.91	16.83	0.968	0.966	576.6
2	251.0	25.33	1875.00	43.30	17.39	0.965	0.964	581.2
3	248.4	24.80	2121.10	46.06	18.49	0.961	0.959	590.7
4	249.1	23.64	1782.60	42.22	16.95	0.968	0.966	578.1
5	252.2	24.36	1793.80	42.35	17.01	0.967	0.965	577.8
6	245.8	25.12	2192.60	46.83	18.80	0.959	0.986	593.3
7	252.6	24.43	1738.70	41.70	16.74	0.968	0.967	575.4
8	250.4	23.78	1716.10	41.43	16.63	0.969	0.967	574.8
Air dried weight								
1	182.8	17.42	1013.50	31.84	17.48	0.966	0.964	534.3
2	183.5	18.79	1099.90	33.16	18.21	0.962	0.961	540.1
3	181.6	18.30	1176.20	34.30	18.83	0.960	0.958	545.3
4	182.2	17.53	1031.90	32.12	17.63	0.966	0.964	536.0
5	184.2	17.85	1032.00	32.12	17.63	0.965	0.963	535.2
6	179.8	18.48	1207.50	34.75	19.07	0.959	0.957	547.3
7	184.5	17.86	999.90	31.62	17.36	0.966	0.964	532.8
8	182.9	17.48	987.10	31.42	17.25	0.967	0.965	532.2
Oven dried weight								
1	139.3	14.29	487.40	22.08	15.80	0.973	0.971	477.9
2	140.2	15.98	634.00	25.18	18.02	0.964	0.963	497.7
3	138.7	14.79	520.90	22.82	16.34	0.971	0.969	482.6
4	139.7	14.29	496.50	22.28	15.95	0.973	0.971	479.7
5	140.0	14.36	493.90	22.22	15.91	0.972	0.971	478.5
6	137.8	15.00	526.00	22.93	16.42	0.970	0.969	483.3
7	140.5	14.33	479.70	21.90	15.68	0.973	0.972	476.3
8	139.5	14.28	466.10	21.59	15.45	0.974	0.973	474.5

Note: values of calculated statistics (Mean, MAE, MSE and RMSE) are in kg tree^{-1}.

4.3.3 Additive nonlinear simultaneous biomass equations system fitted by NSUR

The additive nonlinear simultaneous equation system to be fitted by the nonlinear seemingly unrelated regressions (NSUR) method is written as (Eq. 11):

$$W_{wood} = e^{\,(\beta_{10}+\beta_{11}(lnd)+\beta_{12}h)}$$
$$W_{bark} = e^{\,(\beta_{20}+\beta_{21}(lnd)+\beta_{22}h)}$$
$$W_{top} = e^{\,(\beta_{30}+\beta_{31}(lnd)+\beta_{32}h)}$$
$$W_{branches} = e^{\,(\beta_{40}+\beta_{41}(lnd)+\beta_{42}h)}$$
$$W_{leaves} = e^{\,(\beta_{50}+\beta_{51}(lnd)+\beta_{52}h)}$$
$$W_{AGB=}W_{wood} + W_{bark} + W_{top} + W_{branches} + W_{leaves} \qquad [11]$$

where: W, is the biomass of each tree component (kg tree^{-1}), d is the diameter at breast height of the tree, h is the total height of the tree and β_{1x}..., β_{5x} are the coefficients of the regressions.

The previous models, excepting the top biomass, exhibit heteroscedasticity, in fresh and dry weight, so the standard errors of regression coefficients are biased, as they are if residuals are non-normal, thus leading to less accurate inferences. The scatterplots of the residuals *(ê)* versus the independent variables (*d, h*) is presented in Figures 4.3 to 4.8.

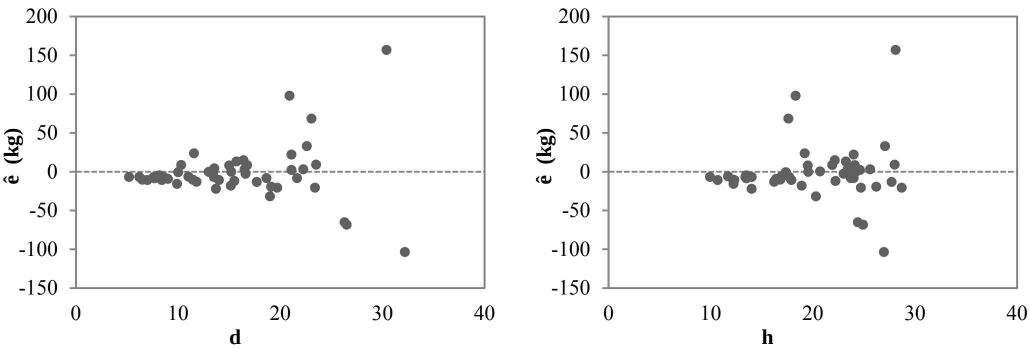

Figure 4.3 - Scatterplots of wood biomass residuals with the independent variables of the unweighted model.

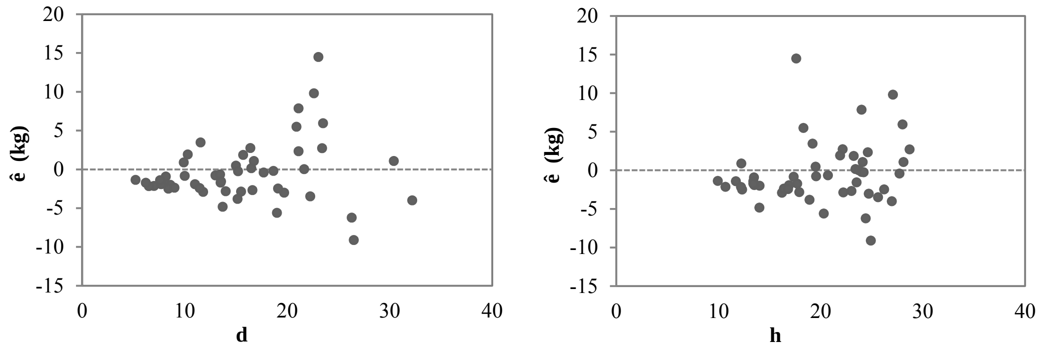

Figure 4.4 - Scatterplots of bark biomass residuals with the independent variables of the unweighted model.

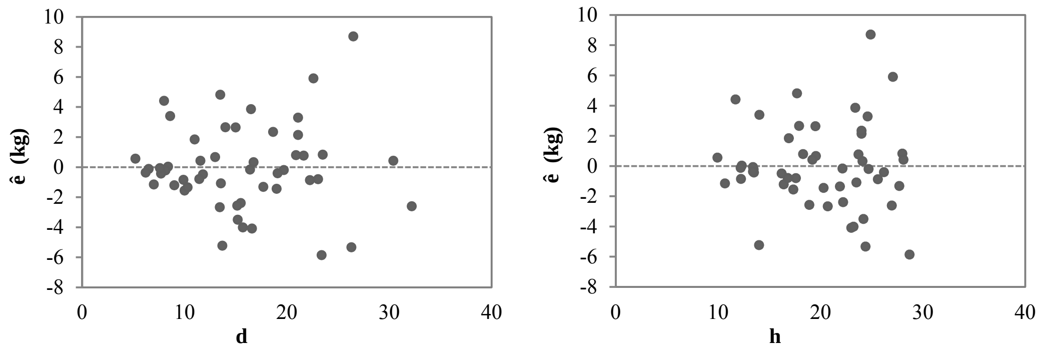

Figure 4.5 - Scatterplots of branches biomass residuals with the independent variables of the unweighted model.

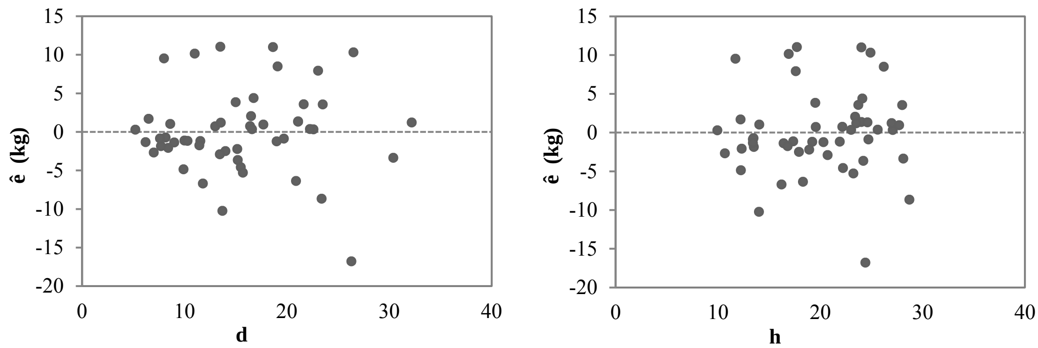

Figure 4.6 - Scatterplots of leaves biomass residuals with the independent variables of the unweighted model.

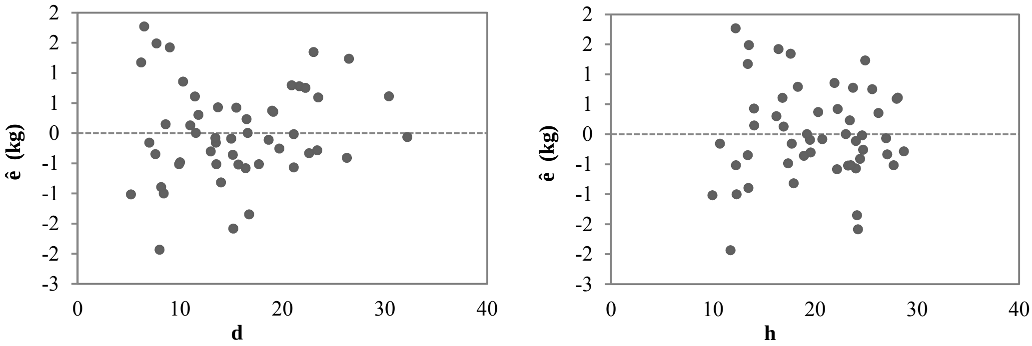

Figure 4.7 - Scatterplots of top biomass residuals with the independent variables of the unweighted model.

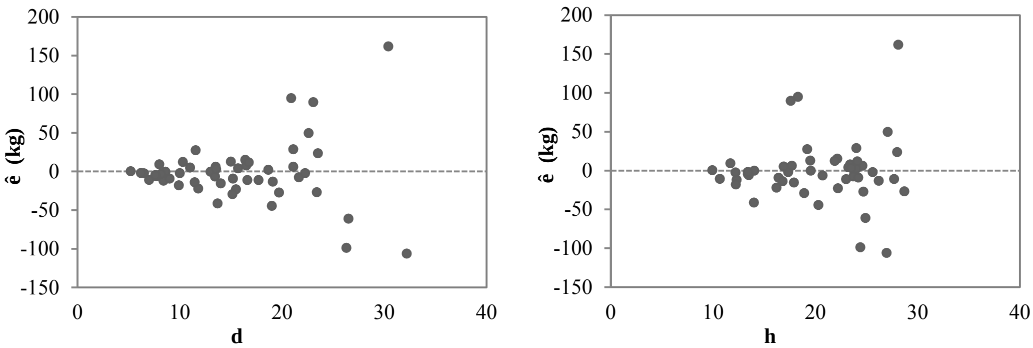

Figure 4.8 - Scatterplots of AGB biomass residuals with the independent variables of the unweighted model.

In order to correct for heteroscedasticity for NSUR system, weights for each biomass equation were derived by modelling the error function presents in Eq. 10. Several error functional forms were modelled and compared using AIC criterion to select the better function (see Parresol, 1999, 2001), as explained in methods and data section.

Tables 4.9 to 4.11 show the parameter estimates and standard errors of the nonlinear unweighted models (NLIN procedure) of the additive nonlinear simultaneous equation system (NSUR procedure) (Eq. 11), for fresh, air and oven dry biomass, respectively. As can be seen the standard errors decreased from the NLIN unweighted estimates to the NSUR estimates, in almost all parameters. By considering the contemporaneous correlation among the components, the process of simultaneous estimation (NSUR) reduces the confidence and prediction intervals of the biomass estimations, resulting from the smaller variance, and so achieving more efficient parameter estimates (Parresol, 2001).

The additive nonlinear simultaneous equation system was derived for the fresh, air and oven dried biomass since they can be used with different purposes. While the information of the oven dry biomass is necessary to assess the carbon stocks, often the information about the air dried biomass is required in studies of biomass energy estimation. In fact, the biomass used for energy purposes is mostly used with moisture content (MC%) in equilibrium with the outdoor atmosphere. On the other hand, after the forest harvesting, the biomass is immediately transported (fresh weight) or transported after air dry in the field. Hence, quantify the biomass weight in these conditions can be useful. However, must be noted that the MC(%) of fresh biomass has big fluctuations between different season and different trees, even from the same species. On the other hand, the air dried biomass will lose its free water depending on the clime conditions in each particular region. By the exposed, the derived equations for predicting the fresh and air dried biomass can be applied, for acquire indicative information, only under the same conditions of the data used in this research,

Table 4.9 - Parameter estimates and standard errors of the nonlinear unweighted models and of the nonlinear simultaneous system of fresh biomass.

		NLIN unweighted		NSUR	
Tree component	**Parameter**	**Estimate**	**Std Err**	**Estimate**	**Std Err**
	β_{10}	-1.3172	0.2662	-1.4540	0.1089
Wood	β_{11}	2.0695	0.1062	1.9884	0.0579
	β_{12}	0.0300	0.0089	0.0452	0.0061
Bark	B_{20}	-2.5694	0.1537	-2.7154	0.1008
	B_{21}	1.9638	0.0626	1.8773	0.0448
	B_{22}	0.0256	0.0052	0.0420	0.0044
	B_{30}	3.5752	0.1357	3.4812	0.1279
Top	B_{31}	-0.8675	0.1090	-0.8468	0.1031
	B_{32}	0.0163	0.0091	0.0180	0.0087
	B_{40}	-4.2368	0.4131	-4.2277	0.4048
Branches	B_{41}	2.6067	0.1682	2.5562	0.1925
	B_{42}	-0.0425	0.0118	-0.0364	0.0151
	B_{50}	-3.1728	0.5414	-3.1440	0.4977
Leaves	B_{51}	2.7420	0.2230	2.5400	0.2465
	B_{52}	-1.3172	0.2662	-1.4540	0.1089

Note: parameters estimates from equations presented in Eq.11

Table 4.10 - Parameter estimates and standard errors of the nonlinear unweighted models and of the nonlinear simultaneous system of air dried biomass.

		NLIN unweighted		NSUR	
Tree component	**Parameter**	**Estimate**	**Std Err**	**Estimate**	**Std Err**
	β_{10}	-1.5259	0.2662	-1.6408	0.1051
Wood	β_{11}	2.0695	0.1062	1.9844	0.0566
	β_{12}	0.0300	0.0089	0.0448	0.0060
Bark	B_{20}	-3.5006	0.1548	-3.6507	0.1029
	B_{21}	1.9601	0.0631	1.8771	0.0455
	B_{22}	0.0255	0.0052	0.0416	0.0045
	B_{30}	3.3665	0.1357	3.2815	0.1273
Top	B_{31}	-0.8675	0.1090	-0.8497	0.1028
	B_{32}	0.0163	0.0091	0.0179	0.0087
	B_{40}	-4.8523	0.4162	-4.7527	0.4205
Branches	B_{41}	2.6145	0.1689	2.5848	0.1994
	B_{42}	-0.0385	0.0119	-0.0386	0.0156
	B_{50}	-3.9221	0.5618	-3.8516	0.5051
Leaves	B_{51}	2.8140	0.2302	2.7037	0.2476
	B_{52}	-1.5259	0.2662	-1.6408	0.1051

Note: parameters estimates from equations presented in Eq.11

Table 4.11 - Parameter estimates and standard errors of the nonlinear unweighted models and of the nonlinear simultaneous system of oven dried biomass.

		NLIN unweighted		NSUR	
Tree component	**Parameter**	**Estimate**	**Std Err**	**Estimate**	**Std Err**
	β_{10}	-2.0695	0.2400	-2.1154	0.1392
Wood	β_{11}	2.0417	0.0940	2.0113	0.0703
	β_{12}	0.0439	0.0081	0.0496	0.0061
Bark	B_{20}	-3.6836	0.1548	-3.8581	0.1087
	B_{21}	1.9601	0.0631	1.8831	0.0465
	B_{22}	0.0255	0.0052	0.0418	0.0046
	B_{30}	3.1856	0.1532	3.1395	0.1354
Top	B_{31}	-1.0415	0.1239	-1.0047	0.1144
	B_{32}	0.0334	0.0103	0.0309	0.0097
	B_{40}	-5.0123	0.4222	-4.9901	0.4058
Branches	B_{41}	2.6176	0.1711	2.7529	0.2031
	B_{42}	-0.0373	0.0121	-0.0555	0.0163
	B_{50}	-4.0483	0.5651	-4.1590	0.4658
Leaves	B_{51}	2.8318	0.2312	2.8993	0.2464
	B_{52}	-2.0695	0.2400	-2.1154	0.1392

Note: parameters estimates from equations presented in Eq.11.

4.3.4 NSUR System evaluation

The statistics of the fitted additive nonlinear simultaneous equations system (NSUR system) for estimating the fresh, air and oven dry biomass tree components of eucalyptus are presented in Table 4.12. The final models show an overall efficiency for the AGB estimations of R^2 = 0.966, R^2 = 0.965 and R^2 = 0.975, respectively.

Table 4.12 - Statistics of the fitted additive nonlinear simultaneous biomass equation system.

Tree component	**Mean**	**MAE**	**MSE**	**RMSE**	**RMSE (%)**	R^2	R^2_{adj}
Fresh weight		R^2					
Wood	184.7	19.7	1418.0	37.7	20.2	0.958	0.957
Bark	34.7	2.7	19.3	4.4	12.6	0.981	0.981
Top	5.2	0.6	0.6	0.8	15.3	0.811	0.809
Branches	9.3	2.0	8.1	2.8	30.7	0.900	0.899
Leaves	12.9	3.7	31.0	5.6	42.6	0.792	0.790
AGB	246.8	24.4	2069.3	45.5	18.3	0.966	0.961
Air dried weight							
Wood	150.1	16.0	931.3	30.5	20.1	0.958	0.957
Bark	13.5	1.0	2.9	1.7	12.6	0.981	0.981
Top	4.2	0.5	0.4	0.6	15.3	0.812	0.810
Branches	5.7	1.2	3.0	1.7	30.6	0.901	0.900
Leaves	7.3	2.2	9.7	3.1	42.7	0.800	0.798
AGB	180.8	17.8	1164.2	34.1	18.7	0.965	0.959
Oven dried weight							
Wood	113.5	12.4	394.3	19.9	17.5	0.969	0.969
Bark	11.2	0.9	2.1	1.4	12.7	0.981	0.981
Top	3.1	0.4	0.3	0.5	16.9	0.779	0.776
Branches	5.0	1.2	2.5	1.6	31.8	0.894	0.893
Leaves	6.7	2.0	8.2	2.9	42.7	0.802	0.800
AGB	139.6	14.6	508.3	22.5	16.1	0.975	0.971

Note: values of calculated statistics (Mean, MAE, MSE and RMSE) are in kg tree^{-1}.

In order to visualise the quality of the fitted NSUR system for estimating the biomass tree components of eucalyptus, the scatterplots of the biomass measured in the field versus the predicted biomass by the NSUR system are presented in Figure 4.9. As can be seen, the nonlinear simultaneous system fitted to the biomass tree components by NSUR method show a good performance in all the biomass tree components. The predictive equations for top and leaves biomass components present higher dispersion in the estimates, comparing with the other biomass tree components. However, attending to the variability of the crown components (top, branches and leaves) comparing with stem and bark components, the model efficiencies can be considered moderate to high. The model efficiencies for fresh biomass of tops and leaves were R^2= 0.811 and R^2=

0.792, respectively; for air dried biomass R^2= 0.812 and R^2= 0.8, respectively; and for oven dried biomass R^2= 0.779 and R^2= 0.802, respectively (Table 4.12).

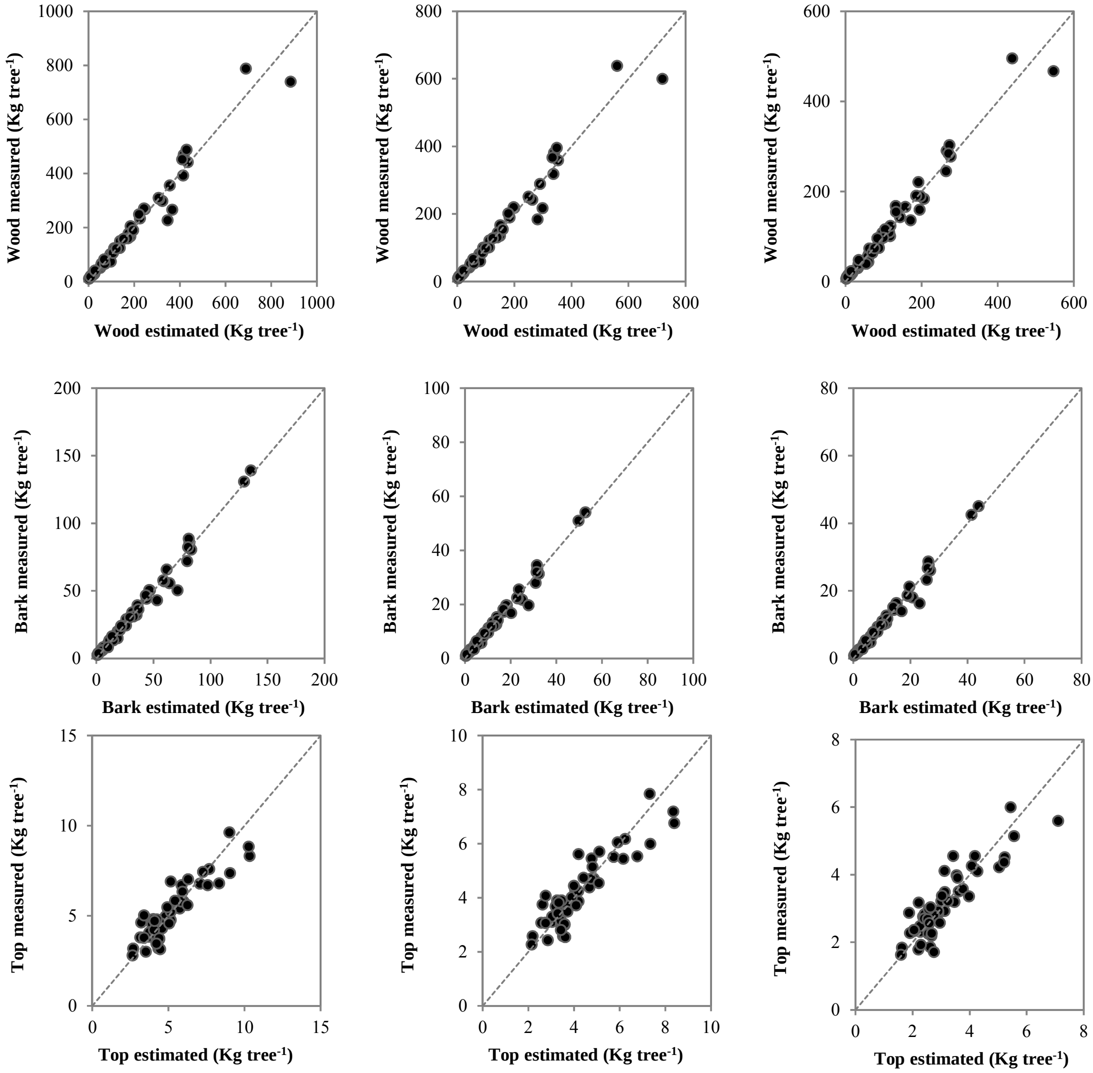

(A) (B) (C)

Figure 4.9 - Scatterplots of the measured versus predicted eucalyptus biomass components fitted by the NSUR system.

(A) fresh biomass, (B) air dried biomass, and (C) oven dried biomass

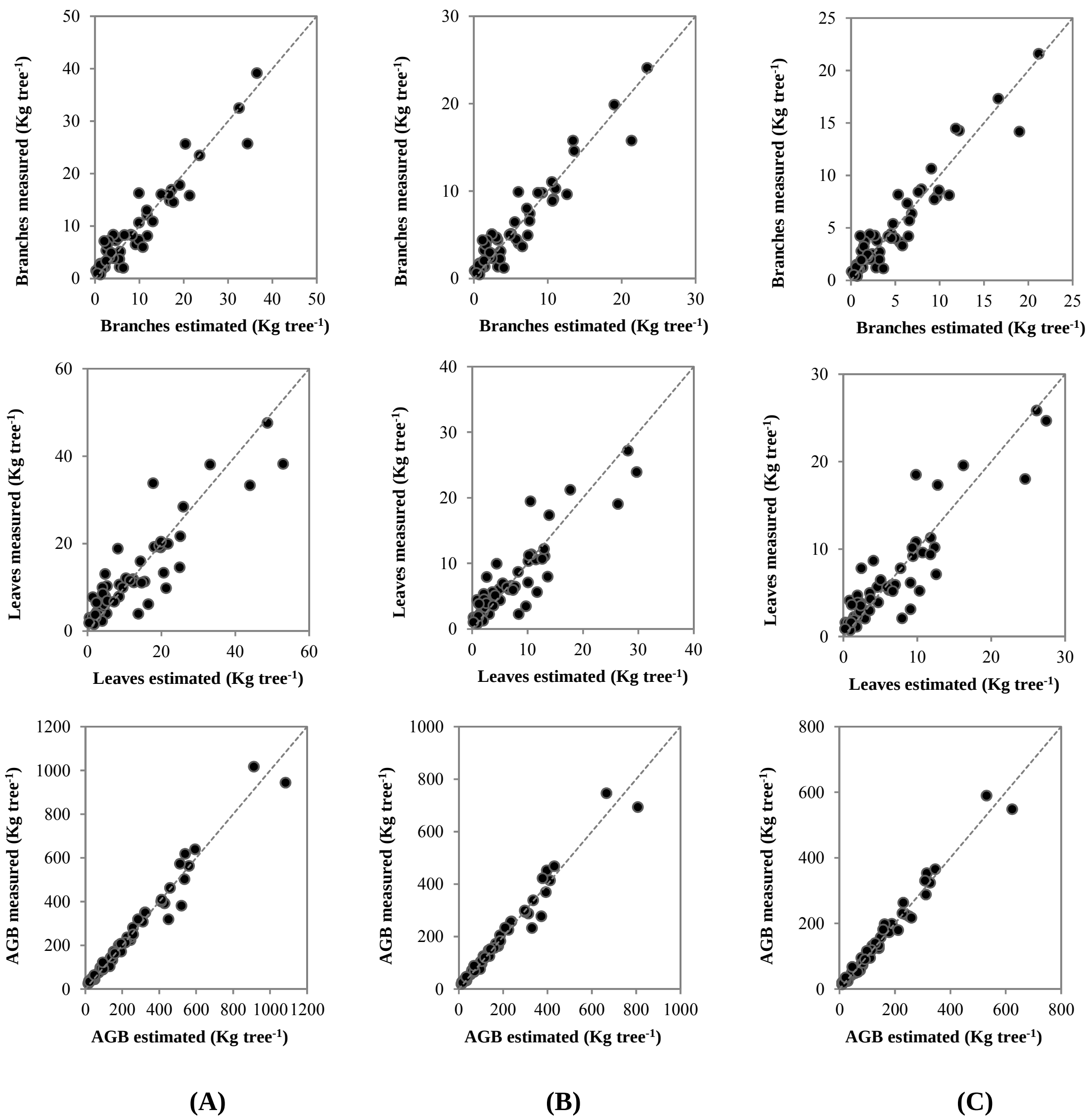

Figure 4.9 - Scatterplots of the measured versus predicted eucalyptus biomass components fitted by the NSUR system (cont.).

(A) fresh biomass, (B) air dried biomass, and (C) oven dried biomass

The nonlinear simultaneous system was also validated using the dataset constituted by the 53 trees only weighted in loco during the field work. The NSUR equations were applied to this dataset and the biomass of wood stem, bark stem, crown (sum of branches, tops and leaves) and total AGB biomass was calculated. Figure 4.10 shows the scatterplots with the measured versus estimated biomass. For all the components the derived models present good performance, despite the estimation of crown biomass presented more dispersion.

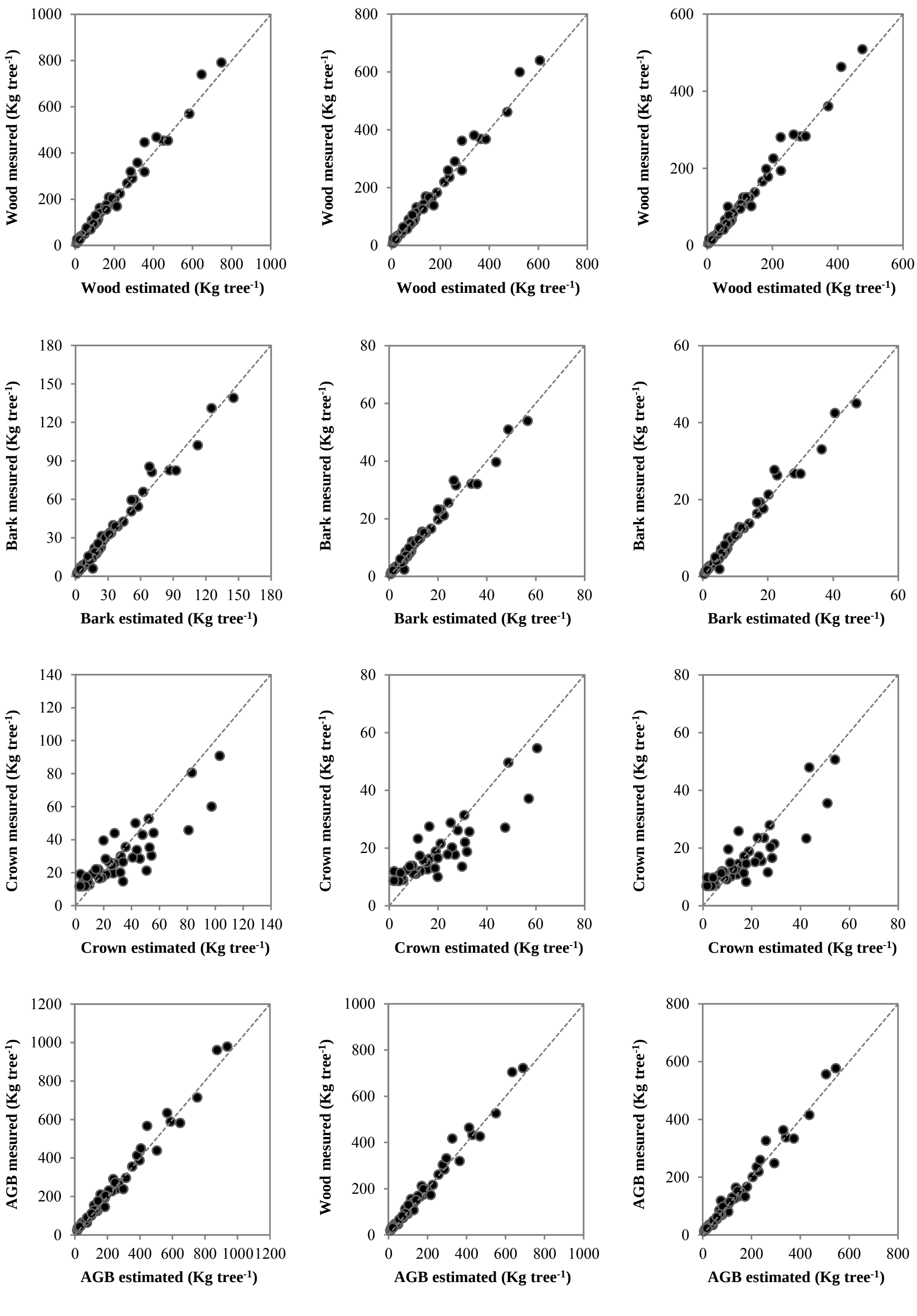

Figure 4.10 - Scatterplots of the measured versus predicted eucalyptus biomass components fitted by the NSUR system in the validation dataset.

(A) fresh biomass (B) air dried biomass and (C) oven dried biomass.

4.3.5 Comparison with other biomass equations for eucalyptus

The models derived by the NSUR approach were compared with equations established by António et al. (2007) and (DNGF, 2010), which were adjusted using seemingly unrelated regressions procedures, for estimating *Eucalyptus globulus* biomass in Portuguese ecosystems (Table 4.13 and Figures 4.11- 4.12).

As scatterplots depict, the equations show substantial differences in the branches and leaves tree's biomass predictions. The RMSE (%) values, presented in Table 4.13, show that the lowest performance. However, the global AGB show good performances with RMSE=21.3% and 16.2%, respectively.

Additional comparisons were made with equations from Arthur D. Little International Inc. (1985), Fabião (1986) and Silva et al. (1991), fitted by OLS (Figure 4.13). The most evident discrepancies are observed in the equations developed by Fabião (1986) to estimate the branches (RMSE=86.7%) and leaves (RMSE=69.6%) biomass, as the equations from Arthur D. Little International Inc. (1985), presented most satisfactory results RMSE=45.9% and 46.7% to dry and fresh crown biomass respectively (Table 4.13).

The observed discrepancies can be explained by the specific characteristics of the eucalyptus trees and stands used in the adjustments, which have distinct growth conditions and silvicultural management. Furthermore, as previous stated the quantification of the individual biomass component certainly contribute to the observed discrepancies.

The comparisons carried out show that significant discrepancies in the biomass estimates can be achieved, particularly in the individual tree components which can lead to misleading assessments of biomass. As most studies make assessments in large areas the individual error obtained at a tree level, could extraordinarily increase proportionally to the study area considered. Hence, the generalization of equations developed to a particular site should be applied prudently as well the quantifications of individual biomass tree components.

Table 4.13 - Statistics of the estimates obtained by the equations from other authors.

Tree component	Mean	MAE	MSE	RMSE	RMSE (%)
(António et al., 2007)					
Wood	107.2	12.3	600.1	24.5	21.6
Bark	15.1	4.0	61.1	7.8	69.3
Branches	9.3	4.5	42.9	6.6	131.0
Leaves	15.7	9.4	190.9	13.8	206.1
AGB	147.4	20.4	988.3	31.4	22.5
(DNGF, 2010)					
Wood	108.3	11.9	567.1	23.8	21.0
Bark	16.1	5.0	87.8	9.4	83.0
Branches	9.1	4.1	30.0	5.5	109.5
Leaves	7.2	2.3	10.9	3.3	49.3
AGB	140.6	15.2	520.3	22.8	16.3
(Arthur D. Little International Inc., 1985)					
Crown (fresh)	30.7	9.7	205.2	14.3	52.0
Crown (dry)	12.9	4.4	35.2	5.9	39.9
(Fabião, 1986)					
Branches	8.66	4.2	56.4	7.5	150.1
Leaves	10.08	4.5	49.2	7.0	104.6
Crown (sum of branches and leaves)	18.75	8.3	182.0	13.5	90.8
(Silva et al., 1991)					
Crown (fresh)	24.5	7.1	104.4	10.2	37.1
Crown (dry)	10.4	5.1	49.6	7.0	47.4
NSUR (fresh)					
Wood	184.7	19.7	1418.0	37.7	20.2
Bark	34.7	2.7	19.3	4.4	12.6
Top	5.2	0.6	0.6	0.8	15.3
Branches	9.3	2.0	8.1	2.8	30.7
Needles	12.9	3.7	31.0	5.6	42.6
AGB	246.8	24.4	2069.3	45.5	18.3
NSUR (Oven dry)					
Wood	113.5	12.4	394.3	19.9	17.5
Bark	11.2	0.9	2.1	1.4	12.7
Top	3.1	0.4	0.3	0.5	16.9
Branches	5.0	1.2	2.5	1.6	31.8
Needles	6.7	2.0	8.2	2.9	42.7
AGB	139.6	14.6	508.3	22.5	16.1

Note: values of calculated statistics (Mean, MAE, MSE and RMSE) are in kg $tree^{-1}$.

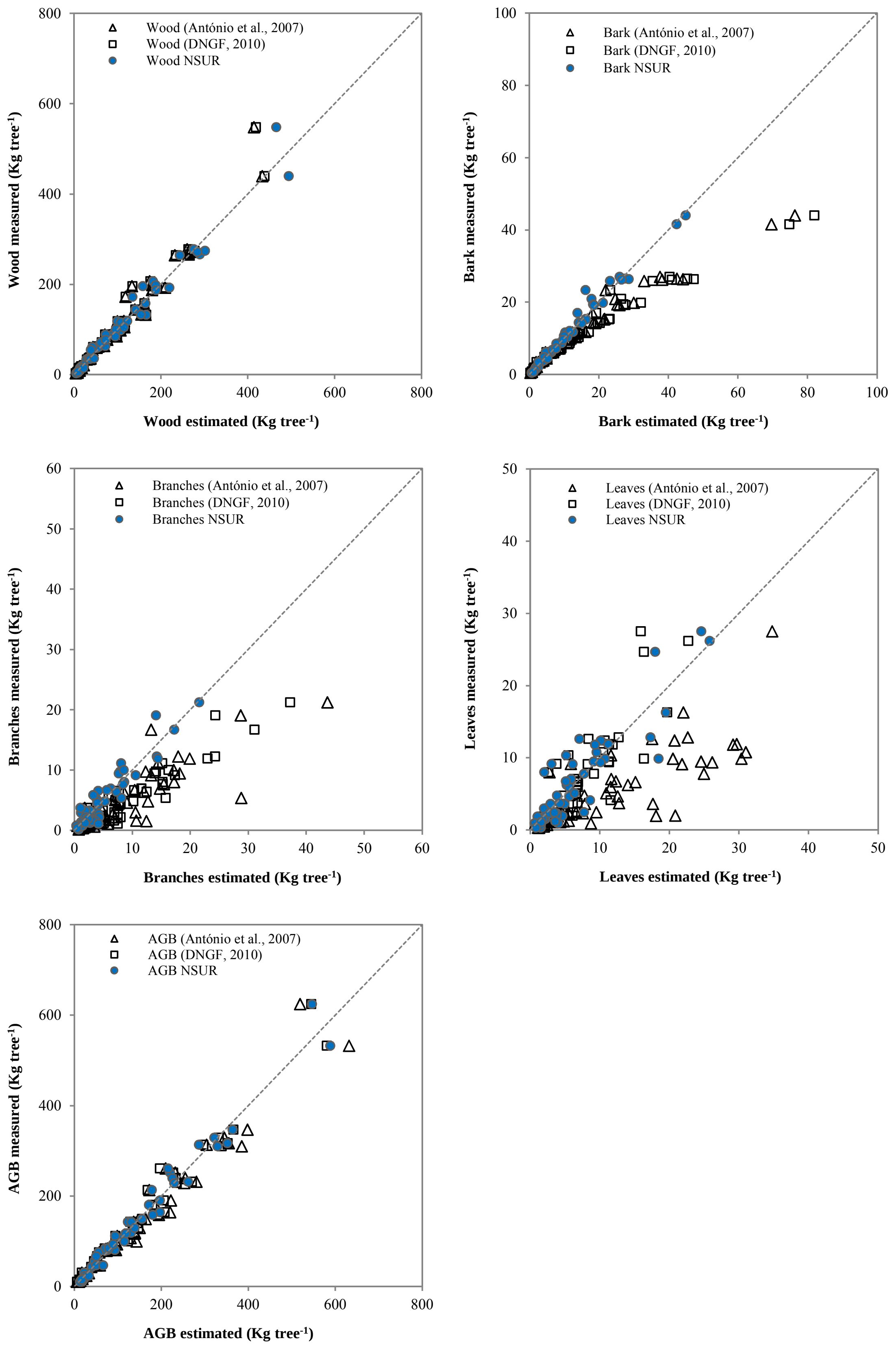

Figure 4.11 - Scatterplots comparing the eucalyptus biomass estimates from the NSUR equation system and from equations adjusted by other authors.

Note: The AGB biomass estimates are the sum of the biomass tree components.

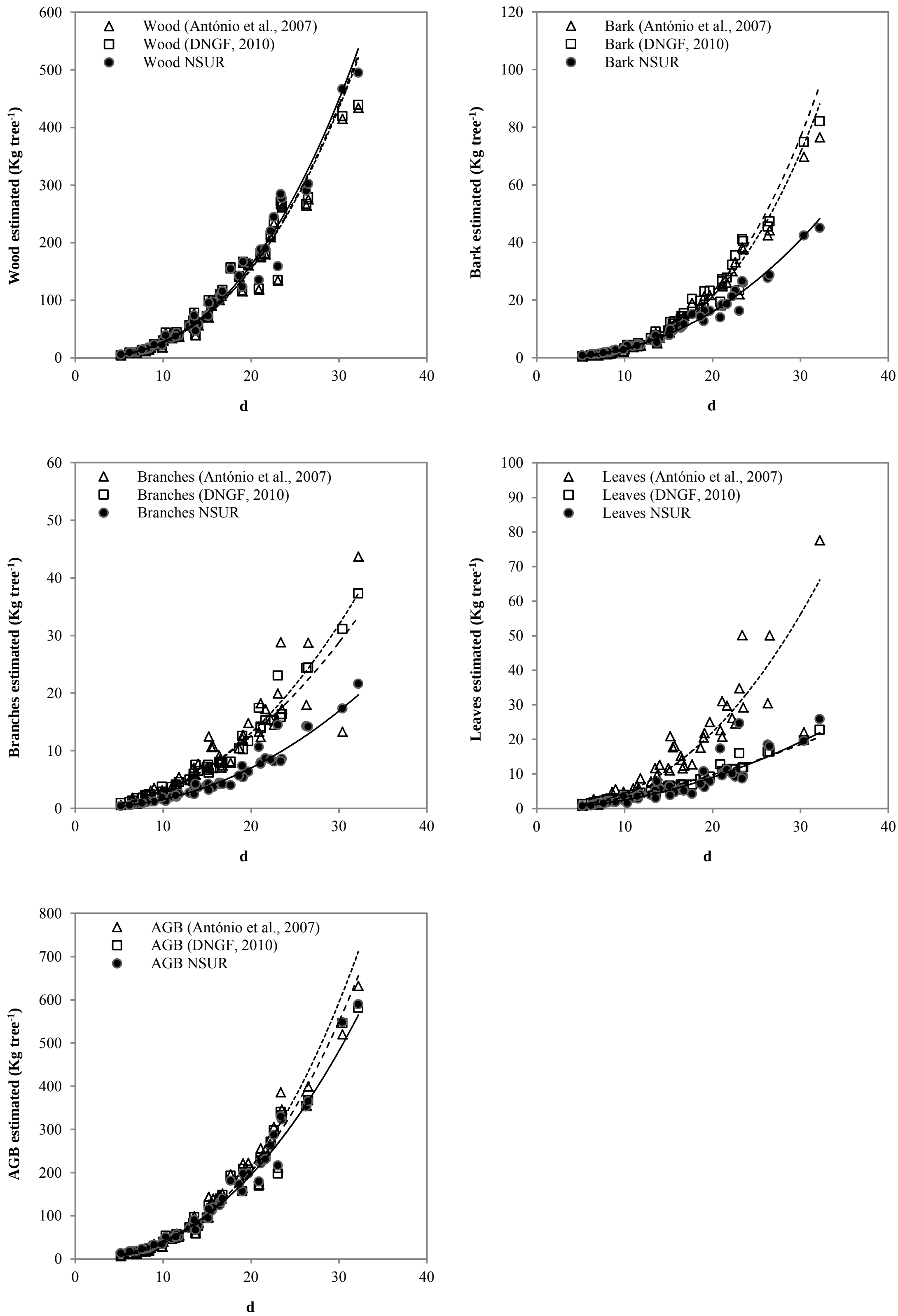

Figure 4.12 - Relationships between the eucalyptus biomass estimates by the NSUR equations system and the diameter at breast height.

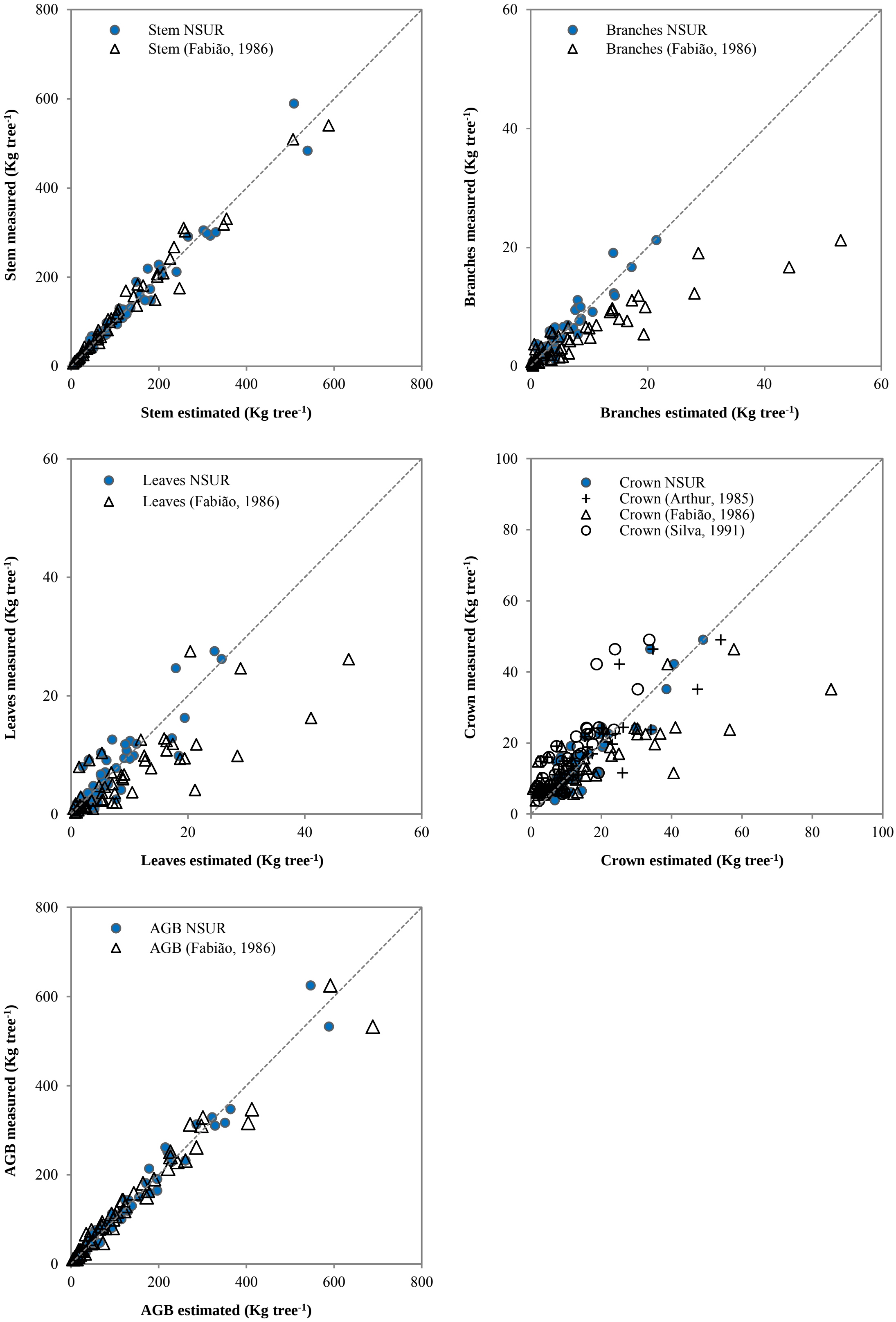

Figure 4.13 - Scatterplots comparing the eucalyptus biomass estimates from the NSUR equation system and from the equations, adjusted by OLS from other authors.

Note: The NSUR Crown and AGB estimates are the sum of top, branches and needles biomass estimates. The equations adjusted by OLS regression analysis are from Arthur D. Little International Inc. (1985), Fabião (1986) and Silva et al. (1991).

4.4 Conclusion

An additive nonlinear simultaneous biomass equations system was derived, by the nonlinear seemingly unrelated regressions (NSUR) method, to estimate the tree biomass components and total aboveground biomass of *Eucalyptus globulus* Labill., in the North-Center region of Portugal. The NSUR approach guarantee the property of additivity among the tree's biomass components and the total tree's AGB, and provide a gain in parameter estimation efficiency as it allows to impose restrictions that involve parameters in different equations, as demonstrated by (Parresol, 1999, 2001). The gain in the accuracies has an important implication in forest inventory estimates because less variation is obtained in reliability analysis.

The comparisons with equations previous developed by other authors for eucalyptus, shows that significant discrepancies in the biomass estimates can be achieved, particularly in the individual fraction of the tree, such as the top, branches or leaves. Furthermore, the generalization of equations developed to a specific site should be made prudently as it can lead to erroneous biomass assessments. Hence, the set of equations developed in this study should be applied to trees and stands with similar characteristics, regarding to stand density and tree sizes. The generalized use in other regions or on national scale can lead to a consistent inaccuracy of the estimates.

References

Akaike, H., 1974. A new look at the statistical model identification. Automatic Control, IEEE Transactions on 19, 716-723.

António, N., Tomé, M., Tomé, J., Soares, P., Fontes, L., 2007. Effect of tree, stand, and site variables on the allometry of *Eucalyptus globulus* tree biomass. Canadian Journal of Forest Research 37, 895-906.

Arthur D. Little International Inc., 1985. Resíduos florestais para produção de energia em Portugal, Tecninvest, SARL ed.

Avery, T.E., Burkhart, H.E., 1983. Forest measurements. McGraw-Hill, pp. 331.

Bartels, R., 2006. Seemingly Unrelated Regressions, Encyclopedia of Environmetrics. John Wiley & Sons, Ltd.

Beal, D.J., 2005. SAS Code to Select the Best Multiple Linear Regression Model for Multivariate Data Using Information Criteria, Science Applications International Corporation. Available online at: *http://analytics.ncsu.edu/ sesug/2005/SA01_05.PDF*, (Accessed January 2012).

Bi, H., Turner, J., Lambert, M.J., 2004. Additive biomass equations for native eucalypt forest trees of temperate Australia. Trees - Structure and Function 18, 467-479.

Bi, H., Long, Y., Turner, J., Lei, Y., Snowdon, P., Li, Y., Harper, R., Zerihun, A., Ximenes, F., 2010. Additive prediction of aboveground biomass for *Pinus radiata* (D. Don) plantations. Forest Ecology and Management 259, 2301-2314.

Burkhart, H.E., 1977. Cubic foot volume of loblolly pine to any merchantable top diameter. Southern Journal of Applied Forestry 1(2), 7-9.

Carvalho, J.P., Parresol, B.R., 2003. Additivity in tree biomass components of Pyrenean oak (*Quercus pyrenaica* Willd.). Forest Ecology and Management 179, 269-276.

CEN EN 14774-1:2009, Solid biofuels - Determination of moisture content – Oven dry method - Part 1: Total moisture - Reference method.

Chiyenda, S.S., Kozak, A., 1984. Additivity of component biomass regression equations when the underlying model is linear. Canadian Journal of Forest Research 14, 441-446.

Clutter, J.L., Fortson, J.C., Pienaar, L.V., Brister, G.H., Bailey, R.L., 1983. Timber management - a quantitative approach. John Wiley & Sons, New York, pp. 333.

Cohen, J., Cohen, P., West, S.G., Aiken, L.S., 2003. Applied Multiple Regression/Correlation Analysis for the Behavioral Sciences, Third ed. Lawrence Erlbaum Associates, Inc., Publishers, London.

Cunia, T., Briggs, R.D., 1984. Forcing additivity of biomass tables: some empirical results. Canadian Journal of Forest Research 14, 376-384.

Cunia, T., Briggs, R.D., 1985. Forcing additivity of biomass tables-use of the generalized least-square method. Canadian Journal of Forest Research 15, 23-28.

DNGF, 2010. 5º Inventário Florestal Nacional. Portugal Continental. 2005-2006. Relatório Final, Direcção Nacional de Gestão Florestal (DNGF). Autoridade Florestal Nacional. Ministério da Agricultura do Desenvolvimento Rural e das Pescas, Lisboa.

Fabião, A., Contribuição para o estudo da dinâmica da biomassa e produtividade primária líquida em eucaliptais. Região Litoral do Centro de Portugal. Tese de Doutoramento. Universidade Técnica de Lisboa, Instituto Superior de Agronomia, Lisboa., 1986.

Freire, J., Tomé, M., Tavares, M., 2003. Equação de Volume Local para a *Pinus pinaster* Aiton na Serra da Lousã. Silva Lusitana 11(2), 207-215.

Goicoa, T., Militino, A., Ugarte, M., 2011. Modelling aboveground tree biomass while achieving the additivity property. Environmental and Ecological Statistics 18, 367-384.

Honer, T.G., 1967. Standard volume tables and merchantable conversion factors for the commercial tree species of Central and Eastern Canada. Information Report FMR-X-5, Forest Management Research and Service Institute, Ottawa, Ontario, p. 21.

Husch, B., Beers, T.W., Kershaw, J.A., 2003. Forest mensuration, 4th ed. John Wiley & Sons, New Jersey, pp. 443.

Jenkins, J.C., Chojnacky, D.C., Heath, L.S., Birdsey, R.A., 2004. Comprehensive Database of Diameter-based Biomass Regressions for North American Tree Species. GTR-NE-319, USDA Forest Service, Northeastern Research Station.

Available online at: *http://www.fs.fed.us/ne/global/pubs/books/dia_biomass/index*, (Accessed May 2012).

Kozak, A., 1970. Methods for ensuring additivity of biomass components by regression analysis. The Forestry Chronicle 46, 402-404.

Lambert, M.C., Ung, C.H., Raulier, F., 2005. Canadian national tree aboveground biomass equations. Canadian Journal of Forest Research 35, 1996-2018.

Loetsch, F., Haller, K.E., Zöhrer, F., 1973. Forest inventory: Inventory data collected by terrestrial measurements. BLV Verlagsgesellschaft, Munchen, pp. 469

Marklund, L.G., 1987. Biomass functions for Norway spruce (Picea abies (l.) Karst.) in Sweden. Sveriges lantbruksuniversitet, Institutionen för skogstaxer-ing, Rapport 43., pp. 127.

Marklund, L.G., 1988. Biomass functions for pine, spruce and birch in Sweden. Report 45, Department of Forest Survey, The Swedish University of Agricultural Sciences. [in Swedish with an English summary] pp. 73.

Metla Project 3306, Database of treewise volume- and biomass equations for common European tree species, Available online at: *http://www.metla.fi/hanke/3306/tietokanta.htm*, (Accessed May 2012).

Meyer, H.A., 1953. Forest mensuration. Pennsylvania Valley Publishers, Inc., pp. 357.

Moon, H.R., Perron, B., 2008. seemingly unrelated regressions, in: Durlauf, S.N., Blume, L.E. (eds.), The New Palgrave Dictionary of Economics. Palgrave Macmillan, Basingstoke.

Motulsky, H., Christopoulos, A., 2003. Fitting models to biological data using linear e nonlinear regression: a pratical guide to curve fitting. GraphPad Software Inc., San Diego CA, pp. 351.

Näslund, M., 1947. Funktioner och tabeller för kubering av stående träd. Tall, gran och björk i södra Sverige samt i hela landet. (Functions and tables for computing of the cubic volume of standing trees. Pine. spruce and birch In southern Sweden. and in the whole of Sweden). (In Swedish with English summary). Meddelanden från Statens Skogsforskningsinstitut (National Forest Research Institute), Stockholm, Sweden, p. 81.

Ogaya, N., Kubierungsformeln und Bestandesmassenformeln, Univ. Freiburg i. Br., Thesis, 1968, pp. 85.

Ostrom, C.W., 1990. Time series analysis: regression techniques. Sage Publications.

Parresol, B.R., 1999. Assessing tree and stand biomass: a review with examples and critical comparisons. J For Sci 45, 573-593.

Parresol, B.R., 2001. Additivity of nonlinear biomass equations. Canadian Journal of Forest Research 31, 865-878.

Pereira, J.S., 2007. Uma espécie altamente produtiva, in: Desenvolvimento, P.C.S.S.F.L.-A.p.o. (ed.), Árvores e Florestas de Portugal. Pinhais e Eucaliptais - A Floresta Cultivada, vol. 4, Lisboa, pp. 167-183.

Prodan, M., 1965. Holzmesslehre. J. D. Sauerlaender´s Verlag, Frankfurt, pp. 644.

Prodan, M., Peters, R., Cox, F., Real, P., 1997. Mensura forestal. GTZ, FmbH: Instituto Interamericano de Cooperación para la Agricultura (IICA), San José, Costa Rica, pp. 586.

Radich, M.C., 2007. Introdução e expansão do eucalipto em Portugal, in: Público Comunicação Social SA / Fundação Luso-Americana para o Desenvolvimento (ed.), Árvores e Florestas de Portugal. Pinhais e eucaliptais - A Floresta Cultivada, vol. 4, Lisboa, pp. 151-165.

Rawlings, J.O., Pantula, S.G., Dickey, D.A., 1998. Applied Regression Analysis: A Research Tool, Second ed. Springer-Verlag New York, Inc.

Reed, D.D., Green, E.J., 1985. A method of forcing additivity of biomass tables when using nonlinear models. Canadian Journal of Forest Research 15, 1184-1187.

Ritz, C., Streibig, J.C., 2008. Nonlinear regression with R. Springer, pp. 144.

SAS Institute Inc., 2004. SAS/ETS ® 9.1 User's Guide. Volumes 1 and 2. SAS Institute Inc. Cary, New York.

Schabenberger, O., Pierce, F.J., 2002. Contemporary statistical models for the plant and soil sciences. CRC PRESS, Boca Raton.

Schumacher, F.X., Hall, F., 1933. Logarithmic expression of timber-tree volume. Journal of Agriculture Research 47(9), 719-734.

Silva, R., Tavares, M., Páscoa, F., 1991. Residual Biomass of Forest Stands. *Pinus pinaster* Ait. and *Eucaliptus globulus* Labill. 10th World Forestry Congress, 5, Food and Agriculture Organization of the United Nations, Paris.

Sit, V., Poulin-Costello, M., 1994. Catalogue of curves for curve fitting. Biometics Information. Handbook nº 4. Forest Science Research Branch. Ministry of Forests, Province of British Columbia, pp. 116.

Spurr, S.H., 1952. Forest inventory. Ronald Press, New York, pp. 476.

Srivastava, V.K., Giles, D.A., 1987. Seemingly unrelated regression equations models: estimation and inference, Dekker, New York.

Stoate, T.N., 1945. The Use of a Volume Equation in Pine Stands. Australian Forestry 9, 48-52.

Takata, K., 1958. Construction of universal diameter-height-curves. Journal of Japanese Forest Society 40: 1, 1-6.

Tsoumis, G.T., 1991. Science and Technology of wood. Structures, Properties, Utilization. Van Nostrand Reinhold, New York.

Viana, H., Cohen, W.B., Lopes, D., Aranha, J., 2010. Assessment of forest biomass for use as energy. GIS-based analysis of geographical availability and locations of wood-fired power plants in Portugal. Applied Energy 87, 2551-2560.

White, H., 1980. A heteroskedastic-consistent covariance matrix estimator and a direct test of heteroskedasticity. Econometrica 48, 817-838.

Zellner, A., 1962. An Efficient Method of Estimating Seemingly Unrelated Regression Equations and Tests of Aggregation Bias. Journal of the American Statistical Association 57, 348–368.

Zianis, D., Muukkonen, P., Mäkipää, R., Mencuccini, M., 2005. Biomass and stem volume equations for tree species in Europe, Silva Fennica Monographs 4. Finnish Society of Forest Science, p. 63.

5

Predictive equations for aboveground biomass and structural characteristics of Mediterranean shrubland

Data from this chapter contributed for the following publications:

[Annex C.1] Viana, H., Aranha, J., Lopes, D., Cohen, W.B., 2012. Estimation of crown biomass of *Pinus pinaster* stands and shrubland above-ground biomass using forest inventory data, remotely sensed imagery and spatial prediction models. Ecological Modelling 226, 22-35.

[Annex E.1] Viana, H., Fernandes, P., Rocha, R., Lopes, D., Aranha, J., 2009. Alometria, Dinâmicas da Biomassa e do Carbono Fixado em Algumas Espécies Arbustivas de Portugal 6º Congresso Florestal Nacional, Ponta Delgada, Açores. 6-9 Outubro, pp. 244-252.

[Annex E.2] Viana, H., Lopes, D., Aranha, J., 2009. Predição de biomassa arbustiva lenhosa empregando dados de inventário e o índice de diferença normalizada extraído em imagens Landsat 5 TM, ISPV Millenium. 37.

[Annex E.3] Aranha, J., Calvão, A., Lopes, D., Viana, H., 2011. Quantificação da biomassa consumida nos últimos 20 anos de fogos florestais no Norte de Portugal. Info 26, 44-49.

Abstract

A study for fuel characterization and development of predictive equations for shrubland aboveground biomass (AGB) estimation was carried out in a Mediterranean-type climate region. A field work and survey was conducted in Dão-Lafões, Tâmega and Serra da Estrela regions located in North-Center Portugal. Data was collected within 53 sample plots and the major native woody species occurring in this shrubland type: *Adenocarpus* sp. (adenocarpus), *Cytisus* sp. (broom), *Erica* sp. (heath), *Pterospartum tridentatum* (L.) Willk (aarquesia) and *Ulex* sp. (furze) were identified and characterized. Temporal evaluation (age) and direct measurements of structural parameters such as height (*h*) and percentage ground cover (*GC%*) was obtained. By destructive sampling, in circular sample plots with $10m^2$, shrubs were harvested, separated by specie and fresh biomass weighted (ton ha^{-1}). Laboratorial analyses of physical properties allowed calculation of the oven dry weight (dry ton ha^{-1}). Regression equations were established between total AGB and collected parameters, using ordinary least squares method. The goodness of fit achieving R^2= 0.85 in the best models assure a good predictive ability attending to the heterogeneity of the specific vegetation found in the studied shrubland. Further comparisons and validation were made with previous published equations for similar shrubland type.

Keywords: Mediterranean shrubland, aboveground biomass, regression equations, Dão-Lafões, Tâmega, Serra da Estrela, Portugal.

5.1 Introduction

Shrubland plays an important role in Mediterranean ecosystems as documented in several studies addressing diverse topics such as biodiversity (e.g. Pérez-Devesa et al., 2008), global climate change (e.g. Riera et al., 2007), biogeochemical cycling of carbon (e.g. Silva et al., 2006; Beier et al., 2009) or wildlife habitat evaluation (e.g. Beja et al., 2007). However, shrubland aboveground biomass (AGB) growing in a Mediterranean-type climate received particular attention in studies to determine fire spread prediction, fire behaviour, fire effects, hazard-reduction evaluation (e.g. Fernandes et al., 2000; Fernandes, 2001; Fernandes and Botelho, 2004; Vega et al., 2006) or studies on regrowth of the aboveground biomass (Baeza and Vallejo, 2007). With the increasing interest, in the last years, of using forest fuels as source of energy (Viana et al., 2010) the assessment of shrubland AGB gained even more attention.

The knowledge of shrubland AGB stocks and growth is essential in these studies but the nature, content and accuracy of this data is highly varied. Shrubland biomass may be measured directly using harvest techniques or estimated indirectly using a variety of non-destructive measurements and regression equations relating biomass to the measures (Husch et al., 2003). However, while herbaceous and dwarf shrubs species can be easily harvested to obtain biomass estimates, for most woody shrubs growing in Mediterranean regions this task is strongly limited by the bigger size of plants, the high heterogeneity of their structural form and by technical limitations caused by the stoniness and slope of the territories where normally these shrubs grow. As a result, biomass estimates in shrublands are commonly achieved from allometric equations. Several indirect relationships have been developed for many years as they prove being suitable and less time-consuming to estimate shrubland AGB (Whittaker and Woodwell, 1968; Brown, 1976; Uresk et al., 1977). In Mediterranean shrubland the most common correlation have been established, in numerous studies, with vegetation's age as compiled by Rambal (2001). For the typical shrub species occurring in the Iberian Peninsula as *Adenocarpus* sp. (adenocarpus), *Cytisus* sp. (broom), *Erica* sp. (heath), *Pterospartum tridentatum* (L.) Willk (carquesia) or *Ulex* sp. (furze), some equations to estimate shrubland AGB are published using this approach (Rego, 1986; Castro et al., 1996; Fernandes and Rego, 1996; Fernandes et al., 2002; Navarro Cerrillo and Blanco Oyonarte, 2006; Krivtsov et al., 2009; Aranha et al., 2011). Several equations relate phytomass with the apparent volume of shrubs (Armand et al., 1993; Pereira et al., 1995; Usó et al., 1997; Fernandes and Rego, 1998; Fernandes et al., 2002; Oyonarte and Cerrillo, 2003) and other studies establishes relationships with phytomass structural characteristics of individual plants such as stem diameter and height (Rego et al., 1994; Pereira et al., 1995; Baeza et al., 2006; Krivtsov et al., 2009). Despite the good correlations presented for some species, the estimation of shrubland AGB by this approach is relatively limited by the difficulty and time-consuming of measuring these individual parameters, particularly the stem diameter since the native woody plants studied generally have multiple basal stems growing from the same root system, as the *Erica* sp. or *Pterospartum tridentatum.* Other models for AGB estimation includes as independent variable shrubland characteristics such as mean vegetation height (*h*), and percentage ground cover (GC%) with good results (Fernandes and Rego, 1998; Fernandes et al., 2002; Viana et al., 2009b; Aranha et al., 2011). These last models have particular interest as their variables can easily be measured in the field, and most of the time it is difficult to determine the vegetation's age.

With the advent of remote sensing a different indirect approach to estimate AGB have been also investigated by relating forest and shrubland biomass and information extracted from satellite sensor data (e.g. Rahman et al., 2005; Aranha et al., 2008; Viana et al., 2009a; Calvão and Palmeirim, 2011; Shoshany and Karnibad, 2011; Viana et al., 2012). However, this approach is limited to experts in remote sensing and GIS tools, the collection of data in field are still necessary and, otherwise, these estimates carry an inherent uncertainty. So, allometric equations continue to be the easiest and accurate method to estimate indirectly AGB.

Although a regression equation developed for a specific site has generalized application in that ecosystem the same equation may not be valid in other areas. In order to minimize the errors of the estimates it may be needed to validate these equations by independent sampling in the areas under study. Hence, this study aims to derive specific allometric equations to predict shrubland AGB in North-Center Portugal and validate and compare previous published equations for estimating shrubland AGB in similar Mediterranean-type climate regions.

5.2 Methods and data

5.2.1 Study area

The data used to fit shrub biomass equations was collected in three different NUT III (Nomenclature of Territorial Units for Statistics) sub-regions in the North-Center Portugal (Dão-Lafões, Tâmega and Serra da Estrela) (Figure 5.1). In these regions, the forest cover is composed mainly by *Pinus pinaster* (maritime pine) and *Eucalyptus globulus* (eucalyptus) stands, and the shrubland occupies the major extensions of the 1.9 million hectares existing in Portuguese territory (DNGF, 2010).

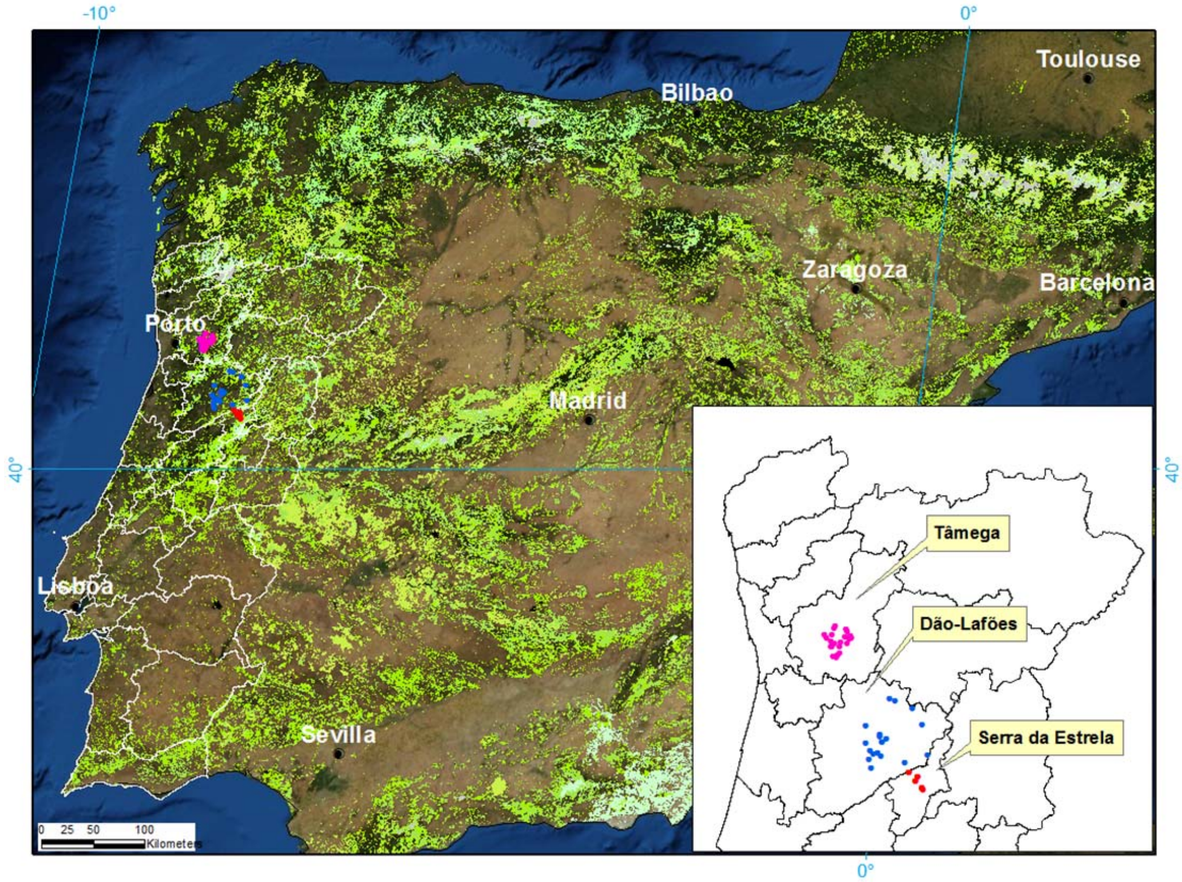

Figure 5.1 - Location of the shrubland sample plots in the NUT III sub-regions.

After a spatial analysis of the wildfires occurrence (AFN, 2011), from 1990 to 2007 (year of data collection), an inventory sampling was applied within the areas burned only one time in the years before 2007 (Figure 5.2) and occupying homogeneously at least one hectare. Under these assumptions, in the NUT III regions of Dão-Lafões and Tâmega, it was possible to identify burned areas from the year 2000 to 2006. In the NUT III region of Serra da Estrela only areas burned from 2002 to 2006 were identified. In the sample plots from 2006 (shrubs with one year) the vegetation presented small growths and low percentage ground cover. Hence, only the shrubland vegetation from 2000 (with 7 years) to 2005 (with 2 years) was considered in the study.

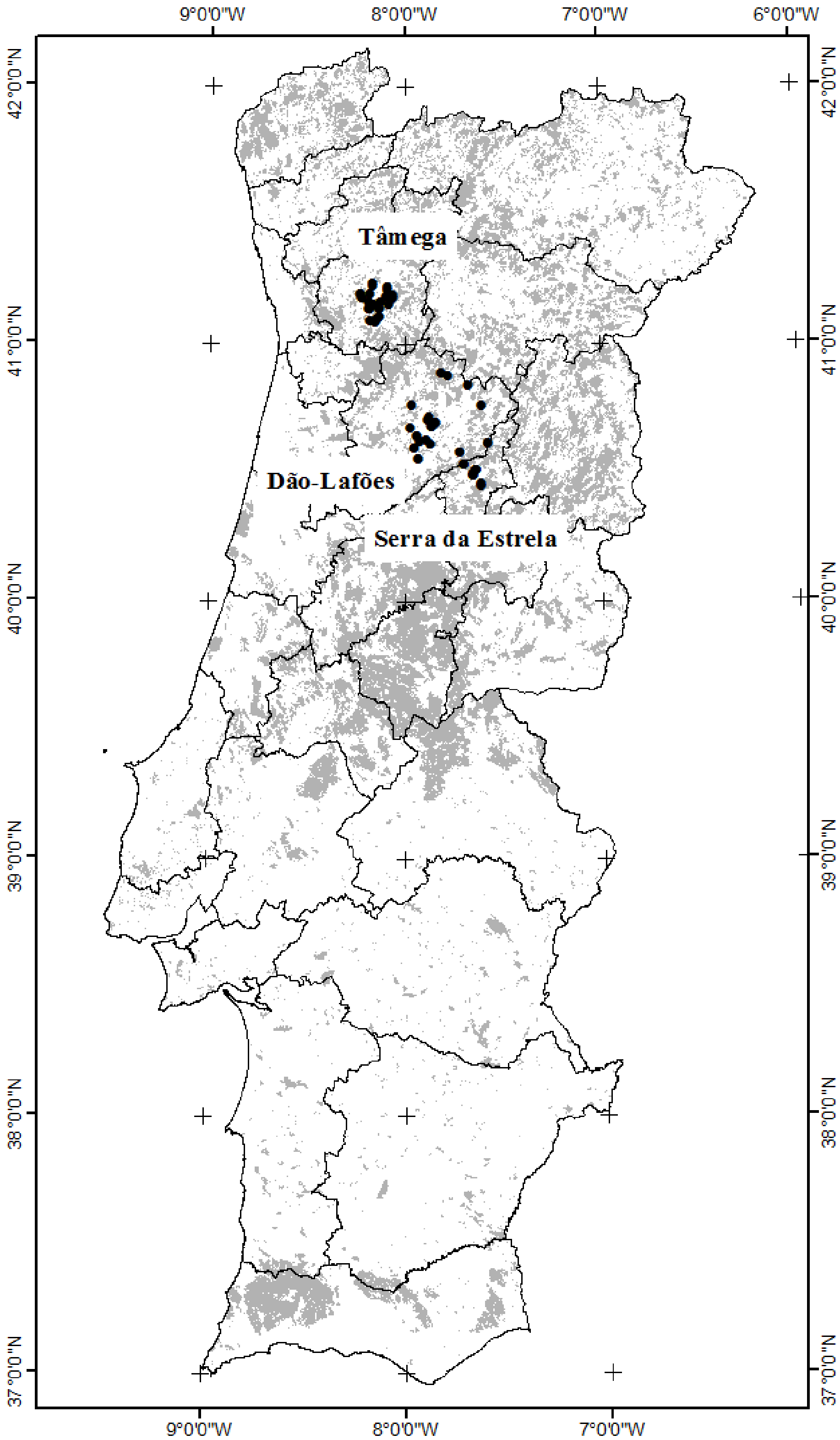

Figure 5.2 - Burnt areas in Portugal from 1990 to 2007 and sample plots location.

5.2.2 Field data collection

A total of 53 sample plots were established in Dão-Lafões, Tâmega and Serra da Estrela regions (18, 23 and 12 sample plots, respectively) and vegetation parameters (e.g. height, crown area, percentage ground cover, etc.) were measured and shrub biomass weighted, using the destructive approach.

The percentage of ground cover was estimated using the line intersection technique. Two transects with 25 meters were implemented in the directions North-South and East-West. In each transect, the length intercepted by the vertical projection of species was measured and the percentage of ground cover was estimated as the ratio of interception length (*I*) to total transect length (L), as (Eq. 1) (Husch et al., 2003):

$$percent\ cover = 100\frac{\sum I}{\sum L} \qquad [1]$$

Within circular plots with an area of 10m^2, the most representative woody shrub species present in each plot (adenocarpus, broom, heath, carquesia and furze) were clipped, separated by species and weighted to determine the biomass per hectare (ton ha^{-1}). A sample of each species was collected and placed into hermetically closed containers to prevent moisture loss, and sent to the laboratory. The moister content was determined following the Technical Specification (DD CEN/TS 14774-1:2004) supersedes by the European Standard (CEN EN 14774-1:2009), which consists in to drying the sample in a drying oven at a temperature within the range of (105 ± 2)°C, in air atmosphere, until constant mass is achieved. After achieving the percentage of moisture, calculated from the loss in mass of the sample, the dry biomass of shrubs (dry ton ha^{-1}) was determined.

5.2.3 Shrubland aboveground biomass models

Plant growth analysis and model fitting of their growth over time was widely investigated (e.g. Causton and Venus, 1981; Hunt, 1982). Nevertheless, many equations have been derived to model plant growth over time, biomass accumulation are commonly described by an exponential or power-function as they seem to explain well the relationship between biomass growths with the temporal change. These models present also strong correlations between biomass stocks and other shrub structural characteristics (e.g. Brown, 1976; Armand et al., 1993; Castro et al., 1996). Hence, these and other regression equations were tested and compared. Linear and non-linear models to predict shrub biomass (ton ha^{-1}) were fitted by the ordinary least squares linear regression analysis using as independent variables the vegetation parameters collected in the field. The non-linear models were linearized by logarithmic transformation, thus overcoming the typical heteroscedasticity of residuals found in the biomass equations (Parresol, 1999, 2001). Nevertheless the logarithmic form of non-linear equations allows to obtain the homoscedasticity of residuals, this transformation produces a systematic underestimation of the dependent variable (Y) when converting the estimated $\ln Y$ back to the original untransformed scale (Y) (Dimitris and Maurizio, 2003). Therefore, several procedures for correcting bias in logarithmic regression estimates have been proposed (e.g. Finney, 1941; Meyer, 1942; Baskerville, 1972; Beauchamp and Olson, 1973; Yandle and Wiant Jr, 1981; Sprugel, 1983; Snowdon, 1991).

Zeng and Tang (2011) comparing several correcting factors recommended the use of a new correction factor or the one proposed by Baskerville (1972). Hence, for example, for the most commonly used power form equation:

$$W_i = \beta_1 x^{\beta_2} \quad [2]$$

the logarithmic transformation comes:

$$lnW_i = ln\beta_0 + \beta_1 lnx \quad [3]$$

so, the back conversion to the original untransformed scale should come as:

$$W_i = e^{ln\beta_0 + \beta_1 lnx + CF} \quad [4]$$

where CF is the correction factor calculated as:

$$CF = SEE^2/2 \quad [5]$$

and SEE is the standard error of the regression estimate, obtained as:

$$SEE = \sqrt{\frac{\sum_1^n (y_i - \hat{y}_i)^2}{n-p}} \qquad [6]$$

where: y_i is the observed value; $\hat{y}_i$ is the predicted value for observation *i*; *n* is the number of observations and *p* is the number of parameters fitted by the regression.

In order to derive a set of allometric equations to predict the shrubland AGB, several models, with different functional form, were compiled in the literature review and fitted to our dataset. Several equations, usually applied to predict individual tree volume and aboveground biomass, were compiled from previous published studies (e.g. Zianis et al., 2005) and from existing databases (e.g. Jenkins et al., 2004; Metla Project 3306, 2006). The model forms of previous published allometric equations derived by other authors to predict similar Mediterranean shrubland AGB were also fitted to our data (Rego, 1986; Fernandes and Rego, 1996, 1998; Rambal, 2001; Fernandes et al., 2002; Aranha et al., 2011). Furthermore, these equations were also applied to our data and their performance validated and compared with the final models derived in this research.

After performing a Pearson Product Moment Correlation (so-called Pearson's correlation) between the vegetation variables and the shrub biomass weight (ton ha^{-1}) the independent variables better correlated were the age (*t*) the mean height (*h*) (weighted according the percentage of each species present in the sample plot) and the percentage ground cover (*GC%*). On the other hand, despite some individual dendrometric variables as stem diameter or basal area are well correlated with shrubland biomass (Pereira et al., 1995; Baeza et al., 2006), these are not easily measured in the studied species. Hence, only age (*t*), height (*h*) and ground cover (*GC%*) were included in the regression models independently and combined. Additionally to the common regression models a stepwise regression was conducted using the JMP Statistical Discovery Software (SAS Institute, 2007) in order to search and select new possible models. Table 5.1 only present the models to predict shrub aboveground biomass with best performance in the fitting stage.

Table 5.1 - Regression models fitted to predict the shrubland aboveground biomass.

Model	Equation	Transformation	Independent variables
1	$W_i = \beta_0 + \beta_1 t^2$		*t*
2	$W_i = at^k = e^{ln\beta_0 + \beta_1 lnt}$	$lnW_i = ln\beta_0 + \beta_1 lnt$	*t*
3	$W_i = ae^{kt} = e^{\beta_0 + \beta_1 t}$	$lnW_i = \beta_0 + \beta_1 t$	*t*
4	$W_i = \beta_0 + \beta_1 t^2 + \beta_2 h^2$		*t, h*
5	$W_i = e^{\beta_0 + \beta_1 lnt + \beta_2 h^2}$	$lnW_i = \beta_0 + \beta_1 lnt + \beta_2 h^2$	*t, h*
6	$W_i = e^{ln\beta_0 + \beta_1 ln(th)}$	$lnW_i = ln\beta_0 + \beta_1 ln(th)$	*t, h*
7	$W_i = \beta_0 + \beta_1 t^2 + \beta_2 (tGC)^2$		*t, GC*
8	$W_i = e^{ln\beta_0 + \beta_1 ln(tGC)}$	$lnW_i = ln\beta_0 + \beta_1 ln(tGC)$	*t, GC*
9	$W_i = e^{\beta_0 + \beta_1 t^2 + \beta_2 (tGC)^2}$	$lnW_i = \beta_0 + \beta_1 t^2 + \beta_2 (tGC)^2$	*t, GC*
10	$W_i = e^{ln\beta_0 + \beta_1 ln(hGC)}$	$lnW_i = ln\beta_0 + \beta_1 ln(hGC)$	*h, GC*
11	$W_i = \beta_0 + \beta_1 h^2 + \beta_2 GC^2$		*h, GC*
12	$W_i = e^{\beta_0 + \beta_1 lnh + \beta_2 GC}$	$lnW_i = \beta_0 + \beta_1 lnh + \beta_1 GC$	*h, GC*
13	$W_i = e^{\beta_0 + \beta_1 t^2 + \beta_2 \ln(hGC)}$	$lnW_i = \beta_0 + \beta_1 t^2 + \beta_2 \ln(hGC)$	*t, h, GC*
14	$W_i = \beta_0 + \beta_1 lnGC + \beta_2 (th)^2$		*t, h, GC*
15	$W_i = \beta_0 + \beta_1 t^2 + \beta_2 (hGC)^2$		*t, h, GC*
16	$W_i = \beta_0 + \beta_1 t^2 + \beta_2 h^2 + \beta_3 GC^2$		*t, h, GC*
17	$W_i = e^{\beta_0 + \beta_1 lnt + \beta_2 h^2 + \beta_3 GC}$	$lnW_i = \beta_0 + \beta_1 lnt + \beta_2 h^2 + \beta_3 GC$	*t, h, GC*

where: W_i is the biomass of shrubland (dry ton ha^{-1}); *t* is the age after wildfire; *h* is the shrubs mean height (m); *GC* is the percentage ground cover (%) and $\beta_0, \beta_1, \beta_2, \beta_3$ are the equation parameter estimates.

5.2.4 Validation and comparison of the derived shrubland AGB models

The shrubland aboveground biomass models were fitted by ordinary least squares (OLS) and the residuals of estimates $e_i = (y_i - \hat{y}_i)$ (difference between the observed and estimated values) were calculated for each equation. The graph analysis (i.e. scatterplots of residuals against the predicted values; scatterplots of residuals against individual predictors and histogram of residuals) and the statistics of regression residuals were examined to check if model assumptions were satisfied (Ostrom, 1990; Rawlings et al., 1998; Ritz and Streibig, 2008).

The following statistical criteria obtained from the residuals were analysed (Sit and Poulin-Costello, 1994): mean absolute error (MAE); residual mean squares error (MSE) defined as the mean of the predicted residual sum of squares (SSE); root mean squared error (RMSE); coefficient of determination (R^2); and adjusted coefficient of determination (R^2_{adj}), (Eqs. 7-11), in order to evaluate each equation's efficiency and their accuracy to estimate shrubland AGB.

Usually, the best model is selected based on measures of goodness-of-fit like the coefficient of determination (R^2_{adj}). However, when the models to be compared do not have the same functional form of the dependent variable, the Furnival Index (FI) (Furnival, 1961) is invariably used to choose the best fitting equation. Hence, the best allometric equations, derived in this study, were selected using FI as main criterion for model comparison, but also taking in account the described statistics, calculated as:

$$MAE = \frac{\sum_1^n |y_i - \hat{y}_i|}{n} = \frac{\sum_1^n |e_i|}{n} \quad [7]$$

$$MSE = \frac{SSE}{n-p} = \frac{\sum_1^n (y_i - \hat{y}_i)^2}{n-p} = \frac{\sum_1^n (e_i)^2}{n-p} \quad [8]$$

$$RMSE = \sqrt{MSE} \quad [9]$$

$$R^2 = 1 - \frac{SSE}{SST} = 1 - \frac{\sum_1^n (y_i - \hat{y}_i)^2}{\sum_1^n (y_i - \bar{y})^2} \quad [10]$$

$$R^2_{adj} = 1 - \frac{SSE*(n-1)}{SST*(n-p)} = 1 - \left[(1 - R^2) * \frac{n-1}{n-p}\right] \quad [11]$$

where: y_i is the observed value; $\hat{y}_i$ is the predicted value for observation *i*; $\bar{y}$ is the mean of the observed values; *n* is the number of observations used to fit the model and *p* is the number of model parameters.

Furnival Index (Eq. 12) is computed as follows (FAO, 1999): the value of the square root of error mean square (MSE) is obtained for each model under consideration through analysis of variance. The geometric mean of the derivative of the dependent variable with respect to *y* is obtained for each model from the observations. Geometric mean of a set of *n* observations is defined by the *n*th root of the product of the observations. The FI for each model is then obtained by multiplying the corresponding values of the square root of mean square error with the inverse of the geometric mean. For instance, the derivative of ln *y* is (1/*y*) and the FI in that case would be:

$$Furnival\ index = \sqrt{MSE}\left(\frac{1}{Geometric\ mean(y^{-1})}\right) \quad [12]$$

Note: Smaller values of the index indicate a better fit.

The developed models were further compared with equations to estimate shrubland AGB, previous published by other authors. These models were developed for similar Mediterranean shrubland. Almost all equations describe the relationship of biomass accumulation over time using the exponential asymptotic (monomolecular) functional form. Other equations were derived using the same independent variables (*h, GC%*) as the ones considered in this research (Table 5.2).

Table 5.2 - Equation models to estimate shrubland AGB in Mediterranean regions.

Equation model	Vegetation	Site	*n*	R^2	*RMSE*	Source
$W_i = 14.43(1 - e^{(-0.18t)})$	*Chamaespartium tridentatum and Erica umbellata*	NW Portugal	-	-	-	(Fernandes and Rego, 1996)
$W_i = 0.443(hGC)^{0.881}$	*Chamaespartium tridentatum and Erica umbellata*	NW Portugal	7	0.92	0.10	(Fernandes and Rego, 1998)
$W_i = 2880(1 - e^{(-0.0896t)})$	*Several Mediterranean shrub species*	Mediterranean type regions	85	0.35	-	(Rambal, 2001)
$W_i = 14.242(1 - e^{(-0.211t)})$ *(shrubs<6 mm)*	*Ulex minor and Chamaespartium tridentatum*	NW Portugal	77	0.95	2.57	(Fernandes et al., 2002) - A
$W_i = 0.555(hGC)^{0.743}$	*Chamaespartium tridentatum, Erica umbellata, Ulex europaeus, Ulex minor, Erica arborea*	North-Center Portugal and NW Spain	66	0.60	3.71	(Fernandes et al., 2002) - B
$W_i = 2.002 - 1.411t + 0.553t^2 - 0.0241t^3$	*Cytisus sp., Erica sp., Pterospartum tridentatum (L.) Willk and Ulex sp.*	North Portugal	50	0.83	2.81	(Aranha et al., 2011) - A
$W_i = e^{(-1.298+1.861\ln t+0.1265\ln h)}$	*Cytisus sp., Erica sp., Pterospartum tridentatum (L.) Willk and Ulex sp.*	North Portugal	50	0.87	2.71	(Aranha et al., 2011) - B
$W_i = e^{(2.070+0.504\ln t+0.057\ln h+1.513\ln GC)}$	*Cytisus sp., Erica sp., Pterospartum tridentatum (L.) Willk and Ulex sp.*	North Portugal	50	0.91	2.74	(Aranha et al., 2011) - C
$W_i = 29.65(1 - e^{(-0.157t)})$	*Pterospartum tridentatum*	Center -East Portugal				(Krivtsov et al., 2009)-A
$W_i = 35.57(1 - e^{(-0.0065t)})$	*Cistus ladanifer*, *Cistus ladanifer* x *Erica australis*	Center -East Portugal				(Krivtsov et al., 2009)-B
$W_i = 37.24(1 - e^{(-0.176t)})$	*Erica australis*	Center -East Portugal				(Krivtsov et al., 2009)-C
$W_i = 16.75(1 - e^{(-0.009t)})$	*Erica umbellatta*	Center -East Portugal				(Krivtsov et al., 2009)-D

where: W_i is the biomass of shrubland (dry ton ha^{-1}); *t* is the vegetation age; *h* is the shrubs mean height (m); *GC* is the percentage ground cover (%).

5.3 Results and discussion

5.3.1 Characteristics of shrubland vegetation

The characteristics of the shrubs measured in the three sites studied: Dão-Lafões, Tâmega and Serra da Estrela, and the global average (53 sample plots) are presented in Table 5.3.

Table 5.3 - Descriptive statistics of the shrub species measured in the sample plots.

Site	Weight-fresh (ton ha^{-1})				Weight-dry (ton ha^{-1})				Height (m)				Ground cover (%)			
Dão-Lafões (n=18)	**Mean**	**Min**	**Max**	**SD**	**Mean**	**Min**	**Max**	**SD**	**Mean**	**Min**	**Max**	**SD**	**Mean**	**Min**	**Max**	**SD**
Cytisus sp.	13.4	1.0	32.1	8.2	6.4	0.5	15.3	4.0	0.8	0.3	1.3	0.3	48.5	11.7	84.7	23.1
Ulex sp.	5.3	1.5	11.0	2.8	2.7	0.7	5.3	1.4	0.6	0.2	1.0	0.3	26.1	7.1	47.9	12.3
Erica sp.	4.9	3.0	9.4	3.0	2.6	1.5	5.5	1.7	0.7	0.2	1.1	0.4	21.4	10.2	54.9	17.2
Pterospartum	2.9	1.0	5.5	2.3	1.6	0.6	2.9	1.2	0.2	0.1	0.3	0.1	12.0	3.5	16.8	7.3
Adenocarpus sp.																
Total average	14.4	1.5	32.1	8.3	7.1	0.7	15.3	4.0	0.7	0.1	1.3	0.3	59.9	16.8	99.6	25.1
Tâmega (n=23)																
Cytisus sp.	12.4	1.2	28.6	9.3	6.4	0.6	15.1	5.0	1.2	0.6	1.7	0.3	44.8	6.2	99.3	26.8
Ulex sp.	13.9	1.6	33.2	10.0	7.5	0.9	18.6	5.4	0.8	0.3	1.5	0.3	39.1	6.2	84.7	27.0
Erica sp.	4.1	0.4	8.2	3.5	2.1	0.2	4.1	1.7	0.6	0.2	1.5	0.6	23.5	2.7	59.0	24.9
Pterospartum																
Adenocarpus sp.	10.6	5.4	13.2	4.5	5.3	3.0	7.0	2.0	1.2	0.5	1.6	0.5	31.4	18.6	44.3	11.6
Total average	18.0	1.9	33.2	9.3	9.5	1.1	18.6	4.9	1.0	0.4	1.6	0.4	60.9	15.1	99.3	23.9
Serra da Estrela (n=12)																
Cytisus sp.	5.7	3.4	10.2	2.0	2.8	1.6	5.1	1.0	0.7	0.4	1.0	0.2	69.9	41.9	97.1	18.3
Ulex sp.	0.2	0.2	0.2		0.1	0.1	0.1		0.4	0.4	0.4		8.0	8.0	8.0	
Erica sp.																
Pterospartum																
Adenocarpus sp.																
Total average	5.7	3.4	10.2	2.0	2.8	1.6	5.1	1.0	0.7	0.4	1.0	0.2	70.6	41.9	97.1	18.2
Global (3 sites) (n=53)																
Cytisus sp.	10.7	1.0	32.1	8.0	5.3	0.5	15.3	4.1	0.9	0.3	1.7	0.4	53.4	6.2	99.3	25.2
Ulex sp.	9.9	0.2	33.2	8.9	5.3	0.1	18.6	4.9	0.7	0.2	1.5	0.3	32.6	6.2	84.7	22.8
Erica sp.	4.6	0.4	9.4	3.0	2.4	0.2	5.5	1.6	0.7	0.2	1.5	0.4	22.3	2.7	59.0	19.3
Pterospartum	2.9	1.0	5.5	2.3	1.6	0.6	2.9	1.2	0.2	0.1	0.3	0.1	12.0	3.5	16.8	7.3
Adenocarpus sp.	10.6	5.4	13.2	4.5	5.3	3.0	7.0	2.0	1.2	0.5	1.6	0.5	31.4	18.6	44.3	11.6
Total average	14.0	1.5	33.2	9.1	7.2	0.7	18.6	4.8	0.8	0.1	1.6	0.4	62.7	15.1	99.6	23.1

The fresh weight of shrubland biomass averages 14 ton ha^{-1}, in the 53 sample plots, achieving higher values in Tâmega region (18 ton ha^{-1}), followed by Dão-Lafões region (14.4 ton ha^{-1}), and Serra da Estrela (5.7 ton ha^{-1}). The oven dried biomass, calculated with the moister content determined in laboratory, ranges from 9.5, 7.1 and

2.8 dry ton ha^{-1} in Tâmega, Dão-Lafões and Serra da Estrela regions, respectively. The vegetation's mean height (m) was obtained by the weighted average of each species height, according to the percentage of occupation (GC%) in the field sample plot. The mean height was superior in Tâmega (1 m), followed by Dão-Lafões (0.7 m) and Serra da Estrela (0.7 m) region. The average percentage ground cover was higher in Serra da Estrela (70.6%) and very similar in Tâmega and Dão-Lafões sample plots (60.9 and 59.9%, respectively).

Figures 5.3 to 5.5, show the composition of shrub species (percentage) observed in each sample plot, in the studied regions. The *Cytisus* sp. and *Ulex* sp. are the most common species, being many times the only species present in the plots, as observed in the sample plots measured in the Serra da Estrela region.

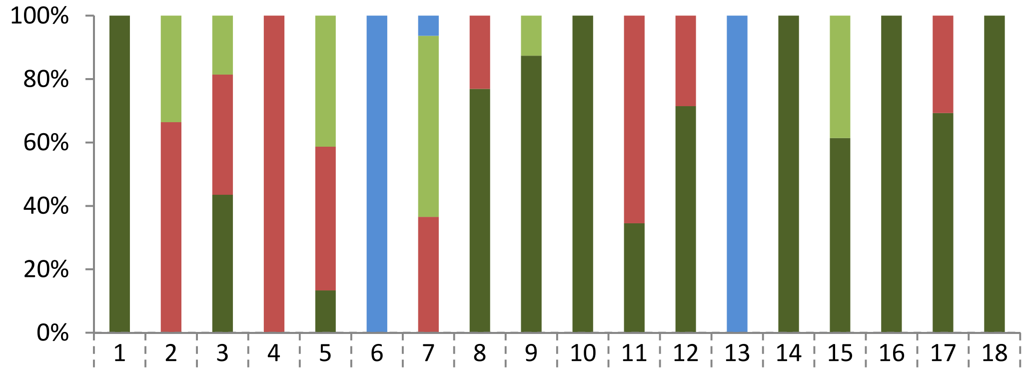

	1	2	3	4	5	6	7	8	9	10	11	12	13	14	15	16	17	18
Pterospartum						2.9	0.6						1.3					
Erica sp.		1.6	1.6		1.5		5.5		1.6						4.0			
Ulex sp.		3.2	3.2	0.7	1.6		3.5	1.5			5.3	3.1					2.3	
Cytisus sp.	5.9		3.7		0.5			4.9	11.	15.	2.8	7.9		6.8	6.4	10.	5.2	2.8

Figure 5.3 - Occurrence of species in the measured sample plots in the Dão-Lafões region. The table attached indicates the dry biomass (ton ha^{-1}).

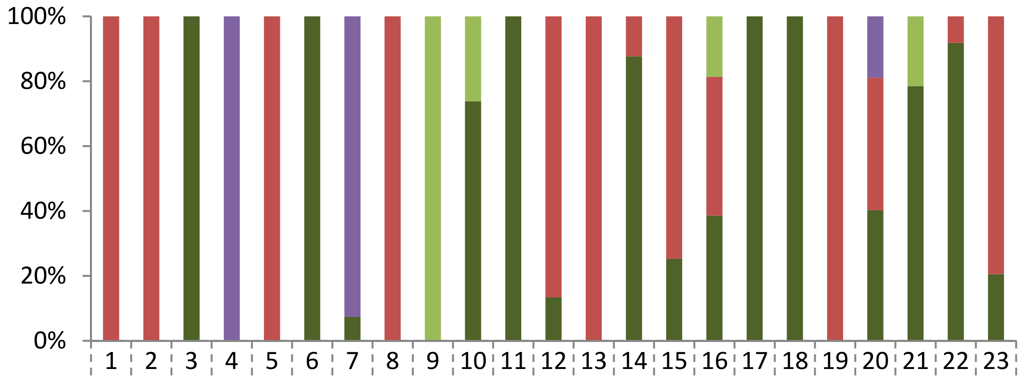

	1	2	3	4	5	6	7	8	9	10	11	12	13	14	15	16	17	18	19	20	21	22	23
Adenocarpus sp.				5.9			7.0													3.0			
Erica sp.									4.1	2.9						1.3					0.2		
Ulex sp.	18.	16.			3.2			10.				7.2	9.4	2.1	10.	3.0			4.7	6.5		0.9	4.5
Cytisus sp.			3.6			7.2	0.6			8.2	8.2	1.1		15.	3.6	2.7	12.	14.		6.4	0.9	9.9	1.2

Figure 5.4 - Occurrence of species in the measured sample plots in Tâmega region.

The table attached indicates the dry biomass (ton ha^{-1}).

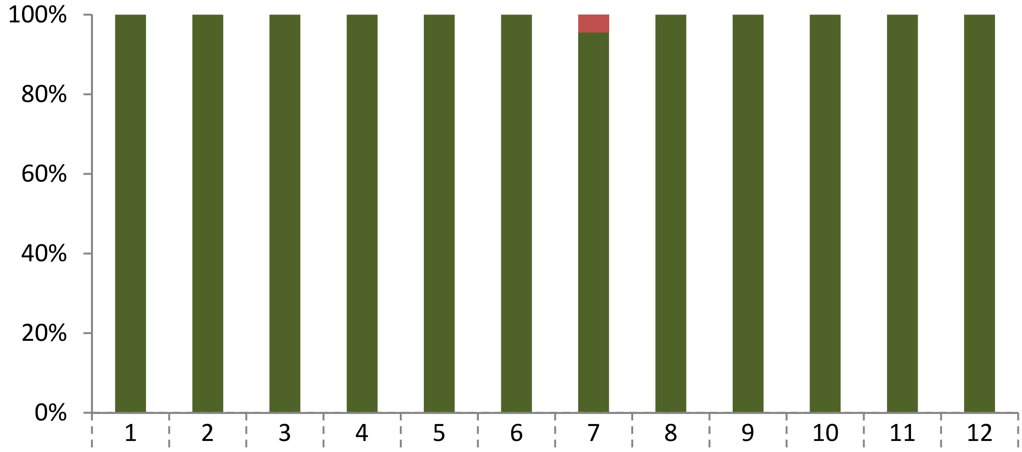

	1	2	3	4	5	6	7	8	9	10	11	12
Ulex sp.							0.1					
Cytisus sp.	4.4	5.1	3.0	2.8	3.2	2.5	2.3	2.4	2.3	2.0	1.9	1.6

Figure 5.5 - Occurrence of species in the measured sample plots in Serra da Estrela region.

The table attached indicates the dry biomass (ton ha^{-1}).

Table 5.4 shows the statistics of the vegetation at each site grouped by age. In Dão-Lafões and Tâmega regions the measurements were made in vegetation with 2-7 years, and in Serra da Estela with 2-5 years. The Tâmega region presented, the highest biomass weights (4 to 31.7 fresh ton ha^{-1}) and (2.2 to 16.8 dry ton ha^{-1}) and Serra da Estrela de lowest values (3.8 to 8.3 fresh ton ha^{-1}) and (1.8 to 4.2 dry ton ha^{-1}). The global sample plots ranged from (3.6 to 26.5 fresh ton ha^{-1}) and (1.8 to 13.6 dry ton ha^{-1}). The average height of vegetation is similar in the three regions however, analysing the most common species (*Cytisus sp.* and *Ulex sp.*) can be seen that in Tâmega region, these have higher growth for all ages.

Table 5.4 - Characteristics of shrubs sampled in the three sites of study grouped by vegetation's age.

Site	Weight-fresh (ton ha^{-1})						Weight-dry (ton ha^{-1})						height (m)						Ground Cover (%)					
Dão-Lafões																								
Sample plots (n=18)	3	2	3	4	2	4	3	2	3	4	2	4	3	2	3	4	2	4	3	2	3	4	2	4
Age of shrubs	2	3	4	5	6	7	2	3	4	5	6	7	2	3	4	5	6	7	2	3	4	5	6	7
Cytisus sp.		6.0	7.4	11.4	15.0	25.0		2.8	3.5	5.5	7.1	12.2	0.3	0.5	0.6	0.9	1.0	1.1	20.4	35.8	33.5	53.3	64.3	66.1
Ulex sp.	1.5	11.0	3.5	5.6	6.5	7.2	0.7	5.3	1.8	3.2	3.1	3.5	0.2	0.5	0.8	0.6	0.9	0.6	25.3	47.9	16.3	26.6	18.2	41.2
Erica sp.			3.0	3.1	8.0	6.2			1.5	1.6	4.0	3.5			1.0	0.3	1.1	0.7			11.1	10.6	17.7	39.2
Pterospartum	3.8					1.0	2.1					0.6	0.2					0.3	16.2					3.5
Adenocarpus sp.																								
Total average	3.0	11.5	11.9	12.9	22.3	23.9	1.6	5.5	5.8	6.5	10.7	12.0	0.2	0.4	0.7	0.7	1.0	1.0	26.0	59.7	53.5	58.6	82.2	80.4
Tâmega																								
Sample plots (n=23)	2	3	5	6	5	2	2	3	5	6	5	2	2	3	5	6	5	2	2	3	5	6	5	2
Age of shrubs	2	3	4	5	6	7	2	3	4	5	6	7	2	3	4	5	6	7	2	3	4	5	6	7
Cytisus sp.	1.5	11.9	7.5	14.6	12.7	28.6	0.9	5.9	3.7	7.8	6.4	15.1	1.1	1.1	1.1	1.4	1.1	1.6	12.4	37.0	29.1	62.4	45.2	68.3
Ulex sp.	6.0		10.1	9.8	20.0	17.4	3.2		5.6	5.2	10.8	9.3	0.5		0.8	1.0	0.9	0.7	21.7		36.8	52.5	36.2	37.0
Erica sp.	0.4		5.2	5.8			0.2		2.7	2.9			0.2		0.4	1.5			2.7		40.6	10.4		
Pterospartum																								
Adenocarpus sp.		13.2		13.2	5.4			5.9		7.0	3.0			1.0		1.3	1.4			31.3		44.3	18.6	
Total average	4.0	12.3	12.6	17.8	27.2	31.7	2.2	5.9	6.7	9.4	14.3	16.8	0.8	1.0	0.8	1.2	1.0	1.1	18.4	45.5	55.8	76.9	68.9	71.1
Serra da Estrela																								
Sample plots (n=12)	3	3	3	3			3	3	3	3			3	3	3	3			3	3	3	3		
Age of shrubs	2	3	4	5			2	3	4	5			2	3	4	5			2	3	4	5		
Cytisus sp.	3.8	4.9	5.8	8.3			1.8	2.3	2.8	4.2			0.4	0.6	0.8	1.0			46.8	64.6	73.1	95.1		
Ulex sp.		0.2						0.1						0.4						8.0				
Erica sp.																								
Pterospartum																								
Adenocarpus sp.																								
Total average	3.8	5.0	5.8	8.3			1.8	2.4	2.8	4.2			0.4	0.5	0.8	1.0			46.8	67.3	73.1	95.1		
Global (3 sites)																								
Sample plots (n=53)	8	8	11	13	7	6	8	8	11	13	7	6	8	8	11	13	7	6	8	8	11	13	7	6
Age of shrubs	2	3	4	5	6	7	2	3	4	5	6	7	2	3	4	5	6	7	2	3	4	5	6	7
Cytisus sp.	3.3	7.2	6.9	11.8	13.5	25.9	1.6	3.5	3.3	6.0	6.6	13.0	0.5	0.7	0.8	1.1	1.0	1.2	34.6	48.5	45.2	69.5	51.6	66.6
Ulex sp.	3.8	5.6	6.8	8.1	17.3	14.0	2.0	2.7	3.7	4.4	9.2	7.4	0.3	0.4	0.8	0.8	0.8	0.6	23.5	27.9	26.5	42.1	32.6	38.4
Erica sp.	0.4		4.4	4.0	8.0	6.2	0.2		2.3	2.0	4.0	3.5	0.2		0.6	0.7	1.1	0.7	2.7		30.7	10.5	17.7	39.2
Pterospartum	3.8					1.0	2.1					0.6	0.2					0.3	16.2					3.5
Adenocarpus sp.		13.2		13.2	5.4			5.9		7.0	3.0			1.0		1.3	1.4			31.3		44.3	18.6	
Total average	3.6	9.4	10.6	14.1	25.8	26.5	1.8	4.5	5.4	7.3	13.3	13.6	0.4	0.7	0.8	1.0	0.9	1.0	31.9	57.2	59.9	75.5	72.7	77.3

5.3.2 Equations fitted to the shrubland aboveground biomass

The computed statistics of the fitted models (Table 5.1) for the three regions (Dão-Lafões, Tâmega and Serra da Estrela) and for the Global data are presented in Tables 5.5 to 5.8. The models that fitted better the data, for each group of independent variables used in the models, are shaded in the tables.

The values of calculated statistics: Mean, MAE, MSE and RMSE for models 1, 4, 7, 11, 14, 15 and 16 are in dry ton ha^{-1}. The values achieved for models 2, 3, 5, 6, 8, 9, 10, 12, 13 and 17 are presented in logarithmic values, according to the mathematical expression transformation (see Table 5.1).

Table 5.5 - Statistics of the fitted models to predict the shrubland AGB in Dão-Lafões region.

Model	Mean	MAE	MSE	RMSE	RMSE (%)	R^2	R^2_{adj}	FI
1	7.1	1.6	4.2	2.04	28.5	0.758	0.743	2.04
2	1.7	0.3	0.2	0.41	20.8	0.760	0.745	2.32
3	1.7	0.3	0.2	0.45	23.1	0.703	0.684	2.58
4	7.1	1.5	3.8	1.94	27.2	0.794	0.766	1.94
5	1.7	0.3	0.2	0.42	21.3	0.764	0.732	2.38
6	1.7	0.2	0.1	0.35	17.8	0.825	0.814	1.99
7	7.1	1.6	4.3	2.08	29.1	0.763	0.732	2.08
8	1.7	0.3	0.1	0.38	19.1	0.797	0.785	2.13
9	1.7	0.4	0.3	0.53	26.8	0.627	0.578	2.99
10	1.7	0.2	0.1	0.32	16.3	0.853	0.843	1.82
11	7.1	1.4	3.4	1.84	25.7	0.815	0.790	1.84
12	1.7	0.2	0.1	0.33	16.6	0.857	0.838	1.85
13	1.7	0.2	0.1	0.31	15.9	0.869	0.851	1.77
14	7.1	1.2	2.5	1.58	22.1	0.864	0.846	1.58
15	7.1	1.5	4.0	2.00	27.9	0.782	0.753	2.00
16	7.1	1.3	3.3	1.81	25.3	0.846	0.813	1.81
17	1.7	0.3	0.1	0.39	19.7	0.812	0.771	2.20

Table 5.6 - Statistics of the fitted models to predict the shrubland AGB in Tâmega region.

Model	Mean	MAE	MSE	RMSE	RMSE (%)	R^2	R^2_{adj}	FI
1	9.5	1.9	6.6	2.57	27.2	0.741	0.729	2.57
2	2.1	0.3	0.1	0.36	15.8	0.729	0.716	2.83
3	2.1	0.3	0.1	0.38	16.7	0.698	0.684	2.99
4	9.5	1.8	5.8	2.41	25.5	0.783	0.761	2.41
5	2.1	0.3	0.1	0.35	15.5	0.752	0.727	2.77
6	2.1	0.3	0.2	0.48	21.6	0.496	0.472	3.86
7	9.5	1.5	3.9	1.97	20.9	0.855	0.840	1.97
8	2.1	0.3	0.1	0.36	16.0	0.722	0.709	2.87
9	2.1	0.3	0.1	0.39	17.2	0.697	0.667	3.07
10	2.1	0.4	0.3	0.54	24.2	0.367	0.337	4.33
11	9.5	3.0	13.9	3.72	39.4	0.484	0.433	3.72
12	2.1	0.4	0.2	0.48	21.3	0.534	0.488	3.80
13	2.1	0.2	0.1	0.36	15.9	0.739	0.713	2.84
14	9.5	2.5	11.9	3.45	36.6	0.556	0.511	3.45
15	9.5	1.7	5.4	2.33	24.6	0.799	0.778	2.33
16	9.5	1.6	4.9	2.20	23.3	0.822	0.794	2.20
17	2.1	0.2	0.1	0.34	15.1	0.776	0.741	2.70

Table 5.7 - Statistics of the fitted models to predict the shrubland AGB in Serra da Estrela region.

Model	Mean	MAE	MSE	RMSE	RMSE (%)	R^2	R^2_{adj}	FI
1	2.8	0.3	0.3	0.51	18.4	0.771	0.748	0.51
2	1.0	0.1	0.0	0.16	15.5	0.799	0.779	0.42
3	1.0	0.1	0.0	0.15	14.3	0.829	0.812	0.39
4	2.8	0.3	0.3	0.54	19.2	0.775	0.725	0.54
5	1.0	0.1	0.0	0.16	15.5	0.817	0.777	0.42
6	1.0	0.1	0.0	0.16	15.5	0.798	0.778	0.42
7	2.8	0.3	0.3	0.52	18.8	0.785	0.737	0.52
8	1.0	0.1	0.0	0.16	15.3	0.803	0.783	0.41
9	1.0	0.1	0.0	0.15	14.9	0.833	0.796	0.40
10	1.0	0.1	0.0	0.15	14.7	0.818	0.800	0.40
11	2.8	0.3	0.3	0.53	19.2	0.777	0.727	0.53
12	1.0	0.1	0.0	0.15	14.7	0.836	0.799	0.40
13	1.0	0.1	0.0	0.15	14.7	0.837	0.801	0.40
14	2.8	0.3	0.3	0.53	19.0	0.780	0.731	0.53
15	2.8	0.3	0.3	0.53	19.1	0.780	0.731	0.53
16	2.8	0.3	0.3	0.57	20.3	0.776	0.692	0.57
17	1.0	0.1	0.0	0.16	15.4	0.840	0.780	0.42

Table 5.8 - Statistics of the fitted models to predict the shrubland AGB for the Global dataset.

Model	Mean	MAE	MSE	RMSE	RMSE (%)	R^2	R^2_{adj}	FI
1	7.2	2.2	7.8	2.78	38.9	0.663	0.657	2.78
2	1.7	0.4	0.2	0.44	25.5	0.694	0.688	2.41
3	1.7	0.4	0.2	0.45	26.2	0.679	0.673	2.47
4	7.2	1.9	6.4	2.53	35.4	0.726	0.715	2.53
5	1.7	0.3	0.2	0.41	24.2	0.730	0.719	2.29
6	1.7	0.4	0.2	0.47	27.7	0.641	0.634	2.62
7	7.2	2.2	7.9	2.81	39.3	0.663	0.650	2.81
8	1.7	0.4	0.3	0.53	31.1	0.546	0.537	2.94
9	1.7	0.4	0.2	0.49	28.5	0.627	0.612	2.69
10	1.7	0.5	0.3	0.59	34.5	0.443	0.432	3.26
11	7.2	2.9	14.4	3.79	53.0	0.387	0.362	3.79
12	1.7	0.5	0.4	0.59	34.6	0.449	0.427	3.27
13	1.7	0.3	0.2	0.44	25.7	0.697	0.685	2.43
14	7.2	2.4	9.9	3.14	43.9	0.580	0.563	3.14
15	7.2	2.0	6.8	2.60	36.4	0.711	0.700	2.60
16	7.2	1.9	6.5	2.55	35.6	0.728	0.711	2.55
17	1.7	0.5	0.2	0.42	24.4	0.732	0.715	2.31

As depicted in the tables, all the considered models present a moderate to high performance attending to the particular characteristics of vegetation under study. As expected the exponential and power functions forms (models 2 and 3, respectively) fitted well the biomass growth over time. Using the FI values to compare and select the best model, Model 2 achieved lower values only in the adjustment of global data. However, as for Dão-Lafões and Tâmega region, the RMSEs(%) were lower than Models 1 and 3, we selected also Model 2 for these regions. For Serra da Estrela region, dominated by (*Cytisus sp.),* the exponential form (Model 3) is selected based in the lower FI. This can be explained by the inferior ages of vegetation (5 years) were the initial growths achieves an exponential behaviour.

The adjustment of equations with height (*h*) and ground cover (*GC*), as independent variables, individually did not produce so god results but the inclusion of these structural variables in combination with age increased slightly the predictive ability of some models.

Analysing and ranking the computed statistics the selected models are: for Dão-Lafões region (2, 4, 7, 10 and 14) and for Tâmega region (2, 4, 7, 11 and 16). The models fitted for Dão-Lafões and Tâmega region have similar performance. However, Serra da Estrela is almost dominated by the same species (*Cytisus sp.)* and with smaller growths (see Tables 5.3 and 5.4), so the performance of the models is distinct. The best models are: 3, 6, 9, 10 and 13. The models fitted to the global data presented a lower efficiency, as result of the vegetation heterogeneity in terms of species and different growths between the distinct geographical locations. The best models are: 2, 5, 9, 10 and 17.

The parameter estimates of the selected models and correction factors of the transformed logarithmic regressions are presented in Table 5.9.

Table 5.9 - Parameter estimates and correction factors of the selected shrubland AGB models.

Model	Equation	$\boldsymbol{\beta_0}$	$\boldsymbol{\beta_1}$	$\boldsymbol{\beta_2}$	$\boldsymbol{\beta_3}$	CF
Dão-Lafões						
2	$W_i = e^{(ln\beta_0 + \beta_1 lnt + CF)}$	-0.600694	1.60337			0.0837
4	$W_i = \beta_0 + \beta_1 t^2 + \beta_2 h^2$	1.78117	0.15992	2.41287		
7	$W_i = \beta_0 + \beta_1 t^2 + \beta_2 (tGC)^2$	1.69775	0.23920	-0.000003526543		
10	$W_i = e^{(ln\beta_0 + \beta_1 ln(hGC) + CF)}$	-0.711501	0.7096			0.0513
14	$W_i = \beta_0 + \beta_1 lnGC + \beta_2 (th)^2$	-10.43477	3.85071	0.11084		
Tâmega						
2	$W_i = e^{(ln\beta_0 + \beta_1 lnt + CF)}$	-0.321772	1.61521			0.0632
4	$W_i = \beta_0 + \beta_1 t^2 + \beta_2 h^2$	0.56365	0.31076	1.33870		
7	$W_i = \beta_0 + \beta_1 t^2 + \beta_2 (tGC)^2$	2.48231	0.16038	0.00002696		
			-			
11	$W_i = \beta_0 + \beta_1 h^2 + \beta_2 GC^2$	4.19159	0.25946	0.00130739		
16	$W_i = \beta_0 + \beta_1 t^2 + \beta_2 h^2 + \beta_3 GC^2$	0.46285	0.26216	0.42678	0.00054186	
Serra da Estrela						
3	$W_i = e^{(\beta_0 + \beta_1 t + CF)}$	0.05022	0.26293			0.0107
6	$W_i = e^{(ln\beta_0 + \beta_1 ln(th) + CF)}$	0.64429	0.43146			0.0126
9	$W_i = e^{(\beta_0 + \beta_1 t^2 + \beta_2 .(tGC)^2 + CF)}$	0.47246	0.03601	0.0000001311		0.01159
10	$W_i = e^{(ln\beta_0 + \beta_1 ln(h.GC) + CF)}$	-0.95480	0.50891			0.01136
13	$W_i = e^{(\beta_0 + \beta_1 t^2 + \beta_2 \ln(hGC) + CF)}$	0.00398	0.02573	0.16364		0.01132
Global						
2	$W_i = e^{(ln\beta_0 + \beta_1 lnt + CF)}$	-0.611667	1.64655			0.0953
5	$W_i = e^{(\beta_0 + \beta_1 lnt + \beta_2 h^2 + CF)}$	-0.54281	1.45222	0.25189		0.0859
9	$W_i = e^{(\beta_0 + \beta_1 t^2 + \beta_2 .(tGC)^2 + CF)}$	0.73804	0.04683	-0.0000003843386		0.1187
10	$W_i = e^{(ln\beta_0 + \beta_1 ln(hGC) + CF)}$	-0.48772	0.58855			0.1739
17	$W_i = e^{(\beta_0 + \beta_1 lnt + \beta_2 h^2 + \beta_3 GC + CF)}$	-0.52150	1.50982	0.258895562	-0.00172503	0.0872

where: W_i is the predicted shrubland biomass (ton ha^{-1}); t is the age after wildfire; h is the shrubs mean height (m); GC is the percentage ground cover (%); $\beta_0, \beta_1, \beta_2$ and β_3 are the parameter estimates; and CF is the correction factor to the transformed logarithmic regressions.

5.3.3 Evaluation of the shrubland aboveground biomass models

The scatterplots presented in Figures 5.6 to 5.9 show the discrepancies between measured aboveground biomass versus the aboveground biomass predicted by the final selected models (Table 5.9). All the models show a good performance as demonstrated by the statistics of fitting, presented in Tables 5.5 to 5.8.

The selected Global equations (2, 5, 9, 10, and 16) were additionally evaluated using the sample data of each region as validation dataset (Table 5.10). The results confirm that the derived Global models (see Table 5.9) are suitable to estimate shrubland AGB, in similar conditions as the used in this research. However, their application in areas dominated by broom is not adequate, as the errors are very high (RMSE of 98.2, 91.5, 69.6 and 85.3%, respectively). So, in this situations, the specific equations derived for Serra da Estrela Region (Table 5.9), are more suitable to estimate these vegetation type AGB.

Despite the global equations can be generalized to predict shrubland AGB in similar ecosystems, for estimations in the regions considered in this study (Dão-Lafões, Tâmega and Serra da Estrela), is always preferable to apply the specific allometric equations derived for each region.

As a final remark, it should be noted that the derived equations are applicable for vegetation up to 7 years. However, given the high frequency of wildfires in these regions (Figure 5.2) is not common to found areas where the shrubland vegetation reaches superior ages.

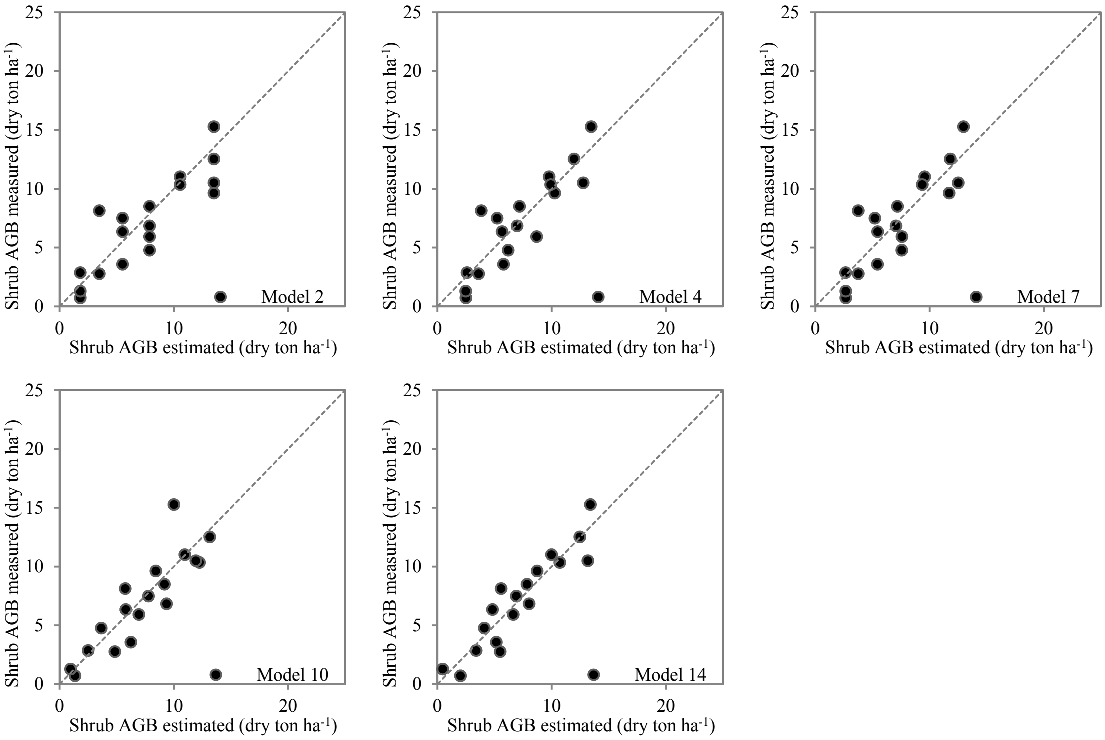

Figure 5.6 - Scatterplots of the measured versus predicted shrubland aboveground biomass for the Dão-Lafões region.

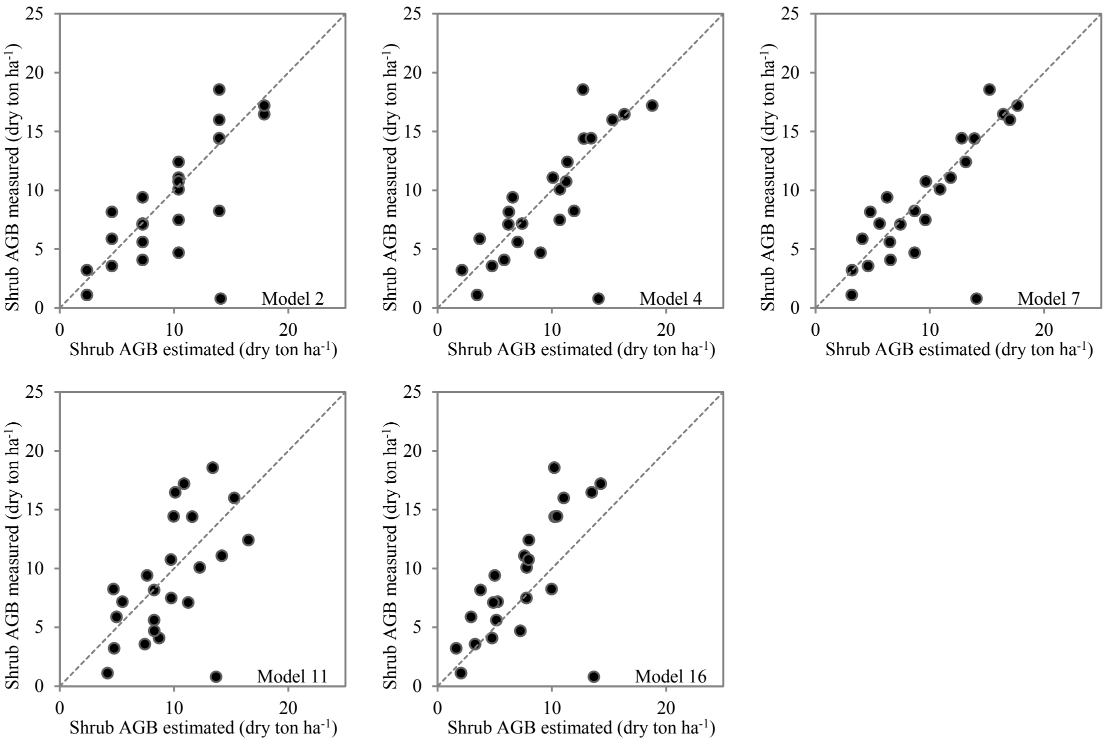

Figure 5.7 - Scatterplots of the measured versus predicted shrubland aboveground biomass for the Tâmega region.

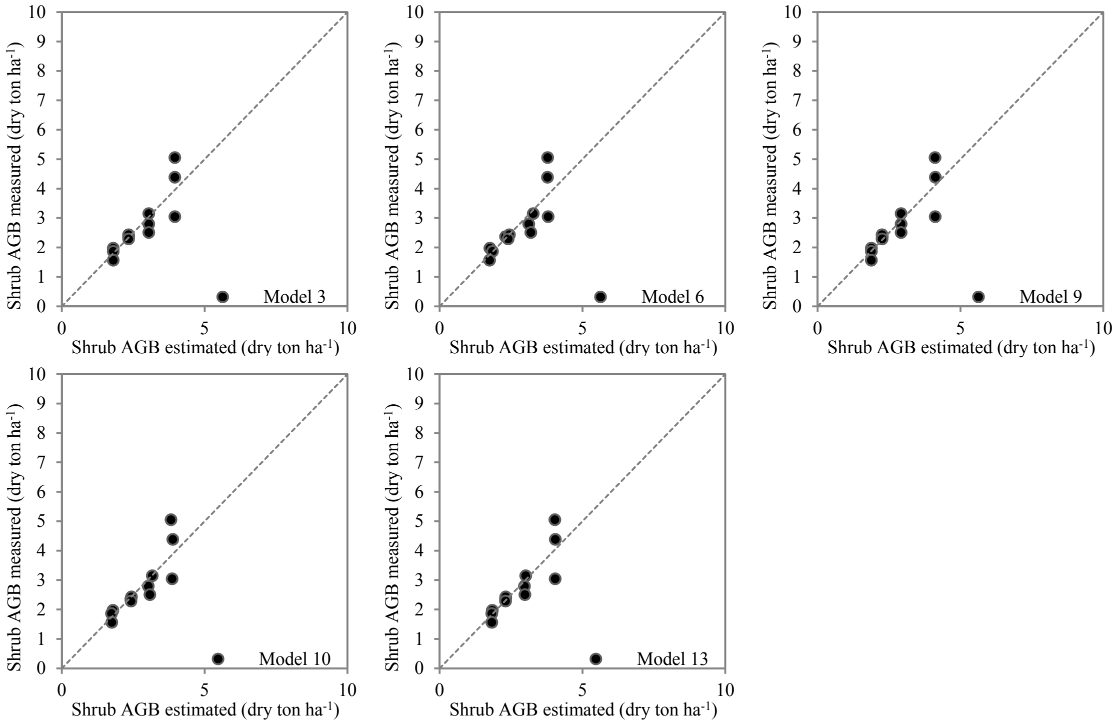

Figure 5.8 - Scatterplots of the measured versus predicted shrubland aboveground biomass for the Serra da Estrela region.

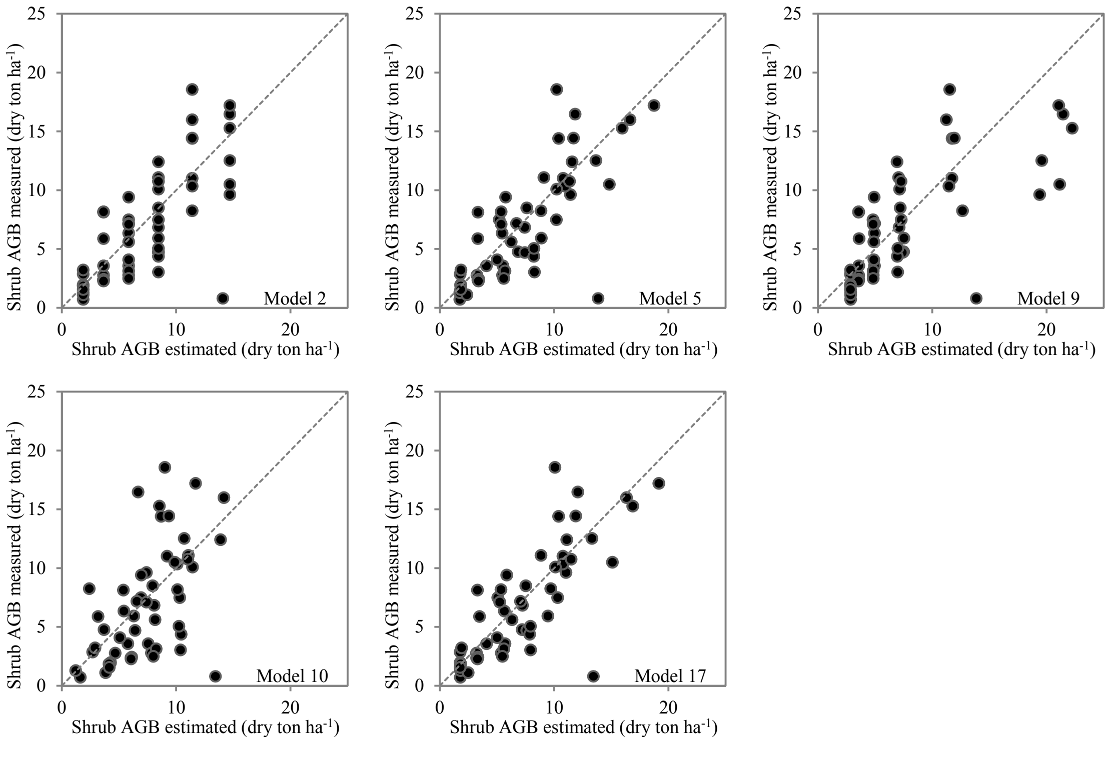

Figure 5.9 - Scatterplots of the measured versus predicted shrubland aboveground biomass for the Global data.

Table 5.10 - Evaluation of the fitted Global models using the data of each region as validation dataset.

Site	Mean	MAE	MSE	RMSE	RMSE (%)
Model 2					
Dão-Lafões	8.1	1.9	5.8	2.4	33.6
Tâmega	7.9	2.5	8.8	3.0	31.4
Serra da Estrela	5.0	2.2	7.5	2.7	98.2
Model 5					
Dão-Lafões	7.4	1.6	4.4	2.1	28.3
Tâmega	8.3	2.1	7.4	2.7	29.1
Serra da Estrela	4.6	1.9	6.0	2.5	91.5
Model 9					
Dão-Lafões	8.0	1.8	5.4	2.3	62.5
Tâmega	7.7	2.6	9.6	3.1	37.0
Serra da Estrela	4.9	2.1	6.3	2.5	69.6
Model 10					
Dão-Lafões	6.4	1.5	4.4	2.1	29.3
Tâmega	8.2	3.0	16.4	4.1	42.9
Serra da Estrela	7.2	4.4	21.4	4.6	166.0
Model 16					
Dão-Lafões	7.5	1.6	4.7	2.2	30.0
Tâmega	8.3	2.1	7.6	2.8	29.6
Serra da Estrela	4.4	1.7	5.1	2.3	85.3

Note: values of calculated statistics (Mean, MAE, MSE and RMSE) are in ton ha^{-1}.

5.3.4 Validations and comparison with other shrubland AGB equations

The developed models were compared with equations previously adjusted for Mediterranean shrubland aboveground biomass by Fernandes and Rego (1996, 1998); Rambal (2001); Fernandes et al. (2002); Aranha et al. (2011) and equations reported in the FIRE PARADOX project (Krivtsov et al., 2009). Figure 5.10 shows the scatterplots of shrubland aboveground biomass estimated by the derived equations and from other authors versus the independent variables used to fit each model. Figure 5.11 shows the scatterplots comparing the AGB measured versus the AGB estimated by equations previously published by other authors. The statistics of the fitting process are presented in Table 5.11, for each region and for the Global data.

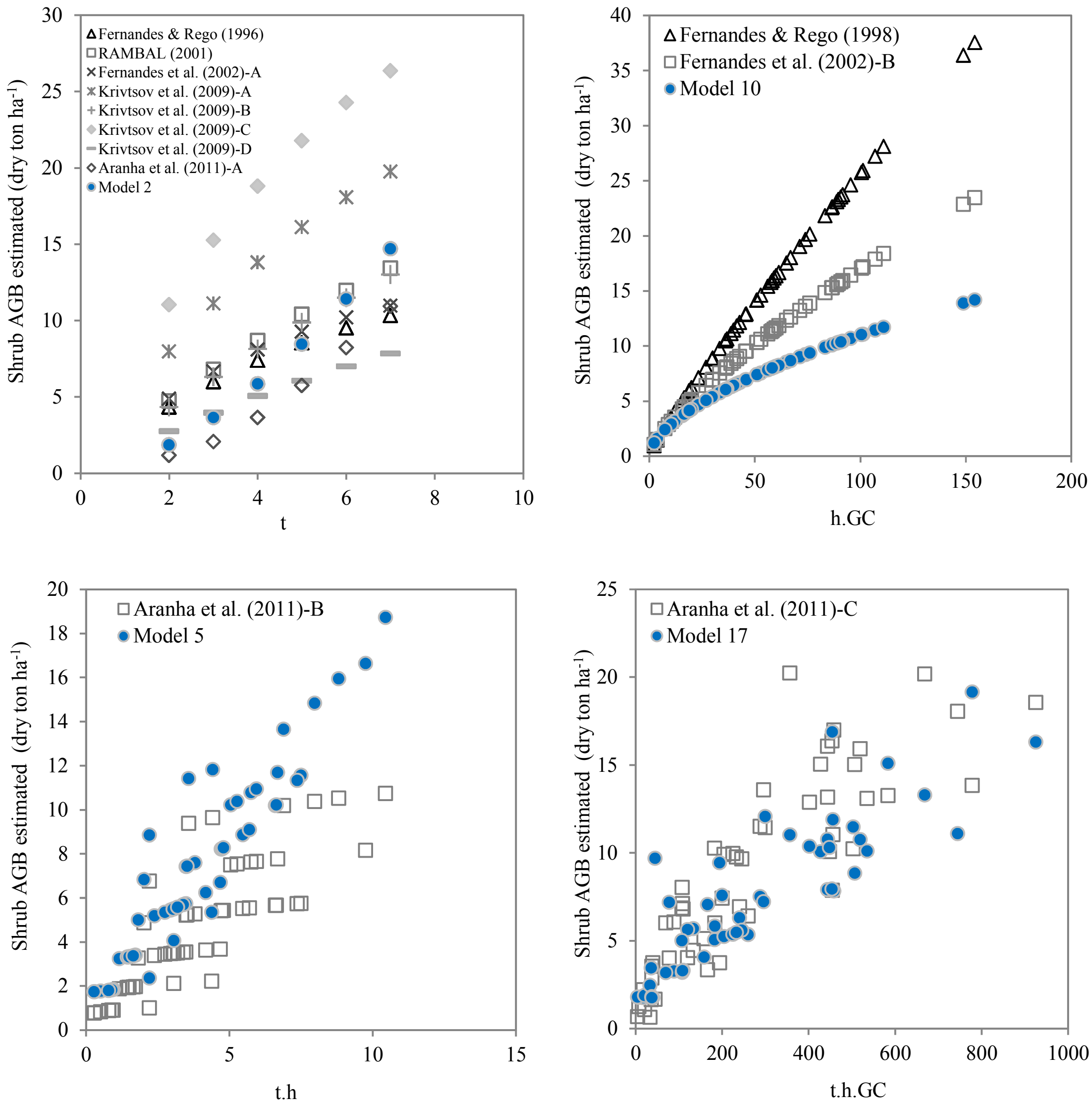

Figure 5.10 - Scatterplots of predicted shrubland aboveground biomass and independent variables.

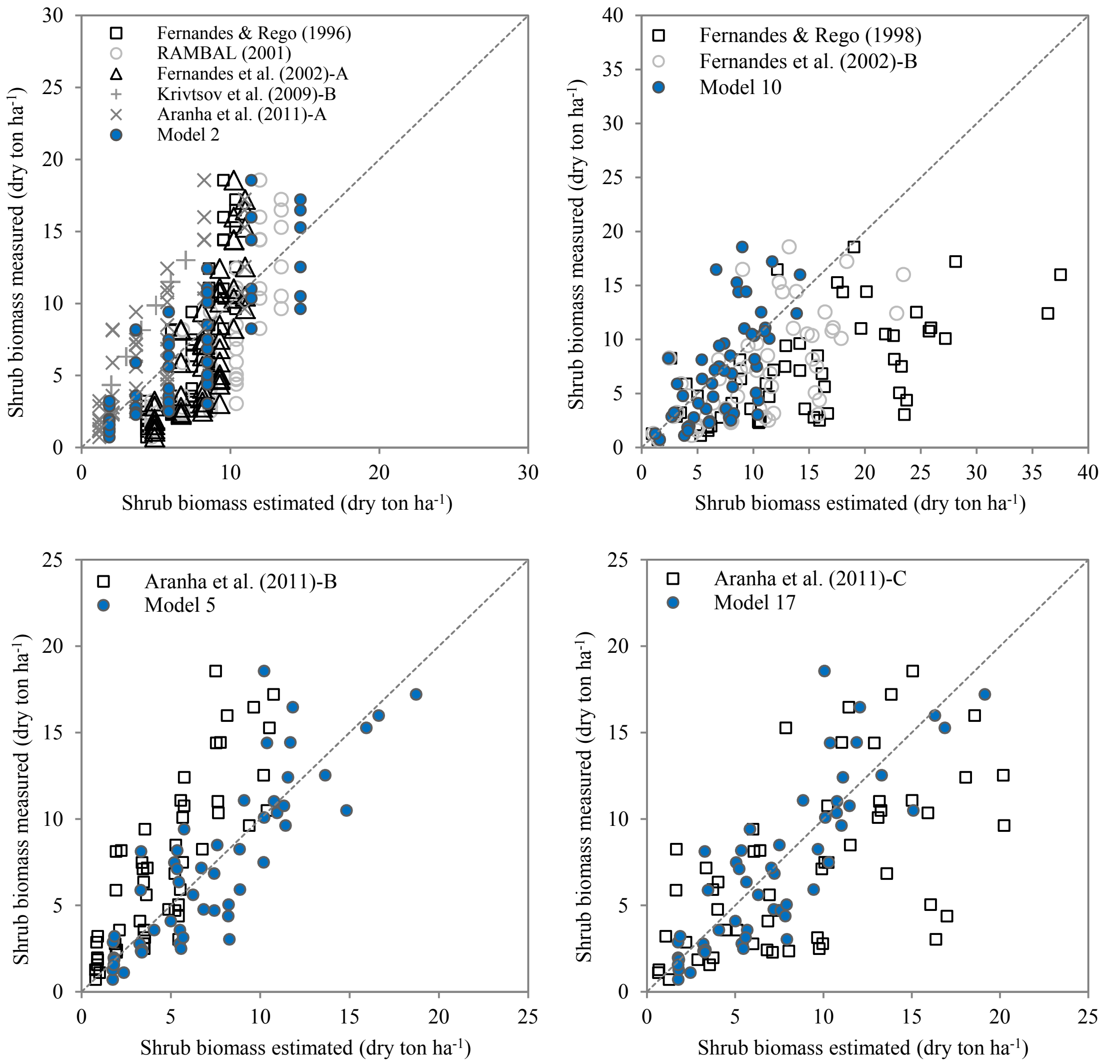

Figure 5.11 - Scatterplots comparing the AGB measured versus the AGB estimated by equations from other authors.

As can be seen in Figures 5.10 and 5.11 and Table 5.11, the biomass equations show discrepancies in the predictions. Nevertheless the low predictive ability of some models, in general the shrubland age is well correlated with biomass (ton ha^{-1}), independently of species and percentage Ground Cover, as also concluded by Rambal (2001). In the predictive models with vegetation age (*t*) as independent variable, the best results are achieved with the models from: Fernandes and Rego (1996) (mean =7.6 ton ha^{-1}, RMSE =48.5%); Rambal (2001) (mean = 9.2 ton ha^{-1}, RMSE = 50.9%); Fernandes et al. (2002) (mean = 8.3 ton ha^{-1}, RMSE = 50.5%); Krivtsov et al. (2009)-B (mean = 8.7 ton ha^{-1}, RMSE = 47.4%).

The equations from Krivtsov et al. (2009) A and C, excessively overestimate the predictions (mean = 14.3 ton ha^{-1}, RMSE = 108.2% and 19.4 ton ha^{-1}, RMSE = 176.8%, respectively). The equations from Aranha et al. (2011)-A (mean = 5.0 ton ha^{-1}, RMSE = 49.8%) and from Krivtsov et al. (2009)-D underestimate the predictions (mean = 5.4 ton ha^{-1}, RMSE = 55.9%). Curiously, Krivtsov et al. (2009)-B equations gives more accurate estimates (mean = 8.7 ton ha^{-1}, RMSE = 47.4%), despite they were developed in shrubland dominated by *Cistus ladanifer, Cistus ladanifer* species, which were not found in the present study.

Considering each studied region independently, the predictive ability of the compared models are very low in Serra da Estrela region, except with equations from Aranha et al. (2011)-A (mean = 3.2 ton ha^{-1}, RMSE = 38%) and Krivtsov et al. (2009)-D (mean = 4.5 ton ha^{-1}, RMSE = 64.5%). Fernandes et al. (2002) cautioned that the predictive ability of his equations (Model A) is very low in shrubland dominated by *Cytisus sp.* This is confirmed by the results achieved for the estimates of AGB in the Serra da Estrela region (mean = 7.2 ton ha^{-1}, RMSE = 163.7%), which is dominated by *Cytisus sp.* species.

Analysing the aboveground biomass models using shrubs height (*h*), and Ground cover (%) as independent variables, the equations from Fernandes and Rego (1998) and Fernandes et al. (2002)-B overestimate the predictions (mean = 14.9 ton ha^{-1}, RMSE = 142.6%; mean = 10.5 ton ha^{-1}, RMSE = 76.1%, respectively).

Aranha et al. (2011)-B equation using age (t) and height (*h*) as independent variables, underestimate the predictions (mean = 4.6 ton ha^{-1}, RMSE = 52.7%) for Global data, giving more accurate results for Serra da Estrela region (mean = 2.9 ton ha^{-1} RMSE = 35.3%). This suggests that Aranha et al. (2011)-A and B equations are suitable for homogenous shrubland dominated by *Cytisus sp.*

The shrubland AGB equation from Aranha et al. (2011)-C combining age (*t*), height (*h*) and Ground Cover (%), as independent variable, did not improved the estimates comparatively to the other equations tested, for the Global data (mean = 9.0 ton ha^{-1}, RMSE= 69.2%). However, for the Dão-Lafões and Tâmega regions showed moderate to high predictive ability (mean=8.8 ton ha^{-1}, RMSE= 62.5% and mean=9.0 ton ha^{-1}, RMSE= 35.3%, respectively).

Table 5.11 - Statistics of the estimates obtained by the equations from other authors.

Site	Mean	MAE	MSE	RMSE	RMSE (%)	Reference
Global	7.6	2.9	12.1	3.5	48.5	(Fernandes and Rego, 1996)
Dão-Lafões	7.9	2.1	6.3	2.5	35.0	
Tâmega	8.0	3.1	14.9	3.9	40.9	
Serra da Estrela	6.6	3.8	15.3	3.9	140.2	
Global	14.9	8.2	104.2	10.2	142.6	(Fernandes and Rego, 1998)
Dão-Lafões	12.3	5.2	43.4	6.6	92.2	
Tâmega	17.4	9.0	123.9	11.1	117.8	
Serra da Estrela	14.0	11.2	157.8	12.6	450.7	
Global	9.2	3.2	13.3	3.6	50.9	(Rambal, 2001)
Dão-Lafões	9.6	2.8	10.0	3.2	44.3	
Tâmega	9.7	2.6	9.5	3.1	32.6	
Serra da Estrela	7.6	4.9	25.5	5.1	181.2	
Global	8.3	3.1	13.1	3.6	50.5	(Fernandes et al., 2002) - A
Dão-Lafões	8.6	2.3	7.7	2.8	38.7	
Tâmega	8.7	3.1	13.3	3.6	38.6	
Serra da Estrela	7.2	4.5	20.8	4.6	163.7	
Global	10.5	4.4	29.7	5.5	76.1	(Fernandes et al., 2002) - B
Dão-Lafões	8.9	2.3	7.8	2.8	39.1	
Tâmega	12.0	4.6	29.4	5.4	57.4	
Serra da Estrela	10.1	7.3	63.1	7.9	284.9	
Global	14.3	7.2	60.0	7.7	108.2	(Krivtsov et al., 2009)-A
Dão-Lafões	14.9	7.7	64.0	8.0	111.9	
Tâmega	15.0	5.6	38.6	6.2	65.8	
Serra da Estrela	12.3	9.5	95.1	9.8	349.8	
Global	8.7	3.0	11.5	3.4	47.4	(Krivtsov et al., 2009)-B
Dão-Lafões	9.1	2.5	7.9	2.8	39.3	
Tâmega	9.2	2.6	9.5	3.1	32.6	
Serra da Estrela	7.2	4.4	20.9	4.6	164.0	
Global	19.4	12.3	160.2	12.7	176.8	(Krivtsov et al., 2009)-C
Dão-Lafões	20.1	12.9	175.0	13.2	185.1	
Tâmega	20.3	10.9	125.2	11.2	118.4	
Serra da Estrela	16.7	13.9	205.0	14.3	513.6	
Global	5.4	3.0	16.0	4.0	55.9	(Krivtsov et al., 2009)-D
Dão-Lafões	5.6	2.4	8.8	3.0	41.6	
Tâmega	5.6	4.2	28.3	5.3	56.3	
Serra da Estrela	4.5	1.7	3.2	1.8	64.5	
Global	5.0	2.6	12.7	3.6	49.8	(Aranha et al., 2011)-A
Dão-Lafões	5.7	1.8	5.9	2.4	34.1	
Tâmega	5.4	4.1	24.0	4.9	51.9	
Serra da Estrela	3.2	0.8	1.1	1.1	38.0	
Global	4.6	2.8	14.3	3.8	52.7	(Aranha et al., 2011)-B
Dão-Lafões	5.2	2.0	7.2	2.7	37.5	
Tâmega	5.1	4.4	26.7	5.2	54.7	
Serra da Estrela	2.9	0.8	1.0	1.0	35.3	
Global	9.0	3.9	24.5	5.0	69.2	(Aranha et al., 2011)-C
Dão-Lafões	8.8	3.4	19.9	4.5	62.5	
Tâmega	9.0	3.0	11.1	3.3	35.3	
Serra da Estrela	9.2	6.5	57.2	7.6	271.3	

Note: values of calculated statistics (Mean, MAE, MSE and RMSE) are in ton ha^{-1}.

In order to analyse the variation of the mean predicted by the models under comparison, a multiple analyses of variance (ANOVA) was performed, using the Statistix Analytical Software (Statistix®8). The results revealed, at alpha level 0.05, significant differences among predictions (Table 5.12). Subsequent pairwise comparisons, by means of post hoc Tukey HSD test, revealed significant differences grouped in eight different sets, in which the means are not significantly different from each other (Table 5.13).

Table 5.12 - One-Way ANOVA performed among shrubland aboveground biomass estimates.

Source	DF	SS	MS	F	P
Between	16	12611.4	788.211	44.1	0.0013
Within	884	15788.6	17.860		
Total	900	28400			

Table 5.13 - Tukey HSD All-Pairwise Comparisons Test performed among shrubland AGB estimates.

Variable	Mean	Homogeneous Groups
Krivtsov et al. (2009)-C	19.42	A
Fernandes and Rego (1998)	14.91	B
Krivtsov et al. (2009)-A	14.34	B
Fernandes et al. (2002) - B	10.52	C
Rambal (2001)	9.19	CD
Aranha et al. (2011)-C	8.98	CD
Krivtsov et al. (2009)-B	8.70	CD
Fernandes et al. (2002)-A	8.31	CD
Model 9	7.64	DE
Fernandes and Rego (1996)	7.64	DE
Model 10	7.34	DEF
Model 17	7.32	DEF
Model 5	7.31	DEF
Model 2	7.29	DEF
Krivtsov et al. (2009)-D	5.39	EF
Aranha et al. (2011)-A	5.00	EF
Aranha et al. (2011)-B	4.64	F

The developed models (2, 5, 10 and 17) in the same group (DEF), indicates that the estimated mean values of biomass are very close confirming the good fitting process. The ranked values of the mean in Table 5.13 confirm (as in Table 5.11) that equations from Krivtsov et al. (2009)-D, Aranha et al. (2011)-A and Aranha et al. (2011)-B slightly underestimate the biomass predictions and the other models overestimate the predictions. The equations from Rambal (2001), Fernandes et al. (2002)-A, Krivtsov et al. (2009)-B, Fernandes and Rego (1996) and Aranha et al. (2011)-C are statistically grouped near to the means estimated from our models. Hence, even overestimating slightly the predictions, we can assume that they can be applied in the shrubland ecosystem studied, except for shrubland homogeneously dominated by *Cytisus sp.* In these situations the equations from Krivtsov et al. (2009)-D and Aranha et al. (2011)-A and B give better results.

5.4 Conclusion

In this study a set of equations to estimate Mediterranean shrubland aboveground biomass were developed. Independent variables were tested in the regression models such as vegetation's age (*t*), height (*h*) and percentage Ground Cover (*GC*%), independently and combined. The best predictive models are able to estimate the shrubland AGB in the studied Mediterranean ecosystem, with moderate to high accuracies. Vegetation's age is well correlated with shrubland AGB. So, if this parameter could be estimated the derived models, only with age as independent variable, are able to predict accurately the shrubland AGB. This was also confirmed by testing equations from other authors (e.g. Rambal, 2001; Fernandes et al., 2002) to our data. However, the inclusion of height and percentage ground cover, in combination with age, slightly increased the prediction ability of some models. Hence, despite the collection of these variables are time-consuming is recommendable, whenever possible, to use equations that include the combination of parameters.

The developed models using the height and GC% as independent variable showed lower predictive ability. However, they may be useful when the age of the vegetation could not be accurately determined.

The type of species and the quantity of AGB vary depending on the geographical region (i.e. latitude, longitude and altitude). Hence, the provided equations can be used in similar Mediterranean ecosystems, but generalization to shrubland composed by different species, with different growth and production can lead to inconsistent estimates of aboveground biomass. Moreover, these equations should not be applied beyond the ranges of the characteristics (e.g. age, height, etc.) of the vegetation measured in this study.

References

AFN, 2011. Estatísticas dos incêndios florestais. Totais Nacionais (2001 - 2010). Autoridade Nacional Florestal, Ministério da Agricultura do Desenvolvimento Rural e das Pescas, Lisboa.

Aranha, J., Calvão, A., Lopes, D., Viana, H., 2011. Quantificação da biomassa consumida nos últimos 20 anos de fogos florestais no Norte de Portugal. Info 26, 44-49.

Aranha, J.T., Viana, H., Rodrigues, R., 2008. Vegetation classification and quantification by satellite image processing. A case study in north Portugal Bioenergy: Challenges and Opportunities. International Conference and Exhibition on Bioenergy Universidade do Minho, Guimarães, Portugal.

Armand, D., Etienne, M., Legrand, C., Marechal, J., Valette, J., 1993. Phytovolume, phytomasse et relations structurales chez quelques arbustes méditerranéens. Ann. For. Sci. 50, 79-89.

Baeza, M.J., Raventós, J., Escarré, A., Vallejo, V.R., 2006. Fire Risk and Vegetation Structural Dynamics in Mediterranean Shrubland. Plant Ecology 187, 189-201.

Baeza, M.J., Vallejo, V.R., 2007. Vegetation recovery after fuel management in Mediterranean shrublands. Applied Vegetation Science 11, 151-158.

Baskerville, G.L., 1972. Use of Logarithmic Regression in the Estimation of Plant Biomass. Canadian Journal of Forest Research 2, 49-53.

Beauchamp, J.J., Olson, J.S., 1973. Corrections for Bias in Regression Estimates After Logarithmic Transformation. Ecology 54, 1403-1407.

Beier, C., Emmett, B.A., Tietema, A., Schmidt, I.K., Peñuelas, J., Láng, E.K., Duce, P., De Angelis, P., Gorissen, A., Estiarte, M., de Dato, G.D., Sowerby, A., Kröel-Dulay, G., Lellei-Kovács, E., Kull, O., Mand, P., Petersen, H., Gjelstrup, P., Spano, D., 2009. Carbon and nitrogen balances for six shrublands across Europe. Global Biogeochem. Cycles 23, GB4008.

Beja, P., Pais, M., Palma, L., 2007. Rabbit *Oryctolagus cuniculus* habitats in Mediterranean scrubland: the role of scrub structure and composition. Wildlife Biology 13, 28-37.

Brown, J.K., 1976. Estimating shrub biomass from basal stem diameters. Canadian Journal of Forest Research 6, 153-158.

Calvão, T., Palmeirim, J.M., 2011. A comparative evaluation of spectral vegetation indices for the estimation of biophysical characteristics of Mediterranean semi-deciduous shrub communities. International Journal of Remote Sensing 32, 2275-2296.

Castro, I., Casado, M.Á., Ramirez-Sanz, L., Miguel, J.M., Costa, M., Diaz Pineda, F., 1996. Funciones de estimación de la biomasa aérea de varias especies del matorral mediterráneo del centro de la peninsula Ibérica. ORSIS 11, 107-116.

Causton, D.R., Venus, J.C., 1981. The biometry of plant growth. Edward Arnold, London

CEN EN 14774-1:2009, Solid biofuels - Determination of moisture content – Oven dry method - Part 1: Total moisture - Reference method.

DD CEN/TS 14774-1:2004, Solid biofuels - Methods for determination of moisture content - Oven dry method - Part 1: Total moisture - Reference method.

Dimitris, Z., Maurizio, M., 2003. Aboveground biomass relationships for beech (*Fagus moesiaca* Cz.) trees in Vermio Mountain, Northern Greece, and generalised equations for Fagus sp. . Ann. For. Sci. 60(5), 439-448.

DNGF, 2010. 5º Inventário Florestal Nacional. Portugal Continental. 2005-2006. Relatório Final, Direcção Nacional de Gestão Florestal (DNGF). Autoridade Florestal Nacional. Ministério da Agricultura do Desenvolvimento Rural e das Pescas, Lisboa.

FAO, 1999. A Statistical Manual For Forestry Research. Forestry research support programme for Asia and the Pacific. Food and Agriculture Organization of the United Nations. Regional office for Asia and the Pacific, Bangkok, pp. 231.

Fernandes, P., Loureiro, C., Botelho, H., Ferreira, A., Fernandes, M., 2002. Avaliação Indirecta da Carga de Combustível em Pinhal Bravo. Silva Lusitana 10(1).

Fernandes, P., Botelho, H., 2004. Analysis of the prescribed burning practice in the pine forest of northwestern Portugal. Journal of Environmental Management 70, 15-26.

Fernandes, P.A.M., 2001. Fire spread prediction in shrub fuels in Portugal. Forest Ecology and Management 144, 67-74.

Fernandes, P.M., Rego, F.C., 1996. Changes in fuel structure & fire behaviour with heath & aging in Northern Portugal.Equations for estimating fuel load in shrub communities dominated by *Chamaespartium tridentatum* and *Erica umbellata*. 13th Conference on Fire and Forest Meteorology, Melbourne, Australia.

Fernandes, P.M., Rego, F.C., 1998. Equations for estimating fuel load in shrub communities dominated by *Chamaespartium tridentatum* and *Erica umbellata*. 3rd International Conference on Forest Fire Research & 14th Fire and Forest Meteorology Conference, II, Luso, pp. 2553-2564.

Fernandes, P.M., Catchpole, W.R., Rego, F.C., 2000. Shrubland fire behaviour modelling with microplot data. Canadian Journal of Forest Research 30, 889-899.

Finney, D.J., 1941. On the distribution of a variate whose logarithm is normally distributed. Journal of the Royal Statistical Society 7, 155-161.

Furnival, G.M., 1961. An Index for Comparing Equations Used In Constructing Volume Tables. Forest Science 7, 337-341.

Hunt, R., 1982. Plant growth curves: the functional approach to plant growth analysis. University Park Press.

Husch, B., Beers, T.W., Kershaw, J.A., 2003. Forest mensuration, 4th ed. John Wiley & Sons, New Jersey, pp. 443.

Jenkins, J.C., Chojnacky, D.C., Heath, L.S., Birdsey, R.A., Comprehensive Database of Diameter-based Biomass Regressions for North American Tree Species. GTR-NE-319, Available online at: *http://www.fs.fed.us/ne/global/pubs/books/dia_biomass/index*, (Accessed February 2012).

Krivtsov, V., Fernandes, P., Higham, B., Pezzatti, G.B., Legg, C., 2009. Release of prototype software for allometric modelling of fuel structure with provisional case studies. Deliverable D3.3-5 of the Integrated project "Fire Paradox", Project no. FP6-018505, European Commission, 33 pp. Available online at,

Metla Project 3306, Database of treewise volume- and biomass equations for common European tree species, Available online at: *http://www.metla.fi/hanke/3306/tietokanta.htm*, (Accessed May 2012).

Meyer, H.A., 1942. A correction factor for a systematic error occurring in the application of the logarithmic volume equation. Penn. State Forestry School Research Paper 7.

Navarro Cerrillo, R.M., Blanco Oyonarte, P., 2006. Estimation of above-ground biomass in shrubland ecosystems of southern Spain. Invest Agrar: Sist Recur For 15(2), 197-207.

Ostrom, C.W., 1990. Time series analysis: regression techniques. Sage Publications.

Oyonarte, P.B., Cerrillo, R.M.N., 2003. Aboveground phytomass models for major species in shrub ecosystems of western Andalusia. Investigación agraria. Sistemas y recursos forestales 12, 47-55.

Parresol, B.R., 1999. Assessing tree and stand biomass: a review with examples and critical comparisons. J For Sci 45, 573-593.

Parresol, B.R., 2001. Additivity of nonlinear biomass equations. Canadian Journal of Forest Research 31, 865-878.

Pereira, J., Sequeira, N., Carreiras, J., 1995. Structural-Properties and Dimensional Relations of Some Mediterranean Shrub Fuels. International Journal of Wildland Fire 5, 35-42.

Pérez-Devesa, M., Cortina, J., Vilagrosa, A., Vallejo, R., 2008. Shrubland management to promote Quercus suber L. establishment. Forest Ecology and Management 255, 374-382.

Rahman, M.M., Csaplovics, E., Koch, B., 2005. An efficient regression strategy for extracting forest biomass information from satellite sensor data. International Journal of Remote Sensing 26, 1511-1519.

Rambal, S., 2001. Hierarchy and productivity of Mediterraneantype ecosystems, in: Roy J, S.B., Mooney HA (ed.), Terrestrial Global Productivity. Academic Press, San Diego, pp. 315-344.

Rawlings, J.O., Pantula, S.G., Dickey, D.A., 1998. Applied Regression Analysis: A Research Tool, Second ed. Springer-Verlag New York, Inc.

Rego, F., Effects of prescribed fire on vegetation and soil properties in *Pinus pinaster* forests of Northern Portugal, University of IDAHO, Ph.D. Dissertation, 1986.

Rego, F.C., Pereira, J.P., Fernandes, P.M., Almeida, A.F., 1994. Biomass and aerial structure characteristics of some mediterranean shrub species. 2nd International Conference on Forest Fire Research, 1, Coimbra, pp. 377 - 384.

Riera, P., Peñuelas, J., Farreras, V., Estiarte, M., 2007. Valuation of Climate-Change Effects on Mediterranean Shrublands. Ecological Applications 17, 91-100.

Ritz, C., Streibig, J.C., 2008. Nonlinear regression with R. Springer, pp. 144.

SAS Institute, 2007. JMP Statistical Discovery Software. SAS Institute. Cary, North Carolina, USA.

Shoshany, M., Karnibad, L., 2011. Mapping shrubland biomass along Mediterranean climatic gradients: The synergy of rainfall-based and NDVI-based models. International Journal of Remote Sensing 32, 9497-9508.

Silva, T., Pereira, J., Paúl, J., Santos, M., Vasconcelos, M., 2006. Estimativa de Emissões Atmosféricas Originadas por Fogos Rurais em Portugal. Silva Lusitana 14, 239-263.

Sit, V., Poulin-Costello, M., 1994. Catalogue of curves for curve fitting. Biometics Information. Handbook nº 4. Forest Science Research Branch. Ministry of Forests, Province of British Columbia, pp. 116.

Snowdon, P., 1991. A ratio estimator for bias correction in logarithmic regressions. Canadian Journal of Forest Research 21, 720-724.

Sprugel, D.G., 1983. Correcting for Bias in Log-Transformed Allometric Equations. Ecology 64, 209-210.

Statistix®8, Analytical Software, Tallahassee, FL, USA.

Uresk, D., Gilbert, R., Menke, J., 1977. Sampling big sagebrush for phytomass. J. Range Manag. 30 311-314.

Usó, J.L., Mateu, J., Karjalainen, T., Salvador, P., 1997. Allometric regression equations to determine aerial biomasses of Mediterranean shrubs. Plant Ecology 132, 59-69.

Vega, J.A., Fernandes, P., Cuiñas, P., Fontúrbel, M.T., Pérez, J.R., Loureiro, C., 2006. Fire spread analysis of early summer field experiments in shrubland fuel types of northwestern Iberia. Forest Ecology and Management 234, S102-S102.

Viana, H., Dias, S., Marques, C., Cruz, M., Lopes, D., Aranha, J., 2009a. Estabelecimento de modelos alométricos para predição da biomassa aérea da *Pinus Pinaster*. Actas do 6º Congresso Florestal Nacional. Ponta Delgada, Açores. 6-9 Outubro, pp. 771-775.

Viana, H., Fernandes, P., Rocha, R., Lopes, D., Aranha, J., 2009b. Alometria, Dinâmicas da Biomassa e do Carbono Fixado em Algumas Espécies Arbustivas de Portugal 6º Congresso Florestal Nacional, Ponta Delgada, Açores. 6-9 Outubro, pp. 244-252.

Viana, H., Cohen, W.B., Lopes, D., Aranha, J., 2010. Assessment of forest biomass for use as energy. GIS-based analysis of geographical availability and locations of wood-fired power plants in Portugal. Applied Energy 87, 2551-2560.

Viana, H., Aranha, J., Lopes, D., Cohen, W.B., 2012. Estimation of crown biomass of *Pinus pinaster* stands and shrubland above-ground biomass using forest inventory data, remotely sensed imagery and spatial prediction models. Ecological Modelling 226, 22-35.

Whittaker, R.H., Woodwell, G.M., 1968. Dimension and production relations of trees and shrubs in the brookhaven forest, New York. Journal of Ecology 56, 1-25.

Yandle, D.O., Wiant Jr, H.V., 1981. Estimation of plant biomass based on the allometric equation. Canadian Journal of Forest Research 11, 833-834.

Zeng, W.S., Tang, S.Z., 2011. Bias Correction in Logarithmic Regression and Comparison with Weighted Regression for Nonlinear Models, Nature Precedings. Available online at: *http://dx.doi.org/10.1038/npre.2011.6708.1*, (Accessed May 2012).

Zianis, D., Muukkonen, P., Mäkipää, R., Mencuccini, M., 2005. Biomass and stem volume equations for tree species in Europe, Silva Fennica Monographs 4. Finnish Society of Forest Science, p. 63.

6

Fuelwood characteristic and ash properties of *Pinus pinaster* Aiton and *Eucalyptus globulus* Labill. species

Data from this chapter contributed for the following published manuscript:

[Annex B.1] Viana, H., Cohen, W.B., Lopes, D., Aranha, J., 2010. Assessment of forest biomass for use as energy. GIS-based analysis of geographical availability and locations of wood-fired power plants in Portugal. Applied Energy 87, 2551-2560.

[Annex B.2] Viana H.; Aranha J.; Lopes D., 2011, Dedicated Biomass Plants for Combined Heat & Power (CHP). The Portuguese National Strategy. 19th European Biomass Conference and Exhibition. ETA-Florence Renewable Energies. Berlin, Germany. June 6-10.

Abstract

An integrated fuel and ash characterization of *Pinus pinaster* Aiton (maritime pine) and *Eucalyptus globulus* Labill. (blue gum eucalyptus) species is presented in this study. Physical, thermal and chemical analysis, including density, moisture content, calorific value, proximate and ultimate analysis, were carried out. The fuel energy density (E_{ar}) and the fuelwood value index were calculated ranking the fuelwood quality. Furthermore, ash elemental metals determination was carried out. The study showed ash content in the range of 0.40-2.88% for *E. globulus* and 0.22-1.92% for *P. pinaster* tree components. The carbon content of biomass tree components ranged from 43.4 to 53.1% for *E. globulus* and 46.5 to 49.3% for *P. pinaster.* The nitrogen content ranged from 0.13 to 1.18%, the sulphur content from 0.056 to 0.148% and hydrogen around 6-7 % for the two species. The average Higher Heating Value (HHV) was inferior to bark stem of eucalyptus and pine (18.48 and 19.57 MJ kg^{-1}, respectively) and superior to eucalyptus and pine leaves (23.48 and 21.61 MJ kg^{-1}, respectively). The effective heating value per unit volume, the Energy Density (E_{ar}), of 2.467 to 3.340 GJ m^{-3} to *E. globulus* and 1.954 to 4.535 GJ m^{-3} to *P. pinaster* biomass tree components confirm the good fuel potential. The Fuelwood Value Index (FVI) ranked the pine wood stem (4658.0) and top (2861.8), followed by the eucalyptus wood stem (2727.4) and top (1857.2) as better quality and the biomass of eucalyptus leaves (374.4) and pine needles (394.2) as inferior quality. Analysis of chemical composition of the ashes revealed elemental contents below the national and most European legislation guidelines for ash application as fertilizer.

Keywords: *Eucalyptus globulus*; *Pinus pinaster*, Heating Value, Fuelwood value index; Energy density; Ash recovery

6.1. Introduction

Maritime pine (*Pinus pinaster* Aiton) and blue gum eucalyptus (*Eucalyptus globulus* Labill.) are the main Portuguese forest species occupying 885 000 hectares and 740 000 hectares, respectively. Planted for commercial purposes for pulp industry and otters consuming industries these forests gained more interest, in the recent years, with the projects of dedicated biomass plants for combined heat and power (CHP) production (DGGE, 2006) as they provide the main source of fuel (the so-called primary residues) (Viana et al., 2010). On the other hand, as these forest ecosystems play an important role in biogeochemical cycling of carbon, the research on quantification and characterization of forest biomass is increasingly necessary.

The identification and characterization of the chemical and phase composition of a given solid fuel is the initial and most important step during the investigation and application of such fuel. This composition is an unique fundamental code that characterizes and determines the properties, quality, potential applications and environmental problems related to any fuel (Vassilev et al., 2010).

The calorific value, defined as the quantity of heat (energy) produced by the complete combustion of a given mass of a fuel, usually expressed in joules per kilogram, is the most important parameter to characterize a substance as combustible and to indicate the quality of a fuel for general utilization. The calorific value of solid fuels is commonly expressed as Higher Heating Value (HHV) at constant volume (dry basis) and Lower Heating Value (LHV) at constant pressure (dry basis or wet basis). The higher heating value at constant volume, also known as Gross Calorific Value (GCV), is the absolute value of the specific energy of combustion, in joules, for unit mass of a solid biofuel burned in oxygen in a calorimetric bomb under the specified conditions. The products of combustion are assumed to consist of gaseous oxygen, nitrogen, carbon dioxide and sulphur dioxide, of liquid water (in equilibrium with its vapour) saturated with carbon dioxide under the conditions of the bomb reaction, and of solid ash, all at the reference temperature (CEN EN 14918:2009). On the other hand, the lower heating value, also known as Net Calorific Value (NCV), at constant pressure is the absolute value of the specific heat (enthalpy) of combustion, in joules, for unit mass of the biofuel burned in oxygen at constant pressure under such conditions that all the water of the reaction products remains as water vapour (at 0.1 MPa), the other products being as for the higher heating value, all at the reference temperature (CEN EN

14918:2009). The HHV value can be estimated by pre-established equations (e.g. Demirbas, 1997; Cordero et al., 2001; Channiwala and Parikh, 2002; Friedl et al., 2005; Yin, 2011) or measured with a bomb calorimeter. The LHV is estimated by the existent relationship (CEN EN 14918:2009) with the HHV. As the effective calorific value depends on the moisture content, being that the higher the moisture content is the less efficient is the wood as a fuel, the LHV (wet basis or as received) is most relevant at the time of characterizing a fuel. The determination of the LHV is not only fundamental at the time of evaluating a substance from an energetic point of view, but also gives an idea of its inflammability or its potential to generate and to propagate fire (Pérez et al., 2006). The knowledge of LHV of the different forest vegetation becomes a realistic indicator of the energetic state of forest biomass of a zone and helps to plan a rational exploitation of the energetic forest resources (Núñez-Regueira et al., 2004).

Any property which influences the heating value, either positively or negatively, defines, therefore, the fuelwood quality and value, and it can be expressed into a fuelwood value index (Senelwa and Sims, 1999). The fuelwood value index (FVI) is an important parameter for ranking fuelwood species (Bhatt and Todaria, 1992) and may be used in the comparison and selection of different feedstock for different applications.

Energy density is an additional parameter that can be calculated to identify the potential and to select a fuel for small-scale heating plants and households usage (DD CEN/TS 15234:2006). The energy density is of importance with regard to wood fuels storage and transport, because the necessary storage and transport capacity decreases with an increasing energy density, and storage and transport thus become more efficient and cheaper (Obernberger and Thek, 2004).

The biomass ash is another factor to take into account either because of the quantities generated in the combustion either on their chemical composition. The knowledge on the quantities of ash generated by combustion is especially important in the technical planning of boilers, where this material will be burned. In respect to chemical composition, the interest relates to the relevance regarding ash melting, deposit and slag formation and corrosion (Miles et al., 1996; Clark and Deswarte, 2008; Loo and Koppejan, 2008). Additionally, the information on the presence of certain elements in biomass is of special importance in environmental terms given to the emission of heavy metals to the environment or the subsequent use that those ashes may have as soil fertilizer. Following Zhan et al. (1996), elements such as Zn, Cu, Cd, Cr and Pb present in the materials applied to the soil, could constitute a potential source of contamination for terrestrial and aquatic ecosystems.

The problems related to biomass ash utilization are only at an initial stage of investigation and they need further clarification. For instance, there is no doubt that biomass ashes contains plant nutrients, namely some compounds of Ca, Mg, Na, K and P, that have to be recycled back to the soil (Vassilev et al., 2010). However, the knowledge about how these compounds are available in the ashes so that they can be assimilated by plants is very low. Moreover, the ash containing heavy metals in its composition, above threshold, can be toxic to plants, precluding their use as fertilizer.

The present chapter was designed to screen the fuel and ash characteristics of maritime pine and blue gum eucalyptus. The quality of fuel was evaluated based in the analysis of physical and thermochemical properties including: (1) physical parameters: density (D) and moisture content (MC%); (2) proximate analysis namely fixed carbon (FC%), volatile matter (VM%) and ash yield (A%); (3) ultimate analysis (C, O, H, S, N); (4) calorific value (Higher and lower heating values); (5) ash elemental metals analysis; and (6) the Fuelwood Value Index (FVI) and energy density (E_{ar}) were calculated.

6.2. Material and methods

6.2.1. Stand measurements and biomass samples for fuel and ash analysis

The biomass samples for fuel and ash analysis were collected within 11 eucalyptus stands and 16 pine stands, located in the North-Center Portugal, extending from 39º 11' 53'' N; 06º 14' 17' W to 42º 50' 50'' N; 08º 19' 02'' W, where these species mainly occur.

The forest stands were sampled and the structural stand variables, such as number of trees per hectare (N), dominant tree height class (h_{dom}), basal area (G), stand age (t), crown closure class (Cc) and site index (SI) were measured and calculated. The aboveground biomass was quantified by means of destructive approach.Within each field plot, a biomass sample of each tree component (wood stem, bark stem, top, branches and leaves) was collected in the average tree. The collected samples were placed into hermetically closed containers to prevent moisture loss, and sent to the laboratory. The preparations and homogenization of the samples, previous to the analytical measurements, were made according to the technical specifications (DD CEN/TS 14780:2005) for sample preparation.

6.2.2. Analytical measurements

6.2.2.1. Physical properties

The moister content (wet basis) was determined following the Technical Specification (DD CEN/TS 14774-1:2004) supersedes by the European Standard (CEN EN 14774-1:2009), which consists in the drying of the sample in a drying oven at a temperature within the range of (105 ± 2°C) in air atmosphere until constant mass is achieved. The percentage moisture was calculated from the loss in mass of the sample. Density (D) and basic density on dry basis (D_b) of tree components was calculated by water displacement technique and is expressed as weight per unit volume (Tsoumis, 1991).

6.2.2.2. Proximate analyses

The determination of ash content (dry basis) was carried out according to the Technical Specification (DD CEN/TS 14775:2004) supersedes by the European Standard (BS EN 14775:2009). The ash content (%) was calculated from the mass of the residue remaining after 1g of oven-dried sample inside a platinum crucible was heated in a muffle furnace at 550 ºC ± 10ºC.

The volatile matter content (dry basis) has been determined according to the Technical Specification (DD CEN/TS 15148:2005) supersedes by the European Standard (CEN EN 15148:2009), by burning 1g of oven-dried sample in a fused silica crucible with lid in a muffle furnace at 900 °C ± 10 °C for 7 min. The percentage of volatile matter was calculated from the loss in mass of the test sample. Fixed carbon content (%) was the difference between the sum of volatile matter and ash contents from 100. For each analyses, a minimum of three test runs were carried out and the means of two closest results (<5% variation) taken as the measured value.

6.2.2.3. Ultimate analyses

Elemental composition of biomass carbon (C), hydrogen (H), nitrogen (N) and sulphur (S) was measured by standard methods of analyses. The Technical Specification (DD CEN/TS 15104:2005) and (DD CEN/TS 15289:2006) describe the instrumental method for determining CHN and S, respectively, in solid biofuels. The simultaneous determination of CHN was carried out in the Leco TruSpec Elemental Determinator. A sample of wood fuel powder (about 0.1g) was burnt in an oxygen/carrier gas mixture under conditions that ensure complete combustion (and conversion of some by-products) to carbon dioxide, water vapour and nitrogen for gas analysis. The determination of Sulphur was done in a Leco SC-144DR using direct combustion and infrared detection. Duplicate determinations and calibration techniques were made to ensure consistency of results. The oxygen content was obtained by subtracting from 100% the sum of (C, H, N, S and ash) contents in percentage.

6.2.2.4. Determination of Higher and Lower Heating Values

The higher heating value (HHV), also called gross calorific value (GCV), of biomass at constant volume in dry basis was determined following the Technical Specification (DD CEN/TS 14918:2005) supersedes by the European Standard (CEN EN 14918:2009). Weighed samples, of the solid biofuel were burned in high-pressure oxygen in an Automated Isoperibol Fixed Bomb Parr 6300 calorimeter (Parr Instruments Company). The 6300 Calorimeter System requires availability of Oxygen, 99.5% purity, with CGA 540 connection, 2500 psig, maximum. A crucible with a pellet containing about 0.5 to 0.6g biomass, to avoid invalid combustion, was inserted into the bomb. After closing the bomb it was filled with oxygen. The calorimeter jacket reservoir was filled with water and the sample ignited electrically. The resulting increase of the water temperature allows the calculation of the HHV of the sample. Three replications for each sample were carried out. The Parr 6300 calorimeter automatically makes all the calculations necessary to produce a gross heat of combustion for the sample. The HHV in dry basis is calculated by Eq. 1 as:

$$q_{v,gr,d} = q_{v,gr} \frac{100}{100 - M_{ad}} \qquad [1]$$

where:

$q_{v,gr,d}$ is the higher heating value at constant volume of the dry (moisture-free) biofuel, in joules per gram;

M_{ad} is the moisture in the analysis sample, in percentage by mass;

$q_{v,gr}$ is the higher heating value at constant volume of the biofuel as analysed, in joules per gram.

The calorific value of the fuel most commonly used for practical purposes is the lower heating value (LHV) at constant pressure for the fuel with some specified moisture content (CEN EN 14918:2009). The main difference between the HHV and LHV is related to the physical state of water in the reaction products. The LHV at constant pressure of the biofuel may be derived from the HHV at constant volume determined on the analysis sample (Eq. 1). The calculation of the LHV at constant pressure requires information about the moisture, hydrogen, oxygen and nitrogen contents of the analysis sample (CEN EN 14918:2009) and was calculated as (Eq. 2):

$$q_{p,net,d} = q_{v,gr,d} - 212{,}2w(H)_d - 0{,}8[w(O)_d + w(N)_d] \qquad [2]$$

where:

$q_{p,net,d}$ is the lower heating value in dry basis at constant pressure, in joules per gram, of the biofuel;

$q_{v,gr,d}$ is the higher heating value at constant volume of the dry (moisture-free) biofuel, in joules per gram;

$w(H)_d$ is the hydrogen content, in percentage by mass, of the moisture-free (dry) biofuel;

$w(O)_d$ is the oxygen content, in percentage by mass of the moisture-free biofuel;

$w(N)_d$ is the nitrogen content, in percentage by mass, of the moisture-free biofuel.

The LHV at constant pressure at a required moisture content M, was calculated as (Eq. 3):

$$q_{p,net,ar} = q_{p,net,d}(1 - 0.01M_{ar}) - 24.43M_{ar} \qquad [3]$$

where:

$q_{p,net,ar}$ is the lower heating value at constant pressure, in joules per gram, of the biofuel with moisture content as received M_{ar} ;

$q_{p,net,d}$ is the lower heating value in dry basis at constant pressure, in joules per gram, of the biofuel;

M_{ar} is the moisture content as received [w-%];

24.43 is the correction factor of the enthalpy of vaporization (constant pressure) for water (moisture) at 25 °C [J g^{-1} per 1 w-% of moisture].

6.2.2.5. Fuelwood Value Index (FVI) and energy density (E_{ar})

Fuel value index is an important parameter for ranking fuelwood species (Bhatt and Todaria, 1992; Goel and Behl, 1996; Bhatt and Tomar, 2002; Bhatt et al., 2004; Nirmal Kumar et al., 2011). The fuelwood value index (FVI) is calculated as the product of calorific value (MJ kg^{-1}) and density (g cm^{-3}) of the biomass by the product of ash content (g g^{-1}) and water content (g g^{-1}) (Eq. 4):

$$FVI = \frac{Calorific \quad value(MJ \quad Kg^{-1}) \times Density(g \quad cm^{-3})}{Ash \quad content(g \quad g^{-1}) \times Moisture \quad content(g \quad g^{-1})} \qquad [4]$$

Since moisture content of the wood varies with the dimensions of the plant, season of the year and other variables, the water content cannot be considered as part of the intrinsic value of a species as a fuel (Bhatt et al., 2004). Therefore, FVI was calculated using the modified formula (Eq. 4), ignoring the moister content, as reported by Bhatt and Todaria (1992).

The energy density as received (E_{ar}) was calculated using the lower heating value as received and the bulk density (BD_{ar}) of each tree component (DD CEN/TS 15234:2006), according to Eq. 5.

$$E_{ar} = \frac{1}{3600} \; q_{p,net,ar} \quad BD_{ar} \qquad [5]$$

where

E_{ar} is the energy density of the biofuel as received (MWh m^{-3} of bulk density);

$q_{p,net,ar}$ is the lower heating value as received (MJ kg^{-1});

BD_{ar} is the bulk density, i.e., volume weight of the biofuel as received (kg m^{-3} bulk volume);

$\frac{1}{3600}$ is the conversion factor for the energy units (MJ to MWh).

The energy density in dry basis (E_{db}) was calculated using the HHV and the bulk density BD_{db} in dry basis.

6.2.2.6. Determination ash elemental metals

After the combustion of biofuel, following the Technical Specification (DD CEN/TS 14775:2004), the ash elemental metals: iron (Fe), aluminium (Al), arsenic (As), cadmium (Cd), lead (Pb), cobalt (Co), copper (Cu) , chromium (Cr), manganese (Mn), zinc (Zn) and nickel (Ni) were analysed according to the Technical Specification of Solid Biofuels to determine major elements (DD CEN/TS 15290:2006) and the Technical Specification of Solid biofuels to determine minor elements (DD CEN/TS 15297:2006). The detection of the major elements (Fe and Al) was done by flame atomic absorption spectrometry (FAAS) and the detection of the minor elements (As, Cd, Pb, Co, Cu , Cr, Mn , Zn and Ni) was done by Graphite furnace atomic absorption spectroscopy (GF-AAS), after the ash digestion with Nitric acid - HNO_3 (65%), Hydrogen peroxide-H_2O_2 (30%), Hydrofluoric acid - HF (40%) and Boric acid - H_3BO_3 (4%). Should be noted, as concluded by Baernthaler et al. (2006), that the method used in the determination of major and minor ash-forming elements in solid biofuels can give values significantly different.

6.3. Results and discussion

6.3.1. Eucalyptus and pine stands characteristics

The characteristics of eucalyptus and pine stands, where the biomass samples were collected to fuel and ash analysis, are presented in Tables 6.1 and 6.2.

The eucalyptus stands are at the first rotation of planted trees, which are managed as a short-rotation coppice system with ages ranging from 8 to 13 years. The maritime pine stands are pure self-thinned even-aged with ages ranging between 20 and 60 years.

Table 6.1 - Descriptive statistics of eucalyptus stands.

Stands plots (n)	N (trees ha^{-1})	t (year)	d_{bh} (cm)	h (m)	BA (m^2 ha^{-1})	SI (m)	Bdry (ton ha^{-1})
1	1400	11.0	14.7	20.0	27.8	20.1	156.1
2	1000	11.0	18.5	21.1	33.8	23.4	218.4
3	1300	11.0	18.8	19.4	29.7	22.9	179.8
4	1300	11.0	11.9	16.8	15.1	19.6	80.2
5	2100	11.0	13.6	16.1	33.5	17.3	171.7
6	800	10.0	12.8	13.6	11.3	19.8	56.7
7	2440	8.0	11.1	6.9	30.9	19.5	144.7
8	800	10.0	12.9	10.1	12.6	19.5	63.9
9	800	13.0	15.4	16.2	17.4	22.3	99.4
10	1320	13.0	12.6	12.7	23.6	20.5	132.4
11	1420	13.0	14.8	13.9	27.4	15.8	137.8
Mean	1335	11.1	14.3	15.2	23.9	20.1	131.0
Min	800	8.0	11.1	6.9	11.3	15.8	56.7
Max	2440	13.0	18.8	21.1	33.8	23.4	218.4
SD	528.3	1.5	2.5	4.3	8.4	2.3	51.1

where: *N* is the number of stems per hectare; *t* is the stand mean age; *h* is the mean height; d_{bh} is the mean diameter at breast height; *BA* is the basal area; *SI* is the site index at 10 years old and Bdry is the dry biomass (ton ha^{-1}).

Table 6.2 - Descriptive statistics of maritime pine stands.

Stands plots (n)	N (trees ha^{-1})	t (year)	d_{bh} (cm)	h (m)	BA (m^2 ha^{-1})	SI (m)	Bdry (ton ha^{-1})
1	700	52	39.8	21.3	59.2	19	420.2
2	800	40	28.6	19.4	55.8	24	260.9
3	600	51	31.5	19.9	49.7	19	232.5
4	600	44	32.0	19.6	50.5	20	231.1
5	600	42	29.5	18.6	43.4	18	193.1
6	600	54	29.4	19.1	43.4	19	194.2
7	620	26	23.6	14.9	30.9	20	123.4
8	460	39	30.6	13.6	38.6	15	158.1
9	900	20	14.1	10.6	16.7	16	58.4
10	620	20	15.0	9.0	15.4	14	53.2
11	460	51	27.4	20.6	29.3	19	132.7
12	2020	27	13.3	12.9	30.1	15	106.3
13	460	60	33.9	22.8	66.9	25	406.2
14	520	48	24.0	16.5	43.1	20	203.7
15	980	26	17.9	11.2	36.7	18	140.1
16	720	35	22.0	15.8	31.0	20	130.1
Mean	729	40	26	17	40	19	190
Min	460	20	13	9	15	14	53
Max	2020	60	40	23	67	25	420
SD	375.6	12.7	7.7	4.2	14.4	3.0	105.3

where: *N* is the number of stems per hectare; *t* is the stand mean age; *h* is the mean height; d_{bh} is the mean diameter at breast height; *BA* is the basal area; *SI* is the site index at 35 years old and Bdry is the dry biomass (ton ha^{-1}).

6.3.2. Proximate analysis and physical properties

Proximate analysis, moisture content and density of eucalyptus and maritime pine tree components are presented in Table 6.3.

Table 6.3 - Proximate analysis and basic density of eucalyptus and maritime pine species.

	Proximate analysis (wt %)					
Species	**Ash**	**VM**	**FC**	**M_{ar} %**	**D ($kg\ m^{-3}$)**	**D_{db} ($kg\ m^{-3}$)**
Eucalyptus globulus						
Wood stem	0.40 (± 0.0024)	85.8 (± 0.0065)	13.8 (± 0.0077)	52.2 (± 3.0)	917.3 (± 0.050)	562.3 (± 0.046)
Bark stem	2.61 (± 0.0039)	79.0 (± 0.004)	18.4 (± 0.0055)	56.6 (± 1.8)	968.0 (± 0.004)	309.6 (± 0.003)
Top	0.62 (± 0.0035)	86.6 (± 0.0031)	12.7 (± 0.0058)	46.4 (± 2.9)	924.0 (± 0.033)	553.6 (± 0.027)
Branches	1.33 (± 0.0019)	82.4 (± 0.0012)	16.3 (± 0.0026)	46.2 (± 3.6)	910.0 (± 0.044)	577.1 (± 0.035)
Leaves	2.88 (± 0.0052)	79.3 (± 0.0043)	17.8 (± 0.0061)	49.4 (± 3.5)	891.8 (± 0.042)	459.1 (± 0.036)
Pinus pinaster						
Wood stem	0.22 (± 0.0011)	85.7 (± 0.0096	14.0 (± 0.0095)	46.6 (± 4.15)	921.2 (± 0.043)	476.4 (± 0.039)
Bark stem	1.31 (± 0.0019)	80.2 (± 0.0082)	19.1 (± 0.0059)	54.1 (± 4.65)	405.5 (± 0.07)	314.9 (± 0.03)
Top	0.24 (± 0.0035)	84.2 (± 0.0031)	15.6 (± 0.0058)	57.0 (± 3.68)	921.1 (± 0.06)	332.7 (± 0.040)
Branches	1.00 (± 0.0023)	80.8 (± 0.0061)	18.2 (±0.0058)	55.0 (± 3.69)	977.2 (± 0.070)	419.6 (± 0.047)
Needles	1.97 (± 0.0022)	79.4 (± 0.0065)	18.7 (± 0.0074)	57.0 (±3.32)	963.2 (± 0.055)	358.6 (± 0.050)

where: Proximate and ultimate analyses are in terms of wt.% dry biomass basis. Ash: Ash percentage (%), VM: Volatile Matter (%), FC: Fixed Carbon (%), Mar %: Moisture content wet basis as received (%); D: density in wet basis ($kg\ m^{-3}$); D_{db}: density in dry basis ($kg\ m^{-3}$). Numbers in parenthesis are the standard deviations.

Ash content ranged from 0.40% to 2.88% for eucalyptus and 0.22 to 1.92% for maritime pine tree components, being that the wood stem presented the lower values and the foliage (leaves and needles) presented the highest values. The values of ash content, collected in the literature review, for both species (eucalyptus and maritime pine) are variable. However, differences in the determination methods were observed, which can influence the results. Vázquez et al. (1995) presented values of 3% for foliage of maritime pine and Hernando et al. (2004) presented values between 1.16 and 2.55% for dead meddles of maritime pine, in Mediterranean countries. Núñez-Regueira et al. (2003) reported lower values for maritime pine biomass ash in Spain, ranging between 0.31-0.69% for needles and between 0.05-0.026% for branches. In other work, Núñez-Regueira et al. (1999) presented, for aboveground biomass ash of pine, values between 0.71-1.04%. Reva et al. (2012) and Telmo et al. (2010) presented values of 0.25% and 0.2%, respectively, in maritime pine wood samples in Portugal. Nunes et al. (1996) reported an ash content of 1.2±0.6% and Vázquez et al. (1987) presented values ranging from 0.3 to 1% for bark of maritime pine in Portugal and Spain, respectively.

For *Eucalyptus globulus*, Gominho et al. (2012) found ash content values of 0.6±0.2% for eucalyptus' stumps in Portugal. Girón et al. (2012) reported an ash content value of 3.75%, in fly ashes from the combustion of eucalyptus' bark, in Spain. Telmo et al. (2010) reported 0.5% for eucalyptus' wood samples. Núñez-Regueira et al. (2002) reported ash content values ranging between 0.6-1.88% for eucalyptus leaves and values ranging from 0.14 to 1.16% for branches in Spain. In other work Núñez-Regueira et al. (1999) presented ash content values between 0.28 and 1.37%, for aboveground biomass of *E. globulus*. Pérez et al. (2006) reported ash content values for young and adult eucalyptus trees of 7.4% and 5.8% for leaves; 2.7 and 2.8% for thin branches and 7.2 and 6.3% for bark, respectively.

The volatile matter observed, between 79.3% and 86.6% dry basis, was similar to typical range found by Franco et al. (2003), Telmo et al. (2010) and Gominho et al. (2012) for eucalyptus and pine biomass, as other biomass types (Parikh et al., 2007; Loo and Koppejan, 2008; Vassilev et al., 2010). The fixed carbon ranging between 12.7% and 19.1% was similar to typical range values found in biomass (Parikh et al., 2007; Loo and Koppejan, 2008; Vassilev et al., 2010).

Moisture content (w%), varied between 46.2% and 57%, which is in accordance with values for the summer season (e.g. Núñez-Regueira et al., 2002; Núñez-Regueira et al., 2003) at the time of harvest. The density of the tree components ranged from 891.8 to 968 kg m^{-3} in eucalyptus and 405.5 to 977.2 kg m^{-3} in maritime pine. However, these values are very variable with the species, age, geographical location, climate, density stock or growth rate, as they depend on the moisture content existent in the biomass. Similar values, with larger ranges, are reported by Núñez-Regueira et al. (2002) for *Pinus pinaster* and by Núñez-Regueira et al. (2003) for *Eucalyptus globulus*. Basic density varying from 309.6 to 577.1 kg m^{-3} for *E. globulus* and 332.7 to 476.4 kg m^{-3} for *P. pinaster* are in the range of average values reported in the literature for *P. pinaster* and *E. globulus* biomass components and total aboveground biomass, e.g. (Senelwa and Sims, 1999; Hernando et al., 2004; Bert and Danjon, 2006; Lousada et al., 2008; Gominho et al., 2012).

6.3.3. Ultimate analysis

Ultimate analysis results for biomass components of eucalyptus and maritime pine are presented in Table 6.4.

Table 6.4 - Ultimate analysis of eucalyptus and maritime pine species.

	Ultimate analysis (wt %)				
	C	**H**	**O**	**N**	**S**
Eucalyptus globulus					
Wood stem	45.4 (±0.129)	6.6 (±0.045)	47.5 (±0.143)	0.17 (±0.016)	0.058 (±0.014)
Bark stem	43.4 (±0.171)	6.2 (±0.108)	47.4 (±0.302)	0.39 (±0.002)	0.031 (±0.005)
Top	45.3 (±0.141)	6.5 (±0.019)	47.5 (±0.153)	0.23 (±0.003)	0.058 (±0.013)
Branches	46.7 (±0.082)	6.5 (±0.101)	45.1 (±0.176)	0.30 (±0.001)	0.020 (±0.004)
Leaves	53.1 (±0.050)	7.3 (±0.034)	35.3 (±0.024)	1.18 (±0.027)	0.148 (±0.036)
Pinus pinaster					
Wood stem	46.5 (±0.107)	6.7 (±0.082)	46.4 (±0.026)	0.13 (±0.025)	0.029 (±0.005)
Bark stem	49.3 (±0.131)	6.8 (±0.054)	42.3 (±0.160)	0.34 (±0.007)	0.026 (±0.005)
Top	48.4 (±0.120)	6.8 (±0.070)	43.8 (±0.060)	0.21 (±0.010)	0.050 (±0.002)
Branches	48.6 (±0.319)	6.8 (±0.050)	43.3 (±0.408)	0.28 (±0.013)	0.032 (±0.010)
Needles	48.2 (±0.225)	6.9 (±0.063)	42.1 (±0.184)	0.74 (±0.063)	0.086 (±0.026)

where: Ultimate analyses are in terms of wt.% dry biomass basis. Numbers in parenthesis are the Standard Deviations

Measured carbon content of *E. globulus* ranged from 43.4 to 53.1%. Lopes (2005) presented for stem 40.4%, for branches 49.1% and for leaves 49.7% in North of Portugal. Núñez-Regueira et al. (2002), found for *E. globulus* in NW Spain values, varying during seven harvest seasons, of 50.1 to 57.7% in leaves and 45.41 to 53.04% in branches. For *P. pinaster* the carbon content ranging from 46.5 to 49.3% differ slightly, in some tree components, from values reported by Lopes (2005), of 44.3% for stem, 50.8% for branches and 47.5% for needles. Reva et al. (2012) report for wood samples 47.68% to Portugal. Values reported by Núñez-Regueira et al. (2003), to NW Spain, are slightly higher in some measurements, ranging from 49.40 to 55.23% in needles, as for branches ranging between 48.33 and 54.92%.

Hydrogen, Oxygen and Nitrogen content, in the range of 6-7%, 35.3-47.5%, and 0.13-1.18%, respectively, are according to measurements reported in the mentioned studies for *E. globulus* and *P. pinaster,* and for general woody biomass (see Vassilev et al., 2010). The sulphur content was below the 0.1% threshold established by Obernberger et al. (2006) for minimizing sulphur-related corrosion risk in biomass boilers combustion, which was similar to average values found in other woody fuels (see Vassilev et al., 2010).

6.3.4. Higher and lower heating values of eucalyptus and maritime pine species

Higher and lower heating values (HHV, LHV) of biomass tree components of *E. globulus* and *P. pinaster* as well as the density in dry base (D_{db}) of fuelwood are presented in Table 6.5. Figures 6.1(a) and 6.1(b) show the maximum, minimum and the average higher heating values for all the tree component of *E. globulus* and *P. pinaster,* respectively.

Table 6.5 - Higher and lower heating values, Moisture content and Density of eucalyptus and maritime pine biomass components.

Species	**HHV ($MJ\ kg^{-1}$)**	**LHV ($MJ\ kg^{-1}$)**	**M_{ar} (%)**	**D_{db} ($kg\ m^{-3}$)**
Eucalyptus globulus				
Wood stem	19.18 (±0.233)	7.42 (±0.666)	52.2	562.3
Bark stem	18.48 (±0.345)	5.48 (±0.060)	56.6	309.6
Top	20.90 (±0.496)	9.20 (±0.744)	46.4	553.6
Branches	20.45 (±0.337)	8.95 (±0.595)	46.2	577.1
Leaves	23.48 (±0.531)	10.66 (±1.009)	49.4	459.1
Pinus pinaster				
Wood stem	21.60 (±0.541)	9.75 (±0.963)	46.6	476.4
Bark stem	19.57 (±1.354)	12.96 (±1.016)	54.1	314.9
Top	20.65 (±0.60)	6.85 (±0.556)	57.0	332.7
Branches	20.92 (±0.555)	7.30 (±0.668)	55.0	419.6
Needles	21.61 (±0.492)	7.22 (±0.732)	57.0	358.6

Where: HHV: Higher Heating Value ($MJ\ kg^{-1}$ at dry basis); LHV: Lower Heating Value ($MJ\ kg^{-1}$) at moisture content as received; M_{ar} %: Moisture content wet basis as received and D_{db}: basic density ($kg\ m^{-3}$). Numbers in parenthesis are the Standard Deviations.

The direct analysis of HHV ranges from 18.48 to 23.48 ($MJ\ kg^{-1}$) and the LHV ranges from 5.48 to 10.66 ($MJ\ kg^{-1}$), for *E. globulus* tree components. For *P. pinaster* HHV ranges from 19.57 and 21.61 ($MJ\ kg^{-1}$) and LHV from 6.85 and 12.96 ($MJ\ kg^{-1}$).

The values compiled in the literature review are in the range to the ones found in this research. Hernando et al. (2004) reported HHV of 23.458 ($MJ\ kg^{-1}$) for leaves, 19.717 ($MJ\ kg^{-1}$) for twigs and 18.870 ($MJ\ kg^{-1}$) for bark of *E. globulus* in Spain. Núñez-Regueira et al. (2002) presented HHV ranging from 20.175 to 22.105 ($MJ\ kg^{-1}$)

for leaves and HHV between 17.67 and 19.07 (MJ kg^{-1}) for branches of *E. globulus* in Spain.

For *P. pinaster* Hernando et al. (2004) reported HHV of 21.487 (MJ kg^{-1}) for live needles, 21.030 to 22.071 (MJ kg^{-1}) for dead twigs, 20.737 (MJ kg^{-1}) for dead cones scales and 20.549 (MJ kg^{-1}) for live bark in Spain. For *P. pinaster* from France, reported HHV of 21.198 (MJ kg^{-1}) for needles and for *P. pinaster* biomass from Portugal, presented HHV ranging between 20.950 and 21.593(MJ kg^{-1}). Núñez-Regueira et al. (2003) presented HHV ranging from 20.423 to 21.713 (MJ kg^{-1}) for needles and HHV between 19.085 and 21.408 (MJ kg^{-1}) for branches of *P. pinaster* in NW Spain. Gillon et al. (1997) presented HHV of 20.83 (MJ kg^{-1}) for *P. pinaster* needles in Spain. The obtained heating values are also in accordance with the ones presented in the most popular biomass databases (e.g. ECN-Biomass; Biolexbase, 2008).

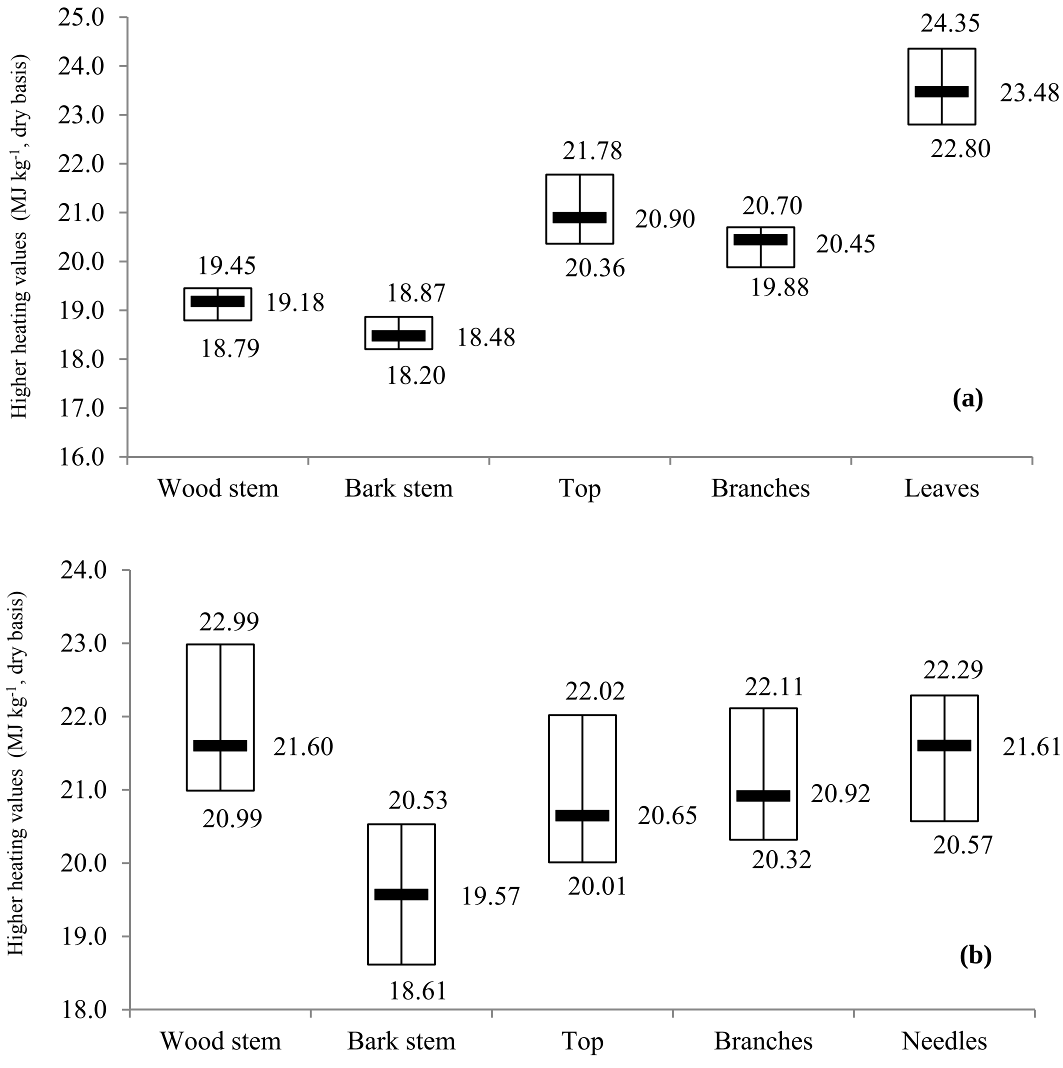

Figure 6.1 - Higher heating values of biomass tree components (a) eucalyptus and (b) maritime pine. Note: The figures show the minimum, maximum and mean HHV measured.

6.3.5. Fuelwood Value Index (FVI) and energy density (E_{ar})

The quality of fuelwood depends on quantitative and qualitative properties of wood. Quantitative properties include calorific value, wood density, moisture content, ash content, drying rate, and chemical composition. Although most of the earlier work emphasized the dried wood calorific value more than calorific value of non-dried wood, it is not as important as there is no significant difference between the majorities of the species. Moreover, effective calorific value also depends on the moisture content. The higher the moisture content, the less efficient is the wood as a fuel since the net calorific value for heating is reduced (Senelwa and Sims, 1999). In general, fuelwood has better quality when the calorific value and density are higher and the ash and moisture content is lower (Goel and Behl, 1996). Therefore, for the estimation of ideal fuelwood, a fuelwood value Index (FVI) was calculated (Table 6.6).

The heating value of a fuel is determined per unit mass, dry or as moisture as received. However, in terms of transport and storage biomass is frequently reported by volume rather than mass. Hence, it is also important to know the effective heating value per unit volume, which is the Energy Density (E) of a woodfuel (Table 6.6).

Table 6.6 - Higher and lower heating values, fuelwood value index and energy density.

Species	HHV (MJ kg^{-1})	LHV (MJ kg^{-1})	D_{db} (kg m^{-3})	BD_{ar} (kg m^{-3})	BD_{db} (kg m^{-3})	Ash (%)	FVI	E_{ar} (GJ m^{-3})	E_{db} (GJ m^{-3})
Eucalyptus globulus									
Wood stem	19.18	7.42	562.3	450.0	230.0	0.40	2727.4	3.340	4.412
Bark stem	18.48	5.48	309.6	400.0	220.0	2.61	219.1	2.193	4.066
Top	20.90	9.20	553.6	285.0	200.0	0.62	1857.2	2.623	4.180
Branches	20.45	8.95	577.1	285.0	200.0	1.33	887.5	2.550	4.090
Leaves	23.48	10.66	459.1	285.0	200.0	2.88	374.4	3.038	4.695
Pinus pinaster									
Wood stem	21.60	9.75	476.4	350.0	190.0	0.22	4658.0	3.414	4.105
Bark stem	19.57	12.96	444.5	200.0	180.0	1.31	468.8	2.591	3.523
Top	20.65	6.85	332.7	285.0	200.0	0.24	2861.8	1.960	4.140
Branches	20.92	7.30	419.6	285.0	200.0	1.00	880.4	2.085	4.192
Needles	21.61	7.22	358.6	285.0	200.0	1.97	394.2	2.058	4.321

Where: HHV: Higher Heating Value (MJ kg^{-1} at dry basis); LHV: Lower Heating Value (MJ kg^{-1}) at moisture content as received; D_{db}: basic density, dry basis (kg m^{-3}); BD_{ar} and BD_{db}: bulk density wet basis and dry basis, respectively (kg m^{-3}); Ash: Ash percentage (%); FVI: fuelwood value Index; E_{ar} and E_{db}: Energy Density, as received and dry basis, respectively (GJ m^{-3}).

As the energy density is based on the heating value and the bulk density of biomass, the differences, on a volume basis, could be very significant, depending if the biomass is processed into denser forms as chips, bundles, or densified into pellets. Some tree components, as the top, branches and leaves, needs great space for transporting and storing, so the low energy density is an evident problem associated with this wood fuel. Moreover, as the characteristics of these biomass components do not allow the processing into chips, the feasible option is transforming it into bundles after harvesting. The compaction into bundles can be very variable depending on the machinery used and type of biomass residues (e.g. Hakkila and Parikka, 2002; McKendry, 2002; Spinelli and Magagnotti, 2009). In order to quantify the energy density after harvesting (E_{ar}) we used for top, branches and leaves of pine and eucalyptus, an average bulk density of 285 kg m^{-3} for green bundles for logging residues. The energy density of stem biomass (wood stem and bark stem) can be calculated depending on the bulk density considered. Usually the stem biomass is transported in log wood (expressed in kg stacked m^{-3}) or after preprocessing into woodchips (expressed in kg bulk m^{-3}). As for energy uses is more suitable preprocess the biomass into woodchips we considered an average bulk density, without pre-drying, (BD_{ar}) of 350 kg m^{-3} for pine stem wood and 450 kg m^{-3} for eucalyptus stem wood (Loo and Koppejan, 2008). For the pine and eucalyptus bark stem we considered an average bulk density (BD_{ar}) of 200 and 400 kg m^{-3}, respectively.

For comparison purposes, the energy density, in dry basis, (E_{db}) was also calculated using the HHV and the bulk density, in dry basis, (BD_{db}). We considered an average bulk density, reported in the literature, of 200 kg m^{-3} for dry logging residues bundles, 190 and 230 kg m^{-3} for the wood stem dry woodchips and 180 and 220 kg m^{-3} for bark stem dry woodchips, for pine and eucalyptus, respectively (e.g. Ragland et al., 1991; McKendry, 2002; Spinelli and Magagnotti, 2009).

The FVI, ranging between 219.2 and 2727.4 in the *E. globulus* biomass components, and 394.2 and 4658.0 in the *P. pinaster* biomass components shows marked differences in the fuelwood properties. As expected, the wood stem achieves the higher values, indicating a superior biomass quality, as the leaves, needles and bark have the lower values.

The Energy Density (E_{ar}) of biomass components ranges from 2.193 to 3.340 GJ m^{-3} in eucalyptus and 1.960 to 3.414 GJ m^{-3} in maritime pine. However, considering the biomass after drying, the Energy Density (E_{db}) increases considerably from from 4.066 to 4.695 GJ m^{-3} in eucalyptus and 3.523 to 4.321 GJ m^{-3} in maritime pine biomass components (Table 6.6), which shows the good quality of this fuelwood when compared with other materials. For example Loo and Koppejan (2008) report the following values (wet basis): woodchips of softwood (2.800 GJ m^{-3}), grass in high pressed bales (2.740 GJ m^{-3}), straw (winter wheat) (1.740 GJ m^{-3}) or triticale (cereals) (1.920 GJ m^{-3}).

If the biomass of eucalyptus and maritime pine is processed into pellets for household usage, the bulk density will be higher ranging in the interval 520-650 kg m^{-3} (Obernberger and Thek, 2004; Loo and Koppejan, 2008), consequently the energy density will increase. For example, considering a conservative average value of 550 kg m^{-3}, in dry basis, the Energy density, in dry basis (E_{db}) will achieve 10.55 and 11.88 GJ m^{-3}, for eucalyptus and maritime pine wood stem respectively.

6.3.6. Ash elemental metals

The analysis results of heavy metals, Fe, Al, As, Cd, Pb, Co, Cu, Cr, Mn, Zn, and Ni, concentrations existent in ash (mg kg^{-1}), generated in the combustion process are presented in Table 6.7. These values are compared to the limit values established by the legislation on ash utilisation as a fertilizer in agriculture and forestry from European countries (Haglund and group, 2008) as: Finland (Maa-ja metsätalousministeriön, 2007b, 2007a), Denmark (Miljøministeriet, 2006), Austria (Asche-Richtlinie, 2006), Sweden (Skogsstyrelsen, 2008) and UK (ICRCL, 1987). The Spanish (Gobierno de España, 1990) and Portuguese (Decreto-Lei nº 118/2006) legislation, reporting the limiting values for these elements, is established for sludge from water treatment plants intended for application in agricultural soils.

Table 6.7 - Concentrations (mg kg^{-1}) of heavy metals in ash of *Eucalyptus globulus* and *Pinus pinaster* and limit values on European countries' legislation.

Species	**Fe**	**Al**	**As**	**Cd**	**Pb**	**Co**	**Cu**	**Cr**	**Mn**	**Zn**	**Ni**
Eucalyptus globulus											
Wood stem	2985.8	1236.5	2.8	0.8	0.4	8.3	479.6	199.9	5253.5	453.5	83.1
Bark stem	10750.0	589.6	2.7	0.6	1.2	7.0	33.6	61.8	13750.0	250.0	27.5
Top	12697.4	1988.1	3.4	0.6	0.8	24.7	211.9	100.0	18277.1	248.5	46.1
Branches	8495.4	1326.8	3.7	0.5	0.3	24.6	72.4	107.1	10528.4	254.1	43.6
Leaves	10525.0	7627.5	3.1	1.7	0.2	14.1	49.4	43.0	9500.0	1200.0	30.0
Pinus pinaster											
Wood stem	29375.0	5884.4	3.8	0.9	13.4	17.1	926.3	109.4	9750.0	1250.0	37.5
Bark stem	9794.0	8231.2	3.0	2.1	0.4	26.3	85.1	8.5	7239.0	1618.1	21.3
Top	4897.2	10980.2	5.7	9.7	10.2	9.0	791.2	10.8	8605.1	2863.7	21.0
Branches	7522.3	8782.3	3.8	4.7	3.9	18.7	333.7	88.8	7346.8	2557.6	20.1
Needles	7758.9	3253.7	2.4	0.7	1.5	5.6	43.2	113.5	21623.2	737.7	25.4
Country (application)											
Denmark (Agriculture/Forestry)				15	120			100			30
Finland (Agriculture)			25	1.5	100		600	300		1500	100
Finland (Forestry)			30	17.5	150		700	300		4500	150
Sweden (Forestry)			30	30	300		400	100		7000	300
Austria (Field and grassland)			20	8	100	100	250	250		1500	100
Portugal (Agriculture)*				20	750		1000	1000		2500	300
Spain (Soils with ph<7)				20	750		1000	1000		2500	300
Spain (Soils with ph>7)				40	1200		1750	1500		4000	400

* limit values of concentration of heavy metals in sludge from water treatment plants.

Heavy metals content in ash (mg $kg^{-1)}$ were similar to the usual ranges commonly found in ash of biomass tree components (wood, bark, leaves, etc.), as reported in several literature (e.g. Misra et al., 1993; Steenari and Lindqvist, 1997; Saarela et al., 2005; Pitman, 2006; Omil et al., 2007; Augusto et al., 2008; Haraldsen et al., 2011; Omil et al., 2011) and in the most popular wood and ash properties databases (e.g. BioBank; ECN-Biomass; SLU; Reisinger et al., 1992; U.S. Department of Energy, 2004; Biolexbase, 2008): Fe (3000-40000), Al (4700-74000), As (3-60), Cd (0-25), Pb (15-650), Co (<1-20), Cu (15-400), Cr (10-250), Mn (1000-30000), Zn (15-4400), and Ni (6-200). Some exceptions were observed in Al content for eucalyptus and pine needles which values were lower than the reported values in the literature. In the wood stem of eucalyptus and pine the Cu content were superior comparing with the mentioned literature. However Núñez-Regueira et al. (1996) presented even superior values of Al content for *E. globulus* and *P. pinaster* biomass, measured in NW Spain.

The measured values were well below the limits established by Portuguese current legislation for all the studied elements (except for Zn content in pine branches and tops), and below the limits from most of the European countries legislation as summarized in Table 6.7. However, some of the observed values in biomass ash would not be met the most conservative thresholds established by North and Central European countries for Cd (<1.5 mg kg^{-1}), Cu (<250 mg kg^{-1}), Cr (<100 mg kg^{-1}), Zn (<1500 mg kg^{-1}) and Ni (<1500 mg kg^{-1}).

The view on ash utilisation in forestry and agriculture varies among the European countries, partly due to the different climate and soil conditions (Haglund and group, 2008). While in some countries, mainly the Nordic countries of Europe, the use of ashes is a key factor for the replenishment of nutrients to the acid and poor soils, in other countries such problems are not so deep and therefore less worrisome. On the other hand, the logging of forest residues for use as energy production is made in a superior extent, extracting a large amount of nutrients in biomass. Hence, the ash recycling in Sweden is considered to be an important part of sustainable forestry; in Finland the ash is considered as a fertilizer to be utilised to increase growth of forests growing on peatlands; and in Denmark ash recycling is considered as a way to compensate for the loss of potassium and phosphorous (Haglund and group, 2008). In consequence, some producers of wood in Europe and Northern America have started to recycle ash on an operational scale. In Finland, more than 10% of wood and bark ash produced by forest industry is returned to the forest (Hakkila, 2002). Wood ash is spread in forests at high rates in Finland (3-5 $t.ha^{-1}$) and in Sweden (1-3 $t.ha^{-1}$).

Despite the potential soil contamination by some elements present in the ash, given their low concentration, especially in the ash-slag, the constraints on the use of this material in soil as fertilizer should be minimal, as referred by Olanders and Steenari (1995). However, Pitman (Pitman, 2006) pointed out that, whereas typical trace elements contents found in forest residues ash should present no risk, as long as fly ash is not used, the variability of Zn, Ni and Cu in bottom ash poses a risk of exceeding permissible levels if ash is applied in large quantities. As the applied quantities and ash form plays an important role in the potential effects on the environment, as example is indicated that applications of ash up to 10 t ha^{-1} from ordinary boilers result in heavy metal soil levels still two orders of magnitude lower than the USEPA (*United States Environmental Protection Agency)* advised loading. In another study, Evans et al. (2011) evaluating the use of pulp mill ash concluded that this ash has the potential to be used as a substrate component for greenhouse container production of tomato. On the other hand, Chirenje et al. (2002) using ash from at a plywood plant mentioned the need to understand the system in which wood ash is applied to minimize potential harmful effects. As highlighted by Vassilev et al. (2010), long-term research in ecological effects of ash application is scarce, and further work on quantifying their potential impact must be conducted.

6.4. Conclusion

Biomass of *Eucalyptus globulus* and *Pinus pinaster* species have been characterized by ultimate analysis, proximate analyses and heating values. A fuelwood value index and the energy density of biomass tree components were calculated. Ash elemental metals were analysed and compared to the limit values established by the legislation on ash utilisation as a fertilizer in agriculture and forestry from European countries.

The elemental analysis showed that high amounts of carbon content are stored in the biomass of tree components 43.4 to 53.1% for *E. globulus* and 46.5 to 49.3% for *P. pinaster*. This knowledge is important in studies aiming to quantify the role of this species in the carbon global cycle.

The high calorific values for *E. globulus* (18.48 to 23.48 MJ kg^{-1}), and for *P. pinaster* (19.57 to 21.61 MJ kg^{-1}) biomass tree components with Energy density of 2.467 to 3.340 GJ m^{-3} in *E. globulus* 1.954 to 4.535 GJ m^{-3} in *P. pinaster* biomass tree components reveal the great potential of this biomass to be used as a valuable source of energy. The Fuelwood Value Index ranks the pine wood stem (4658) and top (2861.8) followed by the eucalyptus wood stem (2727.4) and top (1857.2) as better fuel and the biomass of eucalyptus leaves (374.4) and pine needles (394.2) as inferior quality.

One of the issues that usually arise in the use of biomass in wood-fired power plants is the utilization of ash from combustion. In terms of the ash chemical composition the analysis showed that ash can be used on agriculture or forest soils, since heavy metals are below the legal limits. Compensation for loss of nutrients from the harvesting site could therefore be achieved by the recycling of ash as fertilizer or as a soil improving agent offering environmental and in some cases economic benefits. Nevertheless, as previous highlighted specific research in ecological effects of ash application should be done.

References

Asche-Richtlinie, 2006. Richtlinie für die Aufbringung von Asche aus Holzfeureungsanlagen und landwirtschaftlich genutzte Böden "Asche-Richtlinie 2006", Amt der Salzburger Landesregierung, Austria [Regulation on the utilisation of wood ash].

Augusto, L., Bakker, M., Meredieu, C., 2008. Wood ash applications to temperate forest ecosystems - potential benefits and drawbacks. Plant and Soil 306, 181-198.

Baernthaler, G., Zischka, M., Haraldsson, C., Obernberger, I., 2006. Determination of major and minor ash-forming elements in solid biofuels. Biomass and Bioenergy 30, 983-997.

Bert, D., Danjon, F., 2006. Carbon concentration variations in the roots, stem and crown of mature *Pinus pinaster* (Ait.). Forest Ecology and Management 222, 279-295.

Bhatt, B.P., Todaria, N.P., 1992. Fuelwood characteristics of some Indian mountain species. Forest Ecology and Management 47, 363-366.

Bhatt, B.P., Tomar, J.M.S., 2002. Firewood properties of some Indian mountain tree and shrub species. Biomass and Bioenergy 23, 257-260.

Bhatt, B.P., Tomar, J.M.S., Bujarbaruah, K.M., 2004. Characteristics of some firewood trees and shrubs of the North Eastern Himalayan region, India. Renewable Energy 29, 1401-1405.

BioBank, BIOS Bioenergiesysteme GmbH, Version 2.4, Graz, Austria, Available online at: *http://www.ieabcc.nl/database/ash.php*, (Accessed March 2012).

Biolexbase, Biolex database, properties for the samples of solid biomass fuels., Available online at: *www.biolexbase.dk*, (Accessed March 2012).

BS EN 14775:2009, Solid biofuels - Determination of ash content.

CEN EN 14774-1:2009, Solid biofuels - Determination of moisture content – Oven dry method - Part 1: Total moisture - Reference method.

CEN EN 14918:2009, Solid biofuels - Determination of calorific value.

CEN EN 15148:2009, Solid biofuels - Determination of the content of volatile matter.

Channiwala, S.A., Parikh, P.P., 2002. A unified correlation for estimating HHV of solid, liquid and gaseous fuels. Fuel 81, 1051-1063.

Chirenje, T., Rivero, C., Ma, L.Q., 2002. Leachability of Cu and Ni in wood ash-amended soil as impacted by humic and fulvic acid. Geoderma 108, 31-47.

Clark, J., Deswarte, F. (eds.) 2008. Introduction to Chemicals from Biomass. John Wiley & Sons, Ltd.

Cordero, T., Marquez, F., Rodriguez-Mirasol, J., Rodriguez, J.J., 2001. Predicting heating values of lignocellulosics and carbonaceous materials from proximate analysis. Fuel 80, 1567-1571.

DD CEN/TS 14774-1:2004, Solid biofuels - Methods for determination of moisture content - Oven dry method - Part 1: Total moisture - Reference method.

DD CEN/TS 14775:2004, Solid biofuels - Method for the determination of ash content.

DD CEN/TS 14780:2005, Solid biofuels - Methods for sample preparation.

DD CEN/TS 14918:2005, Solid biofuels - Method for the determination of calorific value.

DD CEN/TS 15104:2005, Solid biofuels – Determination of total content of carbon, hydrogen and nitrogen – Instrumental methods.

DD CEN/TS 15148:2005, Solid biofuels – Method for the determination of the content of volatile matter.

DD CEN/TS 15234:2006, Solid biofuels - Fuel quality assurance. Annex E. Calculation of the net calorific value in different basis and energy density as received.

DD CEN/TS 15289:2006, Solid biofuels – Determination of total content of sulphur and chlorine.

DD CEN/TS 15290:2006, Solid biofuels – Determination of major elements.

DD CEN/TS 15297:2006, Solid biofuels – Determination of minor elements.

Decreto-Lei nº 118/2006, Decreto-Lei nº 118/2006, de 21 de Junho, Estabelece o regime jurídico da utilização agrícola das lamas de depuração [Establishes the legal regime of the agricultural use of sewage sludge].

Demirbas, A., 1997. Calculation of higher heating values of biomass fuels. Fuel 76, 431-434.

DGGE, 2006. Estratégia Nacional para a Energia. A criação de uma rede de Centrais de Biomassa dedicadas, Direcção Geral de Geologia e Energia, Lisboa, p. 19.

ECN-Biomass, Phyllis, database for biomass and waste. Energy research Centre of the Netherlands (ECN). Version: 4.13, Available online at: *http://www.ecn.nl/phyllis/*, (Accessed March 2012).

Evans, W.B., Bi, G., Fain, G.B., 2011. Addition of pulp mill ash raises ph, modifies physical properties, and alters young tomato plant growth and mineral nutrition in a peat-based substrate. Journal of Plant Nutrition 34, 1894-1903.

Franco, C., Pinto, F., Gulyurtlu, I., Cabrita, I., 2003. The study of reactions influencing the biomass steam gasification process☆. Fuel 82, 835-842.

Friedl, A., Padouvas, E., Rotter, H., Varmuza, K., 2005. Prediction of heating values of biomass fuel from elemental composition. Analytica Chimica Acta 544, 191-198.

Gillon, D., Hernando, C., Valette, J.-C., Joffre, R., 1997. Fast estimation of the calorific values of forest fuels by near-infrared reflectance spectroscopy. Canadian Journal of Forest Research 27, 760-765.

Girón, R.P., Suárez-Ruiz, I., Ruiz, B., Fuente, E., Gil, R.R., 2012. Fly Ash from the Combustion of Forest Biomass (*Eucalyptus globulus* Bark): Composition and Physicochemical Properties. Energy & Fuels 26, 1540-1556.

Gobierno de España, 1990. 1990/26940 Real Decreto 1310/1990, de 29 de Octubre, por el que se regula la Utilización de los Lodos de Depuración en el Sector Agrario. BOE 262/1990 de 01-11-1990, pp. 32339. Ministerio de Agricultura, Pesca y Alimentación, Gobierno de España.

Goel, V.L., Behl, H.M., 1996. Fuelwood quality of promising tree species for alkaline soil sites in relation to tree age. Biomass and Bioenergy 10, 57-61.

Gominho, J., Lourenço, A., Miranda, I., Pereira, H., 2012. Chemical and fuel properties of stumps biomass from *Eucalyptus globulus* plantations. Industrial Crops and Products 39, 12-16.

Haglund, N., group, E., 2008. Guideline for classification of ash from solid biofuels and peat utilised for recycling and fertilizing in forestry and agriculture, NT TECHN REPORT 613, Nordic Innovation Centre, Norway.

Hakkila, P., 2002. Operations with reduced environmental impact, in: Richardson, J., Björheden, R., Hakkila, P., Lowe, A.T., Smith, C.T. (eds.), Bioenergy from Sustainable Forestry: Guiding Principles and Practice, vol. 71. Kluwer Academic Publishers, pp. 244-264.

Hakkila, P., Parikka, M., 2002. Fuel Resources from the forest, in: Richardson, J., Björheden, R., Hakkila, P., Lowe, A.T., Smith, C.T. (eds.), Bioenergy from Sustainable Forestry. Guiding Principles and Practice, vol. 71. Kluwer Academic Publishers.

Haraldsen, T.K., Pedersen, P.A., Grønlund, A., 2011. Mixtures of Bottom Wood Ash and Meat and Bone Meal as NPK Fertilizer. Recycling of Biomass Ashes, in: Insam, H., Knapp, B.A. (eds.). Springer Berlin Heidelberg, pp. 33-44.

Hernando, C., Guijarro, M., Madrigal, J., 2004. Physical, chemical and thermal characteristics of the wildland fuel particles. Available online at: *http://www.eufirelab.org/prive/directory/units_section_2/D-02-02/D-02-02.pdf* (Accessed April 2012).

ICRCL, 1987. Guidance on the Assessment and Redevelopment of Contaminated Land. Guidance Note 59/83, Department of the Environment, Interdepartmental Committee on the Redevelopment of Contaminated Land, London.

Loo, S.V., Koppejan, J. (eds.) 2008. The Handbook of Biomass Combustion and Co-firing. Earthscan, London pp. 407.

Lopes, D., Estimating Net Primary Production in *Eucalyptus globulus* and *Pinus pinaster* Ecosystems in Portugal, Kingston University, PhD Thesis, England, 2005.

Lousada, J., Noronha, M., Lopes, D., Silva, M., 2008. Relações entre Peso, Volume e Densidade para a Madeira de Pinheiro Bravo (*Pinus pinaster* Ait.) Cultivado em Portugal. Silva Lusitana 16, 183-196.

Maa-ja metsätalousministeriön, 2007a. Asetus lannoitevalmisteista koskevan toiminnan harjoittamisesta ja sen valvonnasta, nro 13/07. [Ministry of Agriculture and Forestry Decree on the operations concerning fertilizer products and their supervision], Helsinki.

Maa-ja metsätalousministeriön, 2007b. Maa- ja metsätalousministeriön asetus lannoitevalmisteista nro12/07. [Ministry of Agriculture and Forestry Decree on fertilizer products], Helsinki.

McKendry, P., 2002. Energy production from biomass (part 1): overview of biomass. Bioresource Technology 83, 37-46.

Miles, T.R., Miles Jr, T.R., Baxter, L.L., Bryers, R.W., Jenkins, B.M., Oden, L.L., 1996. Boiler deposits from firing biomass fuels. Biomass and Bioenergy 10, 125-138.

Miljøministeriet, 2006. Nr. 1636 af 13. december 2006 Bek. om anvendelse af aske fra forgasning og forbrænding af biomasse og biomasseaffald til jordbrugsformålMiljøministeriet (Miljøstyrelsen) (Ophævet 15/8 2008 ved bekendtgørelse nr. 818 af 21/7 2008), Denmark [Regulation on utilisation of ashes from biomass in agriculture including forestry].

Misra, M.K., Ragland, K.W., Baker, A.J., 1993. Wood ash composition as a function of furnace temperature. Biomass and Bioenergy 4, 103-116.

Nirmal Kumar, J.I., Patel, K., Kumar, R.N., Bhoi, R.K., 2011. An evaluation of fuelwood properties of some Aravally mountain tree and shrub species of Western India. Biomass and Bioenergy 35, 411-414.

Nunes, E., Quilhó, T., Pereira, H., 1996. Anatomy and chemical composition of *Pinus pinaster* bark. IAWA Journal 17(2), 141-149

Núñez-Regueira, L., Añón, J.A.R., Castiñeiras, J.P., 1996. Calorific values and flammability of forest species in Galicia. Coastal and hillside zones. Bioresource Technology 57, 283-289.

Núñez-Regueira, L., Añón, J.A.R., Castiñeiras, J.P., 1999. Design of risk index maps as a tool to prevent forest fires in the northern coast of Galicia (N.W. Spain). Bioresource Technology 69, 23-33.

Núñez-Regueira, L., Proupín-Castiñeiras, J., Rodríguez-Añón, J.A., 2002. Energy evaluation of forest residues originated from *Eucalyptus globulus* Labill. in Galicia. Bioresource Technology 82, 5-13.

Núñez-Regueira, L., Rodríguez-Añón, J., Proupín, J., Romero-García, A., 2003. Energy evaluation of forest residues originated from pine in Galicia. Bioresource Technology 88, 121-130.

Núñez-Regueira, L., Rodríguez-Añon, J.A., Proupín-Castiñeiras, J., 2004. Using calorimetry for determining the risk indices to prevent and fight forest fires. Thermochimica Acta 422, 81-87.

Obernberger, I., Thek, G., 2004. Physical characterisation and chemical composition of densified biomass fuels with regard to their combustion behaviour. Biomass and Bioenergy 27, 653-669.

Obernberger, I., Brunner, T., Bärnthaler, G., 2006. Chemical properties of solid biofuels—significance and impact. Biomass and Bioenergy 30, 973-982.

Olanders, B., Steenari, B.-M., 1995. Characterization of ashes from wood and straw. Biomass and Bioenergy 8, 105-115.

Omil, B., Piñeiro, V., Merino, A., 2007. Trace elements in soils and plants in temperate forest plantations subjected to single and multiple applications of mixed wood ash. Science of The Total Environment 381, 157-168.

Omil, B., Sánchez-Rodríguez, F., Merino, A., 2011. Effects of Ash Applications on Soil Status, Nutrition, and Growth of *Pinus radiata* D. Don Plantations, in: Insam, H., Knapp, B.A. (eds.), Recycling of Biomass Ashes. Springer Berlin Heidelberg, pp. 69-86.

Parikh, J., Channiwala, S.A., Ghosal, G.K., 2007. A correlation for calculating elemental composition from proximate analysis of biomass materials. Fuel 86, 1710-1719.

Parr Instruments Company, The 6300 Parr calorimeter operating instruction manual, Fifty-third street Moline, Illinois 61265 USA.

Pérez, S., Renedo, C.J., Ortiz, A., Mañana, M., Silió, D., 2006. Energy evaluation of the Eucalyptus globulus and the *Eucalyptus nitens* in the north of Spain (Cantabria). Thermochimica Acta 451, 57-64.

Pitman, R.M., 2006. Wood ash use in forestry – a review of the environmental impacts. Forestry 79, 563-588.

Ragland, K.W., Aerts, D.J., Baker, A.J., 1991. Properties of wood for combustion analysis. Bioresource Technology 37, 161-168.

Reisinger, K., Haslinger, C., Herger, M., Hofbauer, H., BIOBIB - a Database for Biofuels. Institute of Chemical Engineering, Fuel and Environmental Technology, Available online at: *http://cdmaster2.vt.tuwien.ac.at/biobib/biobib.html*, (Accessed March 2012).

Reva, V., Fonseca, L., Lousada, J., Abrantes, I., Viegas, D., 2012. Impact of the pinewood nematode, Bursaphelenchus xylophilus, on gross calorific value and chemical composition of *Pinus pinaster* woody biomass. European Journal of Forest Research 131, 1025-1033.

Saarela, K.E., Harju, L., Rajander, J., Lill, J.O., Heselius, S.J., Lindroos, A., Mattsson, K., 2005. Elemental analyses of pine bark and wood in an environmental study. Science of The Total Environment 343, 231-241.

Senelwa, K., Sims, R.E.H., 1999. Fuel characteristics of short rotation forest biomass. Biomass and Bioenergy 17, 127-140.

Skogsstyrelsen, 2008. Rekommendationer vid uttag av avverkningsrester och askåterföring, Meddelande Nr 2/2008 [Approximately Recommendations on ash recycling to the forest, Notice Nr 2/2008], Sweden.

SLU, Wood Ash Database - chemical composition of ashes formed during combustion of biofuels from tree compartments, Available online at: *http://woodash.slu.se/eng/*, (Accessed March 2012).

Spinelli, R., Magagnotti, N., 2009. Logging residue bundling at the roadside in mountain operations. Scandinavian Journal of Forest Research 24, 173-181.

Steenari, B.M., Lindqvist, O., 1997. Stabilisation of biofuel ashes for recycling to forest soil. Biomass and Bioenergy 13, 39-50.

Telmo, C., Lousada, J., Moreira, N., 2010. Proximate analysis, backwards stepwise regression between gross calorific value, ultimate and chemical analysis of wood. Bioresource Technology 101, 3808-3815.

Tsoumis, G.T., 1991. Science and Technology of wood. Structures, Properties, Utilization. Van Nostrand Reinhold, New York.

U.S. Department of Energy, Biomass Feedstock Composition and Property Database, Available online at: *http://www1.eere.energy.gov/biomass/databases.html*, (Accessed March 2012).

Vassilev, S.V., Baxter, D., Andersen, L.K., Vassileva, C.G., 2010. An overview of the chemical composition of biomass. Fuel 89, 913-933.

Vázquez, G., Antorrena, G., Parajó, J.C., 1987. Studies on the utilization of *Pinus pinaster* bark. Wood Science and Technology 21, 155-166.

Vázquez, G., Antorrena, G., González, J., Freire, S., 1995. Studies on the composition of *Pinus pinaster* foliage. Bioresource Technology 51, 83-87.

Viana, H., Cohen, W.B., Lopes, D., Aranha, J., 2010. Assessment of forest biomass for use as energy. GIS-based analysis of geographical availability and locations of wood-fired power plants in Portugal. Applied Energy 87, 2551-2560.

Yin, C.-Y., 2011. Prediction of higher heating values of biomass from proximate and ultimate analyses. Fuel 90, 1128-1132.

Zhan, G., Erich, M.S., Ohno, T., 1996. Release of trace elements from wood ash by nitric acid. Water, Air, & Soil Pollution 88, 297-311.

7

Fuel characterization and biomass combustion properties of selected native woody shrub species from central Portugal and NW Spain

The content of this chapter was fully published in the following manuscript:

[Annex E.4] Viana, H., Vega-Nieva, D., Ortiz Torres, L., Lousada, J., Aranha, J., 2012., Fuel characterization and biomass combustion properties of selected native woody shrub species from central Portugal and NW Spain. Fuel 102, 737-745.

Data from this chapter contributed for the following publication:

[Annex E.1] Viana, H., Fernandes, P., Rocha, R., Lopes, D., Aranha, J., 2009. Alometria, Dinâmicas da Biomassa e do Carbono Fixado em Algumas Espécies Arbustivas de Portugal 6º Congresso Florestal Nacional, Ponta Delgada, Açores. 6-9 Outubro, pp. 244-252.

Abstract

Selected native shrub species from central Portugal and NW Spain, *Cytisus multiflorus* (broom), *Erica australis* (heath), *Pterospartum tridentatum* (L.) Willk (carqueisa) and *Ulex europaeus* (gorse) were characterized for physical, thermal and chemical properties. Proximate and ultimate analysis were carried out and the fuel energy density (Ear) was calculated. Moreover, ash characterization, slagging and fouling indices and associated risk and potential heavy metal contamination risk and emissions risk were evaluated. The studied shrub species showed ash contents in the range of 1-2%. The carbon contents ranged from 46.20 to 49.84 % for aboveground biomass and from 45.49% to 46.50 % for belowground biomass, with the highest carbon content found for aerial biomass of heath. Nitrogen contents ranged from 0.63 to 2.05%, hydrogen ranged from 6.08 to 7.04% and sulphur contents were below 0.1%. The Higher Heating Value (HHV) ranged from 24.44 MJ kg^{-1} for *Erica australis*, 22.46 MJ kg^{-1} for *Cytisus Multiflorus*, 21.94 MJ kg^{-1} for *Pterospartum tridentatum* and 21.16 MJ kg^{-1} for *Ulex europaeus*. A significant effect of species on Higher Heating Value (HHV) was observed, with no significant effect of the location of study, central Portugal or NW Spain. Analysis of the chemical composition of the ashes revealed alkali metals contents of 24-30%, representing a potential sintering, fouling and bed agglomeration risk in the combustion of the studied species. Ash As, Cd, Pb, Co, Cu, Mn, Ni, Cr, and Zn content was below Portuguese, Spanish and most of European legislation maximum levels for these elements for ash application as fertilizer, with the exception of some of the more conservative limits for Cd, Cu, Cr and Zn from Northern and central European countries legislation.

Keywords: shrub biomass; heating value; proximate and ultimate analysis, ash composition; slagging; fouling.

7.1. Introduction

The interest in the utilization of forest biomass for bioenergy has increased exponentially in the last decades in European countries, as an integrated strategy for climate change mitigation, increasing renewable energy security and preventing forest fires. Consequently, Portuguese (DGGE, 2006) and Spanish (Gobierno de España, 2010) National strategies, have established ambitious goals for energy production in dedicated biomass plants for CHP, resulting in a large potential biomass demand in both countries. Given the limited availability of residual forest biomass in Portugal (Viana et al., 2010) and Spain (Bermúdez and Piñeiro, 2000), joined with a growing pellet production in these two countries, potentially utilizing forest residual biomass sources (Miranda et al., 2009), there is an increased interest on the consideration of alternative feedstocks for biomass combustion, such as native woody shrub species.

Shrubland areas currently occupy close to 1 million hectares in the region of Galicia, NW Spain (Núñez-Regueira et al., 2004) and a total of 1.9 million hectares in Portuguese territory (AFN, 2010). Furthermore, abandoned shrubland areas constitute a main fuel for the frequent wildfires in these two countries: approximately half of the 1.5 and 0.2 million hectares burned by wildfires in Portugal and in the region of Galicia, NW Spain, in the period 2001 to 2010, were shrubland areas (AFN, 2011). The regular harvesting of shrubland areas, might therefore additionally be valuable for diminishing the large greenhouse gas emissions associated to these frequent wildfires (Silva et al., 2006), through the reduction of forest fires occurrence.

In order to evaluate their potential as a biomass feedstock for combustion, there is a need for an integrated biomass and ash characterization for the main native species in the shrubland areas of these two countries. Available information on biomass characterization and specific combustion properties of native woody shrub species in this area, however, is relatively scarce, namely the studies by Núñez-Regueira et al. (1999) and Elvira and Hernando (1989) in NW and central Spain, and the studies from Fernandes and Pereira (1993) and from Fernandes and Rego (1998) in Portugal, among others.

Fuel calorific properties are known to be influenced by biomass composition (e.g. Demirbas, 1997; Friedl et al., 2005; Vassilev et al., 2010), this species-specific composition being potentially influenced by growing conditions such as sunlight, geographic location, climate, soil types, available water, soil pH and nutrients (Vassilev et al., 2010). Therefore, it would be of interest to study whether the different local soil and climate conditions from NW Spain and central Portugal have an effect on the calorific properties of the existing native shrub species.

Moreover, available shrub characterization studies for these native species have only focused on selected biomass physical and chemical properties such as basic density (e.g. Fernandes and Rego, 1998), calorific value (e.g. Elvira and Hernando, 1989), and/or fuel proximate and ultimate analysis (e.g. Núñez-Regueira et al., 1999). However, proximate and ultimate analysis brings relatively limited information when the chemical composition of the combusted biomass is not also considered (Vassilev et al., 2010), particularly given the potential ash slagging and fouling risk in biomass fuels with high mobile nutrients contents, specially alkali metals, in their ashes, which can limit boiler efficiency and even lead to bed defluidization through deposit formation and boiler corrosion (e.g. Miles et al., 1996; Fernández Llorente and Carrasco García, 2005; Vega-Nieva et al., 2010). In spite of its relevance on combustion efficiency, slagging and fouling risk, information on the ash composition of these native shrub species is scarce, together with a scarcity of information on the ash composition for shrub species in general: for instance, neither any of the main recent reviews in fuel and ash composition (e.g. Werther et al., 2000; Vassilev et al., 2010; Vega-Nieva et al., 2010), nor any of the main ash composition databases (e.g. BioBank; ECN-Biomass; SLU; Reisinger et al., 1992; U.S. Department of Energy, 2004; Biolexbase, 2008), include any information on shrub ashes composition and/or the associated ash slagging and fouling risk. Additionally, an integrated evaluation of the potential of shrub ashes should consider the monitoring of relevant minor and trace elements contents in the ashes, which are of particular relevance for the environmental impact of the potential ashes reutilization as fertilizer (e.g. Pitman, 2006; Omil et al., 2007; Augusto et al., 2008).

Consequently, the present research aimed to study the fuel and ash characteristics and combustion properties of the selected native shrubs *Cytisus multiflorus* (L'Hér.) Sweet (broom), *Erica australis* (L.) (heath), *Ulex europaeus* (L.) (gorse) and *Pterospartum tridentatum* (L.) Willk (carqueisa), these species being representative of the main genus present in the Mediterranean native shrubland areas of NW Spain and North-Central Portugal. The analysis of physical and thermochemical properties of the shrub biomass including: (1) basic density (Db); (2) proximate analysis, namely moisture content (w%), fixed carbon (FC%), volatile matter (VM%)

and ash yield (A%); (3) ultimate analysis (C, O, H, S, N); (4) calorific value (Higher and Lower Heating Value) and (5) energy density calculation, was conducted for the four species at both areas of study. Additionally, (6) ash chemical composition, including relevant minor and trace elements contents, was analysed.

7.2. Material and methods

7.2.1. Shrub biomass measurement and sampling for fuel and ash analysis

7.2.1.1. Shrub biomass measurement

The areas of study are located in North-Center Portugal (Area 1), extending from 39º 11' 53" N, 06º 14' 17' W to 42º 50' 50" N, 0 8º 19' 02" W and NW Spain (Area 2), extending from 42° 56' 26.06" N, 7° 26' 25.89 W to 42° 31' 28.05" N, 7° 31' 10.41 W. From June to August 2007, 22 and 32 sites were sampled in Area 1 and Area 2, respectively, for aboveground biomass determination. Within each site, occupying homogeneously at least one hectare, a sampling plot with an area of 10 m^2 was established and the aboveground biomass within that plot was clipped, placed into hermetically closed containers to prevent moisture loss and transported to the laboratory, where it was divided by species, oven dried and weighted to determine the dry aboveground biomass per hectare (ton ha^{-1}).

7.2.1.2. Sampling for biomass and ash analysis

The selected species for study of biomass and ash characterization were: *Cytisus multiflorus* (L'Hér.) Sweet (Spanish or Portuguese white broom), *Erica australis* (L.) (Spanish or Portuguese heath), *Ulex europaeus* (L.) (common gorse or furze) and *Pterospartum tridentatum* (L.) Willk (carqueisa).

For each subject woody shrub species, 7 to 9 biomass samples, representative of all the sampled aboveground biomass fractions, were randomly selected from the harvested biomass for fuel and ash laboratory analyses (section 7.2.2). Aboveground biomass samples included leaves and all woody fractions from aboveground biomass. In addition, in Area 1 of study, belowground root biomass samples were taken for proximate and ultimate analyses, by cutting representative small fractions of the exposed root system. Soil particles were carefully removed with high pressure water application.

All samples were prepared according to the technical specifications (DD CEN/TS 14780:2005) for sample preparation for the physical, thermal and chemical characterization of biomass.

7.2.2. Analytical measurements

7.2.2.1. Proximate analysis and basic density

Moisture content (wet basis) was determined following the European Standard (CEN EN 14774-1:2009). The determination of ash content (dry basis) was carried out at 550 ºC ± 10ºC according to (BS EN 14775:2009) The volatile matter content (dry basis) was determined at 900 °C ± 10 °C according to (CEN EN 15148:2009). Fixed carbon content (%) is the difference between the sum of volatile matter and ash contents from 100. Shrub basic density (Db) was calculated by water displacement technique and expressed as dry weight per unit volume (Tsoumis, 1991).

7.2.2.2. Ultimate analysis

Elemental composition of shrub biomass was measured following the Technical standards (DD CEN/TS 15104:2005) for determining Carbon (C), Hydrogen (H) and Nitrogen (N) and the European Standard (DD CEN/TS 15289:2006) for Sulphur (S) content in solid biofuels. The simultaneous determination of CHN was carried out in a Leco TruSpec Elemental Determinator. Sulphur content determination was done in a Leco SC-144DR using direct combustion and infrared detection. The oxygen content was obtained by subtracting from 100% the sum of (C, H, N, S and ash) contents in percentage.

7.2.2.3. Higher and Lower Heating Values

The higher heating value (HHV), also called gross calorific value (GCV), of biomass at constant volume in dry basis was determined following the European Standard (CEN EN 14918:2009). The HHV in dry basis was calculated by Eq. 1:

$$q_{v,gr,d} = q_{v,gr} \frac{100}{100 - M_{ad}} \qquad [1]$$

where:

$q_{v,gr,d}$ is the higher heating value at constant volume of the dry (moisture-free) fuel, in joules per gram;
M_{ad} is the moisture in the analysis sample, in percentage by mass;
$q_{v,gr}$ is the higher heating value at constant volume of the fuel as analysed, in joules per gram.

The LHV was calculated as (Eq. 2):

$$q_{p,net,d} = q_{v,gr,d} - 212{,}2w(H)_d - 0{,}8\left[w(O)_d + w(N)_d\right] \qquad [2]$$

where:

$q_{p,net,d}$ is the lower heating value in dry basis at constant pressure, in joules per gram, of the biofuel;
$q_{v,gr,d}$ is the higher heating value at constant volume of the dry (moisture-free) biofuel, in joules per gram;
$w(H)_d$ is the hydrogen content, in percentage by mass, of the moisture-free (dry) biofuel;
$w(O)_d$ is the oxygen content, in percentage by mass of the moisture-free biofuel;
$w(N)_d$ is the nitrogen content, in percentage by mass, of the moisture-free biofuel.

The LHV at constant pressure at a required moisture content w%, was calculated as (Eq. 3):

$$q_{p,net,ar} = q_{p,net,d}\left(1 - 0.01M_{ar}\right) - 24.43M_{ar} \qquad [3]$$

where:

$q_{p,net,ar}$ is the lower heating value at constant pressure, in joules per gram, of the biofuel with moisture content as received M_{ar} ;
$q_{p,net,d}$ is the lower heating value in dry basis at constant pressure, in joules per gram, of the biofuel;
M_{ar} is the moisture content as received [w-%];
24.43 is the correction factor of the enthalpy of vaporization (constant pressure) for water (moisture) at 25 °C [J g^{-1} per 1 w-% of moisture].

7.2.2.4. Fuel Energy Density

The energy density as received (E_{ar}) was calculated using the lower heating value as received and the bulk density (DD CEN/TS 15234:2006), according to Eq. 4.

$$E_{ar} = \frac{1}{3600} \; q_{p,net,ar} \quad BD_{ar} \qquad [4]$$

where

E_{ar} is the energy density of the biofuel as received (MWh m^{-3} of bulk density);

$q_{p,net,ar}$ is the lower heating value as received (MJ kg^{-1});

BD_{ar} is the bulk density, i.e., volume weight of the biofuel as received (kg m^{-3} bulk volume);

$\frac{1}{3600}$ is the conversion factor for the energy units (MJ to MWh).

Fuel bulk density depends on the utilized biomass logistics: chipping, bundling, etc. The most feasible option for the shrub fuels under study consists on fuel bundling after harvesting. The compaction into bundles can be very variable depending on the machinery used and type of biomass residues (e.g. Hakkila and Parikka, 2002; Spinelli and Magagnotti, 2009). Since it was not the purpose of this paper to explore these issues, an average value of bulk density for green bundles for logging residues (285 kg m^{-3}) reported by Hakkila and Parikka (2002) was utilized for providing an initial estimate of the energy density of the shrub bundles after harvesting. A sensitivity analysis of the effects of varying this average bundling bulk density value on +/- 25 % on calculated energy density was additionally performed.

7.2.2.5. Ash chemical composition

The chemical composition of the biomass ash, obtained at 550 ºC following (BS EN 14775:2009) European Standard, was analysed according to the Solid Biofuels Standards to determine major elements (DD CEN/TS 15290:2006) and the Solid Biofuels Standards to determine minor elements (DD CEN/TS 15297:2006). Ash Si, Al, Ti, Fe, Na, K, Ca, Mg, P determination was done by flame atomic absorption spectrometry (FAAS), and the measurement of ash As, Cd, Pb, Co, Cu , Cr, Mn , Zn and Ni was done by Graphite furnace atomic absorption spectroscopy (GF-AAS), after an ash digestion with Nitric acid - HNO_3 (65%), Hydrogen peroxide-H_2O_2 (30%), Hydrofluoric acid - HF (40%), utilizing a Boric acid - H_3BO_3 (4%) neutralization for the first elements as recommended by Baernthaler et al. (2006).

7.2.2.6. Ash slagging and fouling indices

The following slagging and fouling indices were calculated from ash chemical composition, according to the following expressions (Miles et al., 1996), (Watanabe et al., 1996), (Vamvuka and Zografos, 2004) and (Fernández Llorente and Carrasco García, 2005):

Base to acid index (Watanabe et al., 1996) was calculated according to Eq. 5:

$$B/A = \frac{Fe_2O_3 + CaO + MgO + Na_2O + K_2O}{SiO_2 + Al_2O_3 + TiO_2} \qquad [5]$$

Being that: if B/A < 0.75, slagging trend can be expected (Watanabe et al., 1996).

R_S index (Watanabe et al., 1996) was calculated according to Eq. 6:

$$RS = (B/A)S^d \qquad [6]$$

where: S^d is S in percentage from elementary analysis. If R_S < 0.6 - low fouling trend; if 0.6 < R_S < 2 - medium trend; if 2.0 < R_S < 2.6 - high trend; if R_S > 2.6 - very high trend (Watanabe et al., 1996).

Alkali Index (AI) (Miles et al., 1996) was calculated according to Eq. 7:

$$A.I. = \frac{(K_2O + Na_2O)A(\%)}{HHV} \qquad [7]$$

where: A(%) is the ash percentage obtained at 550 ºC and HHV is the Higher Heating value (MJ kg^{-1}) at w%=0% . If AI > 0.17 kg alkali MJ^{-1} probable slagging and fouling; if AI> 0.34 kg alkali MJ^{-1} slagging and fouling is certain to occur according to Miles et al. (1996).

The following sintering index (SI) (Fernández Llorente and Carrasco García, 2005) was calculated according to Eq. 8:

$$SI = \frac{CaO + MgO}{Na_2O + K_2O} \qquad [8]$$

Being that: no slagging should be expected at values of SI> 2, whereas the slagging risk should be high at SI<2 (Fernández Llorente and Carrasco García, 2005).

For evaluating the risk of bed agglomeration in fluidised bed combustion, the following bed agglomeration index (BAI) (Vamvuka and Zografos, 2004) was calculated according to Eq. 9:

$$BAI = \frac{Fe_2O_3}{Na_2O + K_2O} \qquad [9]$$

Being that: bed agglomeration occurs when BAI <0.15 (Vamvuka and Zografos, 2004).

7.3. Results and discussion

7.3.1. Shrub biomass measurement

Descriptive statistics of the shrub biomass sampling plots at the two areas under study are shown in Table 7.1. All the studied species were characterized by a high weight of fine fractions of < 6mm.

Higher biomass values were found for broom (*Citisus multiflorus*), followed by gorse (*Ulex europaeus*) at both areas of study. Average biomass values for the studied species (Bi) are of a similar range to the values measured in NW Spain shrubland (Núñez-Regueira et al., 1999). In addition to average biomass values for each species, the biomass distribution for an average mixed shrubland plot is given in Table 7.1, resulting in an average total aboveground biomass (Bt) sum of 18.6 and 26 ton ha^{-1} (dry basis) for an average plot in the areas of study in central Portugal and NW Spain, respectively.

Table 7.1 - Descriptive statistics of the shrub biomass sampling plots at the two areas of study.

Area of Study *species*	**ns**	**np**	**h (m)**	**%B (db) < 6 mm**	**CC (%)**	**Bi (dry ton ha^{-1})**	**Bt (dry ton ha^{-1})**
Central Portugal							
Cytisus multiflorus	9	11	0.8 (± 0.3)	85 (± 14)	27.5 (± 22.3)	13.6 (± 7.9)	10.3 (± 9.1)
Erica australis	7	9	0.7 (±0.4)	89 (± 9)	21.4 (± 17.2)	4.9 (± 3.0)	3.9 (± 4.2)
Pterospartum tridentatum	7	10	0.2 (± 0.1)	93 (± 6)	12.0 (± 7.3)	2.9 (± 2.3)	1.7 (± 2.4)
Ulex europaeus	9	12	0.7 (± 0.5)	80 (± 16)	25.4 (± 11.8)	5.5 (± 2.7)	2.9 (± 3.4)
Other species	n	22	0.1 (± 0.2)	99 (± 1)	2.4 (± 2.6)	0.2 (± 0.4)	0.1 (± 0.3)
Sum							18.9 (± 13.4)
NW Spain							
Cytisus multiflorus	9	26	1.6 (± 0.8)	58 (± 35)	83.7 (± 16.1)	30.1 (± 12.3)	8.9 (± 9.6)
Erica australis	7	16	0.9 (± 0.7)	78 (± 17)	85.9 (± 14.3)	26.4 (± 7.4)	4.8 (± 5.3)
Pterospartum tridentatum	7	19	0.4 (± 0.3)	91 (± 4)	38.6 (± 15.7)	16.0 (± 5.9)	3.3 (± 4.8)
Ulex europaeus	9	28	0.9 (± 0.7)	74 (± 21)	87.2 (± 10.4)	28.7 (± 6.8)	9.1 (± 10.2)
Other species	n	32	0.2 (± 0.3)	98 (± 2)	2.6 (± 0.3)	0.3 (± 0.5)	0.2 (± 0.5)
Sum							26.3 (± 16.2)

Where: ns: number of biomass sub-samples selected for biomass and ash analysis at the laboratory; np: number of study plots at each area of study where the species was present; h(m): shrub height (m); % B (db)< 6 mm: Percentage of aboveground biomass (dry weight) corresponding to the fraction of less than 6 mm; CC: shrub canopy cover (%); Bi (ton ha^{-1}) (db): average shrub aboveground biomass (ton ha^{-1} on dry basis), for the plots where the species was present; Bt (ton ha^{-1}) (db): average shrub aboveground biomass (ton ha^{-1} on dry basis), considering all the plots of the area of study. Numbers in parenthesis are the Standard Deviations.

7.3.2. Proximate analysis and basic density

7.3.2.1. Proximate analysis

Proximate analysis and basic density results are shown in Table 7.2. Ash percentage ranged from 1.21 % to 1.56 % for the shrub aboveground biomass of the studied species. Similarly, a seasonal range in ash content for native gorse, broom and heath of 0.71-1.14%, 0.16-0.86% and 0.21-0.79% respectively, were observed in NW Spain (Núñez-Regueira et al., 1999). Ash values of 2.42 % have been reported for *Ulex parviflorus* in France (Doat et al., 1981). The presence of leaves and spines in the evergreen studied species possibly contributed to the relatively high ashes content of the shrub biomass: for instance, Dimitrakopoulos and Panov (2001) reported values of 2.51 % for *Erica arborea* leaves, while the ash content of the same species twigs was 1.63%.

Whereas typical ash content in wood is 0.5%, the ash content in the actively metabolising fractions such as leaves, and in the low diameter branch fractions, where mobile nutrients such as potassium are accumulated, can be as high as 2-5% (e.g. Werkelin et al., 2005; Obernberger et al., 2006; Vassilev et al., 2010). Ash composition will be further discussed in section 7.3.6.2.

The observed values of volatile matter were similar to the usual range of 70 to 86% in volatiles for woody biomass (e.g. Werkelin et al., 2005; Obernberger et al., 2006; Vassilev et al., 2010), with the higher volatile percentages and lower fixed carbon measured for the belowground biomass samples. In high volatiles content fuels, care must be taken to achieve complete combustion of the volatiles to ensure higher combustion efficiency and low emissions of CO, hydrocarbons and PAH (Werther et al., 2000).

Moisture values at the time of reception correspond to the lower values in the reported year-round seasonal ranges in moisture content of 47.5-66.8%, 57.5-62.0%, and 44.4-63.2% for native gorse, broom and heath found in NW Spain (Núñez-Regueira et al., 1999), as it would be expected for a summer harvest of these species. Fuel moisture values should only be regarded as indicative of the conditions at the particular time of sampling at the two areas; furthermore, actual fuel moisture at reception would be influenced both by the season of harvest and the logistics of harvesting and transport.

7.3.2.2. Basic density

Basic density of the shrub aboveground biomass ranged from 404 to 498 kg m^{-3}, the highest values corresponding to heath at both areas of study (Table 7.2). Similar values of 500 to 580 kg m^{-3}, 427 to 484 kg m^{-3}, 356 to 474 kg m^{-3} and 379 to 500 kg m^{-3}, have been reported for Spanish and Portuguese heath, carqueisa, gorse and broom by Elvira and Hernando (1989), Fernandes and Pereira (1993) and Fernandes and Rego (1998), these shrub aboveground biomass samples including leaves and twigs of less than 6 mm, like in the present study. Belowground biomass samples from central Portugal showed higher density values than corresponding aboveground woody biomass samples (Table 7.2).

Table 7.2 - Proximate analysis and basic density of the shrub species at the two areas of study.

Species		Proximate analysis (% by mass, dry basis) Ash %	VM %	FC %	w %	Db (kg m^{-3})
Cytisus multiflorus (Portugal)	shoot	1.32 (± 0.05)	82.48 (± 0.46)	16.20 (± 0.51)	52.3 (± 1.2)	417.5 (± 89.6)
	root	0.71 (± 0.01)	82.73 (± 0.29)	16.57 (± 0.28)	48.7 (± 1.9)	522.7 (± 24.2)
Erica australis (Portugal)	shoot	1.38 (± 0.01)	80.72 (± 0.41)	17.90 (± 0.38)	45.6 (± 2.8)	569.2 (± 183.4)
	root	0.99 (± 0.01)	83.35 (± 0.07)	15.65 (± 0.07)	44.6 (± 1.6)	603.8 (± 30.3)
Pterospartum tridentatum (Portugal)	shoot	1.44 (± 0.01)	81.10 (± 0.30)	17.45 (± 0.29)	47.6 (± 0.5)	485.2 (± 40.0)
	root	0.74 (± 0.02)	83.38 (± 0.14)	15.88 (± 0.39)	37.1 (± 0.9)	739.2 (± 34.0)
Ulex europaeus (Portugal)	shoot	1.47 (± 0.01)	84.46 (± 0.19)	14.06 (± 0.20)	49.6 (± 3.9)	417.9 (± 104.7)
	root	1.38 (± 0.05)	84.31 (± 0.30)	14.31 (± 0.35)	43.6 (± 4.9)	576.9 (± 34.3)
Cytisus multiflorus (NW Spain)	shoot	1.37 (± 0.07)	80.81 (± 0.62)	17.83 (± 0.69)	59.2 (± 1.7)	408.1 (± 53.8)
Erica australis (NW Spain)	shoot	1.38 (± 0.09)	79.65 (± 0.50)	18.97 (± 0.54)	58.9 (± 0.9)	483.3 (± 63.5)
Pterospartum tridentatum (NW Spain)	shoot	1.21 (± 0.05)	80.32 (± 0.44)	18.47 (± 0.46)	46.3 (± 1.5)	420.5 (± 77.5)
Ulex europaeus (NW Spain)	shoot	1.56 (± 0.03)	80.80 (± 0.36)	17.64 (± 0.31)	46.7 (± 2.2)	435.2 (± 66.0)

Where: shoot: aboveground biomass; root: belowground biomass; Ash %: Ash percentage (%), VM %: Volatile Matter (%), FC % Fixed Carbon (%), w %: Moisture content wet basis (%); Db: basic Density (kg m^{-3}), including leaves and twigs < 6 mm. Numbers in parenthesis are the standard Deviations.

7.3.3. Ultimate analysis

Ultimate analysis results for the shrub species at the two areas of study are shown in Table 7.3.

Carbon contents measured on shrub aboveground biomass are similar to the range of 46.02 to 55.51% observed in NW Spain for gorse, broom and heath reported by Núñez-Regueira et al (1999), who also found the highest average carbon content for heath as in the present study. Carbon contents measured on belowground biomass in central Portugal were lower than the corresponding carbon contents for aboveground biomass for all the studied species. Hydrogen and oxygen content, in the range of 6-7% and 41-45%, were within typical ranges for forest biomass fuels (e.g. Vassilev et al., 2010).

All studied species showed a sulphur content below the 0.1% threshold established by Obernberger et al. (2006) for minimizing sulphur-related corrosion risk in biomass boilers combustion, being these measured sulphur content values more similar to average values of <0.1% of woody fuels than to the contents of > 0.2% S commonly found in herbaceous biomass fuels (e.g. Vassilev et al., 2010).

Nitrogen content ranged from 0.63 to 2.05 %, with the highest values found for *Cytisus multiflorus* (broom), followed by *Ulex europaeus* (gorse), at both areas of study. Similarly, Núñez-Regueira et al. (1999) found the highest shrub N content values in NW Spain for the native broom *Cytisus scoparius*, ranging from 1.1 to 4.8 % at four seasons of study, followed by Spanish gorse, with a seasonal N range of 1.0 to 2.8%, and heath, with a N range of 1.0 to 1.7 %. For all the species in the present study, a higher N content was observed in NW Spain area of study, this possibly being a consequence of the higher N content characteristic of the soils in the region (Bará, 1998).

Shrub biomass nitrogen content obtainded in the current study and from Núñez-Regueira et al. (1999) in NW Spain is more similar to the range of 0.5 to 2.8 %, typical of herbaceous biomass fuels, than to the lower range of 0.1-0.7 %, characteristic of woody biomass fuels (e.g. Obernberger et al., 2006; Vassilev et al., 2010). Leguminous shrubs, such as gorse or broom, are characterized by a high nitrogen fixation capacity, accumulating this mobile nutrient in fine fractions such as leaves or twigs, with potential implications for the combustion of these fuels. All of the studied species at both areas of study and in the data of native shrub species ultimate analysis in four seasons of harvest from Núñez-Regueira et al. (1999), in NW Spain, showed N contents above the 0.6 % threshold proposed by Obernberger et al. (2006) for avoiding NOx emissions in combustion.

Table 7.3 - Ultimate analysis of the shrub species at the two areas of study.

		Ultimate analysis (% by mass, dry basis)				
Species		**C**	**H**	**O**	**N**	**S**
Cytisus multiflorus (Portugal)	shoot	46.20 (± 0.26)	6.88 (± 0.09)	44.35 (± 0.29)	1.24 (± 0.06)	<0.1
	root	45.65 (± 0.13)	6.86 (± 0.04)	45.75 (± 0.30)	0.98 (± 0.02)	<0.1
Erica australis (Portugal)	shoot	49.84 (± 0.10)	7.04 (± 0.08)	41.06 (± 0.09)	0.63 (± 0.02)	<0.1
	root	46.50 (± 0.08)	6.71 (± 0.04)	45.32 (± 0.00)	0.45 (± 0.01)	<0.1
Pterospartum tridentatum (Portugal)	shoot	47.95 (± 0.16)	6.97 (± 0.09)	42.96 (± 0.18)	0.67 (± 0.04)	<0.1
	root	46.51 (± 0.08)	6.71 (± 0.04)	45.58 (± 0.09)	0.45 (± 0.01)	<0.1
Ulex europaeus (Portugal)	shoot	46.32 (± 0.43)	6.85 (± 0.04)	44.37 (± 0.52)	0.95 (± 0.01)	<0.1
	root	45.49 (± 0.06)	6.81 (± 0.11)	45.48 (± 0.17)	0.79 (± 0.01)	<0.1
Cytisus multiflorus (NW Spain)	shoot	48.84 (± 0.69)	6.55 (± 0.39)	43.2 (± 0.19)	2.05 (± 0.65)	<0.1
Erica australis (NW Spain)	shoot	48.13 (± 0.46)	6.08 (± 0.55)	42.7 (± 0.33)	0.82 (± 0.08)	<0.1
Pterospartum tridentatum (NW Spain)	shoot	48.78 (± 0.31)	6.65 (± 0.03)	42.3 (± 0.17)	0.96 (± 0.25)	<0.1
Ulex europaeus (NW Spain)	shoot	48.88 (± 0.53)	6.49 (±0.12)	42.4 (± 0.26)	1.72 (±0.09)	<0.1

Where: shoot is the aboveground biomass; root is belowground biomass. Numbers in parenthesis are the Standard Deviations.

7.3.4. Higher and Lower Heating Values

Higher and Lower Heating Values for the studied species at the 2 areas of study are shown in Table 7.4. Higher values were observed for heath HHV at both areas of study. Average HHV and standardized deviations for the four shrub species are shown in Figure 7.1. Using SPSS 19 (SPSS Inc, USA), a General Linear Model ANOVA was performed testing the 3 factors species, area of study and interaction between species and area of study.

A significant (p-value $\leq$ 0.05) effect of species on fuel higher heating value was found, with no significant effect of neither area of study (p-value = 0.105) nor of interaction between species and area of study (p-value = 0.667). A subsequently Student-Newman-Keuls test revealed three groups for HHV, the highest ranking species being heath, with an average HHV of 24.44 MJ kg^{-1}, followed by a second group formed by broom and carqueisa, with values of 22.46 and 21.94 MJ kg^{-1}, respectively, and a third group for gorse, with an average HHV of 21.16 MJ kg^{-1} (Figure 7.1).

Table 7.4 - Higher and lower heating values and energy density of the studied shrub species.

Species	Area	HHV ($MJ\ kg^{-1}$)	LHV ($MJ\ kg^{-1}$)	E_{ar} ($GJ\ m^{-3}$)	E_{ar} ($MWh\ m^{-3}$)
Cytisus multiflorus	1	22.245 (±0.502)	8.455 (±0.361)	2.41	0.67
Erica australis	1	24.117 (±0.668)	11.111 (±0.488)	3.17	0.88
Pterospartum tridentatum	1	21.365 (±0.667)	9.508 (±0.162)	2.71	0.75
Ulex europaeus	1	21.872 (±0.321)	8.702 (±0.396)	2.48	0.69
Cytisus multiflorus	2	22.256 (±0.639)	7.231 (±0.203)	2.06	0.57
Erica australis	2	24.397 (±0.350)	11.208 (±0.234)	3.19	0.89
Pterospartum tridentatum	2	22.144 (±0.656)	7.071 (±0.236)	2.02	0.56
Ulex europaeus	2	21.241 (±0.654)	9.454 (±0.318)	2.69	0.75

Where: Area 1: Central Portugal; Area 2: NW Spain; HHV: Higher Heating Value ($MJ\ kg^{-1}$ at dry basis); LHV: Lower Heating Value ($MJ\ kg^{-1}$) at moisture content as received (see Table 7.2); E_{ar}: Energy Density as received of the shrub fresh bundles ($GJ\ m^{-3}$ and $Mwh\ m^{-3}$). Numbers in parenthesis are the Standard Deviations.

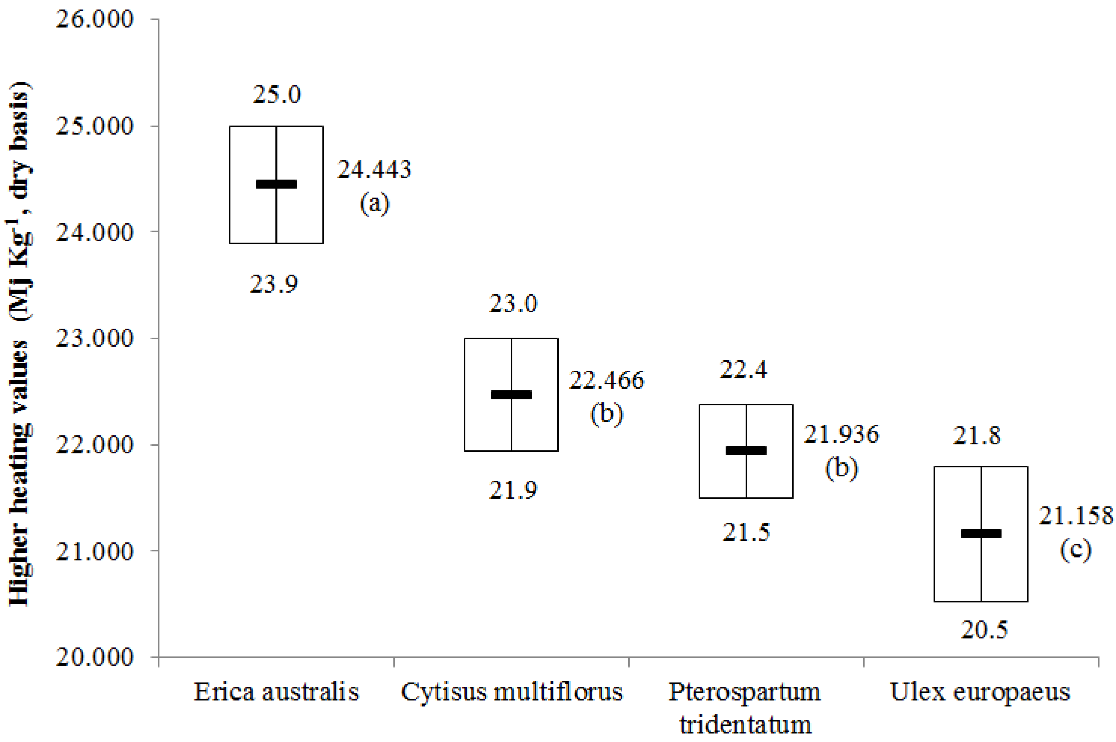

Figure 7.1 - Higher heating values of shrub species for the two areas of study.
Where: letters in brackets stand for signifficant differences at $p<0.05$.

Measured average HHV results are similar to the values measured by Elvira and Hernando (1989), who reported an average HHV of 24.59, 23.44, 22.34 and 20.65 $MJ\ kg^{-1}$ for Spanish broom, heath (*Erica scoparia),* carqueisa and gorse in central Spain, the first three species being classified as high calorific and the latter as medium calorific species following the calorific value classification established by Hough (1969). High calorific values are typical of heath species: values of 24.06, 23.6 and 23.8 MJ kg^{-1} have been measured for *Erica arborea* in France (Doat et al., 1981), Spain (Gillon et al., 1997) and Greece (Dimitrakopoulos and Panov, 2001). This species is reported with the highest ranking in a group of 20 Mediterranean species, in Dimitrakopoulos and Panov (2001) study. Lower calorific values have been reported for other broom species, such as *Cytisus scoparius*, with an average HHV of 21.1 MJ kg^{-1} found in central Spain (Madrigal et al., 2011) and a reported seasonal range from 19.02 to 20.68 MJ kg^{-1} measured in NW Spain (Núñez-Regueira et al., 1999). HHV for gorse measured in the current study are similar to the values reported by Madrigal et al. (2011), who found average calorific values of and 21.43 MJ kg^{-1} for this species, being also similar to the values of 21.32 to 20.62 MJ kg^{-1} reported for *Ulex parviflorus* in France (Doat et al., 1981).

It is interesting to note that the higher HHV was found for heath, which shown also highest average C content and lowest N content. The same was found by Núñez-Regueira et al. (1999) in NW Spain. Various authors have noted the positive role of increasing C and decreasing N in raising the HHV of biomass fuels (e.g. Demirbas, 1997; Friedl et al., 2005), this explaining in part the higher HHV of woody fuels in comparison with herbaceous fuels (Vassilev et al., 2010). In addition, other factors, such as extractive content, not measured in the current study, can be influencing the different HHV of species, this content being linked to season of harvest and associated moisture content (Elvira and Hernando, 1989).

Measured LHV of the freshly harvested shrub biomass samples ranged from 7.07 to 11.21 MJ kg^{-1}, with the highest values found for *Erica australis* at both sites. Lower heating values are highly dependent on fuel moisture content and therefore the values presented are only representative of the calorific value correction for the particular moisture value at the time of sampling. The effects of fuel moisture on effective LHV and associated fuel energy density are discussed in section 7.3.5.

7.3.5. Fuel Energy Density

Energy Density of fresh shrub biomass compacted into bundles (Table 7.4) ranged from 2.2 GJ m^{-3} to 3.2 GJ m^{-3}. These values, which represent a conservative estimate for a summer harvest scenario assuming no drying period of the biomass after harvest, are similar to the energy density values reported for other biomass sources (e.g. Loo and Koppejan, 2008), such as woodchips of softwood (2.8 GJ m^{-3}) or grass in high pressed bales (2.7 GJ m^{-3}) or triticale straw (1.9 GJ m^{-3}).

A +/- 25% variation in the shrub bundle bulk density would result in estimated energy density values of 1.5-2.4 and 2.5-3.9 GJ m^{-3}, respectively, for the summer harvest scenario with the measured moisture contents and associated lower heating values. For a wet season harvest scenario, assuming a moisture content of 65 %, as recorded for the studied fuels in the areas of study by Fernandes and Pereira (1993) and by Núñez-Regueira et al. (1999), the calculated LHV of the studied species would descend to 5.3-6.5 MJ kg^{-1}, resulting in calculated energy density values of 1.1-1.4 GJ m^{-3}, suggesting a greater role of season of harvest and associated moisture content on the energy density of these fuels.

7.3.6. Ash chemical composition and slagging indices

7.3.6.1. Ash chemical composition: major and selected minor elements

Ash contents of Si, Al, Ti, Fe, Na, K, Ca, Mg and P, expressed as oxides referred to ash percentage dry weight and normalized to 100% for slagging indices calculation, are presented in Table 7.5. Shrub ashes were mainly constituted by silica, phosphorus, alkali metals (Na and K) and alkaline earth metals (Ca and Mg). Measured silica content in the ashes, was more similar to the average SiO_2 values of 22.2 % for woody fuels than to the average value of 46.2% for herbaceous fuels reported in the ash composition review by Vassilev et al. (2010).

Table 7.5 - Shrub ash major and selected minor elements composition.

	Ash composition (% oxides referred to ash dry weight)								
Species	**SiO_2**	**Al_2O_3**	**TiO_2**	**Fe_2O_3**	**Na_2O**	**K_2O**	**CaO**	**MgO**	**P_2O_5**
Cytisus multiflorus	16.6	2.0	0.1	1.9	11.6	18.5	8.0	22.0	19.3
Erica australis	17.0	0.1	0.1	1.6	10.4	14.1	17.0	22.1	17.6
Pterospartum tridentatum	23.4	0.1	0.1	1.9	10.4	15.9	18.0	12.1	18.1
Ulex europaeus	33.6	3.9	0.3	3.3	8.5	15.3	13.2	9.0	12.9

All samples showed high alkali metals content, with a total sum of alkali metals (Na and K) oxides ranging from 23.7 to 30.1 %. High alkali metals contents have been recorded in gorse shrub biomass and ash composition: for example, Jobson and Thomas (1964) noted that gorse biomass composition was characterized by high potassium contents, and Soto and Diaz-Fierros (1993) measured alkali metal contents of 30 % in gorse ash in NW Spain. Biomass with high annual growth is abundant in alkaline elements because they are readily taken up from the soil (Vassilev et al., 2010). Consequently, higher alkali metal contents can be found in herbaceous than in woody fuels: Vassilev et al. (2010) reported average K_2O contents of 24.6 % and 10.7% for herbaceous and woody fuels ashes, respectively. Similarly to previous presented in section 7.3.2.1., the mobile nutrient potassium is easily retranslocated and accumulated in low diameter woody fractions as well as in leaves. For instance, Werkelin et al. (2005) observing enriched potassium content in the ashes of young and biologically active tissues found that wood of small-sized branches (1.5–2.5 cm) showed 1.2–1.4 times higher K than wood of branches with larger diameters (3.0–4.8 cm). This high content of potassium, together with other nutrients present in the shrub biomass composition, might be responsible for the relatively high ashes yield of the studied species. For example, Jenkins et al. (1998) observed an increasing potassium concentration in the fuel tended to accompany an increasing ash content. Furthermore, potassium content is important as an indication of the potential for ash fusion or deposition via vaporization and condensation (Miles et al., 1996). Alkali metals, particularly potassium, have the tendency to react with the bed material or with ash silica to form eutectic mixtures with low melting points, forming sticky coatings on the surface of inert material particles and leading to subsequent agglomeration and even defluidization of the bed (Werther et al., 2000). For instance, Fernández Llorente and Carrasco García (2005), in the combustion of herbaceous energy crops such as thistle, straw or brassica, with K_2O contents in the ashes ranging from 10-20%, observed hard sintering and ash deformation at temperatures below 850 ºC, these potassium contents being similar to the values observed in this study. In the present study, all the studied species showed ash potassium contents above the 7% threshold for potassium in ash established by Obernberger et al. (2006) for avoiding ash melting, deposition and corrosion in biomass combustion. Potential ash sintering, slagging and fouling risk is further evaluated in the following section.

7.3.6.2. Ash slagging and fouling indices and risk

Results from the calculation of ash slagging and fouling indices, and associated ash slagging and fouling risk, for the four species of study, are summarized in Table 7.6.

The results of the slagging index Basic to Acid ashes (B/A), with values above the threshold of 0.75 proposed by Watanabe et al. (1996) for the ashes of all the studied species, suggests that the low content of silica found in the ashes would not be expected to lead to significant formation of silicates in reaction with the alkali and alkaline earth metals present in the studied fuels. However, in addition to the intrinsic content of silica in the fuels, other exogenous sources of silica, such as soil contamination associated to the process of biomass harvesting, or potential reactions with silica bed materials, might be regarded as a potential source for the occurrence of ash agglomeration and fusion (Vamvuka and Zografos, 2004; Fernández Llorente and Carrasco García, 2005).

The Rs index value, in the expected range (Table 7.6), suggests a low sulphur-based corrosion risk for all the studied species. The low S content observed for all the studied species are below the 0.1 % threshold for minimizing sulphur-related corrosion risk during combustion established by Obernberger et al. (2006).

Calculated alkali index in the present study was above the 0.17 kg alkali MJ^{-1} threshold for probable slagging and fouling for broom and gorse ashes, whereas heath and carqueisa ashes, with values of 0.14 and 0.16 kg alkali MJ^{-1}, were in the vicinity of the probable slagging and fouling threshold from Miles et al. (1996). The reported alkali index is in the lower range of typical herbaceous fuels values of 0.2 to > 2 kg alkali MJ^{-1}, which contain enough alkali for the ashes to melt in combustion and/or the elements vaporize and condense on boiler tubes and refractories (Miles et al., 1996), but in higher amounts than average reported alkali indexes for woody fuels or leached agricultural fuels with low slagging risk, typically with alkali indexes values of <0.2 (e.g. Miles et al., 1996; Vamvuka and Zografos, 2004).

In addition, the relative amount of alkali metals to alkaline earth metals in the ashes, as evaluated by SI index (Fernández Llorente and Carrasco García, 2005), was below the threshold value of 2 for avoiding ash sintering in the combustion proposed by the authors. Similarly low values of this index (SI <0.3) would be obtained utilizing Spanish gorse ashes composition data from the literature (e.g. Soto and Diaz-Fierros, 1993). This high alkali/ alkaline earth metals content might result in a low fusion temperature of the ashes of the studied species. Increased alkali metal contents together with decreasing alkaline earth metals generally result in lower ash sintering and fusion temperatures, enhancing the probability of ash agglomeration and fusion in the boiler (Werther et al., 2000). Furthermore, according the results from BAI index (Vamvuka and Zografos, 2004), bed agglomeration would expectedly occur in the case of combustion of the studied species in fludized-bed reactors. Boiler-scale combustion tests should be conducted to discriminate the actual slagging and fouling risk of the studied shrub species ashes under different combustion technologies.

Table 7.6 - Ash slagging and fouling indices and risk.

	B/A		**Rs**		**Alkali Index (AI)**		**Sintering Index (SI)**		**Bed Agglomeration Index (BAI)**	
Species	**B/A**	**slagging risk**	**Rs**	**fouling risk**	**AI**	**fouling risk**	**SI**	**sintering risk**	**BAI**	**bed agglomeration**
Cytisus multiflorus	2.06	Low	0.06	Low	0.17	Probable	1.00	High	0.06	Occurs
Erica australis	2.45	Low	0.07	Low	0.14	Low	1.61	High	0.07	Occurs
Pterospartum tridentatum	1.89	Low	0.05	Low	0.16	Low	1.14	High	0.07	Occurs
Ulex europaeus	0.88	Low	0.03	Low	0.17	Probable	0.93	High	0.13	Occurs

Table 7.7 shows the content of trace and selected minor elements As, Cd, Pb and Co, Cu, Cr, Mn, Zn and Ni, measured in the ashes of the studied species. The measured values are compared to the limit values for these elements established by the legislation on ash utilization as a fertilizer in agriculture and forestry from European countries such as Finland, Denmark, Austria, Sweden and UK (see Haglund and group, 2008). The Spanish (Gobierno de España, 1990) and Portuguese (Decreto-Lei nº 118/2006) current legislation with limiting values for these elements is established for sludge from water treatment plants intended for application in agricultural soils. Measured contents of ash As, Cd, Pb, Co, Cu, Cr, Mn, Zn and Ni were similar to the usual ranges of 3-60, 0-25, 15-650, 1-20, 15-400, 10-250, 1000-30000, 15-4400 and 6-200 mg kg^{-1}, respectively, commonly found in wood and bark ash for these elements as reported in the literature (e.g. Steenari and Lindqvist, 1997; Pitman, 2006; Omil et al., 2007; Augusto et al., 2008; Haraldsen et al., 2011). The measured values were well below the limits established by Spanish and Portuguese current legislation for all the studied elements and below the limits from most of the European countries legislation as summarized in

Table 7.7. Some of the most conservative thresholds established by North and Central European countries for Cd (<1.5 mg kg^{-1}), Cu (<250 mg kg^{-1}), Cr (<100 mg kg^{-1}), and Zn (<1500 mg kg^{-1}), however, would not be met neither by some of the observed values in shrub ash, nor by typical values from wood and bark ash (e.g. Steenari and Lindqvist, 1997; Pitman, 2006; Omil et al., 2007; Augusto et al., 2008; Haraldsen et al., 2011).

Table 7.7 - Shrub ash traces and selected minor elements composition.

Species	**As**	**Cd**	**Pb**	**Co**	**Cu**	**Cr**	**Mn**	**Zn**	**Ni**
Cytisus multiflorus	3.2	4.1	5.1	9.9	100.1	20.1	10204.7	3212.6	1.9
Erica australis	4.9	2.5	14.3	2.7	739.9	101.8	5808.8	689.8	2.9
Pterospartum tridentatum	3.4	3.1	11.9	7.3	293.1	128.4	7287.2	2290.3	2.1
Ulex europaeus	4.4	3.3	12.1	5.4	409.2	111.2	4812.2	1660.6	1.7
Country (application)									
Denmark (Agriculture/Forestry)		15	120			100			30
Finland (Agriculture)	25	1.5	100		600	300		1500	100
Finland (Forestry)	30	17.5	150		700	300		4500	150
Sweden (Forestry)	30	30	300		400	100		7000	300
Austria (Field and grassland)	20	8	100	100	250	250		1500	100
Portugal (Agriculture)*		20	750		1000	1000		2500	300
Spain (Soils with ph<7)		20	750		1000	1000		2500	300
Spain (Soils with ph>7)		40	1200		1750	1500		4000	400

* limit values of concentration of heavy metals in sludge from water treatment plants.

Pitman (2006) pointed out that, whereas typical trace elements contents found in forest residues ash should present no risk, as long as fly ash is not used, the variability of Zn, Ni and Cu in bottom ash poses a risk of exceeding permissible levels if ash is applied in large quantities. The applied dose and ash form plays an important role in the potential effects on the environment (Pitman, 2006; Omil et al., 2007; Augusto et al., 2008). Pitman (2006) noted that applications of ash up to 10 ton ha^{-1} from ordinary boilers result in heavy metal soil levels still two orders of magnitude lower than the USEPA (*United States Environmental Protection Agency)* advised loading. However, long-term research in ecological effects of ash application is scarce (Pitman, 2006; Omil et al., 2007; Augusto et al., 2008), particularly under forest mineral soils in Mediterranean countries, and further work on quantifying their potential impact must be conducted in the region.

7.4. Conclusion

Selected native woody shrub species from NW Spain and central Portugal white broom, heath, carqueisa and gorse, showed several advantageous properties as biomass fuels, such as high HHV (21-24 MK kg^{-1}) and interesting energy density values both under a summer (2.2-3.2 GJ m^{-3}) and winter harvest scenario (1.1-1.4 GJ m^{-3}). Further work may focus on detailed moisture content, heating value and associated energy density variations study under different harvesting season and logistic scenarios, as well as on the quantification of calorific values for other native shrubby woody species of the studied genus.

Main drawbacks included high N contents (>0.6-2%) and a relatively high (1-2%) ashes content, combined with a high (20-30%) alkali metals contents in the ashes, measured for all of the studied species at the two areas of study, resulting in a potential NOx emissions, sintering (Fernández Llorente and Carrasco García, 2005), fouling (Miles et al., 1996), and bed agglomeration (Vamvuka and Zografos, 2004) risk in the combustion of the studied fuels. Research on actual emissions and slagging and fouling risk of the studied fuels under real combustion conditions should be conducted, particularly given the scarcity of boiler-scale combustion studies for shrubby biomass fuels. Preventive measures, such as co-combustion with low-nitrogen and high-calcium biomasses, or the incorporation of additives on the combustion of the studied species under different combustion technologies, might deserve future investigation. The potential influence of logistics, including the effect of rain leaching on the content of shrub biomass and ash nutrient contents, should also be further explored for these and other native woody shrubby species in the region, covering a range of soil types and seasons of harvest.

Measured trace and selected minor elements were below national and most European thresholds for these metals, suggesting potential of the biomass ashes to be utilized as fertilizer, this requiring a comprehensive environmental monitoring of fly and bottom ashes obtained under a variety of combustion technologies and under a variety of soil types.

Acknowledgements

Authors would like to express their acknowledgements to the Portuguese Science and Technology Foundation (FCT), programme SFRH/PROTEC/49626/2009. They also would like to thank Eng. Cristóvão Santos from Mechanical Department of the University of Trás-os-Montes and Alto Douro where calorific analysis were performed and Eng. Rui Rocha from Leco laboratory for the assistance in elemental analysis. The authors would like to sincerely thank the anonymous reviewers for their highly productive suggestions for improving the manuscript.

References

AFN, 2010. FloreStat, 5th National Forest Inventory Information retrieval tool, in: Direcção Nacional de Gestão Florestal (DNGF). Autoridade Florestal Nacional (Ed.). Ministério da Agricultura do Desenvolvimento Rural e das Pescas, Lisboa.

AFN, 2011. Estatísticas dos incêndios florestais. Totais Nacionais (2001 - 2010). Autoridade Nacional Florestal, Ministério da Agricultura do Desenvolvimento Rural e das Pescas, Lisboa.

Augusto, L., Bakker, M., Meredieu, C., 2008. Wood ash applications to temperate forest ecosystems - potential benefits and drawbacks. Plant and Soil 306, 181-198.

Baernthaler, G., Zischka, M., Haraldsson, C., Obernberger, I., 2006. Determination of major and minor ash-forming elements in solid biofuels. Biomass and Bioenergy 30, 983-997.

Bará, S., 1998. Fertilización forestal, Colección técnica Consellería de Agricultura. Xunta de Galicia 9.

Bermúdez, J., Piñeiro, G., 2000. La biomasa forestal en Galicia, situación actual y perspectivas de aprovechamiento. CIS-Madera 5, 27-40.

BioBank, BIOS Bioenergiesysteme GmbH, Version 2.4, Graz, Austria, Available online at: *http://www.ieabcc.nl/database/ash.php*, (Accessed March 2012).

Biolexbase, Biolex database, properties for the samples of solid biomass fuels., Available online at: *www.biolexbase.dk*, (Accessed March 2012).

BS EN 14775:2009, Solid biofuels - Determination of ash content.

CEN EN 14774-1:2009, Solid biofuels - Determination of moisture content – Oven dry method - Part 1: Total moisture - Reference method.

CEN EN 14918:2009, Solid biofuels - Determination of calorific value.

CEN EN 15148:2009, Solid biofuels - Determination of the content of volatile matter.

DD CEN/TS 14780:2005, Solid biofuels - Methods for sample preparation.

DD CEN/TS 15104:2005, Solid biofuels – Determination of total content of carbon, hydrogen and nitrogen – Instrumental methods.

DD CEN/TS 15234:2006, Solid biofuels - Fuel quality assurance. Annex E. Calculation of the net calorific value in different basis and energy density as received.

DD CEN/TS 15289:2006, Solid biofuels – Determination of total content of sulphur and chlorine.

DD CEN/TS 15290:2006, Solid biofuels – Determination of major elements.

DD CEN/TS 15297:2006, Solid biofuels – Determination of minor elements.

Decreto-Lei nº 118/2006, Decreto-Lei nº 118/2006, de 21 de Junho, Estabelece o regime jurídico da utilização agrícola das lamas de depuração [Establishes the legal regime of the agricultural use of sewage sludge].

Demirbas, A., 1997. Calculation of higher heating values of biomass fuels. Fuel 76, 431-434.

DGGE, 2006. Estratégia Nacional para a Energia. A criação de uma rede de Centrais de Biomassa dedicadas, Direcção Geral de Geologia e Energia, Lisboa, p. 19.

Dimitrakopoulos, A.P., Panov, P.I., 2001. Pyric properties of some dominant Mediterranean vegetation species. International Journal of Wildland Fire 10, 23-27.

Doat, J., Valette, J., Ch., Askri, D., Caumartin, L., Bettachine, M., Moro, M., 1981. Le pouvoir calorifique supérieur d'espèces forestières méditerranéennes. Ann. For. Sci. 38, 469-486.

ECN-Biomass, Phyllis, database for biomass and waste. Energy research Centre of the Netherlands (ECN). Version: 4.13, Available online at: *http://www.ecn.nl/phyllis/*, (Accessed March 2012).

Elvira, L.M., Hernando, C., 1989. Inflamabilidad y energía de las especies de sotobosque: estudio piloto con aplicación a los incendios forestales. Monografías INIA.

Fernandes, P.M., Pereira, J.P., 1993. Caracterização de combustíveis na serra da Arrábida. Silva Lusitana 1, 237-260.

Fernandes, P.M., Rego, F.C., 1998. A New Method to Estimate Fuel Surface Area- to-Volume Ratio Using Water Immersion. Int. J. Wildland Fire 8, 121-128.

Fernández Llorente, M.J., Carrasco García, J.E., 2005. Comparing methods for predicting the sintering of biomass ash in combustion. Fuel 84, 1893-1900.

Friedl, A., Padouvas, E., Rotter, H., Varmuza, K., 2005. Prediction of heating values of biomass fuel from elemental composition. Analytica Chimica Acta 544, 191-198.

Gillon, D., Hernando, C., Valette, J.-C., Joffre, R., 1997. Fast estimation of the calorific values of forest fuels by near-infrared reflectance spectroscopy. Canadian Journal of Forest Research 27, 760-765.

Gobierno de España, 1990. 1990/26940 Real Decreto 1310/1990, de 29 de Octubre, por el que se regula la Utilización de los Lodos de Depuración en el Sector Agrario. BOE 262/1990 de 01-11-1990, pp. 32339. Ministerio de Agricultura, Pesca y Alimentación, Gobierno de España.

Gobierno de España, 2010. Plan De Acción Nacional De Energías Renovables De España (PANER) 2011-2020, Ministerio de Industria, Turismo y Comercio, Gobierno de España, p. 138.

Haglund, N., group, E., 2008. Guideline for classification of ash from solid biofuels and peat utilised for recycling and fertilizing in forestry and agriculture, NT TECHN REPORT 613, Nordic Innovation Centre, Norway.

Hakkila, P., Parikka, M., 2002. Fuel Resources from the forest, in: Richardson, J., Björheden, R., Hakkila, P., Lowe, A.T., Smith, C.T. (eds.), Bioenergy from Sustainable Forestry. Guiding Principles and Practice, vol. 71. Kluwer Academic Publishers.

Haraldsen, T.K., Pedersen, P.A., Grønlund, A., 2011. Mixtures of Bottom Wood Ash and Meat and Bone Meal as NPK Fertilizer. Recycling of Biomass Ashes, in: Insam, H., Knapp, B.A. (eds.). Springer Berlin Heidelberg, pp. 33-44.

Hough, W.A., 1969. Calorific values of some forest fuels of southern United States. U.S. For. Serv. South. For. Exp. Stn. Res. Note SE-120.

Jenkins, B.M., Baxter, L.L., Miles Jr, T.R., Miles, T.R., 1998. Combustion properties of biomass. Fuel Processing Technology 54, 17-46.

Jobson, H.T., Thomas, B., 1964. The composition of gorse (*Ulex europaeus*). Journal of the Science of Food and Agriculture 15, 652-656.

Loo, S.V., Koppejan, J. (eds.) 2008. The Handbook of Biomass Combustion and Co-firing. Earthscan, London pp. 407.

Madrigal, J., Guijarro, M., Hernando, C., Díez, C., Marino, E., 2011. Effective Heat of Combustion for Flaming Combustion of Mediterranean Forest Fuels. Fire Technology 47, 461-474.

Miles, T.R., Miles Jr, T.R., Baxter, L.L., Bryers, R.W., Jenkins, B.M., Oden, L.L., 1996. Boiler deposits from firing biomass fuels. Biomass and Bioenergy 10, 125-138.

Miranda, M.T., Arranz, J.I., Rojas, S., Montero, I., 2009. Energetic characterization of densified residues from Pyrenean oak forest. Fuel 88, 2106-2112.

Núñez-Regueira, L., Rodríguez, J., Proupín, J., Mouriño, B., 1999. Forest waste as an alternative energy source. Thermochimica Acta 328, 105-110.

Núñez-Regueira, L., Proupín-Castiñeiras, J., Rodríguez-Añón, J.A., 2004. Energy evaluation of forest residues originated from shrub species in Galicia. Bioresource Technology 91, 215-221.

Obernberger, I., Brunner, T., Bärnthaler, G., 2006. Chemical properties of solid biofuels—significance and impact. Biomass and Bioenergy 30, 973-982.

Omil, B., Piñeiro, V., Merino, A., 2007. Trace elements in soils and plants in temperate forest plantations subjected to single and multiple applications of mixed wood ash. Science of The Total Environment 381, 157-168.

Pitman, R.M., 2006. Wood ash use in forestry – a review of the environmental impacts. Forestry 79, 563-588.

Reisinger, K., Haslinger, C., Herger, M., Hofbauer, H., BIOBIB - a Database for Biofuels. Institute of Chemical Engineering, Fuel and Environmental Technology, Available online at: *http://cdmaster2.vt.tuwien.ac.at/ biobib/biobib.html*, (Accessed March 2012).

Silva, T., Pereira, J., Paúl, J., Santos, M., Vasconcelos, M., 2006. Estimativa de Emissões Atmosféricas Originadas por Fogos Rurais em Portugal. Silva Lusitana 14, 239-263.

SLU, Wood Ash Database - chemical composition of ashes formed during combustion of biofuels from tree compartments, Available online at: *http://woodash.slu.se/eng/*, (Accessed March 2012).

Soto, B., Diaz-Fierros, F., 1993. Interactions Between Plant Ash Leachates and Soil. International Journal of Wildland Fire 3, 207-216.

Spinelli, R., Magagnotti, N., 2009. Logging residue bundling at the roadside in mountain operations. Scandinavian Journal of Forest Research 24, 173-181.

Steenari, B.M., Lindqvist, O., 1997. Stabilisation of biofuel ashes for recycling to forest soil. Biomass and Bioenergy 13, 39-50.

Tsoumis, G.T., 1991. Science and Technology of wood. Structures, Properties, Utilization. Van Nostrand Reinhold, New York.

U.S. Department of Energy, US DOE Biomass Feedstock Composition and Property Database, Available online at: *http://www1.eere.energy.gov/biomass/databases.html*, (Accessed March 2012).

Vamvuka, D., Zografos, D., 2004. Predicting the behaviour of ash from agricultural wastes during combustion. Fuel 83, 2051-2057.

Vassilev, S.V., Baxter, D., Andersen, L.K., Vassileva, C.G., 2010. An overview of the chemical composition of biomass. Fuel 89, 913-933.

Vega-Nieva, D.J., Dopazo, R., Ortiz, L., 2010. Slagging risk of mediterranean biomasses for combustion. World Bioenergy, Jönköping, Sweden, pp. 12-16. 25-27 May.

Viana, H., Cohen, W.B., Lopes, D., Aranha, J., 2010. Assessment of forest biomass for use as energy. GIS-based analysis of geographical availability and locations of wood-fired power plants in Portugal. Applied Energy 87, 2551-2560.

Watanabe, A., Daly, C.C., Devine, C.E., Bryers, R.W., 1996. Fireside slagging, fouling, and high-temperature corrosion of heat-transfer surface due to impurities in steam-raising fuels. Progress in Energy and Combustion Science 22, 29-120.

Werkelin, J., Skrifvars, B.-J., Hupa, M., 2005. Ash-forming elements in four Scandinavian wood species. Part 1: Summer harvest. Biomass and Bioenergy 29, 451-466.

Werther, J., Saenger, M., Hartge, E.U., Ogada, T., Siagi, Z., 2000. Combustion of agricultural residues. Progress in Energy and Combustion Science 26, 1-27.

8

Estimation of crown biomass of *Pinus pinaster* stands and shrubland aboveground biomass using forest inventory data, remotely sensed imagery and spatial prediction models

The content of this chapter was fully published in the following manuscript:

[Annex C.1] Viana, H., Aranha, J., Lopes, D., Cohen, W.B., 2012. Estimation of crown biomass of *Pinus pinaster* stands and shrubland above-ground biomass using forest inventory data, remotely sensed imagery and spatial prediction models. Ecological Modelling 226, 22-35.

Data and methodologies from this chapter contributed for the following published book chapter:

[Annex C.2] Viana, H., Lopes, D., Aranha, J., 2011. Assessment of Forest Aboveground Biomass Stocks and Dynamics with Inventory Data, Remotely Sensed Imagery and Geostatistics, in: Shaukat, S.S. (ed.), Progress in Biomass and Bioenergy Production. InTech, pp. 107-130.

Abstract

Spatially crown biomass of *Pinus pinaster* stands and shrubland above-ground biomass (AGB) estimation was carried-out in a region located in North-Center Portugal, by means of different approaches including forest inventory data, remotely sensed imagery and spatial prediction models. Two cover types (pine stands and shrubland) were inventoried and biomass assessed in a total of 276 sample field plots. We compared AGB spatial predictions derived from Direct Radiometric Relationships (DRR) of remotely sensed data; and the geostatistical method Regression-kriging (RK), using remotely sensed data as auxiliary variables. Also, Ordinary Kriging (OK), Universal Kriging (UK), Inverse Distance Weighted (IDW) and Thiessen Polygons estimations were performed and tested. The comparison of AGB maps shows distinct predictions among DRR and RK; and Kriging and deterministic methods, indicating the inadequacy from these later ones to map AGB over large areas. DRR and RK methods produced lower statistical error values, in pine stands and shrubland, when compared to kriging and deterministic interpolators. Since forest landscape is not a continuous variable, the tested forest variables showed low spatial autocorrelation, which makes kriging methods unsuitable to these purposes. Despite the geostatistical method RK did not increase the accuracy of estimates developed by DRR, denser sampling schemes and different auxiliary variables should be explored, in order to test if the accuracy of predictions is improved.

Keywords: Above-ground Biomass, Remote Sensing, Geostatistics, Regression-kriging, *Pinus pinaster*, Shrubland.

8.1. Introduction

8.1.1 Biomass spatial prediction

Estimates of above-ground biomass (AGB) of forested areas have been used to address a broad range of questions including estimations of forest productivity (Chirici et al., 2007; Palmer et al., 2009), studying the impacts of forest fires or other disturbances (García-Martín et al., 2008), monitoring the biomass changes over time (Hu and Wang, 2008), assessing the forest biomass for use as energy (Viana et al., 2010) or to estimate the global carbon balance (Hese et al., 2005). Nowadays, the analysis of these issues over large areas is a common practice. The need of continuous maps where the phenomenon under study can be individually analysed or used as auxiliary variable in a specific model requires that the spatial predictions are represented in the most accurate way. Estimation of AGB has been made by a range of methods, from field measurements to remote sensing-based methods, as well GIS-based modelling approaches using auxiliary data (Lu, 2006).

Traditional approaches to estimate forest AGB over a large area consist in the implementation of forest inventories where a statistical sampling design is established to acquire data, or using data aggregated from stand level management inventories (McRoberts et al., 2010). Estimation using sample-based inventories involves field measurements where AGB is commonly assessed by applying allometric equations for specific species (Ter-Mikaelian and Korzukhin, 1997; Foroughbakhch et al., 2005; Zianis et al., 2005; Peichl and Arain, 2007), at the tree or shrub level, using the dendrometric variables (e.g. diameter-at-breast height, tree height, crown size and crown length) measured in each sample plot. The total biomass for a given area is achieved by applying expansion factors to the area of the sample plot and stand conversion tables. These approaches are widely used in several studies (e.g. Brown et al., 1989; Brown and Lugo, 1992; Fearnside, 1992; Gillespie et al., 1992; Fearnside, 1997; Houghton et al., 2001; Fournier et al., 2003). These estimation models are considered non-spatial as they do not provide the spatial distribution of AGB. To predict the spatial distribution of AGB throughout the territory, the calculated AGB in the forest inventory dataset is usually assigned to the forest polygons, stratified by species, and mapped by aerial photo interpretation.

Despite the field measurements being the most accurate methods for collecting biomass data, the level of precision of the resultant biomass map will depend of the land cover classification detail and of the sample intensity. In fact, forest inventories data at regional or national scale are usually not spatially exhaustive to generate spatially AGB estimates, thus limiting the use of this approach over large areas. An additional limitation is the long temporal resolution of these estimations, which are made in cycles of 10 or more years. This is not compatible with the need of information on shorter time intervals, to analyse land cover changes, to quantify forest resources, or to monitor other environmental variables. In order to overcome these limitations and the need to produce more accurate spatially explicit large area biomass estimates led the researchers to explore different approaches to mapping biomass.

With the increasing availability of satellite imagery, remote sensing-based methods have been the most widely used approach to predict AGB over large areas, in recent years. The utility of the spectral information recorded by remote sensing for monitoring vegetation or gathering ecophysiological information over large areas is very well recognized (Jong et al., 2006), since satellite data became accessible for land cover dynamic studies. It has been demonstrated in several studies that the satellite spectral information (spectral band, band ratios, band transformations, etc.) has a good correlation with forest biomass and when combined with field measurements, is suitable for AGB estimation. Previous research using imagery data provided by distinct sensors and employing different approaches are summarized by Lu (2006). Although remotely sensed data cannot completely replace field sample data, it has been incorporated into operational forest inventories (McRoberts et al., 2010).

Several studies using remotely sensed data sources with different spatial-resolution and applying distinct approaches have been conducted in AGB spatial predictions. These approaches include direct estimations by means of Direct Radiometric Relationships (DRR), between spectral data response and biomass amount, using multiple regression analysis (Hame et al., 1997; Cohen et al., 2001; Cohen et al., 2003; Reich et al., 2004; Labrecque et al., 2006; Muukkonen and Heiskanen, 2007; Zheng et al., 2007); by nonparametric approaches including K nearest neighbour (KNN) (Tomppo, 1991; Reese et al., 2002; Tomppo et al., 2002; Labrecque et al., 2006; Chirici et al., 2008; Tomppo et al., 2008) and neural network (Atkinson and Tatnall, 1997; Blackard and Dean, 1999; Muukkonen and Heiskanen, 2005), or indirect estimations. In this case, characteristics such as crown diameter or leaf area index (LAI) are firstly derived from the remotely sensed data and subsequently are used in regression analysis to estimate biomass.

GIS-based approaches (Iverson et al., 1994; Magcale-Macandog et al., 2006) using ancillary data (e.g. elevation, slope, soil, precipitation, etc.) have not been applied extensively for AGB estimation given the low availability of data, often not sufficiently precise, and the frequent low correlation between AGB and ancillary data.

Spatial models (algorithms) have been also used for spatially predict vegetation attributes. In general, these interpolation techniques are classified in deterministic and probabilistic models (Isaaks and Srivastava, 1989; Goovaerts, 1997; Burrough and McDonnell, 1998; Hengl, 2009). The deterministic approaches are models where arbitrary or empirical model parameters are used. No estimate of the model error is available and usually no strict assumptions about the variability of a feature exist (Hengl, 2009). Inverse distance weighting (IDW) and Thiessen polygons are the most widely used approach to execute interpolations and, in some situations, these can perform as well, or even better, than other spatial prediction methods (Weber and Englund, 1992; Hengl, 2009). Attending that in Earth sciences there is usually a lack of sufficient knowledge concerning how properties vary in space, a deterministic model may not be appropriate. Therefore, to make predictions at locations for which observations do not exist, with inherent uncertainty in predictions, the use of probabilistic models are necessary (Lloyd, 2007).

Spatial statistics and geostatistics were developed to describe and analyse the variation in both natural and man-made phenomena on, above or below the land surface (Cressie, 1993). Geostatistical models are reported in numerous textbooks (e.g. Isaaks and Srivastava, 1989; Cressie, 1993; Goovaerts, 1997; Deutsch and Journel, 1998; Hengl, 2009) such as Kriging (plain geostatistics); environmental correlation (e.g. regression-based); Bayesian-based models (e.g. Bayesian Maximum Entropy) and hybrid models (e.g. regression-kriging). Largely developed by Matheron (1963) in the 1960s, to evaluate recoverable reserves for the mining industry, over the years geostatistical models have been applied in a wide range of fields including modelling forest structure and attributes. Geostatistics and the theory of regionalized variables

(Matheron, 1971) has been used to (Curran and Atkinson, 1988): explore and describe the presence of spatial variation that occur in most natural resource variables and in remotely sensed data (Curran, 1988; Woodcock et al., 1988); to design optimum sampling schemes for image data and ground data (McBratney and Webster, 1981; Hernández and Emery, 2009); and to increase the accuracy in which remotely sensed data can be used to classify land cover (Zhang and Franklin, 2002; Buddenbaum et al., 2005).

In recent years, several works have been conducted using geostatistical approaches to predict continuous forest variables. The motivation for using geostatistical analysis is that classical design-based methods are often weak for small area estimation within global inventories, and there is also an increasing demand to use regional or national inventory data for local estimation purposes (Mandallaz, 1993). However, the major limitation in using spatial statistical models is when forest variable datasets are spatially independent the lack of spatial structure makes it difficult, if not impossible to use optimal predictors such as Ordinary kriging for modelling the spatial variability in the data (Reich et al., 2011). In a particular stand level spatial distribution of tree attributes i.e., basal area, height and density can be thought to be directly influenced by different spatially continuous variables such as solar radiation, soil characteristics and water nutrient availability, thus allowing considered spatially continuous (Kint et al., 2003).

Geostatistics has been used for mapping forest variables (e.g. basal area, density, LAI, tree height, standing volume, above-ground biomass, productivity, etc.) based on forest inventory data where these variables seemingly have spatial autocorrelation (Dungan, 1998; Nanos et al., 2004; Berterretche et al., 2005; Maselli and Chiesi, 2006; Mutanga and Rugege, 2006; Sales et al., 2007; Meng et al., 2009; Palmer et al., 2009; Pierce et al., 2009; Akhavan and Kia-Daliri, 2010). However, in large areas forest variables as AGB are not always spatially continuous because they are highly dependent on forest landscape structure and boundaries of forest patches affected by clear-cuttings of commercial forest management. Gilbert and Lowell (1997) trying to predict stem volume measured the spatial autocorrelation of two interpolation methods, Thiessen polygons and kriging, concluded that although areas of high volume do tend to forn clusters, i.e. are positively spatially autocorrelated, the forest did not behave as a continuous surface relative even to the densest sampling schema. Gunnarsson et al.

(1998) used kriging estimation of stand variables such as total volume, annual volume increment, mean diameter and age and found positive autocorrelation. However, some variables (e.g. hardwood volume) does not exhibited any spatial autocorrelation in the scales studied, suggesting that only conducting an a priori assessment of spatial autocorrelation to determine interpolability may be misleading. Tuominen et al. (2003) combining data from remote sensing imagery with field measurements, and geostatistical interpolation for estimation of five forest variables (mean diameter, mean height, mean age, basal area, and volume) per sample plot and stand, found that the geostatistical interpolation, tested on the stand level estimation, did not improve the accuracy of the estimates. The same conclusion was reported by Freeman and Moisen (2007) who evaluating Kriging as a tool to improve forest biomass estimates concluded that map accuracy was not increased.

While some geostatistical models, such as Kriging, may not provide the desired solution to map AGB over large areas, it is necessary to explore new approaches. The studies exploring spatial prediction models Regression-kriging (RK) using field observations, in combination with various GIS data sources (e.g. remotely sensed data, soil and topographic variables, forest structure, etc.), as auxiliary information are not plentiful. However, some studies indicated good improvements using these approaches on forest variable estimation as volume mean annual increment (Palmer et al., 2009); basal area (Meng et al., 2009) and above-ground biomass (Sales et al., 2007), in comparison with other prediction methods.

In this study, we analysed different approaches to estimate crown biomass of *Pinus pinaster* stands and above-ground biomass of shrubland, including: direct radiometric relationships (DRR) methods and Regression-kriging (RK) with remotely sensed data as predictor. Moreover, deterministic interpolation techniques as Inverse distance weighting (IDW) and Thiessen polygons, and Kriging estimations are presented in order to compare the performance of these methods in large-scale mapping of forest biomass.

8.1.2 Direct Radiometric Relationships (DRR)

This method consist in establishing regression relationships, such as ordinary least squares (OLS), between the satellite spectral data, which can include the individual spectral bands, band ratios, vegetation indices and other possible transformations as independent variables, and the measured biomass at each corresponding inventory sample plot position. In this work, Landsat 5 TM and MODIS Vegetation indices were used as independent variables since they are referred in the literature as being well correlated with biomass availability.

8.1.3 Inverse Distance Weighting (IDW)

Inverse distance weighting (IDW) is a quick deterministic local interpolator that is exact and can be a good method to perform a preliminary analysis of an interpolated surface. It is often used as the default surface generation method to attribute sample locations (Lu and Wong, 2008). IDW explicitly implements the assumption that a value of an attribute at an unsampled location is a weighted average of known data points within a local neighbourhood surrounding the unsampled location (Burrough and McDonnell, 1998). To predict a value for any unsampled location, IDW will use the measured values surrounding the prediction location. Those measured values closest to the prediction location will have more influence on the predicted value than those farther away. Thus, the IDW formula has the effect of giving data points close to the interpolation point relatively large weights while those far away exert little influence. The higher the weight used the more influence points close to prediction location are given. The IDW predictor can be given as Eq. (1):

$$\hat{z}(x_0) = \frac{\sum_{i=1}^{n} z(x_i).d_{i0}^{-r}}{\sum_{i=1}^{n} d_{i0}^{-r}} \qquad [1]$$

where: the prediction for the location x_0 is a function of the *n* neighbouring observations, $z(x_i)$, i = 1; 2;…; n, *r* is an exponent which determines the weight assigned to each of the observations, and *d* is the distance by which the prediction location x_0 and the observation location x_i are separated.

As the exponent becomes larger the weight assigned to observations at large distance from the prediction location becomes smaller. That is, as the exponent is increased, the predictions become more similar to the closest observations.

8.1.4 Thiessen polygons: nearest neighbours

Thiessen polygons also called Dirichlet or Voronoi polygons assign values to unsampled locations that are equal to the value of the nearest observation (Lloyd, 2007). This method is one of the earliest and simplest interpolation methods. They have been considered one of the fundamental structures in computational geometry and other fields such as GIS. In this method, the study area is partitioned into a set of polygons, each containing only one measurement point. Every point within a given polygon is closer to the measurement point than any other measurement points.

The region sampled, *R*, is divided by perpendicular bisectors between the *N* sampling points into polygons or tiles, V_i, i=1, 2, ... , *N*, such that in each polygon all points are nearer to its enclosed sampling point x_i than to any other sampling point. The prediction at each point in V_i is the measured value at x_i , i.e. $z^*(x_0) = Z(x_i)$. The weights are (Webster and Oliver, 2007):

$$\lambda_i = \begin{cases} 1 & f\, x_i \in V_i \\ 0 & otherwise \end{cases}$$

The shortcomings of the method are evident; each prediction is based on just one measurement, there is no estimate of the error, and information from neighbouring points is ignored. When used for mapping the result is basic (Webster and Oliver, 2007). However, Thiessen polygons are used widely to provide a simple overview of the spatial distribution of values.

8.1.5 Ordinary Kriging (OK)

Kriging originated by (Krige, 1951) and developed by (Matheron, 1971) is widely known by the acronym BLUP, because it is the best linear unbiased predictor. The theory and mathematical formulation of kriging have been discussed thoroughly by several authors (e.g. Journel and Huijbregts, 1978; Isaaks and Srivastava, 1989; Cressie, 1993; Goovaerts, 1997). Kriging is a geostatistical method that takes into account both the distance and the degree of variation between known data points. The extent to which this assumption is true can be examined in the computed variogram. The several kriging models (kriging family) are elaborations of the basic generalized linear regression algorithm and corresponding estimator (Eq. 2) differing by some assumptions (or knowledge) on the data (process) (Goovaerts, 1997; Deutsch and Journel, 1998):

$$\left[\hat{Z}_k(u) - m(u)\right] = \sum_{\alpha=1}^{n} \lambda_\alpha(u)\left[Z(u_\alpha) - m(u_\alpha)\right] \qquad [2]$$

where *Z(u)* is the random variable at location *u*, the u_α is the *n* data locations, $\lambda_\alpha(u)$ is the weight assigned to datum $Z(u_\alpha)$ which is a realization of $Z(u_\alpha)$, $m(u)$ and $m(u_\alpha)$ are the location-dependent expected value of *Z(u)* and $Z(u_\alpha)$, and $\hat{Z}_k(u)$ is the linear regression estimator.

Ordinary Kriging (OK) filters the mean from Eq. (2) by requiring that the Kriging weights sum to one. The OK prediction $\hat{Z}_{OK}(u)$ is a linear weighted moving average of the available *n* observations defined as (Deutsch and Journel, 1998) Eq.(3):

$$\hat{Z}_{OK}(u) = \sum_{\alpha=1}^{n} \lambda_\alpha^{OK}(u) Z(u_\alpha) \qquad [3]$$

Using Lagrange form, OK system is written as:

$$\begin{cases} \sum_{\beta=1}^{n} \lambda_\beta^{OK}(u) C(u_\beta - u_\alpha) + \mu_{OK}(u) = C(u - u_\alpha) \\ \sum_{\beta=1}^{n} \lambda_\beta^{OK}(u) = 1 \end{cases} \qquad (\alpha = 1,\ldots,n)$$

where $\lambda_\beta^{OK}(u)$ is the optimal weight, $C(u - u_\alpha)$ is the covariance function between two points, and $\mu_{OK}(u)$ is the Lagrange parameter.

The corresponding minimized error variance, also called OK variance is expressed as Eq. (4):

$$\sigma_{OK}^2 = C(0) - \sum_{\alpha=1}^{n} \lambda_{\alpha}^{OK} C(u_{\alpha} - u) - \mu_{OK}(u) \qquad [4]$$

The Ordinary Kriging cannot be used unless the regionalized variable has a constant mean although it is not known. Because the successive differences conceal the regional mean in the semivariogram calculations, this means that in the case of a systematic variation in the regional average such as abrupt changes, trends, oscillations, the Ordinary Kriging assumption of constant mean is violated. Therefore other estimation procedure, which should take into consideration these systematic mean variations, must be used (Sen, 2009).

8.1.6 Universal Kriging (UK) or kriging with internal drift

"Universal kriging" (UK), first introduced by Matheron (1969), is as a special case of kriging with changing mean where the trend is modelled as a function of cartographic coordinates (Deutsch and Journel, 1998; Webster and Oliver, 2007). Deutsch and Journel (1998) define this method as kriging with a trend model since the underlying random function model *Z(u)* is the sum of a trend component, *m(u)* plus a residual *R(u)* (Eq. 5):

$$Z(u) = m(u) + R(u) \qquad [5]$$

The trend *m* is a deterministic, structural component that represents large scale variation. The residual is a stochastic component representing small scale, 'noisy' variation. The trend component is defined as *m(u)* = E{*Z(u)*}, and is fitted as $m(u) = \sum_{k=0}^{K} a_k f_k(u)$. The $f_k(u)$'s are known functions of the location coordinates and the a_k's are unknown parameters. The trend value *m(u)* is itself unknown since the parameters a_k are unknown. The residual component *R(u)* is usually modelled as a stationary random function with zero mean and covariance $C_R(h)$.

Using Lagrange formalism, UK system is written as:

$$\begin{cases} \sum_{\beta=1}^{n} \lambda_{\beta}^{UK}(u) C_R(u_\alpha - u_\beta) + \sum_{k=0}^{K} u_k^{UK}(u) f_k(u_\alpha) = C_R(u_\alpha - u) \\ \sum_{\beta=1}^{n} \lambda_{\beta}^{UK}(u) = 1, \sum_{\beta=1}^{n} \lambda_{\beta}^{UK}(u) f_k(u_\beta) = f_k(u) \end{cases} \quad (\alpha = 1,...,n), (k = 0,...,k)$$

where $\lambda_{\beta}^{UK}(u)$ is the optimal weight, $C_R(u_\alpha - u_\beta)$ is the covariance function between two residual points, and $u_k^{UK}(u)$ is the Lagrange parameter.

The corresponding UK variance σ_{UK}^2 is (Eq. 6):

$$\sigma_{UK}^2(u) = C_R(0) - \sum_{\alpha=1}^{n} \lambda_{\alpha}^{UK} C_R(u_\alpha - u) - \sum_{k=0}^{k} u_k^{UK}(u) f_K(u) \qquad [6]$$

8.1.7 Regression-kriging (RK)

Regression-kriging (RK) (Odeh et al., 1994, 1995) is a hybrid method that involves either a simple or multiple-linear regression model (or a variant of the generalized linear model and regression trees) between the target variable and ancillary variables, calculating residuals of the regression, and combining them with kriging. Different types or variant of this process, but with similar procedures, can be found in literature, which can cause confusion in the computational process. RK defined by Ahmed and De Marsily (1987) as “Kriging with a guess field” involves regression, and calculation of the residuals. This is followed by kriging of the regression predicted values and the residuals separately, and summing both values together to obtain the final prediction. Knotters et al. (1995) define this method as “kriging combined with regression” where regression is performed, and followed by kriging of regressed values, whereas Goovaerts (1999) uses the term ‘‘Kriging after detrending” to refer the RK method. Hengl et al. (2004; 2007) makes a comprehensive analysis to the RK spatial prediction technique and compared it with the Kriging with external drift (KED) method (Goovaerts, 1997) concluding that they are equivalent and should, under the same assumptions, yield the same predictions.

In this paper we refer to RK according to Hengl et al. (2007) and Hengl (2009) and the proposed methodology of implementation (*http://spatial-analyst.net*) is followed. In the process of RK the predictions are combined from two parts; one is the estimate $\hat{m}(s_0)$ obtained by regressing the primary variable on the *k* auxiliary variables $q_k(s_0)$ and $q_0(s_0)=1$; the second part is the residual estimated from kriging. RK is estimated as follows Eqs. (7) and (8):

$$\hat{z}_{rk}(s_0) = \hat{m}(s_0) + \hat{e}(s_0) \qquad [7]$$

$$\hat{z}_{rk}(s_0) = \sum_{k=0}^{v} \hat{\beta}_k \cdot q_k(s_0) + \sum_{i=1}^{n} w_i(s_0) \cdot e(s_i) \qquad [8]$$

where $\hat{\beta}_k$ are estimated drift model coefficients ($\hat{\beta}_0$ is the estimated intercept), optimally estimated from the sample by some fitting method, e.g. ordinary least squares (OLS) or, optimally, using generalized least squares (GLS), to take the spatial correlation between individual observations into account (Cressie, 1993); w_i are kriging weights determined by the spatial dependence structure of the residual and $e(s_i)$ are the regression residuals at location s_i.

8.2. Methods and data

8.2.1 Study area

The study area is located in the North-Center Portugal, extending from 39º 11' 53" N, 06º 14' 17' W to 42º 50' 50" N, 08º 19' 02" W (Figure 8.1a). This is a heterogeneous region with a complex topography where the elevations ranging from 130 to 1500m (Figure 8.1b). The climatic factors are very variable during the year, with annual mean precipitation in the range of 800 - 2800 mm and annual mean temperatures ranging from 7.5 to 16 ºC. These physical conditions make this region well-suited for forest growth. The land cover is fragmented with small amount of suitable soils for agriculture and the main areas are occupied by forest spaces. Forest activity is a direct source of income for a vast forest products industry, which employs a significant part of the population.

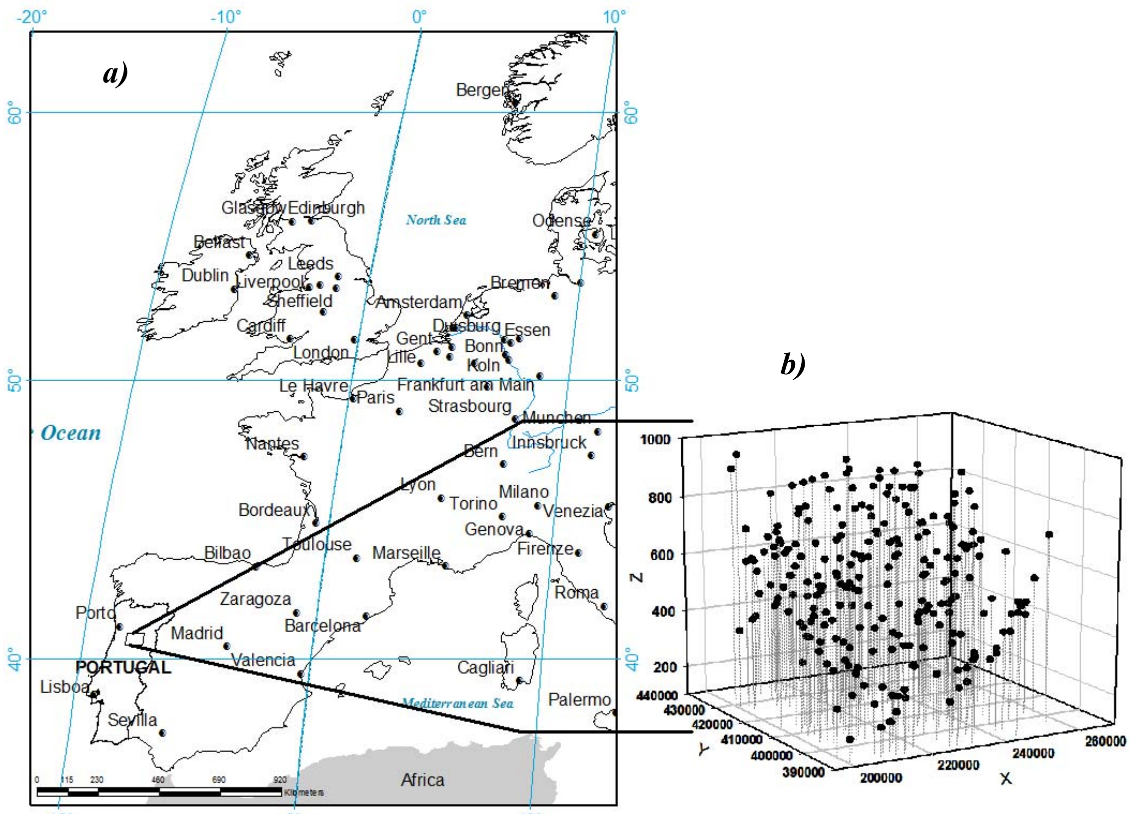

Figure 8.1 - Study area.

(*a*) Geographical location, (*b*) Distribution of inventory samples plots, where *x*, *y* are the cartographic coordinates (Hayford-Gauss, Datum of Lisbon, IGeoE) and *z* is the altitude (m).

8.2.2 Field data

A systematic sampling design was implemented in the study area which include productive forest stands and shrubland areas. A total of 276 sample plots were located being 102 from shrubs, 132 from pure *Pinus pinaster* Aiton (maritime pine) stands and the remaining 42 plots from *Eucalyptus globulus* (eucalyptus) and mixed stands. For the purpose of the present study, only the pure pine stands and shrubland areas were considered. The field data was collected in circular temporary sample plots within a fixed-area of 500m^2, in the year 2006. The geographical locations of the plots were recorded by global navigation satellite systems (GNSS), georeferenced and structured in a geographic information system (GIS) database. In pine stands, the dendrometric parameters: diameter at breast height (dbh), total height of the tree (h) and canopy height (hc) were measured. The structural stand variables recorded in each plot were used to determine the stand characteristics such as age (t), number of trees per hectare (N), dominant tree height class (h_{dom}), basal area (G), crown closure class and site index (SI). In the shrubland areas the dominant height of vegetation (h_{dom}), the vegetation cover (%) and species composition were determined. This data was recorded in a GIS geodatabase, in the Portuguese Cartographic coordinates, to further analysis.

8.2.3 Biomass calculation from the inventory dataset

In order to achieve the biomass in the inventory dataset, different methodologies were followed for the two cover classes considered in the present study. In the pine stands only the so-called primary residues (parts of trees, unsuitable for saw timber such as branches and tops) were calculated and used in the spatially explicit biomass estimation (crown biomass), while for the shrub biomass the entire above-ground biomass was used. This option was due to the fact that the primary residues from pine stands and the shrubland biomass are often ignored in biomass estimations, and their use for energy has being increasing in the last years. As example, the Portuguese political strategy to generate combined heat and power (CHP) from biomass states that the main source of fuel should come from the residual biomass generated by forest activity, where the crown biomass represents the majority, and the other source of fuel should come from shrubs with the intention of reducing the wildfire hazard (see Viana et al., 2010). On the other hand, the isolated canopy cover had better adjustments with the spectral information extracted from the Landsat TM imagery data, than the biomass of the entire tree (stem and crown). In fact, after the canopy cover reaches its maximum the stem keeps growing but the changes in reflectance are very small.

The crown biomass of pine stands was calculated using an allometric equation adjusted for the study area, which are presented further in section 8.3.2, Table 8.2. A total of 100 trees were sampled within 10 maritime pine stands, using the destructive method. The trees were logged, measured (e.g. diameter at breast height, total height, canopy height) and the live crown weighted *in situ*. The moist content was determined in laboratory, for the conversion of biomass to dry weight. The measured variables were then used for adjustment of regression models, using the crown biomass (kg tree^{-1}) as dependent variable. To estimate the shrubland biomass 20 sample plots, with an area of 10m^2 were established and the vegetation parameters measured (shrubs density, height and estimated age) using the line intersection method. The vegetation was divided by species composition and the total biomass was weighted *in loco*. The measured variables were used for adjustment of regression models using shrub AGB (ton ha^{-1}) as dependent variable, which are presented further in section 8.3.2, Table 8.2. These equations were then applied to calculate the AGB in the inventory dataset, according to the characteristics of the stand and shrub of each sample plot.

8.2.4 Remote sensing procedures

8.2.4.1 Remote sensing data

Two different remote sensing imagery data freely available from the US Geological Survey (USGS) Earth Resources Observation and Science (EROS) Centre were used in this research. A Landsat 5 Thematic Mapper (TM) image (Path/row: 204/032) was acquired on 10 December 2006 and the Global MODIS vegetation indices dataset (h17v04) from the Moderate Resolution Imaging Spectroradiometer (MODIS) from 29 August 2006 (MOD13Q1.A2006241.h17v04.005.2008105184154.hdf). Atmospheric conditions were clear at the time of image acquisition, and the data had been corrected for the radiometric and geometric distortions of the images to the standard Level 1G before delivery.

8.2.4.2 Satellite image processing

All images pre-processing and processing procedures were executed using the IDRISI GIS and Image Processing software (Eastman, 2006). Landsat 5 TM and MODIS were projected to the same Portuguese coordinate system (Hayford-Gauss, Datum Lisbon). Landsat 5 TM image geometric correction (Lillesand et al., 2004; Eastman, 2006) was made using ground control points (Toutin, 2004) and was radiometrically resampled by nearest neighbour. The overall root mean square error (RMSE) was 13.93 m. The Landsat 5 TM image raw digital numbers were then transformed to percent reflectance according Chavez (1996). MODIS data were brought to the same grid resolution as Landsat 5 TM (30m) and it was coregistered to Landsat 5 TM image as base, with a RMSE of 14.54m. Supervised classifications of multi-spectral images were carried out, based in the Maximum Likelihood classifier (MLC) using the six reflective bands (1-5 and 7) of TM sensor, covering the spectral ranges from 0.45 to 1.75 μm and 2.09 to 2.35 μm. The cover types, pine and shrubs, were isolated and subsequently validated with the Corine Land Cover map from 2006 (CLC 06, IGP, 2010). These two maps were further used as a mask and AGB estimations were made inside these areas.

8.2.4.3. Vegetation indices development

Vegetation indices, specially the Normalized Difference Vegetation Index (NDVI), have been extensively applied in studies of vegetation biomass (Atkinson et al., 2000; Chirici et al., 2007; Viana et al., 2009). The provided bands (1-5 and 7) from the TM sensor allowed to compute the Normalized Difference Vegetation Index (NDVI) as NDVI = (NIR - R) / (NIR + R), where Near-infrared (NIR) is radiation in waveband 4 and red (R) is radiation in waveband 3. NDVI measures both the amount of green vegetation and vegetation health, but it also is a basic indicator of changes in vegetation over space and time. The Global MOD13Q1 data includes the MODIS Normalized Difference Vegetation Index (NDVI) and a new Enhanced Vegetation Index (EVI) provided every 16 days at 250-m spatial resolution as a gridded level-3 product in the Sinusoidal projection **(***https://lpdaac.usgs.gov/lpdaac/products/modis_products_table/vegetation_indices/16_day_l3_global_250m/mod13q1***).**

Additionally the Tasseled Cap transformation was performed, which is an orthogonal transformation, and the green vegetation index was expressed through the development of their second component (Eastman, 2006).

8.2.5 Direct Radiometric Relationships (DRR)

The field inventory data, within the GIS database, was superimposed on the Landsat 5 TM and MODIS images data and then the individual pixel value (30 m x 30 m) and the nearest pixel values (90 m x 90 m) were attached to the field records. Regressions were performed for the two strata (pine forest and shrubs) individually and for all plots combined. The spectral information extracted from these images (NDVI, EVI and Tasseled Cap) was used as independent variables for developing regression models. Linear, logarithmic, exponential, power, and second-order polynomial functions were tested on the data. Multiple linear regressions were also tested to determine if a combination of several variables (e.g, crown closure, age, elevation, etc.) could improve the associations. The best models, for each stratum, were applied to the imagery data where the independent variable was derived, and the predicted above-ground biomass maps were produced. Depending on the applied model some biomass values predicted by the regression equations were negative. This happened in the low Vegetation index values, so these pixels were removed, because in reality negative biomass values are not possible. The imagery data in which the independent variable (vegetation index) presented the best regression with the AGB was subsequently used as predictor (auxiliary map) in the Regression-kriging spatial prediction method.

8.2.6 Geostatistical modelling

Geostatistics offers a collection of deterministic and statistical tools aimed at understanding and modelling spatial variability through prediction and simulation (Journel and Huijbregts, 1978; Goovaerts, 1997; Deutsch and Journel, 1998). Geostatistical procedures were performed with the GSTAT package included in IDRISI software both to automatically fit the variograms of residuals and to produce final predictions (Pebesma, 2001, 2004). GSTAT produces the predictions and variance map, which is the estimate of the uncertainty of the prediction model, i.e. precision of prediction. In this research, we employed Ordinary kriging (OK), Universal kriging (UK) and Regression-kriging (RK) spatial models. Geostatistical methods such as the semivariogram, also called the variogram, can be used to quantify the spatial variability of a random variable. The first stage of geostatistical modelling consists in computing the experimental variograms using the classical formula (Eq. 9):

$$\hat{\gamma}(h) = \frac{1}{2N(h)} \sum_{i=1}^{N(h)} \left[z(x_i) - z(x_i + h) \right]^2 \quad [9]$$

where: $\hat{\gamma}(h)$ is the semivariance for distance *h*, *N(h)* the number of pairs for a certain distance and direction of *h* units, while z(xi) and $Z(x_i + h)$ are measurements at locations x_i and $x_i + h$, respectively.

Two variogram models were developed: one for the pine crown biomass and one for the shrub AGB, which is satisfactory according to Webster and Oliver (1992). For fitting the experimental variograms we used the exponential, Gaussian, spherical models using iterative reweighted least squares estimation (WLS, Cressie, 1993). Semivariogram gives a measure of spatial correlation of the studied attribute. The variogram is a discrete function of variogram values at all considered lags (Curran, 1988; Isaaks and Srivastava, 1989). Typically, the semivariance values exhibit an ascending behaviour near the origin of the variogram and they usually level off at larger distances (the sill of the variogram). The semivariance value at distances close to zero is called the nugget effect. The distance at which the semivariance levels off is the range of the variogram and represents the separation distance at which two samples can be considered to be spatially independent.

At locations where two properties *u* and *v* have been measured it is possible to estimate the cross-variogram. The cross-variogram is used to characterize spatial dependency between two variables. This is given as (Lloyd, 2007) (Eq.10):

$$\hat{\gamma}_{uv}(h) = \frac{1}{2N(h)} \sum_{i=1}^{N(h)} \left\{ \left[z_u(x_i) - z_u(x_i + h) \right] \left[z_v(x_i) - z_v(x_i + h) \right] \right\} \quad [10]$$

where: $\hat{\gamma}_{uv}(h)$ is the cross-semivariance between variables *u* and *v*, *N(h)* is the number of pairs of data locations separated by lag distance *h*, z_u is the value of variable *u* at locations x_i and $(x_i + h)$ and z_v is the data value of variable v at the same locations.

8.2.7 Validation and assessment of the prediction techniques

To compare the different AGB prediction approaches, we examined the discrepancies between the known data and the predicted data. It is common to check the consistency of interpolation methods using the cross-validation procedure, in which each sample value is removed one at a time from the data set (Leave-One-Out), and that location is predicted from the remaining data (Goovaerts, 1997; Deutsch and Journel, 1998). However, according (Davis, 1987) cross-validation cannot confirm that a particular model is or is not the optimum. It is a method to better examine and understand the phenomenon under study using the available data. On the other side, as we intended to compare the geostatistical approaches with the deterministic (IDW and Thiessen polygons) and DRR predictions, we adopted the methodology of dividing the locations randomly into two sets: the prediction set and the validation set. Webster and Oliver (1992) consider that more reliable estimation of semivariogram values requires at least 150 observations, and larger samples are needed to describe anisotropic direction-dependent variation. This does not mean, however, that geostatistics cannot be applied to smaller data sets (Goovaerts, 1997). The prediction approaches were evaluated by comparing the basic statistics of predicted AGB maps (i.e., mean and standard deviation) and the difference between the known data and the predicted data were examined using the mean error, or bias mean error (ME), the mean absolute error (MAE), standard deviation (SD) and the root mean squared error (RMSE), which measures the accuracy of predictions, as described in Eqs. (11 - 14):

$$SD = \sqrt{\frac{1}{N-1}\sum_{i=1}^{N}\left(e_i - \bar{e}\right)^2} \qquad [11]$$

$$ME = \frac{1}{N}\sum_{i=1}^{N}\left(\hat{e}_i - e_i\right) \qquad [12]$$

$$MAE = \frac{1}{N}\sum_{i=1}^{N}\left|\hat{e}_i - e_i\right| \qquad [13]$$

$$RMSE = \sqrt{\frac{1}{N}\sum_{i=1}^{N}\left(\hat{e}_i - e_i\right)^2} \qquad [14]$$

where: N is the number of values in the dataset, $\hat{e}_i$ is the estimated biomass, e_i is the biomass values measured on the validation plots and $\bar{e}$ is the mean of biomass values of the sample.

8.3 Results and discussion

8.3.1 Descriptive statistics of study sites

The descriptive statistics of pine stands' crown biomass and shrubland´s above-ground biomass, measured during field work and recorded in the inventory dataset, are presented in Table 8.1. The pine stands are highly heterogeneous, with ages ranging from 8 to 51 years old and the crown biomass ranging from 1.3 to 36 ton ha^{-1}. The shrubland areas are also heterogeneous, with canopy density ranging from 5 to 100%, and the biomass per hectare ranging from 0.79 to 36 ton ha^{-1}.

Table 8.1 - Descriptive statistics of data measured in the inventory dataset.

	Pine stands plots (n = 132)								Shrubland plots (n = 102)	
	N (trees ha^{-1})	**t** (year)	**h$_{dom}$** (m)	**dbh$_{dom}$** (cm)	**SI** (m)	**BA** (m^2 ha^{-1})	**V** (m^3 ha^{-1})	**B$_{cb}$** (ton ha^{-1})	**Canopy cover** (%)	**B$_{sr}$** (ton ha^{-1})
Mean	550.8	24.4	15.3	29.7	25.7	20.1	164.6	17.7	56.1	12.0
Min	20.0	8.0	6.0	10.8	16.5	0.4	1.4	1.3	5.0	0.795
Max	2138.5	51.0	29.4	69.9	40.1	68.3	574.1	39.9	100.0	36
SD	372.0	12.0	5.7	10.7	4.6	13.1	129.3	10.1	25.33	8.12

Where: N is the number of stems; t is the stand age; h_{dom} is the dominant height; dbh_{dom} is the dominant diameter at breast height; SI is the site index and is presented as meters at 35 years old; BA is the basal area; V is the stand commercial volume; B_{cb} is the biomass of crown and B_{sr} is the weight on dry base of biomass measured in the shrubland sample plots and n is the number of sampling plots established.

8.3.2 Above-ground biomass calculation from the inventory dataset

Based on the destructive sample approach, several allometric equations were adjusted, at plot level, to calculate the AGB in the inventory dataset. The analysis of the correlation coefficients (R), coefficients of determination (R^2), adjusted coefficients of determination (R^2_{adj}), the significance of the Student t-test, and the root mean square error ($RMSE$) allowed to select the best equations to predict the biomass of pine (R^2 = 0,81) and shrub (R^2 = 0,89), as presented in Table 8.2.

Table 8.2 - Allometric equations used to estimate biomass in the field plots.

Cover type	**Equation**	**R^2**
Pine	$AGB_{pine} = 19284.26 d_{bh}^{2.299} h_t^{-0.7902}$	0.81
Shrub	$AGB_{Srb} = 0.0258[(Cc)(h_{srb})]^{0.754}$	0.89

Where: AGB_{pine} is the crown biomass (kg tree^{-1}), d_{bh} is the diameter at breast height (m), h_t is the height of tree (m), AGB_{srb} *is* the biomass of shrub (ton ha^{-1}), *Cc* is the crown closure (from 0-100 %) and h_{srb} is the mean height of shrubs (cm).

8.3.3 Relation between above-ground biomass and remote sensing data

The correlation analyses between calculated AGB in sample plots and predictors (spectral bands, vegetation indices, Tasseled Cap transformation, principal components), shows that vegetation indices were better correlated with biomass. Hence, several regression models were developed using stand-wise forest inventory data and Landsat TM and MODIS vegetation indices. The best results are presented in Table 8.3.

The best equations were achieved with NDVI derived from Landsat 5 TM, as independent variable, both for pine stands and shrub land, as presented in Figure 8.2. The better results using the higher spatial resolution of Landsat TM data are due to the fact that the effect of mixed pixels is reduced compared to coarse resolution MODIS data. In TM data (30m) the average reflectance of forest stands and shrubland is more pure than that of 250 m resolution MODIS pixels. These regression models were further used to map the biomass by the DRR method and the NDVI TM image was used as an auxiliary variable in RK spatial prediction method.

Table 8.3 - Regression models developed using stand-wise forest inventory data and Landsat 5 TM and MODIS image data.

Model	Independent variable	α	β	δ	R^2	RMSE (ton ha^{-1})	Average Predict biomass (ton ha^{-1})
Pine stands							
$y=\alpha.x^{\beta}$	NDVI (TM)	112.9820	2.4018		0.52	7.48	16.1
$y=\alpha+\beta x+\delta x^2$		-14.0787	62.0106	25.335	0.49	7.24	17.7
$y=\alpha.e^{\beta x}$		1.0957	5.9478		0.51	7.88	16.2
$y=\alpha+\beta x$		-18.4745	83.5498		0.49	7.22	17.7
$y=\alpha.x^{\beta}$	NDVI (MODIS)	49.2270	2.4034		0.22	6.52	15.1
$y=\alpha+\beta x+\delta x^2$		-76.1399	271.2939	-188.857	0.17	9.28	17.7
$y=\alpha.e^{\beta x}$		1.2411	4.0514		0.21	9.89	15.1
$y=\alpha+\beta x$		-12.1289	49.3060		0.15	9.35	17.7
$y=\alpha.x^{\beta}$	EVI (MODIS)	151.1559	2.0062		0.23	3.89	15.2
$y=\alpha+\beta x+\delta x^2$		-34.9565	252.3460	-262.456	0.20	9.07	17.7
$y=\alpha.e^{\beta x}$		1.9357	6.3878		0.22	9.64	15.2
$y=\alpha+\beta x$		-9.2017	85.6510		0.20	9.08	17.7
Shrubland							
$y=\alpha.x^{\beta}$	NDVI (TM)	33.9450	1.1064		0.50	5.73	10.5
$y=\alpha+\beta x+\delta x^2$		2.9293	3.3927	57.4804	0.59	5.28	12.0
$y=\alpha.e^{\beta x}$		2.2121	4.1548		0.55	5.43	10.9
$y=\alpha+\beta x$		-2.6106	42.6519		0.56	5.38	12.0
$y=\alpha.x^{\beta}$	NDVI (MODIS)	39.9192	2.2160		0.32	7.38	10.1
$y=\alpha+\beta x+\delta x^2$		-12.5798	54.86892	-14.8373	0.25	7.12	12.0
$y=\alpha.e^{\beta x}$		0.9470	4.322952		0.31	7.45	10.1
$y=\alpha+\beta x$		-8.6513	39.3024		0.25	7.08	12.0
$y=\alpha.x^{\beta}$	EVI (MODIS)	73.6125	1.5601		0.24	7.47	9.9
$y=\alpha+\beta x+\delta x^2$		-4.7182	67.3874	-20.3535	0.23	7.19	12.0
$y=\alpha.e^{\beta x}$		2.1054	5.4164		0.23	7.51	9.9
$y=\alpha+\beta x$		-3.0693	55.4241		0.23	7.16	12.0

Where: y is the biomass (ton ha^{-1}) and α, β, δ are the coefficients of regression.

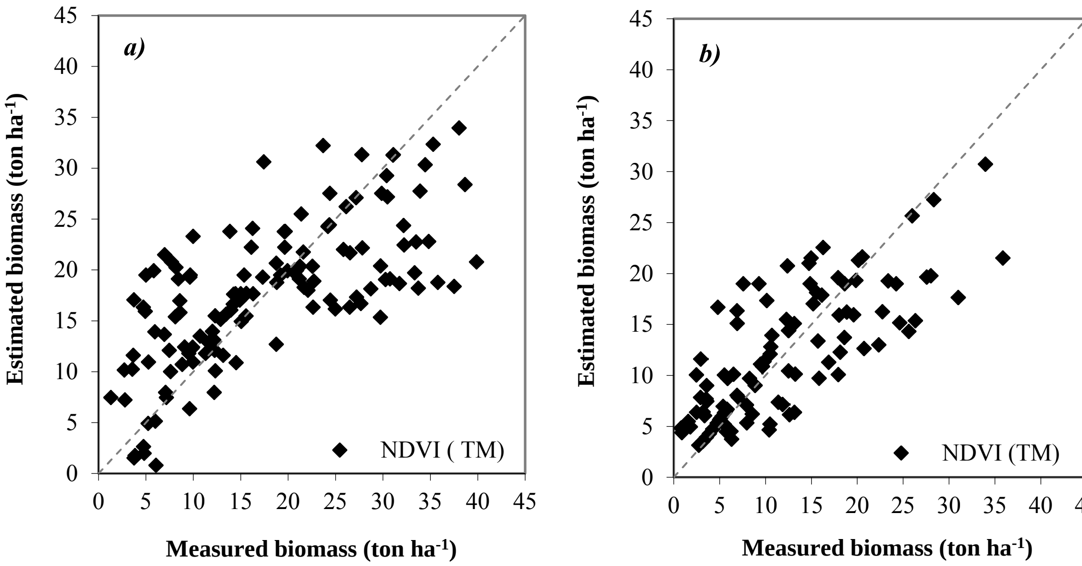

Figure 8.2 - Scatterplots of measured biomass versus estimated biomass from regression equations with NDVI as independent variable.
(a) pine and *(b)* shrubland. A 1:1 line (black, dashed) is provided for reference.

8.3.4 Geostatistical predictions

To spatially estimate AGB by geostatistical modelling the experimental semivariograms were computed and analysed at the first stage. The directional semivariograms of the residuals did not show an evident behaviour of anisotropy, thus an isotropic pattern was considered. The omnidirectional semivariograms were tested and its Exponential, Gaussian and Spherical models were fitted using Eq. (9). While the shrub biomass showed a clear spatial dependence (Figure 8.3) the crown biomass of pine stands presented lower spatial autocorrelation (Figure 8.4). The high nugget effect, visible in the figure, which under ideal circumstances should be zero, indicates that there is a significant amount of error present in the data due to the short scale variation, principally in pine data. In fact, in surveys covering large geographical regions, the residuals from the regression model may lack spatial structure because of the large distances separating sample data locations. As reported by different authors (Gilbert and Lowell, 1997; Gunnarsson et al., 1998) forest variables are not always spatially continuous because it is highly dependent on forest landscape structure even to the densest sampling schema. In shrubland this is not so evident, since these areas have a higher spatial continuity, thus presenting an autocorrelation on the variable studied. For shrub, automated variograms modelling gave a small nugget and larger range parameter (6.35 Km, 7.09 Km and 13.09 Km for exponential, Gaussian and spherical models, respectively), whereas for pine the range parameter was fairly shorter (2.3 Km, 2.9 Km and 6.3 Km for exponential, Gaussian and spherical models, respectively). Despite the exponential model fit better the shrub biomass (nugget of 22, a partial sill of 56, and a range of 6.35 Km) and the spherical model fit better the pine stand biomass (nugget of 88, a partial sill of 19, and a range of 6.3 Km) we used all the fitted models in the geostatistical spatial predictions (OK, UK and RK) to evaluate which is more effective in the predictions all over the study area.

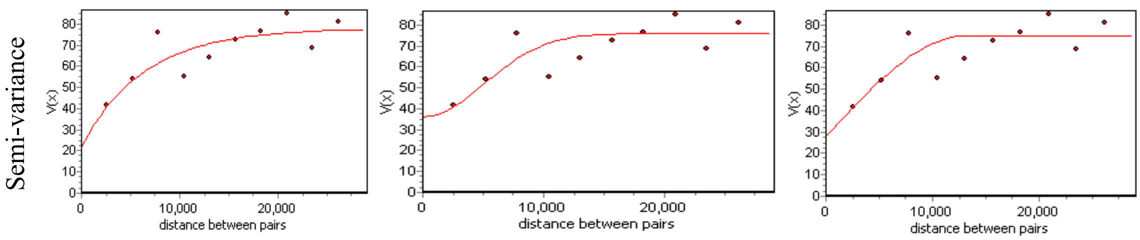

Figure 8.3 - Experimental omnidirectional semivariogram for shrub biomass.

(*a*) exponential [22.000000 Nug(0) + 56 Exp(6350)]; (*b*) gaussian [36.000000 Nug(0) + 40 Gau(7090)] and *(c)* spherical models [28.000000 Nug(0) + 47 Sph(13090)].

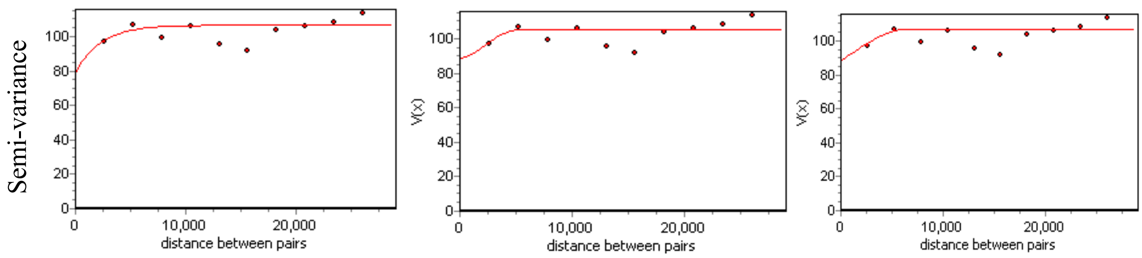

Figure 8.4 - Experimental omnidirectional semivariogram for pine biomass.

(a) exponential [79.000000 Nug(0) + 28 Exp(2300)]; *(b)* gaussian [89.000000 Nug(0) + 17 Gau(2900)] and *(c)* spherical models [88.000000 Nug(0) + 19 Sph(6300)].

8.3.5 Validation of spatial distribution methods of above-ground biomass

The validation of spatial prediction methods, based on random samples outside of the training data set, was made by comparing the basic statistics of predicted AGB maps (Table 8.4). In the pine AGB predictions 100 observations were used for the prediction and 32 for validation. In the shrub AGB predictions 81 observations were used for predictions and 21 for validation. Training and validation sets were compared, by means of a Student's t test (t_{pine} = 0.856 ns; t_{shrub} = 0.746 ns), in order to check if they provided unbiased sub-sets of the original data.

In both shrub and pine biomass estimations the mean error (ME), which should ideally be zero if the interpolation method is unbiased, suggests that all predictions are slightly biased. Analysing the mean absolute errors (MAE) it is clear that DRR approach achieved the lowest errors however, RK method had a similar performance. The archived RMSE in pine estimations was lower in RK than in DRR approach but in shrub estimations DRR provided inferior RMSE values than RK approach (Table 8.4 and Figure 8.5). The best results in pine biomass predictions originated a RMSE=32.2% of the mean (17.4 ton ha^{-1}) for DRR approach and a very similar result for the RK(exponential) approach, with a RMSE=31.4% of the mean (17.4 ton ha^{-1}). Shrub biomass estimation based on DRR approach resulted in a RMSE=31.8% of the mean (11.6 ton ha^{-1}) and RK(spherical) resulted in a RMSE=35.6% of the mean (12 ton ha^{-1}).

The results indicate that determinists and geostatistical (OK and UK) approaches are not efficient to map these type of forest variables, as spatial structure in field biomass data is weak, as concluded by others (Gilbert and Lowell, 1997; Gunnarsson et al., 1998; Tuominen et al., 2003; Freeman and Moisen, 2007). Nevertheless, despite DRR was the most efficient method to map AGB, RK approach can be considered to be explored in future studies with the aim of improving biomass estimation accuracy, were autocorrelation between variables exists.

Table 8.4 - Shrub and Pine AGB estimation models evaluation using the validation sample plots.

	ME (ton ha^{-1})		**MAE (ton ha^{-1})**		**RMSE (ton ha^{-1})**		**SD (ton ha^{-1})**	
	Pine	**Shrub**	**Pine**	**Shrub**	**Pine**	**Shrub**	**Pine**	**Shrub**
IDW	0.33	0.23	8.34	5.74	10.56	7.46	3.44	4.39
Thiessen	-0.39	8.89	9.10	10.30	11.68	12.23	10.34	6.20
DRR	0.62	0.34	3.93	2.87	5.60	3.69	7.84	4.85
OK(exponential)	1.35	0.52	6.77	6.18	8.02	7.60	4.24	4.39
OK(gaussian)	1.46	0.77	6.76	6.41	7.79	7.52	4.03	4.01
OK(spherical)	1.36	0.65	6.80	6.36	8.03	7.56	4.17	4.07
UK(exponential)	1.17	0.39	6.59	6.35	7.64	7.57	3.09	4.69
UK(gaussian)	1.37	0.22	6.87	6.25	8.06	7.62	4.11	4.82
UK(spherical)	1.32	0.48	6.60	5.69	7.71	6.85	3.61	3.47
RK(exponential)	0.61	0.74	4.05	3.65	5.46	4.33	8.11	5.82
RK(gaussian)	0.55	1.01	4.09	3.99	5.52	4.61	8.16	5.98
RK(spherical)	0.62	0.75	4.04	3.65	5.53	4.27	8.13	5.77

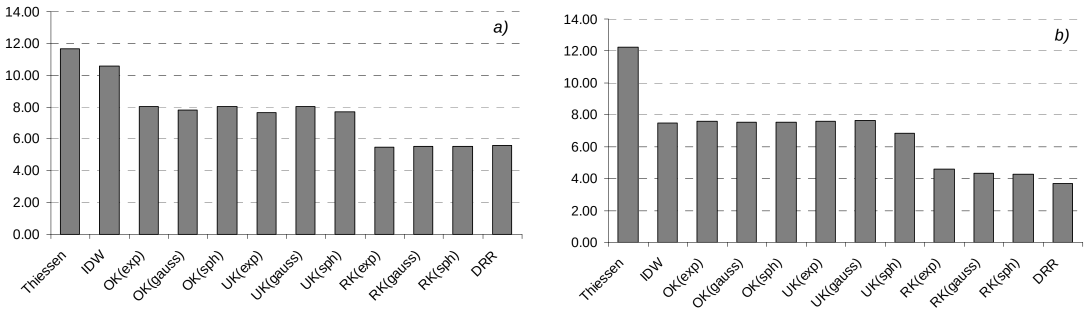

Figure 8.5 - Comparison of Root Mean Square Errors (RMSE).
(*a)* pine stands; (*b)* shrubland.

In order to compare the mean values, of crown biomass and shrub biomass estimated by the interpolation methods, analysis of variance (ANOVA) was performed (Table 8.5). The results show that, at alpha level 0.05, the differences between the means are not significant between the pine AGB maps, but for shrub AGB maps the test failed to reject the null hypothesis that means were equal. Hence, the Tukey HSD All-Pairwise Comparisons Test was carried out to examine the differences between the interpolation methods used (Table 8.6). For pine AGB maps the test confirmed that there are no significant pairwise differences among the biomass means that emanated from all the interpolation methods used, but for shrub AGB maps there are 2 groups (A and B) in which the Thiessen method is statistically different from the other studied methods, as indicated in Table 8.6. Despite that, curiously, the average values of biomass were statistically similar between almost all methods, it just means that interpolations over large areas based on these methods (deterministic and geostatistical where there is no apparent autocorrelation of the variables) can be misleading. In fact, spatially explicit biomass estimation is only reliable by using remote sensing (e.g. DRR or k-NN) or by using remote sensing data, as auxiliary variable, in techniques such as RK, where the existence of autocorrelation between the variables could improve the estimates.

Table 8.5 - Results from ANOVA to compare the differences between the means of the different prediction methods.

Source	DF	SS	MS	F	P
Pine					
Between	11	279.5	25.407	0.65	0.7863
Within	372	14564.5	39.152		
Total	383	14844			
Shrub					
Between	11	1348.08	122.553	5.01	0
Within	240	5866.51	24.444		
Total	251	7214.59			

Table 8.6 - Tukey HSD all-pairwise comparisons test.

	Pine AGB		Shrub AGB	
Method	**Mean (ton ha^{-1})**	**Tukey Group**	**Mean (ton ha^{-1})**	**Tukey Group**
IDW	15.25	A	11.49	B
Thiessen	16.40	A	20.14	A
DRR	17.41	A	11.60	B
OK(exponential)	18.14	A	11.78	B
OK(gaussian)	18.25	A	12.03	B
OK(spherical)	18.15	A	11.91	B
UK(exponential)	17.96	A	11.64	B
UK(gaussian)	18.16	A	11.48	B
UK(spherical)	18.11	A	11.74	B
RK(exponential)	17.40	A	12.00	B
RK(gaussian)	17.35	A	12.26	B
RK(spherical)	17.41	A	12.01	B

8.3.6 Quantitative comparison of AGB mapping methods

Estimates of the crown biomass of pine stands and shrubland AGB (ton ha^{-1}) are shown in Tables 8.7 and 8.8, respectively. Furthermore, Figure 8.6 shows the biomass maps derived by DRR method for the entire study area. The biomass estimates, both the average values (ton ha^{-1}) and the total biomass, shows a clear distinction between the DRR and RK methods and the other spatial prediction methods. As concluded by the analysis of the statistics of the validation dataset, the deterministic approaches and Kriging methods are unsuitable to these mapping purposes as they tend to suppress variance of estimations (Tables 8.7 and 8.8). Hence, comparing the DRR and RK approaches the differences in the total biomass is less than 1% in the best estimates. Another interesting conclusion is that the differences between the total biomass estimated by RK approach are minor using the Exponential, Gaussian or Spherical models in the experimental variogram. The correlation coefficients, presented in Tables 8.9 and 8.10 calculated for comparing pine and shrub AGB maps, respectively, confirm the similar results between DRR and RK estimations. Figures 8.7a) and 8.7b) shows the high correlation existent between the two biomass maps (DRR x RK) of pine stand and shrubland, respectively.

Despite these results, RK method did not improve the biomass map estimation, given the low spatial autocorrelation observed on the data (Figures 8.3 and 8.4). However, this method can be exploited in the case of geographical location of sample plots are denser, or forested areas have a greater spatial continuity, not being so dependent on forest landscape structure and boundary lines of forest patches, as these Mediterranean forests.

Table 8.7 - Summary statistics of crown biomass of pine stands maps estimated from spatial prediction methods.

Method	Pixels	Area (ha)	Mean (ton ha^{-1})	Std (ton ha^{-1})	AGB (total tonnes)
IDW	842408	75816.7	18.24	5.70	1383156
Thiessen	842408	75816.7	18.08	10.31	1370511
DRR	815697	73412.7	19.78	8.14	1452329
OK(exponential)	842408	75816.7	18.11	4.01	1373003
OK(gaussian)	842408	75816.7	18.21	3.81	1380243
OK(spherical)	842408	75816.7	18.10	3.96	1372373
UK(exponential)	842408	75816.7	18.04	3.19	1367642
UK(gaussian)	842408	75816.7	18.04	3.20	1367498
UK(spherical)	842408	75816.7	18.04	3.19	1367642
RK(exponential)	810690	72962.1	20.07	8.09	1464183
RK(gaussian)	809462	72851.6	20.06	8.10	1461312
RK(spherical)	809372	72843.5	20.08	8.09	1462572

Table 8.8 - Summary statistics of shrub AGB maps estimated from spatial prediction methods.

Method	Pixels	Area (ha)	Mean (ton ha^{-1})	Std (ton ha^{-1})	AGB (total tonnes)
IDW	1268228	114141	11.36	4.46	1296347
Thiessen	1268228	114141	10.83	8.13	1235867
DRR	1268228	114141	10.80	5.54	1232276
OK(exponential)	1268228	114141	11.69	4.02	1333860
OK(gaussian)	1268228	114141	11.85	3.88	1352688
OK(spherical)	1268228	114141	11.83	3.85	1350573
UK(exponential)	1268228	114141	11.67	4.62	1331610
UK(gaussian)	1268228	114141	11.62	4.63	1326543
UK(spherical)	1268228	114141	11.90	3.45	1357917
RK(exponential)	1237251	111353	11.18	5.98	1245362
RK(gaussian)	1238493	111464	11.22	6.01	1250744
RK(spherical)	1238644	111478	11.23	6.00	1251459

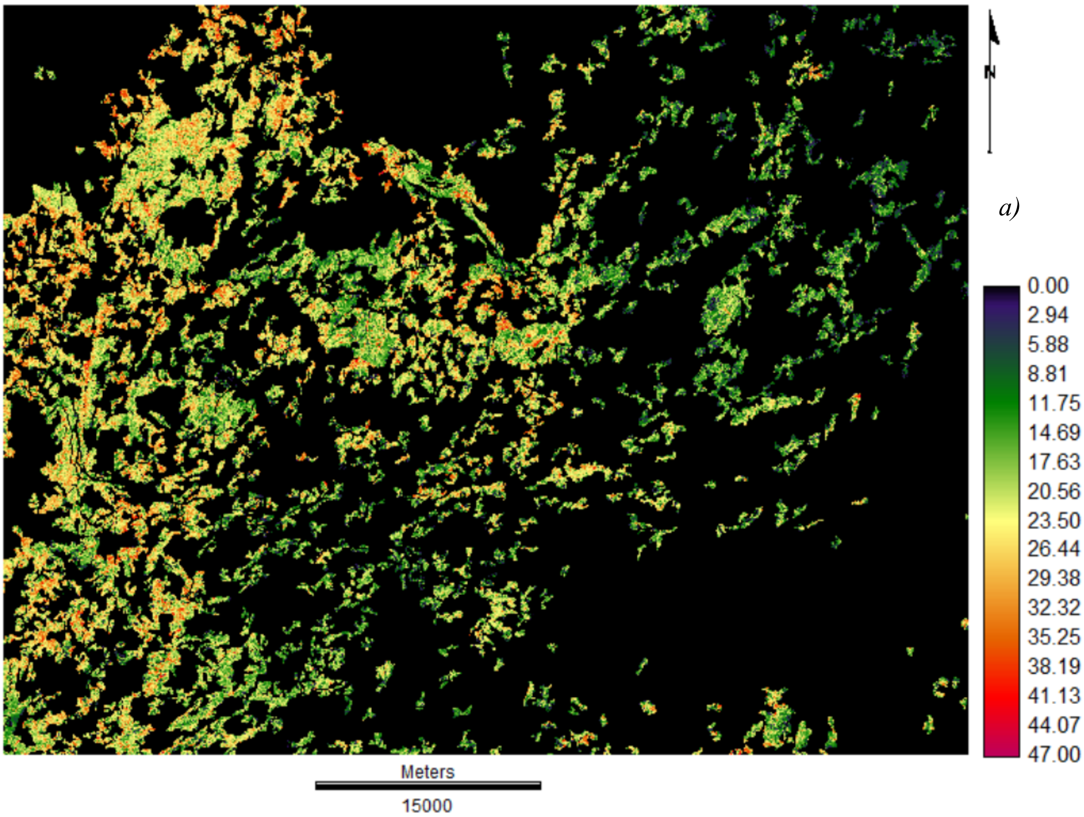

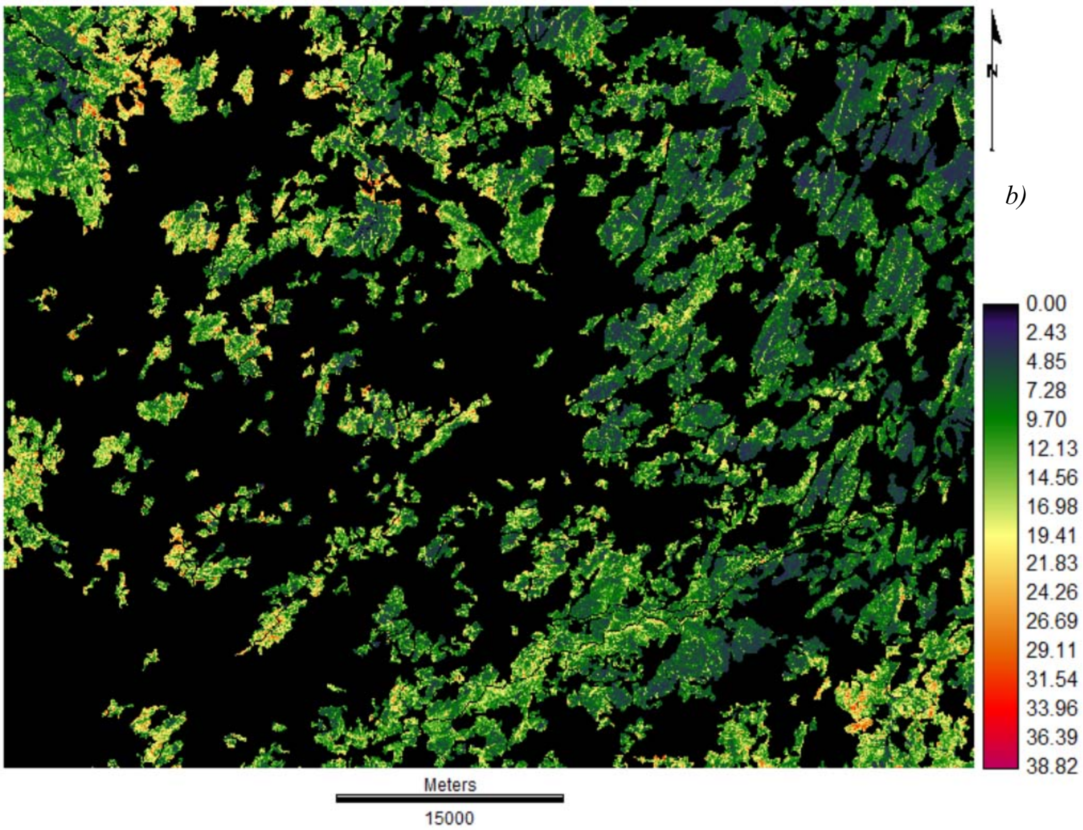

Figure 8.6 - Spatially explicit AGB estimates (ton ha^{-1}) for the study area generated from DRR spatial prediction method (*a)* pine stands (*b)* shrubland.

Note: (the colour gradation represents the vegetation and the black colour represents other land cover types, i.e. no data).

Table 8.9 - Spatial Correlation coefficients calculated between pine crown biomass maps.

	IDW	Thiessen	DRR	OK (exp)	OK (gauss)	OK (sph)	UK (exp)	UK (gauss)	UK (sph)	RK (exp)	RK (gauss)	RK (sph)
IDW	1											
Thiessen	0.81	1										
DRR	0.19	0.10	1									
OK(exponential)	0.74	0.49	0.26	1								
OK(gaussian)	0.66	0.41	0.26	0.95	1							
OK(spherical)	0.70	0.46	0.27	1.00	0.95	1						
UK(exponential)	0.60	0.34	0.30	0.90	0.91	0.91	1					
UK(gaussian)	0.60	0.34	0.30	0.90	0.91	0.91	1.00	1				
UK(spherical)	0.70	0.44	0.29	0.97	0.96	0.97	0.97	0.97	1			
RK(exponential)	0.28	0.17	0.99	0.35	0.34	0.35	0.37	0.37	0.37	1		
RK(gaussian)	0.27	0.16	0.99	0.31	0.30	0.31	0.33	0.33	0.34	1.00	1	
RK(spherical)	0.25	0.15	0.99	0.30	0.29	0.30	0.33	0.33	0.33	1.00	1.00	1

Table 8.10 - Spatial Correlation coefficients calculated between shrub AGB map estimates.

	IDW	Thiessen	DRR	OK (exp)	OK (gauss)	OK (sph)	UK (exp)	UK (gauss)	UK (sph)	RK (exp)	RK (gauss)	RK (sph)
IDW	1											
Thiessen	0.84	1										
DRR	0.24	0.18	1									
OK(exponential)	0.90	0.73	0.28	1								
OK(gaussian)	0.80	0.62	0.28	0.97	1							
OK(spherical)	0.84	0.66	0.29	0.98	0.99	1						
UK(exponential)	0.87	0.69	0.26	0.94	0.91	0.92	1					
UK(gaussian)	0.87	0.72	0.26	0.94	0.92	0.93	0.99	1				
UK(spherical)	0.90	0.69	0.30	0.92	0.85	0.88	0.85	0.86	1			
RK(exponential)	0.42	0.35	0.90	0.44	0.42	0.42	0.41	0.41	0.40	1		
RK(gaussian)	0.39	0.32	0.90	0.43	0.43	0.43	0.41	0.41	0.38	0.99	1	
RK(spherical)	0.41	0.35	0.90	0.42	0.41	0.41	0.40	0.40	0.39	1.00	0.99	1

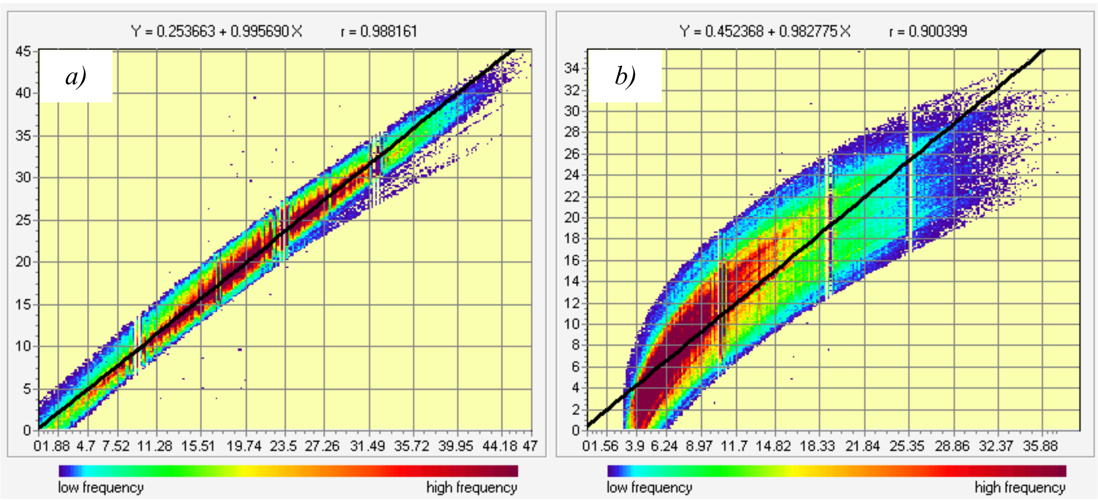

Figure 8.7 - Regression performed between DRR and RK Biomass maps.

Where: *x* and *y* is the biomass in ton ha^{-1}. *(a)* pine stands; *(b)* shrubland.

8.4. Conclusion

This study compared the spatial prediction methods Direct Radiometric Relationships (DRR) and Regression-kriging (RK), to estimate crown biomass of *Pinus pinaster* stands and shrubland above-ground biomass. Moreover, Ordinary Kriging (OK), Universal Kriging (UK), Inverse Distance Weighted (IDW) and Thiessen Polygons estimations were performed. The results showed, as expected, that the deterministic approaches are not suitable for mapping biomass. The same occurs with geostatistical interpolation methods as kriging, as they are dealing with the idea that it occurs spatial autocorrelation between neighbouring field measurement points, which is not a reality in the scattered mosaic of the studied forest landscape. However, as in much of the time the users employ spatial prediction techniques to visually understand the distribution of biomass, Kriging or deterministic models can be used, as they are easily implemented. Remote sensing is the only way, to provide spatially distributed information of the landscape structure (Jong et al., 2006) of intermediate areas between field measurements so, methods using remotely sensed data, as DRR, are the suitable way to map biomass. RK predictions, using remotely sensed data as auxiliary predictor, did not improve the AGB estimations, which is associated to the low spatial dependence observed on the data. Thus, denser sampling schemes and different auxiliary variables should be explored, in order to test if the accuracy of predictions is improved.

The results provided by DRR and RK methods showed the advantages of using the association between remotely sensed data and ground inventory data in spatial mapping. However, it should be noted that the cover types under study presented a homogeneous diversity (pure pine stands and shrubland) which allows a moderately to high correlation between vegetation characteristics and spectral response. Thus, if the objective is to map heterogeneous land cover types (e.g. mixed stands, different crown closure, etc.) the differences between spectral characteristics will increase, which will add noise to the prediction models based in remote sensed data. So, stratification of forest cover should be needed before using this approach.

The RK method has the advantage of generating estimates for the spatial distribution of AGB and its uncertainty for the study area. The uncertainty maps allow the evaluation of the reliability of estimates by identifying the places with major uncertainties which can be useful for example to select different estimation methods for those areas.

Despite RK has been increasingly used, this method has some obstacles which difficult its popularization. Since then, different names and approaches are presented in the literature about the regression-kriging theory, which leads to a confusion by the common users. An additional limitation is that RK is more sophisticated and computationally demanding than other techniques, and therefore still exist a lack of user-friendly GIS environments to run RK.

Independently of the spatial prediction method applied, these techniques are a complement to the traditional field inventories as surveys continue to be needed to collect the input data and to assess the results of spatial prediction.

References

Ahmed, S., De Marsily, G., 1987. Comparison of geostatistical methods for estimating transmissivity using data on transmissivity and specific capacity. Water Resour. Res. 23, 1717-1737.

Akhavan, R., Kia-Daliri, H., 2010. Spatial variability and estimation of tree attributes in a plantation forest in the Caspian region of Iran using geostatistical analysis Caspian J. Env. Sci. 8, 163-172.

Atkinson, P.M., Tatnall, A.R.L., 1997. Introduction Neural networks in remote sensing. International Journal of Remote Sensing 18, 699-709.

Atkinson, P.M., Foody, G.M., Curran, P.J., Boyd, D.S., 2000. Assessing the ground data requirements for regional scale remote sensing of tropical forest biophysical properties. International Journal of Remote Sensing 21, 2571-2587.

Berterretche, M., Hudak, A.T., Cohen, W.B., Maiersperger, T.K., Gower, S.T., Dungan, J., 2005. Comparison of regression and geostatistical methods for mapping Leaf Area Index (LAI) with Landsat ETM+ data over a boreal forest. Remote Sensing of Environment 96, 49-61.

Blackard, J.A., Dean, D.J., 1999. Comparative accuracies of artificial neural networks and discriminant analysis in predicting forest cover types from cartographic variables. Computers and Electronics in Agriculture 24, 131-151.

Brown, S., Gillespie, A.J.R., Lugo, A.E., 1989. Biomass Estimation Methods for Tropical Forests with Applications to Forest Inventory Data. Forest Science 35, 881-902.

Brown, S., Lugo, A., 1992. Aboveground biomass estimates for tropical moist forests of Brazilian Amazon. Interciencia 17, 8-18.

Buddenbaum, H., Schlerf, M., Hill, J., 2005. Classification of coniferous tree species and age classes using hyperspectral data and geostatistical methods. International Journal of Remote Sensing 26, 5453-5465.

Burrough, P.A., McDonnell, R.A., 1998. Principles of Geographical Information Systems. Oxford University Press Inc., New York, pp. 333.

Chavez, P.S.J., 1996. Image-based atmospheric corrections-revisited and improved. Photogrammetric Engineering and Remote Sensing 62, 1025-1036.

Chirici, G., Barbati, A., Maselli, F., 2007. Modelling of Italian forest net primary productivity by the integration of remotely sensed and GIS data. Forest Ecology and Management 246, 285-295.

Chirici, G., Barbati, A., Corona, P., Marchetti, M., Travaglini, D., Maselli, F., Bertini, R., 2008. Non-parametric and parametric methods using satellite images for estimating growing stock volume in alpine and Mediterranean forest ecosystems. Remote Sensing of Environment 112, 2686-2700.

Cohen, W.B., Maiersperger, T.K., Spies, T.A., Oetter, D.R., 2001. Modelling forest cover attributes as continuous variables in a regional context with Thematic Mapper data. International Journal of Remote Sensing 22, 2279-2310.

Cohen, W.B., Maiersperger, T.K., Gower, S.T., Turner, D.P., 2003. An improved strategy for regression of biophysical variables and Landsat ETM+ data. Remote Sensing of Environment 84, 561-571.

Cressie, N.A.C., 1993. Statistics for Spatial Data. John Wiley & Sons, New York, USA, pp. 416.

Curran, P.J., 1988. The semivariogram in remote sensing: An introduction. Remote Sensing of Environment 24, 493-507.

Curran, P.J., Atkinson, P.M., 1988. Geostatistics and remote sensing. Progress in Physical Geography 22, 61-78.

Davis, B., 1987. Uses and abuses of cross-validation in geostatistics. Mathematical Geology 19, 241-248.

Deutsch, C.V., Journel, A.G., 1998. Geostatistical Software Library and User's Guide, 2nd ed. Oxford University Press, New York, USA, pp. 369.

Dungan, J., 1998. Spatial prediction of vegetation quantities using ground and image data. International Journal of Remote Sensing 19, 267-285.

Eastman, J.R., 2006. Idrisi Andes. Guide to GIS and Image Processing. Clark Labs. Clark University, USA, pp. 328.

Fearnside, P.M., 1992. Forest biomass in Brazilian Amazônia: comments on the estimate by Brown and Lugo. Interciencia 17, 19-27.

Fearnside, P.M., 1997. Greenhouse gases from deforestation in brazilian amazonia: Net committed emissions. Climatic Change 35, 321-360.

Foroughbakhch, R., Reyes, G., Alvarado-Vázquez, M.A., Hernández-Piñero, J., Rocha-Estrada, A., 2005. Use of quantitative methods to determine leaf biomass on 15 woody shrub species in northeastern Mexico. Forest Ecology and Management 216, 359-366.

Fournier, R.A., Luther, J.E., Guindon, L., Lambert, M.C., Piercey, D., Hall, R.J., Wulder, M.A., 2003. Mapping aboveground tree biomass at the stand level from inventory information: test cases in Newfoundland and Quebec. Canadian Journal of Forest Research 33, 1846-1863.

Freeman, E., Moisen, G., 2007. Evaluating Kriging as a Tool to Improve Moderate Resolution Maps of Forest Biomass. Environmental Monitoring and Assessment 128, 395-410.

García-Martín, A., Pérez-Cabello, F., de la Riva, J.R., Montorio, R., 2008. Estimation of crown biomass of *Pinus* spp. from Landsat TM and its effect on burn severity in a Spanish fire scar. IEEE Journal of Selected Topics in Applied Earth Observations and Remote Sensing 1, 254-265.

Gilbert, B., Lowell, K., 1997. Forest attributes and spatial autocorrelation and interpolation: effects of alternative sampling schemata in the boreal forest. Landscape and Urban Planning 37, 235-244.

Gillespie, A.J.R., Brown, S., Lugo, A.E., 1992. Tropical forest biomass estimation from truncated stand tables. Forest Ecology and Management 48, 69-87.

Goovaerts, P., 1997. Geostatistics for Natural Resources Evaluation Oxford University Press, Inc., New York, USA.

Goovaerts, P., 1999. Using elevation to aid the geostatistical mapping of rainfall erosivity. Catena 34(3-4), 227-242.

Gunnarsson, F., Holm, S., Holmgren, P., Thuresson, T., 1998. On the potential of Kriging for forest management planning. Scandinavian Journal of Forest Research 13, 237-245.

Hame, T., Salli, A., Andersson, K., Lohi, A., 1997. A new methodology for the estimation of biomass of conifer dominated boreal forest using NOAA AVHRR data. International Journal of Remote Sensing 18, 3211-3243.

Hengl, T., Heuvelink, G.B.M., Stein, A., 2004. A generic framework for spatial prediction of soil variables based on regression-kriging. Geoderma 120, 75-93.

Hengl, T., Heuvelink, G.B.M., Rossiter, D.G., 2007. About regression-kriging: From equations to case studies. Computers & Geosciences 33, 1301-1315.

Hengl, T., 2009. A Practical Guide to Geostatistical Mapping. 2nd ed. University of Amsterdam, Amsterdam.

Hernández, J., Emery, X., 2009. A geostatistical approach to optimize sampling designs for local forest inventories. Canadian Journal of Forest Research 39, 1465-1474.

Hese, S., Lucht, W., Schmullius, C., Barnsley, M., Dubayah, R., Knorr, D., Neumann, K., Riedel, T., Schröter, K., 2005. Global biomass mapping for an improved understanding of the CO_2 balance--the Earth observation mission Carbon-3D. Remote Sensing of Environment 94, 94-104.

Houghton, R.A., Lawrence, K.T., Hackler, J.L., Brown, S., 2001. The spatial distribution of forest biomass in the Brazilian Amazon: a comparison of estimates. Global Change Biology 7, 731-746.

Hu, H., Wang, G.G., 2008. Changes in forest biomass carbon storage in the South Carolina Piedmont between 1936 and 2005. Forest Ecology and Management 255, 1400-1408.

IGP, CLC2006 - Cartografia CORINE Land Cover 2006 para Portugal Continental; 2009. Available online at: *http://www.igeo.pt/gdr/projectos/clc2006/* (Accessed January 2010).

Isaaks, E.H., Srivastava, R.M., 1989. An Introduction to Applied Geostatistics. Oxford University Press, New York, USA, pp. 542.

Iverson, L.R., Brown, S., Prasad, A., Mitasova, H., Gillespie, A.J.R., Lugo, A.E., 1994. Use of GIS for estimating potential and actual forest biomass for continental South and Southeast Asia, in: Dale, V.H. (ed.), Effects of Land-Use Change on Atmospheric CO_2 Concentrations: South and Southeast Asia as a Case Study. Springer-Verlag, New York, pp. 67-116.

Jong, S.M.d., Pebesma, E.J., Meer, F.D.v.d., 2006. Spatial Variability, Mapping Methods, Image Analysis and Pixels, in: Jong, S.M., Meer, F.D. (eds.), Remote

Sensing Image Analysis: Including The Spatial Domain, vol. 5. Springer Netherlands, pp. 17-35.

Journel, A.G., Huijbregts, C.J., 1978. Mining Geostatistics. Academic Press, London.

Kint, V., van Meirvenne, M., Nachtergale, L., Geudens, G., Lust, N., 2003. Spatial Methods for Quantifying Forest Stand Structure Development: A Comparison Between Nearest-Neighbor Indices and Variogram Analysis. Forest Science 49, 36-49.

Knotters, M., Brus, D.J., Oude Voshaar, J.H., 1995. A comparison of kriging, co-kriging and kriging combined with regression for spatial interpolation of horizon depth with censored observations. Geoderma 67, 227-246.

Krige, D.G., A statistical approach to some mine valuations and allied problems at the witwatersrand, University of Witwatersrand, Master's thesis, South Africa, 1951.

Labrecque, S., Fournier, R.A., Luther, J.E., Piercey, D., 2006. A comparison of four methods to map biomass from Landsat-TM and inventory data in western Newfoundland. Forest Ecology and Management 226, 129-144.

Lillesand, T.M., Kiefer, R.W., Chipman, J.W., 2004. Remote Sensing and image Interpretation, 5th ed. John Wiley and Sons Inc., New York, pp. 764.

Lloyd, C.D., 2007. Local Models for Spatial Analysis. CRC Press, Taylor & Francis Group, Boca Raton, pp. 244.

Lu, D., 2006. The potential and challenge of remote sensingbased biomass estimation. International Journal of Remote Sensing 27, 1297-1328.

Lu, G.Y., Wong, D.W., 2008. An adaptive inverse-distance weighting spatial interpolation technique. Computers & Geosciences 34, 1044-1055.

Magcale-Macandog, D.B., Delgado, M.E.M., Ty, E., Villarin, J.R.T.A., 2006. A Gis-based model to improve estimation of aboveground biomass of secondary forests in the Philippines. Journal of Tropical Forest Science 18, 8-21.

Mandallaz, D., Geostatistical methods for double sampling schemes: application to combined forest inventories Chair of Forest Inventory and Planning, Swiss Federal Institute of Technology (ETH) Zürich, 1993, pp. 133.

Maselli, F., Chiesi, M., 2006. Evaluation of Statistical Methods to Estimate Forest Volume in a Mediterranean Region. IEEE TRANSACTIONS ON GEOSCIENCE AND REMOTE SENSING 44, 2239-2250.

Matheron, G., 1963. Principles of geostatistics. Economic Geology 58, 1246-1266.

Matheron, G., 1969. Le krigeage universel (Universal kriging). (Vol. 1). Cahiers du Centre de Morphologie Mathematique. Ecole des Mines de Paris, Fontainebleau, pp. 83.

Matheron, G., 1971. The theory of regionalised variables and its applications. Les Cahiers du Centre de Morphologie Mathematique de Fontainblue. Ecole Nationale Superiore de Paris, Paris, pp. 212.

McBratney, A.B., Webster, R., 1981. The design of optimal sampling schemes for local estimation and mapping of regionalized variables—II: Program and examples. Computers & Geosciences 7, 335-365.

McRoberts, R.E., Tomppo, E.O., Næsset, E., 2010. Advances and emerging issues in national forest inventories. Scandinavian Journal of Forest Research 25, 368-381.

Meng, Q., Cieszewski, C., Madden, M., 2009. Large area forest inventory using Landsat ETM+: A geostatistical approach. ISPRS Journal of Photogrammetry and Remote Sensing 64, 27-36.

Mutanga, O., Rugege, D., 2006. Integrating remote sensing and spatial statistics to model herbaceous biomass distribution in a tropical savanna. International Journal of Remote Sensing 27, 3499-3514.

Muukkonen, P., Heiskanen, J., 2005. Estimating biomass for boreal forests using ASTER satellite data combined with standwise forest inventory data. Remote Sensing of Environment 99, 434-447.

Muukkonen, P., Heiskanen, J., 2007. Biomass estimation over a large area based on standwise forest inventory data and ASTER and MODIS satellite data: A possibility to verify carbon inventories. Remote Sensing of Environment 107, 617-624.

Nanos, N., Calama, R., Montero, G., Gil, L., 2004. Geostatistical prediction of height/diameter models. Forest Ecology and Management 195, 221-235.

Odeh, I.O.A., McBratney, A.B., Chittleborough, D.J., 1994. Spatial prediction of soil properties from landform attributes derived from a digital elevation model. Geoderma 63, 197-214.

Odeh, I.O.A., McBratney, A.B., Chittleborough, D.J., 1995. Further results on prediction of soil properties from terrain attributes: heterotopic cokriging and regression-kriging. Geoderma 67, 215-226.

Palmer, D.J., Höck, B.K., Kimberley, M.O., Watt, M.S., Lowe, D.J., Payn, T.W., 2009. Comparison of spatial prediction techniques for developing *Pinus radiata* productivity surfaces across New Zealand. Forest Ecology and Management 258, 2046-2055.

Pebesma, E.J., 2001. Gstat user's manual. University of Utrecht, pp. 108.

Pebesma, E.J., 2004. Multivariable geostatistics in S: the gstat package. Computers & Geosciences 30, 683-691.

Peichl, M., Arain, M.A., 2007. Allometry and partitioning of above- and belowground tree biomass in an age-sequence of white pine forests. Forest Ecology and Management 253, 68-80.

Pierce, K.B., Ohmann, J.L., Wimberly, M.C., Gregory, M.J., Fried, J.S., 2009. Mapping wildland fuels and forest structure for land management: a comparison of nearest neighbor imputation and other methods. Canadian Journal of Forest Research 39, 1901-1916.

Reese, H., Nilsson, M., Sandström, P., Olsson, H., 2002. Applications using estimates of forest parameters derived from satellite and forest inventory data. Computers and Electronics in Agriculture 37, 37-55.

Reich, R.M., Lundquist, J.E., Bravo, V.A., 2004. Spatial models for estimating fuel loads in the Black Hills, South Dakota, USA. Robin M. ReichA,C. International Journal of Wildland Fire 13, 119-129.

Reich, R.M., Aguirre-Bravo, C., Bravo, V.A., Briseño, M.M., 2011. Empirical evaluation of confidence and prediction intervals for spatial models of forest structure in Jalisco, Mexico. Journal of Forestry Research 22, 159−166.

Sales, M.H., Souza Jr, C.M., Kyriakidis, P.C., Roberts, D.A., Vidal, E., 2007. Improving spatial distribution estimation of forest biomass with geostatistics: A case study for Rondônia, Brazil. Ecological Modelling 205, 221-230.

Sen, Z., 2009. Spatial Modeling Principles in Earth Sciences. Springer Dordrecht Heidelberg, London, New York, pp. 351.

Ter-Mikaelian, M.T., Korzukhin, M.D., 1997. Biomass equations for sixty-five North American tree species. Forest Ecology and Management 97, 1-24.

Tomppo, E., 1991. Satellite image-based national forest inventory of Fin-land. In: Proceedings of the symposium on global and environmental monitoring, techniques and impacts. International Archives of Photogrammetry and Remote Sensing, 28, Victoria, British Columbia, Canada, pp. 419-424.

Tomppo, E., Nilsson, M., Rosengren, M., Aalto, P., Kennedy, P., 2002. Simultaneous use of Landsat-TM and IRS-1C WiFS data in estimating large area tree stem volume and aboveground biomass. Remote Sensing of Environment 82, 156-171.

Tomppo, E., Olsson, H., Ståhl, G., Nilsson, M., Hagner, O., Katila, M., 2008. Combining national forest inventory field plots and remote sensing data for forest databases. Remote Sensing of Environment 112, 1982-1999.

Toutin, T., 2004. Review article: Geometric processing of remote sensing images: models, algorithms and methods. International Journal of Remote Sensing 25, 1893-1924.

Tuominen, S., Fish, S., Poso, S., 2003. Combining remote sensing, data from earlier inventories, and geostatistical interpolation in multisource forest inventory. Canadian Journal of Forest Research 33, 624-634.

Viana, H., Lopes, D., Aranha, J., 2009. Predição de biomassa arbustiva lenhosa empregando dados de inventário e o índice de diferença normalizada extraído em imagens Landsat 5 TM, ISPV Millenium. 37. Available online at: *http://www.ipv.pt/millenium/Millenium37/15.pdf*, (Accessed May 2012).

Viana, H., Cohen, W.B., Lopes, D., Aranha, J., 2010. Assessment of forest biomass for use as energy. GIS-based analysis of geographical availability and locations of wood-fired power plants in Portugal. Applied Energy 87, 2551-2560.

Weber, D., Englund, E., 1992. Evaluation and comparison of spatial interpolators. Mathematical Geology 24, 381-391.

Webster, R., Oliver, M.A., 1992. Sample adequately to estimate variograms of soil properties. Journal of Soil Science 43, 177-192.

Webster, R., Oliver, M.A., 2007. Geostatistics for Environmental Scientists, 2nd ed. John Wiley & Sons Ltd, England, pp. 332.

Woodcock, C.E., Strahler, A.H., Jupp, D.L.B., 1988. The use of variograms in remote sensing: II. Real digital images. Remote Sensing of Environment 25, 349-379.

Zhang, C., Franklin, S.E., 2002. Forest Structure Classification using Airborne Multispectral Image Texture and Kriging Analysis Geoscience and Remote Sensing Symposium, 2002. IGARSS '02. 2002 IEEE International.

Zheng, D., Heath, L.S., Ducey, M.J., 2007. Forest biomass estimated from MODIS and FIA data in the Lake States: MN, WI and MI, USA. Forestry 80, 265-278.

Zianis, D., Muukkonen, P., Mäkipää, R., Mencuccini, M., 2005. Biomass and stem volume equations for tree species in Europe, Silva Fennica Monographs 4. Finnish Society of Forest Science, p. 63.

9

Assessment of forest biomass for use as energy. GIS-based analysis of geographical availability and locations of wood-fired power plants in Portugal

---

The content of this chapter was fully published in the following manuscript and conference proceedings:

[Annex B.1] Viana, H., Cohen, W.B., Lopes, D., Aranha, J., 2010. Assessment of forest biomass for use as energy. GIS-based analysis of geographical availability and locations of wood-fired power plants in Portugal. Applied Energy 87, 2551-2560.

[Annex B.2] Viana H.; Aranha J.; Lopes D., 2011, Dedicated Biomass Plants for Combined Heat & Power (CHP). The Portuguese National Strategy. 19th European Biomass Conference and Exhibition. ETA-Florence Renewable Energies. Berlin, Germany. June 6-10.

Abstract

Following the European Union strategy concerning renewable energy (RE), Portugal established in their national policy programmes that the production of electrical energy from RE should reach 45 % of the total supply by 2010. Since Portugal has large forest biomass resources, a significant part of this energy will be obtained from this source. In addition to the two existing electric power plants, with 22 MW of power capacity, 13 new power plants having a total of 86.4 MW capacity are in construction. Together these could generate a combination of electrical and thermal energy, known as combined heat and power (CHP) production. As these power plants will significantly increase the exploitation of forests resources, this article evaluates the potential quantities of available forest biomass residue for that purpose. In addition to examining the feasibility of producing both types of energy, we also examine the potential for producing only electric energy. Results show that if only electricity is generated some regions will need to have alternative fuel sources to fulfil the demand. However, if cogeneration is implemented the wood fuel resource will be sufficient to fulfil the required capacity demand.

Keywords: Bioenergy; Biomass; wood fuel; Logging residues; Mapping, Combined heat and power plant; Power generation

9.1. Introduction

There is an emerging consensus on the need to reverse the trend of global warming associated with climate change. The main goal is to quickly reduce emissions of greenhouse gases.

The European Union (EU) is resolved to reduce country member greenhouse gas emissions (GGE) and is promoting the development of new energy policies as one important means to that end. These policies should lead both to the development of new and more secure energy sources and contribute to a reduction in the growing dependency of EU member states on imported fossil fuels.

9.1.1. Renewable energy strategy and policy

To implement its renewable energy (RE) strategy, in March 2007 (Council of the European Union, 2007) the EU formally committed to the "20-20-20" initiative, which set as target and objectives for 2020 (Commission of the European Communities, 2008a, 2008b). These include (i) reducing greenhouse gas emissions by at least 20% of 1990 levels (30% if other developed countries commit to comparable cuts), (ii) increasing the share of RE (wind, solar, biomass, etc.) consumption to 20% compared to 8.5% today, and (iii) cutting energy consumption by 20% of projected 2020 levels by improving energy efficiency.

Renewable energy has gained greater importance over the years, and is today considered the solution to the energy future in Europe. Since 1990, the EU has been engaged in an ambitious and successful plan to become a world leader in RE production and use. The strategic energy plans and policies of the EU, as well as those individual member states, established concrete targets for exploitation of indigenous renewable energy sources (RES), and for bioenergy in particular. As a first step towards a strategy for RE the Commission adopted a Green Paper on 20 November 1996 (Commission of the European Communities, 1996). The most ambitious strategic goals were defined in 1997 in a European Commission White Paper (***European Commission, 1997***), where the EU set the target to increase the share of renewable up to 12% by 2010. The White Paper also contains a comprehensive Strategy and Action Plan setting out the means to reach this objective.

After the order Green Paper (2000) on security of energy supply (European Commission, 2001a), diverse and concrete proposals were made. One of these proposals, directive 2001/77/EC (European Commission, 2001b) on electricity production from renewable sources, was adopted in 2001. Under this directive 22% of the electricity consumed in the EU by 2010 should be produced from renewable energy sources.

According to the national targets for future consumption of electricity produced from renewable energy sources, defined for each member state, Portugal committed to 39% (including large hydro). These goals were also stated in the National E4 Programme (Energy Efficiency and Endogenous Energies) launched in 2001 (Resolução do Conselho de Ministros n.º 154/2001 de 27 de Setembro), and subsequently in the National Strategy for energy launched in 2003 (Resolução do Conselho de Ministros nº 63/2003) and 2005 (Resolução do Conselho de Ministros nº 169/2005). In 2007 Portugal established a more ambitious strategic target in its National Strategy of Sustainable Development (Energia e Alterações Climáticas, 2007). This new National Strategy for energy (Resolução do Conselho de Ministros n.º 1/2008) establishes that 45% of the national energy consumption in 2010 should be exclusively produced from renewable energy sources. In this way Portugal intends to set an example in the fulfilment of the EU objectives to reduce emissions of greenhouse gases.

9.1.2. Biomass energy policy

Amongst renewable resources, paramount importance has been given to the bioenergy because it has low negative environmental impact in terms of CO_2 emissions for the entire fuel cycle and zero CO_2 emissions from fossil fuels during operation.
The European Commission White Paper (European Commission, 1997) recognised bioenergy as the most promising area within the biomass sector for several reasons. First, because it would increase the amount of people working in the forestry sector. Second, because the combined use of heat and power (CHP) has the greatest potential per unit volume among all renewable energy sources. They also issued the opinion that the contribution of biomass-derived energy to the primary energy mix should reach 10% by 2010. The European Commission's Green report (2000) (European Commission, 2001a), also recognized that biomass is a versatile energy resource, with a widespread availability through forest and agricultural residues that has so far not been fully exploited. Consistent with the Green report, in Green paper technical document (2002) (European Commission, 2002), emphasis is given to the electricity generation from

biomass energy plants, and some success examples of implementation in some member states are presented.

The strongest incentive of the EU towards development of biomass energy was given in 2005 with the Biomass Action Plan (Commission of the European Communities, 2005a). In this plan, the EU stated that the increased use of renewable energy is essential for environmental and competitiveness reasons, and recognized that "biomass has many advantages over conventional energy sources, as well as over some other renewable energies, in particular, relatively low costs, less dependence on short-term weather changes, promotion of regional economic structures and provision of alternative sources of income for farmers" (Commission of the European Communities, 2005a). This action plan established several measures to promote biomass in heating, electricity and transport, followed by crosscutting measures affecting biomass supply, financing and research (Commission of the European Communities, 2005a; European Commission, 2005a). According to this EU strategy, the goal of reaching 45% of national energy consumption in 2010 from renewable energy sources will be achieved in part from biomass energy production. Hence, the Portuguese government decided to extend the current installed power (two electric power plants, with 22 MW of power) to 250 MW by 2010 (Energia e Alterações Climáticas, 2007). Therefore, in 2006, fifteen new power plant (90 MW) exploration licenses were made available to achieve this aim. However, because only 13 licenses were applied for, presently new power plants will only provide 86.4 MW of additional power. These new power plants will be capable of generating both electrical and thermal energy, or CHP.

The new power plants locations were defined by the Portuguese government with the double objective of increasing the quota of renewable energy in the global production of electricity and to promote the development of forest residues harvesting. This will also serve to remove shrub competition in forest groves and reduce wildfire hazard (DGGE, 2006). These power plants will have variable power generation capabilities and combine different technologies, as appropriate to local circumstances. Two power plant models are planed: small units, with power production ranging from 1.8 to 4.5 MW, and large ones with power production ranging from 9 to 9.9 MW. Considering that wood-fuel demand will increase significantly and will be variable across regions, it will be necessary to apply rational resource exploitation actions associated with regional and local needs. For example, there may be significant competition in some areas due to the presence of pulp mills or other biomass consuming industries. In these cases special solutions and compromises will be needed, or it may not be feasible to construct a power plant in such a location. As stated in the 2005 EU's report '*The support of electricity from renewable energy sources*' (Commission of the European Communities, 2005b) future development of RES projects in a specific area must taken into account spatial aspects of planning. This is especially fundamental for projects in the field of wind and biomass.

In this context the objectives of this paper are to: (1) assess Portugal's current forest biomass resource potential for commercial generation of electricity at regional and national levels, (2) assess the spatial distribution of biomass availability, and (3) evaluate the suitability of existing and proposed wood-fired power plant locations in Portugal.

9.2. Study area

Portugal is located between the latitudes of 36º 57' 23" and 42º 09' 15"N and the longitudes of 09º 30' 40" and 06º 10' 45" W. This area includes two distinctive bioclimatic regions: a Mediterranean bioclimate everywhere except in a small area in the North with a temperate bioclimate (Rivas-Martínez et al., 2004). With four distinct weather seasons, the average annual temperatures range from about 7 °C in the highlands of the interior North and Center and about 18 °C in the south coast. Average annual precipitation is more than 3000 mm in the North and < 600 mm in the south.

With complex topography and elevations ranging from the sea level to 2000m, and a small amount of suitable soils for agriculture, Portuguese land is well-suited for forest growth. Forest activity is a direct source of income for a vast forest products industry, which employs a significant part of the population.

9.3. Methodology

The framework of this study followed four main steps. The first step consisted of forest cover classification and mapping, within Portugal. In a second step, we estimated the available forest biomass and annual growth at national and regional levels. In the third step, the geographical location of existing power plants was evaluated, and a GIS-based analysis was applied to examine the relationship between existing biomass and the power plants wood-fuel demand. Finally, based on the available quantities of biomass and growth we compared the maximum theoretical potential of energy production for two scenarios (fully condensing plants and cogeneration plants).

9.3.1. Forest land cover of study area

To calculate woody biomass, it was necessary to identify and classify forest cover, as well as to characterize forest stand structure. In Portugal, forests cover approximately 3.4 million hectares (DGRF, 2007b) and represents 38 % of the national territory.

The main trees species, which are widely planted for commercial purposes and capable of providing a regular supply to meet fuel demand, are *Pinus pinaster* (maritime pine) and *Eucalyptus globulus* (eucalyptus). Thus, only these stands (710.300 hectares of maritime pine and 646.700 hectares of eucalyptus, according to the National Forestry Inventory (DGRF, 2007b)) were considered in the calculations of potential biomass.

The spatial distribution of forested land cover was made at regional level, using a so-called NUT III sub-regions (Nomenclature of Territorial Units for Statistics) boundaries (Figure 9.1). The pine and eucalyptus stands occur mainly in the North and Center of Portugal as ecological conditions limit their growth in the south part of Portugal.

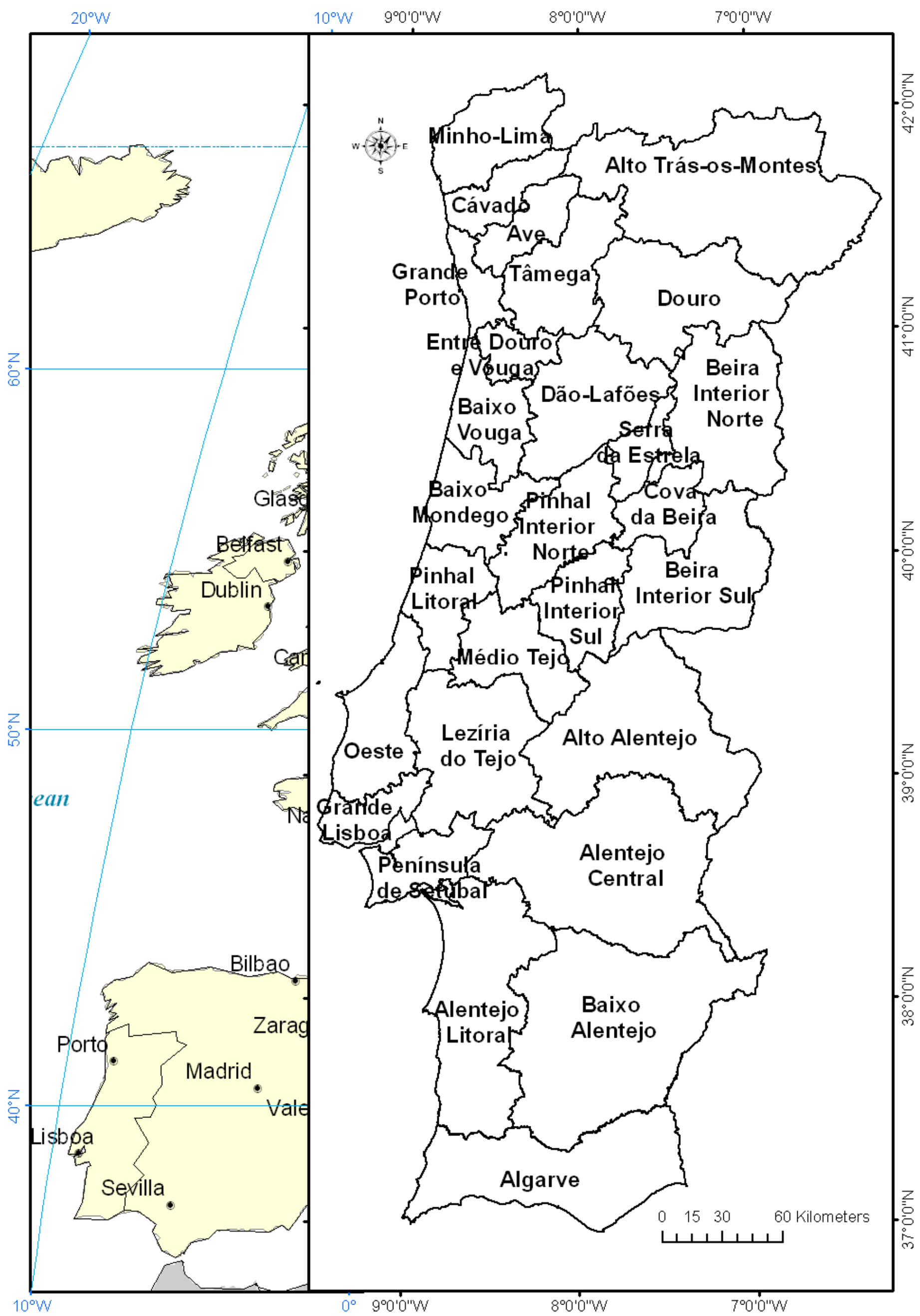

Figure 9.1 - NUT III sub-regions.

9.3.2 Forest biomass calculation

The biomass potentially suitable for energy use is commonly classified into primary residues, secondary residues, tertiary residues and energy crops (BFIN; Easterly and Burnham, 1996; European Commission, 2000; Berndes et al., 2003; Hoogwijk et al., 2003; European Commission, 2005b; WESST, 2008).

Portuguese political strategy to implement the new power plants states that the main source of fuel should come from the residual biomass generated by forest activity.

Because of this policy, only primary residues availability (parts of trees, unsuitable for saw timber such us branches and tops) were used in the calculations. Also industrial byproducts, such us sawdust and woodchips, could constitute an alternative source of fuel; however as they are widely used by plywood and fibreboard industries, this could result in a restriction of biomass supply.

The potential supply of woody biomass resources was achieved through different calculation processes based on pine and eucalyptus stands dendrometric data, of each considered region. In North and Center regions the data was collected by field inventory, within maritime pine and blue-gum eucalyptus stands. For the other regions the data were collected in the NFI 2005/2006 (DGRF, 2007b) and in some previous published studies (ADIV, 2006; UTAD, 2006). Several specific allometric equations for maritime pine (Table 9.1) and for eucalyptus (Table 9.2) were used to calculate residual biomass quantities for all the regions (Eq. 1 - 8) (Arthur D. Little International Inc., 1985; Fabião, 1986; Silva et al., 1991; Barreto, 2005; Lopes, 2005; Tomé, 2007). The total available biomass for the whole country, which can be transformed into energy, is the sum of the estimates for each region.

9.3.3. Spatial distribution of forest biomass and geographical location of power plants

After the wood fuel quantities were calculated, the spatial assessment of forest biomass availability by region was mapped. As the data provided by forest inventories (DGRF, 2007b) did not include the sample plot coordinates, and because no accurate map existed of forest land cover distribution, it was not possible to modulate biomass spatial distribution using real data. Hence, the resultant map expresses the theoretical biomass quantities per year, assuming that they are uniformly distributed all over the region.

As previously presented, this case study analysis was carried out considering the existence of the two actual power plants (Mortágua - M, with 9 MW, and Vila Velha de Ródão - VVR, with 13 MW), and the anticipated location of 13 new power plants (86.4 MW), to the Portuguese electric network (Figure 9.2). The spatial forest biomass availability and the anticipated geographical locations of new power plants were recorded in a GIS database. Spatial and query tools, provided by the GIS, were used to analyse the available wood fuel in each power plant's influence area.

Table 9.1 - Allometric equations used to estimate the residual forest biomass of maritime pine stands.

Source	Allometric Equation (kg tree^{-1})	
(Arthur D. Little International Inc., 1985)	$B = 0.656\ d_{bh}^{2.364}\ h^{-0.977}$	[1]
(Silva et al., 1991)	$B = 0.463\ d_{bh}^{1.604}$	[2]
(Lopes, 2005)	$Log(B_d) = 2.911 + 2.130\ log(d_{bh})$	[3]
(Barreto, 2005)	$y_{ijt} = \beta_{0ij} \times y_{11t}^{\beta_{1ij}}$	[4]
	Leaves:	
	β_{021}=(-30,760406+ 0,58157013 x y_{1110}-2,50380386E-04 x y_{1110}^2 + 3,07544565E-08 x y_{1110}^3) / 10000	
	β_{121} = 2,013	
	Live branches:	
	β_{022} = (-59,521553 + 1,068209 x y_{1110} - 4,5891371E-04 x y_{1110}^2+ 5,62875901E-08 x y_{1110}^3) / 10000	
	β_{122} = 2,013	
	Dead branches	
	β_{023}= (-17,410039 + 0,262031 x y_{1110}- 1,1243324E-04 x y_{1110}^2+ 1,38169184E-08 x y_{1110}^3) / 10000	
	β_{123}= 2,013	

Table 9.2 - Allometric equations used to estimate the residual forest biomass of eucalyptus stands.

Source	Allometric Equation (kg tree^{-1})	
(Arthur D. Little International Inc., 1985)	$B = 8.54 - 1.537\ d_{bh} + 0.163\ d_{bh}^2$ (North and Center) $B = 7.615 + 0.102\ d_{bh}^2$ (South)	[5]
(Silva et al., 1991)	$B = 0.1785\ d_{bh}^{1.756}$	[6]
(Fabião, 1986)	$B_d = Wbr + Wl$ $Ln(Wbr) = -6.989 + 3.157\ ln(d_{bh})$ $Ln(Wl) = -4.902 + 2.524\ ln(d_{bh})$	[7]
(Tomé, 2007)	$B_d = Wbr + Wl$ $Wbr = 0.0956\ d_{bh}^{1.6746} \times h^{-0.8507}$ $Wl = 0,2490\ d_{bh}^{1.2640} \times h^{-0.7121}$	[8]

Where: B - Total weight of biomass (tops and branches); B_d - Total weight of dry Biomass; d_{bh} - Diameter Breast Height; h - Total height of the tree; Wbr - Weight of branches; Wl - Weight of leaves y_{ijt} - Diameter Breast Height at the age *t;* y_{ijt} - Weight of each component of the crown biomass.

9.3.4. Comparison of fully condensing and cogeneration plants scenarios

To analyse the maximum potential of energy production, based on power plant geographical locations and according to their fuel demands, we compared two scenarios: fully condensing plants and cogeneration plants.

The conversion of residual forestry biomass into electrical power, heating power, or both (CHP) is made typically through simple combustion, but alternative processes such as co-firing, in particular coal-fired, or gasification are often used in some EU countries. Conversion process efficiency depends upon the final result products. In stand-alone plants, the efficiency of biomass combustion for electricity production typically varies between 25% and 30% (Breeze, 2004; Faaij, 2006), but if the electrical production is combined with heat production (CHP), the efficiency can rise to 80-100%, in power plants having capacities ranging between 1 and 10 MW (Breeze, 2004; Faaij, 2006). The technical parameters used in this study, adopted from (Fiala et al., 1997; Prasertsan and Krukanont, 2003; Krukanont and Prasertsan, 2004) and (PER, 2009) are presented in Table 9.3.

At this point, it is important to clarify that our results are related to *theoretical biomass potential*; e.g. the annual production of forest residues in a region. However, since the theoretical biomass potential is subject to restrictions (Voivontas et al., 2001), e.g. the efficiency of the residues collection procedure, the amount of biomass that can be technically and economically harvested and is suitable to be used for energy purposes, is defined as *available biomass potential*. In this research, the biomass calculation was made assuming that the *available biomass potential* is only limited by the distance from collection area to the power plant. No other technical, ecological or economical restrictions were considered in this evaluation, which obviously differs from the reality. Thus, two approaches were considered:

- the *theoretical forest biomass potential* of each region, the *maximum theoretical power plant capacity*, optimum thermal boiler load - Q_B (MW_{th}) and the electricity output (E) that can be calculated, e.g. if all the biomass is collected across the region and used into energy production, the possible maximum size of power plant(s) (non considering any restriction of exploitation of fuel) is obtained (Prasertsan and Krukanont, 2003; Krukanont and Prasertsan, 2004) (Eqs. (9) and 10).
- the *available biomass potential*, where the viable fuel collection area for each power plant, is a circular area with a radius of R km, being the power plant located at the

centre. After calculation of R_O (optimum radius), it is possible to obtain the *available power plant capacity,* Q_B (MW_{th}) and respective maximum energy production potential (E).

The optimum radius is calculated as a function of the cost of wood waste and density of wood fuel availability, Ψ (ton ha^{-1} $year^{-1}$), as described in Eqs. 11 and 12, for fully condensing plant and cogeneration plant, respectively (Fiala et al., 1997; Prasertsan and Krukanont, 2003; Krukanont and Prasertsan, 2004).

$$Q_B = \frac{\psi \pi R^2 (LHV) \eta_B}{t} \quad [9]$$

$$E = \frac{\psi \pi R^2 (LHV) \eta_B \eta_{CO}}{t} - Q_D \quad [10]$$

$$R_O = \left(\frac{3(C_{ls} N)}{\psi \pi C_{ts}} \right)^{\frac{1}{3}} \quad [11]$$

$$R_O = \left(\frac{2\alpha}{\beta} \right)^{\frac{1}{3}} \quad [12]$$

Thus, the optimal cost of wood waste at source $(C_{ws})_O$ (maximum affordable fuel cost obtained at the expense of a fixed capacity of the power plant, fixed by a radius R_O), is obtainable by substituting R_O into Eq. 13:

$$(C_{ws})_O = \alpha R_O^{-2} + \beta R_O + \gamma \quad [13]$$

Being:

$$\alpha = \frac{1}{\psi \pi} \left\{ t Q_D p_d - t Q_D \left(f_e p_{ee} + f_e p_{ec} \frac{m}{t} - \frac{I_s [K_m f_a + 1]}{t f_a} \right) - (C_{ls} N) \right\},$$

$$\beta = -\frac{2 C_{ts}}{3}$$

$$\gamma = (LHV) \eta_B \eta_{CO} \left\{ f_e p_{ee} + \frac{m f_e p_{ec}}{t} - \frac{I_s [K_m f_a + 1]}{t f_a} \right\},$$

$$f_a = \frac{(1+i)^n - 1}{i(1+i)^n},$$

where:

f_e is the electricity export factor (% or decimal); *(Cws)o* the optimal unit cost of wood wastes (€ Cent/t); C_{ls} the specific wage per capita of labour cost (€/person/year); C_{ts} the unit cost of transportation (€/t/km); C_{ws} the unit cost of wood wastes (at the site of source) (€ Cent/t); *E* the electricity output (MW_e); *i* the discount rate (%); *Is* the specific cogeneration investment (€/MW_e); K_m the maintenance coefficient (% or decimal); *LHV* the lower heating value of fuel (MJ kg^{-1}); *m* the number of months (month); *n* the economic cogeneration lifetime (year); *N* the number of workers (person); *pd* the price of thermal energy (€ Cent/kWh); *pec* the price of electricity capacity (€ Cent/MW/month); *pee* the price of electricity energy (€ Cent/kWh); Q_B the boiler thermal load (MW_{th}); Q_D the process heat demand (MW_{th}); *R* the radius of biomass supply area (km); R_O the optimal radius of biomass supply area (km); *t* the annual cogeneration operating time (h); η_B the boiler efficiency (%); η_{CO} the cogeneration efficiency (%); Ψ the annual specific wood waste availability (ton ha^{-1} $year^{-1}$).

Table 9.3 - Technical parameters for a wood fired plant.

Parameters			**Unit**
Power plant			
Running time	t	8000	h $year^{-1}$
Process Steam Demand (fully condensing plant)	Q_D	0	MW_{th}
Process Steam Demand (cogeneration plant)	Q_D	27.2	MW_{th}
Overall efficiency (fully condensing plant)	η	25	%
Overall efficiency (cogeneration plant)	η_{CO}	60	%
Boiler efficiency	η_B	80	%
Electrical export factor	*fe*	90	%
Biomass			
Nominal higher heating value	*LHV*	13.8	MJ kg^{-1}
Moisture content (wet basis)	*MCwet*	30	%

The size of a power plant is directly influenced by the biomass availability, Ψ (ton ha^{-1} $year^{-1}$) and the boiler efficiency (η_B) (Eq. 9), which prescribes the biomass demanding area, with a radius of *R* km.

The optimum collection area (with radius *R*) depends on biomass-associated costs. According to (Carinhas, 2006) and (CBE, 2009) biomass-associated costs could be summarized by four major factors: harvesting, transportation, biomass origin (pure and dense stands, burnt areas, shrub areas with scattered trees) and characteristics (e.g. coniferous or hardwood, logs or branches). These factors can also vary according to several variables as:

Machinery: harvester, forwarder, crane, chainsaw; Transportation: tractor and trailer; lorry (2, 4 or 6 wheel drive); Terrain morphology: slope, presence of rocks; Stands types - area, number of trees per hectare, age, species; Operation: tillage, final cut; Man-labour - cutter qualification, driver qualification, operation time; Biomass format: slash, wood and wood parts, chips, bundles, round wood.

This analysis is comprehensively presented by (Carinhas, 2006; Spinelli, 2006; CBE, 2009) in Pinus and Eucalyptus stands, at a local scale. Different methodologies and cost calculation models to calculate the different biomass-associated costs (feeling, bucking, forwarding, transport and chips) can be found in (Leduc et al., 2010) and (Kinoshita et al., 2009).

Given the impossibly of implementing a detailed analysis throughout the entire study area, the achieved optimum radius results from the knowledge of the general exploitation that exists in Portugal. The considered biomass costs were calculated (e.g. Carinhas, 2006; CBE, 2009) for Eucalyptus stands at final harvest (1200 trees per hectare in average (see Lopes, 2005)) using a harvester and a forwarder for cutting and loading and a tractor and trailer for transportation, and Pinus stands at final harvest (600 trees per hectare in average (see Lopes, 2005), using a chainsaw and manual loading and a lorry (two wheel drives) for transportation.

Based in the abovementioned studies (Carinhas, 2006; Spinelli, 2006; CBE, 2009) and on the available knowledge about the existent power plants in Portugal (PER, 2009), the achieved R_0 was approximately 35 km for a 9 MW power plant.

After superimposing within a GIS the projected power plant locations with a land cover map, such as Corine Land Cover (CLC2006) (IGP, 2009), it was possible to realise that the biggest power plants are locate within forested areas. They require a large amount of biomass but they are surrounded by large amounts of biomass. Small power plants are located within less forested areas. They require small amount of biomass but biomass could be far away from the power plant location. Therefore, for the purpose of this study, a radius of 35 km for all the power plants was considered optimum (Figure 9.2). Given the resource competition that will exist, we can assume that, independently of power plant size, the collection area will be the same for all power plants. On the other hand, as the goal of this work is to know the maximum power capacity which should be installed in the best case, we consider the same optimum radius (35 km).

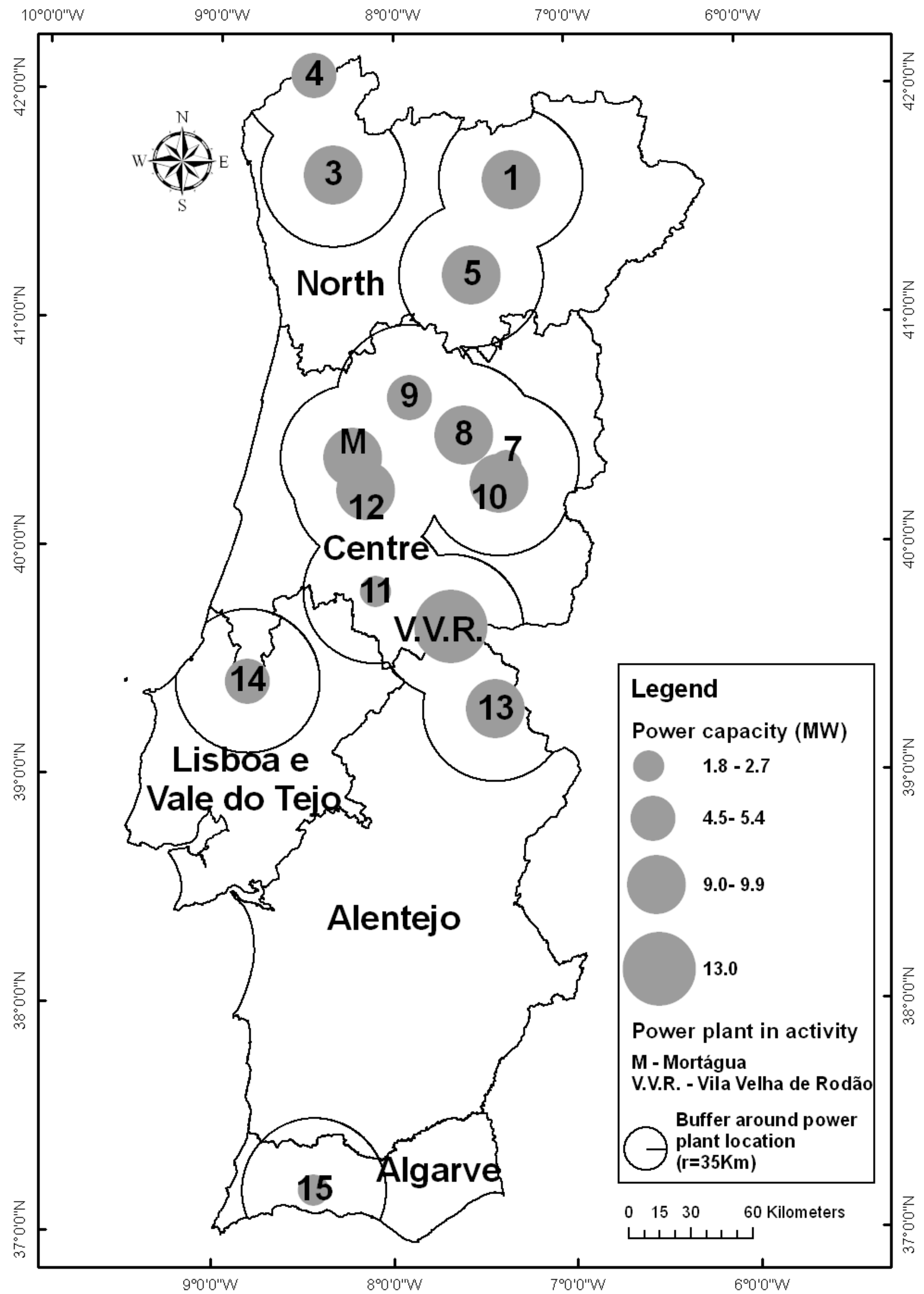

Figure 9.2 - Power plants location with the identification of the NUT II sub-regions boundaries, and the optimum biomass supply area (*R*=35km).

9.4. Results and discussion

The estimated total amount of biomass averages around 1.097 million dry ton year^{-1}, with 579.91 thousand dry ton year^{-1} from maritime pine and 517.23 thousand dry ton year^{-1} from eucalyptus. However, these values range from 874.66 thousand dry ton year^{-1} (473.70 thousand dry ton year^{-1} of pine and 400.96 thousand dry ton year^{-1} of eucalyptus) to 1.41 million dry ton year^{-1} (673.54 thousand dry ton year^{-1} from pine and 737.03 thousand dry ton year^{-1} from eucalyptus). These results are presented in Table 9.4, grouped by NUT II regions (see Figure 9.2).

Table 9.4 - Total amount of theoretical and available residual biomass from maritime pine and eucalyptus, by NUT II sub-region.

NUT II Sub-region	**Area (ha)**	**Forest Area (ha)**	**B_d Total (ton)**	**B_d (ton yr^{-1})**	**B_d (ton ha^{-1})**	**B_d available (tonnes) (R=35Km)**	**B_d available (ton yr^{-1}) (R=35Km)**
Mean values achieved							
North	2128898.8	314400.0	4844028.5	273045.2	27.7	2610138.4	147126.7
Center	2367489.4	668000.0	11313251.0	569601.1	28.2	7693256.4	387341.1
L.V.T.	1170004.6	211100.0	2657602.4	190005.1	32.7	882065.7	63063.2
Alentejo	2727597.4	146100.0	836241.9	55658.5	14.0	116367.3	7745.2
Algarve	499487.9	17400.0	88337.3	8829.1	13.6	38929.7	3890.9
Total	**8893478.1**	**1357000.0**	**19739461.0**	**1097139.0**	**23.2**	**8312368.8**	**609167.1**
Maximum values achieved							
North	2128898.8	314400.0	6016987.5	342774.1	34.5	3242171.3	184699.1
Center	2367489.4	668000.0	13450714.0	723436.6	34.2	9146777.7	491952.6
L.V.T.	1170004.6	211100.0	3238889.0	247294.1	38.7	1074996.4	82077.6
Alentejo	2727597.4	146100.0	1197319.7	85551.2	18.3	166613.1	11904.9
Algarve	499487.9	17400.0	111278.6	11510.5	16.3	49039.8	5072.6
Total	**8893478.1**	**1357000.0**	**24015188.8**	**1410566.5**	**28.4**	**10112895.4**	**775706.8**
Minimum values achieved							
North	2128898.8	314400.0	3935660.0	224821.6	22.8	2120676.5	121142.0
Center	2367489.4	668000.0	9220289.3	461185.8	22.8	6269997.0	313616.4
L.V.T.	1170004.6	211100.0	2182931.3	156861.2	26.8	724521.1	52062.7
Alentejo	2727597.4	146100.0	479470.0	25795.8	9.8	66720.7	3589.6
Algarve	499487.9	17400.0	64777.9	5994.4	10.8	28547.3	2641.7
Total	**8893478.1**	**1357000.0**	**15883128.5**	**874658.7**	**18.6**	**6688451.2**	**493052.4**

When considering only an area of 35 km radius circle around each power plant (installed and planned), the exploitable biomass is considerably less. The estimated total amount of biomass averages 609.17 thousand dry ton year^{-1}, and the maximum and minimum values are 775.71 thousand dry ton year^{-1} and 493.05 thousand dry ton year^{-1}, respectively.

The differences among estimates are due to the use of different biomass allometric equations (Table 9.1 and 9.2). As the growth of trees varies among regions of Portugal with differences in environmental conditions, region-specific equations were required. Furthermore, some equations directly quantify dry biomass and others quantify wet biomass, which then has to be converted by a multiplicative dry factor.

The biomass availability maps, presented in the Figures 9.3 and 9.4, show the spatial distribution of biomass by the NUT III regions. The higher quantities of logging residues generated per year of maritime pine and eucalyptus are located at the Northern and Central regions. In the southern regions (Alentejo and Algarve) the biomass amount is significantly lower. This was expected since, in North and Central Portugal, pinus and eucalyptus species are dominant, while in the south cork oak and holly oak are the most abundant species.

A GIS-based analysis allowed for assessment of both the theoretical maximum and the available potential power installation. In the future, the 15 power plants' (two installed and 13 planed) total power capability will be 108.4 MW (Table 9.5). Our results illustrated that the theoretical maximum power potential (Q_B) of fully condensing power plants is 131.4 MW. However, when calculation is performed using logging residue availability, for the maximum transport distance of 35 km, the real maximum power potential is just 73.0 MW. This means that the power plant capacity to be installed in the country (108.4 MW) is very high even if only logging residues from maritime pine and eucalyptus will be used as fuel source. However, only the region of LVT (see Figure 9.2) could possibly supply the demand (7.6 MW) using only this fuel source.

This problem could be overcome by the use of second-generation power plants that use cogeneration. Results from GIS-based analysis enabled us to estimate a theoretical maximum and a real maximum power potential of 315.4 and 175.1 MW_{th}, respectively. However, even using second-generation power plants the Alentejo and Algarve regions do not produce enough forest biomass and will need other fuel source to supply their biomass needs.

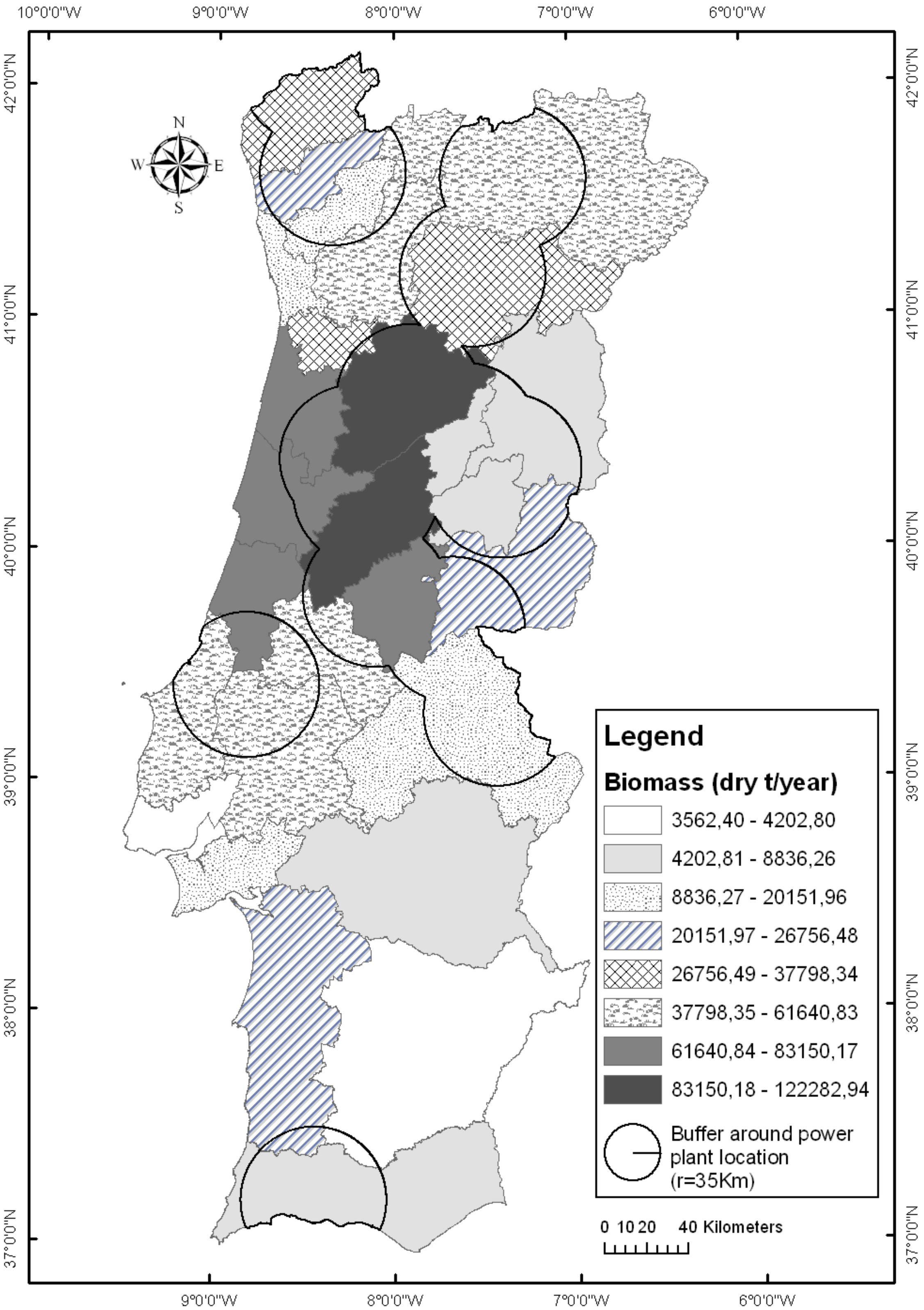

Figure 9.3 - Logging residues availability at regional scale.

The biomass supply area (exploitable radius of 35 Km) is identified.

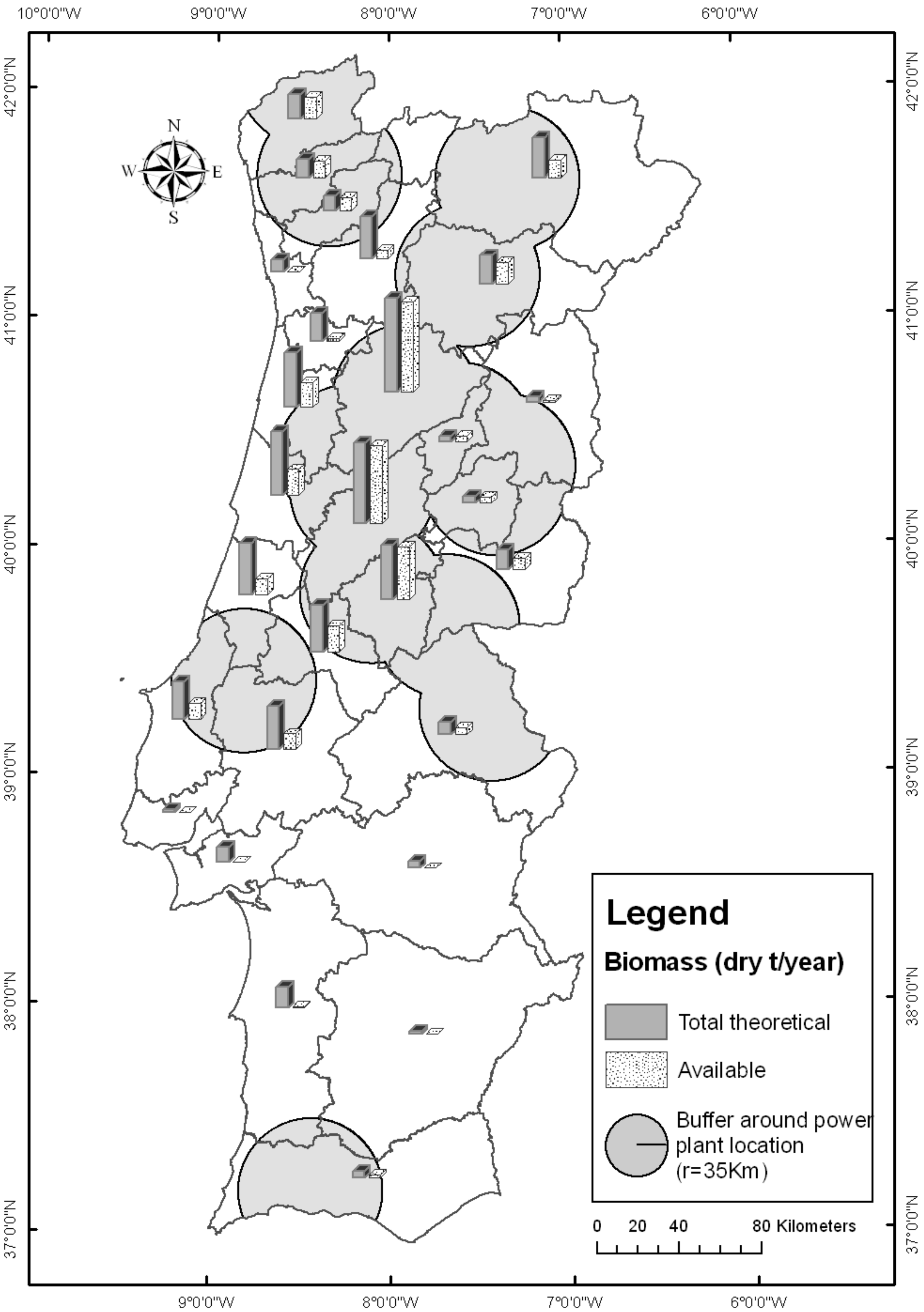

Figure 9.4 - Total theoretical and available (within a radius of 35Km) biomass potential supply.

Table 9.5 - Potential power production of fully condensing plants and cogeneration plants.

Power plant	**Installed Capacity (MW)**	**Theoretical biomass (ton year^{-1})**	**Available biomass (ton year^{-1}) (R=35Km)**	**Fully condensing plant**		**Cogeneration plant**	
				Maximum theoretical potential, Q_B (MW)	**Maximum available potential (R=35Km), Q_B (MW)**	**Maximum theoretical potential, Q_B (MW_{th})**	**Maximum available potential (R=35Km), Q_B (MW_{th})**
1	9.9						
3	9.0						
4	4.5						
5	9.9						
North	33.3	273045.24	147126.69	32.7	17.6	78.5	42.3
7	1.8						
8	9.0						
9	4.5						
10	9.0						
11	2.7						
12	9.0						
M	9.0						
VVR	13.0						
Center	58.0	569601.1	387341.1	68.2	46.4	163.8	111.4
13							
Alentejo	9.0	55658.5	7745.2	6.7	0.9	16.0	2.2
14							
LVT	5.4	190005.1	63063.2	22.8	7.6	54.6	18.1
15							
Algarve	2.7	8829.1	3890.9	1.1	0.5	2.5	1.1
	108.4	**1097139.0**	**609167.1**	**131.4**	**73.0**	**315.4**	**175.1**

9.5. Conclusions

Our results, regarding logging residues availability and future demand of biomass for energy production, enabled identification of the most suitable regions for increasing forest fuel usage.

In this study, biomass available quantities were estimated in respect to the optimum transport allocation areas. However, it is important to take in account that this biomass would not be fully used, as there exist technical limitations (e.g. slope) which limit the collection process. Although this study quantified logging residues existence, the annual biomass availability will depend on forest management, such as tree thinning and pruning, applied to a forest stand during its life cycle. Furthermore, because logging residue supplies depend on harvest activity (e.g. the exploitable residues are different for manual or mechanised harvesting), annual variation in residue amount must also be expected.

The present analysis was made for all power plants as a whole, considering the same collecting area (35 km radius) for all, but removing the overlapping areas. However, as the power plants will have different power capability and different ownership, in practice the biomass needs calculation must be made for each one separately. Furthermore, according to competition rules, the collection area radius will overlap, in particularly in the central region. As a consequence, competition for resources within an area, will affect biomass acquisition costs, leading to enlarged collection area radii. Even considering the best estimates, amounts of biomass will strongly limit the potential energy conversions, as the demand of installed power is very high.

Power plant location was not designed according to local needs of energy or according to local biomass availability, but according to energy transformers' station location, were energy could be injected in Portuguese energy network. Following Leduc et al. (2009) the resolution of an optimization model, addressing constrains (cost for supply of biomass, operation of production plants, investment in plants, and transportation of biomass) would have been essential to generate the optimal locations of power plants.

In this research we did not explore other vegetation biomass sources, which could have a strong contribute to biomass supply. These other sources are: the biomass from stands under grove bush, shrub land and shrubs growing in burnt areas. These types of biofuel are very significant and cannot be discarded, as 1.8 million hectares are shrub land (DGRF, 2007b) and 3.1 million hectares (DGRF, 2007a) are burnt areas (1.5 million hectares from shrub land and 1.6 million hectares from stands), just in the 2001-2006 period, which can generate millions of dry tonnes of biomass each year. A third important biomass source is the agricultural sector, where the residues from vineyard thinning, wine industry, olive groves and fruit trees orchard pruning, olive pulp remaining from olive oil production, etc., can have a considerable exploratory interest.

Portugal has a high biomass potential which can be used in energy production, although it is already used by pulp, plywood and fibreboard industry. The use and probable competition for the same biomass resource requires special concern, to avoid the excess of exploitation, and consequent disequilibrium of ecosystems.

This case study does not end here, as it continues to undergo new surveys and computer calculations, which will be reported in due course.

References

ADIV, 2006. Avaliação da sustentabilidade do recurso florestal para avaliação da viabilidade da instalação de centrais termoeléctricas a biomassa florestal na região Centro. ADIV-IPV, Viseu.

Arthur D. Little International Inc., 1985. Resíduos florestais para produção de energia em Portugal, Tecninvest, SARL ed.

Barreto, L.S., 2005. Pinhais Bravos - Ecologia e Gestão. Departamento de Engenharia Florestal, Instituto Superior de Agronomia, Universidade Técnica de Lisboa, Lisboa, p. 162.

Berndes, G., Hoogwijk, M., van den Broek, R., 2003. The contribution of biomass in the future global energy supply: a review of 17 studies. Biomass and Bioenergy 25, 1-28.

BFIN, Biomass Resources. Bioenergy Feedstock Information Network. Available online at: *http://bioenergy.ornl.gov/*, (Accessed September 2008).

Breeze, P., 2004. The Future of Global Biomass Power Generation. The technology, economics and impact of biomass power generation. Business Insights Ltd, London.

Carinhas, J.C.V., A study on eucalyptus residual biomass exploitation. MPhil thesis, UTAD, Vila Real, Portugal, 2006.

CBE, 2009. Portuguese Centre for Biomass and Energy. Evaluation of associated costs to forest residual biomass economic exploitation. Available online at: *http://www.drapc.min-agricultura.pt/base/geral/files/. avaliacao_custos_aprov_biomassa.pdf*, (Accessed November 2009).

Commission of the European Communities, 1996. Communication from the Commission. Energy for the Future: Renewable Sources of Energy. Green Paper for a Community Strategy. COM(96) 576 final. Brussels, 20 November 1996.

Commission of the European Communities, 2005a. Communication from the Commission. Biomass action plan. COM(2005) 628 final. Brussels.

Commission of the European Communities, 2005b. Communication from the Commission. The support of electricity from renewable energy sources. COM(2005) 627 final. Brussels, 7 December 2005.

Commission of the European Communities, 2008a. Communication from the Commission to the European Parliament, the Council, the European Economic and Social Committee and the Committee of the Regions - 20 20 by 2020 - Europe's climate change opportunity. COM(2008) 30 final. Brussels.

Commission of the European Communities, 2008b. Communication from the Commission to the European Parliament, the Council, the European Economic and Social Committee and the Committee of the Regions - 20 20 by 2020 - Europe's climate change opportunity. COM(2008) 30 final. Brussels, 23 January 2008.

Council of the European Union, 2007. Presidency conclusions of the Brussels European Council 8/9 March 2007. Brussels, 2 May 2007.

DGGE, 2006. Estratégia Nacional para a Energia. A criação de uma rede de Centrais de Biomassa dedicadas, Direcção Geral de Geologia e Energia, Lisboa, p. 19.

DGRF, 2007a. Estatísticas dos incêndios florestais. Totais Nacionais (1980 - 2006). Direcção geral dos Recursos Florestais. Ministério da Agricultura do Desenvolvimento Rural e das Pescas.

DGRF, 2007b. Resultados do Inventário Florestal Nacional 2005/06. Planeamento e Estatística. Direcção Geral dos Recursos Florestais. Ministério da Agricultura do Desenvolvimento Rural e das Pescas, Lisboa.

Easterly, J.L., Burnham, M., 1996. Overview of biomass and waste fuel resources for power production. Biomass and Bioenergy 10, 79-92.

Energia e Alterações Climáticas, 2007. Mais investimento, melhor ambiente. Ministério da Economia e da Inovação. Lisboa, p. 32.

European Commission, 1997. Communication from the Commission. Energy for the Future: Renewable Sources of Energy. White Paper for a Community Strategy and Action Plan: COM(97)599 final. Brussels, Belgium.

European Commission, 2000. BIOMASS: An Energy Resource for the European Union. European Communities, Programme "Energy, Environment and Sustainable Development". Office for Official Publications of the European Communities, Luxembourg. EUR 19424, p. 17.

European Commission, 2001a. Green Paper: Towards a European strategy for the security of energy supply. COM(2000)769 final, Brussels.

European Commission, 2001b. Directive of the European Parliament and the Council on the promotion of electricity produced from renewable energy sources in the internal electricity market, Directive 2001/77/EC, Brussels, Belgium.

European Commission, 2002. Green Paper: Towards a European strategy for the security of energy supply. Technical Document, Brussels, p. 68.

European Commission, 2005a. Commission staff working document. Annex to the Communication from the Commission. Biomass action plan. Impact Assessment. [COM(2005) 628 final].

European Commission, 2005b. BIOMASS - Green energy for Europe. Luxembourg: Office for Official Publications of the European Communities, p. 46.

Faaij, A.P.C., 2006. Bio-energy in Europe: changing technology choices. Energy Policy 34, 322-342.

Fabião, A., Contribuição para o estudo da dinâmica da biomassa e produtividade primária líquida em eucaliptais. Região Litoral do Centro de Portugal. Tese de Doutoramento. Universidade Técnica de Lisboa, Instituto Superior de Agronomia, Lisboa., 1986.

Fiala, M., Pellizzi, G., Riva, G., 1997. A Model for the Optimal Dimensioning of Biomass-fuelled Electric Power Plants. Journal of Agricultural Engineering Research 67, 17-25.

Hoogwijk, M., Faaij, A., van den Broek, R., Berndes, G., Gielen, D., Turkenburg, W., 2003. Exploration of the ranges of the global potential of biomass for energy. Biomass and Bioenergy 25, 119-133.

IGP, 2009. CLC2006 - Cartografia CORINE Land Cover 2006 para Portugal Continental. Available online at: *http://www.igeo.pt/gdr/projectos/clc2006/*, (Accessed November 2009).

Kinoshita, T., Inoue, K., Iwao, K., Kagemoto, H., Yamagata, Y., 2009. A spatial evaluation of forest biomass usage using GIS. Applied Energy 86, 1-8.

Krukanont, P., Prasertsan, S., 2004. Geographical distribution of biomass and potential sites of rubber wood fired power plants in Southern Thailand. Biomass and Bioenergy 26, 47-59.

Leduc, S., Natarajan, K., Dotzauer, E., McCallum, I., Obersteiner, M., 2009. Optimizing biodiesel production in India. Applied Energy 86, Supplement 1, S125-S131.

Leduc, S., Lundgren, J., Franklin, O., Dotzauer, E., 2010. Location of a biomass based methanol production plant: A dynamic problem in northern Sweden. Applied Energy 87, 68-75.

Lopes, D., Estimating Net Primary Production in *Eucalyptus globulus* and *Pinus pinaster* Ecosystems in Portugal, Kingston University, PhD Thesis, England, 2005.

PER, 2009. Central de Biomassa de Mortágua. Portal das Energias Renovávies (PER). Available online at: *http://www.energiasrenovaveis.com/DetalheEstados.asp?ID_conteudo= 22&ID_area=2&ID_sub_area=37*, (Accessed November 2009).

Prasertsan, S., Krukanont, P., 2003. Implications of fuel moisture content and distribution on the fuel purchasing strategy of biomass cogeneration power plants. Biomass and Bioenergy 24, 13-25.

Resolução do Conselho de Ministros n.º 1/2008, Diário da República, 1.ª série - N.º 3 - 4 de Janeiro de 2008.

Resolução do Conselho de Ministros n.º 154/2001 de 27 de Setembro, Programa E4. Eficiência Energética e Energias Endógenas. Ministério Da Economia. Lisboa; 2001.

Resolução do Conselho de Ministros nº 63/2003, Diário da República - I Série-B, Nº 98, 28 de Abril de 2003.

Resolução do Conselho de Ministros nº 169/2005, Diário da República - I Série - B Nº 204 - 24 de Outubro de 2005.

Rivas-Martínez, Díaz, S., Penas, A., 2004. Bioclimatic Map of Europe. Bioclimates. Cartographic Service, University of León, Spain.

Silva, R., Tavares, M., Páscoa, F., 1991. Residual Biomass of Forest Stands. *Pinus pinaster* Ait. and *Eucaliptus globulus* Labill. 10th World Forestry Congress, 5, Food and Agriculture Organization of the United Nations, Paris.

Spinelli, R., A Decision support System for assisting harvesting system choice in eucaliptus spp. fast growing short rotation plantations, College of Life Sciences, University College Dublin, National University of Ireland, PhD, Dublin, 2006, pp. 115.

Tomé, M., 2007. Inventariação de recursos florestais, volume II - Caracterização e monitorização de povoamentos florestais e matos. Publicações GIMREF, TP 2/2007. Universidade Técnica de Lisboa, Instituto Superior de Agronomia, Centro de Estudos Florestais, Lisboa.

UTAD, 2006. Avaliação da sustentabilidade do recurso florestal para avaliação da viabilidade da instalação de centrais termoeléctricas a biomassa florestal na região Norte. UTAD, Vila Real.

Voivontas, D., Assimacopoulos, D., Koukios, E.G., 2001. Aessessment of biomass potential for power production: a GIS based method. Biomass and Bioenergy 20, 101-112.

WESST, 2008. Wood Energy Resources. Module 5. Wood Energy Supply System Training. Available online at: *http://www.wesst.com/*, (Accessed September 2008).

10

Conclusions

The conclusions are stated according to the three questions defined in the beginning of the thesis:

In order to estimate aboveground biomass stocks of maritime pine and eucalyptus, a specific system of nonlinear allometric equation to predict biomass tree components was developed for each species the North-Center region of Portugal. As for shrubland, the set of specific allometric equations developed allow estimating the AGB, with moderate to high accuracy. The comparison with other allometric equations from other author shows important differences in estimates, showing that the generalization of equations developed in other regions is not recommended. Hence, as a reminder, the allometric equations derived in the present study should not be extrapolated to use in extensive forest inventories.

The remote sensing approaches either alone or combined with geostatistical techniques (in particular Regression-kriging) showed the advantages in spatial mapping to predict aboveground biomass. The estimation of biomass amounts with higher accuracies lead to the reduction of the widely recognized uncertainties, inherent in studies evaluating terrestrial resources.

As a contribute to estimate, more accurately, the biomass carbon stocks of maritime pine and eucalyptus species, the elemental chemical analysis of maritime pine and eucalyptus biomass was carried out. The results showed different rates of the carbon fraction, varying in the tree components. These values differ from the carbon fraction of 50%, usually used to quantify carbon uptake and emissions. Hence, the new values found can be used in future works contributing to reduce the uncertainties of carbon gains and loss estimation, in similar forest types. The fuelwood characteristic and combustion properties analysis, of the most common shrubland species, showed that they can store important amounts of carbon. By combining the specific allometric equations developed in this study and mapping approaches it is possible to quantify with good reliability the amounts of biomass carbon and therefore the possible contribution of this vegetation to the greenhouse gas emissions.

The assessment of forest biomass for use as energy shows that Portugal has a high biomass potential which can be used in energy generation. However, the several projects under course, which aim to produce energy in large scale, can lead to overexploitation of forest resources. Therefore, the fuelwood analysis made to the shrubland vegetation show that this biomass can be used as a fuel source, contributing to the implementation of some of the foreseen projects. The field measurements show that shrubland areas contain big amounts of biomass per unit area, and the fuelwood characteristic and biomass combustion show that this biomass has high calorific values. Moreover, measured trace and selected minor elements of ashes resulting from combustion were below national and most European thresholds, suggesting potential of the biomass ashes to be utilized as fertilizer, this requiring a comprehensive environmental monitoring of fly and bottom ashes obtained under a variety of combustion technologies and under a variety of soil types. However, it is important to take into account that some technical limitations (e.g. slope, rocky areas, costs, etc.) will limit the harvesting and transportation process.

Finally, despite the potential of biomass for use as energy there should be an integrated analysis, considering the various industries consuming biomass (e.g. pulp, plywood and fibreboard), in order to avoid future disequilibrium of ecosystems.

11

Future work

This thesis focused in the modelling and mapping of aboveground biomass of two main forest species (maritime pine and eucalyptus) and shrubland vegetation. Future work should apply the developed specific models and the found values, *inter alia*, of carbon fraction of dry matter and heating values per tree component, in conjunction with the mapping techniques studied to produce biomass carbon stocks and energy potential spatial maps. These procedures shall be expedited in a workflow model allowing continuous updating of estimates.

As the biomass growth is usually reported in terms of merchantable volume, another work stream should focus the validation of existing biomass conversion and expansion factors (BCEF), as well the development of specific factors to the region species. A bigger challenge is to study the belowground biomass and develop specific belowground biomass to aboveground biomass ratios, in order to estimate more accurately the belowground biomass of these forest ecosystems.

Another work stream is to consider other species growing in the studied area. Despite having a smaller representation, they play also an important role in carbon cycle and their biomass can be interesting for energy production.

Annexes

Annex A

Viana, H., Dias, S., Marques, C., Cruz, M., Lopes, D., Aranha, J., 2009. Estabelecimento de modelos alométricos para predição da biomassa aérea da *Pinus Pinaster*. Actas do 6º Congresso Florestal Nacional, Ponta Delgada, Açores. 6-9 Outubro, pp. 771-775.

Estabelecimento de Modelos Alométricos para Predição da Biomassa Aérea de *Pinus pinaster*

Helder Viana[1], Sara Dias[1], Carla Marques[1], Marco Cruz[1] Domingos Lopes[2] e José Aranha[2]
[1]Escola Superior Agrária de Viseu. Secção Florestal. Quinta da Alagoa - Ranhados, 3500-606 VISEU
[2]Universidade de Trás-os-Montes e Alto Douro. Departamento de Ciências Florestais e Arquitectura Paisagista. Apartado 1014, 5000-911 VILA REAL

Resumo. O presente trabalho apresenta o estabelecimento de modelos alométricos para predição da biomassa aérea total e das diferentes componentes da espécie *Pinus pinaster*.
A avaliação da biomassa aérea foi feita pelo método destrutivo em povoamentos de pinheiro bravo. Os dados foram recolhidos em 61 árvores, distribuídas por 6 locais na região de Dão Lafões. As medições foram feitas durante 2007 e 2008, em áreas sujeitas a corte final. Foram feitas medições, prévias ao abate e após o abate nas árvores amostra, de vários parâmetros como diâmetro à altura do peito, altura da copa e altura total. A biomassa residual total, de cada árvore, foi recolhida e pesada no local. A biomassa aérea foi separada em componentes (tronco, ramos grossos, ramos finos, folhas e casca), tendo-se retirado uma amostra de cada uma, para posterior análise em laboratório. Foram ajustados vários modelos alométricos não lineares, para a predição da biomassa individual e das suas componentes, individualmente e combinadas. Dos modelos ajustados, seleccionaram-se os que apresentaram melhor qualidade no ajustamento, avaliando os coeficientes de regressão, de determinação (R^2), e de determinação ajustados (R^2_{adj}), bem como os resíduos e a significância do teste de t de Student. Os modelos encontrados apresentam uma boa aptidão de predição da biomassa residual de pinheiro podendo constituir uma ferramenta útil na gestão florestal dos povoamentos desta espécie.
Palavras-chave: *Pinus pinaster*, Biomassa aérea, Modelos alométricos, Região Dão-Lafões

***

Introdução e objectivos

Cada vez mais a gestão dos recursos florestais tem que assentar no conhecimento dos ecossistemas e, particularmente, das existências de biomassa. Os propósitos de quantificar a biomassa florestal são variados, como sejam a utilização dos recursos para a indústria, para a produção energética ou para estudos de fixação de carbono.
As florestas oferecem grande potencial, num prazo relativamente curto, para fixação de CO_2 que removem da atmosfera. Ao contrário de plantas de ciclo de vida curto, que morrem e se decompõem rapidamente, as árvores são indivíduos de ciclo de vida longo que acumulam carbono ao produzirem biomassa (SEDJO *et al.,* 2001). A biomassa é uma valiosa ferramenta na avaliação de ecossistemas, em virtude da sua aplicação na análise da produtividade, conversão de energia, reciclagem de nutrientes, absorção e armazenagem de energia solar, possibilitando conclusões para a exploração racional dos mesmos.
Sendo o pinheiro bravo a espécie mais difundida no país, com 30% dos cerca de 3,240 milhões de hectares ocupados com floresta (DGRF, 2007), é sempre útil dispor de instrumentos que facultem o acesso a informação relativa aos povoamentos florestais. O

trabalho de inventário florestal é sempre uma tarefa dispendiosa, pelo que cada vez mais se procuram modelos que permitam avaliar a floresta de forma expedita. As equações para predição da biomassa aérea do pinheiro bravo são diversas, variando na forma e nas variáveis utilizadas, como as desenvolvidas por: ARTHUR, 1985; SILVA *et al.,* 1985; BARRETO, 1995 ou LOPES, 2005.
Este trabalho procura disponibilizar mais um sistema de equações para estimar a biomassa aérea acima do solo do pinheiro bravo, total e por componentes, ajustadas na região de Dão-Lafões, de forma a poderem ser utilizadas de forma expedita, com parâmetros recolhidos num inventário florestal.

Métodos

Em 6 povoamentos puros de pinheiro bravo, em idade de exploração, com pelo menos 1 ha de área, distribuídos pela região de Dão-Lafões, foram seleccionadas 61 árvores para amostragem destrutiva. Previamente ao abate, foram instaladas parcelas de amostragem circulares com $500m^2$ e avaliados, nas árvores em pé, os seguintes parâmetros dendrométricos: altura total (h); altura da base copa viva (hc); diâmetro a 1,30 m (d); diâmetro da copa (cw), de forma a calcular as variáveis caracterizadoras dos povoamentos: nº de árvores por hectare (N), altura dominante (dom), e área basal (G).
Como critério para selecção das árvores para abate, determinou-se a escolha aleatória no povoamento de pelo menos duas árvores de cada classe de diâmetro e um mínimo total de, pelo menos, 10 árvores por classe. Em todas as árvores foram medidas as seguintes variáveis: altura total (h); altura da base copa viva (hc); altura da bicada (a 7 cm de diâmetro) (hb); diâmetro do cepo (dc); diâmetro a 1,30 m (d) e os diâmetros do tronco de 2 em 2 m, desde do nível de d até à base da bicada e medição da espessura de casca (B) aos vários níveis da medição de d.
Para o âmbito do estudo foram consideradas 5 componentes da biomassa total da árvore: tronco com casca, ramos finos (<3cm de diâmetro na base), ramos grossos (>3cm), bicada e folhas.. Os ramos da copa e a bicada foram separados e pesados integralmente. A bicada cortada (<7cm) e um ramo da copa, recolhido aleatoriamente, em cada andar, foram transportados para laboratório a fim de se separarem e quantificarem por componentes. Ao nível da base do tronco e ao nível da base da bicada foram recolhidas rodelas com a casca, com aproximadamente 2 cm de espessura, para determinação da humidade e da massa volúmica.
Para cada componente foram ajustadas várias equações alométricas, sob a forma não linear, utilizando as variáveis independentes e combinadas, atrás referidas. No caso da bicada os fracos resultados obtidos no ajustamento das equações levaram a incluir esta componente juntamente com os ramos grossos.
Os povoamentos de Pinheiro bravo, onde se instalaram as parcelas, localizam-se nos concelhos de Vila Nova de Paiva, Nelas e Viseu, região Dão-Lafões (Figura 1).

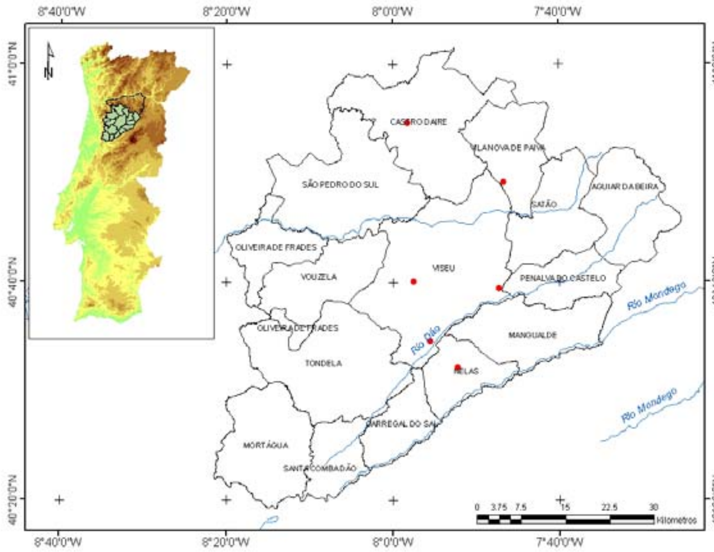

Figura 1 – Localização das parcelas de estudo

Resultados e discussão

Caracterização dos povoamentos

Os povoamentos onde se realizaram os abates, para amostragem destrutiva, apresentavam as seguintes características (Tabela1).

Tabela 1 - Varáveis do povoamento medidas nas parcelas de estudo

LOCAL	t	N (ha)	d (cm)	h(m)	h_{dom}(m)
1	52	700	39,8	21,3	21,5
2	40	800	28,6	19,4	24,7
3	51	600	31,5	19,9	24,1
4	44	600	32,0	19,6	21,8
5	42	600	29,5	18,6	22,4
6	54	600	29,4	19,1	22,8

Caracterização das árvores

Após quantificar as componentes das 61 árvores medidas, obtiveram-se as seguintes proporções médias (Tabela 2).

Tabela 2 - Proporção das componentes da biomassa em relação ao total e em relação à copa da árvore

Componente	Proporção total (%)	Proporção da copa (%)
Agulhas	7,4	43,1
Ramos finos	5,3	30,8
Ramos grossos	3,5	20,1
bicada	1,0	5,9
Tronco	82,8	

Modelos alométricos ajustados

Das funções alométricas ajustadas seleccionaram-se as que permitiram obter as melhores estimativas, cujos parâmetros, R^2_{aj} e EQM são apresentados na tabela 3.

Tabela 3 - Equações ajustadas para a biomassa aérea, estimativa dos parâmetros e coeficientes de determinação ajustados

Componente	Biomassa ($t.ha^{-1}$)	Estimativa dos parâmetros		R^2aj	EQM $t.ha^{-1}$
Copa toda	lnW=α+βd+θ(d.hc)+ δ (d^2h.hc)	α =	1,9967	0,85	0,27
		β =	0,0607		
		θ =	0,0074		
		δ =	-0.00000536		
Agulhas	lnW = α + β bln d	α =	-2,6558	0,72	0,36
		β =	1,9250		
Ramos finos	lnW = α + β bln d	α =	-3,8422	0,76	0,36
		β =	2,1637		
Ramos grossos	lnW = α + β bln d	α =	-4,9524	0,73	0,44
		β =	2,4264		
Tronco	lnW = α + βlnd+θ(hlnd)+ δlnh	α =	-3,8549	0,98	0,10
		β =	2,1770		
		θ =	-0,0059		
		δ =	1,0677		

Nota: diâmetro (d) em centímetros e alturas (h, hc) em metros

Para a obtenção de estimativas da biomassa residual total (biomassa da copa), a equação que apresentou melhor qualidade de ajustamento ($R^2aj = 0,85$) foi a equação de regressão linear múltipla Estas equações são de grande utilidade porque, na maioria dos casos, o interesse prende-se com a estimativa da biomassa total residual dos povoamentos.

Para as componentes individuais da copa (agulhas, ramos finos e ramos grossos) a equação sob a forma de potência (logaritmizada) foi a que apresentou uma melhor qualidade de ajustamento, nas várias relações de variáveis independentes testadas (Tabela 3). A equação para a estimativa da biomassa individual do tronco foi a que apresentou melhor qualidade de ajustamento.

A Biomassa total aérea é dada pela soma das várias componentes individuais:

$$W(t.ha^{-1}) = W_{Agulhas} + W_{Ramosfinos} + W_{Ramosgrossos} + W_{Tronco}$$

Ou

$$W(t.ha^{-1}) = W_{Copa\ total} + W_{Tronco}$$

Conclusão

Os resultados obtidos mostram que os modelos alométricos permitem obter estimativas razoáveis das várias componentes da biomassa dos povoamentos de pinheiro bravo.
Apesar de se terem testado modelos mais complexos, são os modelos mais simples que resultam nos melhores ajustamentos das componentes da biomassa. Os melhores resultados são obtidos incorporando como variável independente o diâmetro à altura do peito (d), a altura (h), a altura de copa (hc) e combinações destas.
A equação ajustada para estimar a biomassa residual (copa total) apresenta uma boa qualidade, sendo aquela que talvez tenha um maior interesse de aplicação prática em estudo de estimação de recursos.
Este trabalho permitiu obter equações de grande utilidade na gestão de povoamentos de pinheiro bravo, uma vez que permitem estimar não só o peso da biomassa gerada sob a forma de troncos, como estimar o peso da biomassa residual (copa total e componentes individuais), recorrendo a parâmetros dendrométricos fáceis de medir, como sejam o diâmetro (d) e a altura (h).

Bibliografia

ARTHUR, D., Little International Inc., 1985. Resíduos florestais para produção de energia em Portugal. Ed. Tecninvest, SARL.

BARRETO, L.S., 1995. Pinhais Bravos. Ecologia e Gestão. Departamento de Engenharia Florestal, Universidade Técnica de Lisboa, Instituto Superior de Agronomia. Lisboa.

DGRF, 2007. Resultados do Inventário Florestal Nacional 2005/06. Planeamento e Estatística. Direcção Geral dos Recursos Florestais. Ministério da Agricultura do Desenvolvimento Rural e das Pescas. Lisboa.

FABIÃO, A.M.D., 1986. Contribuição para o estudo da dinâmica da biomassa e produtividade primária líquida em eucaliptais. Tese de Doutoramento. Universidade Técnica de Lisboa, Instituto Superior de Agronomia, Lisboa, Portugal.

LOPES, DOMINGOS, 2005. Estimating Net Primary Prodution in *Eucalyptus globulus* and *Pinus pinaster* Ecosystems in Portugal. PhD Thesis, Kingston University, England.

PEREIRA, J.S., 2007. *Uma espécie altamente produtiva. In: Pinhais e Eucaliptais- A Floresta Cultivada.* Lisboa. Fundação Luso-Americana. pp167-181.

SEDJO, R., SOHNGEN, B., MENDELSOHN, R., 2001. *Estimating Carbon Supply Curves for Global Forests and Other Land Uses.* Washingt Resources for the Future. 34 p.

SILVA, R., TAVARES, M., PÁSCOA, F., Residual Biomass of Forest Stands., 1991. *Pinus pinaster* Ait. *and Eucaliptus globulus* Labill. Actas nº 5, 10º Congresso Florestal Mundial, Paris.

TOMÉ, M., Inventariação de recursos florestais, 2007. volume II - Caracterização e monitorização de povoamentos florestais e matos. Publicações GIMREF, TP 2/2007. Universidade Técnica de Lisboa, Instituto Superior de Agronomia, Centro de Estudos Florestais, Lisboa.

Annex B

Viana, H., Cohen, W.B., Lopes, D., Aranha, J., 2010. Assessment of forest biomass for use as energy. GIS-based analysis of geographical availability and locations of wood-fired power plants in Portugal. Applied Energy 87, 2551-2560.

[Annexe B.1]

Viana, H., Aranha, J., Lopes, D., 2011. Dedicated Biomass Plants for Combined Heat & Power (CHP). The Portuguese National Strategy. 19th European Biomass Conference and Exhibition, ETA-Florence Renewable Energies, Berlin, Germany. June 6-10.

[Annexe B.2]

Annex B.1

Viana, H., Cohen, W.B., Lopes, D., Aranha, J., 2010. Assessment of forest biomass for use as energy. GIS-based analysis of geographical availability and locations of wood-fired power plants in Portugal. Applied Energy 87, 2551-2560.

Applied Energy 87 (2010) 2551–2560

Contents lists available at ScienceDirect

Applied Energy

journal homepage: www.elsevier.com/locate/apenergy

Assessment of forest biomass for use as energy. GIS-based analysis of geographical availability and locations of wood-fired power plants in Portugal

H. Viana [a,*], Warren B. Cohen [b], D. Lopes [c], J. Aranha [c]

[a] Forestry Sciences, Agrarian Superior School, Polytechnic Institute of Viseu, Quinta da Alagoa, Estrada de Nelas, 3500-606 Viseu, Portugal
[b] USDA Forest Service, 3200 SW Jefferson Way, Corvallis, OR 97331, USA
[c] Forestry Department, University of Trás-os-Montes e Alto Douro, 5000-911 Vila Real, Portugal

ARTICLE INFO

Article history:
Received 20 April 2009
Received in revised form 5 February 2010
Accepted 5 February 2010
Available online 1 March 2010

Keywords:
Bioenergy
Biomass
Wood fuel
Logging residues
Mapping
Combined heat and power plant
Power generation

ABSTRACT

Following the European Union strategy concerning renewable energy (RE), Portugal established in their national policy programmes that the production of electrical energy from RE should reach 45% of the total supply by 2010. Since Portugal has large forest biomass resources, a significant part of this energy will be obtained from this source. In addition to the two existing electric power plants, with 22 MW of power capacity, 13 new power plants having a total of 86.4 MW capacity are in construction. Together these could generate a combination of electrical and thermal energy, known as combined heat and power (CHP) production. As these power plants will significantly increase the exploitation of forests resources, this article evaluates the potential quantities of available forest biomass residue for that purpose. In addition to examining the feasibility of producing both types of energy, we also examine the potential for producing only electric energy. Results show that if only electricity is generated some regions will need to have alternative fuel sources to fulfil the demand. However, if cogeneration is implemented the wood fuel resource will be sufficient to fulfill the required capacity demand.

1. Introduction

There is an emerging consensus on the need to reverse the trend of global warming associated with climate change. The main goal is to quickly reduce emissions of greenhouse gases.

The European Union (EU) is resolved to reduce member country greenhouse gas emissions (GGE) and is promoting the development of new energy policies as one important means to that end. These policies should lead both to the development of new and more secure energy sources and contribute to a reduction in the growing dependency of EU member states on imported fossil fuels.

1.1. Renewable energy strategy and policy

To implement its renewable energy (RE) strategy, in March 2007 [1] the EU formally committed to the "20–20–20" initiative, which set as target and objectives for 2020 [2,3]. These include (i) reducing greenhouse gas emissions by at least 20% of 1990 levels (30% if other developed countries commit to comparable cuts), (ii) increasing the share of RE (wind, solar, biomass, etc.) consumption to 20% compared to 8.5% today, and (iii) cutting energy consumption by 20% of projected 2020 levels by improving energy efficiency.

Renewable energy has gained greater importance over the years, and is today considered the solution to the energy future in Europe. Since 1990, the EU has been engaged in an ambitious and successful plan to become a world leader in RE production and use. The strategic energy plans and policies of the EU, as well as those individual member states, established concrete targets for exploitation of indigenous renewable energy sources (RES), and for bioenergy in particular. As a first step towards a strategy for RE the Commission adopted a Green Paper on 20 November 1996 [4]. The most ambitious strategic goals were defined in 1997 in a European Commission White Paper [5], where the EU set the target to increase the share of renewable up to 12% by 2010. The White Paper also contains a comprehensive Strategy and Action Plan setting out the means to reach this objective.

After the order Green Paper (2000) on security of energy supply [6], diverse and concrete proposals were made. One of these proposals, directive 2001/77/EC [7] on electricity production from renewable sources, was adopted in 2001. Under this directive 22% of the electricity consumed in the EU by 2010 should be produced from renewable energy sources.

According to the national targets for future consumption of electricity produced from renewable energy sources, defined for each member state, Portugal committed to 39% (including large hydro). These goals were also stated in the National E4 Programme (Energy Efficiency and Endogenous Energies) launched in 2001 [8], and subsequently in the National Strategy for the energy launched

* Corresponding author. Tel.: +351 232 446 600; fax: +351 232 426 536.
E-mail address: hviana@esav.ipv.pt (H. Viana).

0306-2619/$ - see front matter © 2010 Elsevier Ltd. All rights reserved.
doi:10.1016/j.apenergy.2010.02.007

in 2003 [9] and 2005 [10]. In 2007 Portugal established a more ambitious strategic target in its National Strategy of Sustainable Development [11]. This new National Strategy for the energy establishes that 45% of the national energy consumption in 2010 should be exclusively produced from renewable energy sources. In this way Portugal intends to set an example in the fulfilment of the EU objectives to reduce emissions of greenhouse gases.

1.2. Biomass energy policy

Amongst renewable resources, paramount importance has been given to the bioenergy because it has low negative environmental impact in terms of CO_2 emissions for the entire fuel cycle and zero CO_2 emissions from fossil fuels during operation.

The European Commission White Paper [10] recognized bioenergy as the most promising areas within the biomass sector for several reasons. First, because it would increase the amount of people working in the forestry sector. Second, because the combined use of heat and power (CHP) has the greatest potential per unit volume among all renewable energy sources. They also issued the opinion that the contribution of biomass-derived energy to the primary energy mix should reach 10% by 2010. The European Commission's Green report (2000) [12], also recognized that biomass is a versatile energy resource, with a widespread availability through forest and agricultural residues that has so far not been fully exploited. Consistent with the Green report [13], emphasis is given to the electricity generation from biomass energy plants, and some successfully examples of implementation in some member states are presented.

The strongest incentive of the EU towards development of biomass energy was given in 2005 with the Biomass Action Plan [14]. In this plan, the EU stated that the increased use of renewable energy is essential for environmental and competitiveness reasons, and recognized that "biomass has many advantages over conventional energy sources, as well as over some other renewable energies, in particular, relatively low costs, less dependence on short-term weather changes, promotion of regional economic structures and provision of alternative sources of income for farmers" [14]. This action plan established several measures to promote biomass in heating, electricity and transport, followed by crosscutting measures affecting biomass supply, financing and research [14,15].

According to this EU strategy, the goal of reaching 45% of national energy consumption in 2010 from renewable energy sources will be achieved in part from biomass energy production. Hence, the Portuguese government decided to extend the current installed power (two electric power plants, with 22 MW of power) to 250 MW by 2010 [11]. Therefore, in 2006, fifteen new power plant (90 MW) exploration licenses were made available to achieve this aim. However, because only 13 licenses were applied for, presently new power plants will only provide 86.4 MW of additional power. These new power plants will be capable of generating both electrical and thermal energy, or CHP.

The new power plants locations were defined by the Portuguese government with the double objective of increasing the quota of renewable energy in the global production of electricity and to promote the development of forest residues harvesting. This will also serve to remove shrub competition in forest groves and reduce wildfire hazard [16].

These power plants will have variable power generation capabilities and combine different technologies, as appropriate to local circumstances. Two power plant models are planed: small units, with power production ranging from 1.8 to 4.5 MW, and large ones with power production ranging from 9 to 9.9 MW. Considering that wood-fuel demand will increase significantly and will be variable across regions, it will be necessary to apply rational resource exploitation actions associated with regional and local needs. For example, there may be significant competition in some areas due to the presence of pulp mills or other biomass consuming industries. In these cases special solutions and compromises will be needed, or it may not be feasible to construct a power plant in such a location. As stated in the 2005 EU's report '*The support of electricity from renewable energy sources*' [17] the future development of RES projects in a specific area must taken into account spatial aspects of planning. This is especially fundamental for projects in the field of wind and biomass.

In this context the objectives of this paper are to: (1) assess Portugal's current forest biomass resource potential for commercial generation of electricity at regional and national levels, (2) assess the spatial distribution of biomass availability, and (3) evaluate the suitability of existing and proposed wood-fired power plant locations in Portugal.

2. Study area

Portugal is located between the latitudes of 36° 57′ 23″ and 42° 09′ 15″N and the longitudes of 09° 30′ 40″ and 06° 10′ 45″ W. This area includes two distinctive bioclimatic regions: a Mediterranean bioclimate in everywhere except a small area in the North with a temperate bioclimate [18]. With four distinct weather seasons, the average annual temperatures range from about 7 °C in the highlands of the interior north and center and about 18 °C in the south coast. Average annual precipitation is more than 3000 mm in the north and <600 mm in the south.

With complex topography and elevations ranging from the sea level to 2000 m, and a small amount of suitable soils for agriculture, Portuguese land is well-suited for forest growth. Forest activity is a direct source of income for a vast forest products industry, which employs a significant part of the population.

3. Methodology

The framework of this study followed four main steps. The first step consisted of forest cover classification and mapping, within Portugal. In a second step, we estimated the available forest biomass and annual growth at national and regional levels. In the third step, the geographical location of existing power plants was evaluated, and a GIS-based analysis was applied to examine the relationship between existing biomass and the power plants wood-fuel demand. Finally, based on the available quantities of biomass and growth we compared the maximum theoretical potential of energy production for two scenarios (fully condensing plants and cogeneration plants).

3.1. Forest land cover of study area

To calculate woody biomass, it was necessary to identify and classify forest cover, as well as to characterize forest stand structure. In Portugal, forests cover approximately 3.4 million hectares [19] and represents 38% of the national territory.

The main trees species, which are widely planted for commercial purposes and capable of providing a regular supply to meet fuel demand, are *Pinus pinaster* (maritime pine) and *Eucalyptus globulus* (eucalyptus). Thus, only these stands (710.300 hectares of maritime pine and 646.700 hectares of eucalyptus, according to the National Forestry Inventory [19]) were considered in the calculations of potential biomass.

The spatial distribution of forested land cover was made at regional level, using a so-called NUT III sub-regions (Nomenclature of Territorial Units for Statistics) boundaries (Fig. 1). The pine and eucalyptus stands occur mainly in the north and center of Por-

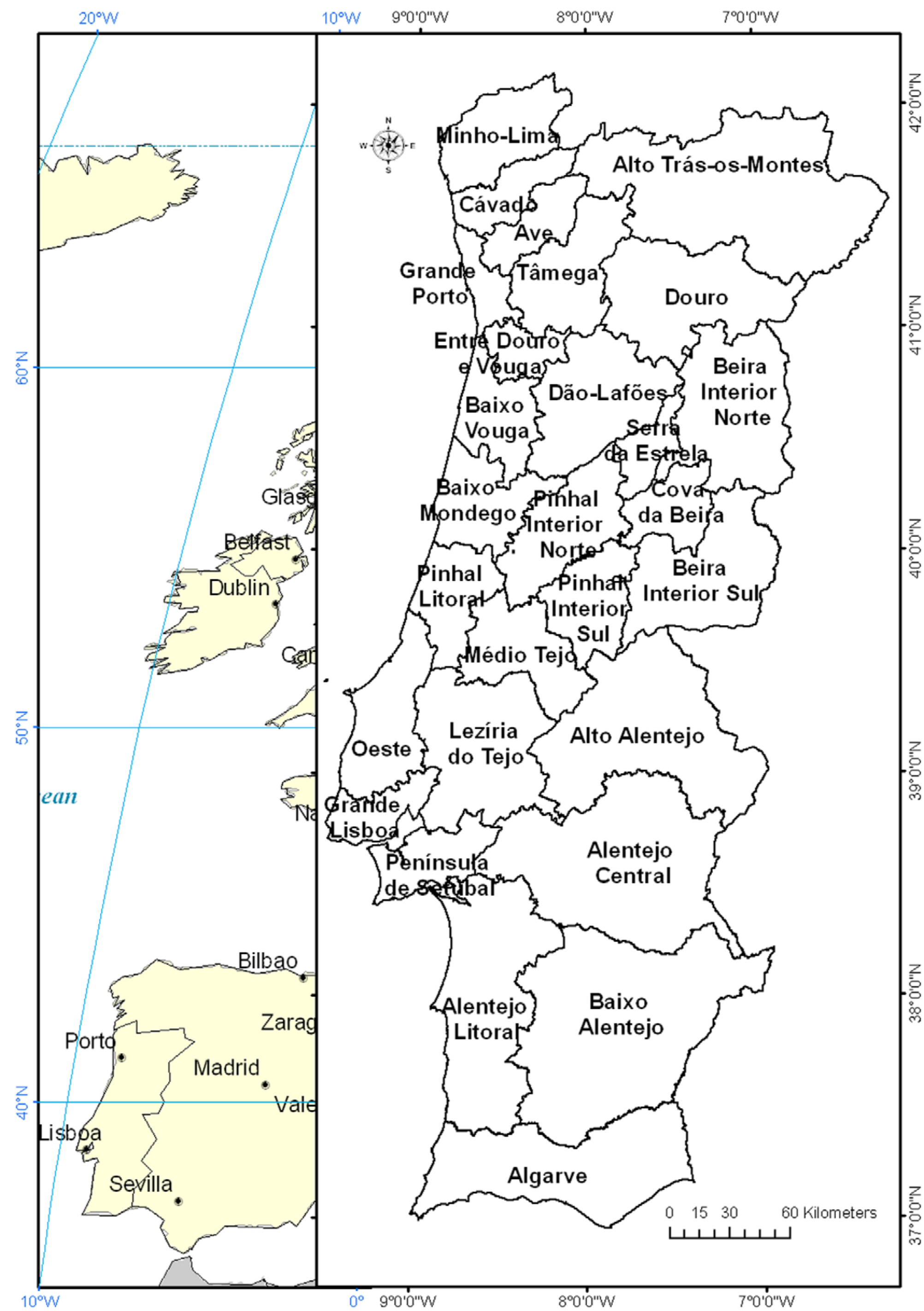

Fig. 1. NUT III sub-regions.

tugal as ecological conditions limit their growth in the south part of Portugal.

3.2. Forest biomass calculation

The biomass potentially suitable for energy use is commonly classified into primary residues, secondary residues, tertiary residues and energy crops [20–26].

Portuguese political strategy to implement the new power plants states that the main source of fuel should come from the residual biomass generated by forest activity. Because of this policy, only primary residues availability (parts of trees, unsuitable for saw timber such us branches and tops [20–26]) were used in the calculations. Also industrial byproducts, such us sawdust and woodchips, could constitute an alternative source of fuel; however, as they are widely used by plywood and fibreboard industries, this could result in a restriction of biomass supply.

The potential supply of woody biomass resources was achieved through different calculation processes based on pine and eucalyptus stands dendrometric data, of each considered region. In North and Center regions the data was collected by field inventory, within maritime pine and blue-gum eucalyptus stands. For the other re-

Table 1
Allometric equations used in the evaluation of the residual forest biomass of maritime pine.

Source	Allometric equation (kg/tree)	
[29]		
	$B = 0.656\ \mathrm{dbh}^{2.364}\ \mathrm{h}^{-0.977}$	(1)
[30]		
	$B = 0.463\ \mathrm{dbh}^{1.604}$	(2)
[31]		
	$\mathrm{Log}(B_d) = 2.911 + 2.130\log(\mathrm{dbh})$	(3)
[32]		
	$y_{\mathrm{ijt}} = \beta_{0\mathrm{ij}\times y11t}^{\beta_{1\mathrm{ij}}}$	(4)
	Leaves: $\beta_{021} = (-30.760406 + 0.58157013 \times y_{1110} - 2.50380386\mathrm{E}{-}04 \times y_{1110}^2 + 3.07544565\mathrm{E}{-}08 \times y_{1110}^3)/10{,}000$ $\beta_{121} = 2.013$ Live branches: $\beta_{022} = (-59.521553 + 1.068209 \times y_{1110} - 4.5891371\mathrm{E}{-}04 \times y_{1110}^2 + 5.62875901\mathrm{E}{-}08 \times y_{1110}^3)/10{,}000$ $\beta_{122} = 2.013$ Dead branches: $\beta_{023} = (-17.410039 + 0.262031 \times y_{1110} - 1.1243324\mathrm{E}{-}04 \times y_{1110}^2 + 1.38169184\mathrm{E}{-}08 \times y_{1110}^3)/10{,}000$ $\beta_{123} = 2.013$	

Table 2
Allometric equations used in the evaluation of the residual forest biomass of blue-gum eucalyptus.

Source	Allometric equation (kg/tree)	
[29]		
	$B = 8.54 - 1.537\ \mathrm{dbh} + 0.163\ \mathrm{dbh}^2$ (North and Center) $B = 7.615 + 0.102\ \mathrm{dbh}^2$ (South)	(5)
[30]		
	$B = 0.1785\ \mathrm{dbh}^{1.756}$	(6)
[33]		
	$B_d = \mathrm{Wbr} + \mathrm{Wl}$ $\mathrm{Ln}\ (\mathrm{Wbr}) = -6.989 + 3.157\ln(\mathrm{dbh})$ $\mathrm{Ln}\ (\mathrm{Wl}) = -4.902 + 2.524\ln(\mathrm{dbh})$	(7)
[34]		
	$B_d = \mathrm{Wbr} + \mathrm{Wl}$ $\mathrm{Wbr} = 0.0956\ \mathrm{dbh}^{1.6746} \times \mathrm{h}^{-0.8507}$ $\mathrm{Wl} = 0.2490\ \mathrm{dbh}^{1.2640} \times \mathrm{h}^{-0.7121}$	(8)

Where B is the total weight of biomass (tops and branches), B_d the total weight of dry biomass, dbh the diameter breast height, h the total height of the tree, Wbr the weight of branches, Wl the weight of leaves, y_{ijt} the diameter breast height at the age t, and y_{ijt} is the weight of each component of the crown biomass.

gions the data were collected in the NFI 2005/2006 [19] and in some previous published studies [27,28]. Several specific allometric equations for maritime pine (Table 1) and for eucalyptus (Table 2) were used to calculate residual biomass quantities for all the regions (Eqs. (1)–(8)) [29–34]. The total available biomass for the whole country, which can be transformed into energy, is the sum of the estimates for each region.

3.3. Spatial distribution of forest biomass and geographical location of power plants

After the wood fuel quantities were calculated, the spatial assessment of forest biomass availability by region was mapped. As the data provided by forest inventories [19] did not include the sample plot coordinates, and because no accurate map existed of forest land cover distribution, it was not possible to modulate biomass spatial distribution using real data. Hence, the resultant map expresses the theoretical biomass quantities per year, assuming that they are uniformly distributed all over the region.

As previously presented, this case study analysis was carried out considering the existence of the two actual power plants (Mortágua – M, with 9 MW, and Vila Velha de Ródão – VVR, with 13 MW), and the anticipated location of 13 new power plants (86.4 MW), to the Portuguese electric network (Fig. 2). The spatial forest biomass availability and the anticipated geographical locations of new power plants were recorded in a GIS database. Spatial and query tools, provided by the GIS, were used to analyse the available wood fuel in each power plant's influence area.

3.4. Comparison of fully condensing and cogeneration plants scenarios

To analyse the maximum potential of energy production, based on power plant geographical locations and according to their fuel demands, we compared two scenarios: fully condensing plants and cogeneration plants.

The conversion of residual forestry biomass into electrical power, heating power, or both (CHP) is made typically through simple combustion, but alternative processes such as co-firing, in particular coal-fired, or gasification are often used in some EU countries. Conversion process efficiency depends upon the resultant final products. In stand alone plants, the efficiency of biomass combustion for electricity production typically varies between 25% and 30% [35,36], but if the electrical production is combined with heat production (CHP), the efficiency can rise to 80–100%, in power plants having capacities ranging between 1 and 10 MW [35,36]. The technical parameters used in this study, adopted from [37–40] are presented in Table 3.

At this point, it is important to clarify that our results are related to *theoretical biomass potential*; e.g. the annual production of forest residues in a region. However, since the theoretical biomass potential is subject to restrictions [41], e.g. the efficiency of the residues collection procedure, the amount of biomass that can be technically and economically harvested and is suitable to be used for energy purposes, is defined as *available biomass potential*. In this research, the biomass calculation was made assuming that the *available biomass potential* is only limited by the distance from collection area to the power plant. No other technical, ecological or economical restrictions were considered in this evaluation, which obviously differs from the reality. Thus, two approaches were considered:

- the *theoretical forest biomass potential* of each region, the *maximum theoretical power plant capacity*, optimum thermal boiler load – Q_B ($\mathrm{MW_{th}}$) and the electricity output (E) that can be calculated, e.g. if all the biomass is collected across the region and used into energy production, the possible maximum size of power plant(s) (non considering any restriction of exploitation of fuel) is obtained [37,38] (Eqs. (9) and (10)).
- the *available biomass potential*, where the viable fuel collection area for each power plant, is a circular area with a radius of R km, being the power plant located at the center. After calculation of R_O (optimum radius), is possible to obtain the *available power plant capacity*, Q_B ($\mathrm{MW_{th}}$) and respective maximum energy production potential (E).

The optimum radius is calculated as a function of the cost of wood waste and density of wood fuel availability, Ψ (t/h/year), as described in Eqs. (11) and (12), for fully condensing plant and cogeneration plant, respectively [37–39].

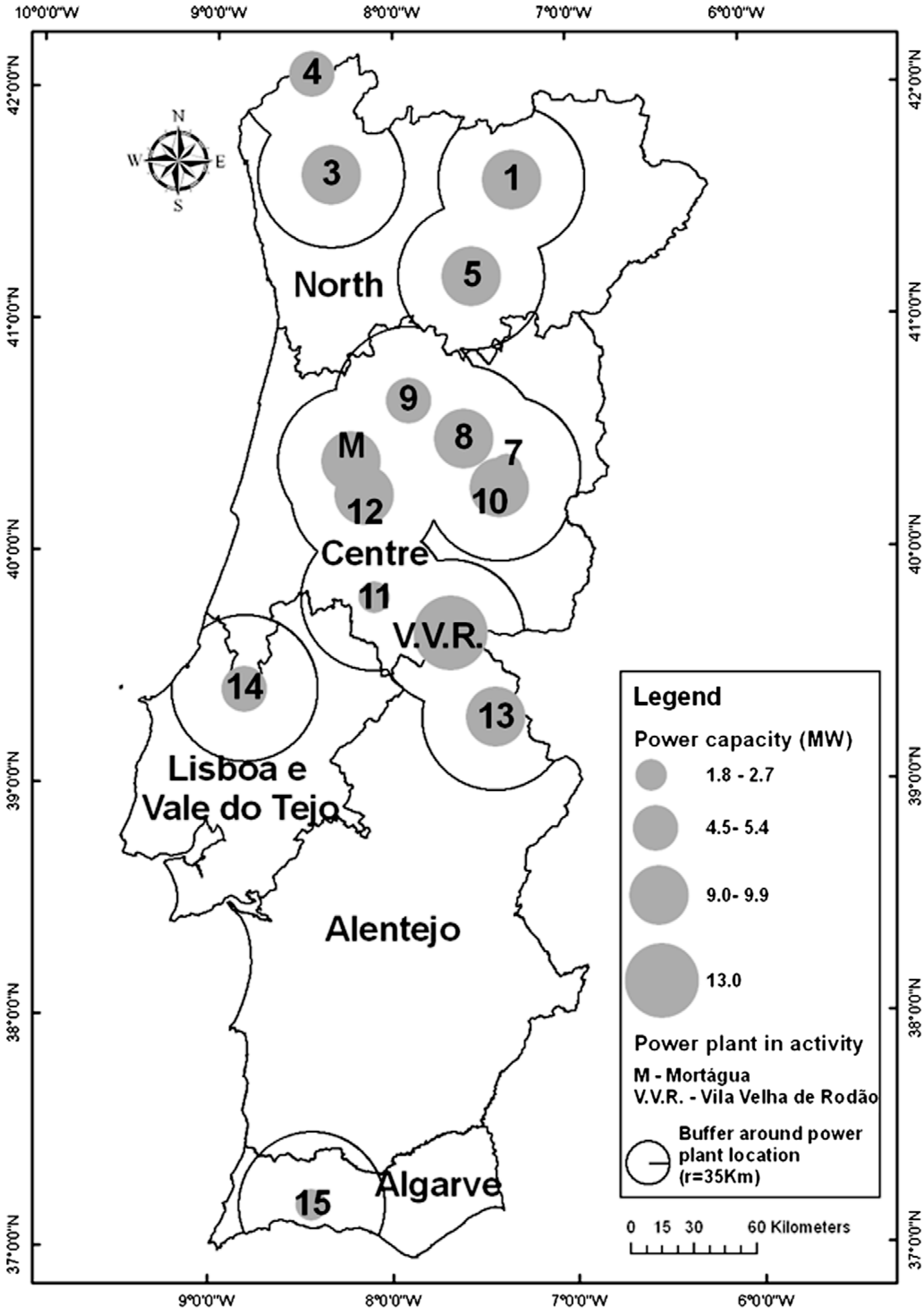

Fig. 2. Power plants location with the identification of the NUT II sub-regions boundaries, and the optimum biomass supply area (R = 35 km).

$$Q_B = \frac{\psi \pi R^2 (LHV)\eta_B}{t} \tag{9}$$

$$E = \frac{\psi \pi R^2 (LHV)\eta_B \eta_{CO}}{t} - Q_D \tag{10}$$

$$R_O = \left(\frac{3(C_{ls}N)}{\psi \pi C_{ts}}\right)^{\frac{1}{3}} \tag{11}$$

$$R_O = \left(\frac{2\alpha}{\beta}\right)^{\frac{1}{3}} \tag{12}$$

Thus, the optimal cost of wood waste at source $(C_{ws})_O$ (maximum affordable fuel cost obtained at the expense of a fixed capacity of the power plant, fixed by a radius R_O), is obtainable by substituting R_O into:

$$(C_{ws})_O = \alpha R_O^{-2} + \beta R_O + \gamma \tag{13}$$

Being:

$$\alpha = \frac{1}{\psi \pi}\left\{tQ_D p_d - tQ_D\left(f_e p_{ee} + f_e p_{ec}\frac{m}{t} - \frac{I_s[K_m f_a + 1]}{tf_a}\right) - (C_{ls}N)\right\},$$

$$\beta = -\frac{2C_{ts}}{3},$$

$$\gamma = (LHV)\eta_B \eta_{CO}\left\{f_e p_{ee} + \frac{mf_e p_{ec}}{t} - \frac{I_s[K_m f_a + 1]}{tf_a}\right\},$$

$$f_a = \frac{(1+i)^n - 1}{i(1+i)^n},$$

Table 3
Technical parameters for a wood fired plant.

Parameters			Unit
Power plant			
Running time	t	8000	h/year
Process steam demand (fully condensing plant)	Q_D	0	MW_{th}
Process steam demand (cogeneration plant)	Q_D	27.2	MW_{th}
Overall efficiency (fully condensing plant)	η	25	%
Overall efficiency (cogeneration plant)	η_{CO}	60	%
Boiler efficiency	η_B	80	%
Electrical export factor	fe	90	%
Biomass			
Nominal higher heating value	LHV	13.8	MJ/kg
Moisture content (wet basis)	$MCwet$	30	%

where f_e is the electricity export factor (% or decimal), $(Cws)o$ the optimal unit cost of wood wastes (€ Cent/t), C_{ls} the specific wage per capita of labour cost (€/person/year), C_{ts} the unit cost of transportation (€/t/km), C_{ws} the unit cost of wood wastes (at the site of source) (€ Cent/t), E the electricity output (MW_e), i the discount rate (%), Is the specific cogeneration investment (€/MW_e), K_m the maintenance coefficient (% or decimal), LHV the lower heating value of fuel (MJ/kg), m the number of months (month), n the economic cogeneration lifetime (year), N the number of workers (person), pd the price of thermal energy (€ Cent/kWh), pec the price of electricity capacity, (€ Cent/MW/month), pee the price of electricity energy (€ Cent/kWh), Q_B the boiler thermal load (MW_{th}), Q_D the process heat demand (MW_{th}), R the radius of biomass supply area (km), R_O the optimal radius of biomass supply area (km), t the annual cogeneration operating time (h), η_B the boiler efficiency (%), $0\eta_{CO}$ the cogeneration efficiency (%) and Ψ is the annual specific wood waste availability (t/ha/year).

The size of a power plant is directly influenced by the biomass availability, Ψ (t/ha/year) and the boiler efficiency (η_B) (Eq. (9)), which prescribes the biomass demanding area, with a radius of R km.

The optimum collection area (with radius R) depends on biomass-associated costs. According to [42,43] biomass-associated costs could be summarized by four major factors: harvesting, transportation, biomass origin (pure and dense stands, burnt areas, shrub areas with scattered trees) and characteristics (e.g. coniferous or hardwood, logs or branches). These factors can also vary according to several variables as:

Machinery: harvester, forwarder, crane, chainsaw; Transportation: tractor and trailer; lorry (2, 4 or 6 wheel drive); Terrain morphology: slope, presence of rocks; Stands types – area, number of trees per hectare, age, species; Operation: tillage, final cut; Man-labour – cutter qualification, driver qualification, operation time; Biomass format: slash, wood and wood parts, chips, bundles, round wood.

This analysis is comprehensively presented by [42–44] in Pinus and Eucalyptus stands, at a local scale. Different methodologies and cost calculation models to calculate the different biomass-associated costs (feeling, bucking, forwarding, transport and chips) can be found in [45,46].

Given the impossibly of implementing a detailed analysis throughout the entire study area, the achieved optimum radius results from the knowledge of the general exploitation existent in Portugal. The considered biomass costs were calculated [42,43] for Eucalyptus stands at final harvest (1200 trees per hectare in average [31]) using a harvester and a forwarder for cutting and loading and a tractor and trailer for transportation, and Pinus stands at final harvest (600 trees per hectare in average [31]), using a chainsaw and manual loading and a lorry (two wheel drives) for transportation.

Based in the abovementioned studies [42–44] and on the available knowledge about the existent power plants in Portugal [40], the achieved R_0 was approximately 35 km for a 9 MW power plant.

After superimposing within a GIS the projected power plant locations with a land cover map, such as Corine Land Cover (CLC2006) [47], it was possible to realise that the biggest power plants are locate within forested areas. They require a large amount of biomass but they are surrounded by large amounts of biomass. Small power plants are located within less forested areas. They require small amount of biomass but biomass could be far way from the power plant location. Therefore, for the purpose of this study, a radius of 35 km for all the power plants was considered optimum (Fig. 2). Given the resource competition that will exist, we can assume that, independently of power plant size, the collection area will be the same for all power plants. On the other hand, as the goal of this work is to know the maximum power

Table 4
Total amount of theoretical and available residual biomass from maritime pine and eucalyptus, by NUT II sub-region.

NUT II Sub-region	Area (ha)	Forest area (ha)	B_d total (tonnes)	B_d (ton/year)	B_d (ton/ha)	B_d available (tonnes) (R = 35 km)	B_d available (ton/year) (R = 35 km)
Mean values achieved							
North	2128898.8	314400.0	4844028.5	273045.2	27.7	2610138.4	147126.7
Center	2367489.4	668000.0	11313251.0	569601.1	28.2	7693256.4	387341.1
L.V.T.	1170004.6	211100.0	2657602.4	190005.1	32.7	882065.7	63063.2
Alentejo	2727597.4	146100.0	836241.9	55658.5	14.0	116367.3	7745.2
Algarve	499487.9	17400.0	88337.3	8829.1	13.6	38929.7	3890.9
Total	8893478.1	1357000.0	19739461.0	1097139.0	23.2	8312368.8	609167.1
Maximum values achieved							
North	2128898.8	314400.0	6016987.5	342774.1	34.5	3242171.3	184699.1
Center	2367489.4	668000.0	13450714.0	723436.6	34.2	9146777.7	491952.6
L.V.T.	1170004.6	211100.0	3238889.0	247294.1	38.7	1074996.4	82077.6
Alentejo	2727597.4	146100.0	1197319.7	85551.2	18.3	166613.1	11904.9
Algarve	499487.9	17400.0	111278.6	11510.5	16.3	49039.8	5072.6
Total	8893478.1	1357000.0	24015188.8	1410566.5	28.4	10112895.4	775706.8
Minimum values achieved							
North	2128898.8	314400.0	3935660.0	224821.6	22.8	2120676.5	121142.0
Center	2367489.4	668000.0	9220289.3	461185.8	22.8	6269997.0	313616.4
L.V.T.	1170004.6	211100.0	2182931.3	156861.2	26.8	724521.1	52062.7
Alentejo	2727597.4	146100.0	479470.0	25795.8	9.8	66720.7	3589.6
Algarve	499487.9	17400.0	64777.9	5994.4	10.8	28547.3	2641.7
Total	8893478.1	1357000.0	15883128.5	874658.7	18.6	6688451.2	493052.4

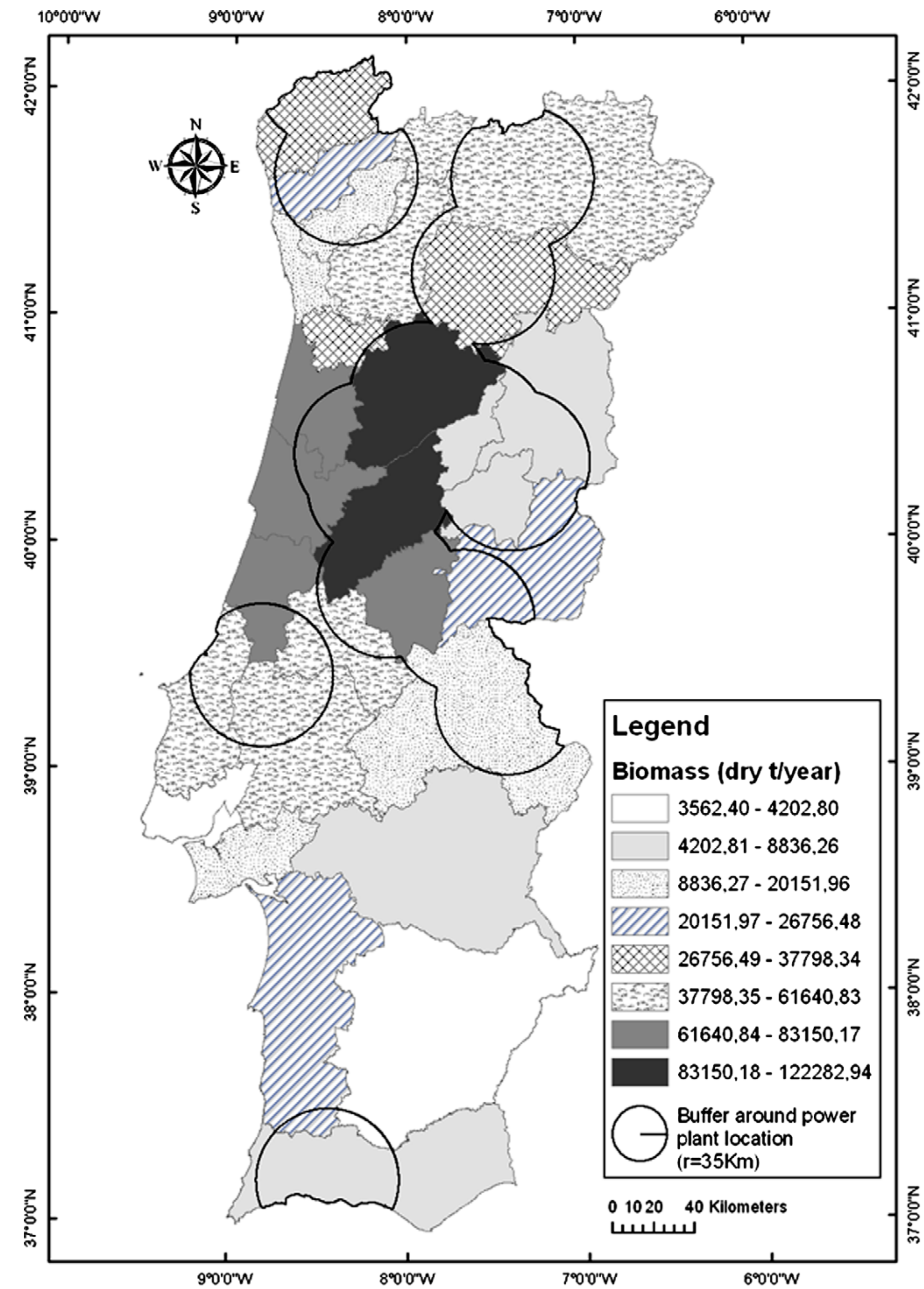

Fig. 3. Logging residues availability at regional scale (t/year). The biomass supply area (exploitable radius of 35 km) is identified.

capacity which should be installed in the best case, we consider the same optimum radius (35 km).

4. Results and discussion

The estimated total amount of biomass averages around 1.097 million dry t/year, with 579.91 thousand dry t/year from maritime pine and 517.23 thousand dry t/year from eucalyptus. However, these values range from 874.66 thousand dry t/year (473.70 thousand dry t/year of pine and 400.96 thousand dry t/year of eucalyptus) to 1.41 million dry t/year (673.54 thousand dry t/year from pine and 737.03 thousand dry t/year from eucalyptus). These results are presented in Table 4, grouped by NUT II regions (see Fig. 2).

When considering only an area of 35 km radius circle around each power plant (installed and planned), the exploitable biomass is considerably less. The estimated total amount of biomass averages 609.17 thousand dry t/year, and the maximum and minimum values are 775.71 thousand dry t/year and 493.05 thousand dry t/year, respectively.

The differences among estimates are due to the use of different biomass allometric equations (Tables 1 and 2). As the growth of trees varies among regions of Portugal with differences in environmental conditions, region-specific equations were required. Furthermore, some equations directly quantify dry biomass and others quantify wet biomass, which then has to be converted by a multiplicative dry factor.

The biomass availability maps, presented in Figs. 3 and 4, show the spatial distribution of biomass by the NUT III regions. The higher quantities of logging residues generated per year of maritime pine and eucalyptus are located at the northern and central regions. In the southern regions (Alentejo and Algarve) the biomass amount is significantly lower. This was expected since, in north and central Portugal, pinus and eucalyptus species are dominant, while in the south cork oak and holly oak are the most abundant species.

A GIS-based analysis allowed for assessment of both the theoretical maximum and the available potential power installation. In a future, the 15 power plants' (two installed and 13 planed) total power capability will be 108.4 MW (Table 5). Our results illustrated that the theoretical maximum power potential (Q_B) of fully condensing power plants is 131.4 MW. However, when calculation is performed using logging residue availability, for the maximum transport distance of 35 km, the real maximum power potential is just 73.0 MW. This means that the power plant capacity to be installed in the country (108.4 MW) is very high even if only logging residues from maritime pine and eucalyptus will be used as fuel source. However, only the region of LVT (see Fig. 2)

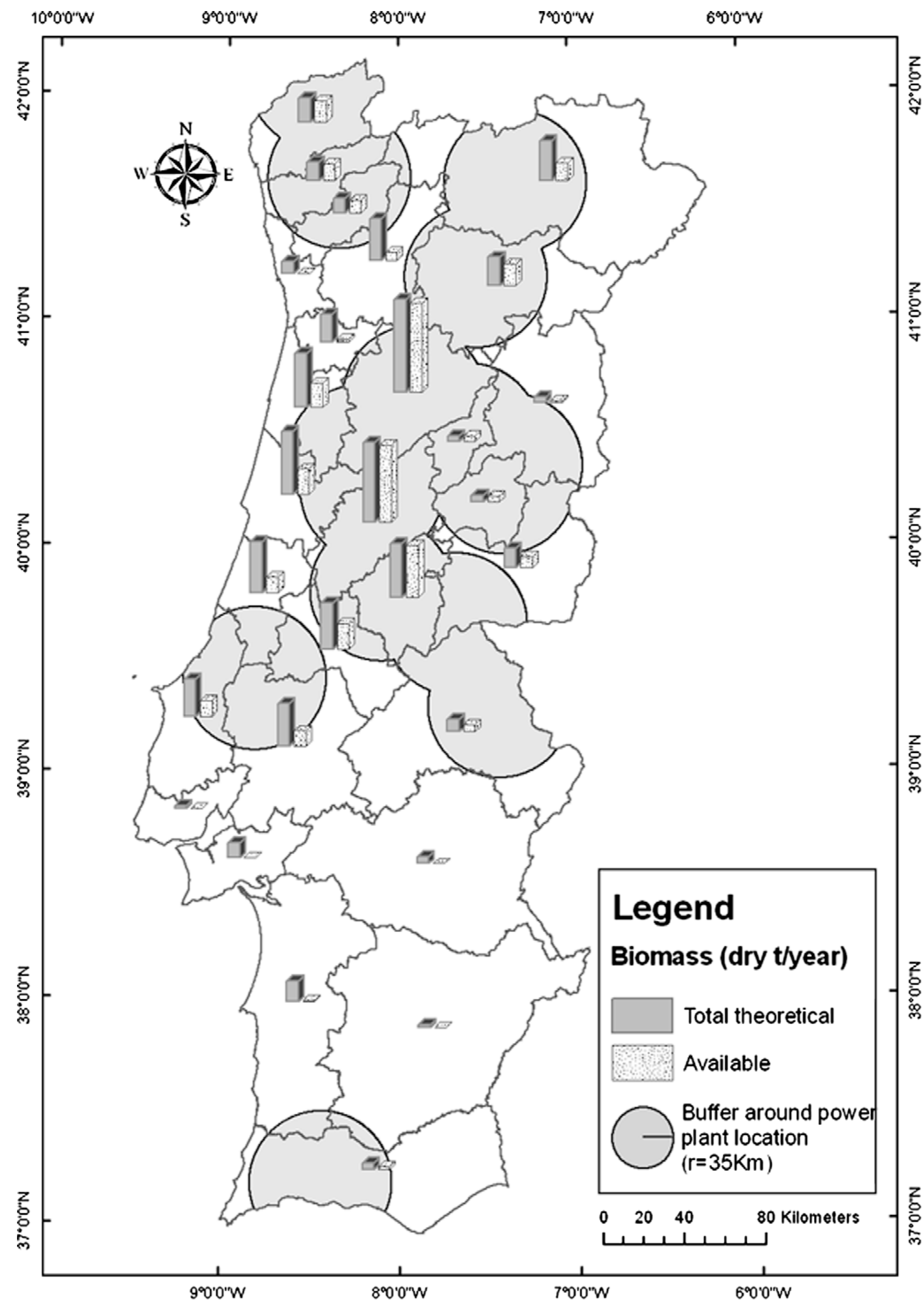

Fig. 4. Total theoretical and available (within a radius of 35 km) biomass potential supply.

Table 5
Potential power production of fully condensing plants and cogeneration plants.

Power plant	Installed capacity (MW)	Theoretical biomass (t/year)	Available biomass (t/year) (R = 35 km)	Fully condensing plant		Cogeneration plant	
				Maximum theoretical potential, Q_B (MW)	Maximum available potential (R = 35 km), Q_B (MW)	Maximum theoretical potential, Q_B (MW_{th})	Maximum available potential (R = 35 km), Q_B (MW_{th})
1	9.9						
3	9.0						
4	4.5						
5	9.9						
North	33.3	273045.24	147126.69	32.7	17.6	78.5	42.3
7	1.8						
8	9.0						
9	4.5						
10	9.0						
11	2.7						
12	9.0						
M	9.0						
VVR	13.0						
Center	58.0	569601.1	387341.1	68.2	46.4	163.8	111.4
13							
Alentejo	9.0	55658.5	7745.2	6.7	0.9	16.0	2.2
14							
LVT	5.4	190005.1	63063.2	22.8	7.6	54.6	18.1
15							
Algarve	2.7	8829.1	3890.9	1.1	0.5	2.5	1.1
	108.4	1097139.0	609167.1	131.4	73.0	315.4	175.1

could possibly supply the demand (7.6 MW) using only this fuel source.

This problem could be overcome by the use of second-generation power plants that use cogeneration. Results from GIS-based analysis enabled us to estimate a theoretical maximum and a real maximum power potential of 315.4 and 175.1 MW_{th}, respectively. However, even using second-generation power plants the Alentejo and Algarve regions do not produce enough forest biomass and will need other fuel source to supply their biomass needs.

5. Conclusions

Our results, regarding logging residues availability and future demand of biomass for energy production, enabled identification of the most suitable regions for increasing forest fuel usage.

In this study, biomass available quantities were estimated with respect to the optimum transport allocation areas. However, it is important to take in account that this biomass would not be fully used, as there exist technical limitations (e.g. slope) which limit the collection process. Although this study quantified logging residues existence, the annual biomass availability will depend on forest management, such as tree thinning and pruning, applied to a forest stand during its life cycle. Furthermore, because logging residue supplies depend on harvest activity (e.g. the exploitable residues are different for manual or mechanised harvesting), annual variation in residue amount must also be expected.

The present analysis was made for all power plants as a whole, considering the same collecting area (35 km radius) for all, but removing the overlapping areas. However, as the power plants will have different power capability and different ownership, in practice the biomass needs calculation must be made for each one separately. Furthermore, according to competition rules, the collection area radius will overlap, in particularly in the central region. As a consequence, competition for resources within an area, will affect biomass acquisition costs, leading to enlarged collection area radii. Even considering the best estimates, amounts of biomass will strongly limit the potential energy conversions, as the demand of installed power is very high.

Power plant location was not designed according to local needs of energy or according to local biomass availability, but according to energy transformers' station location, were energy could be injected in Portuguese energy network. Following [48] the resolution of an optimization model, addressing constrains (cost for supply of biomass, operation of production plants, investment in plants, and transportation of biomass) would have been essential to generate the optimal locations of power plants.

In this research we did not explore other vegetation biomass sources, which could have a strong contribute to biomass supply. These other sources are: the biomass from stands under grove bush, shrub land and shrubs growing in burnt areas. These types of biofuel are very significant and cannot be discarded, as 1.8 million hectares are shrub land [19] and 3.1 million hectares [49] are burnt areas (1.5 million hectares from shrub land and 1.6 million hectares from stands), just in the 2001–2006 period, which can generate millions of dry tonnes of biomass each year. A third important biomass source is the agricultural sector, where the residues from vineyard thinning, wine industry, olive groves and fruit trees orchard pruning, olive pulp remaining from olive oil production, etc., can have a considerable exploratory interest.

Portugal has a high biomass potential which can be used in energy production, although it is already used by pulp, plywood and fibreboard industry. The use and probable competition for the same biomass resource requires special concern, to avoid the excess of exploitation, and consequent disequilibrium of ecosystems.

This case study does not end here, as it continues to undergo new surveys and computer calculations, which will be reported in due course.

References

[1] Council of the European Union. Presidency conclusions of the Brussels European Council 8/9 March 2007. Brussels; 2 May 2007.

[2] Commission of the European Communities. Communication from the Commission to the European Parliament, the Council, the European Economic and Social Committee and the Committee of the Regions – 2020 by 2020 – Europe's climate change opportunity. COM(2008) 30 final. Brussels; 23 January 2008.

[3] Commission of the European Communities. Communication from the Commission to the European Parliament, the Council, the European

Economic and Social Committee and the Committee of the Regions. Second strategic energy review – an EU energy security and solidarity action plan. COM(2008) 781 final. Brussels; 13 November 2008.
[4] Commission of the European Communities. Communication from the Commission. Energy for the Future: Renewable Sources of Energy. Green Paper for a Community Strategy. COM(96) 576 final. Brussels; 20 November 1996.
[5] European Commission. Communication from the Commission. Energy for the future: renewable sources of energy. white paper for a community strategy and action plan: COM(97)599 final. Brussels, Belgium; 1997.
[6] European Commission. Green Paper: Towards a European strategy for the security of energy supply. COM(2000)769 final, Brussels; 2001.
[7] European Commission. Directive of the European Parliament and the Council on the promotion of electricity produced from renewable energy sources in the internal electricity market, Directive 2001/77/EC, Brussels, Belgium; 2001.
[8] Resolução do Conselho de Ministros no. 154/2001 de 27 de Setembro. Programa E4. Eficiência Energética e Energias Endógenas. Ministério Da Economia. Lisboa; 2001.
[9] Resolução do Conselho de Ministros no 63/2003. Diário da República – I Série-B, No 98, 28 de Abril de; 2003.
[10] Resolução do Conselho de Ministros no 169/2005. Diário da República – I Série – B No 204 – 24 de Outubro de; 2005.
[11] Energia e Alterações Climáticas. Mais investimento, melhor ambiente. Ministério da Economia e da Inovação. Lisboa; 2007. p. 32.
[12] Resolução da Assembleia da República no 40/2007. Diário da República, 1.ª série - No.159 – 20 de Agosto de; 2007.
[13] European Commission. Green Paper: Towards a European strategy for the security of energy supply. Technical Document, Brussels; 2002. p. 68.
[14] Commission of the European Communities. Communication from the Commission. Biomass action plan. COM(2005) 628 final. Brussels; 2005.
[15] European Commission. Commission staff working document. Annex to the Communication from the Commission. Biomass action plan. Impact Assessment. COM(2005) 628 final; 2005.
[16] DGGE. Estratégia Nacional para a Energia. A criação de uma rede de Centrais de Biomassa dedicadas. Direcção Geral de Geologia e Energia; 2006.
[17] Commission of the European Communities. Communication from the Commission. The support of electricity from renewable energy sources. COM(2005) 627 final. Brussels; 7 December 2005.
[18] Rivas-Martínez, Díaz S, Penas A. Bioclimatic map of Europe. Bioclimates. Cartographic service. Spain: University of León; 2004.
[19] DGRF. Resultados do Inventário Florestal Nacional 2005/06. Planeamento e Estatística. Direcção Geral dos Recursos Florestais. Ministério da Agricultura do Desenvolvimento Rural e das Pescas. Lisboa; 2007.
[20] Berndes Göran, Hoogwijk Monique, van den Broek Richard. The contribution of biomass in the future global energy supply: a review of 17 studies. Biomass Bioenergy 2003;25:1–28.
[21] Hoogwijk M, Faaij A, Van den Broek R, Berndes G, Gielen D, Turkenburg W. Exploration of the ranges of the global potential of biomass for energy. Biomass Bioenergy 2003;25:119–33.
[22] European Commission. BIOMASS – Green energy for Europe. Luxembourg: Office for Official Publications of the European Communities; 2005. p. 46.
[23] WESST. Wood Energy Resources. Module 5. Wood energy supply system training; 2008. <http://www.wesst.com/> (verified 17.09.08).
[24] BFIN. Biomass Resources. Bioenergy feedstock information network; 2008. <http://bioenergy.ornl.gov/> (verified 17.09.08).
[25] Easterly James L, Burnham Margo. Overview of biomass and waste fuel resources for power production. Biomass Bioenergy 1996;10(2–3).
[26] European Commission. BIOMASS: an energy resource for the European Union. European Communities, Programme "energy, environment and sustainable development". Office for Official Publications of the European Communities, Luxembourg. EUR 19424; 2000. p. 17.
[27] ADIV. Avaliação da sustentabilidade do recurso florestal para avaliação da viabilidade da instalação de centrais termoeléctricas a biomassa florestal na região Centro. ADIV-IPV, Viseu; 2006.
[28] UTAD. Avaliação da sustentabilidade do recurso florestal para avaliação da viabilidade da instalação de centrais termoeléctricas a biomassa florestal na região Norte. UTAD, Vila Real; 2006.
[29] Arthur D. Little International, Inc. Resíduos florestais para produção de energia em Portugal. Ed. Tecninvest, SARL; 1985.
[30] Silva R, Tavares M Páscoa F. Residual Biomass of Forest Stands. *Pinus pinaster* Ait. *and Eucaliptus globulus* Labill. Actas n 5, 10 Congresso Florestal Mundial, Paris; 1991.
[31] Domingos L. Estimating net primary production in *Eucalyptus globulus* and *Pinus pinaster* ecosystems in Portugal. PhD thesis, England: Kingston University; 2005.
[32] Barreto LS. Pinhais Bravos. Ecologia e Gestão. Lisboa: Departamento de Engenharia Florestal, Universidade Técnica de Lisboa, Instituto Superior de Agronomia; 1995.
[33] Fabião AM. Contribuição para o estudo da dinâmica da biomassa e produtividade primária líquida em eucaliptais. Lisboa, Portugal: Tese de Doutoramento. Universidade Técnica de Lisboa, Instituto Superior de Agronomia; 1986.
[34] Tomé M. Inventariação de recursos florestais. Caracterização e monitorização de povoamentos florestais e matos. Publicações GIMREF, TP 2/2007, vol. II. Lisboa: Universidade Técnica de Lisboa, Instituto Superior de Agronomia, Centro de Estudos Florestais; 2007.
[35] Faaij, André PC. Bio-energy in Europe: changing technology choices. Energy Policy 2006;34:322–42.
[36] Breeze P. The future of global biomass power generation. The technology, economics and impact of biomass power generation. London: Business Insights Ltd.; 2004.
[37] Prasertsanb S, Krukanonta P. Implications of fuel moisture content and distribution on the fuel purchasing strategy of biomass cogeneration power plants. Biomass Bioenergy 2003;24:13–25.
[38] Krukanonta P, Prasertsanb S. Geographical distribution of biomass and potential sites of rubber wood fired power plants in Southern Thailand. Biomass Bioenergy 2004;26:47–59.
[39] Fiala M, Pellizzi G, Riva G. A model for the optimal dimensioning of biomass-fuelled electric power plants. J Agr Eng 1997;67:17–25.
[40] Central de Biomassa de Mortágua; 2009. <http://www.energiasrenovaveis.com/DetalheEstados.asp?ID_conteudo=22&ID_area=2&ID_sub_area=37> (Verified 05.11.2009).
[41] Voivontas D, Assimacopoulos D, Koukios EG. Assessment of biomass potential for power production: a GIS based method. Biomass Bioenergy 2001;20:101–12.
[42] Carinhas, Joana CV. A study on eucalyptus residual biomass exploitation. MPhil thesis, Portugal: UTAD, Vila Real; 2006.
[43] CBE – Portuguese Centre for Biomass and Energy. Evaluation of associated costs to forest residual biomass economic exploitation; 2009. <http://www.drapc.min-agricultura.pt/base/geral/files/avaliacao_custos_aprov_biomassa.pdf>.
[44] Spinelli Raffaele. A Decision support system for assisting harvesting system choice in eucaliptus spp fast growing short rotation plantations. PhD College of Life Sciences, University College Dublin, National University of Ireland, Dublin; 2006. 115p.
[45] Leduc S, Lundgren J, Franklin O, Dotzauer E. Location of a biomass based methanol production plant: a dynamic problem in northern Sweden. Appl Energy 2010;87:68–75.
[46] Kinoshita Tsuguki, Inoue Keisuke, Iwao Koki, Kagemoto Hiroshi, Yamagata Yoshiki. A spatial evaluation of forest biomass usage using GIS. Appl Energy 2009;86:1–8.
[47] IGP, 2009, CLC2006 – Cartografia CORINE Land Cover 2006 para Portugal Continental; 2009. <http://www.igeo.pt/gdr/projectos/clc2006/> (verified 15.99.09).
[48] Leduc S, Natarajan K, Dotzauer E, McCallum I, Obersteiner M. Optimizing biodiesel production in India. Appl Energy 2009;86:125–31.
[49] DGRF. Estatísticas dos incêndios florestais. Totais Nacionais (1980–2006). Direcção geral dos Recursos Florestais. Ministério da Agricultura do Desenvolvimento Rural e das Pescas; 2007.

Annex B.2

Viana, H., Aranha, J., Lopes, D., 2011. Dedicated Biomass Plants for Combined Heat & Power (CHP). The Portuguese National Strategy. 19th European Biomass Conference and Exhibition, ETA-Florence Renewable Energies, Berlin, Germany. June 6-10.

DEDICATED BIOMASS PLANTS FOR COMBINED HEAT & POWER (CHP). THE PORTUGUESE NATIONAL STRATEGY

Helder Viana[1], Domingos Lopes[2], José Aranha[2]
[1]Centro de Estudos em Educação, Tecnologias e Saúde. Agrarian Superior School, Polytechnic Institute of Viseu, Quinta da Alagoa, Estrada de Nelas, 3500-606 Viseu, Portugal. phone.: +351 232 446 600; fax: +351 232 426 536;e-mail: hviana@esav.ipv.pt
[2]CITAB - University of Trás-os-Montes e Alto Douro, 5000-911 Vila Real, Portugal

ABSTRACT: The present work analyses the suitability of existing and planned wood-fired power plant in Portugal according to the forest biomass resource available for use as energy. Following the European Union strategy in climate and energy, which aims the decrease of greenhouse gas emissions and increasing the share of renewable energies (wind, solar, biomass, etc) consumption, Portugal established, in a first commitment, that the production of electrical energy from renewable sources should reach 45 % of the total supply by 2010. Further to the EU's "20-20-20" initiative, which set the objectives for 2020, the goal was increased to 60%. In order to fulfil this target, part of this energy will be obtained from biomass forest resources. Hence, in addition to the two existing electric power plants, with 22 MW of power capacity, 13 new power plants with 86.4 MW, are in construction. Despite the main goal is the electricity generation, the government incentive the construction of combined heating and power plants. Considering that wood-fuel demand will increase significantly across the different regions, it will be necessary to apply rational resource exploitation actions associated with regional and local needs. For example, there may be significant competition in some areas due to the presence of pulp mills or other biomass consuming industries. In these cases special solutions and compromises will be needed, or it may not be feasible to construct a power plant in such a location. This article evaluates if the biomass availability is sufficient to fulfil the future demands, considering two scenarios (fully condensing plants and cogeneration plants). The results show that if only electricity is generated some regions will need to find alternative fuel sources to fulfil the demand. However, if cogeneration is implemented the exiting wood fuel resource will be sufficient to fulfil the demand.
Keywords: Biomass; Combined heat and power generation (CHP); Forest residues, Energy

1 INTRODUCTION

The discussion about climate change, which has been done worldwide, has today a broad consensus about the need to change the current living standards. Particular attention has been given to the necessity of reducing greenhouse gas emissions (GGE). The European Union (EU) has been a pioneer in taking effective steps, having started from the 90's a strategy on climate and energy. Therefore, the EU intends that all its member states to adopt policies and actions that lead to the development of new and safer energy sources, thus contributing to reducing dependence on fossil fuels and the consequent reduction of GGE.

The strategic objectives, of the EU as well as those individual member states, for the development of energy from renewable sources (RES) have been described over the years in various documents. As a first step, towards a strategy for RE the Commission adopted a Green Paper on 20 November 1996 [1]. The most ambitious strategic goals were defined in 1997 in a European Commission White Paper [2], where the EU set the target to increase the share of renewable up to 12% by 2010 as well an Action Plan setting out the means to reach this objective.

After the order Green Paper (2000) on security of energy supply [3], a concrete proposal was made in 27 September 2001, Directive 2001/77/EC [4], to promote an increase in the contribution of renewable energy sources to electricity production in the internal market for electricity and to create a basis for a future Community framework. Therefore, this directive defined that all Member States should be required to set national indicative targets for the consumption of electricity produced from renewable sources, by 2010. The national indicative targets should be consistent with the global indicative target of 12 % of gross national energy consumption and in particular with the 22.1 % indicative share of electricity produced from renewable energy sources in total Community electricity consumption.

The reference value for Portugal was set by the government at 39% (including large hydro) in the National E4 Programme (Energy Efficiency and Endogenous Energies) launched in 2001 [5], and subsequently in the National Strategy for the Energy launched in 2003 [6] and 2005 [7]. In 2007 Portugal established a more ambitious strategic target in its National Strategy of Sustainable Development [8]. This new National Strategy for the Energy establishes that 45% of the national energy consumption in 2010 should be exclusively produced from renewable energy sources.

In January 2008 the European Commission proposed binding legislation, agreed by the European Parliament and Council in December 2008 [9, 10] and became law in 2009, to implement the 20-20-20 targets for 2020: - cutting greenhouse gases by at least 20% of 1990 levels (30% if other developed countries commit to comparable cuts); - increasing use of renewables (wind, solar, biomass, etc) to 20% of total energy production (currently ± 8.5%) and - cutting energy consumption by 20% of projected 2020 levels - by improving energy efficiency. As a result, In 23 April 2009 the Directive 2009/28/EC [11] of the European Parliament and of the Council, on the promotion of the use of energy from renewable sources, repealed the Directive 2001/77/EC and established new mandatory national targets, consistent with a target of at least 20% share of energy from renewable sources in the Community's gross final energy consumption in 2020. In order to be an example following the policy of the EU, Portugal has set, by the RCM n.º 29/2010, as a new target of 31 % for share of energy from renewable sources in gross final consumption of energy, in 2020 and the production of electricity from RS should reach 60 % of the total supply in 2020 [12].

Amongst renewable resources, bioenergy has been recognized as the most promising areas, within the biomass sector, for several reasons. First and foremost, because it has low negative environmental impact in terms of CO2 emissions for the entire fuel cycle and zero CO2 emissions from fossil fuels during operation. Additionally, as stated in the European Commission White Paper [2] because it would increase the amount of people working in the forestry sector and because the combined use of heat and power (CHP) has the greatest potential per unit volume among all renewable energy sources.

The European Commission's Green paper (2000) [3], also recognized that biomass is a versatile energy resource, with a widespread availability through forest and agricultural residues that has so far not been fully exploited. Furthermore, in the Green paper technical document (2002) [13], emphasis is given to the electricity generation from biomass energy plants, and some successfully examples of implementation in some member states are presented.

The strongest incentive of the EU towards development of biomass energy was given in 2005 with the Biomass Action Plan [14, 15]. In this plan, the EU stated that the increased use of renewable energy is essential for environmental and competitiveness reasons, and recognized that "biomass has many advantages over conventional energy sources, as well as over some other renewable energies, in particular, relatively low costs, less dependence on short-term weather changes, promotion of regional economic structures and provision of alternative sources of income for farmers". This action plan established several measures to promote biomass in heating, electricity and transport, followed by crosscutting measures affecting biomass supply, financing and research.

Following the EU's strategy, and in consequence of severe forest fires that affected Portugal in 2003 and 2005, the government decided to increase the installed power (2 power plants, with 22 MW) for producing electricity from forest biomass to 250 MW, by 2010 [16]. This strategy aims contribute to meet the share of 45% of electricity from RS (increased in 2009to 60%) and secondly to reduce the risk of fire and to promote and develop the forestry sector. Therefore, in 2006, 15 new power plant (90 MW) exploration licenses were made available to achieve this aim. However, because only 13 licenses were applied for, presently new power plants will only provide 86.4 MW of additional power. If the projects submitted to public contest included the use of the heat generated by the power plant, in addition to electrical power (Combined Heat and Power, CHP), a scaling factor a major weight was given to attribute the operating license. Due to the complexity of the contest, and the delay of the decision, most of power plants are still under construction.

The localization of biomass power plants has been defined based on the amount of biomass and wildfire hazard in each region. The power plants will have variable power generation capabilities and combine different technologies, as appropriate to local circumstances. Two power plant models are planed: small units, with power production ranging from 1.8 to 4.5 MW, and large ones with power production ranging from 9 to 9.9 MW.

In addition to these plants, if we consider the pulp mills and otters consuming industries that produce also CHP, the demand for wood-fuel will increase significantly. In fact, they have already high power capacity and some are expanding. While a few years ago they consumed only the commercial part of the trees, remaining in the forests the residual biomass from logging, now they consume all the components of the trees. As it will be necessary to apply rational resource exploitation actions associated with regional and local needs it is needed to study the availability of resources and the potential power capacity that each region can support.

In this context this work assesses Portugal's current forest biomass resource potential for commercial generation of electricity and analyses if is feasible to construct all the planned power capacity at regional and national levels.

2 MATERIAL AND METHODS

2.1 Study area

Portugal is located between the latitudes of 36º 57' 23" and 42º 09' 15"N and the longitudes of 09º 30' 40" and 06º 10' 45" W (Fig. 1). With four distinct weather seasons, the average annual temperatures range from about 7 ° C in the highlands of the interior north and center and about 18 ° C in the south coast. Average annual precipitation is more than 3000 mm in the north and less than 600 mm in the south. These characteristics create good conditions for forest growth. Forest activity is a direct source of income for a vast forest products industry, which employs a significant part of the population.

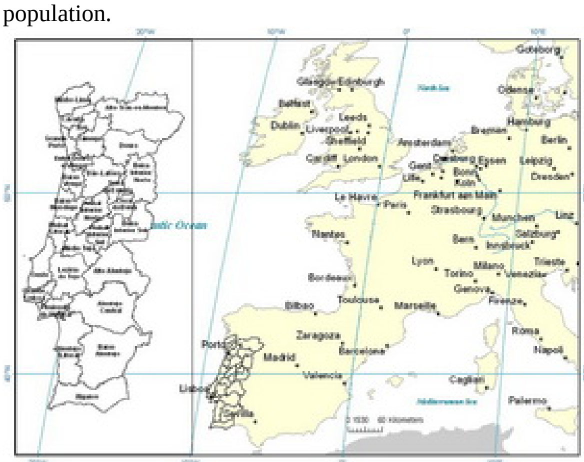

Fig. 1: Geographical location of Portugal and indication of NUT III sub-regions

2.2 Methodology

The first steage of our study consisted on the classification and mapping, of national forest cover. In a second stage, we estimated the available forest biomass and annual growth at national and regional levels. In the third stage, the geographical location of existing power plants was evaluated, and a GIS-based analysis was applied to examine the relationship between existing biomass and the power plants wood-fuel demand. Finally, based on the available quantities of biomass and growth we compared the maximum theoretical potential of energy production for two scenarios (fully condensing plants and cogeneration plants).

2.2.1 Availability of forests resources

Forests cover approximately 3.4 million hectares [17] of Portuguese territory, which represents 38 % of the national territory. *Pinus* pinaster (maritime pine) and *Eucalyptus globulus* (eucalyptus). are the main trees species, planted for commercial purposes and capable of providing a regular amount of biomass. Thus, only these stands (885019.00 hectares of maritime pine and 739514.00 hectares of eucalyptus) were considered in the calculations of biomass availability. The pine and eucalyptus stands occur mainly in the north and centre of Portugal as ecological conditions limit their growth in the south part of Portugal.

As in the basis of the decision of Portuguese strategy to implement the new power plants was the fact that the main source of fuel should come from the residual biomass generated by forest activity, only primary residues availability (parts of trees, unsuitable for saw timber such us branches and tops [18 - 22]) were used in the calculations. The potential supply of woody biomass resources was achieved through different calculation processes based on pine and eucalyptus stands dendrometric data, of each considered NUT III (Nomenclature of Territorial Units for Statistics).sub-region (Fig.1). In the North and Center NUT II regions (Fig. 2) the data was collected by field inventory, within maritime pine and blue-gum eucalyptus stands. The data from NFI (National Forest Inventory) 2005/2006 [19] was used and complemented with a dataset [27, 28] collected by field inventory, in the North and Center of Portugal. The primary residues were estimated, for each NUT III sub-region (Fig. 1), using specific allometric equations [25 - 30] for maritime pine and for eucalyptus. The total available biomass for the whole country, which can be converted into energy, is the sum of the estimates for each region.

2.2.2 Analysis of the spatial distribution of forest biomass and geographical location of power plants

After the wood fuel quantities were calculated, the spatial assessment of forest biomass availability was assigned by NUT III sub-regions region. The final map expresses the theoretical biomass quantities per year, assuming that they are uniformly distributed all over the region. This methodology was considered since, at the time of the calculations, we didn't have the sample plot coordinates of NFI data, neither any land cover accurate map with the classification of pine and eucalyptus stands. The final map expresses the theoretical biomass quantities per year.

Within a GIS environment, the power plants' geographical locations (Fig. 2), and the biomass map allowed analyse the available wood fuel into the influence area of each power plant as well the superimposed area.

2.2.3 Comparison of fully condensing and cogeneration plants scenarios

To analyse the maximum potential of energy production, based on the available biomass around each power plant, and according to their fuel demands, we compared two scenarios: fully condensing plants and cogeneration plants.

The conversion of residual forestry biomass into electrical power, heating power, or both (CHP) is made typically through simple combustion, but alternative processes such as co-firing, in particular coal-fired, or gasification are often used in some EU countries. Conversion process efficiency depends upon the resultant final products. In stand alone plants, the efficiency of biomass combustion for electricity production typically varies between 25% and 30% [31, 32], but if the electrical production is combined with heat production (CHP), the efficiency can rise to over than 80, in power plants having capacities ranging between 1 and 10 MW [31, 32].

We considered a moderate overall efficiency in both situations using the technical parameters adopted from [33-36] as presented in Table 1.

Table 1: Technical parameters for a wood fired plant

Power plant			Unit
Running time	t	8000	h/year
Process Steam Demand (fully condensing plant)	Q_D	0	MW_{th}
Process Steam Demand (cogeneration plant)	Q_D	27.2	MW_{th}
Overall efficiency (fully condensing plant)	η	25	%
Overall efficiency (cogeneration plant)	η_{CO}	60	%
Boiler efficiency	η_B	80	%
Electrical export factor	fe	90	%
Biomass			**Unit**
Nominal higher heating value	LHV	13.8	MJ/kg
Moisture content (wet basis)	$MCwet$	30	%

The analysis was made distinguishing the *theoretical biomass potential* of each region, which mean that all the wood fuel is collected across the region and used into energy production and the *available biomass potential* which mean that only the wood fuel within an area with optimum radius R_0 Km, where is viable collecting the biomass, is used to energy production.

In this research, we considered that the *available biomass potential* is only limited by the distance from collection area to the power plant. No other technical, ecological or economical restrictions were considered in this evaluation, which obviously differs from the reality. In fact, other restrictions must be considered (*e.g.* the efficiency of the residues collection procedure, the amount of biomass that can be technically and economically harvested, etc.).

The *theoretical and available biomass potential* was achieved by calculating the energy output (E - MW) by Equations 9 and 10 [33, 34]. In result, is obtained the *maximum theoretical power plant capacity*, and the *available (viable) power plant capacity.* The optimum radius (R_0) is calculated as a function of the cost of wood waste and density of wood fuel availability, Ψ *(t/ha/year)*, as described in Eqs. 11 and 12 [33-35].

$$Q_B = \frac{\psi \pi R^2 (LHV) \eta_B}{t} \tag{9}$$

$$E = \frac{\psi \pi R^2 (LHV) \eta_B \eta_{CO}}{t} - Q_D \tag{10}$$

$$R_O = \left(\frac{3(C_{ls} N)}{\psi \pi C_{ts}} \right)^{\frac{1}{3}} \tag{11}$$

$$R_O = \left(\frac{2\alpha}{\beta}\right)^{\frac{1}{3}} \quad (12)$$

The optimal cost of wood waste at source $(C_{ws})_O$ (maximum affordable fuel cost obtained at the expense of a fixed capacity of the power plant, fixed by a radius R_O), is obtainable by substituting R_O into Eq. 13:

$$(C_{ws})_O = \alpha R_O^{-2} + \beta R_O + \gamma \quad (13)$$

Being:

$$\alpha = \frac{1}{\psi\pi}\left\{tQ_D p_d - tQ_D\left(f_e p_{ee} + f_e p_{ec}\frac{m}{t} - \frac{I_s[K_m f_a + 1]}{tf_a}\right) - (C_{ls}N)\right\},$$

$$\beta = -\frac{2C_{ts}}{3}$$

$$\gamma = (LHV)\eta_B\eta_{CO}\left\{f_e p_{ee} + \frac{mf_e p_{ec}}{t} - \frac{I_s[K_m f_a + 1]}{tf_a}\right\},$$

$$f_a = \frac{(1+i)^n - 1}{i(1+i)^n},$$

Where:

f_e - electricity export factor, (% or decimal)
$(Cws)_o$ - optimal unit cost of wood wastes, (€ Cent/t)
Cls - specific wage per capita of labour cost, (€/person/year)
Cts - unit cost of transportation, (€/t/km)
Cws - unit cost of wood wastes (at the site of source), (€ Cent/t)
E - electricity output (MWe)
i - discount rate, (%)
Is - specific cogeneration investment, (€/MWe)
Km - maintenance coefficient, (% or decimal)
LHV - lower heating value of fuel, (MJ/kg)
m - number of months (month)
n - economic cogeneration lifetime (year)
N - number of workers, (person)
pd - price of thermal energy, (€ Cent/kWh)
pec - price of electricity capacity, (€ Cent/MW/month)
pee - price of electricity energy, (€ Cent/kWh)
Q_B - boiler thermal load, (MWth)
Q_D - process heat demand, (MW_{th})
R - radius of biomass supply area, (km)
R_O - optimal radius of biomass supply area, (km)
t - annual cogeneration operating time, (h)
η_B - boiler efficiency, (%)
η_{CO} – cogeneration efficiency, (%)
Ψ - annual specific wood waste availability, (t/ha/year)

The size of a power plant is directly influenced by the biomass availability, Ψ (t/ha/year) and the boiler efficiency, (η_B) (Eq. 9), which prescribes the biomass demanding area, with a radius of *R* km. The optimum collection area (with radius *R*) depends on biomass-associated costs which could be summarized by four major factors: harvesting, transportation, biomass origin (pure and dense stands, burnt areas, shrub areas with scattered trees) and characteristics (e.g. coniferous or hardwood, logs or branches). These factors can also vary according to several variables as [37, 38]: type of machinery, type of transportation; Terrain morphology; Stands; Operation; Man-labour and Biomass format. Based in the studies [37 - 39], on the knowledge of the general exploitation existent in Portugal, and on the knowledge about the existent power plants in Portugal [36], the variables used allowed achieved an optimum radius (R_0) with approximately 60 Km driving in national roads far from a power plant. Despite the smaller power plants require low amount of biomass they are located within less forested areas, and by other hand a big percentage of the area overlaps, we assumed that, independently of power plant size, the radius will be the same for all power plants Using Network analyst and the map of the considered distance from the power plant we defined the collection areas (Fig. 2 and 3).

3 RESULTS AND DISCUSSION

Using the biomass allometric equations and the forest inventory data we estimated maximum, minimum and average values.

The estimated total amount of biomass averages around 1.290 million dry ton/year, with 713.5 thousand dry ton/year from maritime pine and 576.5 thousand dry ton/year from eucalyptus. The maximum estimate gave 1.655 million dry ton/year and the minimum estimate gave 1.023 million dry ton/year. When considering only an area within a 35 Km radius distant from each power plant, the exploitable biomass is considerably less. The total amount of biomass estimated averages 710.6 thousand dry ton/year and the maximum and minimum estimates are 901.1 and 574.1 thousand dry ton/year respectively (Table 2). The differences among estimates are due to the use of different equations. So we considered the average values for analyse the energy potential. As the growth of trees varies among the regions, with differences in environmental conditions, region-specific equations were required. Furthermore, some equations directly quantify dry biomass and others quantify wet biomass, which then has to be converted by a multiplicative dry factor.

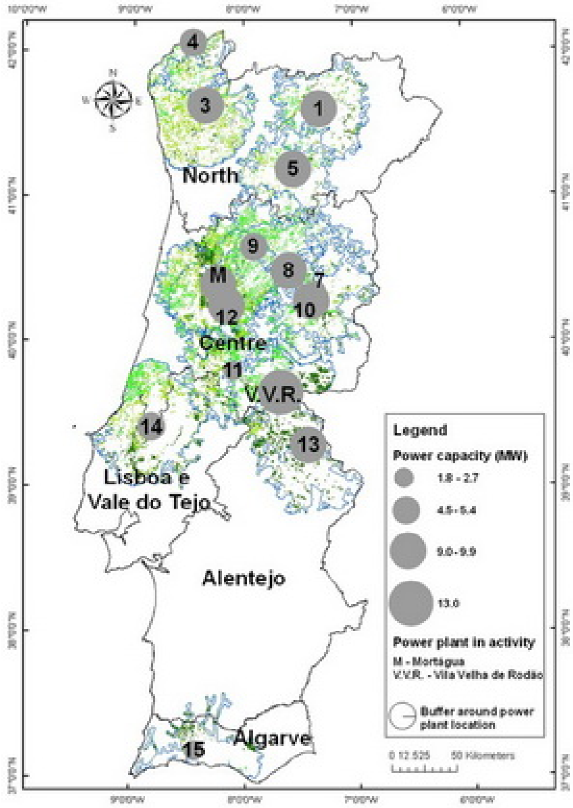

Fig. 2: Power plants location with the identification of the NUT II sub-regions boundaries, and the optimum biomass supply area (R=60km).

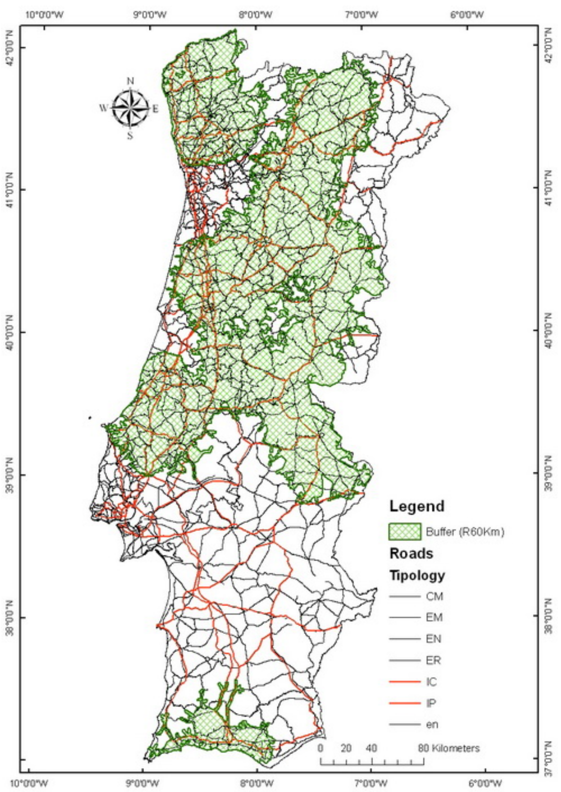

Fig. 3: Buffer of the supply areas around the power plants obtained with the optimum radius of 60 Km in the main roads

Table 2: Total amount of theoretical and available residual biomass from maritime pine and eucalyptus, by NUT II sub-region.

NUT II Sub-region	Forest Area (ha)	B_d Total (tonnes)	B_d (ton/year)
North	387484.0	6244655.4	338828.9
Center	771589.0	13137037.3	646970.9
L.V.T.	235995.0	3042024.8	212601.8
Alentejo	198443.0	1122447.6	75774.7
Algarve	31022.0	154912.4	15841.3
Total	1624533.0	23701077.5	1290017.6

NUT II Sub-region	B_d (ton /ha)	B_d available (tonnes) (R=60Km)	B_d available (ton/year) (R=60Km)
North	27.7	3364847.0	182573.3
Center	28.2	8933470.7	439954.3
L.V.T.	32.7	1009656.6	70563.1
Alentejo	14.0	156194.2	10544.4
Algarve	13.6	68269.0	6981.2
Total	23.2	9980621.9	710616.3

In Figs. 3 is showed the spatial distribution of biomass by the NUT III regions. The higher quantities of logging residues generated per year of maritime pine and eucalyptus are located at the northern and central regions. In the southern regions (Alentejo and Algarve) the biomass amount is significantly lower. This was expected since, in north and central Portugal, pinus and eucalyptus species are dominant, while in the south cork oak and holly oak are the most abundant species.

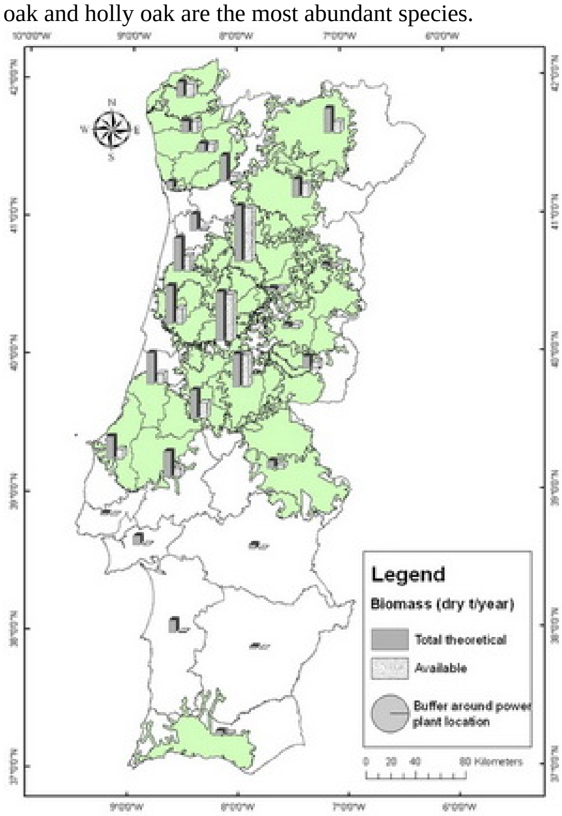

Fig. 4: Theoretical and available (within a radius of 35Km) biomass potential supply

The potential and maximum power capacity with the two scenarios: only electric production or CHP are presented in table 3.

As can be seen the planed capacity (108.4 MW) of the 15 power plants (2 installed and 13 planed) will have sufficient material (pine and eucalyptus residues) if all the theoretical biomass is used. But in an area viable for exploitation only 85.1 MW will be feasible if only logging residues from maritime pine and eucalyptus will be used as fuel source. However, only the region of LVT could supply the demand (8.5 MW).

If cogeneration is used, as the overall efficiency of these plants is superior (electricity and heat), the available biomass is sufficient to supply the demands.

The theoretical and available potential in this situation is 370.9 and 204.3 MWth, respectively. However, even using cogeneration power plants the Alentejo and Algarve regions do not produce enough forest biomass from pinus and eucalyptus, and will need other fuel source to supply their biomass needs.

Table 3: Potential power production of fully condensing plants and combined heating and power plant plants

Region (power plant)	Planned Capacity (MW)	Theoretical potential (MW)	Avaiable potential (MW)	Theoretical potential (MW_{th})	Avaiable potential (MW_{th})
		Condensing plant		CHP	
North (1-5)	33.3	40.6	21.9	97.4	52.5
Center (7-12, M, VVR)	58.0	77.5	52.7	186.0	126.5
LVT (14)	5.4	25.5	8.5	61.1	20.3
Alentejo (13)	9.0	9.1	1.3	21.8	3.0
Algarve (15)	2.7	1.9	0.8	4.6	2.0
Total	108.4	154.5	85.1	370.9	204.3

4 CONCLUSIONS

This study identifies the energetic potential of logging residues from pinus and eucalyptus species in Portugal. The theoretical biomass from this two species is sufficient to fulfil the demand of the planed power plants. However, considering that only the biomass inside an area with an optimum radius will be viably exploited, the demands will not be satisfied with only this type of biomass.

Despite we consider the calculated amounts, inside the buffer area, as *available biomass*, this biomass will not be fully used since we have to consider some technical limitations (e.g. slope) which limit the collection process. Although this study quantified logging residues existence, the annual biomass availability will depend on forest management, such as tree thinning and pruning, applied to a forest stand during its life cycle. Furthermore, because logging residue supplies depend on harvest activity (e.g. the exploitable residues are different for manual or mechanised harvesting), annual variation in residue amount must also be expected.As seen some power plants' influence areas overlaps, particularly in the central region. As a consequence, the competition for resources, will affect biomass acquisition costs, leading to the enlargement of the collection area.

If the planned power could generate heating and power (CHP), then the biomass will be sufficient. However, the decision of install CHP is depended of several factors as the higher installation costs and the existence of demand for heat.

In the future it will be needed to use other biomass sources as vegetation from shrubland (1.8 million hectares). However, the exploitation is not easy which can make the acquisition economically unprofitable. The agricultural residues can have a considerable exploratory interest. The industrial byproducts, such us sawdust and woodchips, could constitute an alternative source of fuel; however as they are widely used by plywood and fibreboard industries.

The use and probable competition for the same biomass resource requires special concern, to avoid the excess of exploitation, and consequent disequilibrium of ecosystems.

5 REFERENCES

[1] Commission of the European Communities. Communication from the Commission. Energy for the Future: Renewable Sources of Energy. Green Paper for a Community Strategy. COM(96) 576 final. Brussels, 20 November 1996.

[2] European Commission. Communication from the Commission. Energy for the Future: Renewable Sources of Energy. White Paper for a Community Strategy and Action Plan: COM(97)599 final. Brussels, Belgium; 1997.

[3] European Commission. Green Paper: Towards a European strategy for the security of energy supply. COM(2000)769 final, Brussels; 2001.

[4] European Commission. Directive of the European Parliament and the Council on the promotion of electricity produced from renewable energy sources in the internal electricity market, Directive 2001/77/EC, Brussels, Belgium; 2001.

[5] Resolução do Conselho de Ministros n.º 154/2001 de 27 de Setembro. Programa E4. Eficiência Energética e Energias Endógenas. Ministério Da Economia. Lisboa; 2001.

[6] Resolução do Conselho de Ministros nº 63/2003. Diário da República - I Série-B, Nº 98, 28 de Abril de 2003.

[7] Resolução do Conselho de Ministros nº 169/2005. Diário da República - I Série - B Nº 204 - 24 de Outubro de 2005.

[8] Resolução do Conselho de Ministros n.º 1/2008. Diário da República, 1.ª série - N.º 3 - 4 de Janeiro de 2008

[9] Commission of the European Communities. Communication from the Commission to the European Parliament, the Council, the European Economic and Social Committee and the Committee of the Regions - 20 20 by 2020 - Europe's climate change opportunity. COM(2008) 30 final. Brussels, 23 January 2008.

[10] Commission of the European Communities. Communication from the Commission to the European Parliament, the Council, the European Economic and Social Committee and the Committee of the Regions. Second Strategic Energy Review - An EU energy security and solidarity action plan. COM(2008) 781 final. Brussels, 13 November 2008.

[11] Directive 2009/28/Ec of the European Parliament and of the Council of 23 April 2009, on the promotion of the use of energy from renewable sources and amending and subsequently repealing Directives 2001/77/EC and 2003/30/EC.
[12] Resolução do Conselho de Ministros n.º 29/2010. Diário da República, 1.ª série - N.º 73 - 15 de Abril de 2010
[13] European Commission. Green Paper: Towards a European strategy for the security of energy supply. Technical Document, Brussels; 2002, 68pp.
[14] Commission of the European Communities. Communication from the Commission. Biomass action plan. COM(2005) 628 final. Brussels; 2005.
[15] European Commission. Commission staff working document. Annex to the Communication from the Commission. Biomass action plan. Impact Assessment. {COM(2005) 628 final}; 2005.
[16] DGGE. Estratégia Nacional para a Energia. A criação de uma rede de Centrais de Biomassa dedicadas. Direcção Geral de Geologia e Energia; 2006.
[17] DGRF. Resultados do Inventário Florestal Nacional 2005/06. Planeamento e Estatística. Direcção Geral dos Recursos Florestais. Ministério da Agricultura do Desenvolvimento Rural e das Pescas. Lisboa; 2007.
[18] Berndes, Göran; Hoogwijk, Monique and Broek, Richard van den. The contribution of biomass in the future global energy supply: a review of 17 studies. Biomass and Bioenergy 25 (2003) 1-28.
[19] Hoogwijk, M.; Faaij, A.; Van den Broek, R.; Berndes, G.; Gielen, D.; Turkenburg, W. Exploration of the ranges of the global potential of biomass for energy. Biomass and Bioenergy 25 (2003) 119 - 133.
[20] European Commission. BIOMASS - Green energy for Europe. Luxembourg: Office for Official Publications of the European Communities; 2005, 46 pp.
[21] Easterly James L., Margo Burnham. Overview of biomass and waste fuel resources for power production. Biomass and Bioenergy. Volume 10, Issues 2-3, 1996.
[22] European Commission. BIOMASS: An Energy Resource for the European Union. European Communities, Programme “Energy, Environment and Sustainable Development”. Office for Official Publications of the European Communities, Luxembourg. EUR 19424; 2000, 17pp.
[23] ADIV. Avaliação da sustentabilidade do recurso florestal para avaliação da viabilidade da instalação de centrais termoeléctricas a biomassa florestal na região Centro. ADIV-IPV, Viseu; 2006.
[24] UTAD. Avaliação da sustentabilidade do recurso florestal para avaliação da viabilidade da instalação de centrais termoeléctricas a biomassa florestal na região Norte. UTAD, Vila Real; 2006.
[25] Arthur D. Little International, Inc. Resíduos florestais para produção de energia em Portugal. Ed. Tecninvest, SARL; 1985.
[26] Silva, R.; Tavares, M. and Páscoa, F. Residual Biomass of Forest Stands. Pinus pinaster Ait. and Eucaliptus globulus Labill. Actas nº 5, 10º Congresso Florestal Mundial, Paris; 1991.
[27] Domingos, L. Estimating Net Primary Production in Eucalyptus globulus and Pinus pinaster Ecosystems in Portugal. PhD Thesis, Kingston University, England; 2005.
[28] Barreto, L. S. Pinhais Bravos. Ecologia e Gestão. Departamento de Engenharia Florestal, Universidade Técnica de Lisboa, Instituto Superior de Agronomia. Lisboa; 1995.
[29] Fabião, A.M. Contribuição para o estudo da dinâmica da biomassa e produtividade primária líquida em eucaliptais. Tese de Doutoramento. Universidade Técnica de Lisboa, Instituto Superior de Agronomia, Lisboa, Portugal; 1986.
[30] Tomé, M. Inventariação de recursos florestais, volume II - Caracterização e monitorização de povoamentos florestais e matos. Publicações GIMREF, TP 2/2007. Universidade Técnica de Lisboa, Instituto Superior de Agronomia, Centro de Estudos Florestais, Lisboa; 2007.
[31] Faaij, André P.C. Bio-energy in Europe: changing technology choices. Energy Policy, 34; 2006, 322–342.
[32] Breeze, P. The Future of Global Biomass Power Generation. The technology, economics and impact of biomass power generation. Business Insights Ltd. London; 2004.
[33] Prasertsanb, S. and Krukanonta, P. Implications of fuel moisture content and distribution on the fuel purchasing strategy of biomass cogeneration power plants. Biomass and Bioenergy 24 (2003) 13 - 25.
[34] Krukanonta, P. and Prasertsanb, S. Geographical distribution of biomass and potential sites of rubber wood fired power plants in Southern Thailand. Biomass and Bioenergy 26 (2004) 47 - 59.
[35] Fiala, M.; Pellizzi, G. and Riva, G. A Model for the Optimal Dimensioning of Biomass-fuelled Electric Power Plants. Journal of Agricultural Engineering 67 (1997) 17-25.
[36] Central de Biomassa de Mortágua. [On-line] Available at: http://www.energiasrenovaveis.com/DetalheEstados.asp?ID_conteudo=22&ID_area=2&ID_sub_area=37
[37] Carinhas, Joana C. V. A study on eucalyptus residual biomass exploitation. MPhil thesis, UTAD, Vila Real, Portugal. 2006
[38] CBE – Portuguese Centre for Biomass and Energy. Evaluation of associated costs to forest residual biomass economic exploitation. 2009. http://www.drapc.min-agricultura.pt/base/geral/files/avaliacao _custos_aprov_biomassa.pdf.
[39] Spinelli, Raffaele, 2006. A Decision support System for assisting harvesting system choice in eucaliptus spp fast growing short rotation plantations. PhD. College of Life Sciences, University College Dublin, National University of Ireland, Dublin. 115pp.

6 ACKNOWLEDGEMENTS

Authors would like to express their acknowledgement to the Portuguese Science and Technology Foundation (FCT), programme SFRH/PROTEC/49626/2009.

Annex C

Viana, H., Aranha, J., Lopes, D., Cohen, W.B., 2012. Estimation of crown biomass of *Pinus pinaster* stands and shrubland above-ground biomass using forest inventory data, remotely sensed imagery and spatial prediction models. Ecological Modelling 226, 22-35.

[Annex C.1]

Viana, H., Lopes, D., Aranha, J., 2011. Assessment of Forest Aboveground Biomass Stocks and Dynamics with Inventory Data, Remotely Sensed Imagery and Geostatistics, in: Shaukat, S.S. (ed.), Progress in Biomass and Bioenergy Production. InTech, pp. 107-130.

[Annex C.2]

Annex C.1

Viana, H., Aranha, J., Lopes, D., Cohen, W.B., 2012. Estimation of crown biomass of *Pinus pinaster* stands and shrubland above-ground biomass using forest inventory data, remotely sensed imagery and spatial prediction models. Ecological Modelling 226, 22-35.

Ecological Modelling 226 (2012) 22–35

Contents lists available at SciVerse ScienceDirect

Ecological Modelling

journal homepage: www.elsevier.com/locate/ecolmodel

Estimation of crown biomass of *Pinus pinaster* stands and shrubland above-ground biomass using forest inventory data, remotely sensed imagery and spatial prediction models

H. Viana[a,b,*], J. Aranha[b], D. Lopes[b], Warren B. Cohen[c]

[a] Centro de Estudos em Educação, Tecnologias e Saúde, Agrarian Superior School, Polytechnic Institute of Viseu, Quinta da Alagoa, 3500-606 Viseu, Portugal
[b] CITAB, University of Trás-os-Montes e Alto Douro, Apartado 1014, 5001-801 Vila Real, Portugal
[c] USDA Forest Service, 3200 SW Jefferson Way, Corvallis, OR 97331, USA

ARTICLE INFO

Article history:
Received 28 March 2011
Received in revised form
16 November 2011
Accepted 25 November 2011

Keywords:
Above-ground biomass
Remote sensing
Geostatistics
Regression-kriging
Pinus pinaster
Shrubland

ABSTRACT

Spatially crown biomass of *Pinus pinaster* stands and shrubland above-ground biomass (AGB) estimation was carried-out in a region located in Centre-North Portugal, by means of different approaches including forest inventory data, remotely sensed imagery and spatial prediction models. Two cover types (pine stands and shrubland) were inventoried and biomass assessed in a total of 276 sample field plots. We compared AGB spatial predictions derived from Direct Radiometric Relationships (DRR) of remotely sensed data; and the geostatistical method Regression-kriging (RK), using remotely sensed data as auxiliary variables. Also, Ordinary Kriging (OK), Universal Kriging (UK), Inverse Distance Weighted (IDW) and Thiessen Polygons estimations were performed and tested. The comparison of AGB maps shows distinct predictions among DRR and RK; and Kriging and deterministic methods, indicating the inadequacy from these later ones to map AGB over large areas. DRR and RK methods produced lower statistical error values, in pine stands and shrubland, when compared to kriging and deterministic interpolators. Since forest landscape is not continuous variable, the tested forest variables showed low spatial autocorrelation, which makes kriging methods unsuitable to these purposes. Despite the geostatistical method RK did not increase the accuracy of estimates developed by DRR, denser sampling schemes and different auxiliary variables should be explored, in order to test if the accuracy of predictions is improved.

1. Introduction

1.1. Biomass spatial prediction

Estimates of above-ground biomass (AGB) of forested areas have been used to address a broad range of questions including estimations of forest productivity (Chirici et al., 2007; Palmer et al., 2009), studying the impacts of forest fires or other disturbances (García-Martín et al., 2008), monitoring the biomass changes over time (Hu and Wang, 2008), assessing the forest biomass for use as energy (Viana et al., 2010) or to estimate the global carbon balance (Hese et al., 2005). Nowadays, the analysis of these issues over large areas is a common practice. The need of continuous maps where the phenomenon under study can be individually analysed or used as auxiliary variable in a specific model requires that the spatial predictions are represented in the most accurate way. Estimation of AGB has been made by a range of methods, from field measurements to remote sensing-based methods, as well GIS-based modelling approaches using auxiliary data (Lu, 2006).

Traditional approaches to estimate forest AGB over a large area consist in the implementation of forest inventories where a statistical sampling design is established to acquire data, or using data aggregated from stand level management inventories (McRoberts et al., 2010). Estimation using sample-based inventories involves field measurements where AGB is commonly assessed by applying allometric equations for specific species (Ter-Mikaelian and Korzukhin, 1997; Foroughbakhch et al., 2005; Zianis et al., 2005; Peichl and Arain, 2007), at the tree or shrub level, using the dendrometric variables (e.g. diameter-at-breast height, tree height, crown size and crown length) measured in each sample plot. The total biomass for a given area is achieved by applying expansion factors to the area of the sample plot and stand conversion tables. These approaches are widely used in several studies (e.g. Brown et al., 1989; Brown and Lugo, 1992; Fearnside, 1992; Gillespie et al., 1992; Fearnside, 1997; Houghton et al., 2001; Fournier et al., 2003). These estimation models are considered non-spatial as they do not provide the spatial distribution of AGB. To predict the spatial distribution of AGB throughout the territory, the calculated AGB in the

* Corresponding author at: Agrarian Superior School, Polytechnic Institute of Viseu, Quinta da Alagoa, 3500-606 Viseu, Portugal. Tel.: +351 232 446 600; fax: +351 232 426 536.
E-mail addresses: hviana@esav.ipv.pt, viana.h@gmail.com (H. Viana).

0304-3800/$ – see front matter © 2011 Elsevier B.V. All rights reserved.
doi:10.1016/j.ecolmodel.2011.11.027

forest inventory dataset is usually assigned to the forest polygons, stratified by species, and mapped by aerial photo interpretation.

Despite the field measurements being the most accurate methods for collecting biomass data, the level of precision of the resultant biomass map will depend of the land cover classification detail and of the sample intensity. In fact, the forest inventories data at regional or national scale are usually not spatially exhaustive to generate spatially AGB estimates, thus limiting the use of this approach over large areas. An additional limitation is the long temporal resolution of these estimations, which are made in cycles of 10 or more years. This is not compatible with the need of information on shorter time intervals, to analyse land cover changes, to quantify forest resources, or to monitor other environmental variables. In order to overcome these limitations and the need to produce more accurate spatially explicit large area biomass estimates led the researchers to explore different approaches to mapping biomass.

With the increasing availability of satellite imagery, remote sensing-based methods have been the most widely used approach to predict AGB over large areas, in recent years. The utility of the spectral information recorded by remote sensing for monitoring vegetation or gathering ecophysiological information over large areas is very well recognized (Jong et al., 2006), since satellite data became accessible for land cover dynamic studies. It has been demonstrated in several studies that the satellite spectral information (spectral band, band ratios, band transformations, etc.) has a good correlation with forest biomass and when combined with field measurements, is suitable for AGB estimation. Previous research using imagery data provided by distinct sensors and employing different approaches are summarized by Lu (2006). Although remotely sensed data cannot completely replace field sample data, it have been incorporated into operational forest inventories (McRoberts et al., 2010).

Several studies using remotely sensed data sources with different spatial-resolution and applying distinct approaches have been conducted in AGB spatial predictions. These approaches include direct estimations by means of Direct Radiometric Relationships (DRR), between spectral data response and biomass amount, using multiple regression analysis (Hame et al., 1997; Cohen et al., 2001, 2003; Reich et al., 2004; Labrecque et al., 2006; Muukkonen and Heiskanen, 2007; Zheng et al., 2007); by nonparametric approaches including K nearest neighbour (KNN) (Tomppo, 1991; Reese et al., 2002; Tomppo et al., 2002; Labrecque et al., 2006; Chirici et al., 2008; Tomppo et al., 2008) and neural network (Atkinson and Tatnall, 1997; Blackard and Dean, 1999; Muukkonen and Heiskanen, 2005), or indirect estimations. Is this case, characteristics such as crown diameter or leaf area index (LAI) are firstly derived from the remotely sensed data and subsequently are used in regression analysis to estimate biomass.

GIS-based approaches (Iverson et al., 1994; Magcale-Macandog et al., 2006) using ancillary data (e.g. Elevation, slope, soil, precipitation, etc.) have not been applied extensively for AGB estimation given the low availability of data, often not sufficiently precise, and the frequent low correlation between AGB and ancillary data.

Spatial models (algorithms) have been also used for spatially predict vegetation attributes. In general, these interpolation techniques are classified in deterministic and probabilistic models (Isaaks and Srivastava, 1989; Goovaerts, 1997; Burrough and McDonnell, 1998; Hengl, 2009). The deterministic approaches are models where arbitrary or empirical model parameters are used. No estimate of the model error is available and usually no strict assumptions about the variability of a feature exist (Hengl, 2009). Inverse distance weighting (IDW) and Thiessen polygons are the most widely used approach to execute interpolations and, in some situations, these can perform as well, or better, than other spatial prediction methods (Weber and Englund, 1992; Hengl, 2009). Attending that in the Earth sciences there is usually a lack of sufficient knowledge concerning how properties vary in space, a deterministic model may not be appropriate. Therefore, to make predictions at locations for which observations do not exist, with inherent uncertainty in predictions, the use of probabilistic models are necessary (Lloyd, 2007).

Spatial statistics and geostatistics were developed to describe and analyse the variation in both natural and man-made phenomena on, above or below the land surface (Cressie, 1993). Geostatistical models are reported in numerous textbooks (e.g. Isaaks and Srivastava, 1989; Cressie, 1993; Goovaerts, 1997; Deutsch and Journel, 1998; Hengl, 2009) such as Kriging (plain geostatistics); environmental correlation (e.g. regression-based); Bayesian-based models (e.g. Bayesian Maximum Entropy) and hybrid models (e.g. regression-kriging). Largely developed by Matheron (1963) in the 1960s, to evaluate recoverable reserves for the mining industry, over the years geostatistical models have been applied in a wide range of fields including modelling forest structure and attributes. Geostatistics and the theory of regionalized variables (Matheron, 1971) has been used to (Curran and Atkinson, 1988): explore and describe the presence of spatial variation that occur in most natural resource variables and in remotely sensed data (Curran, 1988; Woodcock et al., 1988); to design optimum sampling schemes for image data and ground data (McBratney and Webster, 1981; Hernández and Emery, 2009); and to increase the accuracy in which remotely sensed data can be used to classify land cover (Zhang and Franklin, 2002; Buddenbaum et al., 2005).

In recent years, several works has been conducted using geostatistical approaches to predict continuous forest variables. The motivation for using geostatistical analysis is that classical design-based methods are often weak for small area estimation within global inventories, and there is also an increasing demand to use regional or national inventory data for local estimation purposes (Mandallaz, 1993). However, the major limitation in using spatial statistical models is when forest variable datasets are spatially independent the lack of spatial structure makes it difficult, if not impossible to use optimal predictors such as Ordinary Kriging for modelling the spatial variability in the data (Reich et al., 2011). In a particular stand level spatial distribution of tree attributes i.e., basal area, height and density can be thought to be directly influenced by different spatially continuous variables such as solar radiation, soil characteristics and water nutrient availability, thus allowing considered spatially continuous (Kint et al., 2003).

Geostatistics has been used for mapping forest variables (e.g. basal area, density, LAI, tree height, standing volume, above-ground biomass, productivity, etc.) based on forest inventory data where these variables seemingly have spatial autocorrelation (Dungan, 1998; Nanos et al., 2004; Berterretche et al., 2005; Maselli and Chiesi, 2006; Mutanga and Rugege, 2006; Sales et al., 2007; Meng et al., 2009; Palmer et al., 2009; Pierce et al., 2009; Akhavan and Kia-Daliri, 2010). However, in large areas forest variables as AGB is not always spatially continuous because it is highly dependent on forest landscape structure and boundaries of forest patches affected by clear-cuttings of commercial forest management. Gilbert and Lowell (1997) trying to predict stem volume measured the spatial autocorrelation of two interpolation methods Thiessen polygons and kriging concluded that although areas of high volume do tend to cluster, i.e. are positively spatially autocorrelated, the forest did not behave as a continuous surface relative even to the densest sampling schema. Gunnarsson et al. (1998) used kriging estimation of stand variables such as total volume, annual volume increment, mean diameter and age and found positive autocorrelation. However, some variables (e.g. hardwood volume) does not exhibited any spatial autocorrelation in the scales studied, suggesting that only conducting an a priori assessment of spatial autocorrelation to determine interpolability may be misleading. Tuominen et al. (2003) combining data from remote sensing imagery with field measurements, and geostatistical interpolation for estimation of five forest variables (mean diameter, mean height, mean age, basal area, and volume) per sample plot and stand, found that the geostatistical interpolation, tested on the stand level estimation, did not improve the accuracy of the estimates. The same conclusion was reported by Freeman and Moisen (2007) who evaluating Kriging as a tool to improve forest biomass estimates concluded that map accuracy was not increased.

While some geostatistical models, such as Kriging, may not provide the desired solution to map AGB over large areas, it is necessary to explore new approaches. The studies exploring spatial prediction models Regression-kriging (RK) using field observations, in combination with various GIS data sources (e.g. remotely sensed data, soil and topographic variables, forest structure, etc.), as auxiliary information are not plentiful. However, some studies indicated good improvements using these approaches on forest variable estimation as volume mean annual increment (Palmer et al., 2009); basal area (Meng et al., 2009) and above-ground biomass (Sales et al., 2007), in comparison with other prediction methods.

In this study, we analysed different approaches to estimate crown biomass of *Pinus pinaster* stands and above-ground biomass of shrubland, including: direct radiometric relationships (DRR) methods and Regression-kriging (RK) with remotely sensed data as predictor. Moreover, deterministic interpolation techniques as Inverse distance weighting (IDW) and Thiessen polygons, and Kriging estimations are presented in order to compare the performance of these methods in large-scale mapping of forest biomass.

1.2. Direct Radiometric Relationships (DRR)

This method consist in establishing regression relationships, such as ordinary least squares (OLS), between the satellite spectral data, which can include the individual spectral bands, band ratios, vegetation indices and other possible transformations as independent variables, and the measured biomass at each corresponding inventory sample plot position. In this work, Landsat 5 TM and MODIS Vegetation indices were used as independent variables since they are referred in the literature as being well correlated with biomass availability.

1.3. Inverse Distance Weighting (IDW)

Inverse distance weighting (IDW) is a quick deterministic local interpolator that is exact and can be a good method to perform a preliminary analysis of an interpolated surface. It is often used as the default surface generation method to attribute sample locations (Lu and Wong, 2008). IDW explicitly implements the assumption that a value of an attribute at an unsampled location is a weighted average of known data points within a local neighbourhood surrounding the unsampled location (Burrough and McDonnell, 1998). To predict a value for any unsampled location, IDW will use the measured values surrounding the prediction location. Those measured values closest to the prediction location will have more influence on the predicted value than those farther away. Thus, the IDW formula has the effect of giving data points close to the interpolation point relatively large weights while those far away exert little influence. The higher the weight used the more influence points close to prediction location are given. The IDW predictor can be given as (Eq. (1)):

$$\hat{z}(x_0) = \frac{\sum_{i=1}^{n} z(x_i).d_{i0}^{-r}}{\sum_{i=1}^{n} d_{i0}^{-r}} \quad (1)$$

where the prediction for the location x_0 is a function of the n neighbouring observations, $z(x_i)$, $i = 1; 2; \ldots; n$, r is an exponent which determines the weight assigned to each of the observations, and d is the distance by which the prediction location x_0 and the observation location x_i are separated.

As the exponent becomes larger the weight assigned to observations at large distance from the prediction location becomes smaller. That is, as the exponent is increased, the predictions become more similar to the closest observations.

1.4. Thiessen polygons: nearest neighbours

Thiessen polygons also called Dirichlet or Voronoi polygons assign values to unsampled locations that are equal to the value of the nearest observation (Lloyd, 2007). This method is one of the earliest and simplest interpolation methods. They have been considered one of the fundamental structures in computational geometry and other fields such as GIS. In this method, the study area is partitioned into a set of polygons, each containing only one measurement point. Every point within a given polygon is closer to the measurement point than any other measurement points.

The region sampled, R, is divided by perpendicular bisectors between the N sampling points into polygons or tiles, V_i, $i = 1, 2, \ldots, N$, such that in each polygon all points are nearer to its enclosed sampling point x_i than to any other sampling point. The prediction at each point in V_i is the measured value at x_i, i.e. $z^*(x_0) = Z(x_i)$. The weights are (Webster and Oliver, 2007):

$$\lambda_i = \begin{cases} 1 & fx_i \in V_i \\ 0 & \text{otherwise} \end{cases}$$

The shortcomings of the method are evident; each prediction is based on just one measurement, there is no estimate of the error, and information from neighbouring points is ignored. When used for mapping the result is basic (Webster and Oliver, 2007). However, Thiessen polygons are used widely to provide a simple overview of the spatial distribution of values.

1.5. Ordinary Kriging (OK)

Kriging originated by (Krige, 1951) and developed by (Matheron, 1971) is widely known by the acronym BLUP, because it is the best linear unbiased predictor. The theory and mathematical formulation of kriging have been discussed thoroughly by several authors (e.g. Journel and Huijbregts, 1978; Isaaks and Srivastava, 1989; Cressie, 1993; Goovaerts, 1997). Kriging is a geostatistical method that takes into account both the distance and the degree of variation between known data points. The extent to which this assumption is true can be examined in the computed variogram. The several kriging models (kriging family) are elaborations of the basic generalized linear regression algorithm and corresponding estimator (Eq. (2)) differing by some assumptions (or knowledge) on the data (process) (Goovaerts, 1997; Deutsch and Journel, 1998):

$$[\hat{Z}_k(u) - m(u)] = \sum_{\alpha=1}^{n} \lambda_\alpha(u)[Z(u_\alpha) - m(u_\alpha)] \quad (2)$$

where $Z(u)$ is the random variable at location u, the u_α is the n data locations, $\lambda_\alpha(u)$ is the weight assigned to datum $Z(u_\alpha)$ which is a realization of $Z(u_\alpha)$, $m(u)$ and $m(u_\alpha)$ are the location-dependent expected value of $Z(u)$ and $Z(u_\alpha)$, and $\hat{Z}_k(u)$ is the linear regression estimator.

Ordinary Kriging (OK) filters the mean from Eq. (2) by requiring that the Kriging weights sum to one. The OK prediction $\hat{Z}_{OK}(u)$ is a linear weighted moving average of the available n observations defined as (Deutsch and Journel, 1998) (Eq. (3)):

$$\hat{Z}_{OK}(u) = \sum_{\alpha=1}^{n} \lambda_\alpha^{OK}(u) Z(u_\alpha) \quad (3)$$

Using Lagrange form, OK system is written as:

$$\begin{cases} \sum_{\beta=1}^{n} \lambda_{\beta}^{OK}(u)C(u_{\beta}-u_{\alpha})+\mu_{OK}(u)=C(u-u_{\alpha}) \\ \sum_{\beta=1}^{n} \lambda_{\beta}^{OK}(u)=1 \end{cases} \quad (\alpha=1,\ldots,n)$$

where $\lambda_{\beta}^{OK}(u)$ is the optimal weight, $C(u-u_{\alpha})$ is the covariance function between two points, and $\mu_{OK}(u)$ is the Lagrange parameter.

The corresponding minimized error variance, also called OK variance is expressed as (Eq. (4)):

$$\sigma_{OK}^2 = C(0) - \sum_{\alpha=1}^{n} \lambda_{\alpha}^{OK} C(u_{\alpha}-u) - \mu_{OK}(u) \tag{4}$$

The Ordinary Kriging cannot be used unless the regionalized variable has a constant mean although it is not known. Because the successive differences conceal the regional mean in the semivariogram calculations, this means that in the case of a systematic variation in the regional average such as abrupt changes, trends, oscillations, the Ordinary Kriging assumption of constant mean is violated. Therefore other estimation procedure, which should take into consideration these systematic mean variations, must be used (Sen, 2009).

1.6. Universal Kriging (UK) or kriging with internal drift

"Universal kriging" (UK), first introduced by Matheron (1969), is as a special case of kriging with changing mean where the trend is modelled as a function of cartographic coordinates (Deutsch and Journel, 1998; Webster and Oliver, 2007). Deutsch and Journel (1998) define this method as kriging with a trend model since the underlying random function model $Z(u)$ is the sum of a trend component, $m(u)$ plus a residual $R(u)$ (Eq. (5)):

$$Z(u) = m(u) + R(u) \tag{5}$$

The trend m is a deterministic, structural component that represents large scale variation. The residual is a stochastic component representing small scale, 'noisy' variation. The trend component is defined as $m(u) = E\{Z(u)\}$, and is fitted as $m(u) = \sum_{k=0}^{K} a_k f_k(u)$. The $f_k(u)$'s are known functions of the location coordinates and the a_k's are unknown parameters. The trend value $m(u)$ is itself unknown since the parameters a_k are unknown. The residual component $R(u)$ is usually modelled as a stationary random function with zero mean and covariance $C_R(h)$.

Using Lagrange formalism, UK system is written as:

$$\begin{cases} \sum_{\beta=1}^{n} \lambda_{\beta}^{UK}(u)C_R(u_{\alpha}-u_{\beta}) + \sum_{k=0}^{K} u_k^{UK}(u) f_k(u_{\alpha}) = C_R(u_{\alpha}-u) \\ \sum_{\beta=1}^{n} \lambda_{\beta}^{UK}(u)=1, \quad \sum_{\beta=1}^{n} \lambda_{\beta}^{UK}(u) f_k(u_{\beta}) = f_k(u) \end{cases} \quad (\alpha=1,\ldots,n),(k=0,\ldots,k)$$

where $\lambda_{\beta}^{UK}(u)$ is the optimal weight, $C_R(u_{\alpha}-u_{\beta})$ is the covariance function between two residual points, and $u_k^{UK}(u)$ is the Lagrange parameter.

The corresponding UK variance σ_{UK}^2 is (Eq. (6)):

$$\sigma_{UK}^2(u) = C_R(0) - \sum_{\alpha=1}^{n} \lambda_{\alpha}^{UK} C_R(u_{\alpha}-u) - \sum_{k=0}^{k} u_k^{UK}(u) f_K(u) \tag{6}$$

1.7. Regression-kriging (RK)

Regression-kriging (RK) (Odeh et al., 1994, 1995) is a hybrid method that involves either a simple or multiple-linear regression model (or a variant of the generalized linear model and regression trees) between the target variable and ancillary variables, calculating residuals of the regression, and combining them with kriging. Different types or variant of this process, but with similar procedures, can be found in literature, which can cause confusion in the computational process. RK defined by Ahmed and De Marsily (1987) as "Kriging with a guess field" involves regression, and calculation of the residuals. This is followed by kriging of the regression predicted values and the residuals separately, and summing both values together to obtain the final prediction. Knotters et al. (1995) define this method as "kriging combined with regression" where regression is performed, and followed by kriging of regressed values, whereas Goovaerts (1999) uses the term "Kriging after detrending" to refer the RK method. Hengl et al. (2004, 2007) makes a comprehensive analysis to the RK spatial prediction technique and compared it with the Kriging with external drift (KED) method (Goovaerts, 1997) concluding that they are equivalent and should, under the same assumptions, yield the same predictions.

In this paper we refer to RK according to Hengl et al. (2007) and Hengl (2009) and the proposed methodology of implementation (http://spatial-analyst.net) is followed. In the process of RK the predictions are combined from two parts; one is the estimate $\hat{m}(s_0)$ obtained by regressing the primary variable on the k auxiliary variables $q_k(s_0)$ and $q_0(s_0) = 1$; the second part is the residual estimated from kriging. RK is estimated as follows (Eqs. (7) and (8)):

$$\hat{z}_{rk}(s_0) = \hat{m}(s_0) + \hat{e}(s_0) \tag{7}$$

$$\hat{z}_{rk}(s_0) = \sum_{k=0}^{v} \hat{\beta}_k \cdot q_k(s_0) + \sum_{i=1}^{n} w_i(s_0) \cdot e(s_i) \tag{8}$$

where $\hat{\beta}_k$ are estimated drift model coefficients ($\hat{\beta}_0$ is the estimated intercept), optimally estimated from the sample by some fitting method, e.g. ordinary least squares (OLS) or, optimally, using generalized least squares (GLS), to take the spatial correlation between individual observations into account (Cressie, 1993); w_i are kriging weights determined by the spatial dependence structure of the residual and $e(s_i)$ are the regression residuals at location s_i.

2. Methods and data

2.1. Study area

The study area is located in the Centre-North of Portugal, extending from 39°11′53″N, 06°14′17″W to 42°50′50″N, 08°19′02″W (Fig. 1a). This is a heterogeneous region with a complex topography where the elevations ranging from 130 to 1500 m (Fig. 1b). The climatic factors are very variable during the year, with annual mean precipitation in the range of 800–2800 mm and annual mean temperatures ranging from 7.5 to 16 °C. These physical conditions make this region well-suited for forest growth. The land cover is fragmented with small amount of suitable soils for agriculture and the main areas are occupied by forest spaces. Forest activity is a direct source of income for a vast forest products industry, which employs a significant part of the population.

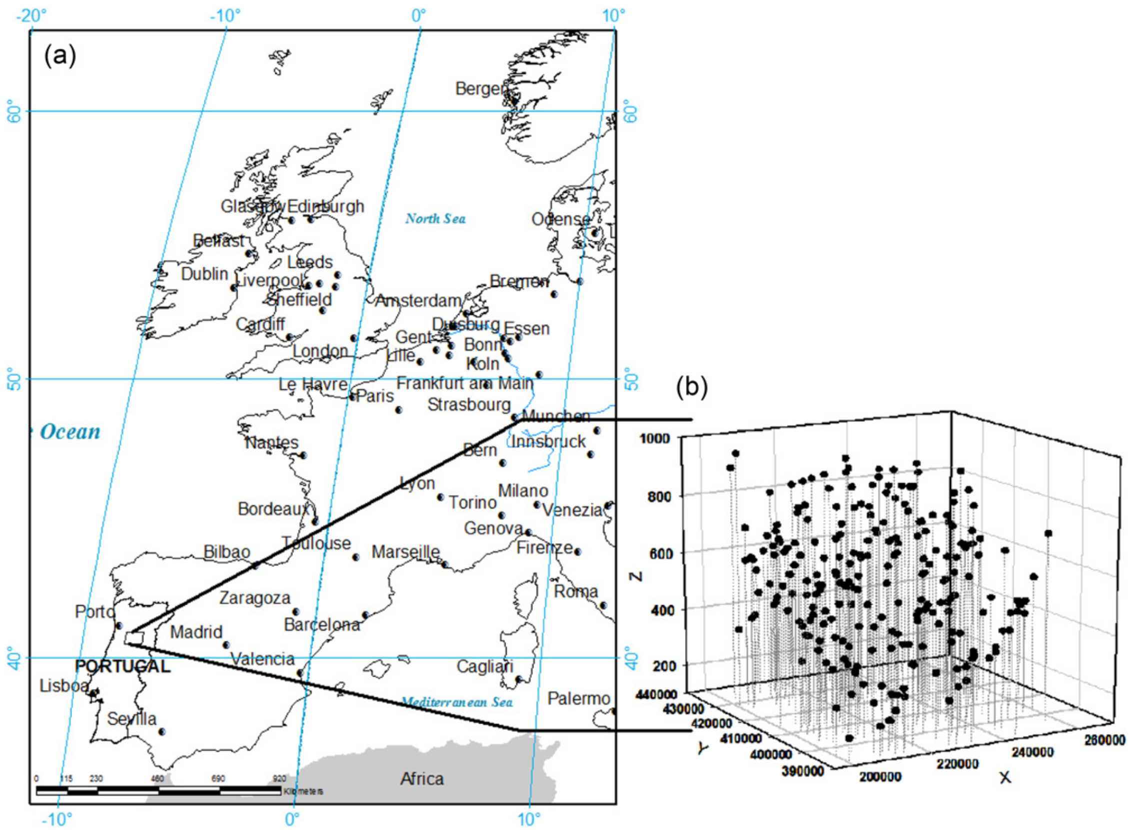

Fig. 1. Study area: (a) Geographical location, (b) Distribution of inventory samples plots, where x, y are the cartographic coordinates (Hayford-Gauss, Datum of Lisbon, IGeoE) and z is the altitude (m).

2.2. Field data

A systematic sampling design was implemented in the study area which include productive forest stands and shrubland areas. A total of 276 sample plots were located being 102 from shrubs, 132 from pure *P. pinaster* Aiton (maritime pine) stands and the remaining plots from *Eucalyptus globulus* (eucalyptus) and mixed stands. For the purpose of the present study, only the pure pine stands and shrubland areas were considered. The field data was collected in circular temporary sample plots within a fixed-area of 500 m^2, in the year 2006. The plots geographical locations were recorded by global navigation satellite systems (GNSS), georeferenced and structured in a geographic information system (GIS) database. In pine stands, the dendrometric parameters: diameter at breast height (dbh), total height of the tree (h) and canopy height (hc) were measured. The structural stand variables recorded in each plot were used to determine the stand characteristics such as age (t), number of trees per hectare (N), dominant tree height class (h_{dom}), basal area (G), crown closure class and site index (SI). In the shrubland areas the dominant height of vegetation (h_{dom}), the vegetation cover (%) and species composition were determined. This data was recorded in a GIS geodatabase, in the Portuguese Cartographic coordinates, to further analysis.

2.3. Biomass calculation from the inventory dataset

In order to achieve the biomass in the inventory dataset, different methodologies were followed for the two cover classes considered in the present study. In the pine stands only the so-called primary residues (parts of trees, unsuitable for saw timber such as branches and tops) were calculated and used in the spatially explicit biomass estimation (crown biomass), while for the shrub biomass the entire above-ground biomass was used. This option was due to the fact that the primary residues from pine stands and the shrubland biomass are often ignored in biomass estimations, and their use for energy has being increasing in the last years. As example, the Portuguese political strategy to generate combined heat and power (CHP) from biomass states that the main source of fuel should come from the residual biomass generated by forest activity, where the crown biomass represents the majority, and the other source of fuel should come from shrubs with the intention of reducing the wildfire hazard (see Viana et al., 2010). On the other hand, the isolated canopy cover had better adjustments with the spectral information extracted from the Landsat TM imagery data, than the biomass of the entire tree (stem and crown). In fact, after the canopy cover reaches its maximum the stem keep growing but the changes in reflectance are very small.

The crown biomass of pine stands was calculated using an allometric equation adjusted for the study area, which are presented further in Section 3.2, Table 2. A total of 100 trees were sampled within 10 maritime pine stands, using the destructive method. The trees were logged, measured (e.g. diameter at breast height, total height, canopy height) and the live crown weighted in situ. The moist content was determined in laboratory, for the conversion of biomass to dry weight. The measured variables were then used for adjustment of regression models, using the crown biomass (kg tree^{-1}) as dependent variable. To estimate the shrubland biomass 20 sample plots, with an area of 10 m^2, were established and the vegetation parameters measured (shrubs density, height and estimated age) using the line intersection method. The vegetation was divided by species composition and the total biomass was weighted in loco. The measured variables were used for adjustment of regression models using shrub AGB (ton ha^{-1}) as dependent variable, which are presented further in Section 3.2,

Table 1
Descriptive statistics of data measured in the inventory dataset.

	Pine stands plots ($n = 132$)								Shrubland plots ($n = 102$)	
	N (trees ha^{-1})	t (year)	h_{dom} (m)	dbh$_{dom}$ (cm)	SI (m)	BA (m^2 ha^{-1})	V (m^3 ha^{-1})	B_{cb} (ton ha^{-1})	Canopy cover (%)	B_{sr} (ton ha^{-1})
Mean	550.8	24.4	15.3	29.7	25.7	20.1	164.6	17.7	56.1	12.0
Min	20.0	8.0	6.0	10.8	16.5	0.4	1.4	1.3	5.0	0.795
Max	2138.5	51.0	29.4	69.9	40.1	68.3	574.1	39.9	100.0	36
SD	372.0	12.0	5.7	10.7	4.6	13.1	129.3	10.1	25.33	8.12

Where N is the number of stems; t is the stand age; h_{dom} is the dominant height; dbh$_{dom}$ is the dominant diameter at breast height; SI is the site index and is presented as meters at 35 years old; BA is the basal area; V is the stand commercial volume; B_{cb} is the biomass of crown and B_{sr} is the weight on dry base of biomass measured in the shrubland sample plots and n is the number of sampling plots established.

Table 2. These equations were then applied to calculate the AGB in the inventory dataset, according to the stand and shrub characteristics of each sample plot.

2.4. Remote sensing procedures

2.4.1. Remote sensing data

Two different remote sensing imagery data freely available from the US Geological Survey (USGS) Earth Resources Observation and Science (EROS) Centre were used in this research. A Landsat 5 Thematic Mapper (TM) image (Path/row: 204/032) acquired on 10 December 2006 and the Global MODIS vegetation indices dataset (h17v04) from the Moderate Resolution Imaging Spectroradiometer (MODIS) from 29 August 2006 (MOD13Q1.A2006241.h17v04.005.2008105184154.hdf). Atmospheric conditions were clear at the time of image acquisition, and the data had been corrected for the radiometric and geometric distortions of the images to the standard Level 1G before delivery.

2.4.2. Satellite image processing

All images pre-processing and processing was executed using the IDRISI GIS and Image Processing software (Eastman, 2006). Landsat 5 TM and MODIS were projected to the same Portuguese coordinate system (Hayford-Gauss, Datum Lisbon). Landsat 5 TM image geometric correction (Lillesand et al., 2004; Eastman, 2006) was made using ground control points (Toutin, 2004) and was radiometrically resampled by nearest neighbour. The overall root mean square (RMS) was 13.93 m. The TM raw digital numbers were then transformed to percent reflectance according Chavez (1996). MODIS data were brought to the same grid resolution as Landsat 5 TM (30 m) and it was coregistered to Landsat 5 TM image as base, with a RMS of 14.54 m. Supervised classifications of multispectral images were carried out, based in the Maximum Likelihood classifier (MLC) using the six reflective bands (1–5 and 7) of TM sensor, covering the spectral ranges from 0.45 to 1.75 μm and 2.09 to 2.35 μm. The cover types, pine and shrubs, were isolated and subsequently validated with the Corine Land Cover map from 2006 (CLC 06, IGP, 2010). These two maps were further used as mask and AGB estimations were made inside these areas.

2.4.3. Vegetation indices development

Vegetation indices, specially the Normalized Difference Vegetation Index (NDVI), have been extensively applied in studies of vegetation biomass (Atkinson et al., 2000; Chirici et al., 2007; Viana et al., 2009). The provided bands (1–5 and 7) from the TM sensor allowed to compute the Normalized Difference Vegetation Index (NDVI) as NDVI = (NIR − R)/(NIR + R), where Near-infrared (NIR) is radiation in waveband 4 and red (R) is radiation in waveband 3. NDVI measures both the amount of green vegetation and vegetation health, but it also is a basic indicator of changes in vegetation over space and time. The Global MOD13Q1 data includes the MODIS Normalized Difference Vegetation Index (NDVI) and a new Enhanced Vegetation Index (EVI) provided every 16 days at 250-m spatial resolution as a gridded level-3 product in the Sinusoidal projection (https://lpdaac.usgs.gov/lpdaac/products/modis_products_table/vegetation_indices/16_day_l3_global_250m/mod13q1). Additionally the Tasseled Cap transformation was performed, which is an orthogonal transformation, and the green vegetation index was expressed through the development of their second component (Eastman, 2006).

2.5. Direct Radiometric Relationships (DRR)

The field inventory data, within the GIS database, was superimposed on the TM and MODIS images data and then the individual pixel value (30 m × 30 m) and the nearest pixel values (90 m × 90 m) were attached to the field records. Regressions were performed for the two strata (pine forest and shrubs) individually and for all plots combined. The spectral information extracted from these images (NDVI, EVI and Tasseled Cap) was used as independent variables for developing regression models. Linear, logarithmic, exponential, power, and second-order polynomial functions were tested on the data. Multiple linear regressions were also tested to determine if a combination of several variables (e.g., crown closure, age, elevation, etc.) could improve the associations. The best models, for each stratum, were applied to the imagery data where the independent variable was derived, and the predicted aboveground biomass maps were produced. Depending on the applied model some biomass values predicted by the regression equations were negative. This happened in the low Vegetation index values, so these pixels were removed, because in reality negative biomass values are not possible. The imagery data in which the independent variable (vegetation index) presented the best regression with the AGB was subsequently used as predictor (auxiliary map) in the Regression-kriging spatial prediction method.

2.6. Geostatistical modelling

Geostatistics offers a collection of deterministic and statistical tools aimed at understanding and modelling spatial variability through prediction and simulation (Journel and Huijbregts, 1978; Goovaerts, 1997; Deutsch and Journel, 1998). Geostatistical procedures were performed with the GSTAT package included in IDRISI software both to automatically fit the variograms of residuals and to produce final predictions (Pebesma, 2001, 2004). GSTAT produces the predictions and variance map, which is the estimate of the uncertainty of the prediction model, i.e. precision of prediction. In this research, we employed Ordinary kriging (OK), Universal kriging (UK) and Regression-kriging (RK) spatial models. Geostatistical methods such as the semivariogram, also called the variogram, can be used to quantify the spatial variability of a random variable. The first stage of geostatistical modelling consists in computing the experimental variograms using the classical formula (Eq. (9)):

$$\hat{\gamma}(h) = \frac{1}{2N(h)} \sum_{i=1}^{N(h)} [z(x_i) - z(x_i + h)]^2 \qquad (9)$$

where $\hat{\gamma}(h)$ is the semivariance for distance h, $N(h)$ the number of pairs for a certain distance and direction of h units, while $z(x_i)$ and $Z(x_i+h)$ are measurements at locations x_i and x_i+h, respectively.

Two variogram models were developed: one for the pine crown biomass and one for the shrub AGB, which is satisfactory according to Webster and Oliver (1992). For fitting the experimental variograms we used the exponential, Gaussian, spherical models using iterative reweighted least squares estimation (WLS, Cressie, 1993). Semivariogram gives a measure of spatial correlation of the studied attribute. The variogram is a discrete function of variogram values at all considered lags (Curran, 1988; Isaaks and Srivastava, 1989). Typically, the semivariance values exhibit an ascending behaviour near the origin of the variogram and they usually level off at larger distances (the sill of the variogram). The semivariance value at distances close to zero is called the nugget effect. The distance at which the semivariance levels off is the range of the variogram and represents the separation distance at which two samples can be considered to be spatially independent.

At locations where two properties u and v have been measured it is possible to estimate the cross-variogram. The cross-variogram is used to characterize spatial dependency between two variables. This is given as (Lloyd, 2007) (Eq. (10)):

$$\hat{\gamma}_{uv}(h)=\frac{1}{2N(h)}\sum_{i=1}^{N(h)}\{[z_u(x_i)-z_u(x_i+h)]\cdot[z_v(x_i)-z_v(x_i+h)]\} \quad (10)$$

where $\hat{\gamma}_{uv}(h)$ is the cross-semivariance between variables u and v, $N(h)$ is the number of pairs of data locations separated by lag distance h, z_u is the value of variable u at locations x_i and (x_i+h) and z_v is the data value of variable v at the same locations.

2.7. Validation and assessment of the prediction techniques

To compare the different AGB prediction approaches, we examined the discrepancies between the known data and the predicted data. It is common to check the consistency of interpolation methods using the cross-validation procedure, in which each sample value is removed one at a time from the data set (Leave-One-Out), and that location is predicted from the remaining data (Goovaerts, 1997; Deutsch and Journel, 1998). However, according (Davis, 1987) cross-validation cannot confirm that a particular model is or is not the optimum. It is a method to better examine and understand the phenomenon under study using the available data. On other side, as we intended to compare the geostatistical approaches with the deterministic (IDW and Thiessen polygons) and DRR predictions, we adopted the methodology of dividing the locations randomly into two sets: the prediction set and the validation set. Webster and Oliver (1992) consider that more reliable estimation of semivariogram values requires at least 150 observations, and larger samples are needed to describe anisotropic direction-dependent variation. This does not mean, however, that geostatistics cannot be applied to smaller data sets (Goovaerts, 1997). The prediction approaches were evaluated by comparing the basic statistics of predicted AGB maps (i.e., mean and standard deviation) and the difference between the known data and the predicted data were examined using the mean error, or bias mean error (ME), the mean absolute error (MAE), standard deviation (SD) and the root mean squared error (RMSE), which measures the accuracy of predictions, as described in Eqs. (11)–(14).

$$\mathrm{SD}=\sqrt{\frac{1}{N-1}\sum_{i=1}^{N}(e_i-\bar{e})^2} \quad (11)$$

Table 2
Allometric equations used to estimate biomass in the field plots.

Cover type	Equation	R^2
Pine	$\mathrm{AGB_{pine}}=19,284.26d^{2.299}h^{-07902}$	0.81
Shrub	$\mathrm{AGB_{Srb}}=0.0258[(\mathrm{Cc})(h_{\mathrm{srb}})]^{0.754}$	0.89

Where $\mathrm{AGB_{pine}}$ is the crown biomass (kg tree^{-1}), d_{bh} is the diameter at breast height (m), h_t is the mean height of tree (m), h_c is the height of live canopy (m), $\mathrm{AGB_{srb}}$ is the biomass of srub (ton ha^{-1}), Cc is the crown closure (%) and h_{srb} is the mean height of shrubs (cm).

$$\mathrm{ME}=\frac{1}{N}\sum_{i=1}^{N}(\hat{e}_i-e_i) \quad (12)$$

$$\mathrm{MAE}=\frac{1}{N}\sum_{i=1}^{N}|\hat{e}_i-e_i| \quad (13)$$

$$\mathrm{RMSE}=\sqrt{\frac{1}{N}\sum_{i=1}^{N}(\hat{e}_i-e_i)^2} \quad (14)$$

where N is the number of values in the dataset, $\hat{e}_i$ is the estimated biomass, e_i is the biomass values measured on the validation plots and $\bar{e}$ is the mean of biomass values of the sample.

3. Results and discussion

3.1. Descriptive statistics of study sites

The descriptive statistics of pine stands' crown biomass and shrubland's above-ground biomass, measured during field work and recorded in the inventory dataset, are presented in Table 1. The pine stands are highly heterogeneous, with ages ranging from 8 to 51 years old and the crown biomass ranging from 1.3 to 36 ton ha^{-1}. The shrubland areas are also heterogeneous, with canopy density ranging from 5 to 100%, and the biomass per hectare ranging from 0.79 to 36 ton ha^{-1}.

3.2. Above-ground biomass calculation from the inventory dataset

Based on the destructive sample approach, several allometric equations were adjusted, at plot level, to calculate the AGB in the inventory dataset. The analysis of the correlation coefficients (R), coefficients of determination (R^2), adjusted coefficients of determination (R^2_{adj}), the significance of the Student t-test, and the root mean square error (RMSE) allowed to select the best equations to predict the biomass of pine ($R^2=0.81$) and shrub ($R^2=0.89$), as presented in Table 2.

3.3. Relation between above-ground biomass and remote sensing data

The correlation analyses between calculated AGB in sample plots and predictors (spectral bands, vegetation indices, Tasseled Cap transformation, principal components), shows that vegetation indices were better correlated with biomass. Hence, several regression models were developed using stand-wise forest inventory data and Landsat TM and MODIS vegetation indices. The best results are presented in Table 3.

The best equations were achieved with NDVI derived from Landsat 5 TM, as independent variable, both for pine stands and shrub land, as presented in Fig. 2. The better results using the higher spatial resolution of Landsat TM data are due to the fact that the effect of mixed pixels is reduced compared to coarse resolution MODIS

Table 3
Regression models developed using stand-wise forest inventory data and Landsat 5 TM and MODIS image data.

Cover type	Model	Independent variable	α	β	δ	R^2	RMSE (ton ha^{-1})	Average predict biomass (ton ha^{-1})
Pine stands	$y=\alpha \cdot x^{\beta}$	NDVI (TM)	112.9820	2.4018	25.335	0.52	7.48	16.1
	$y=\alpha+\beta x+\delta x^2$		−14.0787	62.0106		0.49	7.24	17.7
	$y=\alpha \cdot e^{\beta x}$		1.0957	5.9478		0.51	7.88	16.2
	$y=\alpha+\beta x$		−18.4745	83.5498		0.49	7.22	17.7
	$y=\alpha \cdot x^{\beta}$	NDVI (MODIS)	49.2270	2.4034	−188.857	0.22	6.52	15.1
	$y=\alpha+\beta x+\delta x^2$		−76.1399	271.2939		0.17	9.28	17.7
	$y=\alpha \cdot e^{\beta x}$		1.2411	4.0514		0.21	9.89	15.1
	$y=\alpha+\beta x$		−12.1289	49.3060		0.15	9.35	17.7
	$y=\alpha \cdot x^{\beta}$	EVI (MODIS)	151.1559	2.0062	−262.456	0.23	3.89	15.2
	$y=\alpha+\beta x+\delta x^2$		−34.9565	252.3460		0.20	9.07	17.7
	$y=\alpha \cdot e^{\beta x}$		1.9357	6.3878		0.22	9.64	15.2
	$y=\alpha+\beta x$		−9.2017	85.6510		0.20	9.08	17.7
Shrubland	$y=\alpha \cdot x^{\beta}$	NDVI (TM)	33.9450	1.1064	57.4804	0.50	5.73	10.5
	$y=\alpha+\beta x+\delta x^2$		2.9293	3.3927		0.59	5.28	12.0
	$y=\alpha \cdot e^{\beta x}$		2.2121	4.1548		0.55	5.43	10.9
	$y=\alpha+\beta x$		−2.6106	42.6519		0.56	5.38	12.0
	$y=\alpha \cdot x^{\beta}$	NDVI (MODIS)	39.9192	2.2160	−14.8373	0.32	7.38	10.1
	$y=\alpha+\beta x+\delta x^2$		−12.5798	54.86892		0.25	7.12	12.0
	$y=\alpha \cdot e^{\beta x}$		0.9470	4.322952		0.31	7.45	10.1
	$y=\alpha+\beta x$		−8.6513	39.3024		0.25	7.08	12.0
	$y=\alpha \cdot x^{\beta}$	EVI (MODIS)	73.6125	1.5601	−20.3535	0.24	7.47	9.9
	$y=\alpha+\beta x+\delta x^2$		−4.7182	67.3874		0.23	7.19	12.0
	$y=\alpha \cdot e^{\beta x}$		2.1054	5.4164		0.23	7.51	9.9
	$y=\alpha+\beta x$		−3.0693	55.4241		0.23	7.16	12.0

Where y is the biomass (ton ha^{-1}) and α, β, δ are the coefficients of regression.

data. In TM data (30 m) the average reflectance of forest stands and shrubland is more pure than that of 250 m resolution MODIS pixels. These regression models were further used to map the biomass by the DRR method and the NDVI TM image was used as auxiliary variable in RK spatial prediction method.

3.4. Geostatistical predictions

To spatially estimate AGB by geostatistical modelling the experimental semivariograms were computed and analysed at first stage. The directional semivariograms of the residuals did not show an evident behaviour of anisotropy, thus an isotropic pattern was considered. The omnidirectional semivariograms were tested and its Exponential, Gaussian and Spherical models were fitted using Eq. (9). While the shrub biomass showed a clear spatial dependence (Fig. 3) the crown biomass of pine stands presented lower spatial autocorrelation (Fig. 4). The high nugget effect, visible in the figure, which under ideal circumstances should be zero, indicates that there is a significant amount of error present in the data due to the short scale variation, principally in pine data. In fact, in surveys covering large geographical regions, the residuals from the regression model may lack spatial structure because the large distances separating sample data locations. As reported by different authors (Gilbert and Lowell, 1997; Gunnarsson et al., 1998) forest variables are not always spatially continuous because it is highly dependent on forest landscape structure even to the densest sampling schema. In shrubland this is not so evident, since these areas have a higher spatial continuity, thus presenting an autocorrelation on the variable studied. For shrub, automated variograms modelling gave a small nugget and larger range parameter (6.35 km, 7.09 km and 13.09 km for exponential, Gaussian and spherical models, respectively), whereas for pine the range parameter was fairly shorter

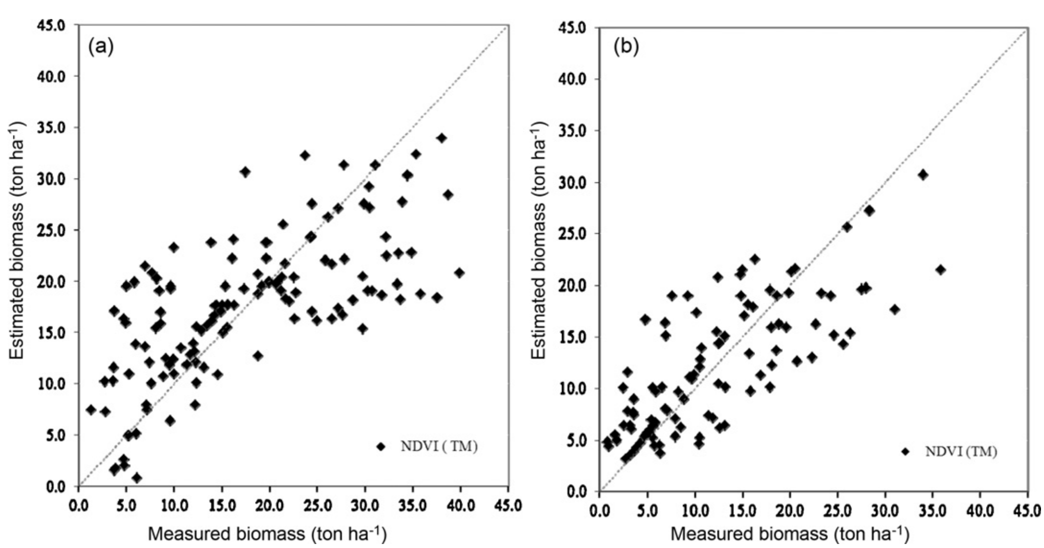

Fig. 2. Scatter plots of measured biomass versus estimated biomass from regression equations with NDVI as independent variable (a) pine and (b) shrubland. A 1:1 line (black, dashed) is provided for reference.

Table 4
Shrub and Pine AGB estimation models evaluation using the validation sample plots.

	ME (ton ha^{-1})		MAE (ton ha^{-1})		RMSE (ton ha^{-1})		SD (ton ha^{-1})	
	Pine	Shrub	Pine	Shrub	Pine	Shrub	Pine	Shrub
IDW	0.33	0.23	8.34	5.74	10.56	7.46	3.44	4.39
Thiessen	−0.39	8.89	9.10	10.30	11.68	12.23	10.34	6.20
DRR	0.62	0.34	3.93	2.87	5.60	3.69	7.84	4.85
OK (exponential)	1.35	0.52	6.77	6.18	8.02	7.60	4.24	4.39
OK (Gaussian)	1.46	0.77	6.76	6.41	7.79	7.52	4.03	4.01
OK (spherical)	1.36	0.65	6.80	6.36	8.03	7.56	4.17	4.07
UK (exponential)	1.17	0.39	6.59	6.35	7.64	7.57	3.09	4.69
UK (Gaussian)	1.37	0.22	6.87	6.25	8.06	7.62	4.11	4.82
UK (spherical)	1.32	0.48	6.60	5.69	7.71	6.85	3.61	3.47
RK (exponential)	0.61	0.74	4.05	3.65	5.46	4.33	8.11	5.82
RK (Gaussian)	0.55	1.01	4.09	3.99	5.52	4.61	8.16	5.98
RK (spherical)	0.62	0.75	4.04	3.65	5.53	4.27	8.13	5.77

(2.3 km, 2.9 km and 6.3 km for exponential, Gaussian and spherical models, respectively). Despite the exponential model fit better the shrub biomass (nugget of 22, a partial sill of 56, and a range of 6.35 km) and the spherical model fit better the pine stand biomass (nugget of 88, a partial sill of 19, and a range of 6.3 km) we used all the fitted models in the geostatistical spatial predictions (OK, UK and RK) to evaluate which is more effective in the predictions all over the study area.

3.5. *Validation of spatial distribution methods of above-ground biomass*

The validation of spatial prediction methods, based on random samples outside of the training data set, was made by comparing the basic statistics of predicted AGB maps (Table 4). In the pine AGB predictions 100 observations were used for the prediction and 32 for validation. In the shrub AGB predictions 81 observations were used for predictions and 21 for validation. Training and validation sets were compared, by means of a Student's *t* test (t_{pine} = 0.856 ns; t_{shrub} = 0.746 ns), in order to check if they provided unbiased subsets of the original data.

In both shrub and pine biomass estimations the mean error (ME), which should ideally be zero if the interpolation method is unbiased, suggests that all predictions are slightly biased. Analysing the mean absolute errors (MAE) it is clear that DRR approach achieved the lowest errors however, RK method had a similar performance. The archived RMSE in pine estimations was lower in RK than in DRR approach but in shrub estimations DRR provided inferior RMSE values than RK approach (Table 4 and Fig. 5). The best results in pine biomass predictions originated a RMSE = 32.2% of the mean (17.4 ton ha^{-1}) for DRR approach and a very similar result for the RK(exponential) approach, with a RMSE = 31.4% of the mean (17.4 ton ha^{-1}). Shrub biomass estimation based on DRR approach resulted in a RMSE = 31.8% of the mean (11.6 ton ha^{-1}) and RK(spherical) resulted in a RMSE = 35.6% of the mean (12 ton ha^{-1}).

Table 5
Results from ANOVA to compare the differences between the means of the different prediction methods.

Source	DF	SS	MS	*F*	*P*
Pine					
Between	11	279.5	25.407	0.65	0.7863
Within	372	14564.5	39.152		
Total	383	14844			
Shrub					
Between	11	1348.08	122.553	5.01	0
Within	240	5866.51	24.444		
Total	251	7214.59			

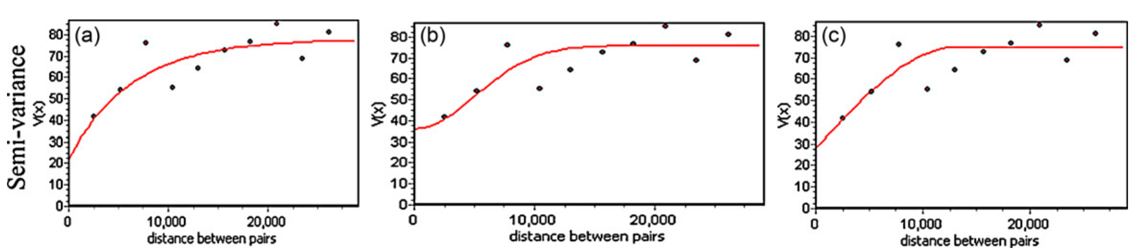

Fig. 3. Experimental omnidirectional semivariogram for shrub biomass: (a) exponential [22.000000 Nug(0) + 56 Exp(6350)]; (b) Gaussian [36.000000 Nug(0) + 40 Gau(7090)] and (c) spherical models [28.000000 Nug(0) + 47 Sph(13090)].

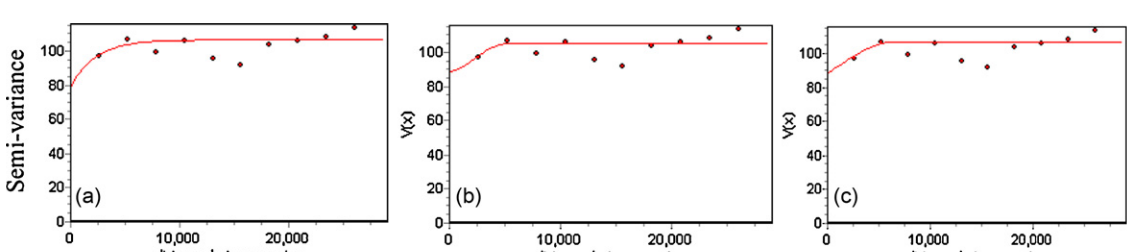

Fig. 4. Experimental omnidirectional semivariogram for pine biomass: (a) exponential [79.000000 Nug(0) + 28 Exp(2300)]; (b) Gaussian [89.000000 Nug(0) + 17 Gau(2900)] and (c) spherical models [88.000000 Nug(0) + 19 Sph(6300)].

Table 6
Tukey HSD all-pairwise comparisons test.

Method	Pine AGB		Shrub AGB	
	Mean	Tukey group	Mean	Tukey group
IDW	15.25	A	11.49	B
Thiessen	16.40	A	20.14	A
DRR	17.41	A	11.60	B
OK (exponential)	18.14	A	11.78	B
OK (Gaussian)	18.25	A	12.03	B
OK (spherical)	18.15	A	11.91	B
UK (exponential)	17.96	A	11.64	B
UK (Gaussian)	18.16	A	11.48	B
UK (spherical)	18.11	A	11.74	B
RK (exponential)	17.40	A	12.00	B
RK (Gaussian)	17.35	A	12.26	B
RK (spherical)	17.41	A	12.01	B

Table 7
Summary statistics of crown biomass of pine stands maps estimated from spatial prediction methods.

Method	Pixels	Area (ha)	Mean (ton ha^{-1})	Std (ton ha^{-1})	AGB (total ton)
IDW	842,408	75,816.7	18.24	5.70	1,383,156
Thiessen	842,408	75,816.7	18.08	10.31	1,370,511
DRR	815697	73,412.7	19.78	8.14	1,452,329
OK (exponential)	842,408	75,816.7	18.11	4.01	1,373,003
OK (Gaussian)	842,408	75,816.7	18.21	3.81	1,380,243
OK (spherical)	842,408	75,816.7	18.10	3.96	1,372,373
UK (exponential)	842,408	75,816.7	18.04	3.19	1,367,642
UK (Gaussian)	842,408	75,816.7	18.04	3.20	1,367,498
UK (spherical)	842,408	75,816.7	18.04	3.19	1,367,642
RK (exponential)	810,690	72,962.1	20.07	8.09	1,464,183
RK (Gaussian)	809,462	72,851.6	20.06	8.10	1,461,312
RK (spherical)	809,372	72,843.5	20.08	8.09	1,462,572

Table 8
Summary statistics of shrub AGB maps estimated from spatial prediction methods.

Method	Pixels	Area (ha)	Mean (ton ha^{-1})	Std (ton ha^{-1})	AGB (total ton)
IDW	1,268,228	114,141	11.36	4.46	1,296,347
Thiessen	1,268,228	114,141	10.83	8.13	1,235,867
DRR	1,268,228	114,141	10.80	5.54	1,232,276
OK (exponential)	1,268,228	114,141	11.69	4.02	1,333,860
OK (Gaussian)	1,268,228	114,141	11.85	3.88	1,352,688
OK (spherical)	1,268,228	114,141	11.83	3.85	1,350,573
UK (exponential)	1,268,228	114,141	11.67	4.62	1,331,610
UK (Gaussian)	1,268,228	114,141	11.62	4.63	1,326,543
UK (spherical)	1,268,228	114,141	11.90	3.45	1,357,917
RK (exponential)	1,237,251	111,353	11.18	5.98	1,245,362
RK (Gaussian)	1,238,493	111,464	11.22	6.01	1,250,744
RK (spherical)	1,238,644	111,478	11.23	6.00	1,251,459

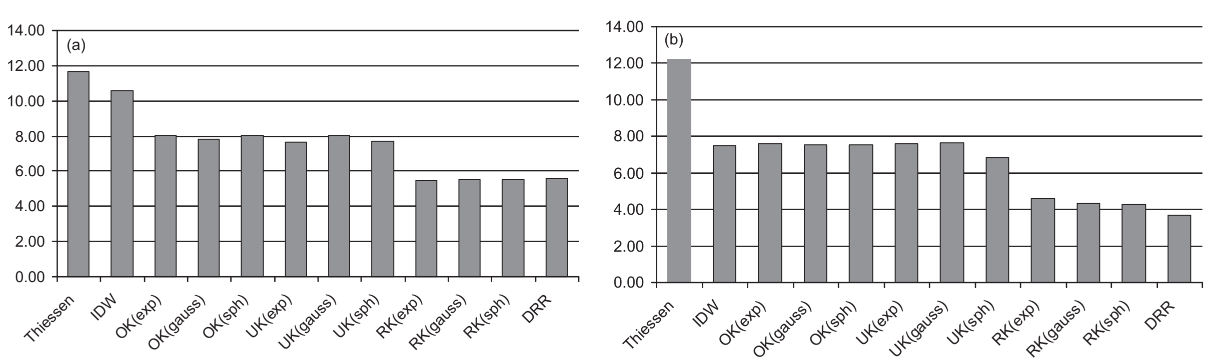

Fig. 5. Comparison of Root Mean Square Errors (RMSE) (a) pine and (b) shrub.

Table 9
Spatial correlation coefficients calculated between pine crown biomass maps.

	IDW	Thiessen	DRR	OK (exp)	OK (gauss)	OK (sph)	UK (exp)	UK (gauss)	UK (sph)	RK (exp)	RK (gauss)	RK (sph)
IDW	1											
Thiessen	0.81	1										
DRR	0.19	0.10	1									
OK (exponential)	0.74	0.49	0.26	1								
OK (Gaussian)	0.66	0.41	0.26	0.95	1							
OK (spherical)	0.70	0.46	0.27	1.00	0.95	1						
UK (exponential)	0.60	0.34	0.30	0.90	0.91	0.91	1					
UK (Gaussian)	0.60	0.34	0.30	0.90	0.91	0.91	1.00	1				
UK (spherical)	0.70	0.44	0.29	0.97	0.96	0.97	0.97	0.97	1			
RK (exponential)	0.28	0.17	0.99	0.35	0.34	0.35	0.37	0.37	0.37	1		
RK (Gaussian)	0.27	0.16	0.99	0.31	0.30	0.31	0.33	0.33	0.34	1.00	1	
RK (spherical)	0.25	0.15	0.99	0.30	0.29	0.30	0.33	0.33	0.33	1.00	1.00	1

Table 10
Spatial correlation coefficients calculated between shrub AGB map estimates.

	IDW	Thiessen	DRR	OK (exp)	OK (gauss)	OK (sph)	UK (exp)	UK (gauss)	UK (sph)	RK (exp)	RK (gauss)	RK (sph)
IDW	1											
Thiessen	0.84	1										
DRR	0.24	0.18	1									
OK (exponential)	0.90	0.73	0.28	1								
OK (Gaussian)	0.80	0.62	0.28	0.97	1							
OK (spherical)	0.84	0.66	0.29	0.98	0.99	1						
UK (exponential)	0.87	0.69	0.26	0.94	0.91	0.92	1					
UK (Gaussian)	0.87	0.72	0.26	0.94	0.92	0.93	0.99	1				
UK (spherical)	0.90	0.69	0.30	0.92	0.85	0.88	0.85	0.86	1			
RK (exponential)	0.42	0.35	0.90	0.44	0.42	0.42	0.41	0.41	0.40	1		
RK (Gaussian)	0.39	0.32	0.90	0.43	0.43	0.43	0.41	0.41	0.38	0.99	1	
RK (spherical)	0.41	0.35	0.90	0.42	0.41	0.41	0.40	0.40	0.39	1.00	0.99	1

The results indicate that determinists and geostatistical (OK and UK) approaches are not efficient to map these type of forest variables, as spatial structure in field biomass data is weak, as concluded by others (Gilbert and Lowell, 1997; Gunnarsson et al., 1998; Tuominen et al., 2003; Freeman and Moisen, 2007). Nevertheless, despite DRR was the most efficient method to map AGB, RK approach can be considered to explore in future studies with the aim of improve biomass estimation accuracy, were autocorrelation between variables exists.

In order to compare the mean values, of crown biomass and shrub biomass estimated by the interpolation methods, analysis of variance (ANOVA) was performed (Table 5). The results show that, at alpha level 0.05, the differences between the means are not significant between the pine AGB maps, but for shrub AGB maps the test failed to reject the null hypothesis that means were equal. Hence, the Tukey HSD All-Pairwise Comparisons Test was carried out to examine the differences between the interpolation methods used (Table 6). For pine AGB maps the test confirmed that there are no significant pairwise differences among the biomass means that emanated from all the interpolation methods used, but for shrub AGB maps there are 2 groups (A and B) in which the Thiessen method is statistically different from the other studied methods, as indicated in Table 6. Despite that, curiously, the average values of biomass were statistically similar between almost all methods, it just means that interpolations over large areas based on these methods (deterministic and geostatistical where there is no apparent autocorrelation of the variables) can be misleading. In fact, spatially explicit biomass estimation is only reliable by using remote sensing (e.g. DRR or k-NN) or by using remote sensing data, as auxiliary variable, in techniques such as RK, where the

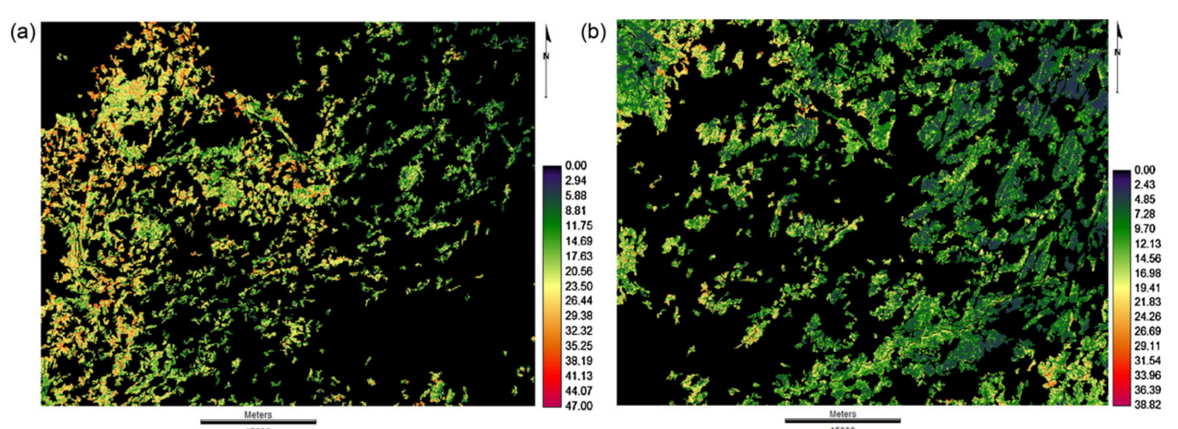

Fig. 6. Spatially explicit AGB estimates (ton ha^{-1}) for the study area (the colour gradation represents the vegetation and the black colour represents other land cover types, i.e. no data) generated from DRR spatial prediction method (a) pine stands and (b) shrubland.

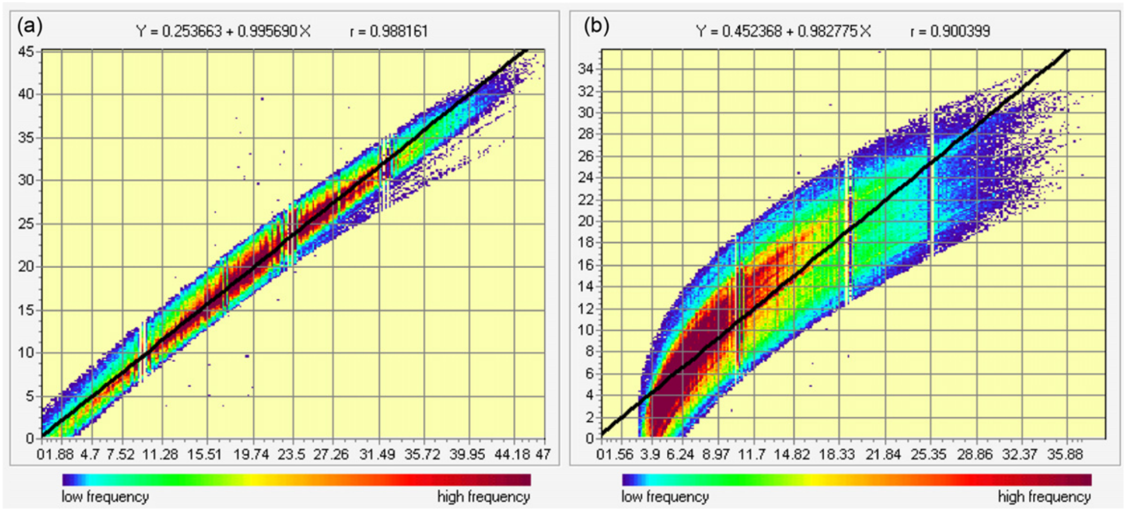

Fig. 7. Regression performed between DRR and RK Biomass maps, where x and y is the biomass in ton ha^{-1} (a) pine stands and (b) shrubland.

existence of autocorrelation between the variables could improve the estimates.

3.6. Quantitative comparison of AGB mapping methods

Estimates of the crown biomass of pine stands and shrubland AGB (ton ha^{-1}) are shown in Tables 7 and 8, respectively. Furthermore, Fig. 6 shows the biomass maps derived by DRR method for the entire study area. The biomass estimates, both the average values (ton ha^{-1}) and the total biomass, shows a clear distinction between the DRR and RK methods and the other spatial prediction methods. As concluded by the analysis of the statistics of the validation dataset, the deterministic approaches and Kriging methods are unsuitable to these mapping purposes as they tend to suppress variance of estimations (Tables 7 and 8). Hence, comparing the DRR and RK approaches the differences in the total biomass is less than 1% in the best estimates. Another interesting conclusion is that the differences between the total biomass estimated by RK approach are minor using the Exponential, Gaussian or Spherical models in the experimental variogram. The correlation coefficients, presented in Tables 9 and 10 calculated for comparing pine and shrub AGB maps, respectively, confirm the similar results between DRR and RK estimations. Fig. 7a and b shows the high correlation existent between the two biomass maps (DRR × RK) of pine stand and shrubland, respectively.

Despite these results, RK method did not improve the biomass map estimation, given the low spatial autocorrelation observed on the data (Figs. 3 and 4). However, this method can be exploited in the case of geographical location of sample plots are denser, or forested areas have a greater spatial continuity, not being so dependent on forest landscape structure and boundary lines of forest patches, as these Mediterranean forests.

4. Conclusion

This study compared the spatial prediction methods Direct Radiometric Relationships (DRR) and Regression-kriging (RK), to estimate crown biomass of *P. pinaster* stands and shrubland above-ground biomass. Moreover, Ordinary Kriging (OK), Universal Kriging (UK), Inverse Distance Weighted (IDW) and Thiessen Polygons estimations were performed. The results showed, as expected, that the deterministic approaches are not suitable for mapping biomass. The same occurs with geostatistical interpolation methods as kriging, as they are dealing with the idea that it occurs spatial autocorrelation between neighbouring field measurement points, which is not a reality in the scattered mosaic of the studied forest landscape. However, as in much of the time the users employ spatial prediction techniques to visually understand the distribution of biomass, Kriging or deterministic models can be used, as they are easily implemented. Remote sensing is the only way, to provide spatially distributed information of the landscape structure (Jong et al., 2006) of intermediate areas between field measurements so, methods using remotely sensed data, as DRR, are the suitable way to map biomass. RK predictions, using remotely sensed data as auxiliary predictor, did not improve the AGB estimations, which is associated to the low spatial dependence observed on the data. Thus, denser sampling schemes and different auxiliary variables should be explored, in order to test if the accuracy of predictions is improved.

The results provided by DRR and RK methods showed the advantages of using the association between remotely sensed data and ground inventory data in spatial mapping. However, it should be noted that the cover types under study presented a homogeneous diversity (pure pine stands and shrubland) which allows a moderately to high correlation between vegetation characteristics and spectral response. Thus, if the objective is to map heterogeneous land cover types (e.g. mixed stands, different crown closure, etc.) the differences between spectral characteristics will increase, which will add noise to the prediction models based in remote sensed data. So, stratification of forest cover should be needed before using this approach.

The RK method has the advantage of generating estimates for the spatial distribution of AGB and its uncertainty for the study area. The uncertainty maps allow the evaluation of the reliability of estimates by identifying the locals with major uncertainties which can be useful for example to select different estimation methods for those areas.

Despite RK has been increasingly used, this method has some obstacles which difficult its popularization. Since then, different names and approaches are presented in the literature about the regression-kriging theory, which leads to a confusion by the common users. An additional limitation is that RK is more sophisticated and computationally demanding than other techniques, and therefore still exist a lack of user-friendly GIS environments to run RK.

Independently of the spatial prediction method applied, these techniques are a complement to the traditional field inventories as surveys continue to be needed to collect the input data and to assess the results of spatial prediction.

Acknowledgement

Authors would like to express their acknowledgement to the Portuguese Science and Technology Foundation (FCT), programme SFRH/PROTEC/49626/2009.

References

Ahmed, S., De Marsily, G., 1987. Comparison of geostatistical methods for estimating transmissivity using data on transmissivity and specific capacity. Water Resources Research 23, 1717–1737.
Akhavan, R., Kia-Daliri, H., 2010. Spatial variability and estimation of tree attributes in a plantation forest in the Caspian region of Iran using geostatistical analysis Caspian. Journal of Environmental Sciences 8, 163–172.
Atkinson, P.M., Foody, G.M., Curran, P.J., Boyd, D.S., 2000. Assessing the ground data requirements for regional scale remote sensing of tropical forest biophysical properties. International Journal of Remote Sensing 21, 2571–2587.
Atkinson, P.M., Tatnall, A.R.L., 1997. Introduction neural networks in remote sensing. International Journal of Remote Sensing 18, 699–709.
Berterretche, M., Hudak, A.T., Cohen, W.B., Maiersperger, T.K., Gower, S.T., Dungan, J., 2005. Comparison of regression and geostatistical methods for mapping Leaf Area Index (LAI) with Landsat ETM+ data over a boreal forest. Remote Sensing of Environment 96, 49–61.
Blackard, J.A., Dean, D.J., 1999. Comparative accuracies of artificial neural networks and discriminant analysis in predicting forest cover types from cartographic variables. Computers and Electronics in Agriculture 24, 131–151.
Brown, S., Gillespie, A.J.R., Lugo, A.E., 1989. Biomass estimation methods for tropical forests with applications to forest inventory data. Forest Science 35, 881–902.
Brown, S., Lugo, A., 1992. Aboveground biomass estimates for tropical moist forests of Brazilian Amazon. Interciencia 17, 8–18.
Buddenbaum, H., Schlerf, M., Hill, J., 2005. Classification of coniferous tree species and age classes using hyperspectral data and geostatistical methods. International Journal of Remote Sensing 26, 5453–5465.
Burrough, P.A., McDonnell, R.A., 1998. Principles of Geographical Information Systems. Oxford University Press Inc., New York, 333 pp.
Chavez, P.S.J., 1996. Image-based atmospheric corrections-revisited and improved. Photogrammetric Engineering and Remote Sensing 62, 1025–1036.
Chirici, G., Barbati, A., Corona, P., Marchetti, M., Travaglini, D., Maselli, F., Bertini, R., 2008. Non-parametric and parametric methods using satellite images for estimating growing stock volume in alpine and Mediterranean forest ecosystems. Remote Sensing of Environment 112, 2686–2700.
Chirici, G., Barbati, A., Maselli, F., 2007. Modelling of Italian forest net primary productivity by the integration of remotely sensed and GIS data. Forest Ecology and Management 246, 285–295.
Cohen, W.B., Maiersperger, T.K., Gower, S.T., Turner, D.P., 2003. An improved strategy for regression of biophysical variables and Landsat ETM+ data. Remote Sensing of Environment 84, 561–571.
Cohen, W.B., Maiersperger, T.K., Spies, T.A., Oetter, D.R., 2001. Modelling forest cover attributes as continuous variables in a regional context with Thematic Mapper data. International Journal of Remote Sensing 22, 2279–2310.
Cressie, N.A.C., 1993. Statistics for Spatial Data. John Wiley & Sons, New York, USA, 416 pp.
Curran, P.J., 1988. The semivariogram in remote sensing: an introduction. Remote Sensing of Environment 24, 493–507.
Curran, P.J., Atkinson, P.M., 1988. Geostatistics and remote sensing. Progress in Physical Geography 22, 61–78.
Davis, B., 1987. Uses and abuses of cross-validation in geostatistics. Mathematical Geology 19, 241–248.
Deutsch, C.V., Journel, A.G., 1998. Geostatistical Software Library and User's Guide, 2nd ed. Oxford University Press, New York, USA, 369 pp.
Dungan, J., 1998. Spatial prediction of vegetation quantities using ground and image data. International Journal of Remote Sensing 19, 267–285.
Eastman, J.R., 2006. Idrisi Andes. Guide to GIS and Image Processing. Clark Labs, Clark University, USA, 328 pp.
Fearnside, P.M., 1992. Forest biomass in Brazilian Amazônia: comments on the estimate by Brown and Lugo. Interciencia 17, 19–27.
Fearnside, P.M., 1997. Greenhouse gases from deforestation in Brazilian Amazonia: net committed emissions. Climatic Change 35, 321–360.
Foroughbakhch, R., Reyes, G., Alvarado-Vázquez, M.A., Hernández-Piñero, J., Rocha-Estrada, A., 2005. Use of quantitative methods to determine leaf biomass on 15 woody shrub species in northeastern Mexico. Forest Ecology and Management 216, 359–366.
Fournier, R.A., Luther, J.E., Guindon, L., Lambert, M.C., Piercey, D., Hall, R.J., Wulder, M.A., 2003. Mapping aboveground tree biomass at the stand level from inventory information: test cases in Newfoundland and Quebec. Canadian Journal of Forest Research 33, 1846–1863.
Freeman, E., Moisen, G., 2007. Evaluating kriging as a tool to improve moderate resolution maps of forest biomass. Environmental Monitoring and Assessment 128, 395–410.
García-Martín, A., Pérez-Cabello, F., de la Riva, J.R., Montorio, R., 2008. Estimation of crown biomass of Pinus spp. from Landsat TM and its effect on burn severity in a Spanish fire scar. IEEE Journal of Selected Topics in Applied Earth Observations and Remote Sensing 1, 254–265.
Gilbert, B., Lowell, K., 1997. Forest attributes and spatial autocorrelation and interpolation: effects of alternative sampling schemata in the boreal forest. Landscape and Urban Planning 37, 235–244.
Gillespie, A.J.R., Brown, S., Lugo, A.E., 1992. Tropical forest biomass estimation from truncated stand tables. Forest Ecology and Management 48, 69–87.
Goovaerts, P., 1997. Geostatistics for Natural Resources Evaluation. Oxford University Press, Inc., New York, USA.
Goovaerts, P., 1999. Using elevation to aid the geostatistical mapping of rainfall erosivity. Catena 34 (3-4), 227–242.
Gunnarsson, F., Holm, S., Holmgren, P., Thuresson, T., 1998. On the potential of Kriging for forest management planning. Scandinavian Journal of Forest Research 13, 237–245.
Hame, T., Salli, A., Andersson, K., Lohi, A., 1997. A new methodology for the estimation of biomass of conifer dominated boreal forest using NOAA AVHRR data. International Journal of Remote Sensing 18, 3211–3243.
Hengl, T., 2009. A Practical Guide to Geostatistical Mapping, 2nd ed. University of Amsterdam, Amsterdam.
Hengl, T., Heuvelink, G.B.M., Rossiter, D.G., 2007. About regression-kriging: from equations to case studies. Computers & Geosciences 33, 1301–1315.
Hengl, T., Heuvelink, G.B.M., Stein, A., 2004. A generic framework for spatial prediction of soil variables based on regression-kriging. Geoderma 120, 75–93.
Hernández, J., Emery, X., 2009. A geostatistical approach to optimize sampling designs for local forest inventories. Canadian Journal of Forest Research 39, 1465–1474.
Hese, S., Lucht, W., Schmullius, C., Barnsley, M., Dubayah, R., Knorr, D., Neumann, K., Riedel, T., Schröter, K., 2005. Global biomass mapping for an improved understanding of the CO_2 balance—the Earth observation mission Carbon-3D. Remote Sensing of Environment 94, 94–104.
Houghton, R.A., Lawrence, K.T., Hackler, J.L., Brown, S., 2001. The spatial distribution of forest biomass in the Brazilian Amazon: a comparison of estimates. Global Change Biology 7, 731–746.
Hu, H., Wang, G.G., 2008. Changes in forest biomass carbon storage in the South Carolina Piedmont between 1936 and 2005. Forest Ecology and Management 255, 1400–1408.
IGP, 2010. CLC2006 – Cartografia CORINE Land Cover 2006 Para Portugal Continental; 2009 (verified 01.01.2010) http://www.igeo.pt/gdr/projectos/clc2006/.
Isaaks, E.H., Srivastava, R.M., 1989. An Introduction to Applied Geostatistics. Oxford University Press, New York, USA, 542 pp.
Iverson, L.R., Brown, S., Prasad, A., Mitasova, H., Gillespie, A.J.R., Lugo, A.E., 1994. Use of GIS for estimating potential and actual forest biomass for continental South and Southeast Asia. In: Dale, V.H. (Ed.), Effects of Land-Use Change on Atmospheric CO_2 Concentrations: South and Southeast Asia as a Case Study. Springer-Verlag, New York, pp. 67–116.
Jong, S.M.d., Pebesma, E.J., Meer, F.D.v.d., 2006. Spatial variability, mapping methods, image analysis and pixels. In: Jong, S.M.d., Meer, F.D.v.d. (Eds.), Remote Sensing Image Analysis: Including the Spatial Domain, vol. 5. Springer, Netherlands, pp. 17–35.
Journel, A.G., Huijbregts, C.J., 1978. Mining Geostatistics. Academic Press, London.
Kint, V., van Meirvenne, M., Nachtergale, L., Geudens, G., Lust, N., 2003. Spatial methods for quantifying forest stand structure development: a comparison between nearest-neighbor indices and variogram analysis. Forest Science 49, 36–49.
Knotters, M., Brus, D.J., Oude Voshaar, J.H., 1995. A comparison of kriging, co-kriging and kriging combined with regression for spatial interpolation of horizon depth with censored observations. Geoderma 67, 227–246.
Krige, D.G., 1951. A Statistical Approach to some Mine Valuations and Allied Problems at the Witwatersrand. University of Witwatersrand, South Africa.
Labrecque, S., Fournier, R.A., Luther, J.E., Piercey, D., 2006. A comparison of four methods to map biomass from Landsat-TM and inventory data in western Newfoundland. Forest Ecology and Management 226, 129–144.
Lillesand, T.M., Kiefer, R.W., Chipman, J.W., 2004. Remote Sensing and Image Interpretation, 5th ed. John Wiley and Sons Inc., New York, 764 pp.
Lloyd, C.D., 2007. Local Models for Spatial Analysis. CRC Press, Taylor & Francis Group, Boca Raton, pp. 244.
Lu, D., 2006. The potential and challenge of remote sensing based biomass estimation. International Journal of Remote Sensing 27, 1297–1328.
Lu, G.Y., Wong, D.W., 2008. An adaptive inverse-distance weighting spatial interpolation technique. Computers & Geosciences 34, 1044–1055.
Magcale-Macandog, D.B., Delgado, M.E.M., Ty, E., Villarin, J.R.T.A., 2006. A Gis-based model to improve estimation of aboveground biomass of secondary forests in the Philippines. Journal of Tropical Forest Science 18, 8–21.
Mandallaz, D., 1993. Geostatistical Methods for Double Sampling Schemes: Application to Combined Forest Inventories. Chair of Forest Inventory and Planning, Swiss Federal Institute of Technology (ETH), Zürich, p. 133.
Maselli, F., Chiesi, M., 2006. Evaluation of Statistical Methods to Estimate Forest Volume in a Mediterranean Region. IEEE Transactions on Geoscience and Remote Sensing 44, 2239–2250.
Matheron, G., 1963. Principles of geostatistics. Economic Geology 58, 1246–1266.
Matheron, G., 1969. Le krigeage Universel, vol. 1. Cahiers du Centre de Morphologie Mathematique, Ecole des Mines de Paris, Fontainebleau, 83 pp.
Matheron, G., 1971. The Theory of Regionalised Variables and its Applications. Les Cahiers du Centre de Morphologie Mathematique de Fontainblue, Ecole Nationale Superiore de Paris, Paris, 212 pp.
McBratney, A.B., Webster, R., 1981. The design of optimal sampling schemes for local estimation and mapping of regionalized variables—II: program and examples. Computers & Geosciences 7, 335–365.

McRoberts, R.E., Tomppo, E.O., Næsset, E., 2010. Advances and emerging issues in national forest inventories. Scandinavian Journal of Forest Research 25, 368–381.

Meng, Q., Cieszewski, C., Madden, M., 2009. Large area forest inventory using Landsat ETM+: a geostatistical approach. ISPRS Journal of Photogrammetry and Remote Sensing 64, 27–36.

Mutanga, O., Rugege, D., 2006. Integrating remote sensing and spatial statistics to model herbaceous biomass distribution in a tropical savanna. International Journal of Remote Sensing 27, 3499–3514.

Muukkonen, P., Heiskanen, J., 2005. Estimating biomass for boreal forests using ASTER satellite data combined with standwise forest inventory data. Remote Sensing of Environment 99, 434–447.

Muukkonen, P., Heiskanen, J., 2007. Biomass estimation over a large area based on standwise forest inventory data and ASTER and MODIS satellite data: a possibility to verify carbon inventories. Remote Sensing of Environment 107, 617–624.

Nanos, N., Calama, R., Montero, G., Gil, L., 2004. Geostatistical prediction of height/diameter models. Forest Ecology and Management 195, 221–235.

Odeh, I.O.A., McBratney, A.B., Chittleborough, D.J., 1994. Spatial prediction of soil properties from landform attributes derived from a digital elevation model. Geoderma 63, 197–214.

Odeh, I.O.A., McBratney, A.B., Chittleborough, D.J., 1995. Further results on prediction of soil properties from terrain attributes: heterotopic cokriging and regression-kriging. Geoderma 67, 215–226.

Palmer, D.J., Höck, B.K., Kimberley, M.O., Watt, M.S., Lowe, D.J., Payn, T.W., 2009. Comparison of spatial prediction techniques for developing Pinus radiata productivity surfaces across New Zealand. Forest Ecology and Management 258, 2046–2055.

Pebesma, E.J., 2001. Gstat User's Manual. University of Utrecht, 108 pp.

Pebesma, E.J., 2004. Multivariable geostatistics in S: the gstat package. Computers & Geosciences 30, 683–691.

Peichl, M., Arain, M.A., 2007. Allometry and partitioning of above- and belowground tree biomass in an age-sequence of white pine forests. Forest Ecology and Management 253, 68–80.

Pierce, K.B., Ohmann, J.L., Wimberly, M.C., Gregory, M.J., Fried, J.S., 2009. Mapping wildland fuels and forest structure for land management: a comparison of nearest neighbor imputation and other methods. Canadian Journal of Forest Research 39, 1901–1916.

Reese, H., Nilsson, M., Sandström, P., Olsson, H., 2002. Applications using estimates of forest parameters derived from satellite and forest inventory data. Computers and Electronics in Agriculture 37, 37–55.

Reich, R.M., Aguirre-Bravo, C., Bravo, V.A., Briseño, M.M., 2011. Empirical evaluation of confidence and prediction intervals for spatial models of forest structure in Jalisco, Mexico. Journal of Forestry Research 22, 159–166.

Reich, R.M., Lundquist, J.E., Bravo, V.A., 2004. Spatial models for estimating fuel loads in the Black Hills, South Dakota. International Journal of Wildland Fire 13, 119–129.

Sales, M.H., Souza Jr., C.M., Kyriakidis, P.C., Roberts, D.A., Vidal, E., 2007. Improving spatial distribution estimation of forest biomass with geostatistics: a case study for Rondônia, Brazil. Ecological Modelling 205, 221–230.

Sen, Z., 2009. Spatial Modeling Principles in Earth Sciences. Springer, Dordrecht/Heidelberg/London/New York, 351 pp.

Ter-Mikaelian, M.T., Korzukhin, M.D., 1997. Biomass equations for sixty-five North American tree species. Forest Ecology and Management 97, 1–24.

Tomppo, E., 1991. Satellite image-based national forest inventory of Finland. In: Proceedings of the Symposium on Global and Environmental Monitoring, Techniques and Impacts, International Archives of Photogrammetry and Remote Sensing, Victoria, British Columbia, Canada, pp. 419–424.

Tomppo, E., Nilsson, M., Rosengren, M., Aalto, P., Kennedy, P., 2002. Simultaneous use of Landsat-TM and IRS-1C WiFS data in estimating large area tree stem volume and aboveground biomass. Remote Sensing of Environment 82, 156–171.

Tomppo, E., Olsson, H., Ståhl, G., Nilsson, M., Hagner, O., Katila, M., 2008. Combining national forest inventory field plots and remote sensing data for forest databases. Remote Sensing of Environment 112, 1982–1999.

Toutin, T., 2004. Review article: geometric processing of remote sensing images: models, algorithms and methods. International Journal of Remote Sensing 25, 1893–1924.

Tuominen, S., Fish, S., Poso, S., 2003. Combining remote sensing, data from earlier inventories, and geostatistical interpolation in multisource forest inventory. Canadian Journal of Forest Research 33, 624–634.

Viana, H., Cohen, W.B., Lopes, D., Aranha, J., 2010. Assessment of forest biomass for use as energy. GIS-based analysis of geographical availability and locations of wood-fired power plants in Portugal. Applied Energy 87, 2551–2560.

Viana, H., Lopes, D., Aranha, J., 2009. Predição de biomassa arbustiva lenhosa empregando dados de inventário e o índice de diferença normalizada extraído em imagens landsat 5 TM. ISPV Millenium.

Weber, D., Englund, E., 1992. Evaluation and comparison of spatial interpolators. Mathematical Geology 24, 381–391.

Webster, R., Oliver, M.A., 1992. Sample adequately to estimate variograms of soil properties. Journal of Soil Science 43, 177–192.

Webster, R., Oliver, M.A., 2007. Geostatistics for Environmental Scientists, 2nd ed. John Wiley & Sons Ltd, England, 332 pp.

Woodcock, C.E., Strahler, A.H., Jupp, D.L.B., 1988. The use of variograms in remote sensing: II. Real digital images. Remote Sensing of Environment 25, 349–379.

Zhang, C., Franklin, S.E., 2002. Forest structure classification using airborne multispectral image texture and kriging analysis. In: IEEE International Geoscience and Remote Sensing Symposium, 2002. IGARSS '02, p. 2002.

Zheng, D., Heath, L.S., Ducey, M.J., 2007. Forest biomass estimated from MODIS and FIA data in the Lake States: MN, WI and MI, USA. Forestry 80, 265–278.

Zianis, D., Muukkonen, P., Mäkipää, R., Mencuccini, M., 2005. Biomass and Stem Volume Equations for Tree Species in Europe, Silva Fennica Monographs 4. Finnish Society of Forest Science, pp. 63.

Annex C.2

Viana, H., Lopes, D., Aranha, J., 2011. Assessment of Forest Aboveground Biomass Stocks and Dynamics with Inventory Data, Remotely Sensed Imagery and Geostatistics, in: Shaukat, S.S. (ed.), Progress in Biomass and Bioenergy Production. InTech, pp. 107-130.

6

Assessment of Forest Aboveground Biomass Stocks and Dynamics with Inventory Data, Remotely Sensed Imagery and Geostatistics

Helder Viana[1], Domingos Lopes[2] and José Aranha[2]

[1]*Polytechnic Institute of Viseu*

[2]*CITAB - University of Trás-os-Montes e Alto Douro*

Portugal

1. Introduction

Several issues, related with forest fires, forest disturbances (García-Martín et al., 2008), forest productivity (Chirici et al., 2007; Palmer et al., 2009), forest changes over time (Hu & Wang, 2008), or the role of forests in the global carbon balance cycle (Hese et al., 2005) are, nowadays, the focus of numerous studies and investigations. All these subjects demand the knowledge about aboveground biomass (AGB) stocks and/or its dynamics. Besides the availability of biomass, the information about the growth of forests is of increasing importance. This variable, which is related with the total biomass growth in a specific ecosystem, is called Net Primary Production (NPP). Annual NPP represents the net amount of carbon captured by plants through photosynthesis each year (Melillo et al., 1993; Cao & Woodward, 1998). In practice, NPP can be defined and measured in terms of either biomass or CO_2 exchange (Field et al., 1995). Waring et al. (1998) define NPP as the sum of live biomass periodic increment (ΔB) and dead biomass (losses, e.g. broken branches, fallen leaves) [NPP = ΔB + losses]. NPP is an important ecological variable due to its relevance for accurate ecosystem management and for monitoring the impact of human activity on ecosystems vegetation at a range of spatial scales: local, regional and global (Melillo et al., 1993). It is one of the most complete and complex variables, since it reflects the growth of the entire ecosystem thus avoiding the analysis of only part of its components. NPP provides a complete view of the ecosystem including information, not only from the arboreal stratum, but also from the shrubs and all the litter produced from each stratum. Thus, the significance of NPP not only reflects the complexity of its measurement or estimation, but also its integrative ecological perspective ecosystems.

Mapping AGB stocks or NPP with the utmost accuracy and expedite methodologies is therefore a challenge. The need of continuous maps where the phenomenon under study can be individually analysed or used as auxiliary variable in a specific model requires that the spatial predictions are represented in the most accurate way. Over the years different spatial prediction methods have been explored in diverse data type (Isaaks & Srivastava, 1989; Goovaerts, 1997; Labrecque et al., 2006; Sales et al., 2007; Meng et al., 2009). Some approaches have a simple application methodology however others are sometimes complex in what concerns to their implementation, or the selection of the variables to be used.

Estimation of AGB has been made by a range of methods, from field measurements to remote sensing-based methods, as well GIS-based modelling approaches with auxiliary data (Lu, 2006). Traditionally, to predict the spatial distribution of AGB throughout the territory, the variables calculated based on the forest inventory dataset were usually assigned to the forest polygons, stratified by species, and mapped by aerial photos interpretation. Despite the field measurements being the most accurate methods for collecting biomass data, the level of precision of the resultant biomass map will depend of the land cover classification detail and of the sample intensity. In fact, the forest inventories data at regional or national scale are often not spatially exhaustive enough to generate continuous AGB estimates, thus limiting the use of this approach over large areas. An additional limitation is the long temporal resolution of these estimations, generally made in cycles of 10 or more years, which could not be compatible with the need of analysis and monitoring of the ecosystems' dynamics.

Remote sensing-based methods have been the most widely used approach to map AGB. The utility of the spectral information recorded by remote sensing for monitoring vegetation or gathering ecophysiological information over large areas is very well recognized, since satellite data became accessible for land cover dynamic studies. Different imagery data have been employed, such as coarse spatial-resolution data as SPOT-VEGETATION (Chirici et al., 2007; Jarlan et al., 2008), NOAA AVHRR (Häme et al., 1997; Atkinson et al., 2000), MODIS (Zheng et al., 2007, Muukkonen & Heiskanen, 2007); medium spatial-resolution data as ASTER (Muukkonen & Heiskanen, 2007), Landsat TM/ETM+ (Tomppo et al., 2002; Rahman et al., 2005; Meng et al., 2009); high spatial-resolution data as IRS P6 LISS-IV (Madugundu et al., 2008) and radar data (Hyde et al., 2007; Liao et al., 2009).

AGB can be estimated by means of Direct Radiometric Relationships (DRR), which consist in establishing regression relationships, such as ordinary least squares (OLS), between the satellite spectral data (e.g. individual spectral bands, band ratios, vegetation indices and other possible transformations) as independent variables, and the measured parameter at each corresponding inventory sample plot position in each forest cover strata. AGB can be directly predicted by multiple regression analysis between spectral data response and biomass amount (Labrecque et al., 2006; Muukkonen & Heiskanen, 2007); by nonparametric approaches including K nearest neighbour (KNN) (Tomppo, 1991; Meng et al., 2007), or by artificial neural network (ANN) (Liao et al., 2009); or indirectly predicted by using characteristic such as crown diameter or leaf area index (LAI). In this case, these variables are firstly derived from the imagery data and subsequently used in regression analysis to estimate AGB.

Spatial prediction models (algorithms) have been used for spatially predicting vegetation attributes. In general, these interpolation techniques are classified in deterministic and statistical (probabilistic) models (Isaaks & Srivastava, 1989; Goovaerts, 1997; Hengl, 2009). Attending that in the Earth sciences there is usually a lack of sufficient knowledge concerning how properties vary in space, a deterministic model may not be appropriate. Therefore, to make predictions at locations for which observations do not exist, with inherent uncertainty in predictions, the use of probabilistic models is necessary (Lloyd, 2007).

Spatial statistics and geostatistics were developed to describe and analyze the variation in both natural and man-made phenomena on above or below the land surface (Cressie, 1993). Largely developed by Matheron (1963) in the 1960s, to evaluate recoverable reserves for the mining industry, geostatistical models have been systematically applied in a wide range of fields (Cressie, 1993; Goovaerts, 1997). Today, geostatistics and the theory of regionalized variables (Matheron, 1971) are used to explore and describe the presence of spatial variation that occur in most natural resource variables. Introduced to remote sensing by Woodcock et al. (1988) and by Curran (1988), geostatistical models have been used to design optimum sampling schemes for image data and ground data; to increase the accuracy in which remotely sensed data can be used to classify land cover; or to estimate continuous variables. Geostatistical models are reported in numerous textbooks (e.g. Isaaks & Srivastava, 1989; Cressie 1993; Goovaerts, 1997; Deutsch & Journel, 1998; Webster & Oliver, 2007; Hengl, 2009; Sen, 2009) such as Kriging (plain geostatistics); environmental correlation (e.g. regression-based); Bayesian-based models (e.g. Bayesian Maximum Entropy) and hybrid models (e.g. regression-kriging).

Despite Regression-kriging (RK) is being implemented in several fields, as soil science, few studies explored this approach to spatially predict AGB with remotely sensed data as auxiliary predictor. Hence, this research makes use of RK and remote sensing data to analyse if spatial AGB predictions could be improved.

This research presents two case studies in order to explore the techniques of remote sensing and geostatistics for mapping the AGB and NPP. The first, aims to compare three approaches to estimate *Pinus pinaster* AGB, by means of remotely sensed imagery, field inventory data and geostatistical modeling. The second aims to analyse if NPP of *Eucalyptus globulus* and *Pinus pinaster* species can easily and accurately be estimated using remotely sensed data.

2. Case study I – Aboveground biomass prediction by means of remotely sensed imagery, field inventory data and geostatistical modeling

2.1 Study area

This study was carry out in Portugal (Continental), extending from the latitudes of 36º 57′ 23″ and 42º 09′ 15″N and the longitudes of 09º 30′ 40″ and 06º 10′ 45″ W (Figure 1). This area

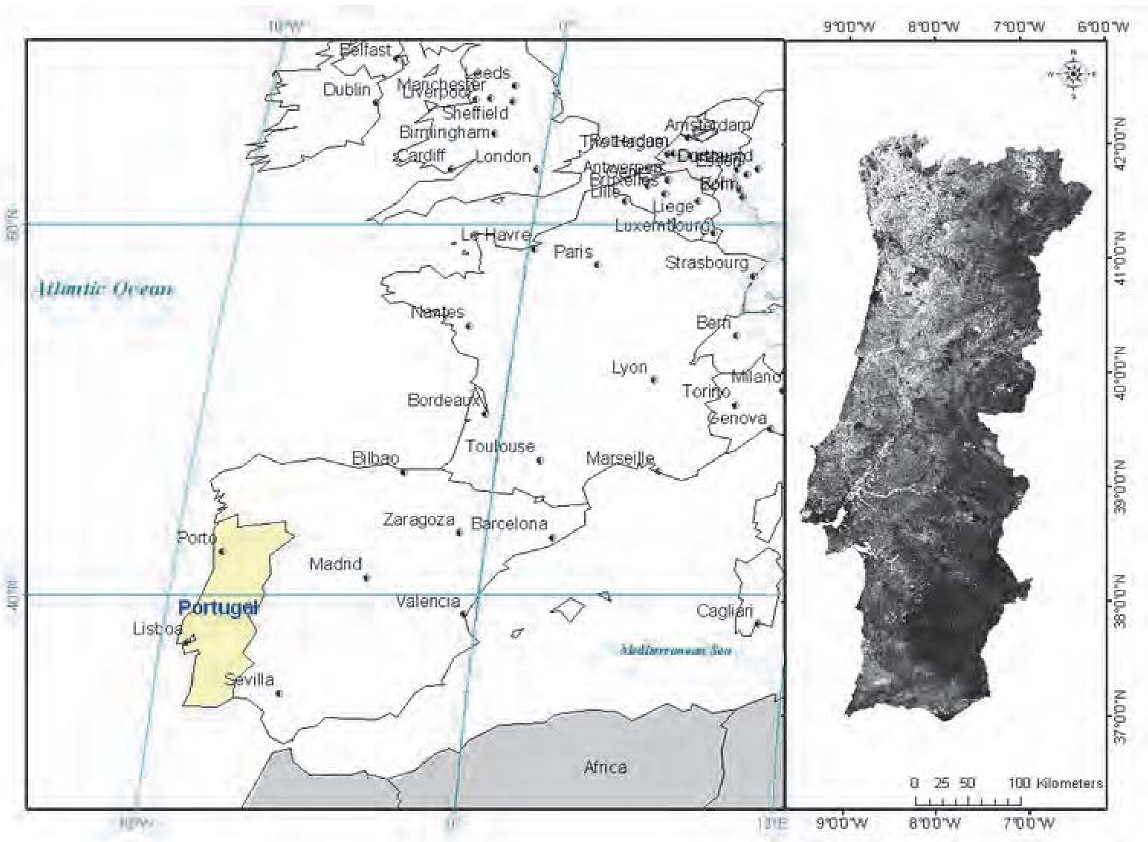

Fig. 1. Study area location

includes two distinctive bioclimatic regions: a Mediterranean bioclimate in everywhere except a small area in the North with a temperate bioclimate. With four distinct weather seasons, the average annual temperatures range from about 7 °C in the highlands of the interior north and center and about 18 ° C in the south coast. Average annual precipitation is more than 3000 mm at the north and less than 600 mm at the south.
Due to a 20 years of severe wild fires during summer time, and intense people movement from rural areas to sea side cities or county capital, forestry landscape changed from large trees' stands interspersed by agricultural lands, to a fragmented landscape. The land cover is fragmented with small amount of suitable soils for agriculture and the main areas occupied by forest spaces. Forest activity is a direct source of income for a vast forest products industry, which employs a significant part of the population.

2.2 Methods and data

2.2.1 GIS and field data

In a first stage a GIS project (ArcGis 9.x), was created in order to identify *Pinus pinaster* pure stands, over a Portuguese Corine Land Cover Map (CLC06, IGP, 2010). In a second stage, GIS project database was updated with the dendrometric data collected during Portuguese National Forestry Inventory (AFN, 2006), in order to derive AGB allometric equations, with Vegetation Indices values as independent variable. A total of 328 field plots of pure pine stands were used. The inventory dataset was further used in spatial prediction analysis, to create continuous AGB maps for the study area.

2.2.2 Biomass estimation from the forest inventory dataset

In order to calculate the biomass exclusively from the forest inventory, the biomass values measured in each field plot were spatially assigned to the pine stands land cover map polygons. In the cases where multiple plots were coincident with the same polygon, weighted averages were calculated proportionally to the area of occupation in that polygon.

2.2.3 Remote sensing imagery

In this research we used the Global MODIS vegetation indices dataset (h17v04 and h17v05) from the Moderate Resolution Imaging Spectroradiometer (MODIS) from 29 August 2006: (MOD13Q1.A2006241.h17v04.005.2008105184154.hdf; and
MOD13Q1.A2006241.h17v05.005.2008105154543.hdf), freely available from the US Geological Survey (USGS) Earth Resources Observation and Science (EROS) Center. The Global MOD13Q1 data includes the MODIS Normalized Difference Vegetation Index (NDVI) and a new Enhanced Vegetation Index (EVI) provided every 16 days at 250-meter spatial resolution as a gridded level-3 product in the Sinusoidal projection.
(https://lpdaac.usgs.gov/lpdaac/products/modis_products_table/vegetation_indices/16_day_l3_global_250m/mod13q1).
MODIS data was projected to the same Portuguese coordinate system (Hayford-Gauss, Datum of Lisbon with false origin) used in the GIS project.

2.2.4 Direct Radiometric Relationships (DRR)

Using GIS tools, field inventory dataset was updated with information from MODIS images. The spectral information extracted (NDVI and EVI) was then used as independent variables for developing regression models. Linear, logarithmic, exponential, power, and second-order polynomial functions were tested on data relationship analysis. The best model achieved was then applied to the imagery data, and the predicted aboveground biomass map was produced. In some pixels where Vegetation index values were very low, the biomass values predicted by the regression equations were negative, so these pixels were removed, because in reality negative biomass values are not possible.

2.2.5 Geostatistical modeling

Regression-kriging (RK) (Odeh et al., 1994, 1995) is a hybrid method that involves either a simple or multiple-linear regression model (or a variant of the generalized linear model and regression trees) between the target variable and ancillary variables, calculating residuals of the regression, and combining them with kriging. Different types or variant of this process, but with similar procedures, can be found in literature (Ahmed & De Marsily, 1987; Knotters et al.; 1995; Goovaerts; 1999; Hengl et al.; 2004, 2007), which can cause confusion in the computational process.

In the process of RK the predictions $\left(\hat{z}_{rk(S_0)}\right)$ are combined from two parts; one is the estimate $\hat{m}(s_0)$ obtained by regressing the primary variable on the k auxiliary variables $\mathrm{q_k(s_0)}$ and $\mathrm{q_0(s_0)=1}$; the second part is the residual estimated from kriging $\left(\hat{e}_{(S_0)}\right)$. RK is estimated as follows (Eqs. 1 and 2):

$$\hat{z}_{rk}(s_0) = \hat{m}(s_0) + \hat{e}(s_0) \tag{1}$$

$$\hat{z}_{rk}(s_0) = \sum_{k=0}^{v} \hat{\beta}_k \cdot q_k(s_0) + \sum_{i=1}^{n} w_i(s_0) \cdot e(s_i) \tag{2}$$

where $\hat{\beta}_k$ are estimated drift model coefficients ($\hat{\beta}_0$ is the estimated intercept), optimally estimated from the sample by some fitting method, e.g. ordinary least squares (OLS) or, optimally, using generalized least squares (GLS), to take the spatial correlation between individual observations into account (Cressie, 1993); w_i are kriging weights determined by the spatial dependence structure of the residual and $e(s_i)$ are the regression residuals at location s_i.

RK was performed using the GSTAT package in IDRISI software (Eastman, 2006) both to automatically fit the variograms of residuals and to produce final predictions (Pebesma, 2001 and 2004). The first stage of geostatistical modeling consists in computing the experimental variograms, or semivariogram, using the classical formula (Eq. 3):

$$\hat{\gamma}(h) = \frac{1}{2N(h)} \sum_{i=1}^{N(h)} \left[z(x_i) - z(x_i + h)\right]^2 \tag{3}$$

where $\hat{\gamma}(h)$ is the semivariance for distance h, $N(h)$ the number of pairs for a certain distance and direction of h units, while z(xi) and $Z(x_i + h)$ are measurements at locations x_i and $x_i + h$, respectively.

Semivariogram gives a measure of spatial correlation of the attribute in analysis. The semivariogram is a discrete function of variogram values at all considered lags (e.g. Curran 1988; Isaaks & Srivastava 1989). Typically, the semivariance values exhibit an ascending

behaviour near the origin of the variogram and they usually level off at larger distances (the sill of the variogram). The semivariance value at distances close to zero is called the nugget effect. The distance at which the semivariance levels off is the range of the variogram and represents the separation distance at which two samples can be considered to be spatially independent.
For fitting the experimental variograms we tested the exponential, the gaussian and the spherical models, using iterative reweighted least squares estimation (WLS, Cressie, 1993). Finally, RK was carried out according to the methodology described in http://spatial-analyst.net. The EVI image was used as predictor (auxiliary map) in RK. GSTAT produces the predictions and variance map, which is the estimate of the uncertainty of the prediction model, i.e. precision of prediction.

2.2.6 Validation of the predicted maps

The validation and comparison of the predicted AGB maps were made by examining the discrepancies between the known data and the predicted data. The dataset was, prior to estimates, divided randomly into two sets: the prediction set (276 plots) and the validation set (52 plots). According to Webster & Oliver (1992), to estimate a variogram 225 observations are usually reliable. The prediction approaches were evaluated by comparing the basic statistics of predicted AGB maps (e.g., mean and standard deviation) and the difference between the known data and the predicted data were examined using the mean error, or bias mean error (ME), the mean absolute error (MAE), standard deviation (SD) and the root mean squared error (RMSE), which measures the accuracy of predictions, as described in Eqs. (4-7).

$$SD = \sqrt{\frac{1}{N-1}\sum_{i=1}^{N}\left(e_i - \overline{e}\right)^2} \tag{4}$$

$$ME = \frac{1}{N}\sum_{i=1}^{N}\left(\hat{e}_i - e_i\right) \tag{5}$$

$$MAE = \frac{1}{N}\sum_{i=1}^{N}\left|\hat{e}_i - e_i\right| \tag{6}$$

$$RMSE = \sqrt{\frac{1}{N}\sum_{i=1}^{N}\left(\hat{e}_i - e_i\right)^2} \tag{7}$$

where: N is the number of values in the dataset, $\hat{e}_i$ is the estimated biomass, e_i is the biomass values measured on the validation plots and $\overline{e}$ is the mean of biomass values of the sample.

2.3 Results and discussion

2.3.1 *Pinus pinaster* stands characteristics

The descriptive statistics of pine stands data are presented in Table 1, where: N is the number of trees; t is the forestry stand age; h_{dom} is the dominant height; dbh_{dom} is the dominant diameter at breast height; SI is the site index; BA is the basal area; V is the stand volume and AGB is the biomass in the sample plot.

The pine stands are highly heterogeneous with ages ranging from 8 to 110 years old and the biomass per hectare ranging from 0.9 to 136.1 ton ha^{-1}. The values of Biomass present a normal distribution with mean m = 52.12 ton ha^{-1} and standard deviation σ = 32.32 ton ha^{-1} (Figure 2).

	Pine stands plots							
	N (trees ha^{-1})	**t** (year)	**h_{dom}** (m)	**dbh_{dom}** (cm)	**SI** (m)	**BA** (m^2 ha^{-1})	**V** (m^3 ha^{-1})	**AGB** (ton ha^{-1})
Mean	566	31	13.4	25.3	11.8	14.39	99.46	52.12
Min	20	8	4.6	8.9	0.0	0.41	1.37	0.85
Max	2219	110	36.5	59.0	69.0	38.34	259.03	136.09
SD	405.2	15.9	4.0	8.0	11.5	7.64	61.86	32.32

Table 1. Descriptive statistics of data measured in the forest inventory dataset

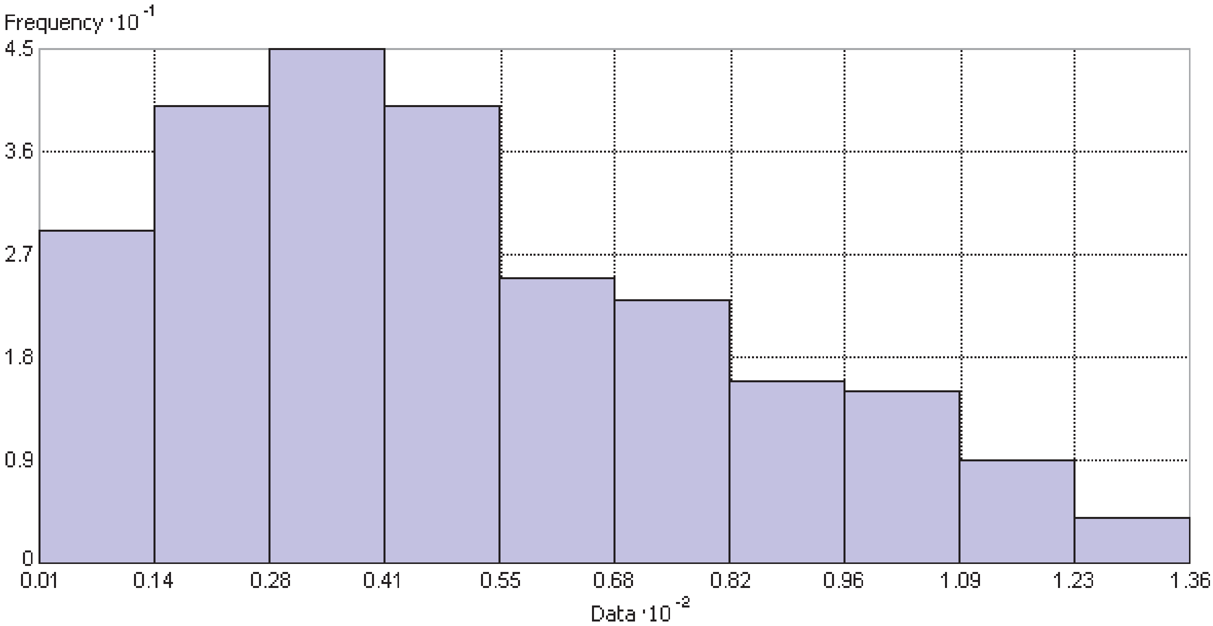

Fig. 2. Histogram of the distribution of the AGB (ton ha^{-1}) in the forest inventory dataset

2.3.2 Aboveground biomass estimation from the inventory dataset

The estimates based in the inventory dataset were achieved by assigning the 328 field plot biomass values (weighted by each polygon area) into all the polygons of the pine cover class. After the global calculation, the dataset used for training (276 plots) was used to make a first validation of this approach. Hence, a regression was established between the biomass values, measured in the field plots, and the forest inventory polygon data. In Figure 3 it is presented the positive relationship between the measured and the predicted data with a coefficient of determination (R^2) of 0.71.

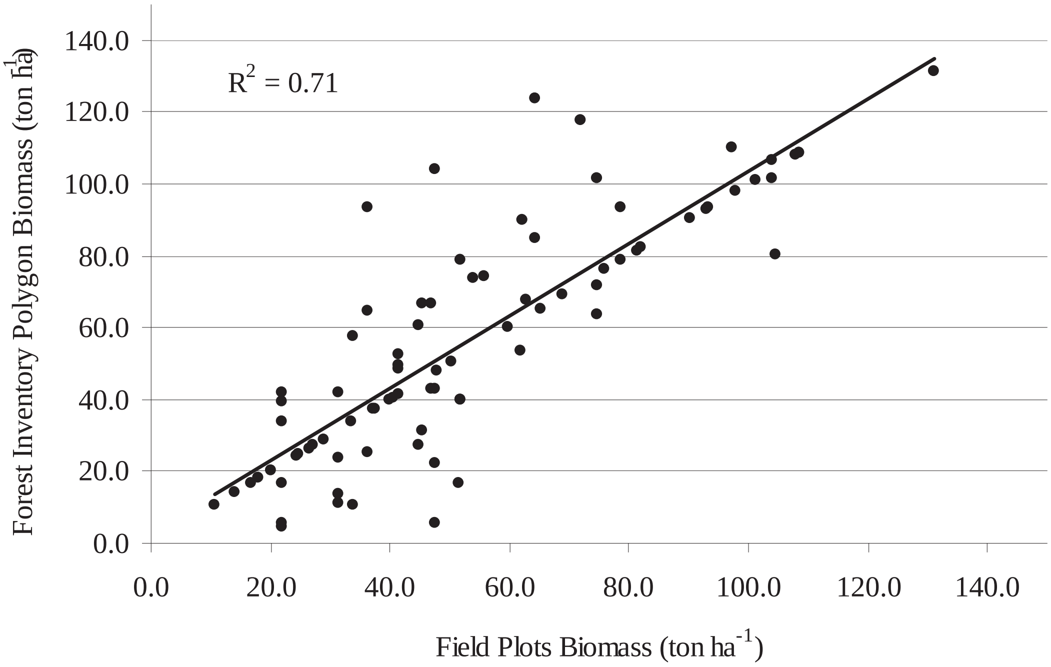

Fig. 3. Relationship between the biomass data measured in field plots and the predicted data extracted in the polygons of land cover map

2.3.3 Aboveground biomass estimation from DRR

After performing correlation analyses, between AGB and Vegetation indices, several regression models were developed using stand-wise forest inventory data and the MODIS vegetation indices (NDVI and EVI) as predictors.

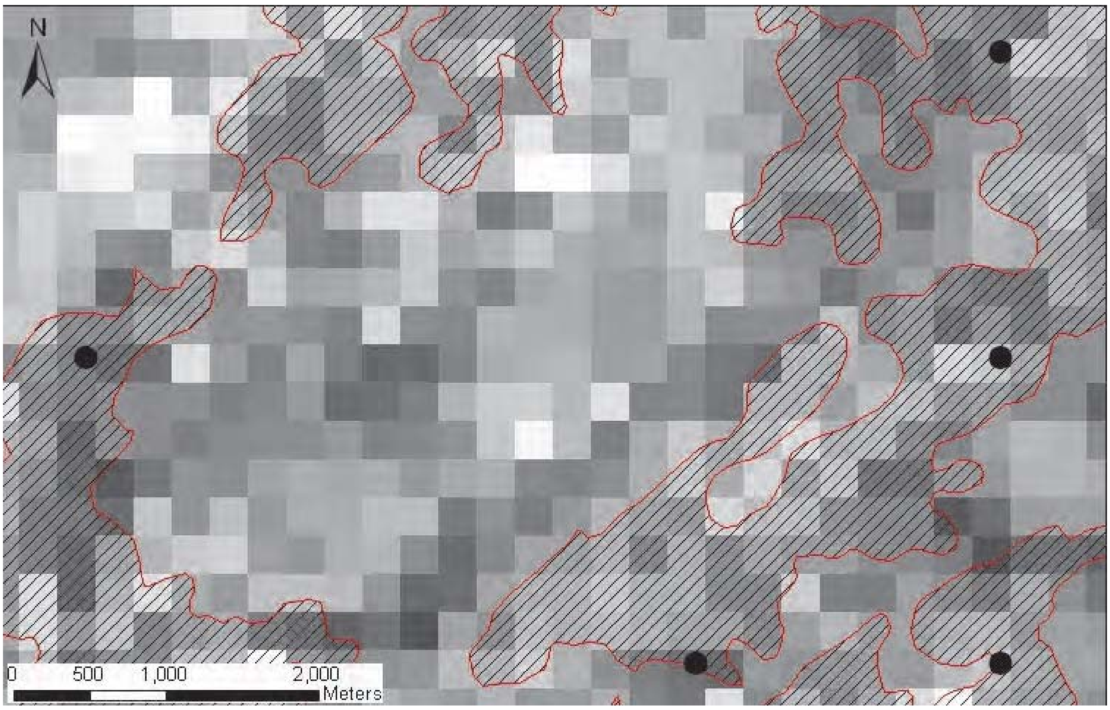

Fig. 4. MODIS image showing the effect of pixels (250m) in the edge of polygons

The best correlation was obtained with EVI as independent variable as (Eq. 8):

$$AGB = 322.4(EVI) - 39.933 \ (R^2 = 0.32) \tag{8}$$

The AGB was then estimated for the entire study area. The low correlation achieved is explained, in part, by the heterogeneity of pine stands and the high effect of mixed pixels (Burcsu et al., 2001) in coarse resolution MODIS data (250 m).

As it can be seen in Figure 4, the reflectance value recorded in the boundary pixels of the polygons limits is not pure, they record both pine stands, and the neighbouring land cover classes reflectance values.

2.3.4 Aboveground biomass estimation from geostatistical methods

To spatially estimate the AGB by geostatistical approach, the first step consisted in the modeling and analysis of the experimental semivariograms (Eq. 3). The directional semivariograms of the residuals showed anisotropy at 38.6°, so at this direction were fitted Exponential, Gaussian and Spherical models. Based on experimentation, the exponential variogram model was fitted better (nugget of 703.75 and a partial sill of 390.17 reaching its limiting value at the range of 43,9Km) to the calculated biomass pine stands data (Figure 5). The present data showed a low spatial autocorrelation. The high nugget effect, visible in the figure, which under ideal circumstances should be zero, suggests that there is a significant amount of measurement error present in the data, possibly due to the short scale variation.

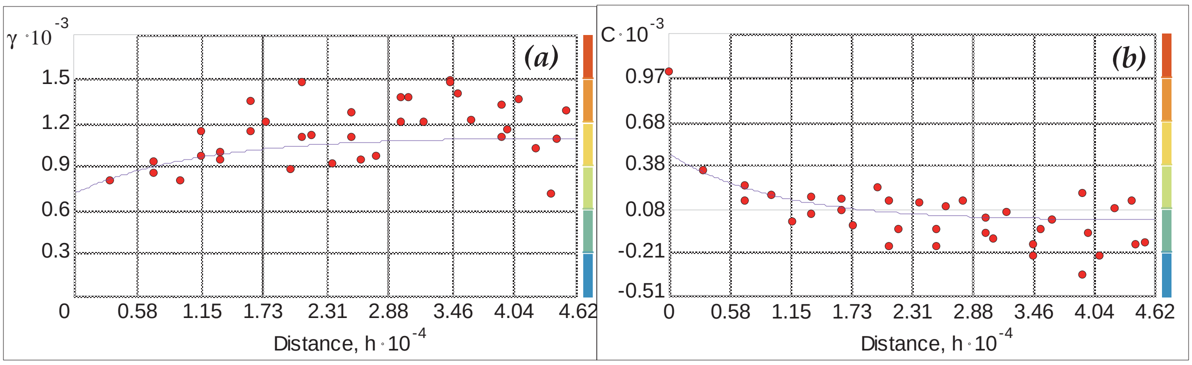

Fig. 5. Directional experimental semivariogram (38.6°) with the exponential model fitted (a) and covariance (b)

2.3.5 Validation and comparison of the aboveground biomass estimation approaches

The validation of the AGB estimation approaches was made by comparing the calculated basic statistics (Table 2) in the 52 validation random samples. Training and validation sets were compared, by means of a Student's *t* test (*t* = 0.882 ns), in order to check if they provided unbiased sub-sets of the original data.

As expected, the Inventory Polygons method produced the best statists. The mean error (ME), which should ideally be zero if the prediction is unbiased, shows a bias in the three approaches, being lower in the Inventory polygons method, and higher in the DRR method.

The analysis of the root mean squared errors (RMSE), shows that Inventory Polygons present the lower discrepancies in the estimations (RMSE=33.53%), and RK achieve estimations under lower errors (RMSE=51.95%) than the DRR approach (RMSE=61.62%). Despite this, the errors from the two prediction approaches are very high, which can be explained by the low correlation found between the vegetation indices data, as explained above. This limitation can be overcome by using remote sensing data with higher spatial resolution. Moreover, the work area must also be sectioned into smaller areas, to minimize the heterogeneity that is observed in very large landscapes.

Method	**Estimated AGB (average - ton ha^{-1})**	**ME (ton ha^{-1})**	**MAE (ton ha^{-1})**	**RMSE (ton ha^{-1})**	**SD (ton ha^{-1})**	**RMSE %**
Inventory Polygons	53.94	-3.11	11.26	18.09	27.70	33.53
DRR	50.23	-6.83	25.84	30.95	22.03	61.62
RK	52.01	-5.05	22.70	27.02	19.67	51.95

Table 2. Statistics of validation plots for the AGB prediction methods

In order to determine the significance of the differences between interpolation methods, analysis of variance (ANOVA) was performed (Table 3). The results show that, at alpha level 0.05, do not exist significant differences between the biomass values, predicted by the different methods.

Source	**DF**	**SS**	**MS**	**F**	**P**
Between	2	122.86	61.432	0.123	0.884
Within	243	113453.67	497.604		
Total	245	113576.54			

Table 3. Results from ANOVA to compare the differences between the means of the different prediction methods

A quantitative comparison of the complete AGB maps, estimated by the three approaches, was additionally made. The estimates (ton ha^{-1}) are shown in the Table 4. In order to better preserve the land cover areas, the maps were brought to the resolution of 50x50m, and then clipped by the pine land cover mask.

Method	**Pixels**	**Area (ha)**	**AGB (average – ton ha^{-1})**	**Std (ton ha^{-1})**	**B (tonnes)**
Inventory Polygons		300446	53.8	30.8	15564351
DRR	1191597	297899	53.8	20.0	16020055
RK	1189213	297303	52.8	21.3	15711245

Table 4. Summary statistics of predicted pine AGB maps

The three AGB maps originates very similar average values (ton ha^{-1}), and the differences between the maximum and minimum values of total biomass (tonnes) estimated by the different methods varies less than 1.6%.
Although there has been a low discrepancy between the total biomass values, estimated by three maps, the analysis of the correlation coefficient of regressions, carried out between the three maps, show low to moderate correlation between *Inventory Polygons x DRR* and *Inventory Polygons x RK* methods (R = 0.27 and 0.40, respectively). Only DRR x RK methods present high correlation values (R = 0.95) indicating a very similar biomass estimation at individual pixels (Figure 6).

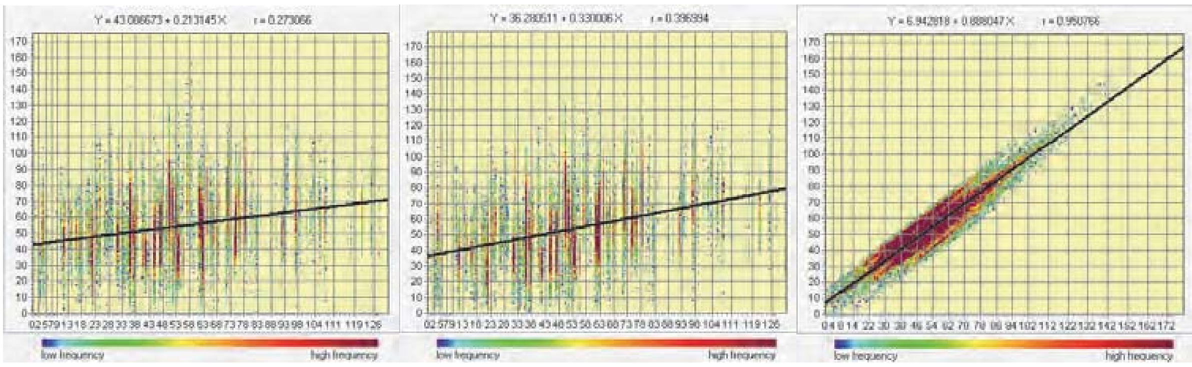

(a) (b) (c)

Fig. 6. Regression performed between AGB maps (a) *Inventory Polygons x DRR; (b) Inventory Polygons x RK*; (c) *DRR x RK*

Based in the calculated statistics of the validation dataset and in the global biomass estimations for entire area, we can consider that the Regression-kriging geostatistical prediction approach, with remotely sensed imagery as auxiliary variable, increases the classifications accuracy when compared with estimates based merely in the Direct Radiometric Relationships (DRR). Furthermore, the accuracy of these estimations could increase by using imagery data with higher spatial resolution, and if the work region is more homogeneous.

The biomass maps derived by the three methods (Inventory Polygons, Direct Radiometric Relationships and Regression-Kriging) for the whole study area are presented in Figure 7.

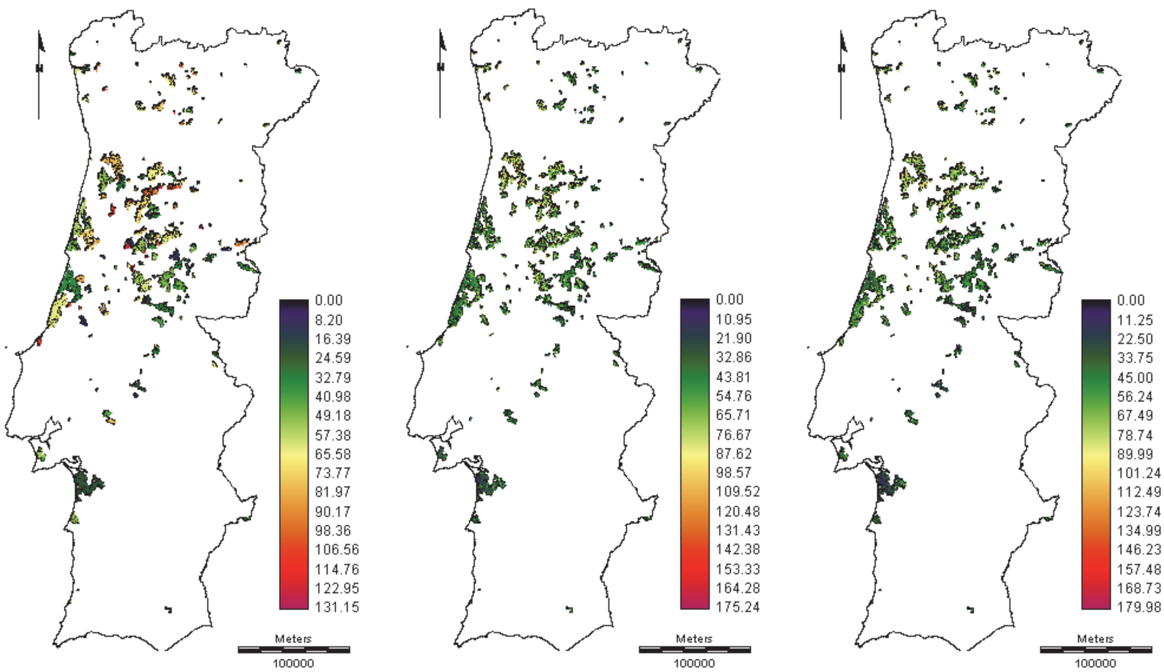

(a) (b) (c)

Fig. 7. Aboveground biomass maps (a) Inventory Polygons (b) DRR and (c) RK

3. Case study II – Biomass growth (NPP) of *Pinus pinaster* and *Eucalyptus globulus* stands, in the north of Portugal. Estimations by means of LANDSAT ETM+ images

3.1 Study area

This research took place within an area in the northern part of Portugal where *Pinus pinaster* Ait. and *Eucalyptus globulus* Labill constitute the two most important forest species in terms of forested area (Figure 8).

The *P. pinaster* study area is a 60 km² rectangle (10 km × 6 km) with extensive stands of this species located at the north of Vila Real (41°39′N, 7°35′W) and the *E. globulus* study area is a 24km² rectangle (4 km × 6 km) of extensive stands of this species located at west of Vila Real (41°2′N, 7°43′W).

Both species are ecologically well adapted, despite *E. globulus* being an exotic tree, and the case study areas are representative of these ecosystems in Portugal. The *P. pinaster* forest is very heterogeneous in canopy density, has experienced only limited human intervention, and covers a wide range of structures, varying widely in terms of number of trees per hectare, average dimensions, and age groups. The *E. globulus* forest is much more homogeneous and has been more extensively investigated to enable greater timber production, which is very valuable for pulp production.

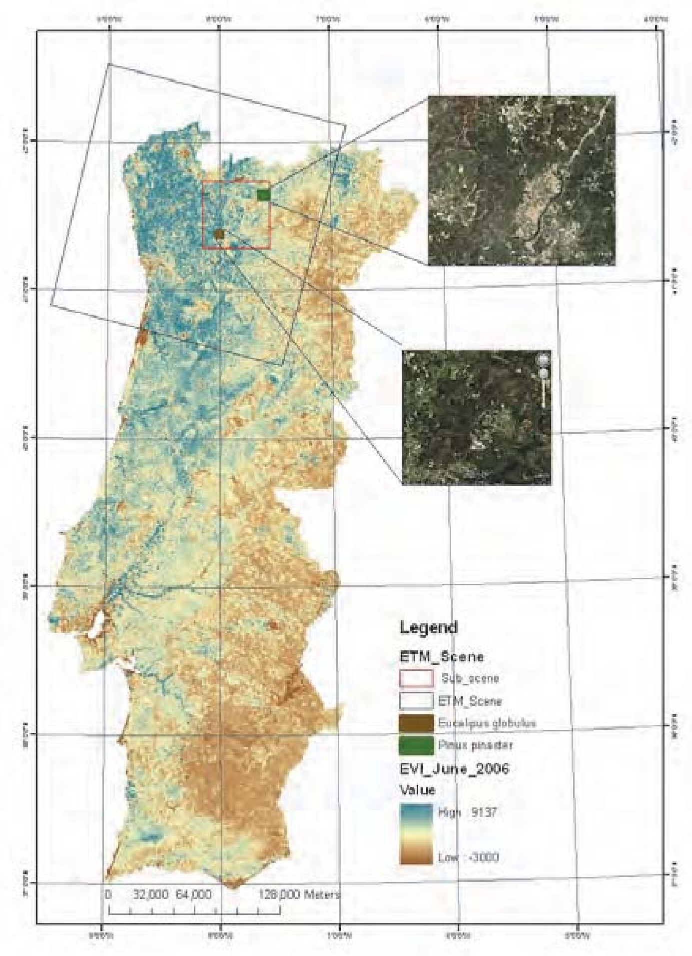

Fig. 8. Study area.

3.2 Methods and data

3.2.1 Methodology used in geometric and radiometric corrections

The available LANDSAT-7 ETM+ Image was acquired on the 15th of September 2001 at 10:02:13 (UTC). The image was geometrically and radiometrically corrected using MiraMon ("WorldWatcher"). This software allows displaying, consulting and editing raster and vector maps and was developed by the Autonomous University of Barcelona (UAB) remote sensing team. The software allows for the geometric correction of raster (e.g., IMG and JPG: satellite images, aerial photos, scan maps) or vector maps (e.g., VEC, PNT, ARC and POL and NOD), based on ground control points coordinates.

In the present research the ground control points were collected from Portuguese topographic maps on a 1/25000-scale, using the original ETM+ Scene. Twenty-five control points were collected (Toutin, 2004) to allow image correction and eleven control points were used for its validation. A first-degree polynomial correction was chosen for the geometric correction, using the nearest neighbour option for the resampling process.

Two Digital Elevation Models (DEMs) were constructed for each study area (*Pinus pinaster* and *Eucaliptus globulus* – see Figure 8), based on 10 m contour lines. The first DEM had a spatial resolution of 15 m and was used to correct the panchromatic band, mainly to allow identification of the ground control points due to its better spatial resolution. The second DEM had a spatial resolution of 20 m and was used for the correction of the LANDSAT ETM+ bands 1, 2, 3, 4, 5, and 7. Those 20 m DEMs were merged with a altitude model for Europe, with a pixel size of 1 Km. The radiometric correction was based on the lowest radiometric value for each band which is well known as the *kl*, and should be collected from the histogram analysis (Pons & Solé-Sugrañes, 1994 and Pons, 2002).

3.2.2 Methodology used to calculate vegetation indices

Within the study area, 31 sampling plots for the *Eucalyptus globulus* and 34 for the *Pinus pinaster* were surveyed and the coordinates of the centre of each plot recorded by Global Positioning System (GPS). The plots' location could then be identified on the geo-corrected images and reflectance data extracted for each ETM+ band. These data were then used to calculate a series of vegetation indices (Table 5), which were further used to analyse potential relationships with the forest variables.

In table 5, G represents the reflectance on the green wavelength; R is the reflectance in the red wavelength; NIR is the reflectance in the near infrared wavelength; and MIR1 and MIR2 are the reflectance in the two middle infrared bands from LANDSAT ETM+ image.

3.2.3 Model adjustment and selection

The available data (31 sampling plots for the *Eucalyptus globulus* and 34 for the *Pinus pinaster*) were divided in two groups, one for the adjustment of mathematical models and the other for the validation. An overall analysis of the correlation matrix allowed to identify the variables strongest related to NPP, which were then selected to establish regression models to Estimate NPP. The best NPP prediction models were selected based in the following statistics: the coefficient of determination (R^2); the adjusted coefficient of determination (R^2adj.); the root mean square error (RMSE); and the percentage root mean square error (RMSE%).

	Designation	Mathematical expression	Source
1	NDI(MIR1)	$\frac{(NIR-MIR1)}{(NIR+MIR1)}$	Lucas (1995)
2	NDI(MIR2)	$\frac{(NIR-MIR2)}{(NIR+MIR2)}$	Lucas (1995)
3	NDVI	$\frac{(NIR-R)}{(NIR+R)}$	Rouse *et al.* (1974); Bouman (1992); Malthus *et al.* (1993); Xia (1994); Nemani *et al*. (1993); Baret *et al.* (1995); Hamar *et al.* (1996); Fassnacht *et al*. (1997); Purevdorj *et al*. (1998); Todd *et al*. (1998); and Singh *et al*. (2003)
4	MVI1	$\frac{MIR1}{MIR2}$	Fassnacht *et al.* (1997)
5	MVI2	$\frac{NIR}{MIR2}$	Fassnacht *et al.* (1997)
6	RVI1	$\frac{NIR}{R}$	Tucker (1979); Xia (1994); Baret *et al.* (1995); Hamar *et al*. (1996); Fassnacht *et al*. (1997); and Xu *et al.* (2003).
7	TVI1	$\sqrt{\frac{NIR}{R}}$	Tucker (1979)
8	TVI2	$\frac{(NIR+R)}{(NIR-R)}$	Tucker (1979)
9	TVI9	$\sqrt{\frac{(G-R)}{(G+R)}+0{,}5}$	Tucker (1979)

Table 5. Vegetation indices used in the research

3.2.4 Comparison of the NPP images

NPP images obtained from different methodologies were compared by the *Kappa* index of agreement. Kappa was adopted by the remote sensing community as a useful measure of classification accuracy Rossiter (2004). The *Kappa* coefficient (*K*) measures pairwise agreement among a set of coders making category judgments, thus correcting values for expected chance of agreement (Carletta, 1996).

The overall *kappa* statistic, defining the overall proportion of area correctly classified, or in agreement, is calculated by the mathematical expression defined by Eq. 9 (Stehman, 1997; Rossiter, 2004):

$$\hat{k} = \frac{\sum_{i=1}^{k} p_{ii} - \sum_{i=1}^{k} P_{i+}.P_{+i}}{1 - \sum_{i=1}^{k} P_{i+}.P_{+i}} \qquad (9)$$

where:

k = number of land-cover categories

$\sum_{i=1}^{k} p_{ii}$ represents the overall proportion of area correctly classified

$\sum_{i=1}^{k} P_{i+}.P_{+i}$ is the expected overall accuracy if there were chance agreement between reference and mapped data

According to Green (1997) when there is complete agreement between two maps K=1, and a kappa value of zero, the two maps are said to be unrelated.

Moss (2004) considers that when Kappa is less than 20 the strength of agreement between both images is poor; between 0.21 and 0.40 fair; between 0.41 and 0.60 moderate; between 0.61 and 0.80 good; higher than 0.81 very good. However, according to Green (1997), kappa lower than 0.40 indicates a low degree of agreement; between 0.40 and 0.75 a fair to good degree of agreement; and higher than 0.75 a high degree of agreement.

3.3 Results and discussion

3.3.1 Identification of the best prediction variables

In order to identify whether if it was possible to directly or indirectly estimate NPP from the remote sensing data, the Vegetation Index better correlated with NPP was identified from the general correlation matrix and analysed. The most relevant results are summarised in Table 6.

	***Pinus* NPP**	***Eucalyptus* NPP**
DN_B	-0.179	-0.739
DN_G	-0.268	-0.692
DN_R	-0.194	-0.688
DN_NIR	0.344	-0.280
DN_MIR1	-0.078	-0.605
DN_MIR2	-0.174	-0.614
TVI2	-0.142	-0.535
TVI9	0.030	0.288
MVI1	0.486	0.427
MVI2	0.435	0.318
NDVI	0.280	0.519
NDI(MIR1)	0.181	0.386
NDI(MIR2)	0.232	0.466

Table 6. Correlation between NPP and the reflectance from each individual band and some vegetation indices

As presented in Table 6, *Pinus* NPP shows the higher correlation (positive) with the near infrared wavelength band, while *Eucalyptus* NPP is better correlated (negatively) whit the middle infrared wavelength band.

The NDVI and TVI2 are the best correlated indices for the *Eucalyptus* and the MVI1 and MVI2 for the *Pinus*. These results reflect the initial observation when only reflectance from each individual band was analysed.
The best correlated vegetation indices were selected as independent variables for adjusting regression models to estimate NPP.

3.3.2 Models for the NPP *Eucalyptus globulus* estimation

The best mathematical models to estimate the NPP for the *Eucalyptus* stands and the basic statistics (ME and MAE) calculated from the validation dataset are presented in Table 7.

Mathematical models	NPP adjusted models statistics				Validation dataset statistics	
	R^2	$R^2_{adj.}$	s_{yx}	s_{yx} (%)	ME	MAE
$NPP=27.644-0.243B-0.0007GR^2-0.00014R^2$	0.613	0.558	2.988	22.5	-1.631	2.758
$NPP_{arboreal}=89.260NDVI^2-117.195NDVI^3$ $NPP=-13.114+12.271NPP_{arboreal}-1.818(NPP_{arboreal})^2+0.091(NPP_{arboreal})^3$	0.936 0.694	0.933 0.695	1.654 2.656	35.4	0.116 -1.198	1.238 3.098
$NPP=3.593+167.750NDVI^2-233.667NDVI^3$	0.493	0.447	3.342	25.2	-0.340	2.959
$NPP_{litter}=56.584NDVI^2-69.233NDVI^3$ $NPP=7.893(NPP_{litter})^{0.412}$	0.812 0.678	0.805 0.666	2.088 2.484	53.0 18.7	-0.150 -0.589	1.309 2.834
$NPP=17.672-0.611TVI2^2+0.048TVI2^3$	0.422	0.370	3.567	26.9	-0.347	2.903
$G=13.431-155.484NDVI+648.846NDVI^2-635.713NDVI^3$ $NPP=-5.787+4.652G-0.339G^2+0.008G^3$	0.657 0.634	0.608 0.581	4.170 2.908	33.1 21.6	1.121 -0.779	2.687 3.347
$G=38.150-0.300GR-0.174MIR1$ $NPP=-5.787+4.652G-0.339G^2+0.008G^3$	0.793 0.634	0.774 0.581	3.168 2.908	33.7 21.6	-1.754 -2.199	2.754 3.662

Table 7. Selected models to estimate *Eucalyptus* NPP, and validation dataset statistics

The observed standard error of the estimates are lower in the model using as independent variable the blue, the green and the red reflectances, and in the model using the NDVI, respectively. However, the model with NDVI as independent variable reveals a lower ME. Additionally, this model has a superior applicability since the individual bands reflectance have a great variation along the year, thus varying from image to image.
Based in the field measurements and in the estimated NPP, by the model using only the NDVI directly as independent variable (R^2=0.493), two images were created for the entire study area (Figures 9a and 9b).
After the classification into four classes (1 – NPP < 5 ton $ha^{-1}year^{-1}$; 2- 5≤ NPP <10 ton $ha^{-1}year^{-1}$; 3 - 10 ≤ NPP < 15 ton $ha^{-1}year^{-1}$; and 4 - NPP > 15 ton $ha^{-1}year^{-1}$) the cross tabulation was carried out and the matrix error table analysed.
Kappa statistic showed a slight agreement around 37%. However, for a first approach these results are a good indicator for further studies. From the analyses of the *Eucalyptus* NPP map, obtained from fieldwork, it can be observed that there are no areas with an NPP lower than 5 ton $ha^{-1}year^{-1}$, and almost the whole *Eucalyptus* stand presents NPP figures between 10 and 15 ton $ha^{-1}year^{-1}$.

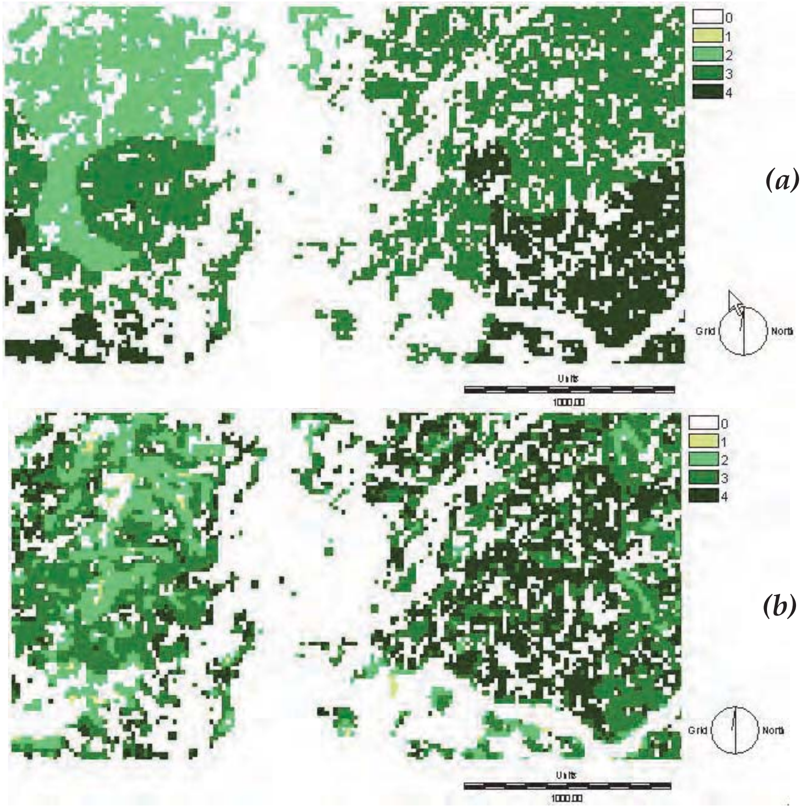

Fig. 9. *Eucalyptus* NPP estimations from field measurements (a) and NDVI model (b).

A significant result to estimate *Eucalyptus* NPP was obtained with the basal area (G) as independent variable (R^2=0.634). In this case, the basal area can be estimated with acceptable confidence, using the NDVI or MIR1 as independent variables (R^2=0.657 and 0.793, respectively). In alternative, *Eucalyptus* NPP can also be estimated indirectly, with acceptable accuracies, by the litter present in the *Eucalyptus* stands (R^2=0.678). A strong relationship was found between NPP from litter and NDVI (R^2=0.812). The same methodology can be used by estimating, in a previous stage, the NPP arboreal with the NDVI as independent variable (R^2=0.936) and subsequently, indirectly estimate the *Eucalyptus* NPP (R^2=0.694).

3.3.3 Models for the NPP *Pinus pinaster* estimation

The best mathematical models to estimate the NPP for the *Pinus* stands and the basic statistics (ME and MAE) calculated from the validation dataset are presented in Table 8. The observed standard error of the estimates, as well the ME achieved from the validation dataset shows that the best model is obtained in the model using as independent variable the MVI1 for estimate the NPP of shrubs. The NPP of pine is subsequently estimated indirectly using this variable.

As in the *Eucalyptus* predictions the same methodology was implemented to compare the final maps achieved for the Pinus stands. The *Pine* NPP model using only the MVI1 as independent variable was used (R^2=0.417). The two created maps for the entire study area (Figures 10a and 10b), were classified into four classes (1 – NPP < 5 ton ha^{-1}year^{-1}; 2- 5≤ NPP <10 ton ha^{-1}year^{-1}; 3 - 10 ≤ NPP < 15 ton ha^{-1}year^{-1}; and 4 - NPP > 15 ton ha^{-1}year^{-1}), a cross tabulation was carried out and the matrix error table analysed. Kappa statistic showed an agreement around 48%, slightly better than in *Eucalyptus* estimations. However, it was observed that the achieved model was not able to identify and locate the extreme values of NPP (e.g. neither the most productive areas nor the least productive ones).

Mathematical models	NPP adjusted models statistics				Validation dataset statistics	
	R^2	$R^2_{adj.}$	s_{yx}	$s_{yx}(\%)$	ME	MAE
$NPP=51.288-32.080MVI1+6.787MVI1^2$	0.417	0.369	4.617	31.7	-0.902	1.974
$NPP_{shrubs}=-0.516MVI1^2+0.414MVI1^3$	0.816	0.809	2.614	71.3	-0.279	2.146
$NPP=10.629+1.071NPP_{shrubs}$	0.649	0.635	3.508	27.5	-0.317	1.677
$NPP_{shrubs}=1.146+0.142MVI2^2$	0.486	0.466	3.196	83.8	-0.490	2.268
$NPP=10.629+1.071NPP_{shrubs}$	0.649	0.635	3.508	27.6	-0.842	2.276

Table 8. Selected models to estimate *Pinus* NPP and validation dataset statistics

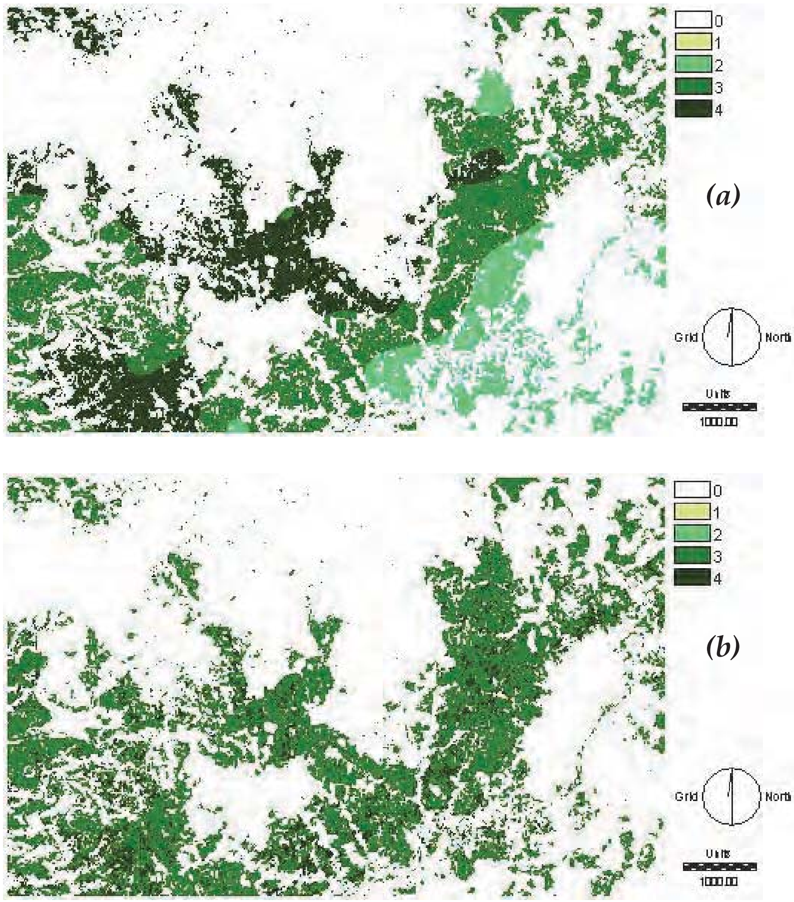

Fig. 10. Pinus NPP estimations from field measurements (a), and the MVI1 model (b).

For the *Pinus* stands, it was possible to estimate the total NPP (R^2=0.816) knowing only the NPP from shrubs. In this case, the NPP from shrubs was predicted using the MVI as auxiliary variable (R^2=0.645).

4. Conclusions

In this research, AGB and NPP estimates were carried out by means of forest inventory data remote sensing imagery and geostatistical modeling. The general conclusions are:

In the case study I, tree Aboveground biomass (AGB) mapping approaches were compared: Inventory Polygons; Direct Radiometric Relationships (DRR) and Regression-kriging (RK). Pure pine stands were mapped and AGB estimates were achieved using data collected in the National Forest inventory dataset. The Inventory polygons method was used since the field plots of forest inventory dataset fall within all the polygons of the forest cover map. At the same time, this approach was used to compare and validate DRR and RK methods.

The results showed that DRR and RK, using Vegetation Indices transformed from MODIS remotely sensed data, can be used for biomass mapping purposes. However, it should be pointed out that, in the present research, the coarse resolution of MODIS (250m) data associated with small polygons of the pine landcover class did not allow to extract the pure spectral response of this vegetation type. Hence, the correlation between AGB and NDVI as independent variable is not as high as desired.

This limitation can be overcome by using images with higher spatial resolution. Moreover, these methodologies can be applied with greater accuracy in areas where land cover polygons are large enough to minimize, as much as possible, the effect of edging.

The analysis of statistical parameters of validation dataset such as the mean error (ME), the mean absolute error (MAE), standard deviation (SD) and the root mean squared error (RMSE) show that RK, making use of geostatistical modeling techniques, combined with remote sensing data as auxiliary variable improves the predictions when compared to DRR. Furthermore, RK has the advantage of generating estimates for the spatial distribution of AGB and its uncertainty for the study area. The uncertainty maps allow the evaluation of the reliability of estimates by identifying the sites with major uncertainties which can be useful to select different estimation methods for those areas.

In the case study II, some simplified methodologies were proposed to estimate NPP. For the *Eucalyptus* ecosystem using the basal area or the NPP from litter, and for the *Pinus* ecosystem using the NPP from shrubs.

Despite the direct NPP estimation from remote sensing data did not provide very promising results, it was possible to establish indirect relationships between some vegetations indices calculated from Landsat ETM+ imagery data and the litter NPP, shrubs NPP and from basal area of the studied forest stands.

Those simplifications can be extremely important when time and economic resources are limited. The importance of those methodologies could become more relevant as NPP is a variable very difficult to obtain, consuming time and demanding hard fieldwork.

The loss in accuracy is certainly compensated by decrease of fieldwork. The balance between both should only be taken in each particular case, considering the general context of each situation (e.g., time and funds available, human resources available, objectives of the research).

5. Acknowledgements

Authors would like to express their acknowledgement to the Portuguese Science and Technology Foundation (FCT), programmes SFRH/PROTEC/49626/2009 and FCT FCOMP-01-0124-FEDER-007010 (PTDC/AGR-CFL/68186/2006).

6. References

AFN (2006). Dados do Inventário Florestal Nacional (05/06) Information retrieval tool. Autoridade Florestal Nacional. Ministério da Agricultura do Desenvolvimento Rural e das Pescas, Lisboa.

Ahmed, S., & de Marsily, G (1987). Comparison of geostatistical methods for estimating transmissivity using data on transmissivity and specific capacity. *Water Resources Research* 23(9): 1717-1737.

Atkinson, P. M.; Foody, G. M.; Curran, P. J., & Boyd D. S. (2000). Assessing the ground data requirements for regional scale remote sensing of tropical forest biophysical properties. *International Journal of Remote Sensing* 21(13-14): 2571-2587.

Baret, F., Clevers, J.G. and Steven, M.D. (1995). The robustness of canopy gap fraction estimates from red and near-infrared reflectances: A comparison of approaches. *Remote Sensing of Environment* 54: 141-151.

Bouman, B.M. (1992). Accuracy of estimating the leaf area index from vegetation indices derived from crop reflectance characteristics: a simulation study. *International Journal of Remote Sensing* 13(16): 3069-3084.

Burcsu, T. K., Robeson, S. M., & Meretsky, V.J. (2001). Identifying the Distance of Vegetative Edge Effects Using Landsat TM Data and Geostatistical Methods. *Geocarto International* 16(4): 61-70.

Cao, M. and Woodward, F.I. (1998). Net primary and ecosystem production and carbon stocks of terrestrial ecosystems and their responses to climate change. *Global Change Biology* 4: 185-198.

Carletta, J. (1996). Assessing agreement on classification tasks: the kappa statistic. *Computational linguistics* 22(2): 1-6.

Chirici, Gherardo; Barbati, Anna, & Maselli, Fabio (2007). Modelling of Italian forest net primary productivity by the integration of remotely sensed and GIS data. *Forest Ecology and Management* 246: 285-295.

Cressie, N. A. C. (1993). *Statistics for Spatial Data*. New York, USA: John Wiley & Sons. pp. 416.

Curran, P.J. (1988). The semivariogram in remote sensing: An introduction. *Remote Sensing of Environment* 24: 493-507.

Deutsch, C. V., & Journel A. G. (1998). *Geostatistical Software Library and User's Guide.* (2nd ed.). New York, USA: Oxford University Press, pp. 369.

Eastman, J. R. (2006). *Idrisi Andes. Guide to GIS and Image Processing*. USA: Clark Labs. Clark University, pp. 328.

Fassnacht, K.S., Gower, S.T., MacKenzie, M.D., Nordheim, E.V. and Lillesand, T.M. (1997). Estimating the leaf area index of north central Wisconsin forests using the Landsat Thematic Mapper. *Remote Sensing of Environment* 61: 229-245.

Field, C.B., Randerson, J.T. and Malmstrom, C.M. (1995). Global net primary production: combining ecology and remote sensing. *Remote Sensing of Environment* 51: 74-88.

García-Martín, A., Pérez-Cabello, F., de la Riva, J. R., & Montorio, R. (2008). Estimation of crown biomass of Pinus spp. from Landsat TM and its effect on burn severity in a Spanish fire scar. *IEEE Journal of Selected Topics in Applied Earth Observations and Remote Sensing 1*(4): 254-265.

Goovaerts, P. (1997). *Geostatistics for Natural Resources Evaluation*. New York, USA: Oxford University Press, Inc., pp. 496.

Goovaerts, P. (1999). Using elevation to aid the geostatistical mapping of rainfall erosivity. *Catena 34*(3-4): 227-242.

Green, A.M. (1997). Kappa statistics for multiple raters using categorical classifications, *Proceedings of the twenty-second annual SAS @Users Group International Conference*, Cary, NC: SAS Institute, Inc: 1110-1115.

Hamar, D., Ferencz, C., Lichtenberger, J., Tarcsa, G. and Ferencz-Árkos, I. (1996). Yield estimation for corn and wheat in the hungarian great plain using landsat MSS data. *International Journal of Remote Sensing* 17(9): 1689-1699.

Häme, T., Salli, A., Andersson, K., & Lohi, A. (1997). A new methodology for estimation of biomass of conifer-dominated boreal forest using NOAA AVHRR data. *International Journal of Remote Sensing* 18: 3211-3243.

Hengl T., Heuvelink G. M. B., & Stein A. (2004). A generic framework for spatial prediction of soil variables based on regression-kriging. *Geoderma 122*(1-2): 75-93.

Hengl T., Heuvelink, G. B. M. & Rossiter, D. G. (2007). About regression-kriging: from equations to case studies. *Computers and Geosciences 33*(10): 1301-1315.

Hengl, T. (2009). *A Practical Guide to Geostatistical Mapping*. Amsterdam, ISBN 978-90-9024981-0.

Hese, S., Lucht, W., Schmullius, C., Barnsley, M., Dubayah, R., Knorr, D., Neumann, K., Riedel, T., & Schröter, K. (2005). Global biomass mapping for an improved understanding of the CO2 balance-the Earth observation mission Carbon-3D. *Remote Sensing of Environment* 94(1): 94-104.

Hu, Huifeng, & Wang, G. G. (2008). Changes in forest biomass carbon storage in the South Carolina Piedmont between 1936 and 2005. *Forest Ecology and Management* 255(5-6): 1400-1408.

Hyde, P., Nelson, R., Kimes, D., & Levine, E. (2007). Exploring LiDAR–RaDAR synergy-predicting aboveground biomass in a southwestern ponderosa pine forest using LiDAR, SAR and InSAR. *Remote Sensing of Environment* 106(1): 28-38.

IGP (2010). *CLC2006 – Cartografia CORINE Land Cover 2006 para Portugal Continental; 2009*. <http://www.igeo.pt/gdr/projectos/clc2006/> (verified 01.01.2010).

Isaaks, E. H., & Srivastava, R. M. (1989). *An Introduction to Applied Geostatistics*. New York, USA: Oxford University Press, pp. 542.

Jarlan, L., Mangiarotti, S., Mougin E., Mazzega, P., Hiernaux, P., & Le Dantec, V. (2008). Assimilation of SPOT/VEGETATION NDVI data into a sahelian vegetation dynamics model. *Remote Sensing of Environment* 112(4): 1381-1394.

Knotters, M., Brus, D. J., & Voshaar, J. H. O. (1995). A comparison of kriging, co-kriging and kriging combined with regression for spatial interpolation of horizon depth with censored observations. *Geoderma* 67(3-4): 227–246.

Labrecque, S., Fournier, R. A., Luther, J. E., & Piercey, D. (2006). A comparison of four methods to map biomass from Landsat-TM and inventory data in western Newfoundland. *Forest Ecology and Management* 226, 129-144.

Liao, J., Dong, L., & Shen, G. (2009). Neural network algorithm and backscattering model for biomass estimation of wetland vegetation in Poyang Lake area using Envisat ASAR data. *Geoscience and Remote Sensing Symposium*, IEEE International, IGARSS 2009.

Lloyd, C. D. (2007). *Local Models for Spatial Analysis*. Boca Raton: CRC Press, Taylor & Francis Group.

Lu, D. (2006). The potential and challenge of remote sensing-based biomass estimation. *International Journal of Remote Sensing* 27: 1297-1328.

Lucas, N.S. (1995). *Coupling remotely sensed data to a forest ecosystem simulation model*. Thesis for the Degree of Doctor of Philosophy, University of Wales, Swansea, England, pp. 375.

Madugundu, R.; Nizalapur, V. & Jha, C. S. (2008). Estimation of LAI and above-ground biomass in deciduous forests: Western Ghats of Karnataka, India. *International Journal of Applied Earth Observation and Geoinformation* 10(2): 211-219.

Malthus, T.J., Andrieu, B., Danson, F.M., Jaggard, K.W. and Steven, M.D. (1993). Candidate high spectral resolution infrared indices for crop cover. *Remote Sensing of Environment* 46: 204-212.

Matheron G. (1963). Principles of geostatistics. *Economic Geology* 58: 1246–1266.

Matheron G. (1971). *The theory of regionalised variables and its applications. Les Cahiers du Centre de Morphologie Mathematique de Fontainblue*. Paris: Ecole Nationale Superiore de Paris, pp. 212.

Melillo, J.M, McGuire, A.D., Kicklighter, D.W., Moore III, B., Vorosmarty, C.J. and Schloss, A.L. (1993). Global climate change and terrestrial net primary production. *Nature* 363: 234-240.

Meng, Q., Cieszewski, C. J., Madden, M., & Borders, B. E. (2007). K Nearest Neighbor method for forest inventory using remote sensing data. *GIScience & Remote Sensing* 44(2): 149-165.

Meng, Q.; Cieszewski, C. J. & Madden, M. (2009). Large area forest inventory using Landsat ETM+: A geostatistical approach. *ISPRS Journal of Photogrammetry and Remote Sensing* 64: 27-36.

Moss, S. (2004). Kappa statistics. The Institute of Cancer Research, http://www.icr.ac.uk/cseu/bc_eqa_kappa.html.

Muukkonen, P., & Heiskanen, J. (2007). Biomass estimation over a large area based on standwise forest inventory data and ASTER and MODIS satellite data: A possibility to verify carbon inventories. *Remote Sensing of Environment* 107: 617–624.

Nemani, R., Pierce, L., Running, S. and Band, L. (1993). Forest ecosystem processes at the watershed scale: sensitivity to remotely-sensed leaf area index estimates. *International Journal of Remote Sensing* 14(13): 2519-2534.

Odeh, I. O. A., McBratney, A. B., & Chittleborough, D. J. (1994). Spatial prediction of soil properties from landform attributes derived from a digital elevation model. *Geoderma,* 63: 197-214.

Odeh, I.O. A., McBratney, A. B., & Chittleborough, D. J. (1995). Further results on prediction of soil properties from terrain attributes: heterotopic cokriging and regression-kriging. *Geoderma* 67(3-4): 215–226.

Palmer, D. J.; Höck, B. K.; Kimberley, M. O.; Watt, M. S.; Lowe, D. J. & Payn, T. W. (2009). Comparison of spatial prediction techniques for developing Pinus radiate productivity surfaces across New Zealand. *Forest Ecology and Management* 258: 2046-2055.

Pebesma, E. (2001). *Gstat user's manual.* University of Utrecht, pp. 108.

Pebesma, E. (2004). Multivariable geostatistics in S: the gstat package. Computers & *Geosciences* 30(7): 683-691.

Pons, X and Solé-Sugrañes, L. (1994). A simple radiometric correction model to improve automatic mapping of vegetation from multispectral satellite data. *Remote Sensing of Environment* 48: 191-204.

Pons, X. (2002). *MiraMon. Geographic information system and remote sensing software* Centre de Recerca Ecològica i Aplicacions Forestals, CREAF. Bellaterra. ISBN: 84-931323-5-7.

Purevdorj, T., Tateishi, R., Ishiyamas, T., and Honda, Y. (1998). Relationships between percent cover and vegetation indices. *International Journal of Remote Sensing* 19(18): 3519-3535.

Rahman, M. M.; Csaplovics, E., & Koch, B. (2005). An efficient regression strategy for extracting forest biomass information from satellite sensor data. *International Journal of Remote Sensing* 26(7): 1511-1519.

Rossiter, D.G. (2004). *Statistical method for accuracy assessment of classified thematic map*. International Institute for Geo-information Science and Earth, Department of Earth Systems Analysis, Enschede, NL, pp. 46.

Rouse, J.W., Haas, R.H., Schell, J.A., Deering, D.W. and Harlan, J.C. (1974). *Monitoring the vernal advancement retrogradiation of natural vegetation*. Final Report Type III, NASA/GSFC, Greenbelt, MD., USA, pp. 371.

Sales, M. H., Souza Jr., C. M., Kyriakidis, P. C.; Roberts, D. A., & Vidal, E. (2007). Improving spatial distribution estimation of forest biomass with geostatistics: A case study for Rondônia, Brazil. *Ecological Modelling* 205: 221-230.

Sen, Zekai (2009). *Spatial Modeling Principles in Earth Sciences*. London, New York: Springer Dordrecht Heidelberg, pp. 351.

Singh, R.P., Roy, S., and Koogan, F. (2003). Vegetation and temperature condition indices from NOAA AVHRR data for drought monitoring over India. *International Journal of Remote Sensing* 24 (22): 4393-4402.

Stehman, S.V. (1997). Selecting and interpreting measures of thematic classification accuracy. *Remote Sensing of Environment* 62: 77-89.

Todd, S.W., Hoffer, R.M., and Milchunas, D.G. (1998). Biomass estimation on grazed and ungrazed rangelands using spectral indices. *International Journal of Remote Sensing* 19 (3): 427-438.

Tomppo, E. (1991). Satellite imagery-based national inventory of Finland. *International Archives of Photogrammetry and Remote Sensing 28*(7-1): 419-424.

Tomppo, E., Nilsson, M., Rosengren, M., Aalto, P., Kennedy, P. (2002). Simultaneous use of Landsat-TM and IRS-1c WiFS data in estimating large area tree stem volume and aboveground biomass. *Remote Sensing of Environment* 82: 156−171.

Toutin, T. (2004). Review article: Geometric processing of remote sensing images: models, algorithms and methods. *International Journal of Remote Sensing* 25(10): 1893-1924.

Tucker, C.J. (1979). Red and photographic infrared linear combinations for monitoring vegetation. *Remote Sensing of Environment* 8: 127-150.

Waring, R.H., Landsberg, J.J. and Williams, M. (1998). Net primary production of forests: a constant fraction of gross primary production? *Tree Physiology* 18: 129-134.

Webster, R. & Oliver, M. A. (1992). Sample adequately to estimate variograms of soil properties. *Journal of Soil Science* 43: 177-192.

Webster, R. & Oliver, M. A. (2007). *Geostatistics for Environmental Scientists.* (2nd ed.), England: John Wiley & Sons Ltd, pp.332.

Woodcock, C. E, Strahler, A. H., & Jupp, D. L. B. (1988). The use of variograms in remote sensing: II. Real digital images. *Remote Sensing of Environment* 25: 349-379.

Xia, L., 1994. A two-axis adjusted vegetation index (TWVI). *International Journal of Remote Sensing* 15(7): 1447-1458.

Xu, B., Gong, P., and Pu, R. (2003). Crown closure estimation of oak savannah in a dry season with Landsat TM imagery: comparison of various indices through correlation analysis. *International Journal of Remote Sensing* 24 (9): 1811-1822.

Zheng, D., Heath, L. S., & Ducey, M. J. (2007). Forest biomass estimated from MODIS and FIA data in the. Lake States: MN, WI and MI, USA. *Forestry* 80(3): 265-278.

Annex D

Viana, H., Dias, S., Marques, C., Cruz, M., Lopes, D., Aranha, J., 2009. Estabelecimento de modelos alométricos para predição da biomassa aérea de *Eucalyptus globulus*. Actas do 6º Congresso Florestal Nacional. Ponta Delgada, Açores. 6-9 Outubro, pp. 765-770.

Estabelecimento de Modelos Alométricos para Predição da Biomassa Aérea de *Eucalyptus globulus*

Helder Viana[1], Ângelo Cardoso[1], Ricardo Correia[1], Domingos Lopes[2] e José Aranha[2]

[1]Escola Superior Agrária de Viseu. Secção Florestal. Quinta da Alagoa - Ranhados, 3500-606 VISEU

[2]Universidade de Trás-os-Montes e Alto Douro. Departamento de Ciências Florestais e Arquitectura Paisagista. Apartado 1014, 5000-911 VILA REAL

Resumo. O presente trabalho apresenta a quantificação da biomassa aérea de *Eucalyptus globulus*, tanto total e como das suas diferentes componentes (tronco, bicada, ramos, folhas, e casca), através de modelos alométricos ajustados para o efeito. A avaliação da biomassa aérea foi feita através de métodos destrutivos em povoamentos de primeira rotação de eucalipto. Os dados foram recolhidos durante 2007 e 2008, em 60 árvores, distribuídas por 6 locais na região de Dão Lafões, em áreas sujeitas a corte final. Foram feitas medições dendrométricas (diâmetro à altura do peito, altura da copa e altura total) nas árvores amostra, antes e após o abate. A biomassa residual de cada árvore foi recolhida e pesada no local. Foi colhida uma amostra para quantificar as diferentes componentes (tronco, bicada, ramos, folhas, e casca) e para posterior análise em laboratório. Foram ajustados vários modelos alométricos não lineares, para a predição da biomassa total da árvore e das suas componentes, recorrendo a variáveis dendrométricas individualmente e combinadas, tendo-se seleccionado os melhores modelos através da análise dos coeficientes de regressão, de determinação (R^2), e de determinação ajustados (R^2_{adj}), bem como os resíduos e a significância do teste de t de Student. Os modelos encontrados apresentam uma boa aptidão de predição da biomassa residual de eucalipto podendo constituir uma ferramenta útil na gestão florestal dos povoamentos desta espécie.

Palavras-chave: *Eucalyptus globulus*, Biomassa aérea, Modelos alométricos, Região Dão-Lafões

***

Introdução e objectivos

O eucalipto é, a seguir ao pinheiro bravo, a espécie mais difundida no país, com 22,9% dos cerca de 3,240 milhões de hectares ocupados com floresta (DGRF, 2007). Controvérsias à parte, as elevadas produtividades do eucalipto no país (16 e 24 $tha^{-1}ano^{-1}$, estimadas por FABIÃO (1986) para a região Centro) levam a que seja explorada fundamentalmente para a utilização pela indústria. O eucalipto assume também uma especial relevância pelas elevadas quantidades de carbono que captura da atmosfera (PEREIRA, 2007). Por outro lado, os sobrantes da exploração florestal, biomassa florestal residual, têm também uma utilidade para fins energéticos, com um interesse crescente. Desta forma, modelos de produção e crescimento e modelos de estimação da biomassa são fundamentais para se conhecerem, de uma forma expedita, as existências dos recursos. A bibliografia consultada refere equações para predição da biomassa aérea do eucalipto no país como as desenvolvidas (ARTHUR, 1985; SILVA *et al.,* 1985; FABIÃO, 1986 ou TOMÉ 2007), no entanto, estas carecem de validação local.

Este trabalho procura contribuir com um sistema de equações que permita estimar a biomassa aérea acima do solo, tanto total como por componentes, ajustadas à região de Dão-Lafões, de forma a poderem ser utilizadas de forma expedita, com base em parâmetros recolhidos num processo de inventário florestal tradicional.

Métodos

Em 6 povoamentos puros de *Eucaliptus globulus*, de 1ª rotação, com pelo menos 1ha de área, distribuídos pela região de Dão-Lafões, foram seleccionadas 60 árvores para amostragem destrutiva. Previamente ao abate, foram instaladas parcelas de amostragem circulares com 500m^2 e avaliados, nas árvores em pé, os parâmetros dendrométricos: altura total (h); altura da base copa viva (hc); diâmetro a 1,30 m (d); diâmetro da copa (cw), de forma a permitir calcular as variáveis dos povoamentos, nº de árvores por hectare (N), altura dominante (dom), e área basal (G).
Foram seleccionadas, aleatoriamente, pelo menos duas árvores por classe de diâmetro e, pelo menos, 10 árvores por parcela. Em todas as árvores foram medidas as seguintes variáveis: altura total (h); altura da base copa viva (hc); altura da bicada (5 cm) (hb); diâmetro do cepo (dc); diâmetro a 1,30 m (d) e os diâmetros do tronco de 2 em 2 m, desde do nível de d até à base da bicada e medição da espessura de casca (B) aos vários níveis da medição de d.
Para o âmbito do estudo foram consideradas 5 componentes da biomassa total da árvore: lenho do tronco, casca, ramos vivos, bicada, folhas. Os ramos da copa e da bicada foram separados e pesados integralmente. A bicada cortada (<5cm) e um ramo da copa, recolhido aleatoriamente, em cada andar, foram transportados para laboratório a fim de se separarem e quantificarem as suas componentes. Ao nível da base do tronco e ao nível da base da bicada foram recolhidas rodelas com a casca, com aproximadamente 2 cm de espessura, para determinação da humidade e massa volúmica.
Para cada componente foram ajustadas várias equações alométricas, sob a forma não linear, utilizando as variáveis independentes, atrás referidas, e simples ou combinadas.
Os povoamentos de eucalipto, onde se instalaram as parcelas, localizam-se nos concelhos de Mortágua, Santa Comba Dão, Tondela, São Pedro do Sul, Vila Nova de Paiva e Viseu, que se inserem na região Dão-Lafões (Figura 1).

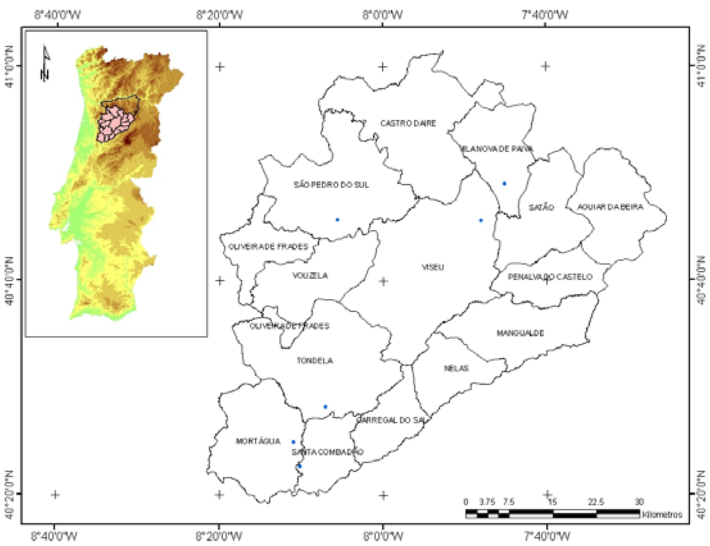

Figura 1 – Localização das parcelas de estudo

Resultados e discussão

Caracterização dos povoamentos

Os povoamentos onde se realizaram os abates, para amostragem destrutiva, apresentavam as seguintes características (Tabela1).

Tabela 1 – Varáveis do povoamento medidas nas parcelas de estudo

LOCAL	t	N (ha)	d (cm)	Gm^2ha^{-1}	h(m)	Abatidas
1	12	800	12,8	10,93	18,37	10
2	8	1220	13,7	15,49	18,05	10
3	10	1260	12,9	18,3	19,97	10
4	13	1220	15,4	26,11	16,97	10
5	13	1320	12,6	19,75	12,71	10
6	12	1420	14,8	28,07	12,83	10

Caracterização das árvores

Após quantificar as componentes das 60 árvores medidas, obtiveram-se as seguintes proporções médias (Tabela 2).

Tabela 2 - Proporção das componentes da biomassa em relação ao total e em relação à copa do eucalipto

Componente	Proporção total (%)	Proporção da copa (%)
Folhas	4,0	43,0
Bicada (<5cm)	0,7	7,4
Ramos	4,7	49,6
Casca	11,3	
Fuste	79,3	

Na Figura 2 apresenta-se a variação das proporções da biomassa aérea da copa em função da classe de d das árvores. Como se pode ver a distribuição das componentes não varia muito de acordo com as classes de diâmetro.

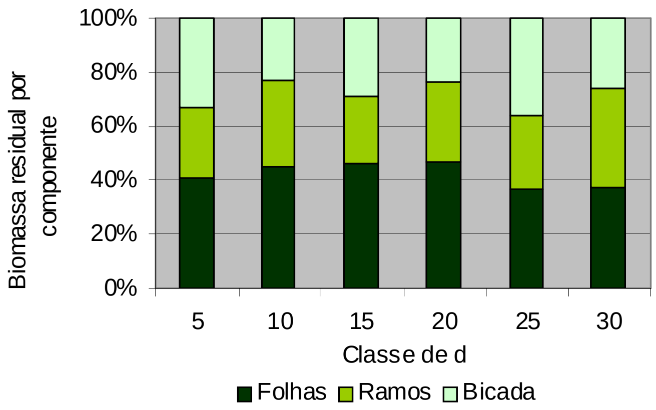

Figura 2 – Proporção média de cada componente em relação à biomassa residual, por classe de d

Modelos alométricos ajustados

Das funções alométricas ajustadas seleccionaram-se as que permitiram obter as melhores estimativas, cujos parâmetros, R^2_{aj} e EQM são apresentados na Tabela 3.

Tabela 3 - Equações ajustadas para a biomassa aérea, estimativa dos parâmetros e coeficientes de determinação ajustados

Componente	**Biomassa ($t.ha^{-1}$)**	**X - variáveis independentes**	**Estimativa dos parâmetros**	**R^2aj**	**EQM $t.ha^{-1}$**
Copa total	$\ln W = \alpha + \beta x_1 + \theta x_2 + \delta\ x_3$		α = -0,0744878	0,85	0,433
		d (cm)	β = 0,1733661		
		d.hc	θ = 0,006707918		
		d^2.h.hc	δ = -0,000012032		
Folhas	$W = \alpha.x^{\beta}$	d(cm)	α = 0,0252	0,78	6,84
			β = 2,1164		
Ramos	$W = \alpha.e^{\beta x}$	d(cm)	α = 0,4339	0,77	12,35
			β = 0,1744		
Bicada	$W = \alpha.e^{\beta x}$	dh	α = 0,6663	0,42	1,36
			β = 0,00002245		
Tronco	$\ln W = \alpha + \beta \ln d + \theta(h \ln d) + \delta \ln h$		α = -2,62352	0,98	0,19
		lnd	β = 2,2249		
		hlnd	θ = 0,004352		
		lnh	δ = 0,44863		
Casca	$W = \alpha.x^{\beta}$	dh	α = 3,42335E-06	0,94	5,20
			β = 1,5207		

Nota: diâmetro (d) em centímetros e alturas (h, hc) em metros

Para a obtenção de estimativas da biomassa residual total (biomassa da copa), ajustou-se uma equação por regressão linear múltipla, uma vez que este tipo de equação apresentou melhor qualidade de ajustamento $R^2aj = 0,85$. Estas equações são de grande utilidade na estimativa da biomassa total residual dos povoamentos, porque, na maioria dos casos, o interesse prende-se com a estimativa da biomassa total residual dos povoamentos.

Para as componentes ajustadas individualmente: folhas, ramos, bicada e casca, as equações sob a forma exponencial e de potência foram as que apresentaram uma melhor qualidade de ajustamento, nas várias relações de variáveis independentes testadas (Tabela 3 e Figura 3). Para o tronco a equação regressão linear múltipla foi a que melhores resultados apresentou.
A Biomassa total aérea é dada pela soma das componentes (W t.ha^{-1}) por:

$$W(t\ ha^{-1}) = W_{Folhas} + W_{Ramos} + W_{Bicada} + W_{Tronco} + W_{Casca.}$$

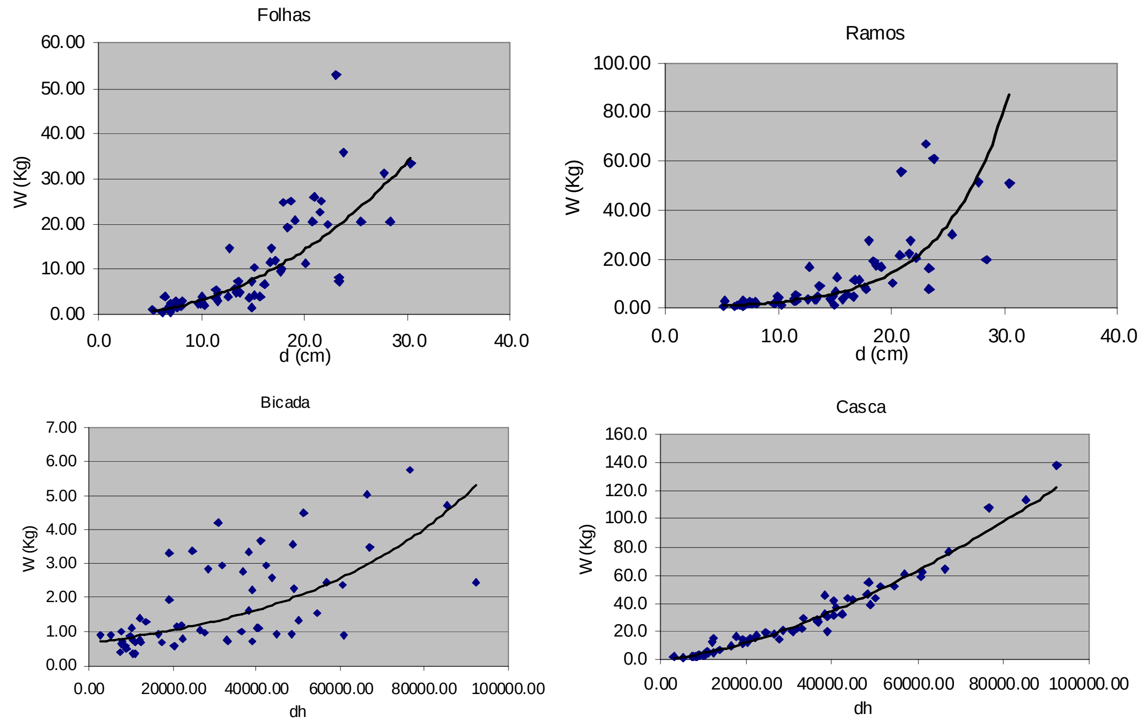

Figura 4 - Representação gráfica das equações alométricas nas componentes de biomassa Folhas, Ramos, Bicada, Casca

Conclusão

O sistema de cinco equações, ajustadas para estimar as componentes individuais da biomassa produzida em povoamentos de *eucalipto globulus*, na região de Dão–Lafões, permitiu obter estimativas razoáveis. A biomassa da bicada apresenta uma qualidade de ajustamento menor, comparativamente com as equações obtidas para as restantes componentes, uma vez que esta componente tanto pode assumir a forma dum único ramo ou ser composta por vários pequenos ramos. Os melhores resultados são obtidos incorporando como variável independente o diâmetro à altura do peito (d), a altura (h), a altura de copa (hc) e combinações destas.
A equação ajustada para a biomassa residual total (copa total) apresenta uma qualidade razoável de ajustamento, sendo aquela que talvez tenha um maior interesse de aplicação prática, uma vez que permite estimar a totalidade da biomassa residual. Este modelo constitui, por isso, uma ferramenta de grande utilidade na gestão florestal deste tipo de povoamentos. Recorrendo a medições simples, como seja o diâmetro (d) e a altura total das árvores, pode-se

fazer a monitorização periódica da biomassa produzida em povoamentos de *eucalipto globulus*.

Bibliografia

ARTHUR, D., Little International Inc., 1985. Resíduos florestais para produção de energia em Portugal. Ed. Tecninvest, SARL.

DGRF, 2007. Resultados do Inventário Florestal Nacional 2005/06. Planeamento e Estatística. Direcção Geral dos Recursos Florestais. Ministério da Agricultura do Desenvolvimento Rural e das Pescas. Lisboa.

FABIÃO, A.M.D., 1986. *Contribuição para o estudo da dinâmica da biomassa e produtividade primária líquida em eucaliptais*. Tese de Doutoramento. Universidade Técnica de Lisboa, Instituto Superior de Agronomia, Lisboa, Portugal.

LOPES, DOMINGOS, 2005. Estimating Net Primary Prodution in *Eucalyptus globulus* and *Pinus pinaster* Ecosystems in Portugal. PhD Thesis, Kingston University, England.

PEREIRA, J.S., 2007. *Uma espécie altamente produtiva. In: Pinhais e Eucaliptais- A Floresta Cultivada.* Lisboa. Fundação Luso-Americana. pp167-181.

SILVA, R., TAVARES, M., PÁSCOA, F., Residual Biomass of Forest Stands., 1991. *Pinus pinaster* Ait. *and Eucaliptus globulus* Labill. Actas nº 5, 10º Congresso Florestal Mundial, Paris.

TOMÉ, M., 2007. Inventariação de recursos florestais. Volume II - Caracterização e monitorização de povoamentos florestais e matos. Publicações GIMREF, TP 2/2007. Universidade Técnica de Lisboa, Instituto Superior de Agronomia, Centro de Estudos Florestais, Lisboa.

Annex E

Viana, H., Fernandes, P., Rocha, R., Lopes, D., Aranha, J., 2009. Alometria, Dinâmicas da Biomassa e do Carbono Fixado em Algumas Espécies Arbustivas de Portugal 6º Congresso Florestal Nacional, Ponta Delgada, Açores. 6-9 Outubro, pp. 244-252.

[Annexe E.1]

Viana, H., Lopes, D., Aranha, J., 2009.Predição de biomassa arbustiva lenhosa empregando dados de inventário e o índice de diferença normalizada extraído em imagens landsat 5 TM, ISPV Millenium. 37.

[Annexe E.2]

Aranha, J., Calvão, A., Lopes, D., Viana, H., 2011. Quantificação da biomassa consumida nos últimos 20 anos de fogos florestais no Norte de Portugal. Info 26, 44-49.

[Annexe E.3]

Viana, H., Vega-Nieva, D., Ortiz Torres, L., Lousada, J., Aranha, J., 2012., Fuel characterization and biomass combustion properties of selected native woody shrub species from central Portugal and NW Spain. Fuel. DOI: 10.1016/j.fuel.2012.06.035.

Annexe E.4]

Annex E.1

Viana, H., Fernandes, P., Rocha, R., Lopes, D., Aranha, J., 2009. Alometria, Dinâmicas da Biomassa e do Carbono Fixado em Algumas Espécies Arbustivas de Portugal 6º Congresso Florestal Nacional, Ponta Delgada, Açores. 6-9 Outubro, pp. 244-252.

Alometria, Dinâmicas da Biomassa e do Carbono Fixado em Algumas Espécies Arbustivas de Portugal

Helder Viana[1], Paulo Fernandes[2], Rui Rocha[3], Domingos Lopes[2] e José Aranha[2]
[1]Escola Superior Agrária de Viseu. Secção Florestal. Quinta da Alagoa - Ranhados, 3500-606 VISEU
[2]Universidade de Trás-os-Montes e Alto Douro. CECAV, Departamento de Ciências Florestais e Arquitectura Paisagista, Quinta de Prados. Apartado 1014, 5000-911 VILA REAL
[3]LECO Instrumentos, S.A. Av. de la Industria, 43 - 28760 Tres Cantos, Madrid, ESPANHA

Resumo. O presente trabalho procurou quantificar as disponibilidades de biomassa arbustiva após a ocorrência de incêndios florestais, avaliar a capacidade de acumulação de carbono, na parte aérea e radicular, e determinar o seu potencial energético. Para o efeito foram instaladas em 2007, aleatoriamente, na região de Viseu, parcelas de amostragem ($10m^2$) com três repetições, num total de 18, em locais ardidos entre 2000 e 2005. As plantas mais representativas e interessantes para o âmbito deste estudo incidiram sobre três grupos: giesta (*Cytisus* sp), tojo (*Ulex* sp.) e urze (*Erica* sp). Foram recolhidas plantas individuais completas em cada parcela, para posterior análise termo-físico-química em laboratório, e pesada, no local, a biomassa total existente. Posteriormente, foram ajustadas equações de regressão para estimar a biomassa. Atendendo à grande variabilidade de espécies, densidades, etc., que se pode encontrar na regeneração arbustiva após o fogo, os modelos alométricos mostram uma boa de qualidade ajustamento para a predição total de biomassa ($t.ha^{-1}$). Os resultados revelam que estas espécies fixam uma elevada percentagem de carbono tanto na parte aérea como radicular e de acordo com os poderes caloríficos avaliados podem ter um aproveitamento energético interessante.
Palavras-chave: Biomassa, Modelos alométricos, Carbono, Arbustivas, Giesta, Tojo, Urze, Poder calorífico

***

Introdução e objectivos

A investigação sobre a quantificação e caracterização da biomassa florestal tem sido crescente nos últimos anos. Se, por um lado, os ecossistemas florestais desempenham um papel importante no ciclo biogeoquímico do carbono, por outro o aproveitamento desta biomassa para fins energéticos apresenta-se como uma possibilidade que importa estudar.

A biomassa arbustiva lenhosa tem vindo a ser estudada com crescente interesse, dados os múltiplos aspectos de que se reveste o conhecimento quer da disponibilidade quer das suas características, tanto em estudos de recuperação pós-fogo, como de balanço do carbono ou redução do perigo de incêndio, como se pode ler em FERNANDES, 1991; NATÁRIO e PEREIRA, 1992; FERNANDES e PEREIRA 1993; BOTELHO *et al.,* 1994; REGO *et al*., 1994; FERNANDES e REGO, 1998a; FERNANDES e REGO, 1998b; FERNANDES *et al.,* 2002. Estes estudos, particularmente direccionados para a predição do comportamento do fogo, ganham, actualmente, maior importância com a dinâmica que se instalou no aproveitamento da vegetação para efeitos energéticos e no papel que esta desenvolve no ciclo global do carbono.

O facto de mais de 1,8 milhões de hectares do país serem ocupados por vegetação arbustiva (DGRF, 2007a) torna ainda mais evidente o interesse em estudar este tipo de vegetação.

Particularmente preocupante é o facto destes espaços arderem ciclicamente. De 1980 a 2006 arderam aproximadamente 3,1 milhões de hectares (1,5 milhões em áreas arbustivas e 1,6 milhões de povoamentos), o que dá uma média anual de cerca de 115 mil hectares (63 mil de povoamentos e 52 mil de matos). Estes incêndios libertam grandes quantidades de gases com efeito de estufa, particularmente dióxido de carbono, para a atmosfera conforme demonstrado por SILVA *et al.,* 2006, pelo que urge encontrar soluções de gestão viáveis para estes espaços.
Os objectivos a alcançar com este trabalho foram o estabelecimento de equações de regressão para estimação da biomassa e a caracterização termo-fisico-química dessa biomassa.

Material e métodos

Enquadramento da área de estudo

As parcelas de estudo foram instaladas no concelho de Viseu e nos concelhos limítrofes, em áreas ardidas entre 2000 e 2005 (Figura 1). Esta região apresenta uma topografia complexa, uma vez que é rodeada por maciços importantes como as Serras do Caramulo, Arada, Montemuro, Lapa e Estrela. As altitudes variam desde aproximadamente 100m no vale do Rio Dão até aos 1800 metros na Serra da Estrela. A variabilidade climática também é acentuada observando-se precipitações médias anuais de 800 a 2800mm no vale do rio Dão e temperaturas médias anuais inferiores que variam de 7,5 até a 16ºC.
A região é ocupada por espaços florestais onde predomina o pinheiro bravo e onde as áreas de matos são significativas. Frequentemente estas áreas são percorridas por incêndios como mostra a Figura 1.

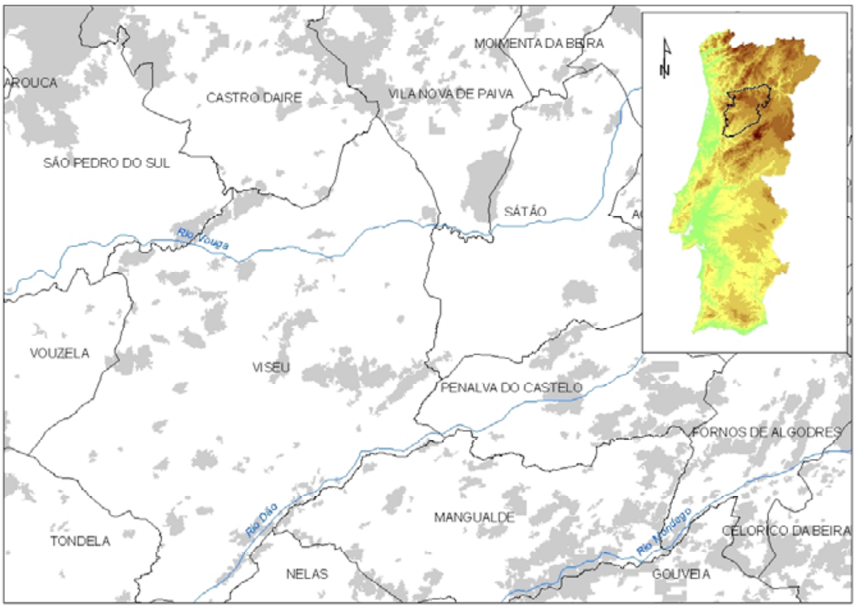

Figura 1 - Localização da área de estudo
(as manchas de cor cinza representam as áreas ardidas entre 2000 e 2007)

Metodologia

O presente trabalho teve como ponto de partida a selecção dos locais de amostragem. Numa primeira abordagem seleccionaram-se as áreas ardidas na região durante o período 2000-2005, sendo apenas considerados os locais ardidos apenas uma vez nos últimos 5 anos, no período de tempo considerado. As áreas amostradas tinham ocupação vegetal homogénea e dimensão superior a 2 hectares. Foram amostrados casualmente três locais dispersos pela região, para cada ano, o que perfez um total de 18 parcelas. As amostragens decorreram entre Março e Maio de 2007.

A carga arbustiva regenerada após o fogo foi agrupada em três grupos de acordo com a vegetação lenhosa mais representativa observada, e de interesse para o estudo: giesta (*Cytisus* sp.), tojo (*Ulex* sp.) e urze (*Erica* sp). Posteriormente, foram instaladas parcelas de amostragem circulares com $10m^2$ e a vegetação foi cortada, agrupada e pesada no local, de forma a determinar a biomassa existente ($t.ha^{-1}$).

De cada grupo foram recolhidas três plantas individuais completas (parte aérea e radicular) de cada espécie, representativas da vegetação média de cada parcela, colocadas num recipiente hermeticamente fechado, para evitar a perda de humidade, e enviadas para laboratório.

Em laboratório as plantas foram medidas (comprimento aéreo e radicular) e pesadas por componentes (raiz, caules e folhas) de forma a estudar o crescimento individual de cada espécie. Deste material foram retiradas diferentes amostras para se fazer a caracterização termo-fisico-química.

A fim de se determinar o conteúdo de humidade presente nas amostras, estas foram introduzidas numa estufa de secagem a uma temperatura constante de 103±2ºC até se obter um peso seco constante. A massa volúmica ($Kg.m^{-3}$) relativa ao peso verde e ao peso seco foi determinada pelo princípio de Arquimedes. Após a secagem, as componentes foram moídas, de forma a homogeneizar o mais possível as amostras, e separadas em diferentes fracções para as análises subsequentes.

A análise da composição elementar (C, H, N, O e S) foi feita com o analisador TruSpect da LECO.

O poder calorífico foi determinado com um calorímetro de combustão isoperibólico, Parr 6300, de acordo com a metodologia descrita na Norma DD CEN/TS 14918:2005 (Solid Biofuels - Method for the determination of calorific value). Os teores de cinzas após combustão foram determinados de acordo com a metodologia descrita na Norma DD CEN/TS 14775:2004 (Solid biofuels - Method for the determination of ash content) e o teor de substâncias voláteis libertadas durante a combustão foram determinadas de acordo com a metodologia descrita na Norma DD CEN/TS 15148:2005 (Solid biofuels - Method for the determination of the content of volatile matter).

Numa fase posterior ao tratamento laboratorial dos dados de campo, fez-se a caracterização da biomassa em função da espécie e das características do coberto vegetal, bem como o ajustamento de equações de regressão que permitissem quantificar essa biomassa com base em variáveis biofísicas de fácil acesso como seja a idade, a altura e o grau de ocupação.

Após o ajustamento de vários modelos para a predição da biomassa por hectare ($t.ha^{-1}$), seleccionaram-se aqueles que apresentaram melhor qualidade de ajustamento, após avaliação dos coeficientes de regressão (R), de determinação (R^2), e de determinação ajustados (R^2_{adj}), bem como os resíduos (EQM) e a significância do teste de t de Student.

Resultados e discussão

Após processar os dados de campo, foi possível verificar que a giesta é a espécie mais frequente, na regeneração vegetal de áreas ardidas, como se apresenta na Tabela 1.

Tabela 1- Caracterização das parcelas amostradas

Parcela	Ano fogo	Idade regeneração	Composição %		
			giesta	tojo	urze
1	2000	7		40,9	59,1
2	2000	7	88,0		12,0
3	2000	7	100,0		
4	2001	6	100,0		
5	2001	6	72,3	27,7	
6	2001	6	61,9		38,1
7	2002	5	100,0		
8	2002	5	47,0	33,7	19,3
9	2002	5	100,0		
10	2003	4	14,3	42,9	42,9
11	2003	4	76,9	23,1	
12	2003	4	70,9	29,1	
13	2004	3	70,8	29,2	
14	2004	3	35,3	64,7	
15	2004	3	100,0		
16	2005	2		100,0	
17	2005	2	100,0		
18	2005	2			100,0

Após o ajustamento de vários modelos de regressão, verificou-se que a equação alométrica que apresentou o melhor desempenho nas várias relações testadas foi:

$Y = \alpha.X^{\beta}$

Onde:
Y - Quantidade de biomassa por hectare ($t.ha^{-1}$), variável dependente
α, β - Parâmetros de regressão
X - Variável independente

Predição da carga arbustiva lenhosa total

Dos vários modelos de regressão ajustados, seleccionaram-se os que permitiram obter as melhores estimativas, que se apresentam na Tabela 2 e Figura 2.
A análise da Tabela 2 indica que os melhores resultados são obtidos quando se recorre a variáveis independentes transformadas ou combinadas. A melhor equação de regressão (R^2_{aj} = 0,89) recorre à combinação grau de ocupação x altura do coberto vegetal, permitindo obter estimativas de biomassa com um erro de 27,9% (EQM = 4,26 $t.ha^{-1}$). O desempenho desta

equação é bastante satisfatório para a vegetação em causa, dada a grande heterogeneidade da distribuição espacial, às distintas espécies presentes.

Tabela 2 - Equações da forma $Y = \alpha.x^{\beta}$ ajustadas à biomassa aérea total ($t.ha^{-1}$), estimativa dos parâmetros e coeficientes de determinação ajustados

Equação	X - variável independente	Estimativa dos parâmetros	R^2aj	EQM ($t.ha^{-1}$)
1	t (anos)	$\alpha = 1,1336$ $\beta = 1,6291$	0,72	5,29
2	h (cm)	$\alpha = 0,1239$ $\beta = 1,1091$	0,78	5,45
3	ln h	$\alpha = 0,035$ $\beta = 4,1632$	0,81	5,18
4	ln t	$\alpha = 6,2667$ $\beta = 2,04$	0,76	4,84
5	t.h (cm)	$\alpha = 0,2026$ $\beta = 0,7362$	0,82	4,73
6	GO(%).h (cm)	$\alpha = 0,0258$ $\beta = 0,754$	0,89	4,26

Sendo: t – idade da regeneração após o fogo; h altura média; GO (%) – grau de ocupação do solo; EQM – Erro Quadrático Médio

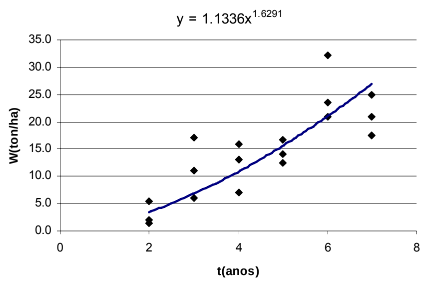

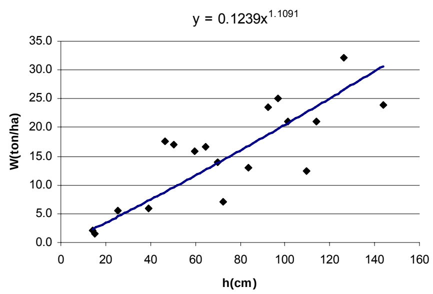

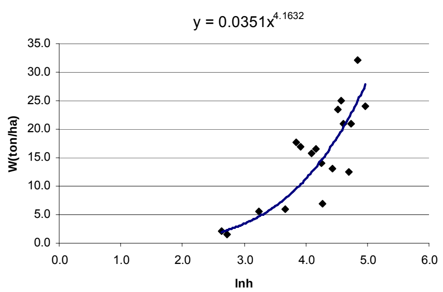

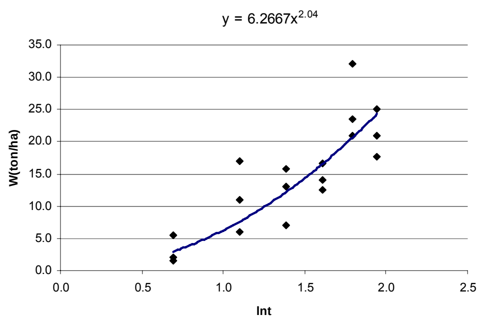

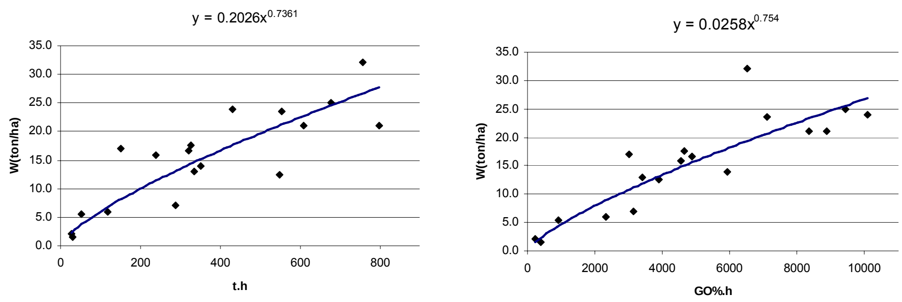

Figura 2 - Relações estabelecidas entre a carga arbustiva total e as variáveis testadas

Predição da altura do coberto vegetal

Da mesma forma que para a predição da carga arbustiva lenhosa total, também foram ajustados diversos modelos de regressão para a predição da altura da vegetação. Os melhores ajustamentos obtidos para a predição da altura da vegetação são apresentados na Tabela 3 e Figura 3.

Tabela 3 - Equações da forma $Y = \alpha.x^{\beta}$ ajustadas para a altura da vegetação (m), estimativa dos parâmetros e coeficientes de determinação ajustados

Equação	X - variável independente	Estimativa dos parâmetros	R^2aj	EQM (m)
1	lnt	$\alpha = 0{,}392$ $\beta = 1{,}5284$	0,62	0,32
2	ln(GO.t)	$\alpha = 0{,}0036$ $\beta = 3{,}0554$	0,58	0,35

Sendo: t – idade da regeneração após o fogo; GO (%) – grau de ocupação do solo

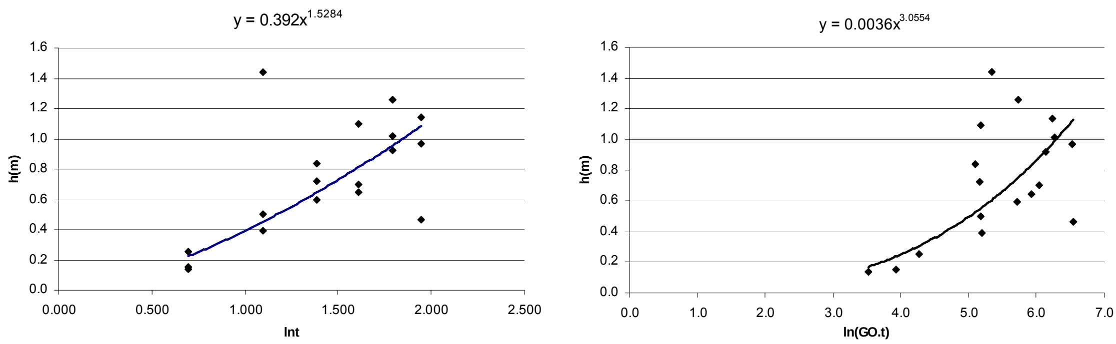

Figura 3 - Relações estabelecidas entre a altura da vegetação e as variáveis t e GO

A qualidade do ajustamento é inferior àquela alcançada na fase anterior, mas atendendo a que a altura ajustada se refere à altura média medida nas várias parcelas, de três tipos de vegetação existente, giesta, tojo e urze, constituem uma indicação razoável deste parâmetro. Estas espécies podem apresentar crescimentos muito diferentes entre si ao longo do tempo e, por outro lado, para uma determinada espécie os crescimentos vão diferir em função das características da estação e da densidade de indivíduos. Desta forma é possível encontrar crescimentos muito díspares no mesmo local percorrido pelo fogo. As equações apresentadas referem-se à relação da altura do coberto vegetal médio com as variáveis t(anos) e Grau de Ocupação GO(%), transformadas e combinadas.

Análise imediata, determinação dos poderes caloríficos e parâmetros físicos

A análise termo-fisico-química da biomassa permitiu obter valores relativos a: humidade (%) e massa volúmica ($kg.m^{-3}$); poder calorífico superior ($kJ.kg^{-1}$); e os resultados da análise imediata, teor de cinzas (%), teor de voláteis (%) e carbono fixo (%) após a combustão, das componentes aéreas e radiculares, cujos resultados se apresentam na Tabela 4.

Tabela 4 - Resultados da análise termo-fisico-química da biomassa vegetal

Vegetação	**PCS ($kJ\ kg^{-1}$)**	**H (%)**		**Massa volúmica ($kg\ m^{-3}$)**		**Cinzas (%)**		**Voláteis (%)**		**Carbono fixo (%)**	
	Aérea	Aérea	Raiz	Aérea	Raiz	Aérea	Raiz	Aérea	Raiz	Aérea	Raiz
Giesta	18669,4	51,9	48,7	862	1018	1,0	0,7	82,5	82,7	16,5	16,6
Tojo	18442,3	51,0	56,7	963	1023	1,5	1,4	84,5	84,3	14,1	14,3
Urze	23454,4	47,2	44,6	901	1090	1,4	2,8	80,7	81,4	17,9	15,8

Os valores apresentados para a parte aérea referem-se a uma amostra média das componentes (caule e folhas), pelo que estes poderão variar se na amostra analisada a proporção de folhas e caule variar. Neste estudo as amostras foram moídas e homogeneizadas de forma a retirar uma amostra representativa para análise (três repetições).
Após a libertação do material volátil, por combustão total, o resíduo remanescente é constituído, quase na totalidade, pelas cinzas e carbono fixado. Os teores de carbono fixado são muito similares nas partes aérea e radicular, excepto para a urze em que o carbono fixado pela parte aérea é superior àquele fixado pela raiz.
Relativamente aos poderes caloríficos, verificou-se que o da giesta e o do tojo são muito aproximados, sendo que a urze apresenta o valor mais elevado (Tabela 4).

Análise química elementar

Em termos de análises químicas elementares, efectuadas nos três tipos de vegetação, os resultados obtidos são apresentadas na Tabela 5.

Tabela 5 - Análise química elementar da vegetação

Vegetação	**C %**		**H %**		**N %**		**S %**		**O %**	
	Aérea	Raiz	Aérea	Raiz	Aérea	Raiz	Aérea	Raiz	Aérea	Raiz
Giesta	46,2	45,7	6,9	6,9	1,2	1,0	0,02	0,2	44,6	45,6
Tojo	46,3	45,5	6,9	6,8	0,9	0,8	0,2	0,2	44,3	45,3
Urze	49,8	45,4	7,0	6,8	0,6	1,1	0,02	0,2	41,1	43,9

Em termos de teor de carbono, verifica-se que a urze apresenta uma taxa ligeiramente superior à giesta e ao tojo sendo que, no sistema radicular os valores encontrados são muito semelhantes nas três espécies.

Conclusões

Os resultados encontrados no presente estudo permitem concluir que a regeneração arbustiva pós-fogo apresenta quantidades significativas passíveis de serem aproveitadas para diversos fins, não considerando os aspectos técnico-económicos de exploração.
Tendo em conta a variabilidade inerente à estrutura da vegetação, a qualidade do ajustamento das equações para predição da carga arbustiva após o fogo foi elevada, podendo ser utilizadas em comunidades arbustivas com estrutura e composição similares.
É elevado o potencial das espécies arbustivas, giesta, tojo e urze, para aproveitamento energético através de combustão, como demonstram os poderes caloríficos avaliados, o que se pode traduzir num aproveitamento comercial para produção de energia.
As espécies estudadas fixam grandes quantidades de carbono, quer no sistema aéreo quer no radicular, sendo um importante recurso para fixação do carbono atmosférico. Caso se opte por as utilizar na produção de energia eléctrica, o carbono fixado pela raiz, ao permanecer no solo por longos períodos, permite produzir energia com taxas de emissão de, aproximadamente, 50%. Acresce que este tipo de plantas rebenta, por toiça, pelo que, após a passagem do fogo, a raiz viva continua a fixar o carbono
Os resultados alcançados com este trabalho mostram que as espécies arbustivas reúnem um potencial interessante, ecológico e económico, o que permite desenhar formas de gestão adequadas para estas áreas, aspecto cada vez mais importante, considerando a elevada extensão do território nacional ocupada com espécies arbustivas e que grandes áreas são consumidas pelo fogo periodicamente.

Agradecimentos

Os autores agradecem ao departamento de Engenharia Mecânica e de Química da UTAD, pelas análises térmicas e químicas, respectivamente. Agradecem também à LECO, pelo apoio na realização das análises elementares dos materiais.

Bibliografia

BOTELHO, H., VEGA, J.A., FERNANDES, P., REGO, F., 1994. Prescribed fire behavior and fine fuel consumption in Northern Portugal and Galiza maritime pine stands. *In* Proc. 2nd Int. Conf. on Forest Fire Research, Viegas, D.X. (Ed.), Coimbra, pp. 343-353.

DGRF, 2007a. Resultados do Inventário Florestal Nacional 2005/06. Planeamento e Estatística. Direcção Geral dos Recursos Florestais. Ministério da Agricultura do Desenvolvimento Rural e das Pescas. Lisboa.

DGRF, 2007b. Estatísticas dos incêndios florestais. Totais Nacionais (1980 - 2006). Direcção geral dos Recursos Florestais. Ministério da Agricultura do Desenvolvimento Rural e das Pescas.

FERNANDES, P., LOUREIRO, C., BOTELHO, H., FERREIRA, A., FERNANDES, M., 2002. Avaliação indirecta da carga de combustível em pinhal bravo. *Silva Lusitana* **10**(1): 73-90.

FERNANDES, P.M., PEREIRA, J.P., 1993. Caracterização de combustíveis na Serra da Arrábida. *Silva Lusitana* **1**(2): 237-260.

FERNANDES, P.M., 1991. Caracterização do combustível florestal em ecossistemas de *Pinus pinaster* Ait.: aplicação do Sistema BEHAVE. Relatório final de estágio, UTAD, Vila Real.

FERNANDES, P.M., REGO, F.C., 1998a. Equations for estimating fuel load in shrub communities dominated by *Chamaespartium tridentatum* and *Erica umbellata*. *In* Proc. 3rdInternational Conf. on Forest Fire Research & 14thFire and Forest Meteorology Conf., D.X. Viegas (Ed.), Luso, Vol. II, pp. 2553-2564.

FERNANDES, P.M., REGO, F.C., 1998b. A new method to estimate fuel surface area-to-volume ratio using water immersion. *Int. J. Wildland Fire* **8**(3): 121-128.

NATÁRIO, R.M., PEREIRA, J.M., 1992. Relatório do projecto de modelação de combustíveis para o pinhal bravo. DGF, D.S. Produção, Div. Defesa e Protecção dos Arvoredos, Lisboa.

REGO, F.C., PEREIRA J.P., FERNANDES, P.M., ALMEIDA, A.F., 1994. Biomass and aerial structure characteristics of some mediterranean shrub species. 2nd International Conference on Forest Fire Research 1B: 377-384.

SILVA, T.P., PEREIRA, J.M.C., PAUL, J.C.P., *et al*., 2006. Estimativa de Emissões Atmosféricas Originadas por Fogos Rurais em Portugal. *Silva Lusitana* **14**(2): 239-263.

Annex E.2

Viana, H., Lopes, D., Aranha, J., 2009.Predição de biomassa arbustiva lenhosa empregando dados de inventário e o índice de diferença normalizada extraído em imagens landsat 5 TM, ISPV Millenium. 37.

PREDIÇÃO DE BIOMASSA ARBUSTIVA LENHOSA EMPREGANDO DADOS DE INVENTÁRIO E O ÍNDICE DE DIFERENÇA NORMALIZADA EXTRAÍDO EM IMAGENS LANDSAT 5 TM

HELDER VIANA [1]
DOMINGOS LOPES [2]
JOSÉ ARANHA [2]

[1] Secção Florestal, Escola Superior Agrária do Instituto Politécnico de Viseu.
[2] Departamento de Ciências Florestais e Arquitectura Paisagista, CECAV, Universidade de Trás-os-Montes e Alto Douro, Vila Real.

RESUMO

Com o intuito de estudar se o Índice de Vegetação de Diferença Normalizada (NDVI), gerado a partir de imagens de satélite de média resolução, pode ser utilizado na quantificação de biomassa vegetal aérea de plantas arbustivas lenhosas, regeneradas após a ocorrência de incêndios florestais, foram instaladas 18 parcelas de amostragem ($10m^2$) em locais ardidos entre os anos de 2000 e 2005 na região de Viseu. A metodologia utilizada baseou-se no ajustamento de modelos de regressão entre a quantidade de biomassa ($t.ha^{-1}$) pesada em campo pelo método destrutivo, em cada parcela, e os valores da resposta espectral referentes ao NDVI, calculados e extraídos de imagens Landsat Thematic Mapper (TM). Os resultados obtidos mostram que a quantidade de biomassa vegetal apresenta uma correlação positiva com os valores de NDVI. A estimativa de biomassa lenhosa aérea forneceu resultados significativos, tendo permitido ajustar uma equação que descreve a quantidade de biomassa ($t.ha^{-1}$) em função do comportamento espectral da vegetação.

Palavras-chave: Biomassa, Arbustivas, Detecção remota, Landsat 5 TM, NDVI, SIG

1 – Introdução e objectivos

Nos últimos anos tem-se observado um interesse crescente na quantificação e caracterização da biomassa vegetal aérea dos espaços florestais. Contudo, a biomassa arbustiva lenhosa sub-arbórea ou aquela regenerada em áreas percorridas pelos incêndios é uma componente muito significativa da biomassa vegetal total que, em grande parte dos casos, não é quantificada nos inventários tradicionais. Esta biomassa tem sido avaliada em estudos sobretudo direccionados para a avaliação da carga combustível lenhosa, regenerada após o fogo, e consequente predição do comportamento do fogo, como se pode ler em Botelho *et al.,* 1994; Rego *et al.*, 1994; Fernandes e Rego, 1998; Fernandes *et al.,* 2002. Porém, a importância que esta vegetação desempenha no ciclo biogeoquímico do carbono e o possível aproveitamento que pode ter para fins energéticos veio aumentar o interesse neste tipo de biomassa. O facto de mais de 1,8 milhões de hectares do país serem ocupados por vegetação arbustiva (DGRF, 2007) torna ainda mais evidente o interesse em estudar este tipo de vegetação.

A estimativa de biomassa lenhosa acima do solo tem sido feita, nos últimos anos, por uma variedade de métodos, desde medições em campo que envolvem a amostragem destrutiva (Peichl *et al*., 2006; Viana *et al,* 2009a), ou medições directas (Foroughbakhch *et al*., 2005; Flombaum *et al*., 2007; Aranha e Viana, 2008). Em resultado destas avaliações diversos modelos alométricos são ajustados com base em parâmetros como altura, diâmetro, idade, grau de ocupação, entre outros (Delphis *et al.*, 2008; Viana *et al.,* 2009a; Viana *et al.,* 2009b; Viana *et al.,* 2009c). No entanto, a recolha destes parâmetros exige tempo e custos que, em áreas de grande extensão, podem limitar determinados estudos. Por conseguinte, o recurso a técnicas expeditas e de baixo custo, para classificar a biomassa vegetal nestas áreas, como a detecção remota é, por vezes, uma alternativa para a estimativa da biomassa vegetal (ex: Suganuma *et al*., 2006). A utilização do comportamento espectral registado pelas imagens de satélite quando associada a modelação baseada em SIG, como informação auxiliar, permite também o mapeamento espacial das estimativas de biomassa (ex: Neeff, 2005; Wulder *et al.,* 2008; Aranha e Viana, 2008).

Desde que as imagens de satélite estão disponíveis para estudos da dinâmica da cobertura do solo, que a utilidade dos índices de vegetação para monitorizar vegetação e recolher informação ecofisiológica sobre grandes áreas é reconhecida. As imagens de satélite com média resolução espacial de sensores como o Landsat TM são as mais utilizadas, uma vez que a informação espectral apresenta uma forte correlação com a biomassa (Muukkonen *et al*., 2007; Zheng *et al.,* 2007; Meng *et al.,* 2007). Por esta razão cada vez mais as recentes estimativas de biomassa se baseiam em metodologias onde os índices de vegetação são utilizados. Embora vários índices de vegetação (NDVI, EVI, SAVI, etc.) sejam utilizados em estudos do género, o NDVI (Índice de Diferença Normalizada) é o mais comummente aplicado (ex: Chirici *et al*. 2007; Wang *et al*. 2005). O NDVI é obtido pelas bandas de reflectância do vermelho e do infravermelho próximo da seguinte forma (Equação 1):

$$\text{NDVI} = (\text{IVP} - \text{V}) / (\text{IVP} + \text{V}) \qquad (1)$$

sendo:

NDVI – Índice de Vegetação de Diferença Normalizada
IVP – Infravermelho próximo
V – Vermelho

Embora os estudos utilizando o NDVI sejam muito utilizados para estudos em povoamentos florestais, não há muitos trabalhos que relacionem o NDVI com variáveis de matos mediterrâneos predominantes na região. Desta forma, este trabalho teve como objectivo (1) analisar a relação existente entre o NDVI, gerado a partir do comportamento espectral de imagens Landsat TM, e variáveis recolhidas nas parcelas de matos, (2) ajustar um modelo de regressão que permita estimar a biomassa de arbustivas utilizando o valor do NDVI como variável independente.

2 - Material e métodos

2.1 - Enquadramento da área de estudo

A área de estudo localiza-se no concelho de Viseu e limítrofes. Esta região apresenta uma topografia complexa, uma vez que é rodeada por maciços importantes como as Serras do Caramulo, Arada, Montemuro, Lapa e Estrela. As altitudes variam desde aproximadamente 100m no vale do Rio Dão até aos 1800 metros na Serra da Estrela. A variabilidade climática também é acentuada observando-se precipitações médias anuais de 800 a 2800mm no vale do rio Dão e temperaturas médias anuais inferiores que variam de 7,5 até 16ºC.

A região é ocupada por espaços florestais onde predomina o pinheiro bravo e por extensas áreas ocupadas com arbustivas. Frequentemente estas áreas são percorridas por incêndios como mostra a Figura 1. Para o âmbito deste trabalho as parcelas para recolha dos dados foram instaladas em áreas ardidas entre 2000 e 2005.

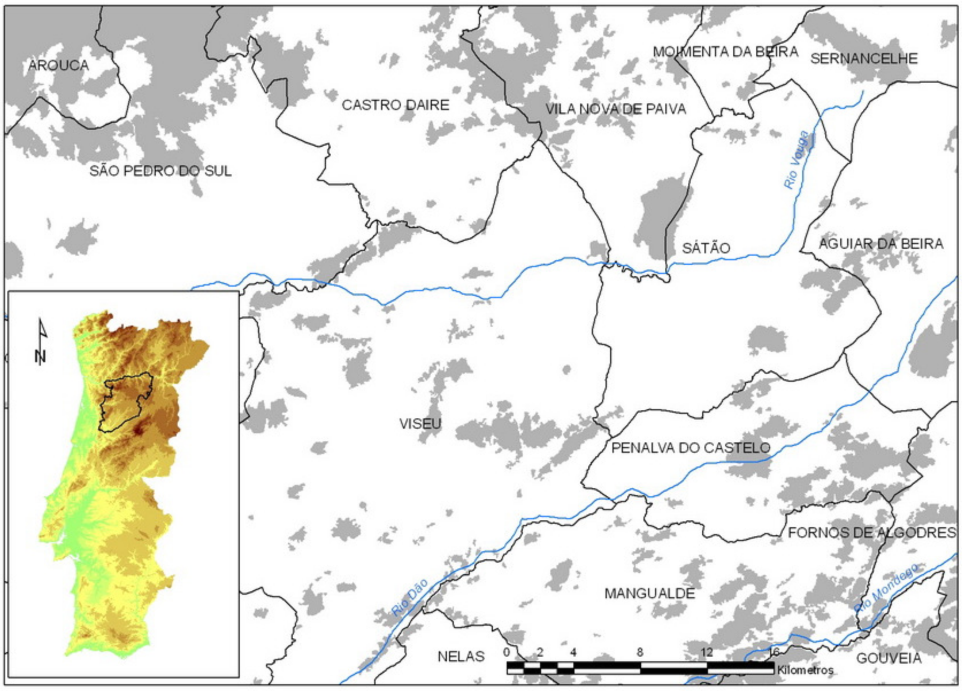

Figura 1. Localização da área de estudo (as manchas de cor cinza representam as áreas ardidas entre 2000 e 2005)

2.2 - Metodologia

Recolha das variáveis em campo

Os levantamentos de campo decorreram entre Março e Maio de 2007. Em áreas ardidas na região durante o período 2000-2005 foram instaladas parcelas de amostragem circulares com $10m^2$, três repetições em cada ano, num total de 18 parcelas. A localização geográfica foi assinalada por meio de GPS (*Global Positioning System).* As áreas amostradas tinham ocupação vegetal homogénea e uma extensão superior a 2 hectares. A carga arbustiva regenerada foi medida pelo método de intersecção comum e as variáveis altura média, área de projecção das copas, grau de ocupação foram recolhidas. Posteriormente a vegetação foi cortada, agrupada por espécie e pesada no local, de forma a determinar a biomassa existente ($t.ha^{-1}$).

Processamento da imagem de satélite

Numa imagem Landsat 5 TM adquirida em 10 de Dezembro de 2006, foi utilizado um excerto com aproximadamente 40 Km x 40 Km. O processamento da imagem de satélite foi levado a cabo no software IDRISI, que apresenta funcionalidades de Detecção Remota e SIG. A imagem foi corrigida geometricamente, com base em 18 pontos de controlo, pelo ajustamento de um polinómio linear, e introduzida no sistema de coordenadas Hayford-Gauss, Datum de Lisboa. O interpolador utilizado na reamostragem foi o vizinho mais próximo (Lillesand *et al.,* 2004).

De forma a reduzir os efeitos atmosféricos foi feita a correcção radiométrica pelo método da subtracção do objecto mais escuro proposto por Chavez (1989). Os valores dos números digitais foram então convertidos em unidades de reflectância e o índice de vegetação de diferença normalizada (Huete and Jackson, 1987; Huete *et al.,* 1997) foi calculado de acordo com a Equação 1. Os valores do NDVI foram extraídos em ArcGIS 9.x, para os 18 locais, pelo método da interpolação bilinear, que calcula a média dos 4 pixéis vizinhos (Lillesand *et al.,* 2004).

Ajustamento dos modelos

A relação entre o NDVI e as variáveis recolhidas em campo foi avaliada pela correlação de Pearson. Após o ajustamento de vários modelos para a predição da biomassa por hectare ($t.ha^{-1}$), seleccionaram-se aqueles que apresentaram melhor qualidade de ajustamento, após avaliação dos coeficientes de regressão (R), de determinação (R^2), e de determinação ajustados (R^2_{adj}), bem como os resíduos (EQM) e a significância do teste de t de Student.

3 - Resultados e discussão

3.1 - Caracterização da vegetação

A vegetação arbustiva amostrada divide-se essencialmente em três grupos: giesta (*Cytisus* sp), tojo (*Ulex* sp.) e urze (*Erica* sp.). A Figura 2 mostra a distribuição da cobertura vegetal em cada parcela.

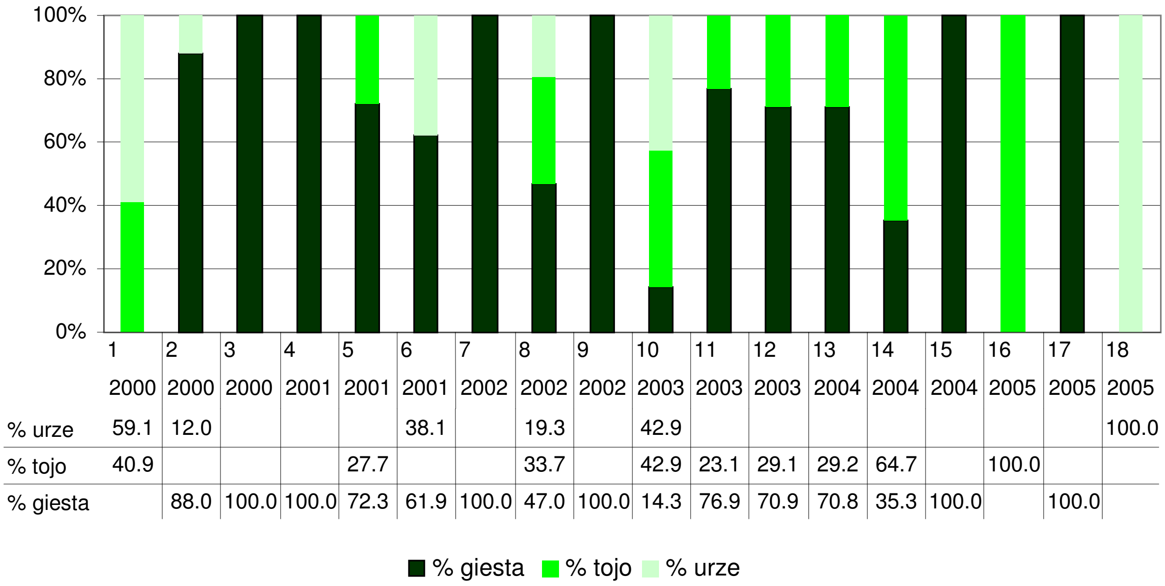

	1	2	3	4	5	6	7	8	9	10	11	12	13	14	15	16	17	18
	2000	2000	2000	2001	2001	2001	2002	2002	2002	2003	2003	2003	2004	2004	2004	2005	2005	2005
% urze	59.1	12.0				38.1		19.3		42.9								100.0
% tojo	40.9				27.7			33.7		42.9	23.1	29.1	29.2	64.7		100.0		
% giesta		88.0	100.0	100.0	72.3	61.9	100.0	47.0	100.0	14.3	76.9	70.9	70.8	35.3	100.0		100.0	

Figura 2. Caracterização da ocupação vegetal nas parcelas amostradas

Como se observa, a giesta é a mais frequente em quase todas as parcelas. Esta apenas não aparece nas parcelas 1 e 18. O grau de ocupação varia entre 16,8% e 99,6% e a biomassa varia entre 1,5 a 32,1 $t.ha^{-1}$.

3.2 - Relações entre o NDVI e as variáveis da vegetação arbustiva

As correlações entre as variáveis medidas em campo foram sempre positivas tendo permitido obter modelos alométricos para predição da biomassa por hectare, com razoável qualidade de ajustamento, como se pode ler em Viana *et al.* (2009a). O NDVI encontra-se positivamente correlacionado com a quantidade de biomassa ($t.ha^{-1}$) bem como com as variáveis da vegetação medidas em campo, como se pode ver na matriz com os coeficientes da correlação de Pearson (Tabela 1).

Tabela 1 – Matriz dos coeficientes da Correlação de Pearson entre o NDVI e as variáveis da vegetação

	W ($t.ha^{-1}$)	*NDVI*	*Idade*	*GO (%)*	*H (m)*
W ($t.ha^{-1}$)	1				
NDVI	0.72	1			
Idade	0.83	0.76	1		
GO (%)	0.63	0.50	0.73	1	
H (m)	0.66	0.41	0.57	0.37	1

3.3 - Modelos alométricos para predição da biomassa arbustiva lenhosa

Após o ajustamento de vários modelos de regressão, seleccionaram-se os que permitiram obter as melhores estimativas, que se apresentam na Tabela 2 e Figura 3.

Tabela 2. Equações ajustadas à biomassa arbustiva aérea total ($t.ha^{-1}$), estimativa dos parâmetros, coeficientes de determinação ajustados e erro quadrático médio

	Equação	X - variável independente	Estimativa dos parâmetros	R^2aj	EQM ($t.ha^{-1}$)
1	$Y = \alpha + \beta x$	NDVI	α = -23.870 β = 113.5396	0,48	5,9
2	$Y = \alpha + \beta x$	ln(NDVI.t)	α = 10,507 β = 12,444	0,70	4,5
3	$Y = \alpha + \beta x_1 + \gamma x_2$	NDVI ln(t)	α = 15,6879 β = 36,8923 γ = 12,5032	0,68	4,7

Sendo: Y - Quantidade de biomassa por hectare ($t.ha^{-1}$), variável dependente; α, β, γ - Parâmetros da regressão; X - Variável independente; NDVI – índice de vegetação de diferença normalizada; t – idade da regeneração após o fogo; R^2aj – coeficiente de determinação ajustado; EQM – Erro Quadrático Médio

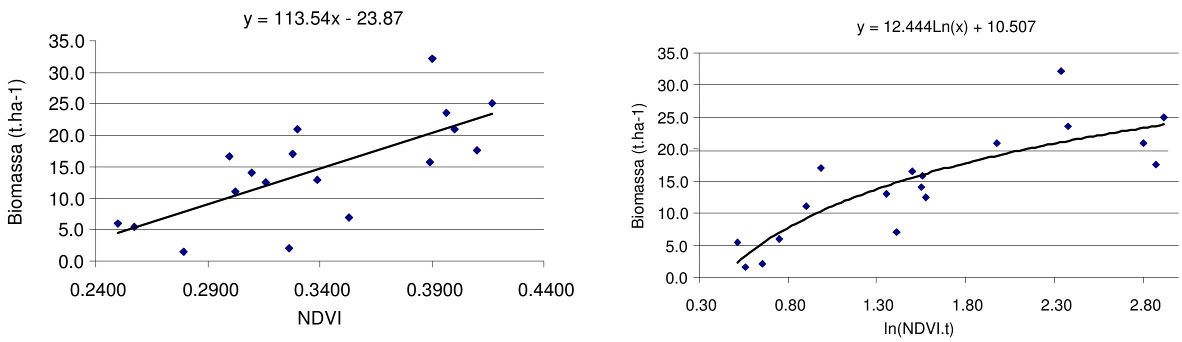

Figura 3. Relações estabelecidas entre a carga arbustiva total e as variáveis testadas

Os melhores resultados são obtidos quando se recorre às variáveis independentes NDVI e t (idade) combinadas (R^2_{aj} = 0,70), permitindo obter estimativas de biomassa com um erro de 31% (EQM = 4,5 $t.ha^{-1}$). O desempenho desta equação é bastante satisfatório para a vegetação em causa, uma vez que esta vegetação apresenta uma distribuição espacial muito heterogénea.

Por outro lado as espécies presentes nas parcelas (giesta, tojo e urze) apresentam crescimentos muito díspares e logo variação de peso muito significativa nas várias idades de regeneração. Estas espécies podem apresentar crescimentos muito diferentes entre si ao longo do tempo e, por outro lado, para uma determinada espécie, os crescimentos vão diferir em função das características da estação e da densidade de indivíduos.

4 – Conclusões

O presente estudo demonstrou ser possível estabelecer um modelo para a predição da carga arbustiva lenhosa após o fogo, relacionando dados de inventário e a resposta espectral extraída em imagens Landsat 5 TM.

A aplicação deste método permite fazer estimativas expeditas, de forma não destrutiva, sobre áreas extensas, e com rapidez.

Tendo em conta a variabilidade inerente à estrutura da vegetação (grande variabilidade de espécies, densidades, etc.), a qualidade do ajustamento das equações foi razoável, pelo que poderão ser utilizadas, com erros aceitáveis para este tipo de vegetação, em comunidades arbustivas com estrutura e composição similares. Estes modelos oferecem um grande interesse uma vez que, para além de estimarem a biomassa, permitem a posterior modelação da distribuição espacial da biomassa em áreas percorridas pelos incêndios. Desta forma, podem constituir um suporte para estudos de estimação da produtividade primária líquida, estudos de avaliação dos impactos de incêndios florestais ou outros distúrbios que possam ocorrer nestas áreas.

Os resultados alcançados mostram que as espécies arbustivas lenhosas, que regeneram após os incêndios, atingem proporções muito significativas, ao fim de poucos anos, pelo que reúnem um potencial interessante. As quantidades geradas podem prever um aproveitamento comercial para produção de energia, nos locais onde as restrições técnico-económicas não sejam limitantes. Por outro lado, as espécies estudadas têm importância ecológica uma vez que, nesta vegetação, estão sequestradas grandes quantidades de carbono, quer no sistema aéreo, quer no radicular, sendo um importante recurso para fixação do carbono atmosférico.

REFERÊNCIAS BIBLIOGRÁFICAS

- ARANHA, J. and Viana, H., 2008. Assessing Shrub Biomass By Means Of Field Work and Geostatistics Processes. A Case Study in North Portugal. Proceedings of the Bioenergy: Challenges and Opportunities. International Conference and Exhibition on Bioenergy. Universidade do Minho, Guimarães, Portugal. April 6th – 9th 2008.
- BOTELHO, H., Vega, J.A., Fernandes, P., Rego, F., 1994. Prescribed fire behavior and fine fuel consumption in Northern Portugal and Galiza maritime pine stands. *In* Proc. 2nd Int. Conf. on Forest Fire Research, Viegas, D.X. (Ed.), Coimbra, pp. 343-353.
- CHAVEZ, P. S. JR., 1989. Radiometric Calibration of Landsat Thematic Mapper Multispectral Images. Photogrammetric Engineering And Remote Sensing. Vol. 55, N.9. Pp. 1285-1294.
- CHIRICI, Gherardo; Barbati, Anna and Maselli, Fabio, 2007. Modelling of Italian forest net primary productivity by the integration of remotely sensed and GIS data. Forest Ecology and Management 246, 285–295.
- DELPHIS F. and Levia Jr, 2008. A generalized allometric equation to predict foliar dry weight on the basis of trunk diameter for eastern white pine (Pinus strobus L.). Forest Ecology and Management, Volume 255, Issues 5-6, 5, 1789-1792.
- DGRF, 2007. Resultados do Inventário Florestal Nacional 2005/06. Planeamento e Estatística. Direcção Geral dos Recursos Florestais. Ministério da Agricultura do Desenvolvimento Rural e das Pescas. Lisboa.
- FERNANDES, P., Loureiro, C., Botelho, H., Ferreira, A., Fernandes, M., 2002. Avaliação indirecta da carga de combustível em pinhal bravo. *Silva Lusitana* 10(1) : 73–90.
- FERNANDES, P.M., Rego, F.C., 1998. Equations for estimating fuel load in shrub communities dominated by *Chamaespartium tridentatum* and *Erica umbellata*. *In* Proc. 3rd International Conf. on Forest Fire Research & 14th Fire and Forest Meteorology Conf., D.X. Viegas (Ed.), Luso, Vol. II, pp. 2553-2564.
- FLOMBAUM, P. and Sala, O.E, 2007. A non-destructive and rapid method to estimate biomass and aboveground net primary production in arid environments. Journal of Arid Environments, Volume 69 (2), 352-358.
- FOROUGHBAKHCH, Rahim; Reyes, Gregorio; Alvarado-Vázquez, Marco A.; Hernández-Piñero, Jorge and Rocha-Estrada, Alejandra, 2005. Use of quantitative methods to determine leaf biomass on 15 woody shrub species in northeastern Mexico. Forest Ecology and Management, Volume 216, Issues 1-3, 12, 359-366.
- HUETE, A. R., Liu, H. Q., Batchily, K. and Leeuwen, W. Van, 1997. A Comparison of Vegetation Indices over a Global Set of TM Images for MODIS-EOS. Remote Sensing Of Environment. Vol. 59. Pp. 440-451.
- HUETE, A.R. and Jackson, R.D., 1987. Suitability of spectral indices for evaluating vegetation characteristics on arid rangelands. Remote Sensing of Environment, 23, 213-232.
- LILLESAND, T.M.; Kiefer, R.W.; Chipman, J.W., 2004. Remote Sensing and image Interpretation. Fifth Edition, John Wiley and Sons Inc., New York, 764p.
- MENG, Qingmin; Cieszewski, Chris J.; Madden, Marguerite and Borders, Bruce, 2007. A linear mixed-effects model of biomass and volume of trees using Landsat ETM+ images. Forest Ecology and Management 244, 93–101.
- MUUKKONEN, P.; Heiskanen, J., 2007. Biomass estimation over a large area based on standwise forest inventory data and ASTER and MODIS satellite data: A possibility to verify carbon inventories. Remote Sensing of Environment, 107, 617-624.
- NEEFF, Till, 2005. Spatial modeling of primary and secondary forest growth in Amazonia. Forest Ecology and Management 219 149–168.
- PEICHL, Matthias and Arain, M. Altaf, 2006. Above and belowground ecosystem biomass and carbon pools in an age-sequence of temperate pine plantation forests. Agricultural and Forest Meteorology, Volume 140, Issues 1-4, Pages 51-63.
- REGO, F.C., Pereira J.P., Fernandes, P.M., Almeida, A.F., 1994. Biomass and aerial structure characteristics of some mediterranean shrub species. 2nd International Conference on Forest Fire Research 1B, 377-384.
- SUGANUMA, Hideki; Abe, Yukuo; Taniguchi, Masahiko; Tanouchi, Hiroyuki; Utsugi, Hajime; Kojima, Toshinori and Yamada, Koichi, 2006. Stand biomass estimation method by canopy coverage for application to remote sensing in an arid area of Western Australia. Forest Ecology and Management, Volume 222, Issues 1-3, 75-87.

- VIANA, H.; Cardoso, A.; Correia, R; Lopes, D.; Aranha, J., 2009b. Estabelecimento de modelos alométricos para predição da biomassa aérea de *Eucalyptus globulus*. Actas do 6º Congresso Florestal Nacional. 6-9 Outubro 2009.
- VIANA, H.; Dias, S.; Marques, C.; Cruz, M..; Lopes, D.; Aranha, J., 2009c. Estabelecimento de modelos alométricos para predição da biomassa aérea da *Pinus Pinaster.* Actas do 6º Congresso Florestal Nacional. 6-9 Outubro 2009.
- VIANA, H.; Fernandes, P.; Rocha, R.; Lopes, Domingos Aranha, J., 2009a. Alometria, dinâmicas da biomassa e do carbono fixado em algumas espécies arbustivas de Portugal. Acta do 6º Congresso Florestal Nacional. 6-9 Outubro 2009.
- WANG, Quan; Adikua, Samuel; Tenhunena, John and Granierb, André, 2005. On the relationship of NDVI with leaf area index in a deciduous forest site. Remote Sensing of Environment 94, 244–255.
- WULDER, Michael A.; White, Joanne C.; Fournier, Richard A.; Luther, Joan E. And Magnussen, Steen, 2008. Spatially Explicit Large Area Biomass Estimation: Three Approaches Using Forest Inventory and Remotely Sensed Imagery in a GIS. Sensors, 8, 529-560.
- ZHENG, G.; Chen, J.M.; Tian, Q.J.; Ju, W.M. and Xia, X.Q., 2007. Combining remote sensing imagery and forest age inventory for biomass mapping. Journal of Environmental Management 85, 616–623.

Annex E.3

Aranha, J., Calvão, A., Lopes, D., Viana, H., 2011. Quantificação da biomassa consumida nos últimos 20 anos de fogos florestais no Norte de Portugal. Info 26, 44-49.

INFELIZMENTE, TEM-SE VERIFICADO QUE OS FOGOS FLORESTAIS EM PORTUGAL CONTINENTAL SÃO UM FENÓMENO RECORRENTE, QUE CAUSA ENORMES PREJUÍZOS AMBIENTAIS, ECOLÓGICOS E ECONÓMICOS

QUANTIFICAÇÃO DA BIOMASSA CONSUMIDA NOS ÚLTIMOS 20 ANOS DE FOGOS FLORESTAIS NO NORTE PORTUGAL

José Aranha [a]
Ana Rita Calvão [b]
Domingos Lopes [a]
Helder Viana [c]
[a] CITAB – Centro de Investigação em Tecnologias Agroambientais e Biológicas – UTAD - 5001-801 Vila Real, Portugal
[b] ESTGA-UA - Escola Superior de Tecnologia e Gestão de Águeda 3754 – 909 Águeda, Portugal
[c] Dept. de Engenharia Florestal, Instituto Politécnico de Viseu, 3500-606 Viseu, Portugal

A análise estatística relativa aos fogos florestais ocorridos, nos últimos 20 anos (1990-2009), em Portugal continental, mostra que ocorreram 22380 fogos, que consumiram 2 443 350ha. Analisando apenas a região Norte de Portugal (distritos da Guarda, de Viseu, do Porto, do Minho, de Vila Real e de Bragança), verificou-se que a tendência foi a mesma, com 15 339 ocorrências e 1 209 976ha ardidos. Com o objectivo de analisar a dinâmica da vegetação arbustiva, que coloniza as áreas ardidas, estabeleceu-se um sistema de amostragem de campo, sobre as áreas ardidas nos últimos 10 anos, composto por 5 amostras por data. Em cada uma destas amostras, quantificou-se a biomassa arbustiva em pé e determinou-se o peso verde e o peso seco. Com estes dados, estabeleceu-se um sistema de equações que permitiu analisar a dinâmica vegetal das espécies arbustivas e quantificar a biomassa consumida pelos fogos.
Os resultados mostram que, nos últimos 20 anos arderam, aproximadamente e só no Norte de Portugal, 749500ha de matos. Considerando um valor médio de 9 t/ha de biomassa (30% de humidade), estima-se que tenham ardido 6 745 500 toneladas de mato.
Fogos florestais, biomassa florestal, centrais termoeléctricas, sistemas de informação geográfica, sistema de posicionamento por satélite.

INTRODUÇÃO E OBJECTIVOS

Durante os últimos 20 anos, uma equipa de investigação do CITAB-UTAD tem monitorizado regularmente as zonas florestais localizadas a norte de Portugal, com o objectivo de quantificar e de avaliar a biomassa florestal (povoamentos e áreas de mato). Durante este trabalho, foram estabelecidas centenas de parcelas de amostragem e foram recolhidos milhares de dados biométricos relativos ao crescimento de árvores florestais e de arbustos (mato). Infelizmente, durante as várias saídas para desenvolver trabalho de campo, tem-se verificado que os fogos florestais em Portugal continental são um fenómeno recorrente, que causa enormes prejuízos ambientais, ecológicos e económicos.

Do acompanhamento, que a equipe de investigação do CITAB-UTAD tem feito em áreas ardidas, verificou-se que a vegetação arbustiva consegue colonizar rapidamente estas áreas e que a floresta continua tem transformado em floresta descontínua e dispersa e em vastas zonas de mato.

Através dum programa de limpeza e ordenamento do espaço florestal, a biomassa, consumida pelos fogos, poderia ser usada como combustível em centrais termoeléctricas, gerar energia eléctrica e minimizar o problema dos fogos florestais.

Com o objectivo de estudar a dinâmica da recuperação vegetal nas áreas ardidas e de quantificar a biomassa arbustiva acumulada, estabeleceu-se um sistema de amostragem de campo, sobre as áreas ardidas nos últimos 10 anos, composto por 5 amostras por data.

Durante a preparação do trabalho, consultou-se informação disponível sobre o assunto, tendo sido recolhidas várias equações alométricas de quantificação de biomassa arbustiva, como se apresenta na Tabela 1.

Tabela 1 – Equações alométricas para estimar biomassa florestal (matos)

Equações alométricas	
$BMG = 5.6680 + 0.00008\,(A\ DC)^2$	[1]
$BMG = 37.634 + 1.010\ Id$	[1]
$BMG = 5.005 + 0.136\ Id$	[1]
Erica sp. - $P = 9.43\ Id^{2} - 184.11\ Id + 1034.2$	[2]
Cistus ladanifer L. and *Erica sp.* - $P = 27.54\ Id^{1.202}$	[2]
Cistus ladanifer L. - $P = 0.064\ Id^{2} + 79.39\ Id - 76.42$	[2]
Genista and Ulex - $P = 1.58\ Id^{2.0714}$	[2]
Mancha - $P = 28.06\ Id^{1.3868}$	[2]
Pistacia lentiscus L. - $P = 1.58\ e^{0.088\ Id}$	[2]
$BMG = 1.1336\ Id^{1.6291}$	[3]
$BMG = 0.1239\ AT^{1.1091}$	[3]
$BMG = 6.2667\ Ln\ Id^{2.040}$	[3]
$BMG = 0.0258\,(DC\ A)^{0.754}$	[3]
Sendo:	
BMG – Biomassa de matos (genérico) - Kg $planta^{-1}$	
P – Peso da copa dos arbustos - g m^{-2}	
A - Altura total - cm	
AC – Tree Canopy Height - m	
Id – Idade (year)	
DC – Densidade de copas - % - 0 a 100)	
Exp – Exponencial	
Ln – Logaritmo Natural	

MATERIAL E MÉTODOS

Para o desenvolvimento do presente trabalho, criou-se um sistema de informação geográfica (SIG), com base na cartografia das áreas ardidas, disponibilizada pela Autoridade Florestal Nacional [4] e nas Cartas CLC1990 e CLC2006 (Corine Land Cover para 1990 e para 2006, IGP, 2009 [5 e 6]). A carta de áreas ardidas foi, posteriormente, processada por datas, de modo a permitir calcular a recorrência dos fogos e a seleccionar áreas que arderam apenas uma vez e a obter uma distribuição espaço-temporal das áreas ardidas e isolar apenas as que ocorreram em áreas de mato ou de floresta degradada.

Esta selecção foi, posteriormente restringida à zona norte de Portugal (distritos da Guarda, de Viseu, do Porto, do Minho, de Vila Real e de Bragança), uma vez que a equipa de investigação do CITB-UTAD se concentra especialmente nesta área do país.

Numa segunda fase, seleccionaram-se apenas as áreas ardidas no ano de 2000 e de 2009 e aplicou-se um sistema de amostragem, que permitiu identificar 5 áreas ardidas em cada ano de fogos. Deste esquema de amostragem, resultaram 45 áreas ardidas, que foram posteriormente visitadas durante o ano de 2009.

Para a fase de recolha de dados de campo, criou-se um projecto SIG de campo, que foi instalado num receptor GPS com capacidade para receber também o sinal EGNOS e, deste modo, poder trabalhar em modo diferencial em tempo real.

Para a recolha de dados de campo, usou-se o método das linhas de intersecção, tendo sido usadas parcelas de 200m^2 e duas linhas perpendiculares, cruzadas no centro da parcela. Os dados recolhidos permitiram determinar, por espécies arbustivas (giesta, urze, carqueja e tojo):

– A percentagem de ocupação;
– Altura média;
– Peso verde
– Peso seco

Posteriormente, os dados de campo e as medições em laboratório, permitiram criar uma base de dados relativa a cada mancha ardida, onde se associou o tempo (idade pós fogo) às medidas biométricas das várias espécies arbustivas.

APRESENTAÇÃO E DISCUSSÃO DOS RESULTADOS

Fogos florestais

A análise estatística relativa aos fogos florestais ocorridos, nos últimos 20 anos (1990-2009), em Portugal continental, mostra que ocorreram 22380 fogos, que consumiram 2 443 350ha. Analisando apenas a região Norte de Portugal, verificou-se que a tendência foi a mesma, com 15339 ocorrências e 1209976ha ardidos. Estes resultados mostram que, nos últimos 20 anos, mais do que 68% dos fogos florestais ocorreram nesta zona, o que representa cerca de 50% da área total ardida, o que evidencia que o problema é particularmente importante no norte do país.

Como se apresenta nas Figuras 1 e 2, nos últimos 20 anos quase todas as áreas florestais (povoamentos e áreas de mato) foram percorridas pelo fogo. Concentrando a análise em termos de valores totais anuais, como se apresenta na Tabela 2, pôde-se verificar que a magnitude dos fogos florestais é cíclica. Quando se analisa a relação entre a área total ardida e o número de ocorrências, verifica-se que os ciclos de fogo são, em média de 10 anos, quer para as grandes

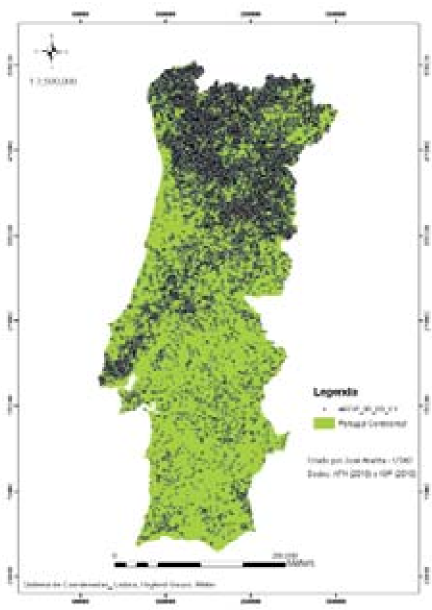

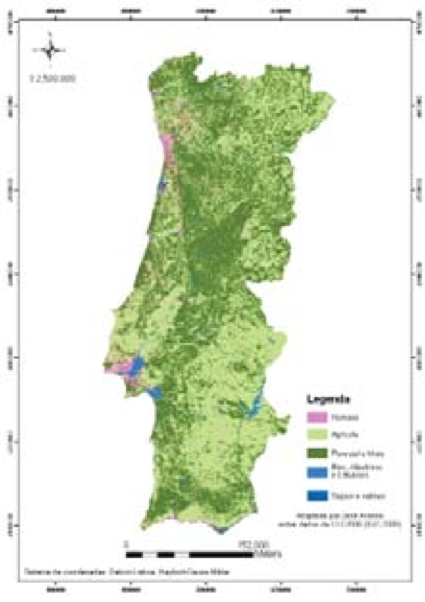

fig. 1 (à esquerda)
Dispersão dos fogos florestais em Portugal Continental entre 1990 e 2009

fig. 2 (à direita)
Adaptação da CLC2006 (Corine Land Cover para 2006)

ocorrências quer para as pequenas, com um desfasamento de 5 anos entre ocorrências extremas, como se mostra na Figura 3.

Tabela 2 – Características dos fogos florestais em Portugal entre 1990 e 2009

Ano	N. de ocorrências	Area_ha	Area_ha / N_ocorrências
1990	1416	105891	74.8
1991	880	182215	207.1
1992	230	34231	148.8
1993	141	40240	285.4
1994	623	72017	115.6
1995	1749	134465	76.9
1996	1477	92942	62.9
1997	755	21265	28.2
1998	1831	216175	118.1
1999	1462	67183	46.0
2000	1731	143285	82.8
2001	1861	97606	52.4
2002	1851	133204	72.0
2003	1186	439918	370.9
2004	722	114975	159.2
2005	1458	346396	237.6
2006	715	72679	101.6
2007	738	38322	51.9
2008	683	11813	17.3
2009	971	78530	80.9
Total	22480	2443350	108.7 (valor médio)

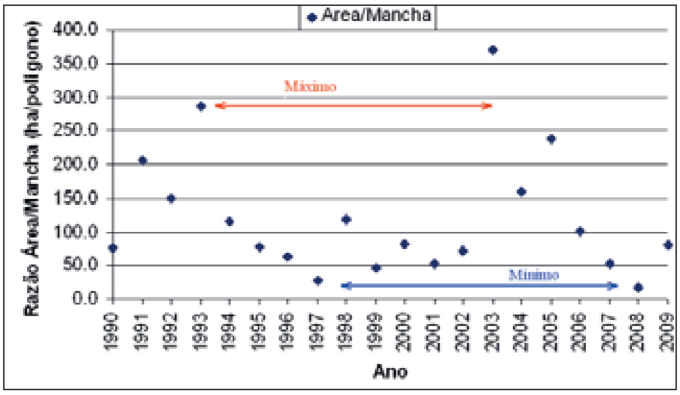

fig. 3 (ao lado)
Ciclo dos fogos florestais em Portugal Continental entre 1990 e 2009

A análise conjunta da carta de áreas ardidas e das cartas CLC1990 e CLC2006, estimou-se que, em 2006, a área florestal de Portugal Continental fosse de 3 400 000ha (38% do território) e que a área de mato e floresta degradada fosse de 1 900 000ha (21% do território)
[5, 6, 7, 8].

Entre 1990 e 2006, estima-se que tenham ocorrido 20 100 fogos florestais, que consumiram, aproximadamente, 2 315 000ha, atribuídos a:

– Agricultura – 12,4%
– Floresta de folhosas (ex. carvalhos ou castanheiros) – 4.7%
– Floresta de resinosas (ex. pinheiro bravo) – 12,5 %
– Florestas mistas de folhosas e de resinosas – 8,1%
– Áreas de mato – 62,3%

Dinâmica de crescimento do mato

Durante o trabalho de campo, verificou-se que as várias espécies arbustivas (mato) conseguiam colonizar completamente uma área ardida, em apenas 5 anos e que atingiam o seu máximo de ocupação entre os 10 e os 12 anos, como se apresenta na Tabela 3 e se mostra na Figura 4.

Tabela 3 – Valores médios de crescimento do mato

Idade pós fogo	2	3	4	5	6	7	8	9	10
Altura (m)	0.74	0.55	0.77	0.86	0.98	0.74	1.21	1.30	1.33
D. de copa (%)	0.19	0.34	0.38	0.43	0.47	0.56	0.7	0.81	0.95
Peso (t/ha)	0.92	2.44	3.84	6.24	7.34	10.1	15.2	16.4	18.9

fig. 4 (ao lado)
Evolução do peso de mato em função da idade pós fogo

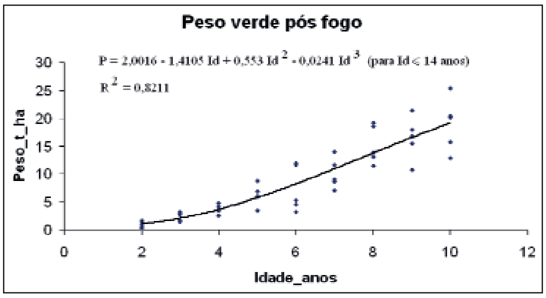

Como se mostra na Figura 3, crescimento do mato apresenta padrões de crescimento muito variado. Esta variação deve-se a diferentes composições de espécies, bem como à relação entre a altura dos arbustos e a densidade de ocupação do território, como se apresenta na Tabela 4.

Tabela 4 – Equações alométricas para o cálculo da biomassa do mato

Equação	R^2_{adj}	RMSE ton/ha	RMSE %	n
BMG = 2.002 - 1.411 Id + 0.553 Id2 - 0.0241 Id3	0.831	2.81	31.06	50
BMG = Exp (- 1.298 + 1.861 Ln Id + 0.1265 Ln AT)	0.865	2.71	30.00	50
BMG = Exp (2.070 + 0.504 Ln Id + 0.057 Ln AT + 1.513 Ln DC)	0.906	2.74	30.29	50

Sendo: BMG – Biomassa do mato (genérico) – t/há (verde)
Id – Idade – anos pós fogo
AT – Altura Total – m
DC – Densidade de Copas - % (0 – 1)
Exp – Exponencial
Ln – Logaritmo Natural

Análise da biomassa perdida nos fogos florestais

De acordo com a bibliografia consultada, [9, 10, 11, 12],

Uma central termoeléctrica a biomassa floresta trabalha, em média, 8000 hora por ano e consome 8200 t/ano de biomassa (30% de humidade) para produzir 1 MW de energia eléctrica (6,3 GWh ano). Os resultados anteriormente apresentados mostram que, nos últimos 20 anos arderam, aproximadamente e só no norte de Portugal, 749 500ha de matos. Considerando um valor médio de 9 t/ha de biomassa (30% de humidade), estima-se que tenham ardido 6 745 500 toneladas de mato. Este valor, transformado em energia, significa 822,62 MW de energia, o que equivale à produção de uma central termoeléctrica de 11 MW durante 75 anos.

Num cenário optimista, a quantidade de biomassa florestal (matos) consumida pelos últimos 20 anos de fogos florestais, teria possibilitado o regular funcionamento de 4 centrais de 11 MW, durante o mesmo período de tempo.

Considerando, de acordo com as limitações sugeridas pelo Centro para a Biomassa e Energia (CBE, 1997), que apenas 50% desta biomassa pudesse ser retirada em condições economicamente viáveis, teríamos um cenário mais conservador, de 2 centrais de 11 MW.

CONCLUSÕES

O fenómeno dos fogos florestais, em Portugal Continental, constitui um sério problema. Com o continuo aumento do abandono da actividade agrária, o envelhecimento das populações rurais e do êxodo para as cidades do litoral ou para as capitais de Concelho, vai agravar o problema.

O desenvolvimento de programas de limpeza, gestão e ordenamento do espaço florestal, permitiria reduzir o perigo de incêndio florestal, minimizar os impactos ambientais e ecológicos e produzir energia eléctrica limpa.

Por outro lado, a dinamização destas actividades, permitiriam criar centenas de postos de trabalho local, contribuindo para um complemento do rendimento das populações rurais e, por ventura, evitar o abandono da actividade agro-florestal [13, 14, 15].

REFERÊNCIAS

[1] Kazanis D, Xanthopoulos G, Arianoutsou M. Understorey fuel load estimation along two post-fire chronosequences of *Pinus halepensis* Mill. forests in Central Greece. J For Res 2011 DOI 10.1007/s10310-011-0250-0. http://uaeco.biol.uoa.gr/files/PDF/papers_int/48_kazanis_et_al_2011. (Last access 11 July 2011)

[2] Cerrillo R M N and Oyonarte P B . Estimation of above-ground biomass in shrubland ecosystems of southern Spain. Invest Agrar: Sist Recur For 15(2): 2006;197-207

[3] Viana H, Fernandes P, Rocha R, Aranha J.. 2009. Alometria, Dinâmicas da Biomassa e do Carbono Fixado em Algumas Espécies Arbustivas de Portugal. Meeting proceedings in CD_ROM. Actas do 6º Congresso Florestal Nacional, Ponta Delgada, Açores; 2009.

[4] AFN – Autoridade Florestal Nacional. Cartografia nacional de areas ardidas entre 1990 e 2009. 2010. http://www.afn.min-agricultura.pt/portal/dudf/cartografia. (Last access in 25 July 2011).

[5] Caetano M., Nunes V and Nunes A. CORINE Land Cover 2006 for Continental Portugal, Technical report, Instituto Geográfico Português. http://www.igeo.pt/gdr/index.php?princ=PROJECTOS/CLC2006&sessao=m_projectos. (Last access in 25 July 2011).

[6] Caetano M., Araújo A, Nunes A, Nunes V and Pereira M. Accuracy assessment of the CORINE Land Cover 2006 map of Continental Portugal, Technical report, Instituto GeográficoPortuguês. http://www.igeo.pt/gdr/index.php?princ=PROJECTOS/CLC2006&sessao=m_projectos. (Last access in 25 July 2011).

[7] DGF – Direcção Geral das Florestas. Inventário Florestal Nacional. 3ª Revisão, Relatório Final. Direcção Geral de Florestas. Ministério da Agricultura do Desenvolvimento Rural e das Pescas. Lisboa; 2001.

[8] AFN – Autoridade Florestal Nacional,. Resultados do Inventário Florestal Nacional 2005/06. 2010. http://www.afn.min-agricultura.pt/portal/ifn/ (Last access in 25 July 2011).

[9] Viana H, Cohen BW, Lopes D, Aranha J. Assessment of forest biomass for use as energy. GIS-based analysis of geographical availability and locations of woodfired power plants in Portugal. Applied Energy 87(8): 2010; 2551-60.

[10] Muukkonen P, Heiskanen, J. Biomass estimation over a large area based on stand wise forest inventory data and ASTER and MODIS satellite data: A possibility to verify carbon inventories. Remote Sensing of Environment 107: 2007; 617-24.

[11] Agencia Portuguesa do Ambiente, 2011. Atlas Digital do Ambiente. http://sniamb.apambiente.pt/webatlas (Last access in 25 July 2011).

[12] Central de Biomassa de Mortágua. http://www.energiasrenovaveis.com/ html/energias/bio_projectos01.asp (Last access in 11 July 2011)

[13] European Commission. BIOMASS - Green energy for Europe.: Office for Official Publications of the European Communities. Luxembourg; 2005.

[14] Openshaw K. Biomass energy: employment generation and its contribution to poverty alleviation. Biomass and Bioenergy 34(3): 2010; 365-78.

[15] Hillebrand B, Buttermann HG, Behringer JM, Bleuel M. The expansion of renewable energies and employment effects in Germany. Energy Policy 34(18): 2006; 3484-94.

[16] Centro para a Biomassa e Energia - www.centrodabiomassa.pt

Agradecimento

Os autores gostavam de agradecer o apoio prestado pela Fundação para a Ciência e Tecnologia (FCT), sob a forma de uma bolsa de estudos SFRH/PROTEC/49626/2009 bem como ao CITAB (http://www.citab.utad.pt)

Annex E.4

Viana, H., Vega-Nieva, D., Ortiz Torres, L., Lousada, J., Aranha, J., 2012., Fuel characterization and biomass combustion properties of selected native woody shrub species from central Portugal and NW Spain. Fuel. DOI: 10.1016/j.fuel.2012.06.035.

Fuel 102 (2012) 737–745

Contents lists available at SciVerse ScienceDirect

Fuel

journal homepage: www.elsevier.com/locate/fuel

Fuel characterization and biomass combustion properties of selected native woody shrub species from central Portugal and NW Spain

H. Viana [a,c,*], D.J. Vega-Nieva [b], L. Ortiz Torres [b], J. Lousada [c], J. Aranha [c]

[a] CI&DETS. Forestry Sciences Section, Agrarian Superior School, Polytechnic Institute of Viseu. Quinta da Alagoa, 3500-606 Viseu, Portugal
[b] Escuela Universitaria de Ingeniería Técnica Forestal, Universidad de Vigo, Spain
[c] CITAB, University of Trás-os-Montes e Alto Douro, Apartado 1014, 5001-801 Vila Real, Portugal

HIGHLIGHTS

- Selected shrub native species from Spain and Portugal were characterized.
- Ashes of 1–2%, N > 0.6%, S < 0.1% and HHV of 21–24 MJ kg^{-1}were found.
- Alkali metal 20–30% denote potential ash bed sintering/agglomeration and fouling risk.
- ash trace elements were below most of European limits.

ARTICLE INFO

Article history:
Received 10 November 2011
Received in revised form 13 March 2012
Accepted 8 June 2012
Available online 23 June 2012

Keywords:
Shrub
Biomass
Heating value
Ash
Slagging

ABSTRACT

Selected native shrub species from central Portugal and NW Spain, *Cytisus multiflorus* (broom), *Erica arborea* (heath), *Pterospartum tridentatum* (carqueisa) and *Ulex europaeus* (gorse) were characterized for physical, thermal and chemical properties for combustion. The studied shrub species showed ash contents in the range 1–2%, nitrogen contents above 0.6%, and sulfur contents below 0.1% at both areas of study. A significant effect of species on Higher Heating Value (HHV) was observed, with no significant effect of the location of study, central Portugal or NW Spain. The higher HHV (24.4 MJ kg^{-1}) was recorded for heath, this species also shows the higher average carbon and lower nitrogen content values of the studied species. Analysis of the chemical composition of the ashes revealed alkali metals contents of 24–30%, representing a potential sintering, fouling and bed agglomeration risk in the combustion of the studied species. Ash As, Cd, Pb, Co, Cu, Mn, Ni, Cr, and Zn content was below national and most of European legislation maximum levels for these elements for ash application as fertilizer, with the exception of some of the more conservative limits for Cd, Cu, Cr, and Zn from Northern and central European countries legislation.

1. Introduction

The interest in the utilization of forest biomass for bioenergy has increased exponentially in the last decades in European countries, as an integrated strategy for climate change mitigation, increasing renewable energy security and preventing forest fires. Consequently, Portuguese [1] and Spanish [2] National strategies, have established ambitious goals for energy production in dedicated biomass plants for CHP, resulting in a large potential biomass demand in both countries. Given the limited availability of residual forest biomass in Portugal [3] and Spain [4], joined with a growing pellet production in these two countries, potentially utilizing forest residual biomass sources [5], there is an increased interest on the consideration of alternative feedstocks for biomass combustion, such as native woody shrub species.

Shrubland areas currently occupy close to 1 million hectares in the region of Galicia, NW Spain [6] and a total of 1.9 million hectares in Portuguese territory [7]. Furthermore, abandoned shrubland areas constitute a main fuel for the frequent wildfires in these two countries: approximately half of the 1.5 and 0.2 million hectares burned by wildfires in Portugal and in the region of Galicia, NW Spain, in the period 2001–2010, were shrubland areas [8]. The regular harvesting of shrubland areas, might therefore additionally be valuable for diminishing the large greenhouse gas emissions associated to these frequent wildfires [9], through the reduction of forest fires occurrence.

In order to evaluate their potential as a biomass feedstock for combustion, there is a need for an integrated biomass and ash

* Corresponding author at: CI&DETS. Forestry Sciences Section, Agrarian Superior School, Polytechnic Institute of Viseu, Quinta da Alagoa, 3500-606 Viseu, Portugal. Tel.: +351 232 446 600; fax: +351 232 426 536.
E-mail address: hviana@esav.ipv.pt (H. Viana).

0016-2361/$ - see front matter © 2012 Elsevier Ltd. All rights reserved.
http://dx.doi.org/10.1016/j.fuel.2012.06.035

characterization for the main native species in the shrubland areas of these two countries. Available information on biomass characterization and specific combustion properties of native woody shrub species in this area, however, is relatively scarce, namely the studies by Núñez-Regueira et al. [10] and Elvira and Hernando [11] in NW and central Spain, and the studies from Fernandes and Pereira [12] and from Fernandes and Rego [13] in Portugal, among others.

Fuel calorific properties are known to be influenced by biomass composition (e.g. [14–16]), this species-specific composition being potentially influenced by growing conditions such as sunlight, geographic location, climate, soil types, available water, soil pH and nutrients [16]. Therefore, it would be of interest to study whether the different local soil and climate conditions from NW Spain and central Portugal have an effect on the calorific properties of the existing native shrub species.

Moreover, available shrub characterization studies for these native species have only focused on selected biomass physical and chemical properties such as basic density (e.g. [13]), calorific value (e.g. [11]), and/or fuel proximate and ultimate analysis (e.g. [10]). However, proximate and ultimate analysis brings relatively limited information when the chemical composition of the combusted biomass is not also considered [16], particularly given the potential ash slagging and fouling risk in biomass fuels with high mobile nutrients contents, specially alkali metals, in their ashes, which can limit boiler efficiency, even lead to bed defluidization through deposit formation and boiler corrosion (e.g. [17–19]). In spite of its relevance on combustion efficiency, slagging and fouling risk, information on the ash composition of these native shrub species is scarce, together with a scarcity of information on the ash composition for shrub species in general: for instance, neither any of the main recent reviews in fuel and ash composition (e.g. [16,19,20]), nor any of the main ash composition databases (e.g. [21–26]), include any information on shrub ashes composition and/or the associated ash slagging and fouling risk. Additionally, an integrated evaluation of the potential of shrub ashes should consider the monitoring of relevant minor and trace elements contents in the ashes, which are of particular relevance for the environmental impact of the potential ashes reutilization as fertilizer (e.g. [27–29]).

Consequently, the present work aimed to study the fuel and ash characteristics and combustion properties of the selected native shrubs *Cytisus multiflorus* (L'Hér.) Sweet (broom), *Erica australis* (L.) (heath), *Ulex europaeus* (L.) (gorse) and *Pterospartum tridentatum* (L.) Willk (carqueisa), these species being representative of the main genus present in the Mediterranean native shrubland areas of NW Spain and North-Central Portugal. The analysis of physical and thermochemical properties of the shrub biomass including: (1) basic density (Db); (2) proximate analysis, namely moisture content (w%), fixed carbon (FC%), volatile matter (VM%) and ash yield (A%); (3) ultimate analysis (C, O, H, S, N); (4) calorific value (Higher and Lower Heating Value) and (5) energy density calculation, was conducted for the four species at both areas of study. Additionally, (6) ash chemical composition, including relevant minor and trace elements contents, was analysed.

2. Material and methods

2.1. Shrub biomass measurement and sampling for fuel and ash analysis

2.1.1. Shrub biomass measurement

The areas of study were Centre – North Portugal (Area 1), extending from 39°11′53″N, 06°14′17′W to 42°50′50″N, 08°19′02″W and NW Spain (Area 2), extending from 42°56′26.06″N, 7°26′25.89W to 42°31′28.05″N, 7°31′10.41W. From June to August 2007, 22 and 32 sites were sampled in Area 1 and Area 2, respectively, for aboveground biomass determination. Within each site, occupying homogeneously at least one hectare, a sampling plot with an area of 10 m^2 was established and the aboveground biomass within that plot was clipped, placed into hermetically closed containers to prevent moisture loss and transported to the laboratory, where it was divided by species, oven dried and weighted to determine the dry aboveground biomass per hectare (t ha^{-1}).

2.1.2. Sampling for biomass and ash analysis

The selected species for study of biomass and ash characterization were: *Cytisus multiflorus* (L'Hér.) Sweet (Spanish or Portuguese white broom), *Erica australis* (L.) (Spanish or Portuguese heath), *Ulex europaeus* (L.) (common gorse or furze) and *Pterospartum tridentatum* (L.) Willk (carqueisa).

For each subject woody shrub species, 7–9 biomass samples, representative of all the sampled aboveground biomass fractions, were randomly selected from the harvested biomass for fuel and ash laboratory analyses (Section 2.2). Aboveground biomass samples included leaves and all woody fractions from aboveground biomass. In addition, in Area 1 of study, belowground root biomass samples were taken for proximate and ultimate analyses, by cutting representative small fractions of the exposed root system. Soil particles were carefully removed with high pressure water application.

All samples were prepared according to the technical specifications CEN/TS 14780:2005 [30] for sample preparation for the physical, thermal and chemical characterization of biomass.

2.2. Analytical measurements

2.2.1. Proximate analysis and basic density

Moisture content (wet basis) was determined following the European Standard CEN EN 14774-1:2009 [31]. The determination of ash content (dry basis) was carried out at 550 °C ± 10 °C according to CEN EN 14775:2009 [32] The volatile matter content (dry basis) was determined at 900 °C ± 10 °C according to CEN EN 15148:2009 [33]. Fixed carbon content (%) is the difference between the sum of volatile matter and ash contents from 100. Shrub basic density (Db) was calculated by water displacement technique and expressed as dry weight per unit volume [34].

2.2.2. Ultimate analysis

Elemental composition of shrub biomass was measured following CEN/TS 15104:2005 [35] European Standard for determining Carbon (C), Hydrogen (H) and Nitrogen (N) and CEN/TS 15289:2006 [36] for Sulfur (S) content in solid biofuels. The simultaneous determination of CHN was carried out in a Leco TruSpec Elemental Determinator. Sulfur content determination was done in a Leco SC-144DR using direct combustion and infrared detection. The oxygen content was obtained by subtracting from 100% the sum of (C, H, N, S and ash) contents in percentage.

2.2.3. Higher and lower heating values

The higher heating value (HHV), also called gross calorific value (GCV), of biomass at constant volume in dry basis was determined following the CEN EN 14918:2009 [37] The HHV in dry basis was calculated by the Eq. (1) [37]:

$$q_{v,gr,d} = q_{v,gr} \frac{100}{(100 - M_{ad})} \tag{1}$$

where $q_{v,gr,d}$ is the higher heating value at constant volume of the dry (moisture-free) fuel, in joules per gram. M_{ad} is the moisture in the analysis sample, in percentage by mass. $q_{v,gr}$ is the higher heating value at constant volume of the fuel as analysed, in joules per gram.

The LHV was calculated as (Eq. (2)) [37]:

$$q_{p,net,d} = q_{v,gr,d} - 212,2w(H)_d - 0,8[w(O)_d + w(N)_d] \quad (2)$$

where $q_{p,net,d}$ is the lower heating value in dry basis at constant pressure, in joules per gram, of the biofuel, $q_{v,gr,d}$ is the higher heating value in dry basis, in joules per gram, of the biofuel, $w(H)_d$ is the hydrogen content, in percentage by mass, of the moisture-free (dry) biofuel, $w(O)_d$ is the oxygen content, in percentage by mass of the moisture-free biofuel, $w(N)_d$ is the nitrogen content, in percentage by mass, of the moisture-free biofuel.

The LHV at constant pressure at a required moisture content w%, was calculated as the following equation:

$$q_{p,net,ar} = q_{p,net,d}(1 - 0.01M_{ar}) - 24.43M_{ar} \quad (3)$$

where $q_{p,net,ar}$ is the lower heating value at constant pressure, in joules per gram, of the biofuel with moisture content as received M_{ar}; $q_{p,net,d}$ is the lower heating value at constant pressure in dry basis, in joules per gram, of the biofuel; M_{ar} is the moisture content as received [w%]; 24.43 is the correction factor of the enthalpy of vaporization (constant pressure) for water (moisture) at 25 °C [J/g per 1 w% of moisture].

2.2.4. Fuel energy density

The energy density as received (E_{ar}) was calculated using the lower heating value as received and the bulk density, according to Eq. (4) [38].

$$E_{ar} = \frac{1}{3600} q_{p,net,ar} BD_{ar} \quad (4)$$

where E_{ar} is the energy density of the biofuel as received (MWh m^{-3}) of bulk density); $q_{p,net,ar}$ the lower heating value as received (MJkg^{-1}), BD_{ar} the bulk density, i.e., volume weight of the biofuel as received (kg m^{-3} bulk volume), $\frac{1}{3600}$ the conversion factor for the energy units (MJ to MWh).

Fuel bulk density depends on the utilized biomass logistics: chipping, bundling, etc. The most feasible option for the shrub fuels under study consists on fuel bundling after harvesting. The compaction into bundles can be very variable depending on the machinery used and type of biomass residues (e.g. [39,40]). Since it was not the purpose of this paper to explore these issues, an average value of bulk density for green bundles for logging residues (285 kg m^{-3} [39]) reported in the literature was utilized for providing an initial estimate of the energy density of the shrub bundles after harvesting. A sensitivity analysis of the effects of varying this average bundling density value on ±25% on calculated energy density was additionally performed.

2.2.5. Ash chemical composition

The chemical composition of the biomass ash, obtained at 550 °C following CEN EN 14775: 2009 [32] was analysed according to CEN/TS 15290:2006 Solid biofuels – Determination of major elements [41] and CEN/TS 15297:2006 Solid biofuels – Determination of minor elements [42]. Ash Si, Al, Ti, Fe, Na, K, Ca, Mg, P determination was done by flame atomic absorption spectrometry (FAAS), and the measurement of ash As, Cd, Pb, Co, Cu, Cr, Mn, Zn and Ni was done by Graphite furnace atomic absorption spectroscopy (GF-AAS), after an ash digestion with Nitric acid – HNO_3 (65%), Hydrogen peroxide – H_2O_2 (30%), Hydrofluoric acid – HF (40%), utilizing a Boric acid – H_3BO_3 (4%) neutralization for the first elements as recommended by Baernthaler et al. [43].

2.2.6. Ash slagging and fouling indices

The following slagging and fouling indices were calculated from ash chemical composition (Table 5), according to the following expressions [17,18,44,45]:

Base to acid index [45] was calculated according to the following equation:

$$B/A = \frac{Fe_2O_3 + CaO + MgO + Na_2O + K_2O}{SiO_2 + Al_2O_3 + TiO_2} \quad (5)$$

Being that: if B/A < 0.75, slagging trend can be expected [45]. R_S index [45] was calculated according to the following equation:

$$R_S = (B/A)S^d \quad (6)$$

where S^d is S in percentage from elementary analysis if $R_S < 0.6$, low fouling trend; if $0.6 < R_S < 2$, medium trend; if $2.0 < R_S < 2.6$, high trend; if $R_S > 2.6$, very high trend [45].

Alkali Index (AI) [17] was calculated according to the following equation:

$$AI = \frac{(K_2O + Na_2O)A(\%)}{HHV} \quad (7)$$

where $A(\%)$ is the ash percentage obtained at 550 °C and HHV is the Higher Heating value (MJ kg^{-1}) at $w\%$ = 0%. If AI > 0.17 kg alkali MJ^{-1} probable slagging and fouling; if AI > 0.34 kg alkali MJ^{-1} slagging and fouling is certain to occur according to Miles et al. [17]

The following sintering index (SI) [18] was calculated according to the following equation:

$$SI = \frac{CaO + MgO}{Na_2O + K_2O} \quad (8)$$

Being that: no slagging should be expected at values of SI > 2, whereas the slagging risk should be high at SI < 2, according to Fernández Llorente and Carrasco García [18]

For evaluating the risk of bed agglomeration in fluidised bed combustion, the following bed agglomeration index (BAI) [44] was calculated according to the following equation:

$$BAI = \frac{Fe_2O_3}{Na_2O + K_2O} \quad (9)$$

Being that: bed agglomeration occurs when BAI < 0.15, following Vamvuka and Zografos [44]

3. Results and discussion

3.1. Shrub biomass measurement

Descriptive statistics of the shrub biomass sampling plots at the two areas of study are shown in Table 1. All the studied species were characterized by a high weight of fine fractions of <6 mm.

Higher biomass values were found for broom (*Citisus multiflorus*), followed by gorse (*Ulex europaeus*) at both areas of study. Average biomass values for the studied species (Bi) are of a similar range to the values measured in NW Spain shrubland [10]. In addition to average biomass values for each species, the biomass distribution for an average mixed shrubland plot is given in Table 1, resulting in an average total aboveground biomass (Bt) sum of 18.6 and 26 t ha^{-1} (dry basis) for an average plot in the areas of study in central Portugal and NW Spain, respectively.

3.2. Proximate analysis and basic density

Proximate analysis and basic density results are shown in Table 2.

3.2.1. Proximate analysis

Ash percentage ranged from 1.21% to 1.56% for the shrub aboveground biomass of the studied species. Similarly, a seasonal range

Table 1
Descriptive statistics of the shrub biomass sampling plots at the two areas of study.

Area of study *species*	ns	np	h (m)	B% (db) <6 mm	CC (%)	Bi (t ha^{-1}) (db)	Bt (t ha^{-1}) (db)
Central Portugal							
Cytisus multiflorus	9	11	0.8 (±0.3)	85 (±14)	27.5 (±22.3)	13.6 (±7.9)	10.3 (±9.1)
Erica australis	7	9	0.7 (±0.4)	89 (±9)	21.4 (±17.2)	4.9 (±3.0)	3.9 (±4.2)
Pterospartum tridentatum	7	10	0.2 (±0.1)	93 (±6)	12.0 (±7.3)	2.9 (±2.3)	1.7 (±2.4)
Ulex europaeus	9	12	0.7 (±0.5)	80 (±16)	25.4 (±11.8)	5.5 (±2.7)	2.9 (±3.4)
Other species	n	22	0.1 (±0.2)	99 (±1)	2.4 (±2.6)	0.2 (±0.4)	0.1 (±0.3)
Sum							18.9 (±13.4)
NW Spain							
Cytisus multiflorus	9	26	1.6 (±0.8)	58 (±35)	83.7 (±16.1)	30.1 (±12.3)	8.9 (±9.6)
Erica australis	7	16	0.9 (±0.7)	78 (±17)	85.9 (±14.3)	26.4 (±7.4)	4.8 (±5.3)
Pterospartum tridentatum	7	19	0.4 (±0.3)	91 (±4)	38.6 (±15.7)	16.0 (±5.9)	3.3 (±4.8)
Ulex europaeus	9	28	0.9 (±0.7)	74 (±21)	87.2 (±10.4)	28.7 (±6.8)	9.1 (±10.2)
Other species	n	32	0.2 (±0.3)	98 (±2)	2.6 (±0.3)	0.3 (±0.5)	0.2 (±0.5)
Sum							26.3 (±16.2)

Where: ns: number of biomass sub-samples selected for biomass and ash analysis at the laboratory; np: number of study plots at each area of study where the species was present; h(m): shrub height (m); %B(db) <6 mm: Percentage of aboveground biomass (dry weight) corresponding to the fraction of less than 6 mm; CC: shrub canopy cover (%); Bi (t ha^{-1}) (db): average shrub aboveground biomass (t ha^{-1} on dry basis), for the plots where the species was present; Bt (t ha^{-1}) (db): average shrub aboveground biomass (t ha^{-1} on dry basis), considering all the plots of the area of study. Numbers in parenthesis are the standard deviations.

Table 2
Proximate analysis and basic density of the shrub species at the two areas of study.

Species		Proximate analysis (% by mass, dry basis)				Db (kg m^{-3})
		Ash%	VM%	FC%	w%	
Cytisus multiflorus (Portugal)	Shoot	1.32 (±0.05)	82.48 (±0.46)	16.20 (±0.51)	52.3 (±1.2)	417.5 (±89.6)
	Root	0.71 (±0.01)	82.73 (±0.29)	16.57 (±0.28)	48.7 (±1.9)	522.7 (±24.2)
Erica australis (Portugal)	Shoot	1.38 (±0.01)	80.72 (±0.41)	17.90 (±0.38)	45.6 (±2.8)	569.2 (±183.4)
	Root	0.99 (±0.01)	83.35 (±0.07)	15.65 (±0.07)	44.6 (±1.6)	603.8 (±30.3)
Pterospartum tridentatum (Portugal)	Shoot	1.44 (±0.01)	81.10 (±0.30)	17.45 (±0.29)	47.6 (±0.5)	485.2 (±40.0)
	Root	0.74 (±0.02)	83.38 (±0.14)	15.88 (±0.39)	37.1 (±0.9)	739.2 (±34.0)
Ulex europaeus (Portugal)	Shoot	1.47 (±0.01)	84.46 (±0.19)	14.06 (±0.20)	49.6 (±3.9)	417.9 (±104.7)
	Root	1.38 (±0.05)	84.31 (±0.30)	14.31 (±0.35)	43.6 (±4.9)	576.9 (±34.3)
Cytisus multiflorus (NW Spain)	Shoot	1.37 (±0.07)	80.81 (±0.62)	17.83 (±0.69)	59.2 (±1.7)	408.1 (±53.8)
Erica australis (NW Spain)	Shoot	1.38 (±0.09)	79.65 (±0.50)	18.97 (±0.54)	58.9 (±0.9)	483.3 (±63.5)
Pterospartum tridentatum (NW Spain)	Shoot	1.21 (±0.05)	80.32 (±0.44)	18.47 (±0.46)	46.3 (±1.5)	420.5 (±77.5)
Ulex europaeus (NW Spain)	Shoot	1.56 (±0.03)	80.80 (±0.36)	17.64 (±0.31)	46.7 (±2.2)	435.2 (±66.0)

Where: shoot: aboveground biomass; root: belowground biomass; Ash%: Ash percentage (%), VM%: Volatile Matter (%), FC% Fixed Carbon (%), w%: Moisture content wet basis (%); Db: basic Density (kg m^{-3}), including leaves and twigs <6 mm. Numbers in parenthesis are the standard deviations.

Table 3
Ultimate analysis of the shrub species at the two areas of study.

Species		Ultimate analysis (% by mass, dry basis)				
		C	H	O	N	S
Cytisus multiflorus (Portugal)	Shoot	46.20 (±0.26)	6.88 (±0.09)	44.35 (±0.29)	1.24 (±0.06)	<0.1
	Root	45.65 (±0.13)	6.86 (±0.04)	45.75 (±0.30)	0.98 (±0.02)	<0.1
Erica australis (Portugal)	Shoot	49.84 (±0.10)	7.04 (±0.08)	41.06 (±0.09)	0.63 (±0.02)	<0.1
	Root	46.50 (±0.08)	6.71 (±0.04)	45.32 (±0.00)	0.45 (±0.01)	<0.1
Pterospartum tridentatum (Portugal)	Shoot	47.95 (±0.16)	6.97 (±0.09)	42.96 (±0.18)	0.67 (±0.04)	<0.1
	Root	46.51 (±0.08)	6.71 (±0.04)	45.58 (±0.09)	0.45 (±0.01)	<0.1
Ulex europaeus (Portugal)	Shoot	46.32 (±0.43)	6.85 (±0.04)	44.37 (±0.52)	0.95 (±0.01)	<0.1
	Root	45.49 (±0.06)	6.81 (±0.11)	45.48 (±0.17)	0.79 (±0.01)	<0.1
Cytisus multiflorus (NW Spain)	Shoot	48.84 (±0.69)	6.55 (±0.39)	43.2 (±0.19)	2.05 (±0.65)	<0.1
Erica australis (NW Spain)	Shoot	48.13 (±0.46)	6.08 (±0.55)	42.7 (±0.33)	0.82 (±0.08)	<0.1
Pterospartum tridentatum (NW Spain)	Shoot	48.78 (±0.31)	6.65 (±0.03)	42.3 (±0.17)	0.96 (±0.25)	<0.1
Ulex europaeus (NW Spain)	Shoot	48.88 (±0.53)	6.49 (±0.12)	42.4 (±0.26)	1.72 (±0.09)	<0.1

Where: shoot: aboveground biomass; root: belowground biomass. Numbers in parenthesis are the standard deviations.

in ash content for native gorse, broom and heath of 0.71–1.14%, 0.16–0.86% and 0.21–0.79% respectively, were observed in NW Spain [10]. Ash values of 2.42% have been reported for *Ulex parviflorus* in France [46]. The presence of leaves and spines in the evergreen studied species possibly contributed to the relatively high ash content of the shrub biomass: for instance, Dimitrakopoulos and Panov [47] reported values of 2.51% for *Erica arborea* leaves, while the ashes content of the same species twigs was 1.63%. Whereas typical ash content in wood is 0.5%, the ash content in the actively metabolising fractions such as leaves, and in the low diameter branch fractions, where mobile nutrients such as potassium are accumulated, can be as high as 2–5% (e.g. [16,48,49]). Ash composition will be further discussed in Section 3.6.2.

Table 4
Higher and lower heating values and energy density of shrub species at the two areas of study.

Species	Area	HHV (MJ kg^{-1})	LHV (MJ kg^{-1})	Ear (GJ m^{-3})	Ear (MW h m^{-3})
Cytisus multiflorus	1	22.245 (±0.502)	8.455 (±0.361)	2.41	0.67
Erica australis	1	24.117 (±0.668)	11.111 (±0.488)	3.17	0.88
Pterospartum tridentatum	1	21.365 (±0.667)	9.508 (±0.162)	2.71	0.75
Ulex europaeus	1	21.872 (±0.321)	8.702 (±0.396)	2.48	0.69
Cytisus multiflorus	2	22.256 (±0.639)	7.231 (±0.203)	2.06	0.57
Erica australis	2	24.397 (±0.350)	11.208 (±0.234)	3.19	0.89
Pterospartum tridentatum	2	22.144 (±0.656)	7.071 (±0.236)	2.02	0.56
Ulex europaeus	2	21.241 (±0.654)	9.454 (±0.318)	2.69	0.75

Where: Area 1: Central Portugal; Area 2: NW Spain; HHV: Higher Heating Value (MJ kg^{-1} at dry basis); LHV: Lower Heating Value (MJ kg^{-1}) at moisture content as received (see Table 2); Ear: Energy Density as received of the shrub fresh bundles (GJ m^{-3} and Mw h m^{-3}). Numbers in parenthesis are the standard deviations.

Table 5
Shrub ash major and selected minor elements composition.

Species	Ash composition (% oxides referred to ash dry weight)								
	SiO_2	Al_2O_3	TiO_2	Fe_2O_3	Na_2O	K_2O	CaO	MgO	P_2O_5
Cytisus multiflorus	16.6	2.0	0.1	1.9	11.6	18.5	8.0	22.0	19.3
Erica australis	17.0	0.1	0.1	1.6	10.4	14.1	17.0	22.1	17.6
Pterospartum tridentatum	23.4	0.1	0.1	1.9	10.4	15.9	18.0	12.1	18.1
Ulex europaeus	33.6	3.9	0.3	3.3	8.5	15.3	13.2	9.0	12.9

The observed values of Volatile matter were similar to the usual range of 70–86% in volatiles for woody biomass [16,48,49] with the higher volatile percentages and lower fixed carbon measured for the belowground biomass samples. In high volatiles content fuels, care must be taken to achieve complete combustion of the volatiles to ensure higher combustion efficiency and low emissions of CO, hydrocarbons and PAH [20].

Moisture values at the time of reception correspond to the lower values in the reported year-round seasonal ranges in moisture content of 47.5–66.8%, 57.5–62.0%, and 44.4–63.2% for native gorse, broom and heath found in NW Spain [10], as it would be expected for a summer harvest of these species. Fuel moisture values should only be regarded as indicative of the conditions at the particular time of sampling at the two areas; furthermore, actual fuel moisture at reception would be influenced both by the season of harvest and the logistics of harvesting and transport.

3.2.2. Basic density

Basic density of the shrub aboveground biomass ranged from 404 to 498 kg m^{-3}, the highest values corresponding to heath at both areas of study (Table 2). Similar values of 500–580 kg m^{-3}, 427–484 kg m^{-3}, 356–474 kg m^{-3} and 379–500 kg m^{-3}, have been reported for Spanish and Portuguese heath, carqueisa, gorse and broom by Elvira and Hernando [11], Fernandes and Pereira [12] and Fernandes and Rego [13], these shrub aboveground biomass samples including leaves and twigs of less than 6 mm, like in the present study. Belowground biomass samples from central Portugal showed higher density values than corresponding aboveground woody biomass samples (Table 2).

3.3. Ultimate analysis

Ultimate analysis results for the shrub species at the two areas of study are shown in Table 3.

Measured shrub aboveground biomass carbon contents are similar to the range of 46.02–55.51% observed in NW Spain for gorse, broom and heath by Núñez-Regueira et al. [11], who also found the highest average carbon content for heath as in the present study. Measured belowground biomass carbon contents results in central Portugal area of study were lower than the corresponding carbon

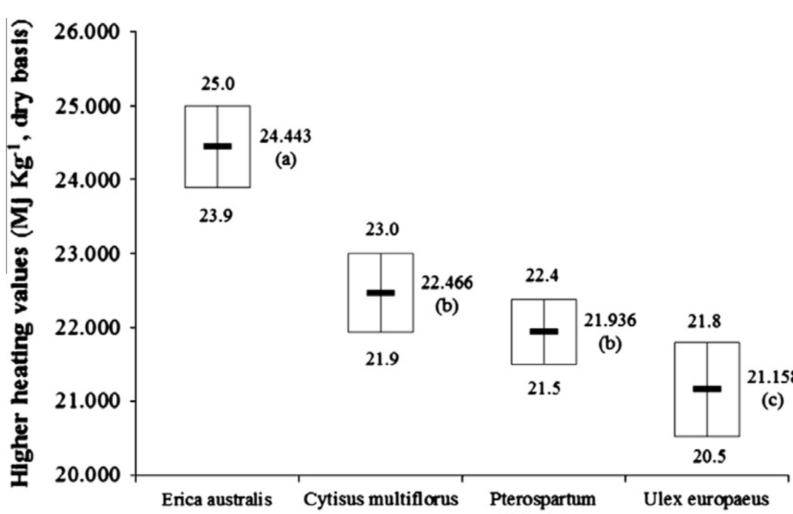

Fig. 1. Average higher heating values of shrub species for the two areas of study *Where*: (letters in brackets) stand for signifficant differences at $p < 0.05$.

Table 6
Ash slagging and fouling indices and risk.

Species	B/A		Rs		Alkali Index (AI)		Sintering Index (SI)		Bed Agglomeration Index (BAI)	
	B/A	Slagging risk	Rs	Fouling risk	AI	Fouling risk	SI	Sintering risk	BAI	Bed agglomeration
Cytisus multiflorus	2.06	Low	0.06	Low	0.17	Probable	1.00	High	0.06	Occurs
Erica australis	2.45	Low	0.07	Low	0.14	Low	1.61	High	0.07	Occurs
Pterospartum tridentatum	1.89	Low	0.05	Low	0.16	Low	1.14	High	0.07	Occurs
Ulex europaeus	0.88	Low	0.03	Low	0.17	Probable	0.93	High	0.13	Occurs

Table 7
Shrub ash trace and selected minor elements composition.

Species	As	Cd	Pb	Co	Cu	Cr	Mn	Zn	Ni
Cytisus multiflorus	3.2	4.1	5.1	9.9	100.1	20.1	10204.7	3212.6	1.9
Erica australis	4.9	2.5	14.3	2.7	739.9	101.8	5808.8	689.8	2.9
Pterospartum tridentatum	3.4	3.1	11.9	7.3	293.1	128.4	7287.2	2290.3	2.1
Ulex europaeus	4.4	3.3	12.1	5.4	409.2	111.2	4812.2	1660.6	1.7
Country (application)									
Denmark (Agriculture/Forestry)		15	120			100			30
Finland (Agriculture)	25	1.5	100		600	300		1500	100
Finland (Forestry)	30	17.5	150		700	300		4500	150
Sweden (Forestry)	30	30	300		400	100		7000	300
Austria (Field and grassland)	20	8	100	100	250	250		1500	100
Portugal (Agriculture)[a]		20	750		1000	1000		2500	300
Spain (Soils with ph < 7)		20	750		1000	1000		2500	300
Spain (Soils with ph > 7)		40	1200		1750	1500		4000	400

[a] Limit values of concentration of heavy metals in sludge from water treatment plants.

contents for aboveground biomass for all the studied species. Hydrogen and oxygen content, in the range of 6–7% and 41–45%, were within typical ranges for forest biomass fuels (e.g. [16]).

All studied species showed a sulfur content below the 0.1% threshold established by Obernberger et al. [49] for minimizing sulfur-related corrosion risk in biomass boilers combustion, these measured sulfur content values being more similar to average values of <0.1% of woody fuels than to the contents of >0.2% S commonly found in herbaceous biomass fuels (e.g. [16]).

Nitrogen content ranged from 0.63% to 2.05%, with the highest values found for *Cytisus multiflorus* (broom), followed by *Ulex europaeus* (gorse), at both areas of study. Similarly, Núñez-Regueira et al. [10] found the highest shrub N content values in NW Spain for the native broom *Cytisus scoparius*, ranging from 1.1% to 4.8% at four seasons of study, followed by Spanish gorse, with a seasonal N range of 1.0–2.8%, and heath, with a N range of 1.0–1.7%. For all the species in the present study, a higher N content was observed in NW Spain area of study, this possibly being a consequence of the higher N content characteristic of the soils in the region (e.g. [50]).

Measured shrub biomass nitrogen content from the current study and from Núñez-Regueira et al. [10] in NW Spain is more similar to the range of 0.5–2.8%, typical of herbaceous biomass fuels, than to the lower range of 0.1–0.7%, characteristic of woody biomass fuels [49,16]. Leguminous shrubs, such as gorse or broom, are characterized by a high nitrogen fixation capacity, accumulating this mobile nutrient in fine fractions such as leaves or twigs, with potential implications for the combustion of these fuels. All of the studied species at both areas of study and in the data of native shrub species ultimate analysis at four seasons of harvest from Núñez-Regueira et al. [10], in NW Spain, showed N contents above the 0.6% threshold proposed by Obernberger et al. [49] for avoiding NO_x emissions in combustion.

3.4. Higher and lower heating values

Higher and lower heating values for the studied species at the 2 areas of study are shown in Table 4. Higher values were observed for heath HHV at both areas of study. Average HHV and standardized deviations for the four shrub species are shown in Fig. 1. Using SPSS 19 (SPSS Inc, USA), a General Linear Model ANOVA was performed testing the three factors species, area of study and interaction between species and area of study.

A significant (p-value $\leqslant$ 0.05) effect of species on fuel higher heating value was found, with no significant effect of neither area of study (p-value = 0.105) nor of interaction between species and area of study (p-value = 0.667). A subsequently Student–Newman-Keuls test revealed three groups for HHV, the highest ranking species being heath, with an average HHV of 24.44 MJ kg^{-1}, followed by a second group formed by broom and carqueisa, with values of 22.46 and 21.94 MJ kg^{-1}, respectively, and a third group for gorse, with an average HHV of 21.16 MJ kg^{-1} (Fig. 1).

Measured average HHV results are similar to the values measured by Elvira and Hernando [11], who reported average HHV of 24.59, 23.44, 22.34 and 20.65 MJ kg^{-1} for Spanish broom, heath (*Erica scoparia*), carqueisa and gorse in central Spain, the first three species being classified as high calorific and the latter as medium calorific species following the calorific value classification established by Hough [51]. High calorific values are typical of heath species: values of 24.06, 23.6 and 23.8 MJ kg^{-1} have been measured for *Erica arborea* in France [46], Greece [47] and Spain [52], this species being the highest ranking of 20 Mediterranean species in Greece in Dimitrakopoulos and Panov study [47]. Lower calorific values have been reported for other broom species, such as *Cytisus scoparius*, with an average HHV of 21.1 MJ kg^{-1} found in central Spain [53] and a reported seasonal range from 19.02 to 20.68 MJ kg^{-1} measured in NW Spain [10]. HHV for gorse measured in the current study agrees with the values reported by Madrigal et al. [53], who found average calorific values of and 21.43 MJ kg^{-1} for this species, being also similar to the values of 21.32–20.62 MJ kg^{-1} reported for *Ulex parviflorus* in France [46].

It is interesting to note that the higher HHV was found for heath, this species having the both the highest average C content and lowest N content in the current study and in Núñez-Regueira et al. [10] study in NW Spain, as discussed in the Section 3.3. Various authors have noted the positive role of increasing C and decreasing N in raising the HHV of biomass fuels (e.g. [14,15]), this explaining in part the higher HHV of woody fuels in comparison with herbaceous fuels [16]. In addition, other factors, such as extractive content, not measured in the current study, can be influencing the different HHV of species, this content being linked to season of harvest and associated moisture content [11].

Measured LHV of the freshly harvested shrub biomass samples ranged from 7.07 to 11.21 MJ kg^{-1}, with the highest values found for *Erica australis* at both sites. Lower heating values are highly dependent on fuel moisture content and therefore the values presented are only representative of the calorific value correction for the particular moisture value at the time of sampling. The effects of fuel moisture on effective LHV and associated fuel energy density are discussed in Section 3.5 below.

3.5. Fuel energy density

Energy density of fresh shrub biomass compacted into bundles (Table 4) ranged from 2.2 GJ m^{-3} to 3.2 GJ m^{-3}. These values, which represent a conservative estimate for a summer harvest scenario assuming no drying period of the biomass after harvest, are similar to the energy density values reported for other biomass sources such as woodchips of softwood (2.8 GJ m^{-3}) or grass in high pressed bales (2.7 GJ m^{-3}) or triticale straw (1.9 GJ m^{-3}) [54].

A ±25% variation in the shrub bundle bulk density would result in estimated energy density values of 1.5–2.4 and 2.5–3.9 GJ m^{-3}, respectively, for the summer harvest scenario with the measured moisture contents and associated lower heating values. For a wet season harvest scenario, assuming a moisture content of 65%, as recorded for the studied fuels in the areas of study by Núñez-Regueira et al. [10] and by Fernandes and Pereira [12], the calculated LHV of the studied species would descend to 5.3–6.5 MJ kg^{-1}, resulting in calculated energy density values of 1.1–1.4 GJ m^{-3}, suggesting a greater role of season of harvest and associated moisture content on the energy density of these fuels.

3.6. Ash chemical composition and slagging indices

3.6.1. Ash chemical composition: major and selected minor elements

Ash contents of Si, Al, Ti, Fe, Na, K, Ca, Mg and P, expressed as oxides referred to ash percentage dry weight and normalized to 100% for slagging indices calculation, are presented in Table 5. Shrub ashes were mainly constituted by silica, phosphorus, alkali metals (Na and K) and alkaline earth metals (Ca and Mg). Measured silica content in the ashes, was more similar to the average SiO_2 values of 22.2% for woody fuels than to the average value of 46.2% for herbaceous fuels reported in the ash composition review by Vassilev et al. [16].

All samples showed high alkali metals content, with a total sum of alkali metals (Na and K) oxides ranging from 23.7% to 30.1%. High alkali metals contents have been recorded in gorse shrub biomass and ash composition: for example, Jobson and Thomas [55] noted that gorse biomass composition was characterized by high potassium contents, and Soto and Diaz-Fierros [56] measured alkali metal contents of 30% in gorse ash in NW Spain. Biomass with high annual growth is abundant in alkaline elements because they are readily taken up from the soil [16]. Consequently, higher alkali metal contents can be found in herbaceous than in woody fuels: Vassilev et al. [16] reported average K_2O contents of 24.6% and 10.7% for herbaceous and woody fuels ashes, respectively. Similarly to what discussed in Sections 3.2.1. and 3.3., the mobile nutrient potassium is easily retranslocated and accumulated in low diameter woody fractions as well as in leaves. For instance, Werkelin et al. [48] observed enriched K content in the ashes of young and biologically active tissues such as leaves, together with 1.4–1.7 times higher K content in the ashes of the wood of small-sized branches and twigs compared to the ashes from branches with diameters larger than 3 cm.

This high content of potassium, together with other nutrients present in the shrub biomass composition, might be responsible for the relatively high ashes yield of the studied species: Jenkins et al. [57] observed an increasing potassium concentration in the fuel tended to accompany an increasing ash content. Furthermore, potassium content is important as an indication of the potential for ash fusion or deposition via vaporization and condensation [17]. Alkali metals, particularly potassium, have the tendency to react with the bed material or with ash silica to form eutectic mixtures with low melting points, forming sticky coatings on the surface of inert material particles and leading to subsequent agglomeration and even defluidization of the bed [20]. For instance, Fernández Llorente and Carrasco García [18], in the combustion of herbaceous energy crops such as thistle, straw or brassica, with K_2O contents in the ashes ranging from 10% to 20%, observed hard sintering and ash deformation at temperatures below 850 °C, these K contents being similar to the values observed in this study. In the present sudy, all the studied species showed ash potasium contents above the 7% threshold for K in ash established by Obernberger et al. [49] for avoiding ash melting, deposition and corrosion in biomass combustion. Potential ash sintering, slagging and fouling risk is further evaluated in the following Section 3.6.2.

3.6.2. Ash slagging and fouling indices and slagging and fouling risk

Results from the calculation of ash slagging and fouling indices, and associated ash slagging and fouling risk, for the four species of study, are summarized in Table 6.

The results of the slagging index Basic to Acid ashes (B/A), with values above the threshold of 0.75 proposed by Bryers [45] for the ashes of all the studied species, suggests that the low content of silica found in the ashes would not be expected to lead to significant formation of silicates in reaction with the alkali and alkaline earth metals present in the studied fuels. However, in addition to the intrinsic content of silica in the fuels, other exogenous sources of silica, such as soil contamination associated to the process of biomass harvesting, or potential reactions with silica bed materials, might be regarded as a potential source for the occurrence of ash agglomeration and fusion (e.g. [18,44]).

The Rs index suggested a low sulfur-based corrosion risk for all the studied species, these results being expected, given the low S content reported for all the studied species in Table 3, below the 0.1% threshold established by Obernberger et al. [49] for minimizing sulfur-related corrosion risk during combustion as discussed in Section 3.3. above.

Calculated alkali index in the present study was above the 0.17 kg alkali MJ^{-1} threshold for probable slagging and fouling for broom and gorse ashes, whereas heath and carqueisa ashes, with values of 0.14 and 0.16 kg alkali MJ^{-1}, were in the vicinity of the probable slagging and fouling threshold from Miles et al. [17]. The reported alkali index is in the lower range of typical herbaceous fuels values of 0.2 to >2 kg alkali MJ^{-1}, which contain enough alkali for the ashes to melt in combustion and/or the elements vaporize and condense on boiler tubes and refractories [17], but in higher amounts than average reported alkali indexes for woody fuels or leached agricultural fuels with low slagging risk, typically with alkali indexes values of <0.2 (e.g. [17,44]).

In addition, the relative amount of alkali metals to alkaline earth metals in the ashes, as evaluated by Fernández Llorente and Carrasco García [18] SI index, was below the threshold value of 2 for avoiding ash sintering in the combustion proposed by the authors. Similarly low values of this index (SI < 0.3) would be obtained utilizing Spanish gorse ashes composition data from the literature [56]. This high alkali/ alkaline earth metals content might result in a low fusion temperature of the ashes of the studied species: as illustrated by [20], increased alkali metal contents together with decreasing alkaline earth metals generally result in lower ash sintering and fusion temperatures, enhancing the probability of ash agglomeration and fusion in the boiler.

Furthermore, as evaluated by [44] BAI index, bed agglomeration would expectedly occur in the case of combustion of the studied species in fludized-bed reactors. Boiler-scale combustion tests should be conducted to discriminate the actual slagging and fouling risk of the studied shrub species ashes under different combustion technologies.

Table 7 shows the content of trace and selected minor elements As, Cd, Pb and Co, Cu, Cr, Mn, Zn and Ni, measured in the ashes of the studied species. The measured values are compared to the limit values for these elements established by the legislation on ash utilization as a fertilizer in agriculture and forestry from European countries such as Finland, Denmark, Austria, Sweden and UK as synthesized in Haglund [58]. The Spanish [59] and Portuguese [60] currently existing legislation with limiting values for these elements is established for sludge from water treatment plants intended for application in agricultural soils. Measured contents of ash As, Cd, Pb, Co, Cu, Cr, Mn, Zn and Ni were similar to the usual ranges of 3–60, 0–25, 15–650, 1–20, 15–400, 10–250, 1000–30000, 15–4400 and 6–200 mg kg^{-1}, respectively, commonly found in wood and bark ash for these elements as reported in the literature [61,27–29,62]. The measured values were well below the limits established by Spanish and Portuguese current legislation for all the studied elements and below the limits from most of the European countries legislation as summarized in Table 7. Some of the most conservative thresholds established by North and Central European countries for Cd (<1.5 mg kg^{-1}), Cu (<250 mg kg^{-1}), Cr (<100 mg kg^{-1}), and Zn (<1500 mg kg^{-1}), however, would not be met neither by some of the observed values in shrub ash, nor by typical values from wood and bark ash (e.g. [61,27–29,62]).

Pitman [27] pointed out that, whereas typical trace elements contents found in forest residues ash should present no risk, as long as fly ash is not used, the variability of Zn, Ni and Cu in bottom ash poses a risk of exceeding permissible levels if ash is applied in large quantities. The applied dose and ash form plays an important role in the potential effects on the environment [27], [28] and [29]. Pitman [27] noted that applications of ash up to 10 t ha^{-1} from ordinary boilers result in heavy metal soil levels still two orders of magnitude lower than the USEPA (*United States Environmental Protection Agency*) advised loading. However, long-term research in ecological effects of ash application is scarce [27–29], particularly under forest mineral soils in Mediterranean countries [28], and further work on quantifying their potential impact must be conducted in the region.

4. Conclusions

Selected native woody shrub species from NW Spain and central Portugal white broom, heath, carqueisa and gorse, showed several advantageous properties as biomass fuels, such as high HHV (21–24 MK kg^{-1}) and interesting energy density values both under a summer (2.2–3.2 GJ m^{-3}) and winter harvest scenario (1.1–1.4 GJ m^{-3}). Further work may focus on detailed moisture content, heating value and associated energy density variations study under different harvesting season and logistic scenarios, as well as on the quantification of calorific values for other native shrubby woody species of the studied genus.

Main drawbacks included high N contents (>0.6–2%) and a relatively high (1–2%) ashes content, combined with a high (20–30%) alkali metals contents in the ashes, measured for all of the studied species at the two areas of study, resulting in a potential NOx emissions, sintering [18], fouling [17] and bed agglomeration [44] risk in the combustion of the studied fuels. Research on actual emissions and slagging and fouling risk of the studied fuels under real combustion conditions should be conducted, particularly given the scarcity of boiler-scale combustion studies for shrubby biomass fuels. Preventive measures, such as co-combustion with low-nitrogen and high-calcium biomasses, or the incorporation of additives on the combustion of the studied species under different combustion technologies, might deserve future investigation. The potential influence of logistics, including the effect of rain leaching on the content of shrub biomass and ash nutrient contents, should also be further explored for these and other native woody shrubby species in the region, covering a range of soil types and seasons of harvest.

Measured trace and selected minor elements were below national and most European thresholds for these metals, suggesting potential of the biomass ashes to be utilized as fertilizer, this requiring a comprehensive environmental monitoring of fly and bottom ashes obtained under a variety of combustion technologies and under a variety of soil types.

Acknowledgements

Authors would like to express their acknowledgements to the Portuguese Science and Technology Foundation (FCT), programme SFRH/PROTEC/49626/2009. They also would like to thank Eng. Cristóvão Santos from Mechanical Department of the University of Trás-os-Montes and Alto Douro where calorific analysis were performed and Eng. Rui Rocha from Leco laboratory for the assistance in elemental analysis. The authors would like to sincerely thank the anonymous reviewers for their highly productive suggestions for improving the manuscript.

References

[1] DGGE. Estratégia Nacional para a Energia. A criação de uma rede de Centrais de Biomassa dedicadas. Direcção Geral de Geologia e Energia, Lisboa; 2006. p. 19.
[2] Plan De Acción Nacional De Energías Renovables De España (PANER) 2011–2020. Ministerio de Industria, Turismo y Comercio, Gobierno de España; 2010. p. 138.
[3] Viana H, Cohen WB, Lopes D, Aranha J. Assessment of forest biomass for use as energy. GIS-based analysis of geographical availability and locations of wood-fired power plants in Portugal. Appl Energy 2010;87:2551–60.
[4] Bermúdez J, Piñeiro G. La biomasa forestal en Galicia, situación actual y perspectivas de aprovechamiento. CIS-Madera 2000;5:27–40.
[5] Miranda MT, Arranz JI, Rojas S, Montero I. Energetic characterization of densified residues from Pyrenean oak forest. Fuel 2009;88:2106–12.
[6] Núñez-Regueira L, Proupín-Castiñeiras J, Rodríguez-Añón JA. Energy evaluation of forest residues originated from shrub species in Galicia. Bioresour Technol 2004;91:215–21.
[7] AFN. FloreStat, 5th national forest inventory information retrieval tool. Ministério da Agricultura do Desenvolvimento Rural e das Pescas, Lisboa; 2010.
[8] AFN. Estatísticas dos incêndios florestais. Totais Nacionais (2001–2010). Autoridade Nacional Florestal. Ministério da Agricultura do Desenvolvimento Rural e das Pescas, Lisboa; 2011.
[9] Silva T, Pereira J, Paúl J, Santos M, Vasconcelos M. Estimativa de Emissões Atmosféricas Originadas por Fogos Rurais em Portugal. Silva Lusitana 2006;14:239–63.
[10] Núñez-Regueira L, Rodríguez J, Proupín J, Mouriño B. Forest waste as an alternative energy source. Thermochim. Acta 1999;328:105–10.
[11] Elvira LM, Hernando C. Inflamabilidad y energía de las especies de sotobosque: estudio piloto con aplicación a los incendios forestales, 68, Monografías INIA; 1989.
[12] Fernandes PM, Pereira JP. Caracterização de combustíveis na serra da Arrábida. Silva Lusitana 1993;1:237–60.
[13] Fernandes PM, Rego FC. A new method to estimate fuel surface area- to-volume ratio using water immersion. Int J Wildland Fire 1998;8:121–8.
[14] Demirbas A. Calculation of higher heating values of biomass fuels. Fuel 1997;76:431–4.
[15] Friedl A, Padouvas E, Rotter H, Varmuza K. Prediction of heating values of biomass fuel from elemental composition. Anal Chim Acta 2005;544:191–8.
[16] Vassilev SV, Baxter D, Andersen LK, Vassileva CG. An overview of the chemical composition of biomass. Fuel 2010;89:913–33.
[17] Miles TR, Miles Jr TR, Baxter LL, Bryers RW, Jenkins BM, Oden LL. Boiler deposits from firing biomass fuels. Biomass Bioenergy 1996;10:125–38.

[18] Fernández Llorente MJ, Carrasco García JE. Comparing methods for predicting the sintering of biomass ash in combustion. Fuel 2005;84:1893–900.
[19] Vega-Nieva DJ, Dopazo R, Ortiz L. Slagging risk of mediterranean biomasses for combustion. In: World bioenergy, Jönköping, Sweden; 2010.p. 12–6.
[20] Werther J, Saenger M, Hartge EU, Ogada T, Siagi Z. Combustion of agricultural residues. Prog Energy Combust Sci 2000;26:1–27.
[21] Phyllis, database for biomass and waste. Energy research Centre of the Netherlands. <http://www.ecn.nl/phyllis/> [accessed March 2012].
[22] Wood Ash Database – chemical composition of ashes formed during combustion of biofuels from tree compartments. <http://woodash.slu.se/eng/ [accessed March 2012].
[23] BioBank. BIOS bioenergiesysteme GmbH, Version 2.4, Graz, Austria. <http://www.ieabcc.nl/database/ash.php> [accessed March 2012].
[24] US DOE Biomass Feedstock Composition and Property Database. <http://www1.eere.energy.gov/biomass/databases.html> [Accessed March 2012].
[25] Biolex database, properties for the samples of solid biomass fuels. <www.biolexbase.dk> [accessed March 2012].
[26] Reisinger K, Haslinger C. Herger M, Hofbauer H. BIOBIB – a database for biofuels. Institute of Chemical Engineering. Fuel and Environmental Technology. <http://www.vt.tuwien.ac.at/biobib/biobib.html> [accessed March 2012].
[27] Pitman RM. Wood ash use in forestry – a review of the environmental impacts. Forestry 2006;79:563–88.
[28] Augusto L, Bakker M, Meredieu C. Wood ash applications to temperate forest ecosystems – potential benefits and drawbacks. Plant Soil 2008;306:181–98.
[29] Omil B, Piñeiro V, Merino A. Trace elements in soils and plants in temperate forest plantations subjected to single and multiple applications of mixed wood ash. Science Total Environ 2007;381:157–68.
[30] DD CEN/TS 14780:2005. Solid biofuels – methods for sample preparation.
[31] CEN EN 14774-1:2009, Solid biofuels – determination of moisture content – oven dry method – Part 1: Total moisture – reference method.
[32] CEN EN 14775:2009. Solid biofuels – determination of ash content.
[33] CEN EN 15148:2009. Solid biofuels – determination of the content of volatile matter.
[34] Tsoumis GT. Science and technology of wood. structures, properties, utilization. New York: Van Nostrand Reinhold; 1991.
[35] DD CEN/TS 15104:2005. Solid biofuels – determination of total content of carbon, hydrogen and nitrogen – instrumental methods.
[36] DD CEN/TS 15289:2006. Solid biofuels – determination of total content of sulphur and chlorine.
[37] CEN EN 14918:2009, Solid biofuels – determination of calorific value.
[38] DD CEN/TS 15234:2006. Solid biofuels – fuel quality assurance. Annex E. Calculation of the net calorific value in different basis and energy density as received.
[39] Hakkila P, Parikka M. Fuel resources from the forest. In: Richardson J, Björheden R, Hakkila P, Lowe AT, Smith CT, editors. Bioenergy from sustainable forestry. Guiding principles and practice, vol. 71. Kluwer Academic Publishers.; 2002.
[40] Spinelli R, Magagnotti N. Logging residue bundling at the roadside in mountain operations. Scand J Forest Res 2009;24:173–81.
[41] DD CEN/TS 15290:2006. Solid biofuels – determination of major elements.
[42] DD CEN/TS 15297:2006, Solid biofuels – determination of minor elements.
[43] Baernthaler G, Zischka M, Haraldsson C, Obernberger I. Determination of major and minor ash-forming elements in solid biofuels. Biomass Bioenergy 2006;30:983–97.
[44] Vamvuka D, Zografos D. Predicting the behaviour of ash from agricultural wastes during combustion. Fuel 2004;83:2051–7.
[45] Watanabe A, Daly CC, Devine CE, Bryers RW. Fireside slagging, fouling, and high-temperature corrosion of heat-transfer surface due to impurities in steam-raising fuels. Progress Energy Combust Sci 1996;22:29–120.
[46] Doat J, Valette J, Askri ChD, Caumartin L, Bettachine M, et al. Le pouvoir calorifique supérieur d'espèces forestières méditerranéennes. Ann Forest Sci 1981;38:469–86.
[47] Dimitrakopoulos AP, Panov PI. Pyric properties of some dominant mediterranean vegetation species. Int J Wildland Fire 2001;10:23–7.
[48] Werkelin J, Skrifvars B-J, Hupa M. Ash-forming elements in four Scandinavian wood species. Part 1: summer harvest. Biomass and Bioenergy 2005;29: 451–66.
[49] Obernberger I, Brunner T, Bärnthaler G. Chemical properties of solid biofuels—significance and impact. Biomass Bioenergy 2006;30:973–82.
[50] Bará S. Fertilización forestal. Colección técnica Consellería de Agricultura. Xunta de Galicia, vol. 9; 1998.
[51] Hough WA. Calorific values of some forest fuels of southern United States. US Forest Serv South For Exp Stn Res Note SE-120; 1969.
[52] Gillon D, Hernando C, Valette J-C, Joffre R. Fast estimation of the calorific values of forest fuels by near-infrared reflectance spectroscopy. Canadian J Forest Res 1997;27:760–5.
[53] Madrigal J, Guijarro M, Hernando C, Díez C, Marino E. Effective heat of combustion for flaming combustion of mediterranean forest fuels. Fire Technol 2011;47:461–74.
[54] Loo Sv, Koppejan J. The handbook of biomass combustion and co-firing. London: Earthscan; 2008.
[55] Jobson HT, Thomas B. The composition of gorse (Ulex europaeus). J Sci Food Agric 1964;15:652–6.
[56] Soto B, Diaz-Fierros F. Interactions between plant ash leachates and soil. Int J Wildland Fire 1993;3:207–16.
[57] Jenkins BM, Baxter LL, Miles Jr, TR, Miles TR. Combustion properties of biomass. Fuel Process Technol 1998;54:17–46.
[58] Haglund N, E. group, guideline for classification of ash from solid biofuels and peat utilised for recycling and fertilizing in forestry and agriculture. Nordic Innovation Centre, Norway; 2008.
[59] 1990/26940 Real Decreto 1310/1990, de 29 de Octubre, por el que se regula la Utilización de los Lodos de Depuración en el Sector Agrario. BOE 262/1990 de 01-11-1990, pp. 32339. Ministerio de Agricultura, Pesca y Alimentación, Gobierno de España.
[60] Decreto-Lei No. 118/2006, de 21 de Junho, Estabelece o regime jurídico da utilização agrícola das lamas de depuração [Establishes the legal regime of the agricultural use of sewage sludge].
[61] Steenari BM, Lindqvist O. Stabilisation of biofuel ashes for recycling to forest soil. Biomass Bioenergy 1997;13:39–50.
[62] Haraldsen TK, Pedersen PA, Grønlund A. Mixtures of bottom wood ash and meat and bone meal as NPK fertilizer. In: Insam H, Knapp BA, editors. Recycling of biomass ashes. Berlin (Heidelberg): Springer; 2011. p. 33–44.